Bruker BioSpin

Solid State NMR

AVANCE Solids
User Manual

Version 002

think forward

NMR Spectroscopy

The information in this manual may be altered without notice.

BRUKER BIOSPIN accepts no responsibility for actions taken as a result of use of this manual. BRUKER BIOSPIN accepts no liability for any mistakes contained in the manual, leading to coincidental damage, whether during installation or operation of the instrument. Unauthorized reproduction of manual contents, without written permission from the publishers, or translation into another language, either in full or in part, is forbidden.

This manual was written by:

Hans Foerster, Jochem Struppe, Stefan Steuernagel, Fabien Aussenacc, Francesca Benevelli, Peter Gierth, and Sebastian Wegner

Desktop Published by:

Stanley J. Niles

Rheinstetten, Germany

P/N: Z31848
DWG-Nr.: Z4D10641 002

For further technical assistance on Solid State NMR, please do not hesitate to contact your nearest BRUKER dealer or contact us directly at:

BRUKER BioSpin GMBH
am Silberstreifen
D-76287 Rheinstetten
Germany

Phone: + 49 721 5161 0
FAX: + 49 721 5171 01
E-mail: solids@bruker.de, service@bruker.de
Internet: www.bruker.com

Contents

Contents 3

1 Introduction 9

1.1 Disclaimer 10
1.2 Safety Issues 10
1.3 Contact for Additional Technical Assistance 10

2 Test Samples 11

3 General Hardware Setup 15

3.1 Connections to the Preamplifier 15
3.2 RF Connections Between Preamplifier and Probe 20
3.3 RF-Filters in the RF Pathway 21
3.4 Connections for Probe Identification and Spin Detection 25
3.5 MAS Tubing Connections 26
3.5.1 Connections 27
Wide Bore (WB) Magnet Probes 28
Standard Bore (SB) Magnet Probes 30
3.6 Additional Connections for VT Operation 31
3.7 Probe Setup, Operations, Probe Modifiers 41
3.7.1 Setting the Frequency Range of a Wideline (single frequency) Probe 41
3.7.2 Shifting the Probe Tuning Range 42
3.7.3 Adding a Frequency Channel to a Probe (WB probes only) 48
3.8 Mounting the Probe in the Magnet/Shim Stack 50
3.9 EDASP Display: Software Controlled Routing 51

4 Basic Setup Procedures 55

4.1 General Remarks 56
4.2 Setting the Magic Angle on KBr 57
4.2.1 RF-Routing 57
4.2.2 Setting Acquisition Parameters 59
4.3 Calibrating 1H Pulses on Adamantane 65
4.4 Calibrating 13C Pulses on Adamantane and Shimming the Probe 73
4.5 Calibrating Chemical Shifts on Adamantane 75
4.6 Setting Up for Cross Polarization on Adamantane 76
4.7 Cross Polarization Setup and Optimization for a Real Solid: Glycine 79
4.8 Some Practical Hints for CPMAS Spectroscopy 85
4.9 Field Setting and Shift Calibration 87
4.10 Literature 88

5 Decoupling Techniques 89

5.1 Heteronuclear Decoupling 89

5.1.1 CW Decoupling 89
5.1.2 TPPM Decoupling 90
5.1.3 SPINAL Decoupling 91
5.1.4 Swept-Frequency-TPPM 91
5.1.5 XiX Decoupling 91
5.1.6 Pi-Pulse Decoupling 91
5.2 Homonuclear Decoupling 92
5.2.1 Multiple Pulse NMR: Observing Chemical Shifts of Homonuclear Coupled Nuclei 92
5.2.2 Multiple Pulse Decoupling 92
BR-24, MREV-8, BLEW-12 92
FSLG Decoupling 92
DUMBO 97
5.3 Transverse Dephasing Optimized Spectroscopy 98

6 Practical CP/MAS Spectroscopy on Spin 1/2 Nuclei 99

6.1 Possible Difficulties 99
6.2 Possible Approaches for 13C Samples 99
6.3 Possible Approaches for Non-13C Samples 101
6.4 Hints, Tricks, Caveats for Multi-nuclear (CP-)MAS Spectroscopy 102
6.5 Setup for Standard Heteronuclear Samples 15N, 29SI, 31P 102

7 Basic CP-MAS Experiments 105

7.1 Pulse Calibration with CP 105
7.2 Total Sideband Suppression TOSS 106
7.3 SELTICS 110
7.4 Non-Quaternary Suppression (NQS) 113
7.5 Spectral Editing Sequences: CPPI, CPPISPI and CPPIRCP 116

8 FSLG-HETCOR 119

8.1 Pulse Sequence Diagram for FSLG HETCOR 120
8.2 Setting up FSLG HETCOR 121
8.3 Results 125

9 Modifications of FSLG HETCOR 127

9.1 Carbon Decoupling During Evolution 128
9.2 HETCOR with DUMBO, PMLG or w-PMLG, Using Shapes 129
9.2.1 The Sequence pmlghet 129
9.2.2 w-pmlghet 132
9.2.3 edumbohet 133
9.2.4 dumbohet 134
9.3 HETCOR with Cross Polarization under LG Offset 135

10 RFDR 137

10.1 Experiment 138
10.2 Set-up 138
10.3 Data Acquisition 139
10.3.1 Set-up 2D Experiment 139
10.4 Spectral Processing 141

11 Proton Driven Spin Diffusion (PDSD) 143

11.1 Pulse Sequence Diagram 145
11.2 Basic Setup 145
11.2.1 2D Experiment Setup 146
11.3 Acquisition Parameters 147
11.3.1 Processing Parameters 149
11.4 Adjust the Rotational Resonance Condition for DARR/RAD 149
11.5 Example Spectra 151

12 REDOR 155

12.1 Pulse Sequence 157
12.2 Setup 157
12.2.1 Data Acquisition 159
12.2.2 Data Processing 160
12.3 Final Remarks 167

13 SUPER 169

13.1 Overview 169
13.2 Pulse Program 170
13.3 2D Experiment Setup 170
13.3.1 Experiment setup 170
13.3.2 Setup 2D Experiment 171
13.4 Data Acquisition 173
13.5 Spectral Processing 174

14 Symmetry Based Recoupling 179

14.1 Pulse Sequence Diagram, Example C7 181
14.2 Setup 181
14.2.1 Spectrometer Setup for 13C 183
14.2.2 Setup for the Recoupling Experiment 183
14.2.3 Setup of the 2D SQ-DQ Correlation Experiment 185
14.3 Data Acquisition 186
14.4 Spectral Processing 188
14.5 13C-13C Single Quantum Correlation with DQ Mixing 189
14.6 Data Acquisition 190
14.7 Spectral Processing 191

15 PISEMA 193

15.1 Pulse Sequence Diagram 194
15.2 Setup 195
15.3 Processing 198

16 Relaxation Measurements 201

16.1 Describing Relaxation 201
16.2 T1 Relaxation Measurements 202
16.2.1 Experimental Methods 202
16.2.2 The CP Inversion Recovery Experiment 203
16.2.3 Data Processing 205
16.2.4 The Saturation Recovery Experiment 208

16.2.5 T1p Relaxation Measurements 209
16.3 Indirect Relaxation Measurements 210
16.3.1 Indirect Proton T1 Measurements 211

17 Basic MQ-MAS 213

17.1 Introduction 213
17.2 Pulse sequences 213
17.3 Data Acquisition 215
17.3.1 Setting Up the Experiment 215
17.3.2 Two Dimensional Data Acquisition 220
17.4 Data processing 222
17.5 Obtaining Information from Spectra 225

18 MQ-MAS: Sensitivity Enhancement 231

18.1 Split-t1 Experiments and Shifted Echo Acquisition 231
18.2 Implementation of DFS into MQMAS Experiments 233
18.2.1 Optimization of the Double Frequency Sweep (DFS) 233
18.2.2 2D Data Acquisition 238
18.2.3 Data Processing 240
18.3 Fast Amplitude Modulation - FAM 242
18.4 Soft Pulse Added Mixing - SPAM 242

19 STMAS 245

19.1 Experimental Particularities and Prerequisites 245
19.2 Pulse Sequences 247
19.3 Experiment Setup 249
19.3.1 Setting Up the Experiment 249
19.3.2 Two Dimensional Data Acquisition 251
19.4 Data Processing 253

20 Double-CP 255

20.1 Pulse Sequence Diagram, Double CP (DCP) 256
20.2 Double CP Experiment Setup 256
20.2.1 Double CP 2D Experiment Setup 256
20.2.2 15N Channel Setup 258
20.2.3 Setup of the Double CP Experiment 259
20.2.4 Setup of the 2D Double CP Experiment 264
20.3 2D Data Acquisition 265
20.4 Spectral Processing 266
20.5 Example Spectra 267

21 CRAMPS: General 271

21.1 Homonuclear Dipolar Interactions 271
21.2 Multiple Pulse Sequences 271
21.3 W-PMLG and DUMBO 272
21.4 Quadrature Detection and Chemical Shift Scaling 273

22 CRAMPS 1D 275

22.1 Pulse Sequence Diagram of W-PMLG or DUMBO 275

22.2 Pulse Shapes for W-PMLG and DUMBO 276
22.3 Analog and Digital Sampling Modi 277
22.3.1 Analog Mode Sampling 278
22.3.2 Digital Mode Sampling 278
22.4 Setup 279
22.5 Parameter Settings for PMLG and DUMBO 279
22.6 Fine Tuning for Best Resolution 281
22.7 Fine Tuning for Minimum Carrier Spike 281
22.8 Correcting for Actual Spectral Width 281
22.9 Digital Mode Acquisition 282
22.10 Examples 282

23 Modified W-PMLG 285

23.1 Pulse Sequence Diagram for Modified W-PMLG 285
23.2 Pulse Shapes for W-PMLG 286
23.3 Setup 287
23.4 Parameter Settings for PMLG and DUMBO 287
23.5 Fine Tuning for Best Resolution 288
23.6 Correcting for Actual Spectral Width 288
23.7 Digital Mode Acquisition 289

24 CRAMPS 2D 291

24.1 Proton-Proton Shift Correlation (spin diffusion) 291
24.2 Pulse Sequence Diagram 292
24.3 Data Processing 293
24.4 Examples 294
24.5 Proton-Proton DQ-SQ Correlation 296
24.6 Pulse Sequence Diagram 297
24.7 Data Processing 299
24.8 Examples 299

A Appendix 303

A.1 Form for Laboratory Logbooks 303

Figures 309

Tables 315

Index 319

Contents

Introduction 1

This manual is intended to help the users set up a variety of different experiments that are nowadays more or less standard in solid state NMR.

Previously, the manuals described the hardware in some detail, and also basic setup procedures. Armed with this knowledge, it was assumed the users would be in a position to manage the setup of even complicated experiments themselves.

In this manual however, the hardware is not discussed in detail, since there is no longer much hardware which is specific to solid-state NMR. There are still transmitters with higher power, and preamps and probes that take this power, but for the purposes of experimental setup, detailed knowledge is not required, since the setup does not generally depend on the details of the hardware. So, this manual is now much more specific to the type of experiment which is to be executed, and includes tricks and hints required to set the experiment up properly for best performance. If any special hardware (or software) knowledge is required, it is indicated within the experimental section.

This manual begins with the most frequently used solid-state NMR experiments, and will be extended as time permits and as it is required by new development in NMR. The manual is written primarily for Bruker AVANCE III instruments, but the experimental part will be identical, or similar, for AVANCE I and AVANCE II instruments. For example, pulse programs will have slightly different names, differing usually in the pulse program name extension. Contact your nearest applications scientist if you do not find the experiment/pulse program that you are looking for. Users of older instruments (DSX, DMX, DRX) should refer to the Solids Users Manual delivered within the Help system at Help -> Other topics -> Solids Users Manual. Even though the pulse programs may look similar, they will not run on these instruments.

The first five chapters deal with basic setup procedures, subsequent chapters are dedicated to specific types of experiments. There may be many different „sub“ experiments within a given type, since the same information can often be obtained with pulse sequences differing by subunits only, or in using a totally different principle. The experiments outlined here are usually the most important ones and/or the ones that were common at the time when the manual was written.

New chapters will be added, as the manual consists of largely self-contained units rather than being a comprehensive single volume. This was done in order to be more flexible in updating/replacing individual chapters. So do not be surprised if some chapters are still missing, they will be completed in the near future and implemented as they are finished and proofread. The individual chapters are written by different people, so there will be some differences in style and composition.

Note Concerning Future TopSpin Release

Upon the release of this manual, a new TopSpin version was in development. In the new version, which is scheduled to be released later this year, there are fairly big changes that will influence all of the setup routines described in this manual.

In the future version of TopSpin there will be a different way of setting pulse powers. There will be a watt scale which refers to the pulse power in watts. This allows you to set pulse powers in a spectroscopically more relevant scale. Moreover, different transmitters and different routings will not anymore have an influence on the pulse power setting, since it is referenced to an absolute, not relative scale. This means however, that some setup routines within this manual will have to be modified to comply with this. The setting will also be possible on a dB scale, however with an absolute reference. Power level changes will therefore be calculated properly using ***calcpowlev.*** Where pulse power recommendations are given in this manual, they will still apply if given in watts, they will however not apply in the future version of TopSpin if given in dB.

We will try to release a new version of this manual when the new TopSpin version is available, whereas possible inconsistencies will be removed. There is no inconsistency with TopSpin vs. 2.1.

Disclaimer *1.1*

Any hardware units mentioned in this manual should only be used for their intended purpose as described in their respective manual. Use of units for any purpose other than that for which they are intended is taken only at the users own risk and invalidates any and all manufacturer warranties.

Service or maintenance work on the units must be carried out by qualified personnel.

Only those persons schooled in the operation of the units should operate the units.

Read the appropriate user manuals before operating any of the units mentioned. Pay particular attention to any safety related information.

Safety Issues *1.2*

Please refer to the corresponding user manuals for any hardware mentioned in this manual for relevant safety information.

Contact for Additional Technical Assistance *1.3*

For further technical assistance please do not hesitate to contact your nearest BRUKER dealer or contact us directly at:

BRUKER BioSpin GMBH
am Silberstreifen
D-76287 Rheinstetten
Germany

Phone: + 49 721 5161 0
FAX: + 49 721 5171 01
E-mail: service@bruker.de
Internet: www.bruker.de

Test Samples 2

Table 2.1. Setup Samples for Different NMR Sensitive Nuclei

Nucleus	Sample	Method	O1P	Remarks
^{3}H				
^{1}H	Silicone paste Silicone rubber Adamantane Glycine Malonic Acid	^{1}HMAS ^{1}HMAS ^{1}HMAS CRAMPS CRAMPS	0 0 0 -3 -3	setup proton channel, shim, set field setup proton channel, set field setup proton channel, set field, shim under CRAMPS conditions setup CRAMPS resolution CRAMPS, d1=60s
^{19}F	PVDF PTFE	^{19F}MAS CP ^{19}FMAS	106 126	direct observe ^{19}F CP $^{1}H/^{19}F$, $^{1}H/^{13}C$, $^{19}F/^{13}C$ (low sensitivity) direct observe
^{3}He				
^{203,209} Tl				
^{31}P	$(NH_4)H_2PO_4$	$^{1}H/^{31}$PCP	0	powdered sample, piezoelectric, 4s
^{7}Li	LiCl	MAS		
$^{117,119}Sn$	Sn (cyclohexyl)$_4$ $Sm_2Sn_2O_7/SnO_2$	CP MAS		5ms contact, d1>10s VT shift thermometer, d1<1s $Sm_2Sn_2O_7$,>60s SnO_2 (temp. independent)
^{87}Rb	$RbNO_3$, $RbClO_4$	MQMAS	0	0.5s repetition
^{11}B	BN Boric Acid	MAS MQMAS		 >5s repetition
^{65}Cu	Cu-metal powder	wideline		knight shift +2500ppm
^{71}Ga	Ga_2O_3	hahn echo		CT 300 kHz wide
^{129}Xe	as hydroquinon Clathrate gas in air	CPMAS	0 0	d1>5s single pulses overnight, 1s
^{23}Na	Na_2HPO_4 $Na_3P_3O_9$	MQMAS MQMAS	0	dep. on crystal water 2-5 lines
^{51}V	NH_4VO_4			
^{123}Te				
^{27}Al	AlPO-14	MQMAS	0	d1 05-1s, 4 lines

Table 2.1. Setup Samples for Different NMR Sensitive Nuclei

^{13}C	Adamantane α-glycine	CP,DEC CP	50 110	HH setup, shim sensitivity,decoupling.Prep.: precipitate with acetone from aq. solution, C,N fully labelled for fast setup, recoupling, REDOR (10% in natrl. abundance)
^{79}Br	KBr	MAS	57	d1< 50msec, angle setting finely powdered, reduced volume
^{59}Co	$Co(CN)_6$	MAS		shift thermometer
^{55}Mn	$KMnO_4$	MAS		>500 kHz pattern
^{93}Nb				
^{207}Pb	$PbNO_3$ $Pb(p\text{-tolyl})_4$	MAS CP	 -150	shift thermometer, 0,753 ppm/degr. d1>10s 5ms, 15s
^{29}Si	Q_8M_8 DSS,TMSS	CPMAS CPMAS	-50 0	d1>5s, reference sample 12.6/-108 ppm reference sample 0 ppm
^{77}Se	H_3SeO_3 $(NH_4)_2SeO_4$	CPMAS CPMAS	1800 -200	HH setup, 8ms contact, d1>10s 3ms, d1>4s
^{113}Cd	$Cd(NO_3)_2{*}4H_2O$	CPMAS	350	15ms contact, d1>8s
^{195}Pt	$K_2Pt(OH)_6$	CPMAS	-12000	1ms contact, d1>4s
^{199}Hg	$Hg(acetate)_2$ Hexakis (dimethyl sulphoxide) Hg(II) trifluorome-thansulfonate	CPMAS	2500 -2313	5ms contact, d1>10s 30-35ms contact, d1>10s *
^{2}H	d-PMMA d-PE $d\text{-}DMSO_2$	WL WL WL	0 0 0	wideline setup d1 5s wideline setup d1 0.5s/10s amorphous/ crystalline exchange expt. at 315K
^{6}Li	LiCl, Li (org.)			make sure it is not ^{6}Li depleted, d1>60s
^{17}O	D_2O		0	pulse determination, 100scans,0.5s
^{15}N	α-glycine	CP	50	sensitivity, 4ms contact,4s labelled for fast setup
^{35}Cl	KCl	WL,MAS	0	pulse determ., 100 scans
^{33}S	K_2S	MAS	0	100 scans in a >=500 MHz instr.
^{14}N	NH_4Cl	MAS,WL	0	100 scans, narrow line.
^{25}Mg				
$^{47/49}Ti$	Anatas	MAS		
^{39}K	KCl	MAS,WL	0	100 scans

Table 2.1. Setup Samples for Different NMR Sensitive Nuclei

^{109}Ag	$AgNO_3$ $AgSO_3CH_3$	MAS CPMAS	70	1scan, 500s, finely powdered 50 ms contact, 10 s repetition, 1 scan.
^{89}Y	$Y(NO_3)_3*6H_2O$	CPMAS	-50	10ms contact, d1>10s
* Literature: J.M. Hook, P.A.W. Dean and L.C.M. van Gorkom, *Magnetic Resonance in Chemistry*, 33, 77 (1995).				

General Hardware Setup

3

Avance instruments are constructed in a way to minimize the requirements to reconnect or readjust hardware for different experiments. Probe changes are however sometimes necessary, and require some manual operations. This chapter deals with connections that need to be done by the operator, and also with other manipulations that are required to set up the instrument in an optimum way.

Since the RF pathways are under software control up to the preamplifier, and under operator control between preamplifier and probe, both setups are considered separately.

All remaining connections (heater cable, thermocouple, gas flow, spin rate cable, PICS cable) can in no way be under software control, so the operator is responsible for proper wiring, cabling, and tubing! Since mistakes (especially in connection with compressed gas tubing) may cause rather expensive repairs, it is recommended to check carefully before an experiment is started.

The following operations will be described and illustrated with suitable images, for WB and SB probes, where non-trivial differences exist.

"Connections to the Preamplifier" on page 15

"RF Connections Between Preamplifier and Probe" on page 20

"RF-Filters in the RF Pathway" on page 21

"Connections for Probe Identification and Spin Detection" on page 25

"MAS Tubing Connections" on page 26

"Additional Connections for VT Operation" on page 31

"Probe Setup, Operations, Probe Modifiers" on page 41

"Mounting the Probe in the Magnet/Shim Stack" on page 50

"The edasp Display for a System with two Receiver Channels" on page 54

Connections to the Preamplifier *3.1*

For solids and liquids there should normally be different sets of preamplifiers. Liquids preamplifiers (HPPR, **H**igh **P**erformance **Pr**eamplifiers) are not suitable for some of the requirements of solid state NMR. Where CP/MAS applications are the only solids applications, it is however possible to use liquids preamplifiers for X-observation. Solids preamplifiers (HPHPPr, **H**igh **P**ower **H**igh **P**erformance **Pr**eamplifiers) are definitely required if high power ≥ 1 kW is used (liquids preamplifiers take max. 500W for X frequencies, 50W for proton and fluorine frequency). For the high frequency range ^{19}F and ^{1}H, two different types of solids preamps are available, the older HPHPPr ^{19}F /^{1}H and the recent replacement HPLNA

(**H**igh **P**ower **L**ow **N**oise **A**mplifier) which is strictly frequency selective, either ^{19}F or ^{1}H.

The connections into (the back) of the preamp stack should normally not be changed. For broadband high power preamplifiers, it is important to insert the appropriate “matching box” into the side of the preamp.

RF cables from transmitter, RS-485 control, DC voltages in, tune and lock RF in, RF signal out to receiver, gate pulses for preamplifier control (multi-receive setup only).

The orange colored cable is the high voltage supply for the HPLNA preamplifier.

Figure 3.1. All Connections to the Back of the Preamplifier

The lock preamplifier is located at the bottom of the stack, the transmitter cable carries the lock pulses. For solids, this preamp is normally not required.

When the transmitter cables are rewired to different preamp modules, the changes must be entered into the ***edasp*** routing (type ***edasp setpreamp***, NMRSU password required).

Figure 3.2. Transmitter Cables (only) Wired to Back of the Preamplifier

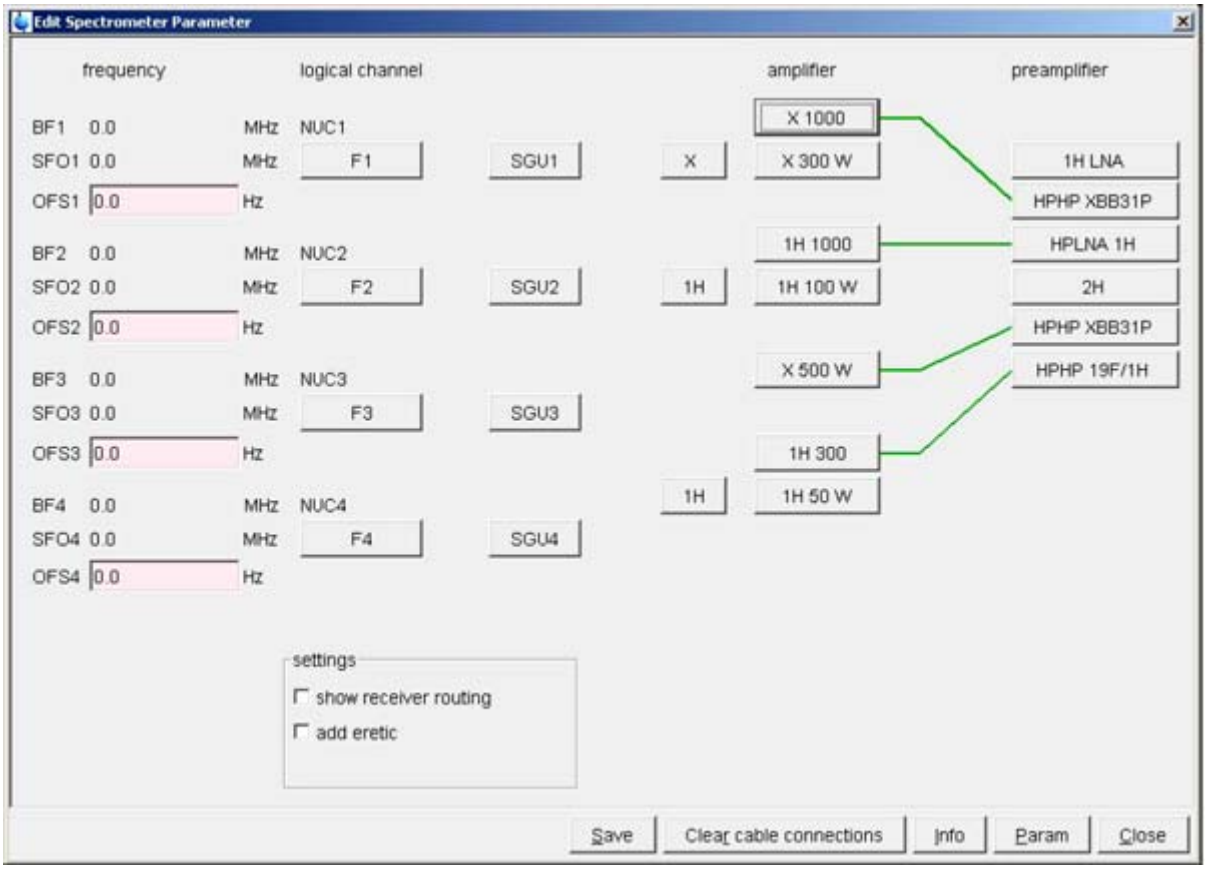

Figure 3.3. The edasp setpreamp Display

Note for ***Figure 3.3.***: Transmitter to preamplifier wiring must reflect hardware connections!

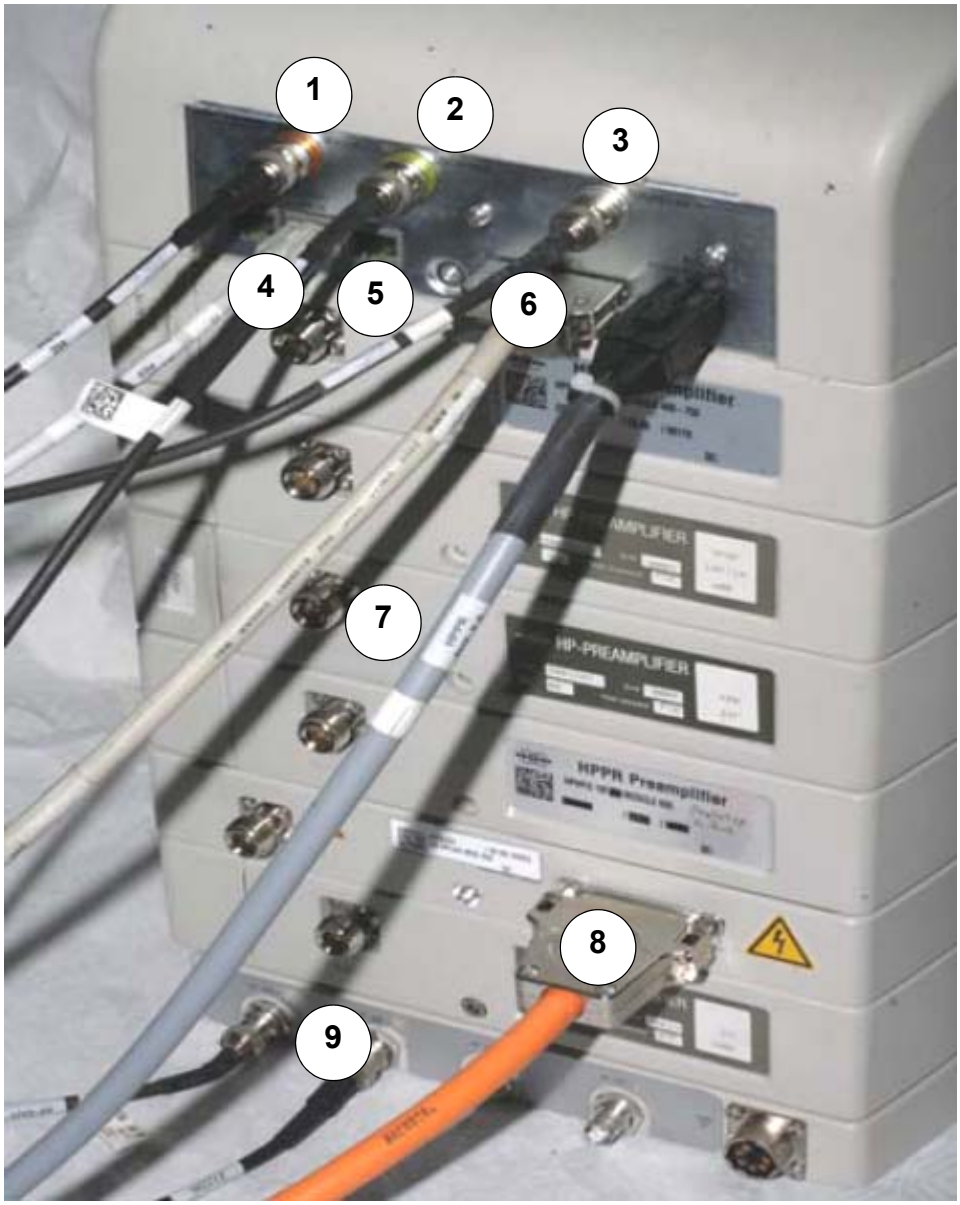

1. RF signal out to receiver
2. Lock signal out to lock receiver
3. Tune RF in (from SGU 2 aux out)
4. PICS probe ID cable to probe
5. ATMA and AUX connectors
6. RS 485 control connection and DCin
7. Additional DC supply for >3 preamps
8. High voltage DC for HPLNA-preamp
9. Additional controls for multi-receiver

Figure 3.4. Additional Connections to the Preamplifier Stack.

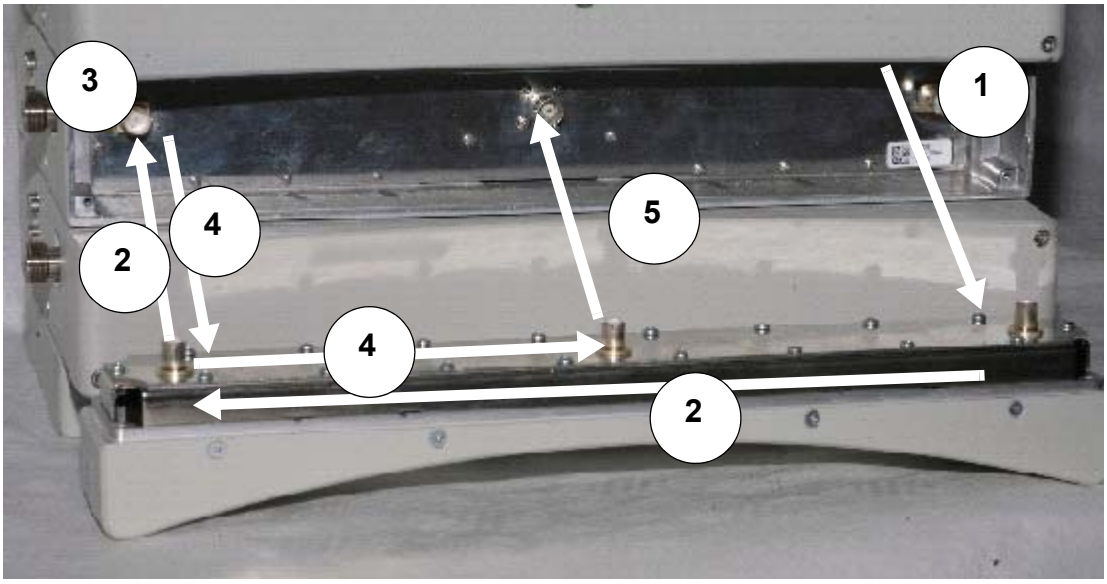

1. Pulse from TX
2. Pulse pathway to probe
3. To probe
4. Signal from probe
5. Signal to preamplifier

Figure 3.5. Matching Box Setup for High Power X-BB Preamplifiers

The frequency of the observed nucleus must be within the bandwidth of the matching box (the matching box contains a low pass filter to suppress frequencies above the X-nucleus frequency range (^{1}H, ^{19}F) and a passive diode multiplexer, which directs the RF pulse into the probe, and the NMR signal into the preamplifier). High resolution preamplifiers use actively switched pin diodes for this purpose and are therefore broadbanded, so there is no exchangeable box.

Pulsing with high power into an RF circuit which is not properly set up to pass this frequency may result in damage to the RF circuit (in this case, the “matching box”) or to the transmitter. This applies to filters, preamplifiers and matching boxes. Especially, if liquids preamps are used for solids work, as well power limitations as frequency limitations must be strictly observed!

RF Connections Between Preamplifier and Probe *3.2*

These connections must be done with high quality cable, with suitable length. It should be short, but not too short so that the cable must not be severely bent. Higher quality cable is fairly stiff; the flexible ones are of less quality.

N.B.: It is extremely important that RF cables are not bent to a radius of less than 30 cm, and that no force is exerted on the RF connectors. Adapters should be avoided; since every connector may change the impedance to deviate from the required 50 Ω. Cables with loose connectors should be discarded, unless they

can be repaired by a skilled RF engineer. BNC connectors should be avoided; they are usually off 50 Ω.

As pulses in solids NMR can be rather long, and rather high power, it is also necessary to consider the preamplifier's power limitations.

Proton high resolution preamps are unsuitable for high power pulses, especially for durations required for decoupling. High resolution X-BB preamplifiers are limited to 10 msec pulses at 300 (500) watts. If the back label does not say 500W, it is 300W max.

$^{1}H/^{19}F$ high power preamps need not necessarily be bypassed, but may gradually deteriorate under many decoupling pulses. It is therefore recommended to bypass these for decoupling unless the experiment requires that the preamp remain in line.

Warning: These preamps are not optimized for ^{19}F, so ^{19}F decoupling should never be done through this preamp.

^{1}H HPLNA preamplifiers need not be bypassed. HPLNA preamplifiers are strictly frequency selective; a ^{19}F pulse through a ^{1}H HPLNA will destroy it!

RF-Filters in the RF Pathway 3.3

RF filters are frequently required if more than one frequency is transmitted to the probe.

Without filtering, the noise and spurious outputs from the transmitter of one channel would severely interact with signal detection on another channel. One has to keep in mind that pulse voltages are in the order of hundreds of volts, but NMR signals are in the order of microvolt. In High Resolution, where the selection of nuclei to run is rather limited, it is possible to apply the necessary filtering inside the preamplifier. For solids, this is not easily possible, due to the wide range of possible detection frequencies, but also due to the additional dead time that filters may cause. So all filtering is done with external filters. If a single channel NMR experiment is run, no filters are required.

Usually, one filter per RF channel is required. Both filters should mutually exclude the frequency of the other channel(s). Usual attenuations of the frequency to be suppressed should be around > 80 dB, in special cases, when both frequencies

are rather close, >140 dB may be necessary (as in the case $^{1}H/^{19}F$). More than 90 dB is usually hard to achieve with one filter.

Using external filters has three principal safety aspects:

1. Make sure you do not pulse into a filter with a frequency that this filter does not pass.

2. Make sure the pulse power you apply does not exceed the power rating of this filter. Most modern Bruker filters will survive 1 kW pulses of 5msec, but older filters (or non-Bruker filters) may not.

3. Remember that filters may attenuate the pulse RF voltage by as much as 1.5 dB (about 20%!)

The following figures illustrate the most common filter combinations.

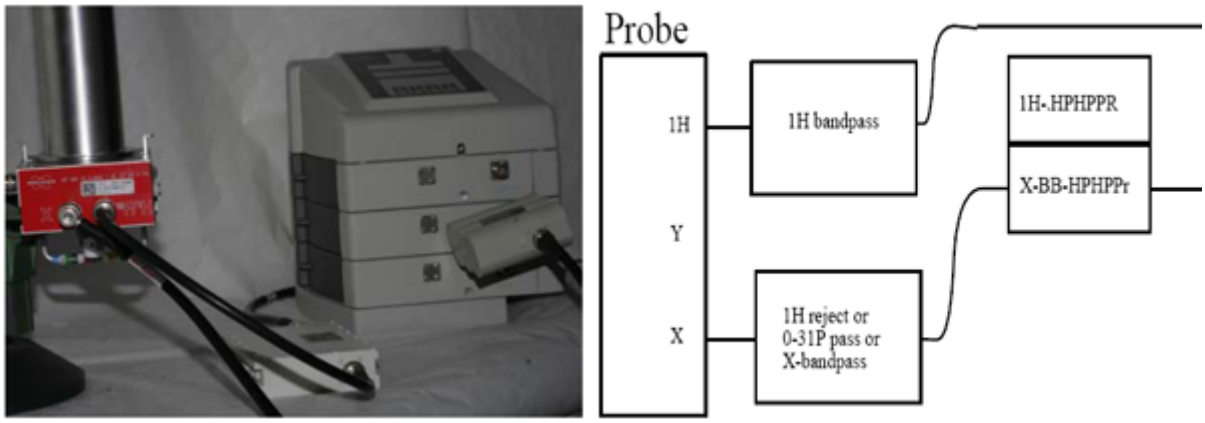

Figure 3.6. Standard Double Resonance CP Experiment, Bypassing the Proton Preamp

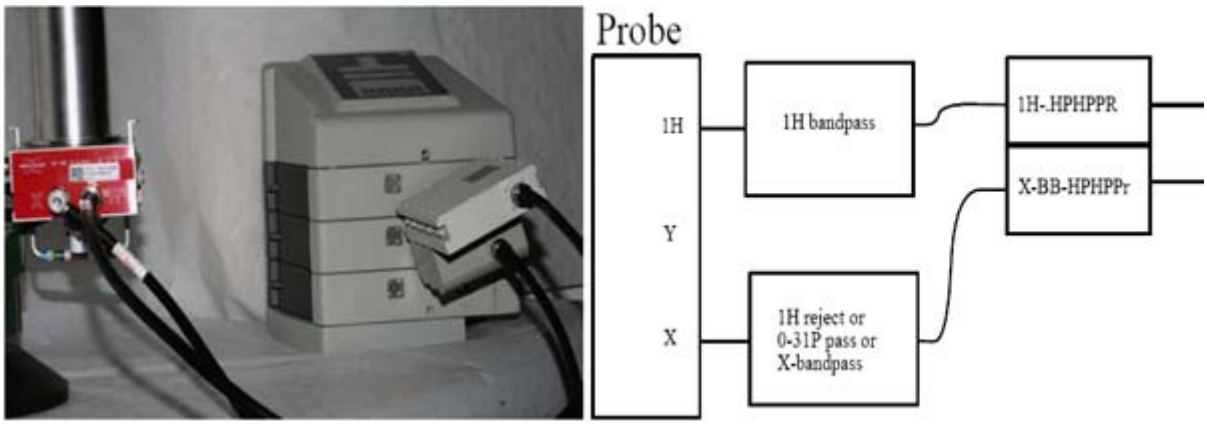

Figure 3.7. Standard CP Experiment, Proton Preamp in Line

Please note in ***Figure 3.7.***: Only high power preamps allow decoupling through the preamp.

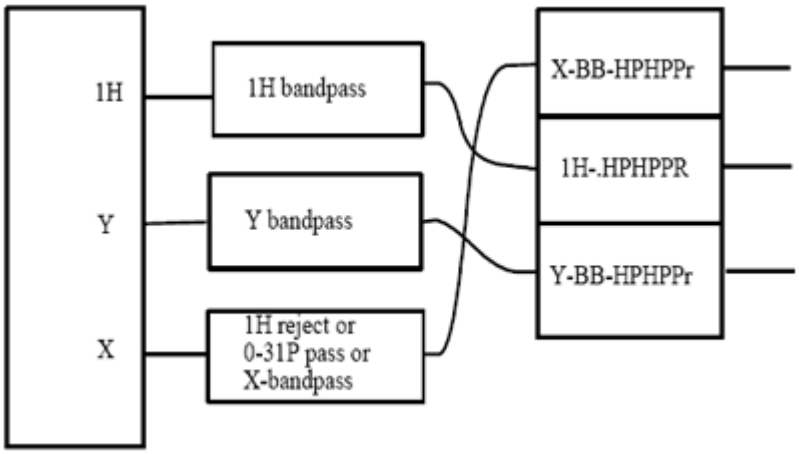

Figure 3.8. Triple Resonance Experiment, without X-Y Decoupling

Figure 3.8. is a triple resonance experiment, without X-Y decoupling (one bandpass will suffice), note the preamp configuration. It is recommended not to put two preamps of the same kind next to each other in order to avoid incorrect wiring of probe and filters. For the X-channel, only the proton frequency needs to be filtered out if X or Y is not decoupled while Y or X is observed (protons are usually decoupled).

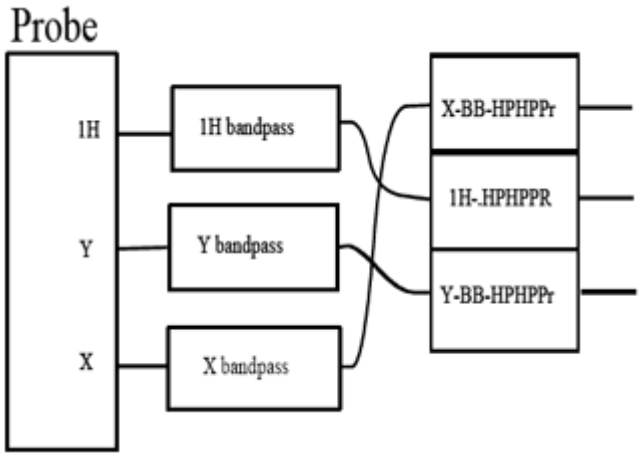

Figure 3.9. Triple Resonance Experiment, with X-Y Decoupling

Figure 3.9. is a triple resonance experiment, with X-Y decoupling (two band passes required! Care should be taken that the two bandpass filters mutually exclude the other frequency as efficiently as possible. Low pass filters will not allow X or Y observe while Y or X is decoupled!).

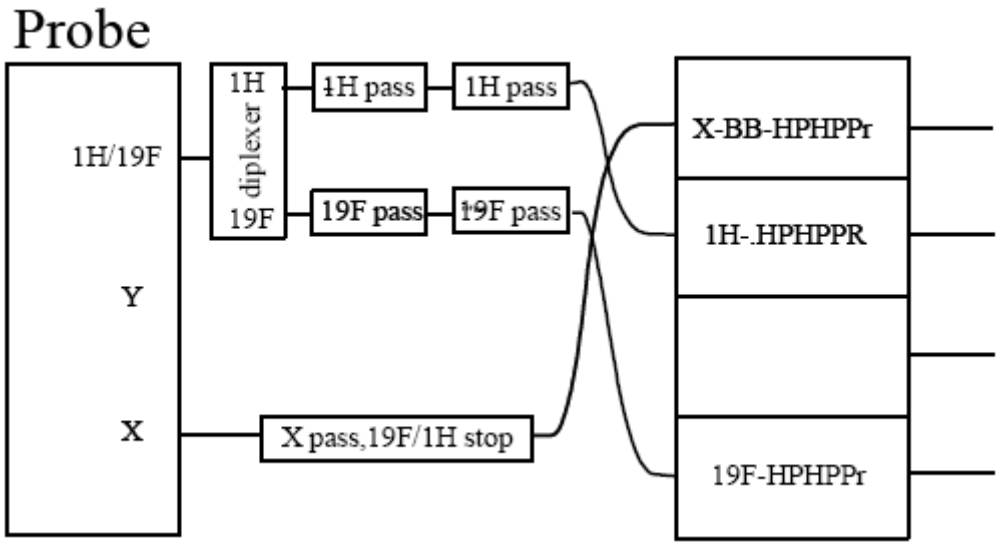

Figure 3.10. Triple Resonance 1H/19F-Experiment

Figure 3.10. is a double/triple resonance HF-experiment, with ^{19}F observation and ^{1}H decoupling or X-observation with ^{19}F and ^{1}H decoupling (WB probes ≥ 400 MHz only! For SB probes and <400 MHz different hardware is used). A set of ^{1}H-transmitter/bandpass/preamp and ^{19}F-transmitter/bandpass/preamp is required.

Note: a standard $^{1}H/^{19}F$ preamplifier will not allow long 19F pulses through it! For short pulses it is ok, for decoupling it must be bypassed, or a dedicated ^{19}F preamp must be used.

Figure 3.11. 19F/1H Combiner/Filter Set

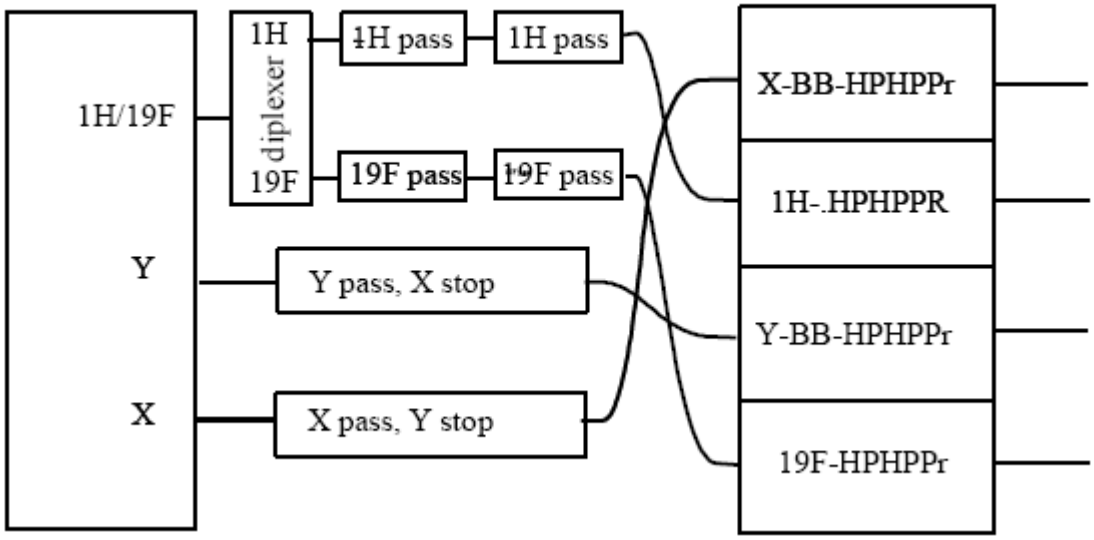

Figure 3.12. Quadruple Resonance HFXY Experiment (WB probes ≥ 400 MHz only!)

Connections for Probe Identification and Spin Detection *3.4*

Most solids probes were delivered without **P**robe **I**dentification **S**ystem (PICS). Probes delivered since 2007 are equipped with PICS. Please refer to ***Figure 3.4.*** to identify the PICS port at the preamplifier cover module. The probe connections for the spin rate cable and the PICS cable are shown in ***Figure 3.13.*** for a WB and in ***Figure 3.14.*** for a SB probe.

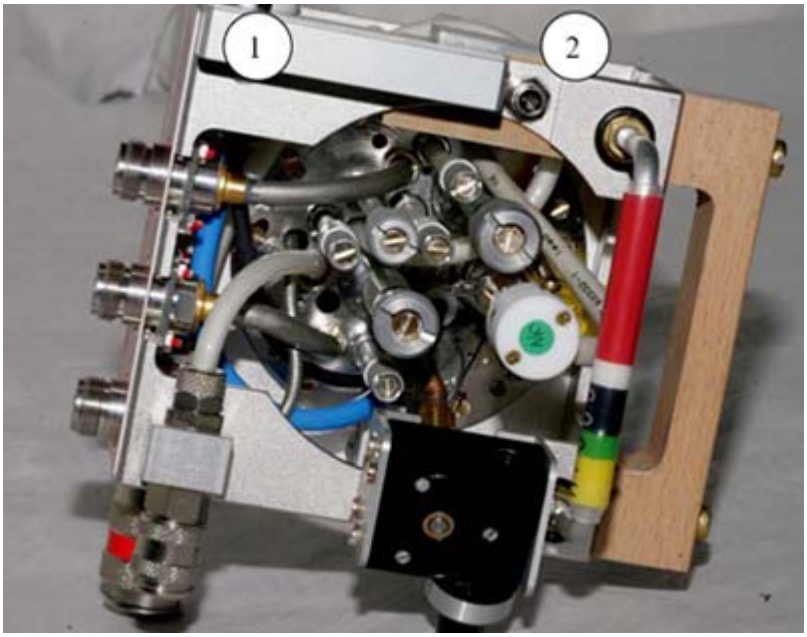

1. PICS probe connector **2. Spin rate monitor cable**

Figure 3.13. PICS Probe Connector and Spin Rate Monitor Cable on a WB Probe

On SB probes the location may differ, but the connectors are (if present in the case of PICS) easily identified by the type of connector.

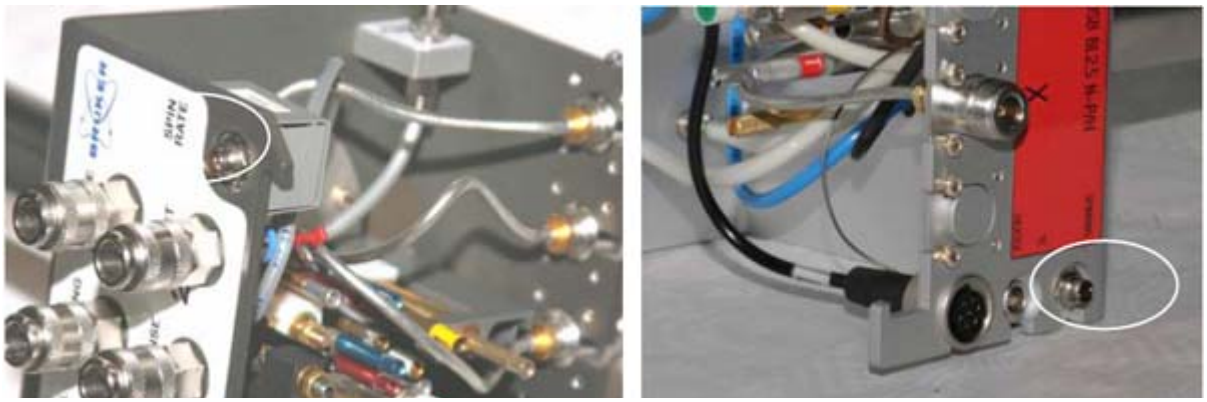

Figure 3.14. Spin Rate Monitor Cable Connector for 2 Different Types of SB Probes

Warning: The spin rate monitor cable has a probe side connector that is exactly the same as the power supply cable for the B-TO thermocouple oven used with many high resolution probes. If this cable is connected to the spin rate monitor assembly at the probe, the latter will be destroyed. Make sure the B-TO cable and the MAS cable (labelled "probe" at the probe side) are labelled such that they cannot be mistaken!

MAS Tubing Connections *3.5*

For any type of fast spinning probe, compressed gas is used to provide the spinner bearing and drive gas. Please refer to the installation or site planning manuals to learn about the gas requirements. The most important parameters are:

- Mains pressure (should be at least maximum required pressure +1 bar, to provide pressure regulation range).
- Bearing pressure: up to 4.5 bar (as of February 2008)
- Drive pressure: up to 4.5 bar (as of February 2008)

This means that at least 5.5 bars of pressure should be available at the outlet. If the pressure droop along the supply tube is substantial, the internal pressure may drop below 5 bars, then the MAS unit stops to regulate and gives a warning.

Consequently, we recommend a primary (inlet) pressure of min. 6 bar, preferably 7-8 bar (max. 10 bar) and a low loss gas line (8mm inner diameter, distance ≤5 meters) between the instrument and the gas supply, to assure trouble free operation even under conditions of high gas throughput. The maximum throughput depends on the experimental conditions and the probe type.

The following gas requirements exist:

1. At room temperature or higher: dew point min. -30 °C, compressed air will do.
2. At temperatures 200 °C or higher (suitable probe required!): nitrogen is required to prevent coil oxidation.
3. At temperatures between room temperature and -50 °C (using a B-CUX cryo cooler with -80 °C exchanger temperature): nitrogen or compressed air with a dew point ≤ -100 °C.
4. At temperatures below -50 °C (using liquid nitrogen and heat exchanger): boil-off nitrogen with a dew point -196 °C.

Any compressed gas used in NMR probes must be free of any liquid droplets or of oil (from compressor lubrication). Especially oil (even smallest amounts) will lead to probe arcing, and/or spinning problems and potentially expensive repair. Using boil-off nitrogen should be carefully considered, since it is by far the most reliable, stable and trouble free source of compressed gas, to be used at any temperature!

Connections *3.5.1*

MAS tubing connections are quite different between different types of probes (for stationary, non spinning probes, only frame flush and VT gas are required:

1. WB probes, VTN, WVT and DVT probes (VTN: VT-normal range, WVT: VT-wide range). These probes have a diameter of 72 mm and are longer than SB probes. Probe lengths are the same up to 400 MHz, the same for 500 and 600 MHz, and longer for higher fields.
2. SB probes, VTN and DVT type probes, also major differences between older and more modern probes. Furthermore, probes with sample insert/eject and probes without insert/eject exist.

The major difference between DVT and VTN/WVT probes is that for VTN/WVT probes the bearing gas is used for temperature control, whereas for DVT probes, bearing, drive and VT gas are separate.

Wide Bore (WB) Magnet Probes

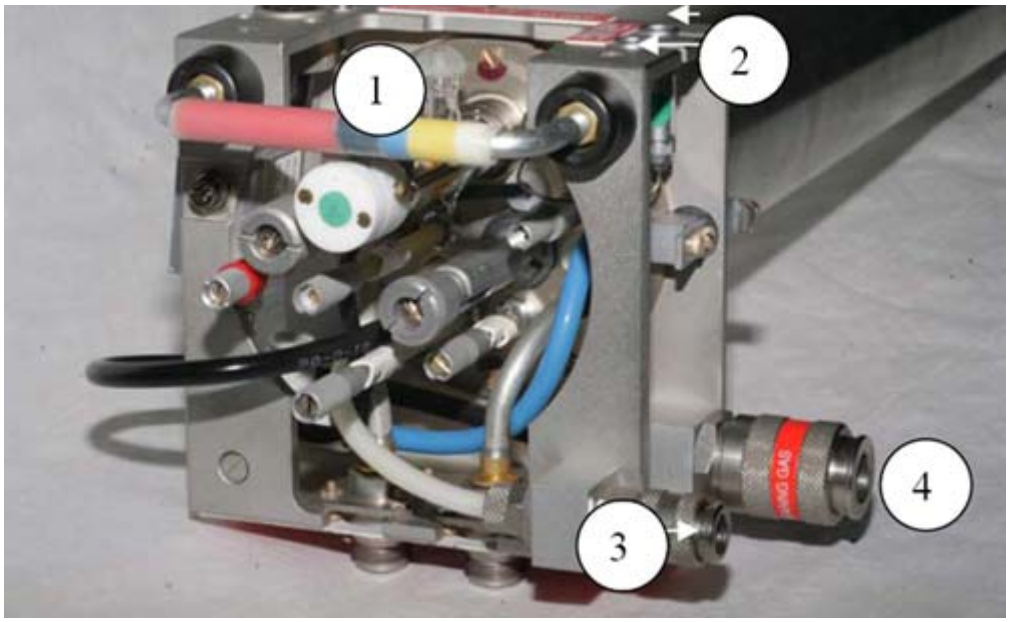

1. VT gas only input into dewar
2. Two thermocouple connectors
3. Drive gas in
4. Bearing gas in

Figure 3.15. WB DVT Probe MAS Tubing Connections

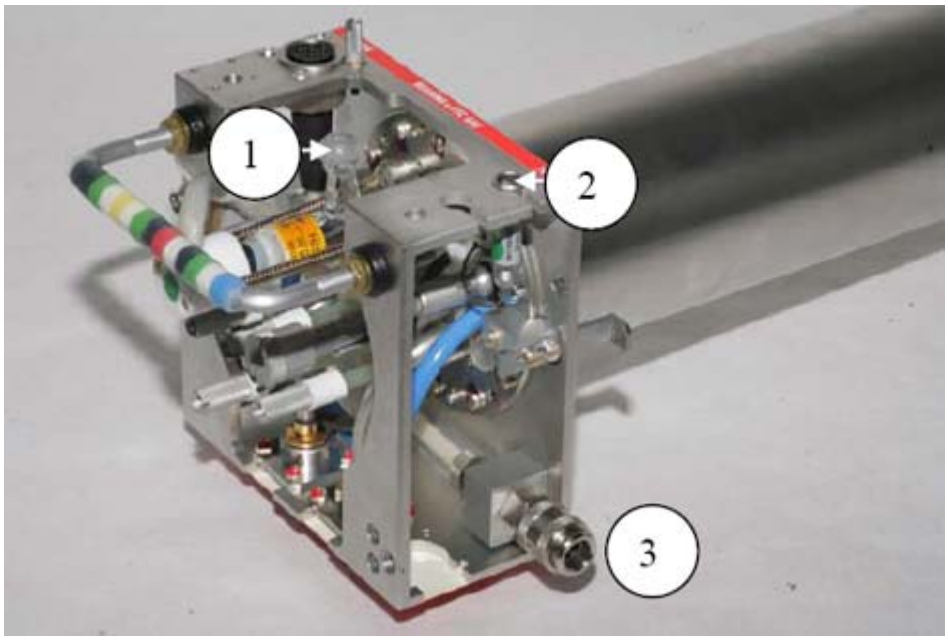

1. VT plus bearing gas
2. One thermocouple connector at stator inlet
3. Drive gas

Figure 3.16. VTN Probe MAS Tubing Connections Note: WVT Probes are VTN-Type Probes

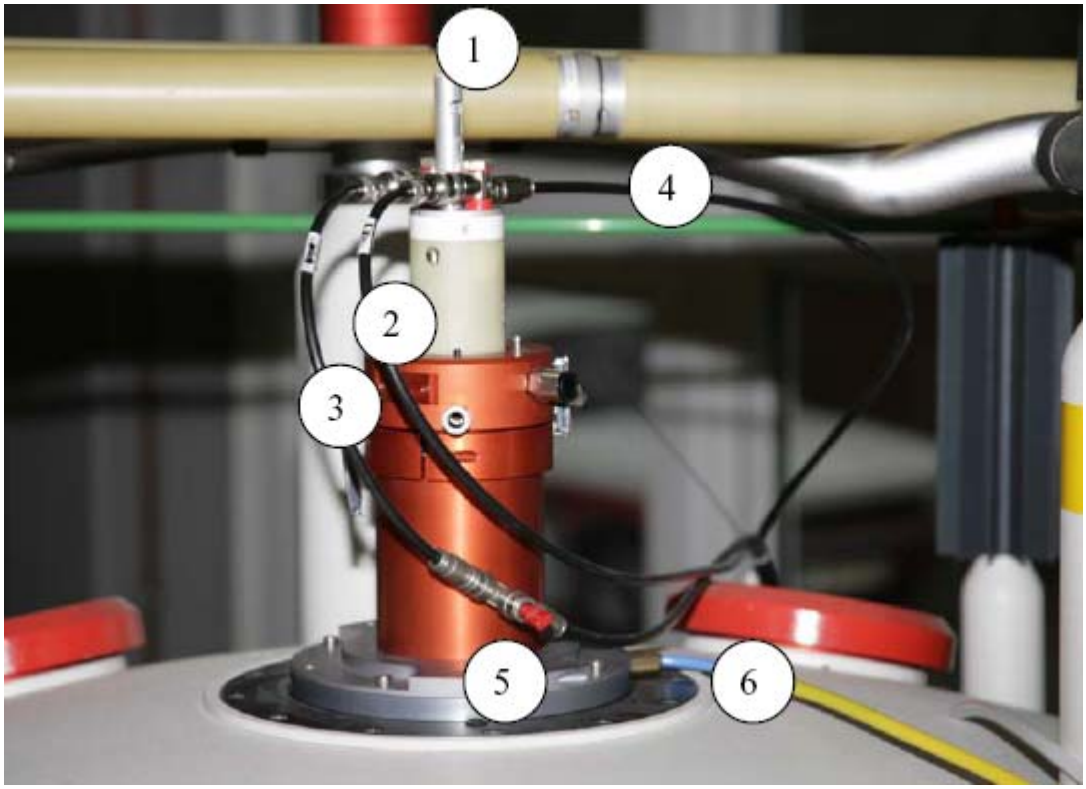

1. Sample insert/eject
2. Eject gas in
3. Insert gas in
4. Flush gas for transfer tube
5. T-piece to insert tube (allows the flush gas to be fed in at low temperature to avoid ice formation on spinner cap)
6. Shim stack flush connection

Figure 3.17. WB Probes: Eject/Insert Connections

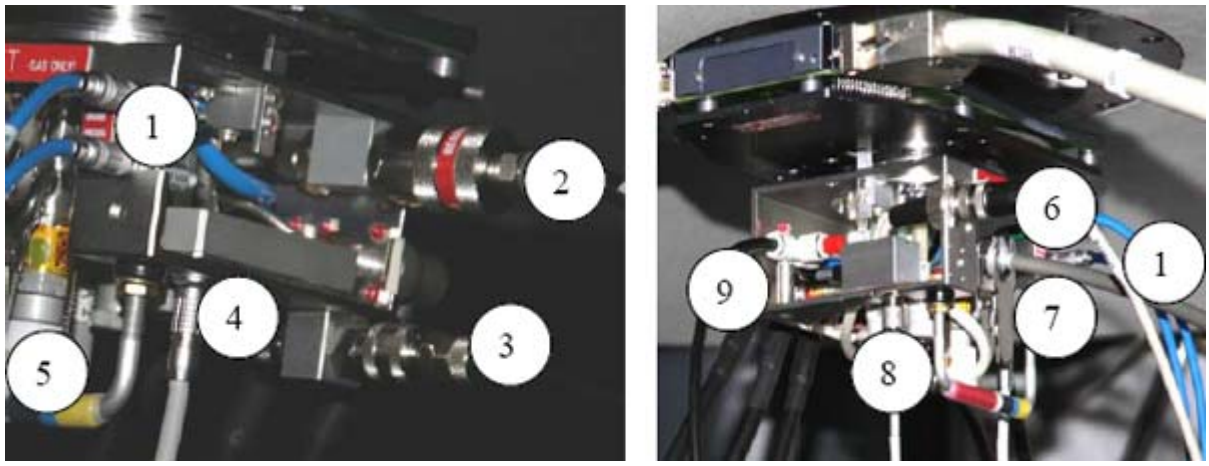

1. Thermocouple(s)
2. Bearing gas in
3. Drive gas in
4. PICS cable
5. Heater
6. Heater cable in
7. VT gas in
8. Spin rate cable
9. Flush gas in

Figure 3.18. WB Probes: DVT, Probe Connections for RT and HT Measurements

Standard Bore (SB) Magnet Probes

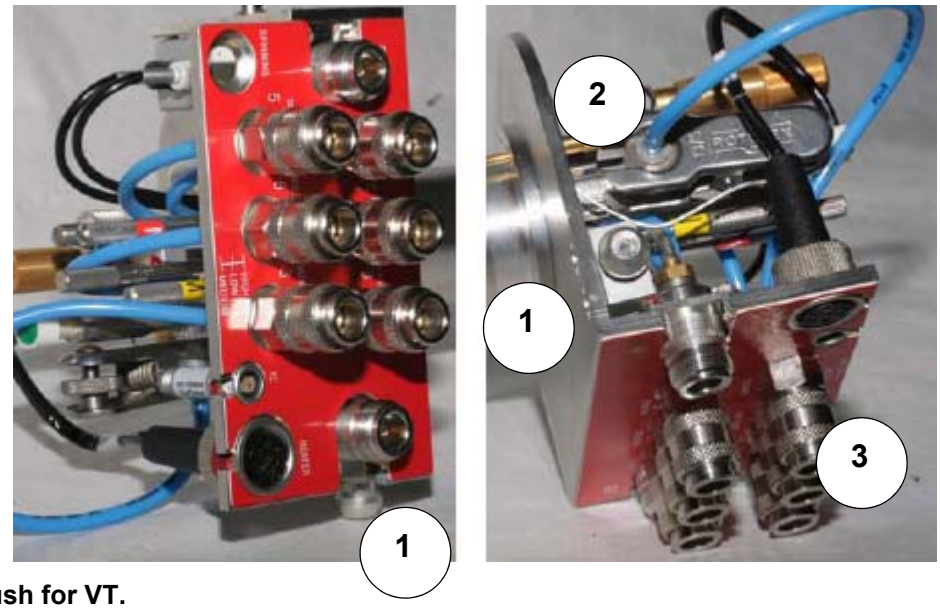

1. Frame flush for VT.
2. Ball joint takes bearing gas from the Quickfit connector at the front into the heater dewar.
3. Bearing connector for ambient temperature gas.

Figure 3.19. SB VTN Probe MAS Connections

With the standard bore VTN probe, quick fit connectors include:

- Bearing (3).
- Eject (2).
- Drive (5).
- Vertical (7) to the tilt stator for eject.
- Magic Angle (8) to tilt stator into the magic angle.
- Bearing sense (to supervise bearing pressure, shut down in case of a pressure loss).

For LT experiments, the ball joint at the heater dewar must be opened and the transfer line of the heat exchanger or the cooling unit must be connected.

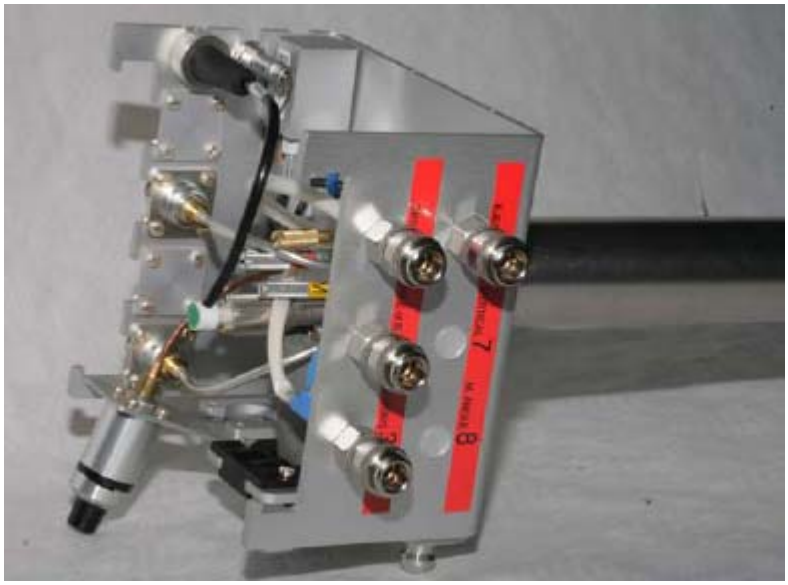

Figure 3.20. SB DVT probe MAS connections.

The numbered connectors are the same as the VTN probe. Connectors 7 and 8 are not present since the probe does not tilt the stator for eject (not required for 2.5 mm probes).

Additional Connections for VT Operation *3.6*

If **V**ariable **T**emperature experiments must be run, there are a few connections to be done which are not required for room temperature experiments.

First of all, there must be a flow of VT control gas. For MAS probes, this flow can be the bearing gas (VTN) or it can be separate (DVT). In any case, the VT control gas will flow through a dewar which contains a heater. There will be at least one thermocouple which senses the temperature as close as possible to the sample. Several requirements must be fulfilled to obtain precise and stable temperature readings as close as possible to the real sample temperature. This will however be part of a different chapter.

Some connections are required to control the temperature of the probe/sample, others are necessary to protect the probe and the magnet from illegal temperatures. MAS probes are usually not as well insulated as for instance a wideline or PE stationary probe is. Therefore the probe outer shell warms/cools down during the experiment. The heat transfer between heater and probe electronics/probe environment must be kept at a safe level.

Safety precautions involve flushing the probe frame, this serves to keep the tuning elements at decent temperatures. Furthermore, the magnet must be kept at legal temperatures to prevent freezing of O-rings or excessive expansion of the inner bore tube. The shim stack must be kept at temperatures below 70 °C, else the shim coils might be damaged. With MAS probes, it must be made sure that no wet air is sucked into the eject tube, which would lead to formation of ice on low temperature runs. This requires to maintain some overpressure above the spinner (usually by applying some flow to the insert gas line).

Heat exchangers must be dried with a flow of dry gas before use, so there is no water left in which will ice up the exchanger loop. After use, they must be warmed up and dried with a dry gas flow so that there is no water in leading to corrosion.

The following figures show the various connections to different probes.

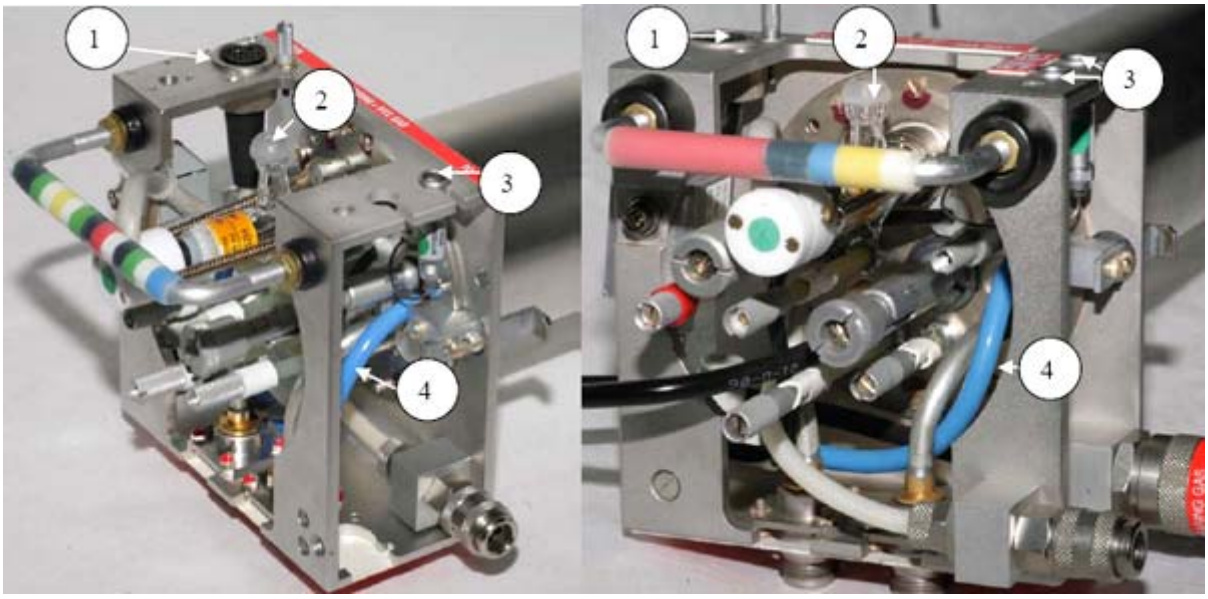

1. Probe heater connector
2. VT gas in
3. TC connector (s)
4. Frame flush gas

Figure 3.21. WB Probe MAS VTN and WVT, and DVT Probe Connections

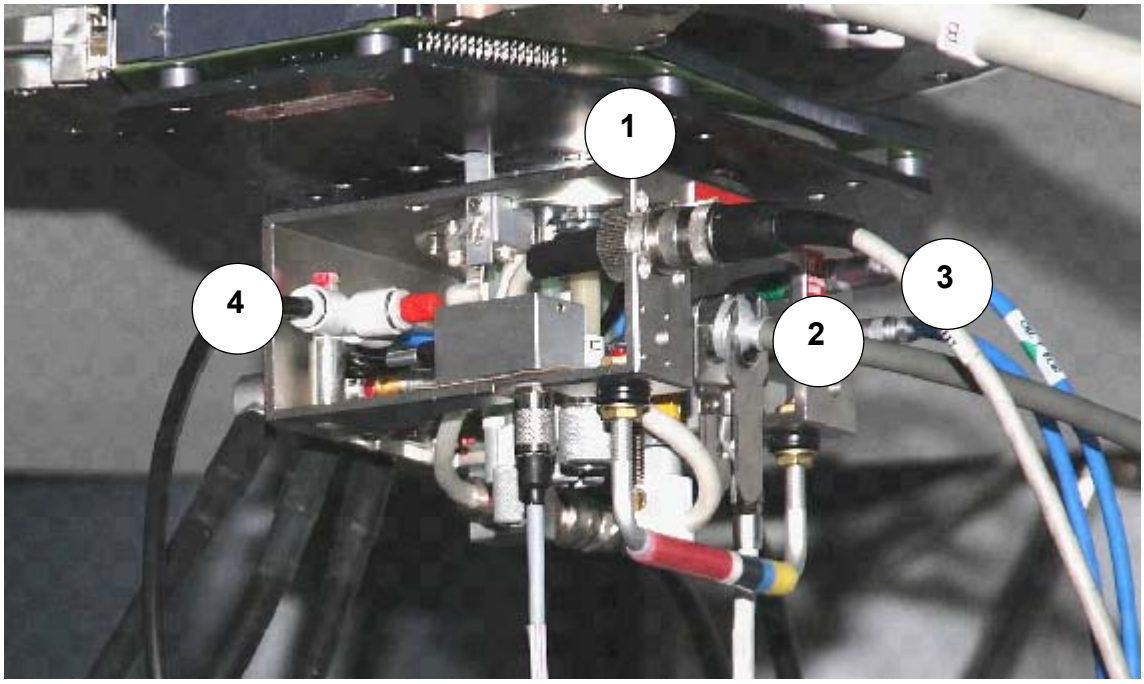

1. Probe heater connector **3. TC connector (s)**
2. VT gas in **4. Frame flush gas**

Figure 3.22. WB Probe MAS DVT Connections

In the figure above the upper thermocouple connector (read), located at stator out, lower thermocoupler connector (regul), located at stator inlet are connected. The VT unit must have the auxiliary sensor module to read more than one temperature. Only the TC labelled "regul" is used for regulation.

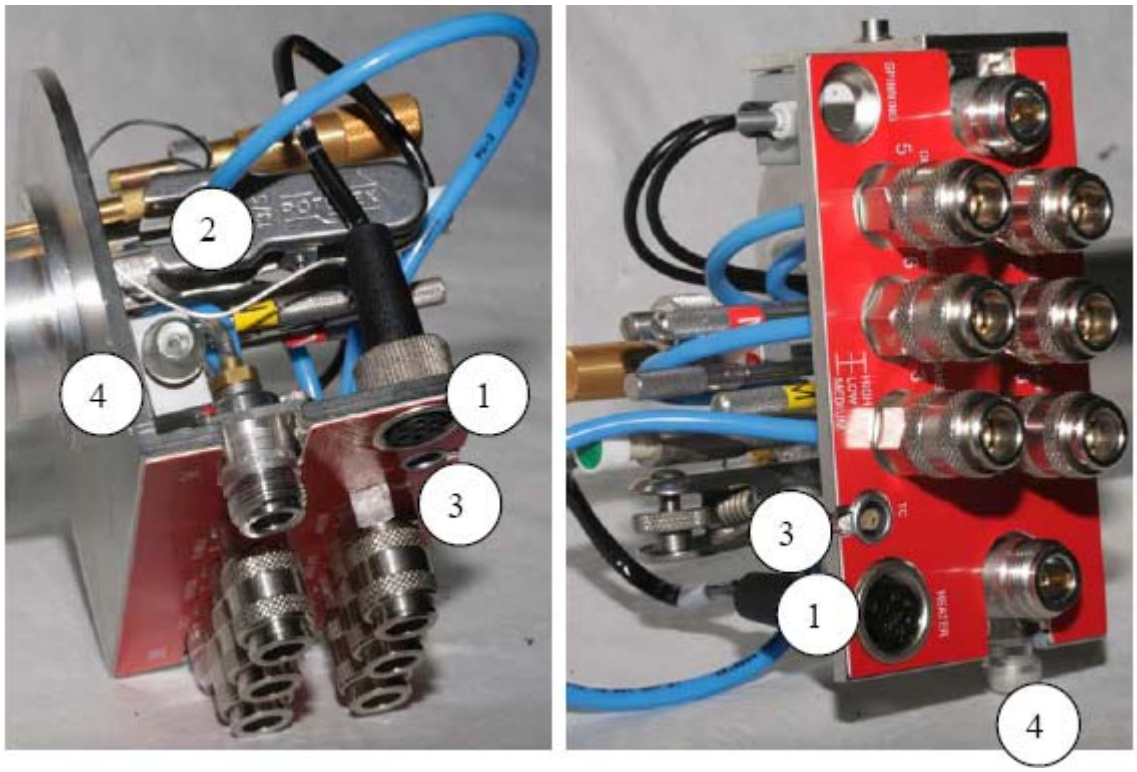

1. Probe heater connector
2. VT gas in
3. TC connector (s)
4. Frame flush gas

Figure 3.23. SB Probe MAS VTN

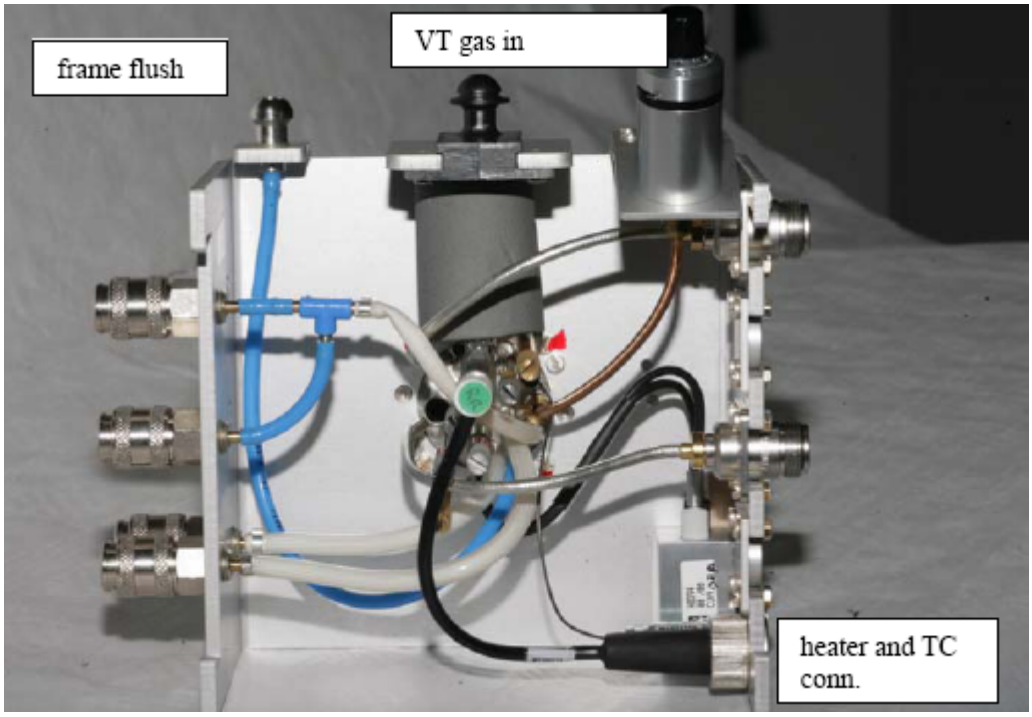

Figure 3.24. SB Probe MAS DVT Connections

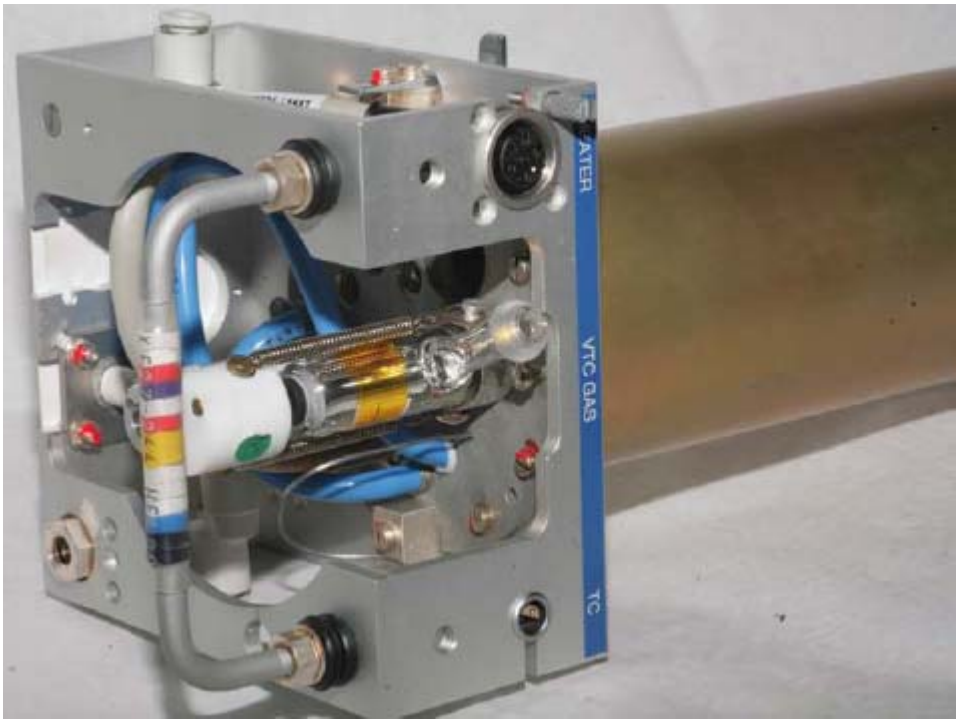

Figure 3.25. WB Wideline or PE Probes

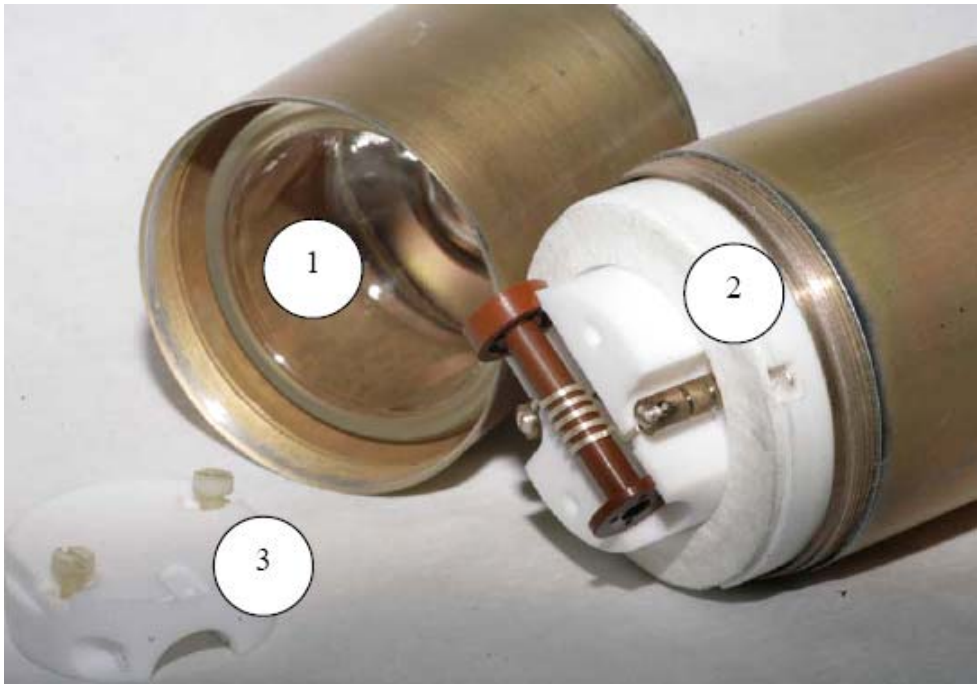

1. Bell shaped glass dewar around sample chamber
2. Insulating and sealing Al_2O_3 - felt ring
3. Cover for coil/sample compartment, fixed with plastic or metal screws

Figure 3.26. WB Wideline or PE Probe Connections

Figure 3.27. Low Temperature Heat Exchanger for VTN Probes (old style)

In the figure above is a low temperature heat exchanger for VTN probes (old style):

- 1 turn exchanger loop for SB probes;
- 2 turn loop for WB probes;
- 4 turn loop for DVT probes.

Figure 3.28. Low Temperature Heat Exchanger for DVT Probes

The low temperature heat exchanger for DVT probes in the figure above uses the exchanger coil with 6 turns, the larger one may be used for high resolution probes. To use the spring loaded connection device shown in the close-up:

1. Compress the spring.
2. Move the hollow part over the ball joint.
3. Release the spring.

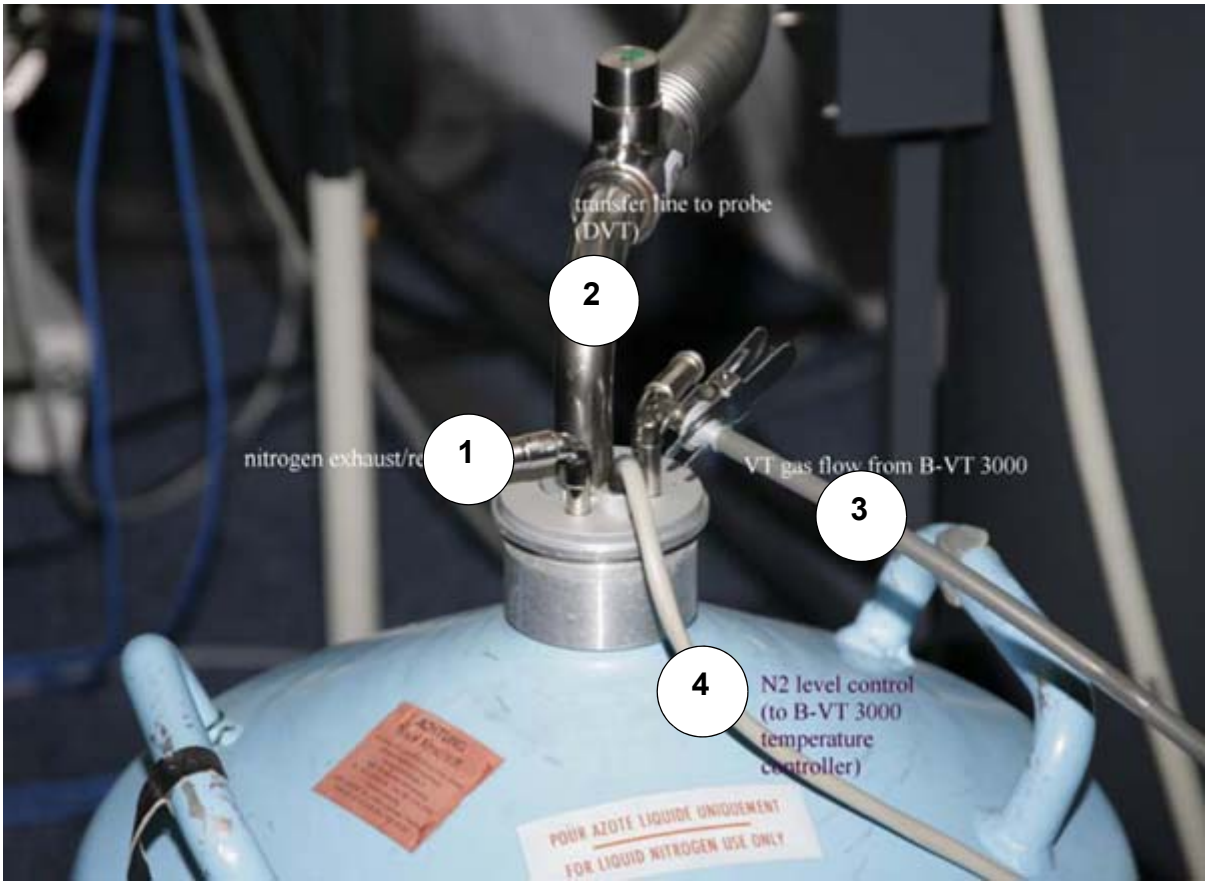

1. Nitrogen exhaust/refill
2. Transfer line to probe (DVT)
3. VT Gas flow from B-VT 3000
4. N2 level control (to B-VT 3000 temperature controller)

Figure 3.29. Low Temperature Liquid N_2 Dewar with DVT Probe/Heat Exchanger

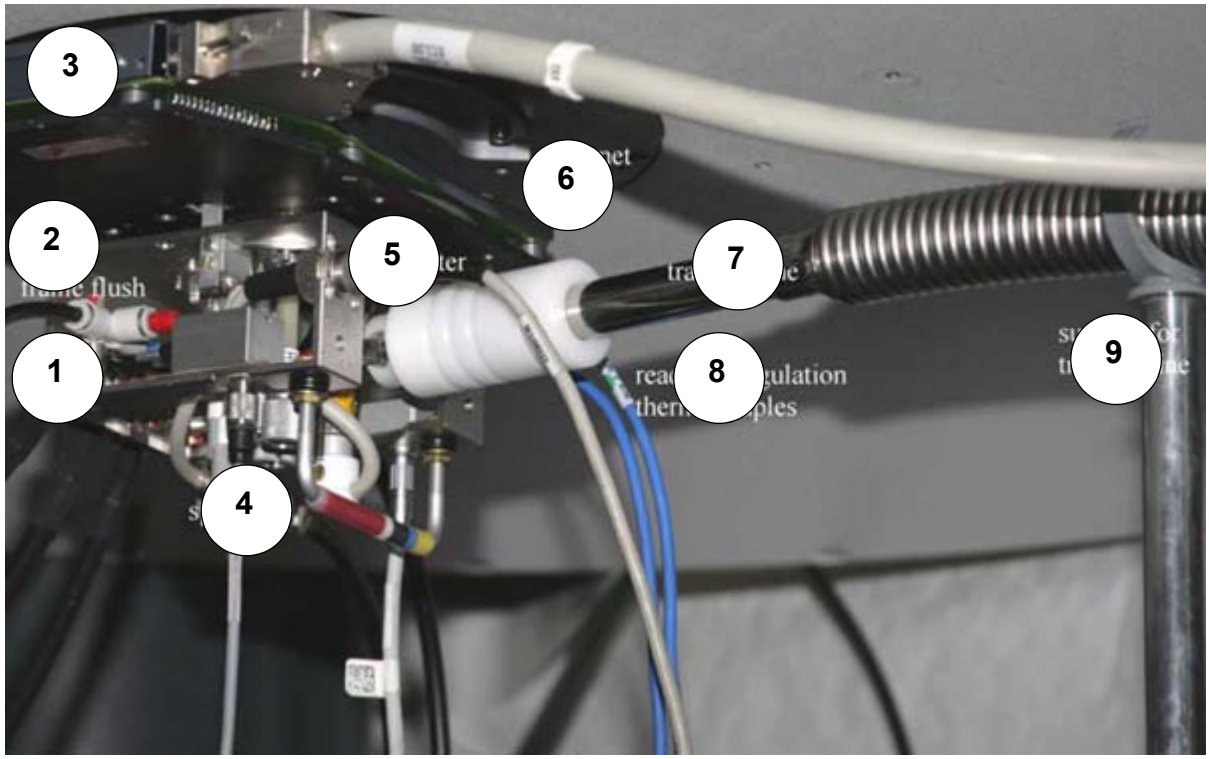

1. Gas in
2. Frame flush
3. Shims
4. Spin rate
5. Heater
6. Magnet bore
7. Transfer line
8. Read and regulation thermocouples
9. Support for transfer line

Figure 3.30. Bottom view of Low Temperature DVT Probe/Heat Exchanger

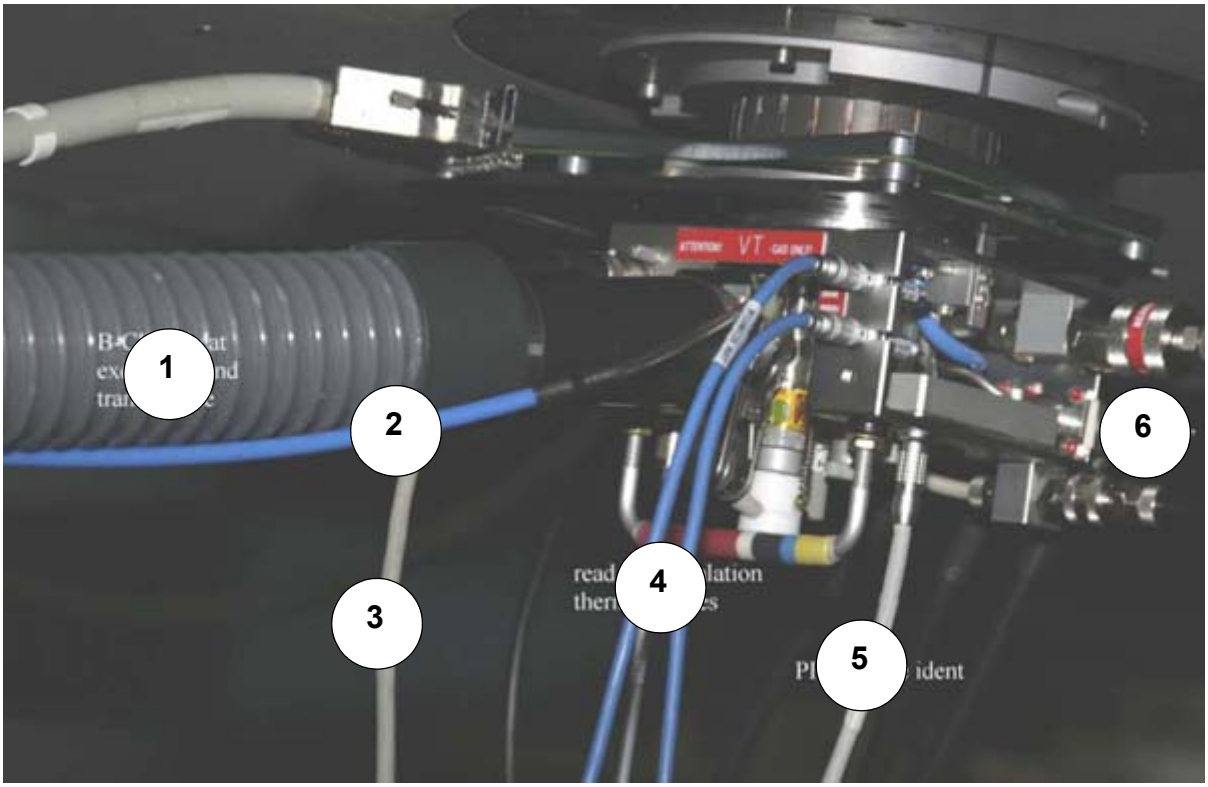

1. B-CU X heat exchanger and transfer line
2. Bypass
3. Heater
4. Read and regulation thermocouples
5. PICS probe identification
6. Bearing, drive

Figure 3.31. Low Temperature Setup with B-CU X (or B-CU 05)

In the figure above is the low temperature setup with a B-CU X (or B-CU 05) for DVT probes only, shown from the probe/magnet side.

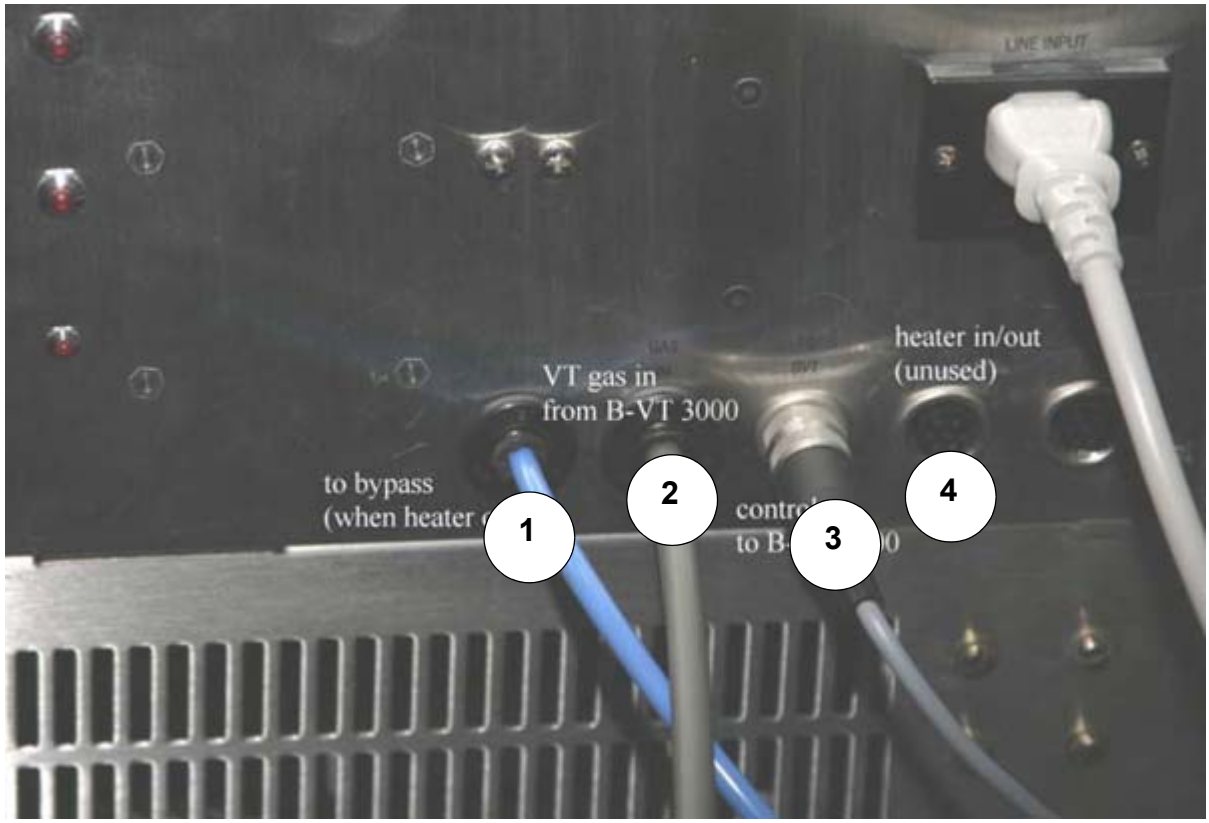

1. To bypass (when heater is off)
2. VT gas in, from B-VT 3000
3. Control, to B-VT 3000
4. Heater in/out (unused)

Figure 3.32. Low temperature setup with B-CU X

Probe Setup, Operations, Probe Modifiers *3.7*

Setting the Frequency Range of a Wideline (single frequency) Probe *3.7.1*

In a single frequency design, there are more degrees of freedom in tuning the circuit. The frequency range is set by a suitable NMR coil (see ***Figure 3.26.***). Fine tuning is done by a variable capacitance (1) and a fixed capacitance inside an exchangeable tuning insert (3). The purpose of this setup is to adapt the probe to the desired task as much as possible. A wideline probe has to cope with a large range of frequencies and line widths, and must provide the shortest possible pulses and highest possible sensitivity at the shortest possible dead time. These requirements cannot be met with one standard setup. Principles of setting up such a probe are:

1. Select an NMR coil (2) with highest inductance that can still be tuned to the required frequency. Choose the smallest coil diameter permitted by your sample, reduce the sample diameter if appropriate
2. Select the symmetrization insert such that the desired frequency is close to the upper end of the available tuning range

3. Select the Q value of the insert according to the expected line widths (higher Q for line widths up to 100 kHz). Please note that multiturn coils, especially multi-filament coils, have an intrinsically low Q.

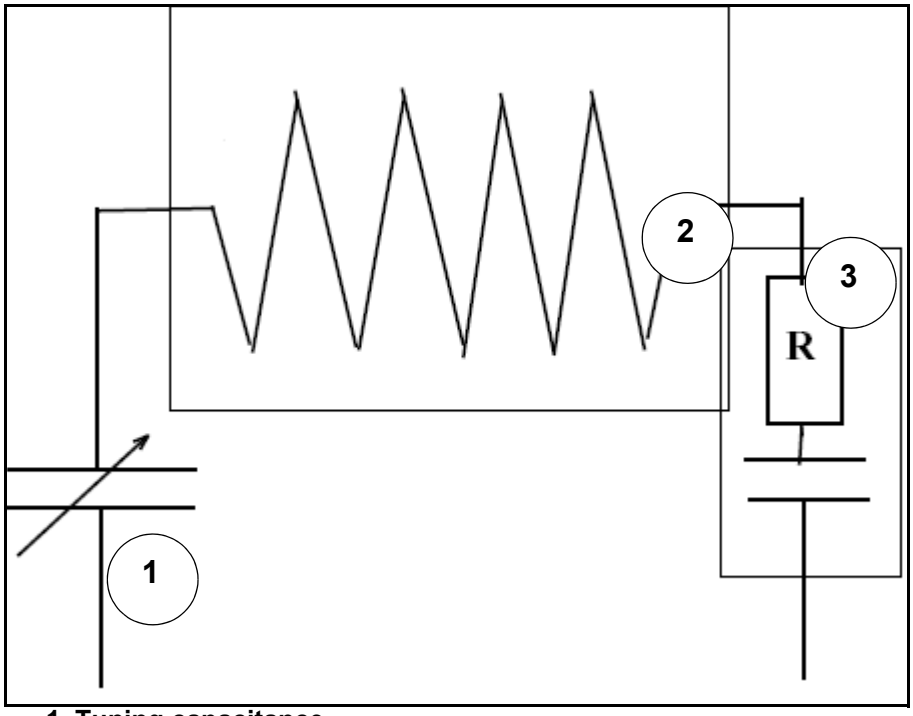

1. Tuning capacitance
2. Exchangeable NMR coil
3. Exchangeable symmetrization and Q-reduction

Figure 3.33. RF Setup of a Wideline Single Frequency Probe

Shifting the Probe Tuning Range *3.7.2*

Most probes cover a fairly wide frequency range. Changing the frequency range of a probe requires either a change in the inductance or capacitance of the circuit. The inductance of a circuit is hard to change unless a coil is mechanically lengthened or shortened. Most probes are tuned over a certain range by variation of a capacitance. The frequency range is then determined by the minimum and maximum capacitance that can be set. In order to make the inductance as high as possible (since the signal from the oscillating magnetization is detected in the inductive part), one usually chooses a capacitance with very small minimum capacitance, which again means a not large enough maximum capacitance. So in most probes additional tuning components must be inserted (removed) to achieve the full tuning range. The highest signal to noise is always reached with maximum inductance and minimum capacitance, i.e. at the high end of the tuning frequency achieved with maximum inductance.

In a wideline probe the NMR coil is easily replaced. So with a few coils of different inductance one can extend the tuning range determined by the tuning capacitor inside the probe. This cannot easily be done in a MAS probe for two reasons:

1. The coil must be carefully aligned such that it does not touch the spinning rotor
2. There are two frequency ranges to be set- the X-tuning range and the proton tuning frequency.

In such a probe, changing the coil would throw off the proton tuning totally, so a coil change is not possible.

Extending the tuning range of a CP/MAS probe can be done in the following ways (***Figure 3.34.***):

1. Switch the proton transmission line between λ/4 (low range) and λ/2 mode (high range). The proton transmission line is also part of the X-circuit and is higher (lower) in capacitance in λ/4 (λ/2) mode (only 400 MHz and up).
2. Add a parallel capacitance to the X-tuning capacitance, which makes the capacitance bigger (tunes to lower frequency). This is normally done to shift the tuning range to or below ^{15}N.
3. Add a capacitance in series to another capacitance. This reduces the total capacitance and shifts to higher frequency. A capacitance in series to the λ/4 line will reduce its total capacitance and shift the X tuning to higher frequency.
4. Add a parallel coil to the NMR coil. This reduces the total inductance and shifts to higher frequency, however at the cost of filling factor. The bigger the parallel inductance, the smaller the high frequency shift and the loss.

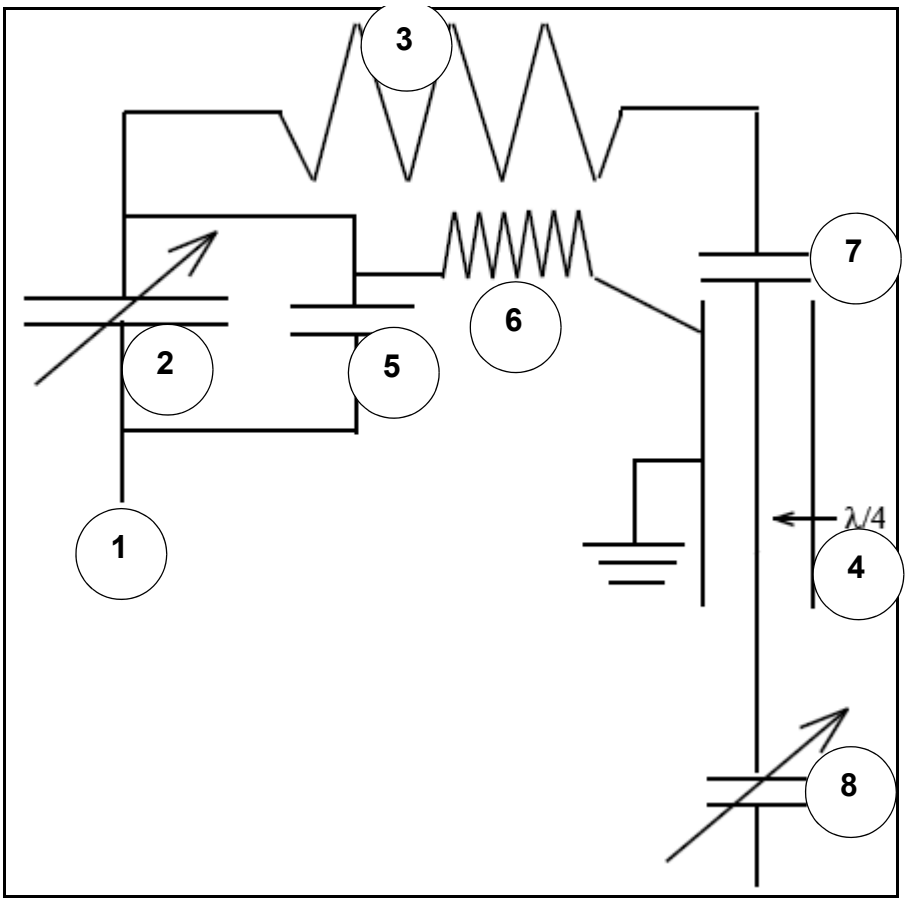

1. X-frequency in
2. X-tuning
3. NMR Coil
4. lambda/4 switch
5. Parallel capacitance
6. Parallel inductance
7. Serial capacitance
8. H-tuning

Figure 3.34. Possible Modifiers for Probe Tuning Ranges (400 MHz and up only)

Figure 3.34. *illustrates modifiers for probe tuning ranges for 400 MHz and up only. In 300 MHz and lower probes only a λ/4 line can be used, because a λ/2 would be too long, but here λ/4 can be tuned over the full range.*

All these modifications may be available for WB probes. In SB probes, they are usually built in (if necessary) and operated by a switch.

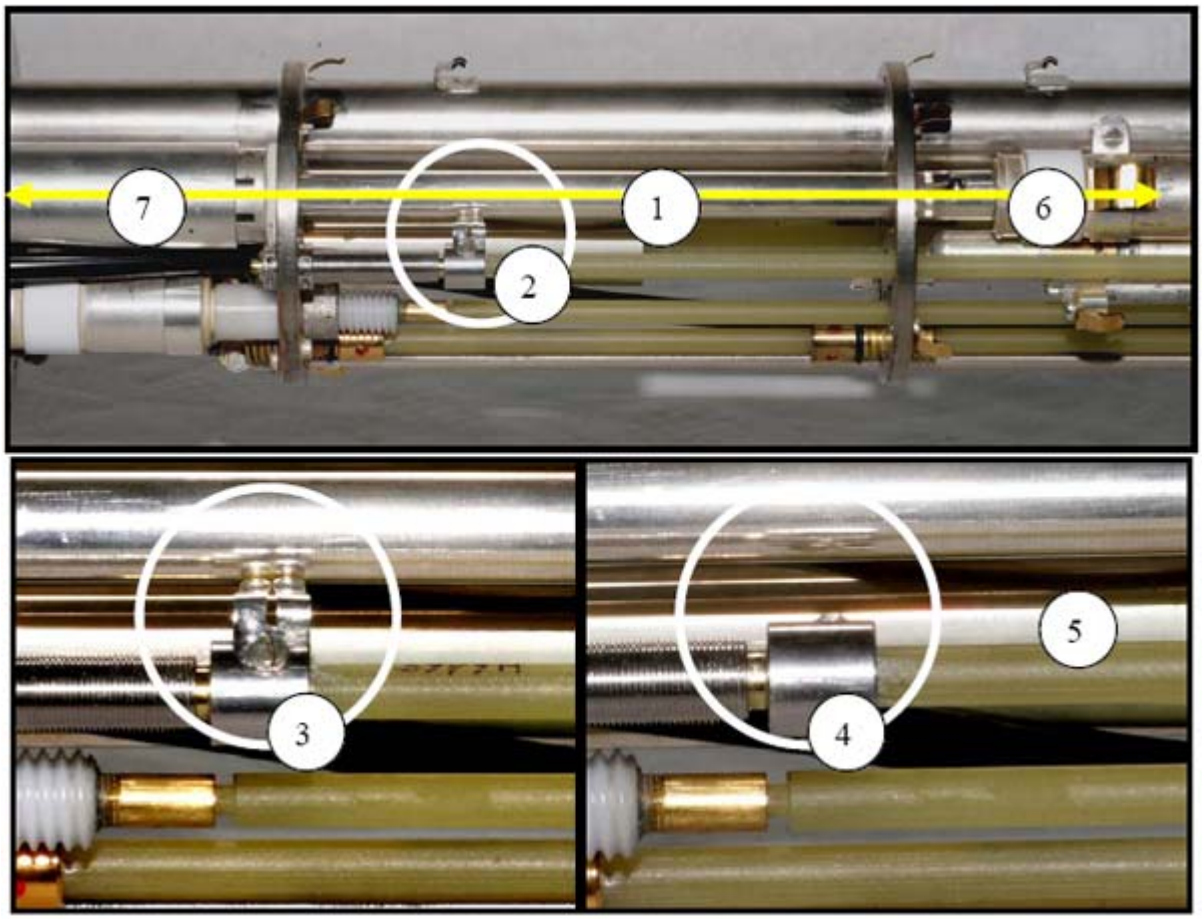

1. **λ-line inner conductor**
2. **Rotating switch at λ/4 position**
3. **Switch closed rotating counterclockwise** (seen from probe lower end). Contact springs (grounded) touch the λ-line at the λ/4 position
4. **Switch open rotating clockwise.**
5. **Switch operating rod**
6. **Tuning capacitor** at the end of the λ-line inner conductor: Fine tunes the effective length and therefore resonating frequency of the λ-line. This tunes the proton channel frequency (“tune”).

Figure 3.35. λ/4 (low range) and λ/2 Mode (high range), 400 MHz Probe

At 400 MHz, the wavelength is large, so the λ/4 point is below the closed section (7) of the λ-line. At higher frequencies, the λ/4 point may fall within the closed section 7.

The proton channel (decoupling channel) is usually tuned via a so-called λ-line (“transmission line”). This is just a coaxial cable or a coaxial conductor with an arrangement of an outer conductor (a tube) and an inner conductor (a rod). The relative diameters and distances and also the dielectric in between (usually air in WB probes) determine the impedance of the transmission line. Since such a line is as well an inductance as a capacitance, it is a resonating circuit. If the length of the transmission line equals λ/4 or λ/2 of the RF-wave, it is a λ/4 or λ/2 line. Since the upper end of the transmission line (inner conductor) is connected to the coil, high voltage is required there. This means that the λ/4 point has low voltage but high current, whereas the λ/2 point is at high voltage and low current. A short between

inner and outer conductor at the λ/4 position enforces a low voltage/high current and fixes a certain resonance frequency.Some probes are tuned for the proton resonance frequency by a tunable capacitor at the end of the λ/2-line (400 MHz and up) which changes the effective length of the λ/2-line. Some probes (400 MHz and below) are tuned by shifting the position of the λ/4 short to a higher (higher frequency, shorter length) or lower (lower frequency, longer length) position.

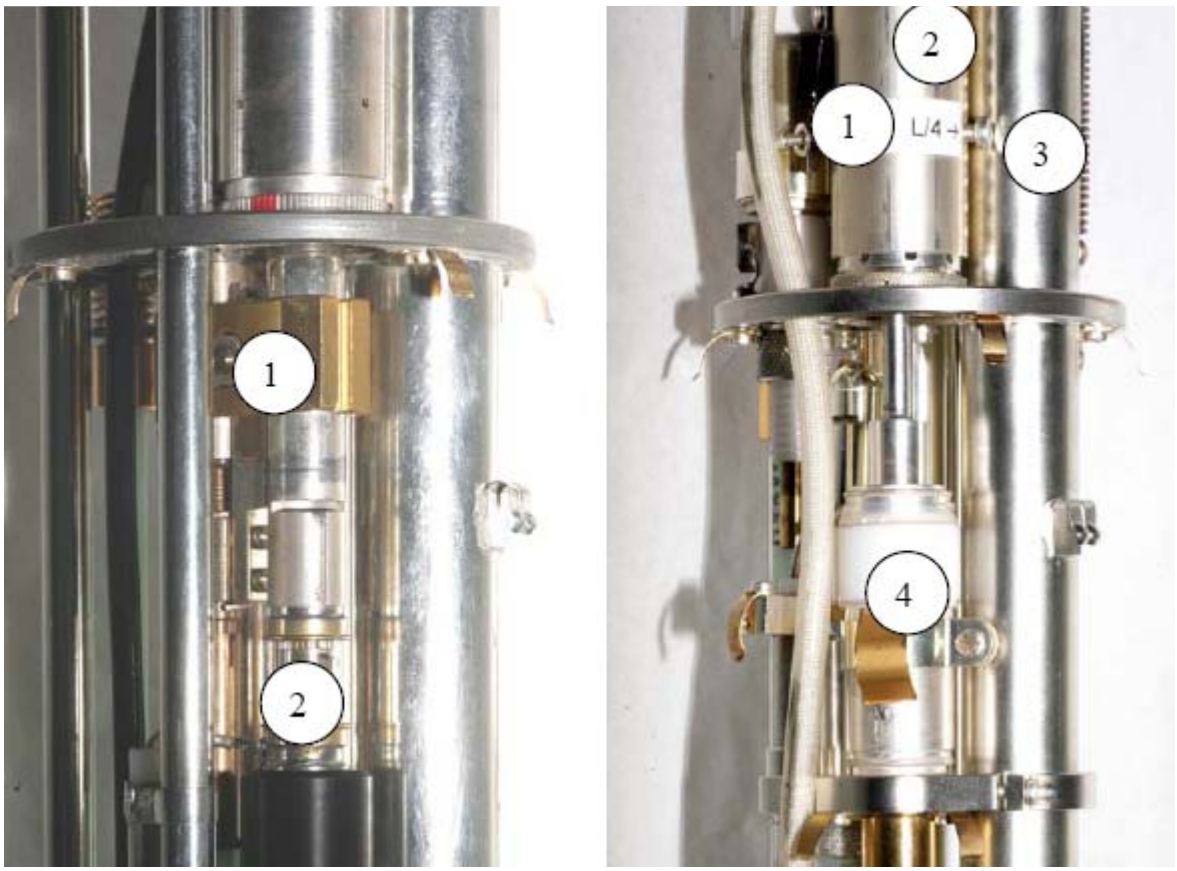

Figure 3.36. A λ/4 only probe (left) and a λ/4 - λ/2 probe (right)

On the left side of the figure above is a λ/4 only probe (200, 300 MHz, 400 low range only probes). The transmission line is only λ/4, proton tuning is done by moving the brass block to ground (1). Proton matching is done with capacitor 2.

On the right side of the figure above is a λ/4 - λ/2 probe 600 MHz. Due to the high proton frequency the λ/4-length shortens, the λ/4 point (1) moves inside the transmission line outer conductor (2). The screw (3) is used to set λ/4 (screw in) and λ/2 –mode (screw out). (4) proton tuning capacitor.

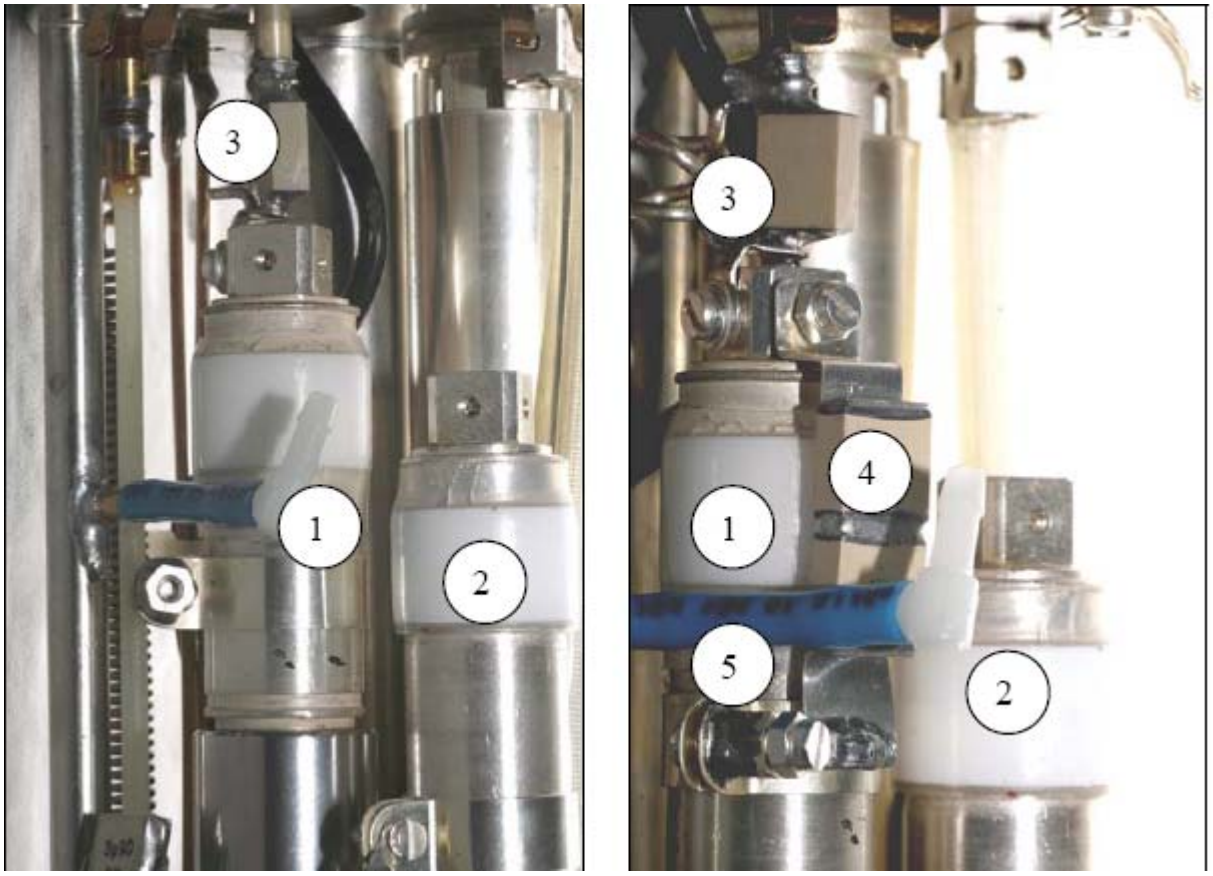

1. X-tuning variable capacitance
2. Y-tuning capacitance
3. Proton reject filter
4. Low range extension with parallel capacitance
5. Frame flush air outlet (to protect sensitive capacitors)

Figure 3.37. Without/with Parallel Capacitance to Shift the Tuning Range to Lower Frequency

Adding a parallel capacitance does not decrease the efficiency of a circuit. However, a certain circuit has the highest possible efficiency if it is tuned with maximum inductance and minimum capacitance. Maximum inductance can usually not be achieved due to spacial restrictions in the stator (MAS probes) or due to losses in Q if the coil becomes too large (increase in resistance). Furthermore, capacitances are tunable, inductances usually are not, so a wide tuning range can only be achieved via exchangeable inductances and/or capacitance with a wide tuning range. Capacitances may look different than the one shown in the picture. Frequently, two larger capacitances are used in series to form a smaller capacitance withstanding higher voltage. A parallel capacitance lowers and narrows the tuning range.

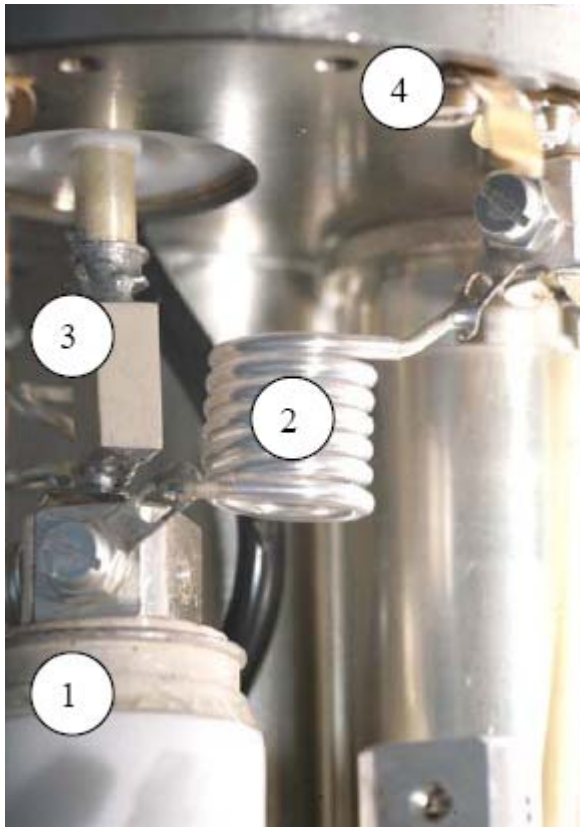

1. X-Tuning cap
2. Parallel coil
3. Proton reject filter („trap“)
4. Probe ground

Figure 3.38. Parallel Coil to Shift the Tuning Range to Higher Frequency

This additional coil is electrically connected in parallel to the detection coil. Since it is connected behind the proton trap, the proton channel is not influenced, but as well the X and Y channel will be affected, because only part of the inductance is now filled with sample. A parallel coil therefore reduces the RF efficiency quite substantially. The losses increase as the inductance (size and number of turns) of the parallel coil decreases. A coil of the same inductance as the detection coil will cost 50% in S/N and pulse voltage. Usually, these coils introduce about 30% loss.

Adding a Frequency Channel to a Probe (WB probes only) *3.7.3*

Probes are produced as single channel, double (channel), triple or quadruple probes (1, 2, or 3 RF connectors on the probe). It is not possible to modify a probe produced as a double channel probe into a triple probe, but a triple probe may be used as triple or double probe. As multiple tuning will reduce the RF performance of a probe on the other channels (if they are part of the same RF network), it is better to remove an unused RF channel, if this is possible.

The usual case is triple probes or quadruple probes. A triple probe can be tuned to ^{1}H, X and Y (where X is the higher frequency, Y is the lower frequency, both in the X-nuclei range). A triple probe X/F/H only has 2 RF connectors, because 1H and 19F are tuned to the same RF connector simultaneously. Likewise, a quadruple probe is an X/Y/F/H probe, with the X channel tuned to X and Y, and the pro-

ton channel tuned to ^{19}F and ^{1}H, so there are only 3 RF connectors. Check ***Figure 3.9.***, ***Figure 3.10.***, ***Figure 3.11.***, ***Figure 3.12.*** for the connection of such probes.

So the double tuning of the X channel into an X and a Y channel is an optional operation available for WB probes. SB probes are always fixed multi channel probes, with no option to insert/remove an RF channel.

Such probes have 2 complete X-tuning circuits, almost identical in construction. Activating the second channel means: Insert a filter which is tuned to reject at the exact X-frequency (exactly to ^{13}C frequency for a $^{13}C/^{15}N$-^{2}H probe). The X channel frequency is fixed to the specified frequency (in this case, ^{13}C), while the Y frequency has a broader tuning range (in this case ^{15}N-^{2}H). With different filter-inserts, that same probe can be modified to different frequency combinations, with the following restrictions:

1. A frequency outside the tuning range of the probe in double mode cannot be reached in triple mode (for instance, if the probe in double mode does not tune to ^{31}P, a triple insert for ^{31}P-^{13}C cannot be provided (without a frequency range shift shown in ***Figure 3.34.***). As the triple tuning insert will act as a load to the whole circuit, the frequency range will shift a bit to lower frequencies.
2. Both frequencies (X and Y) should be within the same basic probe tuning range high or low (λ/2 (high range) or (λ/4 (low range)) mode.

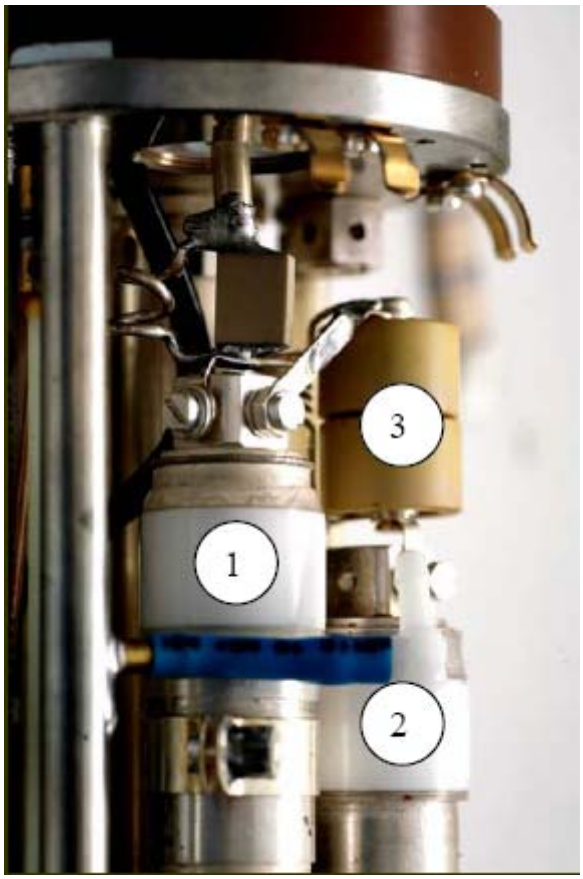

1. X-Tuning capacitor
2. Y-Tuning capacitor
3. X-Y trap (stops X-frequency into Y-channel, but not Y into X-channel)

Figure 3.39. Mounting a Triple Insert Into a Triple Probe

These inserts can be made to optimize the X or the Y channel. They should be mounted in exactly the position as indicated on the information sheet included with the probe.

Reversing the trap may mess up tuning! Observe probe manual instructions! For low range (below ^{13}C) nuclei, the probe must be in λ/4 mode. Combinations of low/high range nuclei are difficult/impossible and always lossy!

Mounting the Probe in the Magnet/Shim Stack *3.8*

Usually, the service engineer installing the magnet and the rack has considered the local restrictions, and placed the system such that all operations which may be required for the proper probe installation are conveniently possible. This refers to the ease of access of the magnet bore from below and above, to mount the probe and the sample insert devices, and also to the possibility to place VT equipment (liquid N_2 dewar, B-CU 05 or B-CU X) in a convenient location that allows access without restricting standard operations.

Depending on the type of probe, VT control gas enters the probe from the side or from behind. So it must be possible to attach the heat exchanger transfer line from the appropriate side. Furthermore, the weight of the transfer line must be relieved from the probe dewar ball joint, so there should be appropriate fixation points for the transfer line. It is important that the transfer line enters the ball joint as straight as possible, as a ball joint will cut off the flow when strongly tilted to an angle.

It should also be possible to reach the probe tuning elements (since they need to be operated frequently) as easily as possible from the operators chair. Also, when tuning the probe, the video screen and the preamplifier display should be easily visible.

Figure 3.40. Example of a 600 WB NMR Instrument Site

The example of a 600 WB NMR instrument site in the figure above provides easy access to the probe from either side.

EDASP Display: Software Controlled Routing *3.9*

The menu **edasp** shows all relevant RF routing and allows the routing which are under software control to be changed. The following restrictions apply:

- Connections between transmitter and preamplifier cannot be changed (the command **edasp setpreamp** with NMR Super user permissions does that).
- Channel F1 is the detection channel by default (which is no limitation).
- Detection must usually be routed via the same SGU as the F1 pulses are, since that SGU will supply the phase coherent reference signal. In some cases, pulsing and detection may use different SGU's, but provisions must be made to add the signal up coherently (using exactly the same frequency on both channels is usually coherent).
- Routing between SGU's and transmitters can only be selected if **cf** (the configuration routine) has found a hardware connection that supports this routing.
- Most routine applications will route correctly if the “default” button is pressed in the short menu version (receiver routing not shown).

- If an illegal or potentially dangerous routing is selected, an error message or a warning will pop up. Error messages will not allow selection of this routing.
- On AVIII instruments (with SGU/2), one SGU can produce two pulse trains (within the same NCO-frequency-setting range, 5 MHz).

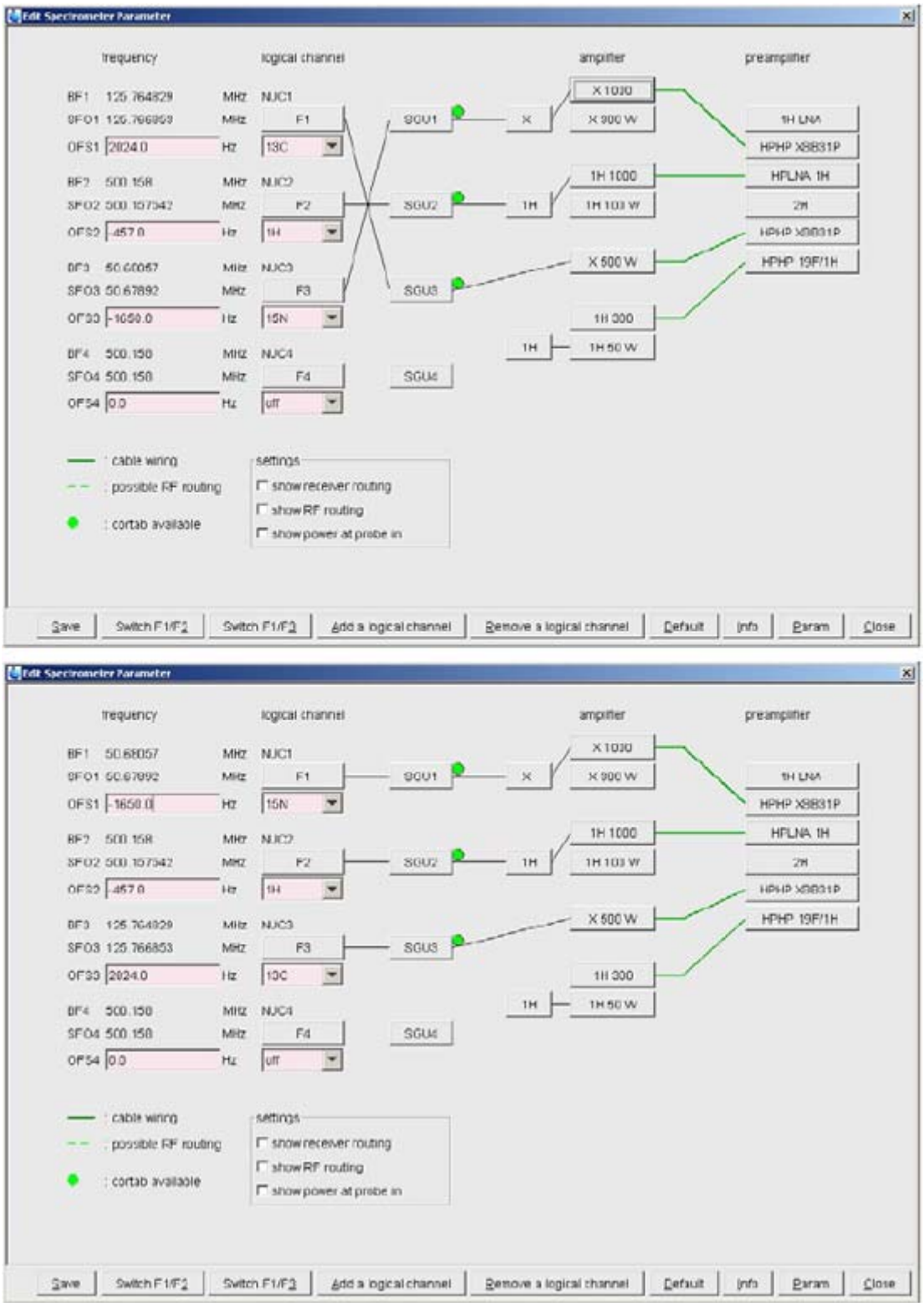

Figure 3.41. Short Display, Pulse Routing Only for C/N/H DCP or REDOR Experiment, observing ^{13}C (above) and ^{15}N (below)

In the figures above is a “short” display, pulse routing only, for a C/N/H DCP or REDOR experiment, observing C and observing N (without any hardware change!). Green dots indicate CORTAB linearization. ^{13}C routed via 500W transmitter since ^{13}C requires less power than ^{15}N.

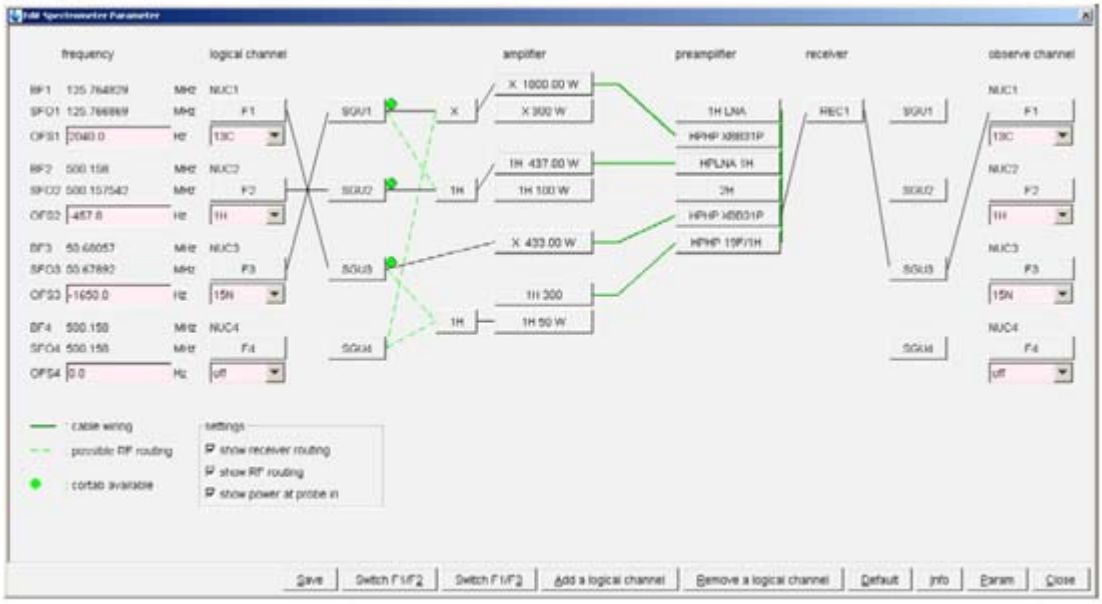

Figure 3.42. Long Display, Pulse and Receiver Routing

The figure above is a “long” display, with pulse and receiver routing:

- Green dots: CORTAB done for this path, transmitter linearized.
- Dotted green lines: Possible (hardwired) routing are shown (“show RF routing”).
- Receiver routing: SGU3 used for transmit and receive (“show receiver routing”).
- Power indication: Maximum possible power output (as measured, “show power at probe in”).

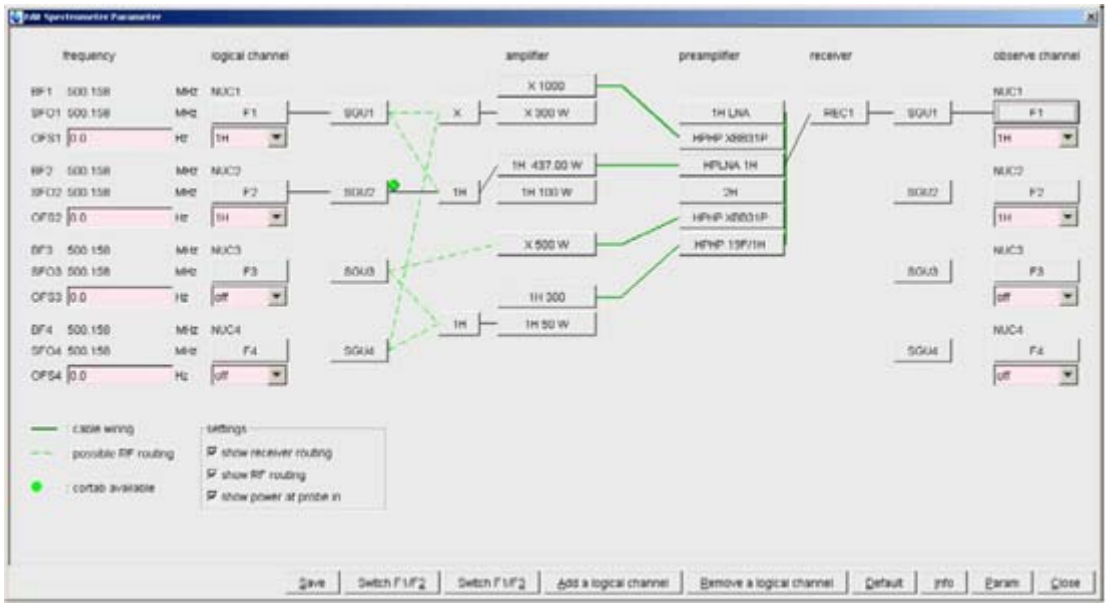

Figure 3.43. Pulse on F2, Observe on F1 - Routing

In the figure above the SGU2 is used for pulsing and the SGU1 is used to receive.

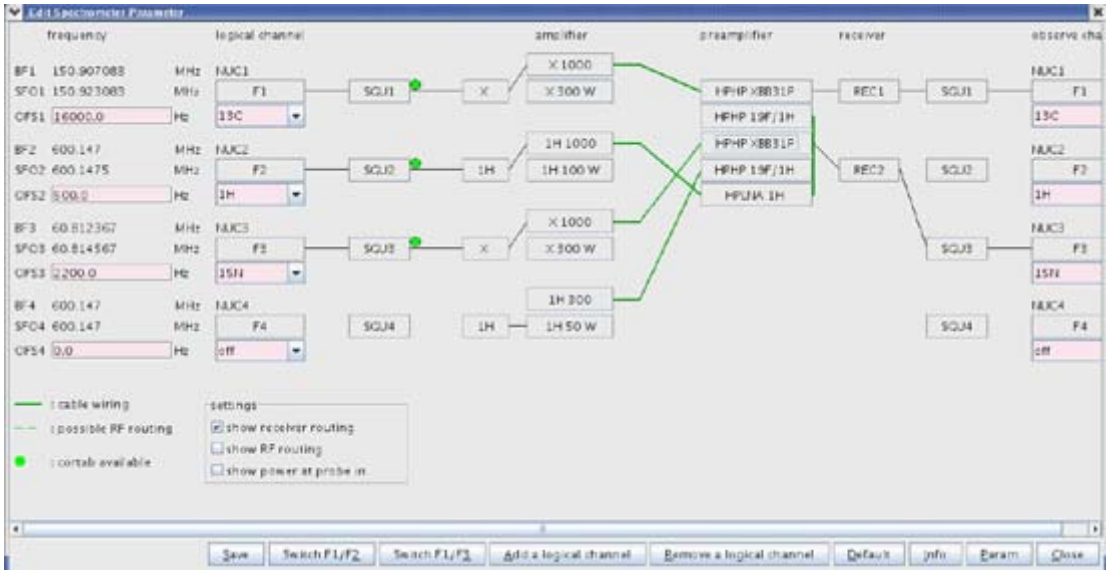

*Figure 3.44. The **edasp** Display for a System with two Receiver Channels*

In the figure above the ***edasp*** display for a system with two receiver channels, set for observe on ^{13}C and ^{15}N, while decoupling on protons. The same SGU is used for pulse and detection on both receiver channels.

Basic Setup Procedures

4

This chapter contains information and examples on how to set up basic solid-state NMR (SSNMR) experiments. We'll begin with the settings for the RF-routing of the spectrometer, some basic setup procedures for MAS probes and how to measure their (radio frequency) RF-efficiency and RF-performance. Accurate measurement of the pulse lengths and the associated RF-power levels is essential for solid-state NMR experiments. In SSNMR, RF-field amplitudes are often expressed as spin nutation frequencies instead of 90° pulse widths. Spin nutation frequency n_{rf} and 90° pulse width are related through the reciprocal of the 360° pulse duration $4t_{p90}$ such that:

$$n_{rf} = 1/(4t_{p90}) = \text{RF-field in Hz (with } t_{p90} \text{ in µsec)}$$

Setting up the magic angle, shimming a CPMAS probe, setting up cross polarization and measuring probe sensitivity for ^{13}C will also be explained. This is part of probe setup and performance assessment during installation. However, regularly scheduled performance measurements should be part of the hardware, probes and spectrometer maintenance. Therefore, these checks should be performed periodically.

The checks also need to be performed if an essential piece of hardware has been exchanged. In the following, we describe all steps which are necessary to assess performance of a CPMAS probe, along with all necessary settings. Detailed information about TopSpin software commands is available in the help section within the appropriate chapter.

Setting up a CPMAS probe from scratch requires the following steps:

1. Mount the probe in the magnet and connect the RF connectors of the probe to the appropriate preamps.
2. Connect the spinning gas connectors and the spin rate monitor cable.
3. Insert a spinner with finely ground KBr and spin at 5 kHz.

It is assumed that these operations are known. If not, please refer to the following sources:

- Probe manual.
- MAS-II pneumatic unit manual in TopSpin/help.
- SBMAS manual in TopSpin/help.

This chapter will include:

"Setting the Magic Angle on KBr"

"Calibrating 1H Pulses on Adamantane"

"Calibrating 13C Pulses on Adamantane and Shimming the Probe"

"Calibrating Chemical Shifts on Adamantane"

"Setting Up for Cross Polarization on Adamantane"

"Cross Polarization Setup and Optimization for a Real Solid: Glycine"

"Some Practical Hints for CPMAS Spectroscopy"

"Literature"

General Remarks *4.1*

Despite the fact that most spectra taken on a CP/MAS probe look like liquids spectra, the conditions under which they are taken must account for the presence of strong interactions. This basically means that:

- Fast spinning, and
- high power pulses are applied.

Fast spinning requires a high precision mechanical system to allow spinning near the speed of sound. This requires careful operation of the spinning devices. Please read the probe manual carefully!

High power decoupling in solids requires 20-fold RF fields compared to liquids spectroscopy, since we are dealing with >20 kHz dipolar couplings rather than maximum 200 Hz J-couplings! This means that RF voltages near the breakthrough limit must be applied, and that currents of far more than 20 A occur.

It is therefore essential that:

- Power levels for pulses must be carefully considered before they are applied. Always start at very moderate power levels with an unknown probe, find the associated RF field or pulse length and then work your way towards specified values. The same applies for pulse lengths, especially decoupling periods, since the power dissipation inside the probe is proportional to pulse power and duration. Always observe the limits for duty cycle and maximum pulse power. Please refer to the probe specifications for more information. Never set acquisition times longer than required!
- Spinners and turbine must be kept extremely clean. Any dirt, especially oil, sweat from fingers, water will decrease the breakthrough voltage dramatically. Make sure the spinner is always clean (wipe before inserting, touch the drive cap only) and the spinning gas supply is carefully checked to provide oil-free and dry (dew point below 0 °C) spinning gas. Compressors and dryers must be checked and maintained on a regular basis. Any dirt inside the turbine will eventually cause expensive repairs.

The following setup steps need only be executed upon installation or after a probe repair. The test spectrum on glycine should be repeated in regular intervals to assure probe performance.

Setting the Magic Angle on KBr 4.2

For all following steps, generate new data sets with appropriate names using the ***edc*** command to record all individual setup steps.

RF-Routing 4.2.1

The spectrometer usually has 2 or more RF generation units (SGU's), transmitters and preamplifiers. In order to connect the appropriate SGU to the appropriate transmitter and the transmitter to the associated preamp where the probe channels are connected, there are several routing possibilities. In order to minimise errors in hardware connections, the routing is under software control where possible. Where cable connections need to be done manually, the software does not allow a change. These connections are made during instrument installation.

Enter the "***edasp***" command (or click the **Edit** button in the nucleus section in the acquisition parameter window ***eda***) in order to get the spectrometer router display.

Alternatively, click on the routing icon in ***eda***.

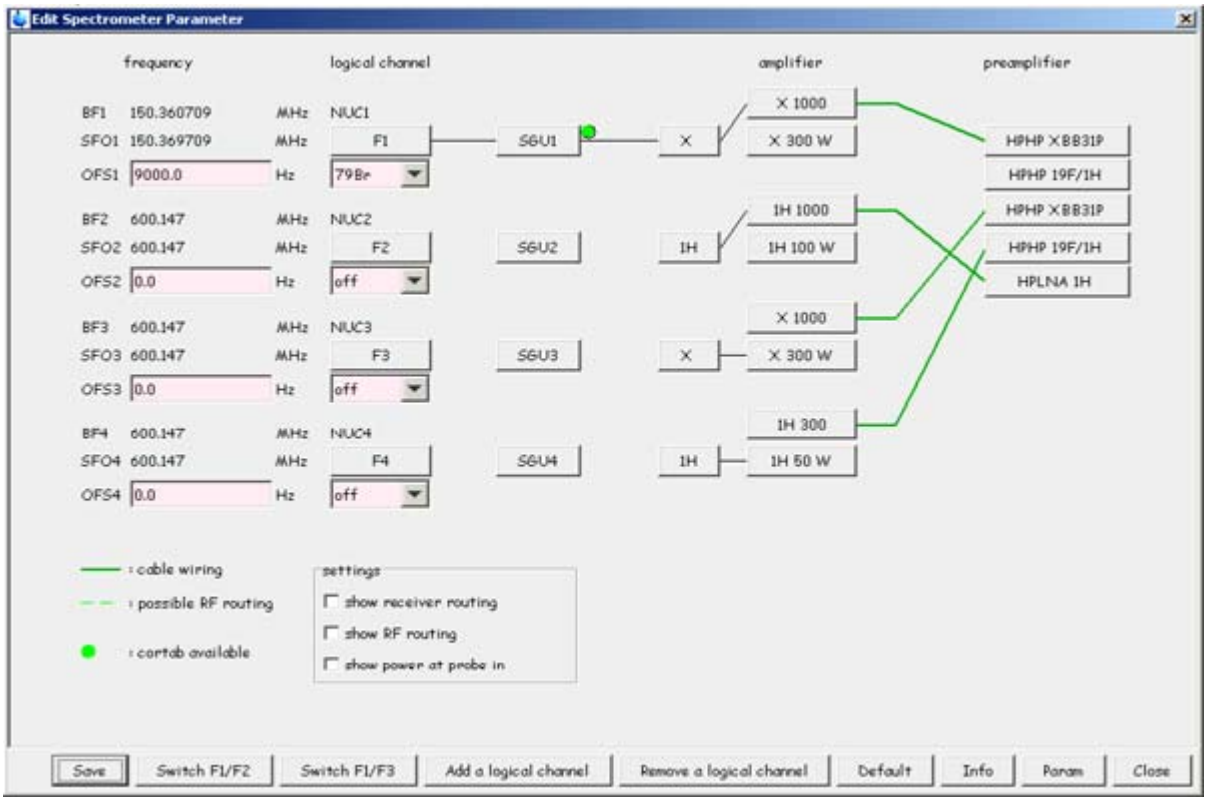

Figure 4.1. Routing for a Simple One Channel Experiment

The figure above shows the routing for a simple one channel NMR experiment using the 1000 W output from the high power amplifier.

In this menu, 4 RF channels are available. These 4 RF channels can be set up for 4 different frequencies. The two left most columns labelled frequency and logical

channel define the precise irradiation frequency by setting the nucleus and the offset ***O1*** from the basic frequency. In this example, we want to set up for pulsing/observe on the nucleus ^{79}Br. Selecting ^{79}Br for channel F1 defines the basic frequency ***BF1*** of ^{79}Br (in this case on a 600 MHz spectrometer, 150.360709) and the adjustable offset (9000 Hz in this case). Both values are added to show the actual frequency setting, ***SFO1***. The frequency setting is taken from a nucleus table which is calculated for the respective magnetic field B_0. The index 1 in ***O1, BF1, and SFO1*** refers to the RF channel 1 (which is also found in the pulse program where the pulse is defined as p1:f1. Note that this index does not exist for the following columns which represent the hardware components (SGU1-4 refers to the slot position in the AQS-rack). The lines connecting the (software) channel F1 to the actual frequency generation and amplification hardware can be drawn ad libitum as long as the required hardware connections are present. The connections between transmitter and preamp cannot be routed arbitrarily, because every transmitter output is hardwired to a preamplifier, so the lines are drawn in green. Please note that the nucleus in channel F1 is always the observe nucleus.

To set up for ^{79}Br observation, click on **Default** and the correct routing will be shown.

The green dot between SGU1 and amplifier 1 indicates that for this nucleus in this connection, the transmitter has been calibrated for amplitude and phase linearity (CORTAB).

For example, if you select a nucleus where this has not been calibrated and the green dot is not visible, the same power level setting in dB will produce >6 dB more power (> 4-fold power) which may destroy your probe. Calibrate power levels in such a case starting with 10 dB less power (higher *pl(n)*-value) to prevent destruction of your probe!

The connections between SGU(n) and transmitter (n) can be altered by clicking on either side of the connecting line (removes the connection), and clicking again on both units you want to connect (route). In case of high power transmitters, you have two power stages which you select by clicking on the desired stage. High power stages require the parameter ***powmod*** to be set to “high”. Selecting a path which is not fully routed will generate an error message.

To leave the display, click on **Save**. Make sure your probe X-channel is connected to the selected preamplifier (the sequence of preamplifiers in ***edasp*** represents the physical position of the preamplifier in the stack). If the preamp is a high power type, make sure the correct matching box is inserted into the preamp (for 500-800 MHz systems, it would be labelled for the frequency range 120-205 MHz). Connections are shown in the figure below:

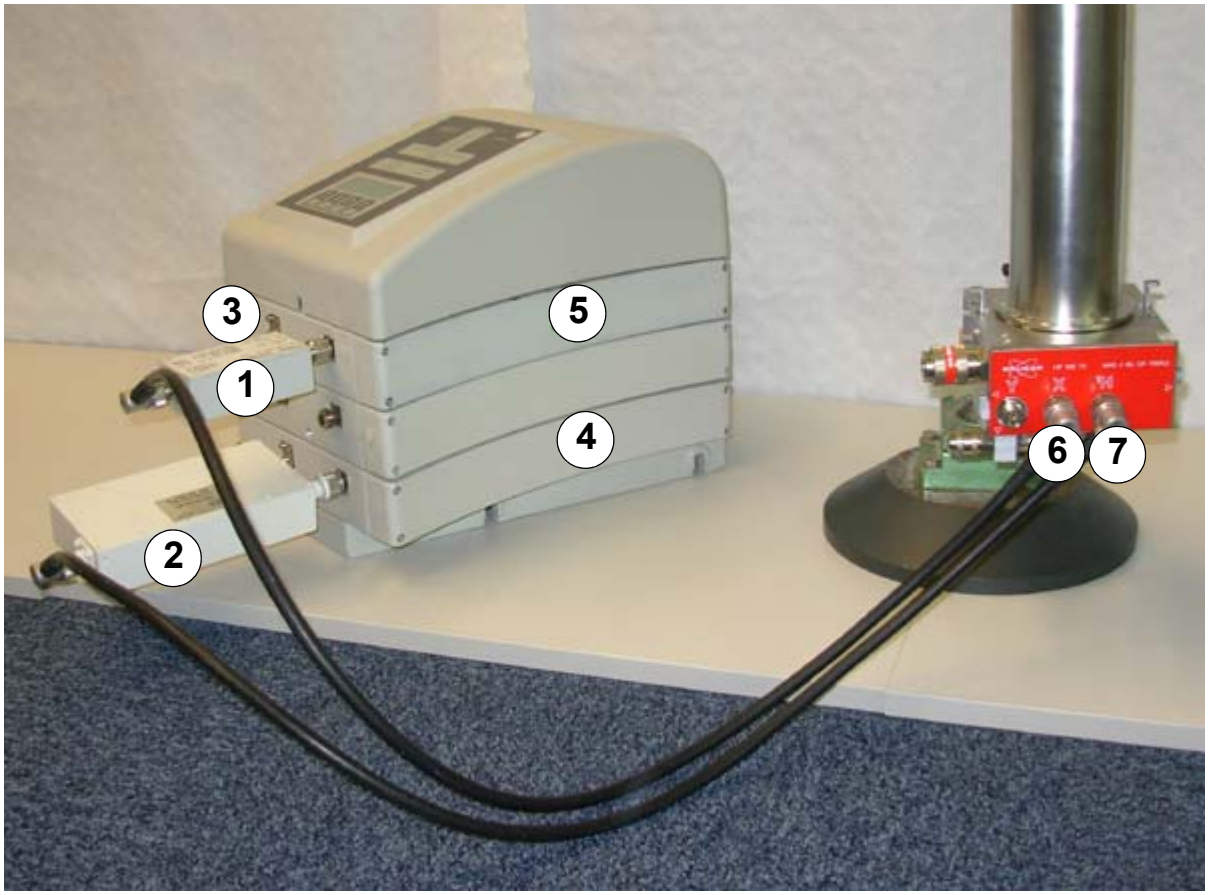

1: X Low Pass Filter
2: Proton Bandpass Filter
3: X-BB Preamplifier
4: 1H HP Preamplifier
5: 13C Matching Box
6: X Probe Connector
7: 1H Probe Connector

Figure 4.2. Probe Connections to the Preamplifier

The figure above shows the probe connections to the preamplifier with appropriate filters, placed on a table for better illustration.

Setting Acquisition Parameters *4.2.2*

Create a new data set for the experiment by typing ***edc*** in the command line.

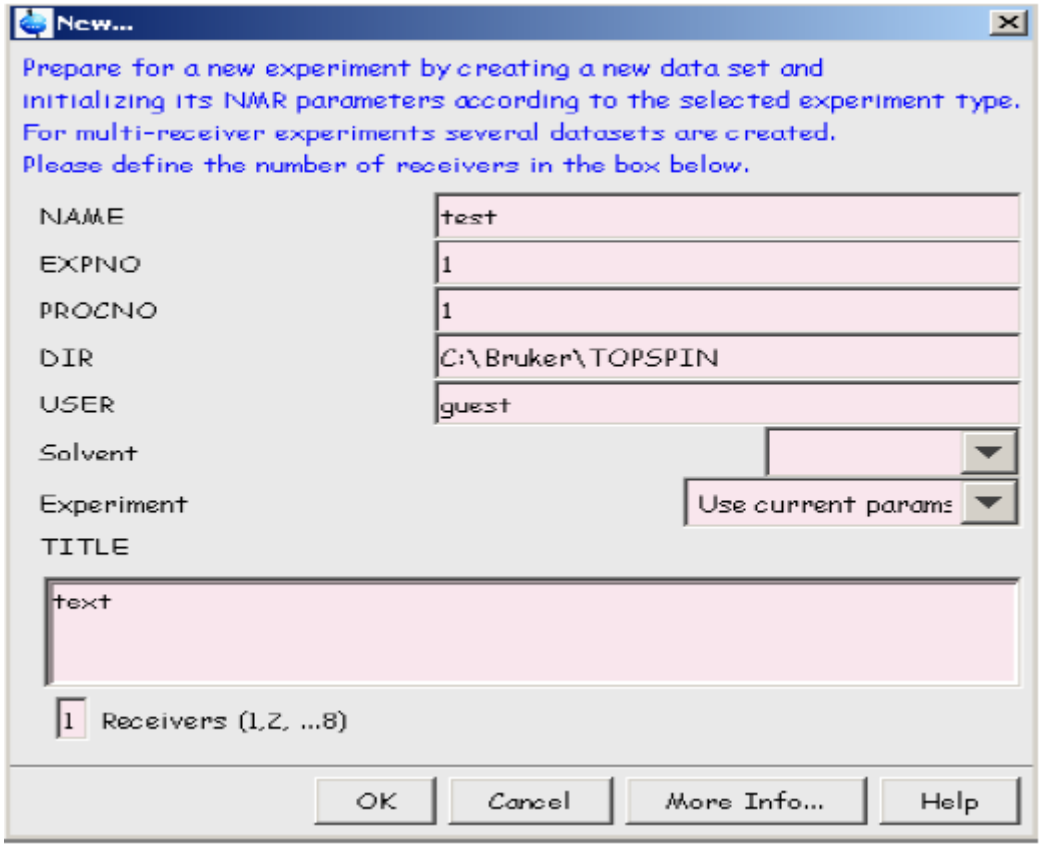

Figure 4.3. Pop-up Window for a New Experiment

Spin the KBr sample moderately (~5, 2.5 mm: 10 kHz). In order to set up the experiment, type ***ased*** in the command line to open the table with parameters used for this experiment.

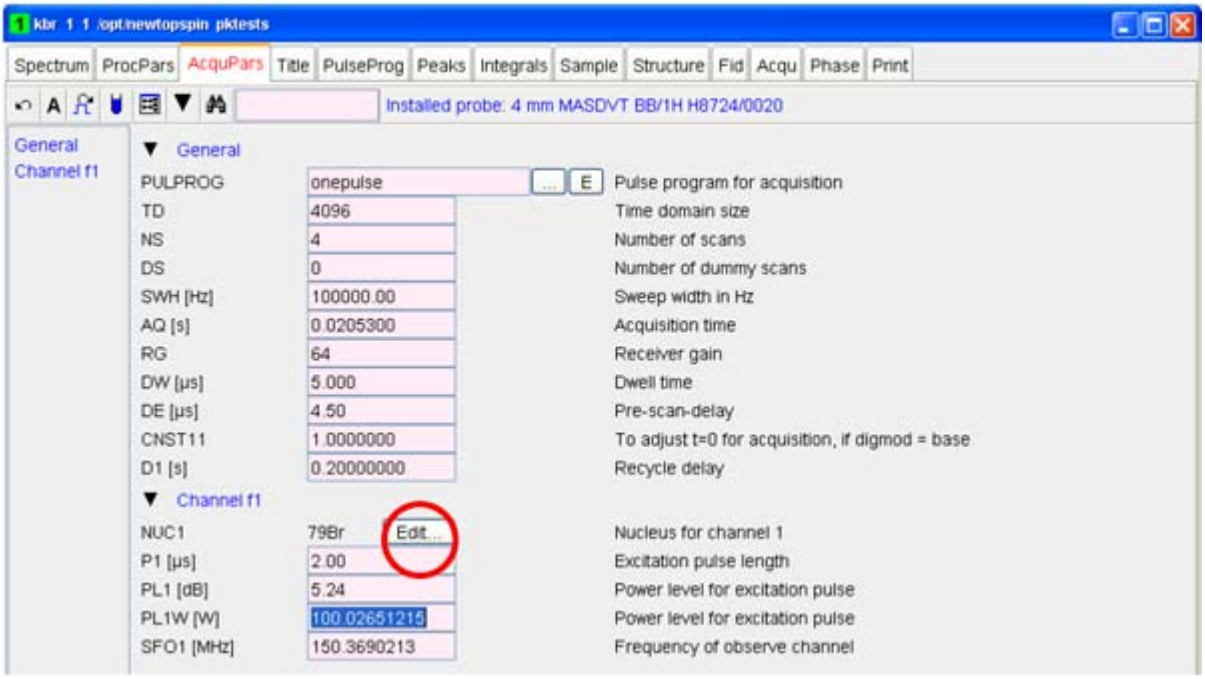

Figure 4.4. ased Table with Acquisition Parameters for the KBr Experiment

Then check rf routing by clicking on the **Edit** button in figure 4 or by typing ***edasp*** in the command line and check ***powmod*** by clicking the *default* button (as described above). The rf routing for this experiment is shown in figure 1. Next set ***p1*** = 2 µs***, ns*** = 8 or 16. The power level at which ***p1*** is executed is ***pl1***. Having high power transmitters it is important to be aware of the pulse power that is applied. With TopSpin 2.0 and later, ***ased*** shows ***pl1*** and ***pl1w***, if the transmitter has been linearized (green dot in ***edasp***) and the transmitter power has been measured. Set the power to about 100W.

For a non linearized transmitter, ***pl1*** should be set to 10 in case of a 1000W transmitter and to 4 (5) for a 300W or 500W transmitter. You can also check durations and power levels in a graphical display by clicking the *experiment* button in the ***Pulprog*** window as it is shown in the figure below.

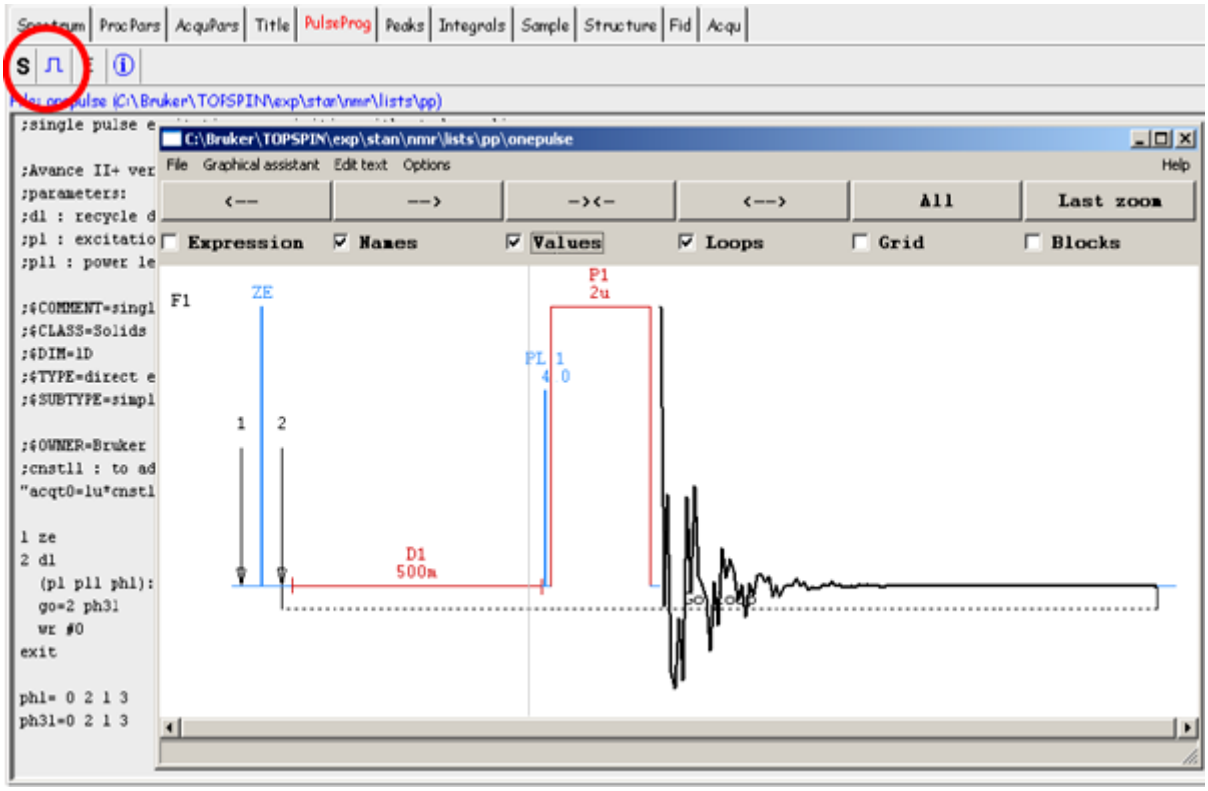

Figure 4.5. Graphical Pulse Program Display

In the figure above, the experiment button for opening the graphical display is marked with a red circle.

Then match and tune the probe for this sample using the command ***wobb***. This will start a frequency sweep over the range of ***SFO1***+/-***WBSW***/2. The swept frequency will only be absorbed by the probe at the frequency to which it is tuned.

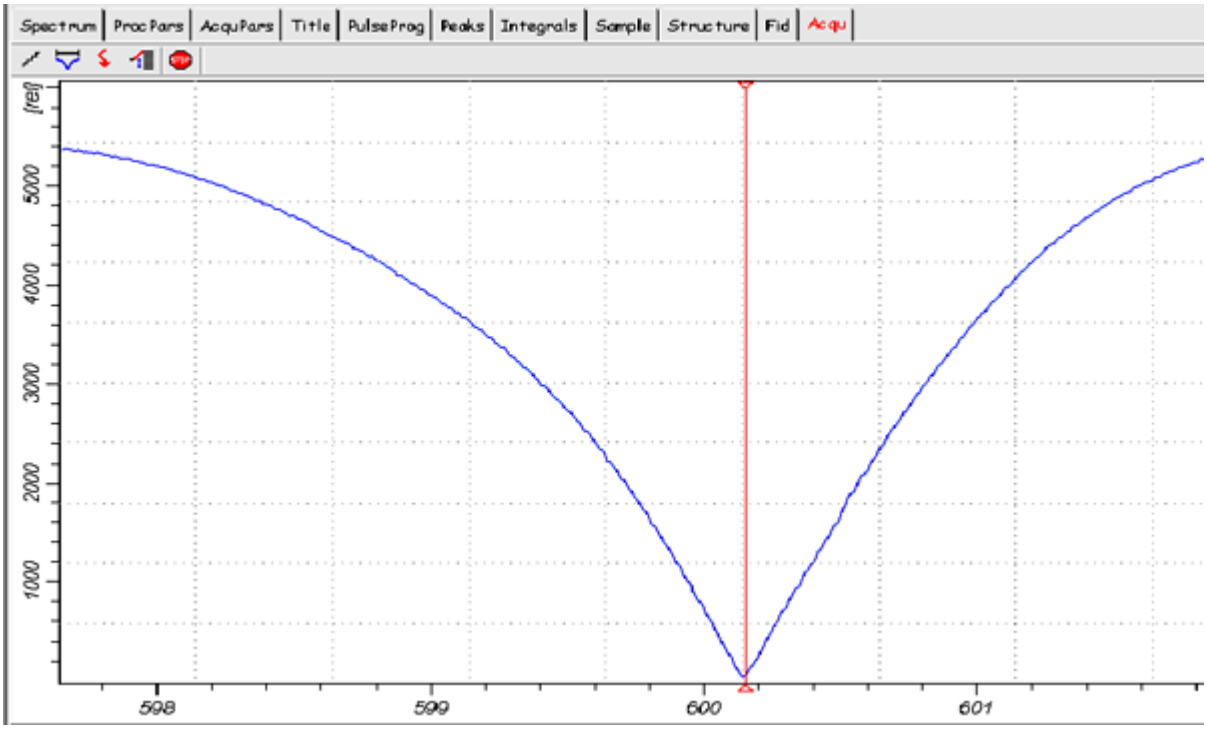

Figure 4.6. Display Example of a Well-tuned Probe

At frequencies, where the probe is not matched to 50 Ohms, the curve will lift off the zero line. If tuned to a frequency within ***SFO1***+/-***WBSW***/2, but ≠ ***SFO1***, the probe response will be off center.

N.B.: Fake resonances may appear which do not shift with probe tuning. It is always a good idea to keep track which nucleus was tuned last so it is clear what direction to tune to. Usually, turning the tuning knob counter clockwise (looking from below) will shift to higher tuning frequency.

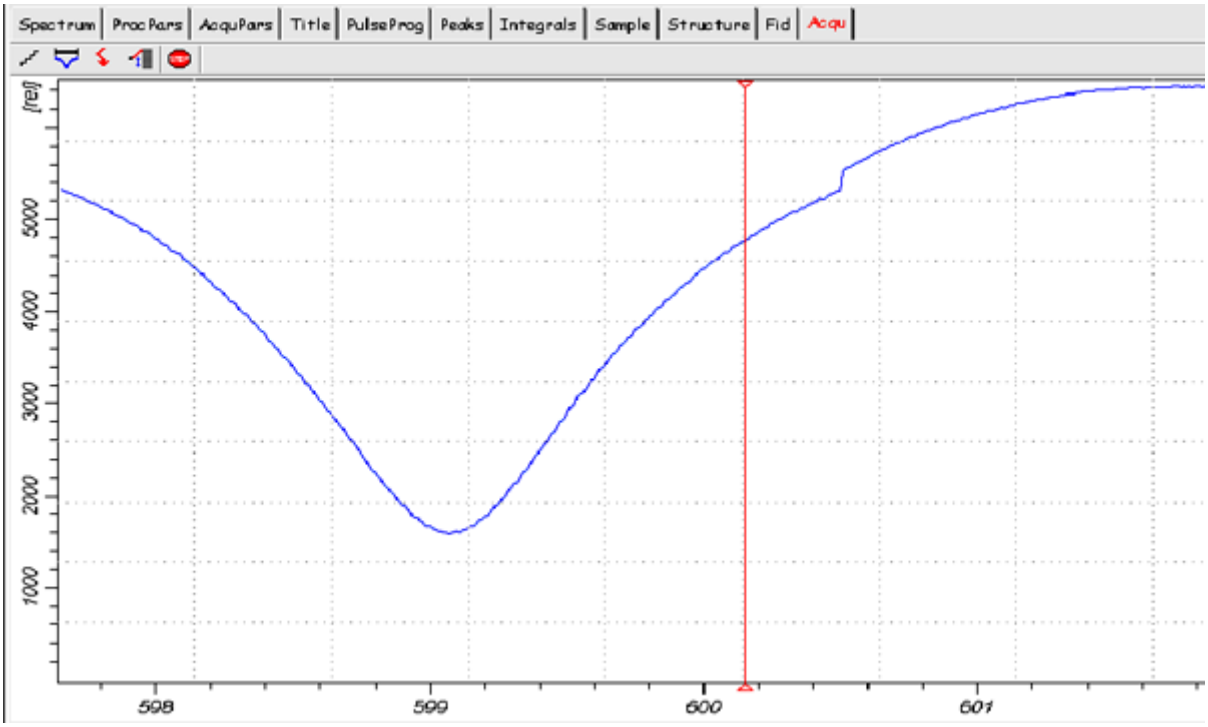

Figure 4.7. Display Example of an Off-Matched and Off-Tuned Probe

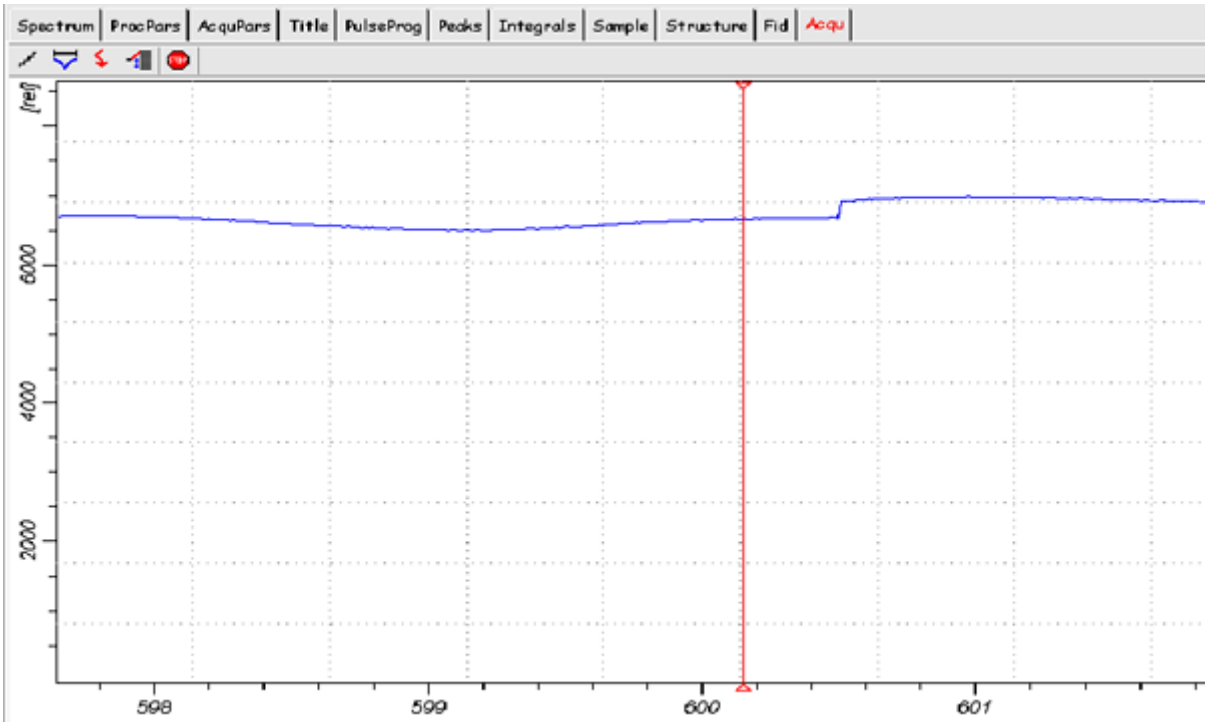

Figure 4.8. Display Example Where Probe is Tuned to a Different Frequency

The figure above is an example of where the probe is either tuned to a completely different frequency outside this window or the probe is not connected to the selected preamp. Check ***edasp*** for correct routing, Check for correct matching box frequency range. Increase WBSW to 50 or 100 and try to find the probe resonance position.

When the probe is tuned well, as shown in ***Figure 4.6.***, start an acquisition by typing *zg* in the command line or clicking on the black triangle (upper left side) in the acquisition display. Do a Fourier transformation and a phase correction by typing *ft* and phase correct.

Set offset ***O1*** to the value obtained for the center peak (see ***Figure 4.13.***) and start *"**xau angle**"*. This will allow you to view the fourier transformed spectrum or the FID after ***ns*** scans. The magic angle is adjusted best when the spikes on the FID or the spinning sidebands in the *Spectrum* display have maximum size, like shown in ***Figure 4.9.***. This is most easily seen with the carrier exactly on resonance and the un-shuffled FID display mode. The spinning sidebands should have maximum intensity, the rotational echoes on the FID should extend out to at least 8msec in the FID-display.

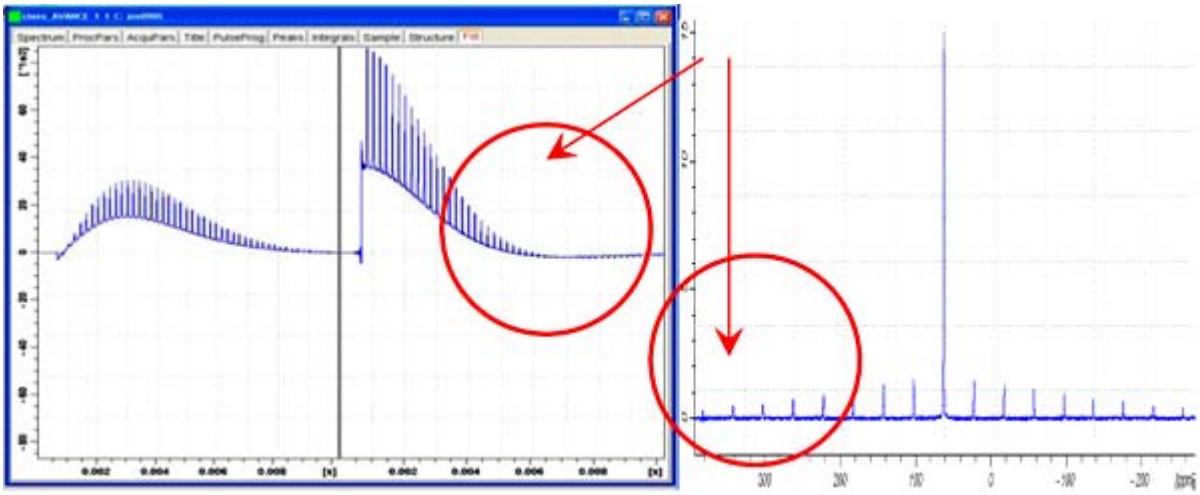

Figure 4.9. FID and Spectrum of the ^{79}Br Signal of KBr used to Adjust the Magic Angle

Calibrating 1H Pulses on Adamantane *4.3*

Spin the KBr sample down and change to a spinner filled with adamantane. Spin at 5-10 kHz. Generate a new data set from the KBr data set by typing ***new***. Set the instrument routing for ^{13}C observe and ^{1}H decoupling, as shown in the following figure:

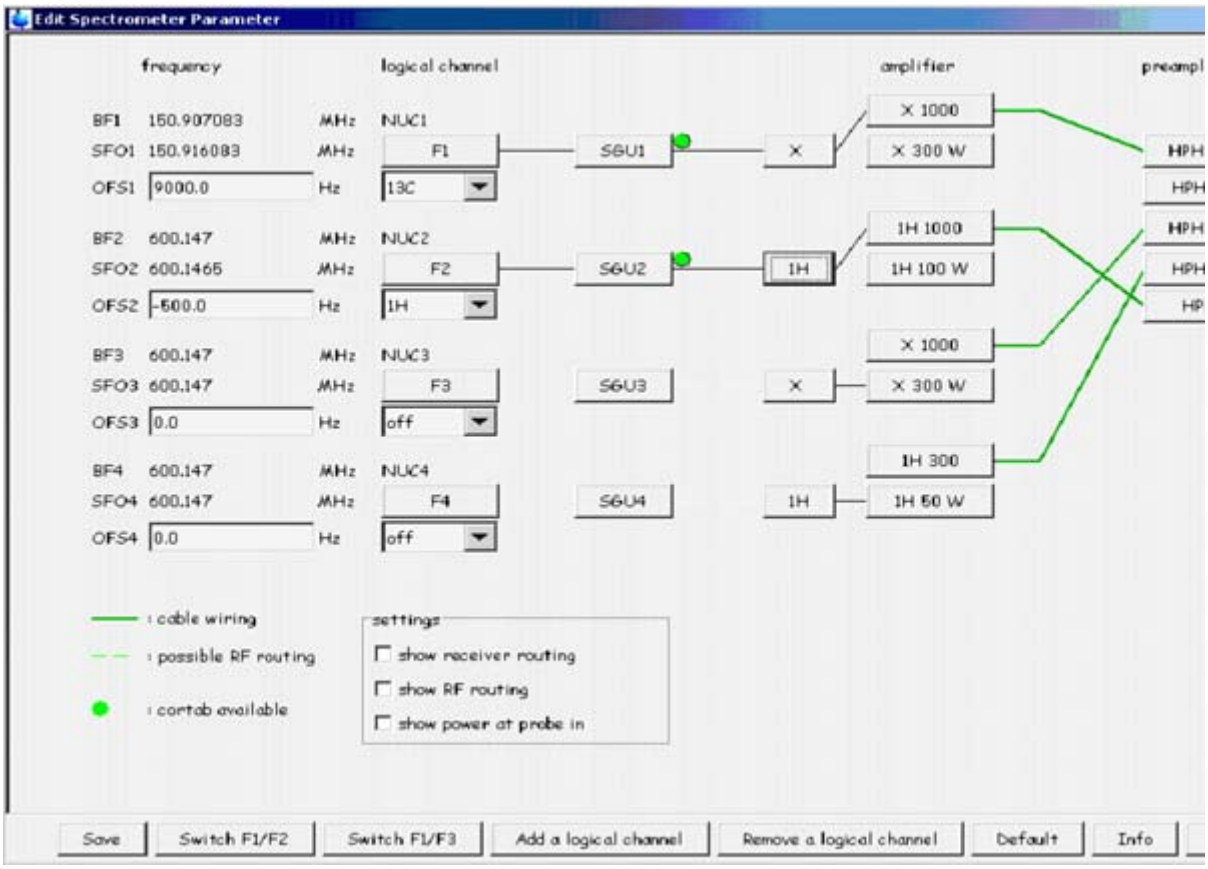

Figure 4.10. Routing for a Double Resonance Experiment using High Power Stage for H and X-nucleus

The figure above shows the routing for a double resonance experiment, e.g. a ^{13}C experiment with ^{1}H decoupling. For high power transmitters, the parameter ***powmod*** must be set to ***high***. To check which power mode is selected, one may click the **default** button, change to ***powmod high*** in the command line if necessary. Note: the routing is only effective if the parameter *powmod* = *high*.

To change to proton observe, click **SwitchF1/F2**.

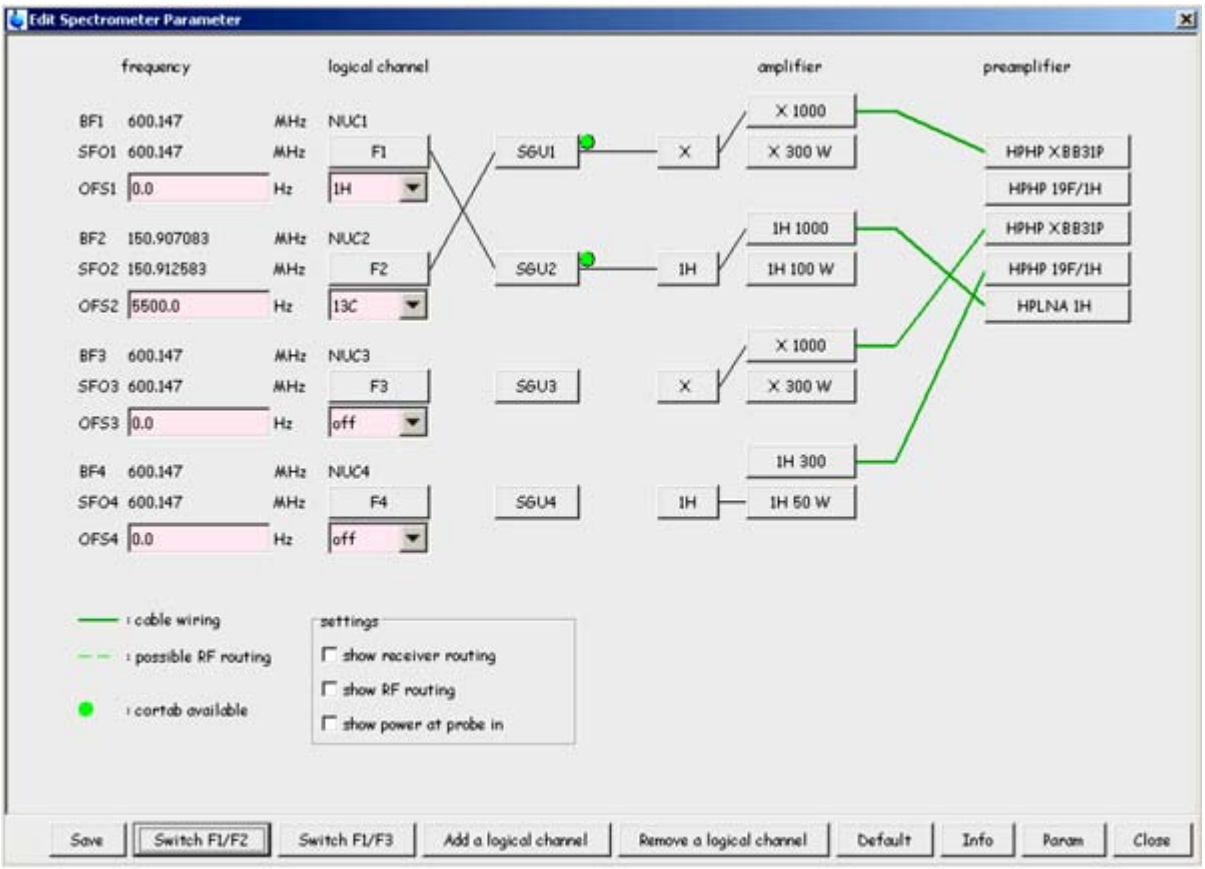

Figure 4.11. Routing for a Double Resonance Experiment, Changed for Proton Observation

In the figure above channel F2 need not be used.

The settings for F1 and F2 are interchanged. Change ***rg*** to 8-16 and ***d1*** to 4 sec. Set ***pl1w*** to 50W, or to 10 dB (high power proton transmitter), 7 dB (500W proton transmitter), 5dB (300W proton transmitter) or -4 (100W transmitter), if the green dot does not appear in the ^{1}H channel in ***edasp***. Connect the probe proton channel to the proton preamp. A proton band pass filter must be inserted between preamp and probe. Tune the proton channel of the probe using the command ***wobb high***. This means that the highest frequency is tuned first. Stop and type ***wobb*** again. Then adjust the tuning of the X channel to ^{13}C. Alternatively, you can switch to the lower frequency channel within ***wobb high*** by clicking on the frequency table symbol in the ***wobb*** display or by pressing the second touch button on the preamp cover module twice. Then acquire ***ns*** =2 scans on the protons of adamantane.

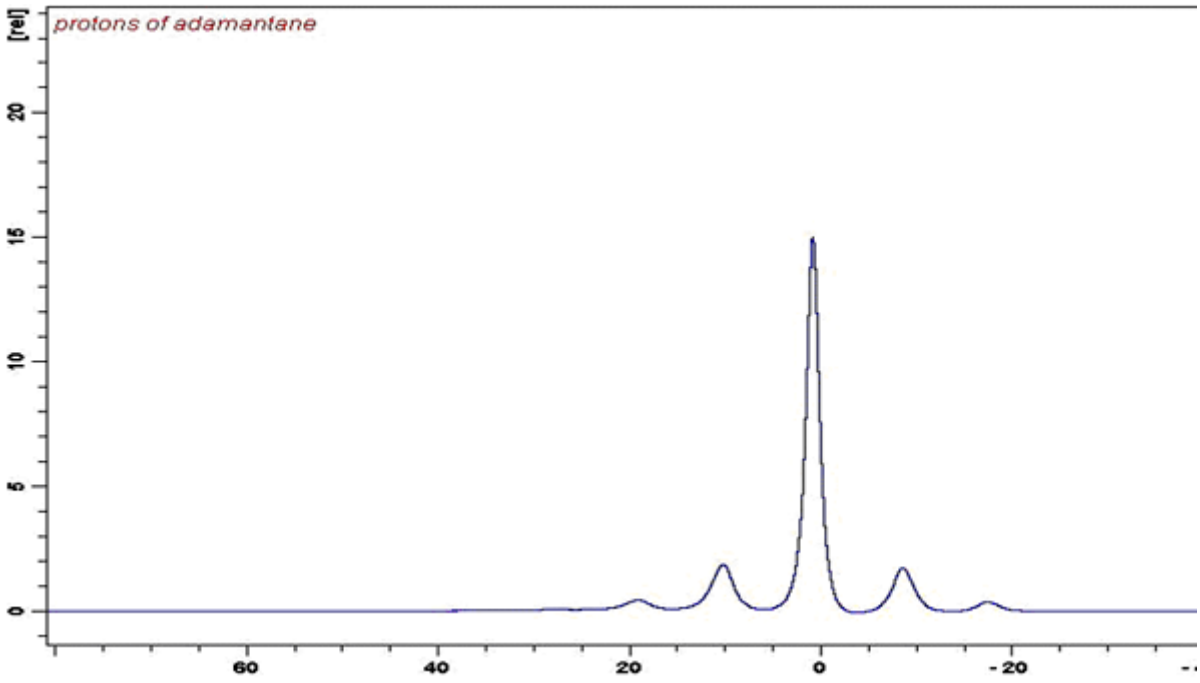

Figure 4.12. Proton Spectrum of Adamantane at Moderate Spin Speed

Set the carrier frequency O1 on top of the biggest peak using the encircled button in TopSpin.

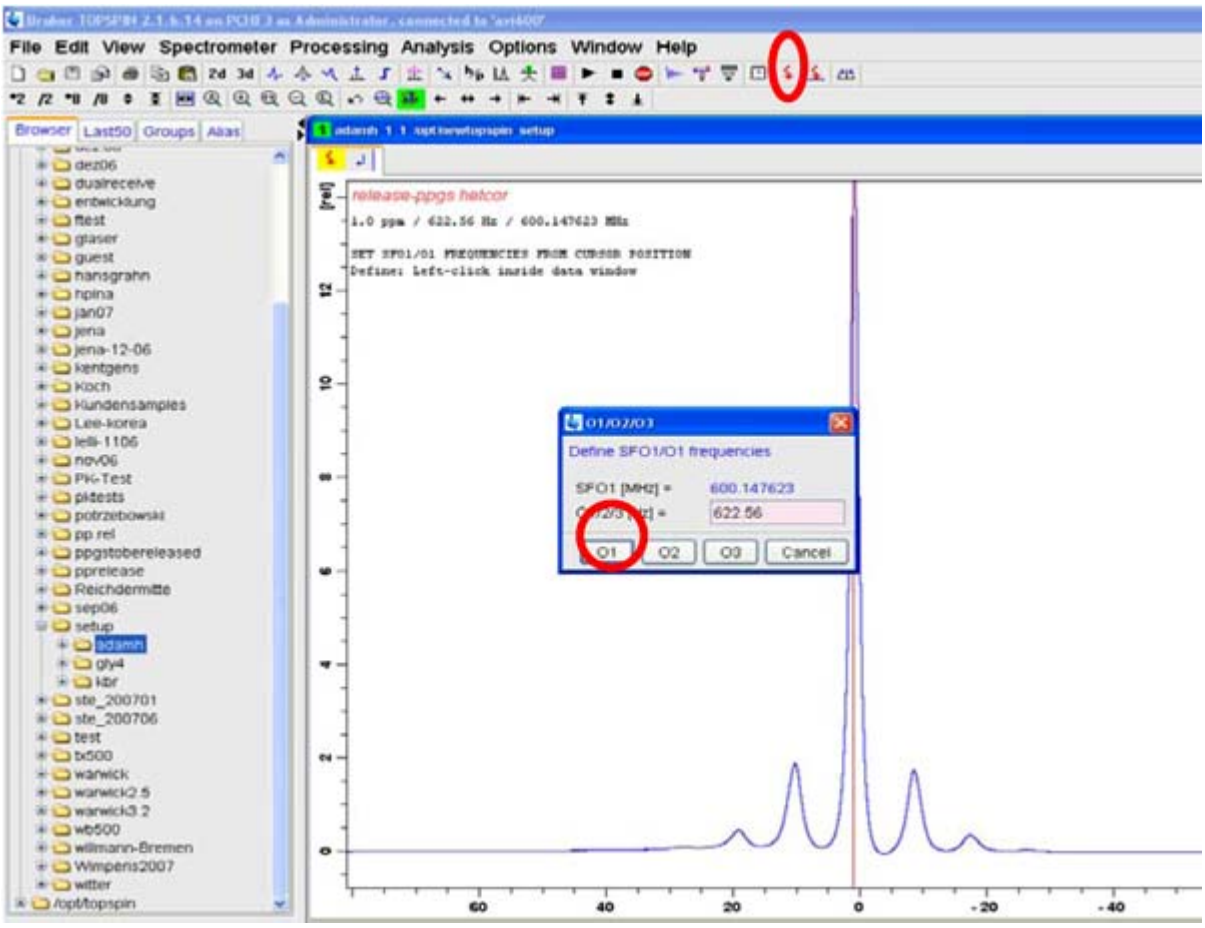

Figure 4.13. Setting the Carrier on Resonance

Click on the marked red arrow to set the observe frequency, set the position of the cursor line, and left click on the **o1** button. Acquire another spectrum, ft and phase.

Then expand the spectrum around the adamantane proton signal including the spinning sidebands by clicking on the left margin of the region of interest and pulling the mouse to the right margin of the region of interest as shown in the following figure:

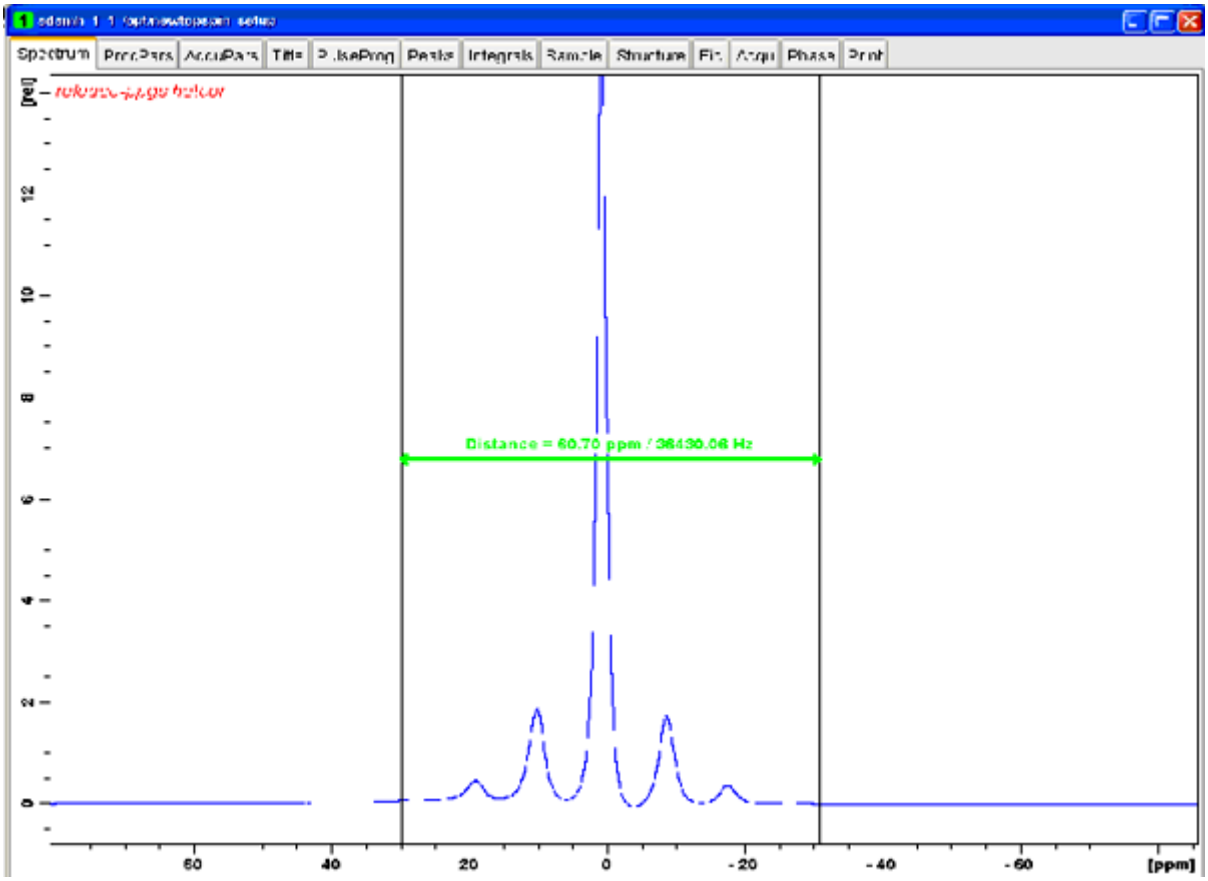

Figure 4.14. Expanding the Region of Interest

Click right mouse button in the **Spectrum** window. When the **Save Display Region to** menu pops up, select *Parameters F1/2* and OK or type ***dpl*** in the command line.

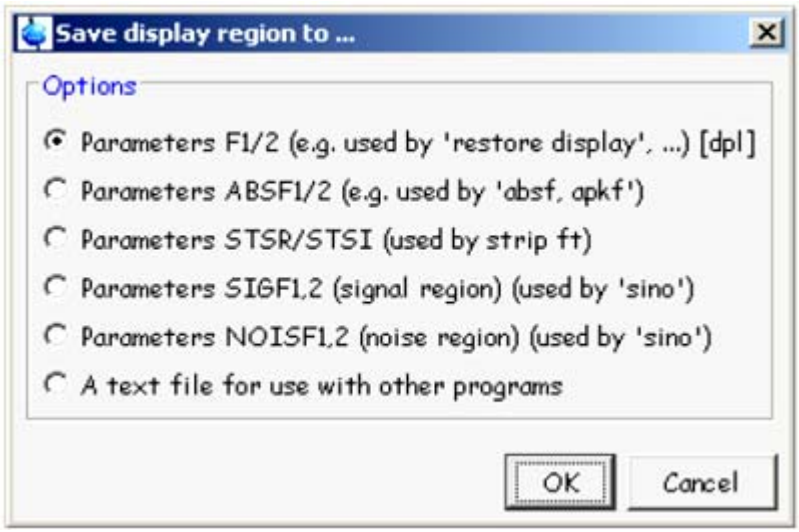

Figure 4.15. Save Display Region to Menu

Start parameter optimization by typing ***popt*** in the command line. The ***popt*** window will appear.

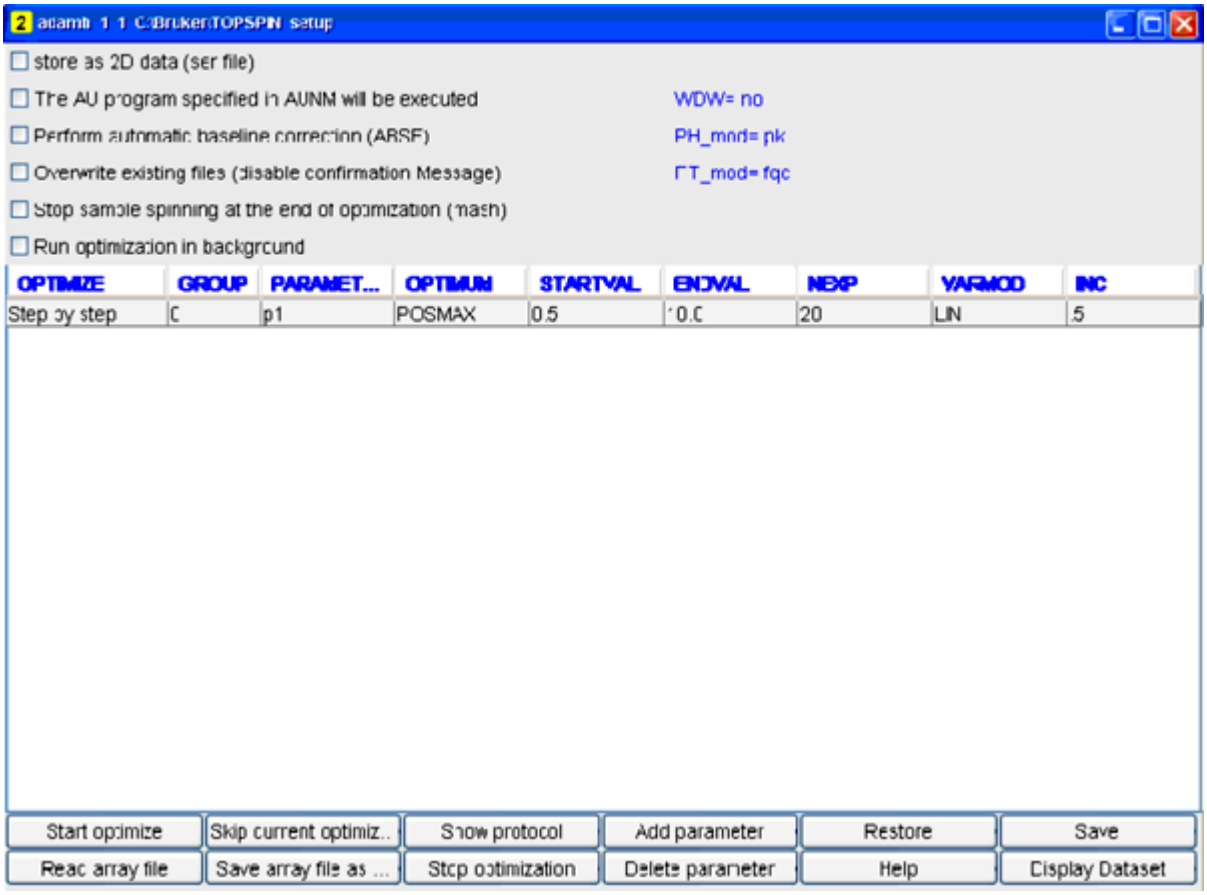

Figure 4.16. The popt Window

Use **optimize** *step by step*, **parameter** *p1* to optimize parameter ***p1***, **optimum** *posmax* to find the highest signal intensity (90 degree pulse) for the given value of ***pl1w*** or ***pl1***,and **varmod** *lin* to use linear increments for optimization. The value for **group** is not used for optimizing only one parameter and the number of experiments **nexp** is set automatically when clicking on the save button. Then save table by clicking on the **save** button and click on **start optimize** to start the optimization procedure.

The parameter value obtained by the program is written into the parameter set of the actual experiment at the end of the optimization.

In order to stop the execution of *popt* use the **skip** or **stop optimization** buttons. **Skip optimization** will evaluate the obtained data as if *popt* had finished regularly and writes the parameter into the parameter set. **Stop optimization** will stop without evaluation of the data. You can also type *kill* in the command line and click on the bar with "***poptau.exe***" to stop optimization. This will work like **stop optimization**.

Popt will generate a data set, where the selected expansion part of the spectrum is concatenated for all different parameter values (in this case, for ***p1***). It will have a ***procno*** around 999. To achieve this, processing parameters are changed ap-

propriately. Fourier transforming a normal FID in such a window will generate an incorrect spectrum window.

Therefore:

Never start an acquisition in such a window, first read in the ***procno*** where popt was started using the ***rep*** n command where n is the source ***procno***.

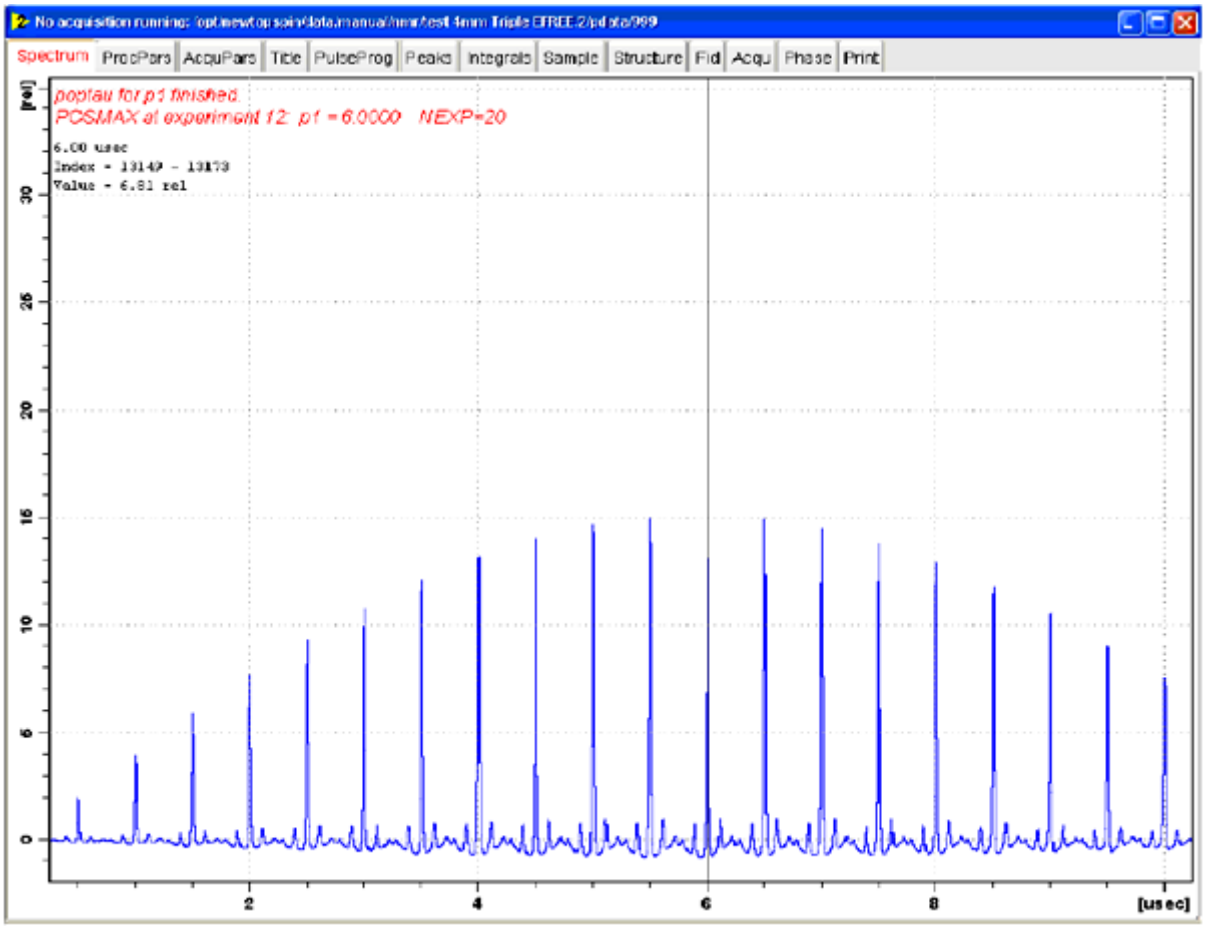

*Figure 4.17. The **popt** Display after Proton p1 Optimization*

The figure above shows the ***popt*** display after proton p1 optimization, the biggest signal is obtained at 6 µsec in this case.

Once you have obtained a 90-degree pulse for a given power setting, you can calculate power levels for different rf fields using the AU program ***calcpowlev***. Type ***xau calcpowlev*** into the command line and follow the instructions in the popup window.

Calculate the power level (in Watts or dB) required to achieve a 4.5 µsec proton 90 degree pulse. In this case, 6 µsec were obtained. The command ***calcpowlev*** calculates a power level 2.5 dB higher than used above to achieve 4.5 µsec pulse length. Set the new pl1 as calculated and check whether 2*4.5 µsec for ***p1*** will give a close to zero signal. This is a safe power level for all probes for pulses up to 100 msec. length.

Calibrating 13C Pulses on Adamantane and Shimming the Probe *4.4*

A high power decoupling experiment on ^{13}C of adamantane is used to measure ^{13}C pulse parameters.

NOTE: For experiments where long decoupling pulses on protons are executed, the proton preamplifier must be bypassed, i.e. the transmitter should be wired to the probe directly (via the proton bandpass filter) without going through the preamp if a high power proton preamplifier is not available. For HP-HPPR modules $^{1}H/^{19}F$ this is not absolutely necessary, but recommended. For HPLNA ^{1}H modules it is not required to bypass. Note that when bypassing the preamp which attenuates by about 1 dB, the proton power levels should be corrected by adding 1 dB to the pl-values.

Type ***edasp*** in the command line. You should get a display like in ***Figure 4.11.***. Click on **SwitchF1/F2** to set for ^{13}C observation with proton decoupling. Load the pulse program *hpdec*. Set ***cpdprg2***=cw. Set ***pl12*** to the power level that yields a 4.5 µsec proton pulse. Set ***pl1*** such that in ***ased*** the power displayed is 200W for ^{13}C (7mm probe), 150W (4mm probe) or 80W (2.5 mm probe). If the green dot is not visible in ***edasp*** for the ^{13}C channel, set pl1 to 12 dB (1 kW transmitter), 9 dB (500W transmitter) or 7 dB (300W transmitter) for any probe. Make sure the proton channel is tuned (***wobb high***) and the carbon channel is also tuned (***wobb***). With ***d1*** = 4s, ***rg*** = 256 ***swh*** = 100000, ***td*** = 4k, ***o2*** set to be on resonance on the adamantane protons as found above, accumulate 4 scans. Set the carrier frequency between both adamantane ^{13}C peaks. Reduce the spectral width swh to 50 kHz, set ***aq*** =50 msec.

Acquire 2-4 scans and define the plot limits (as shown in ***Figure 4.14.***) for the larger of the two peaks. Define the plot limits and determine the 90 degree carbon pulse ***p1***, using ***popt***. Recalculate ***pl1*** for a 4.5 µsec carbon pulse using ***calcpowlev***.

Pulse continuously using ***gs*** and shim the z gradient for highest FID integral.

The gradient settings can be conveniently changed in the ***setsh*** display. ***Figure 4.18.*** and ***Figure 4.19.*** show the adamantane ^{13}C FID without shims, with z-shim adjusted and the corresponding ***setsh*** displays.

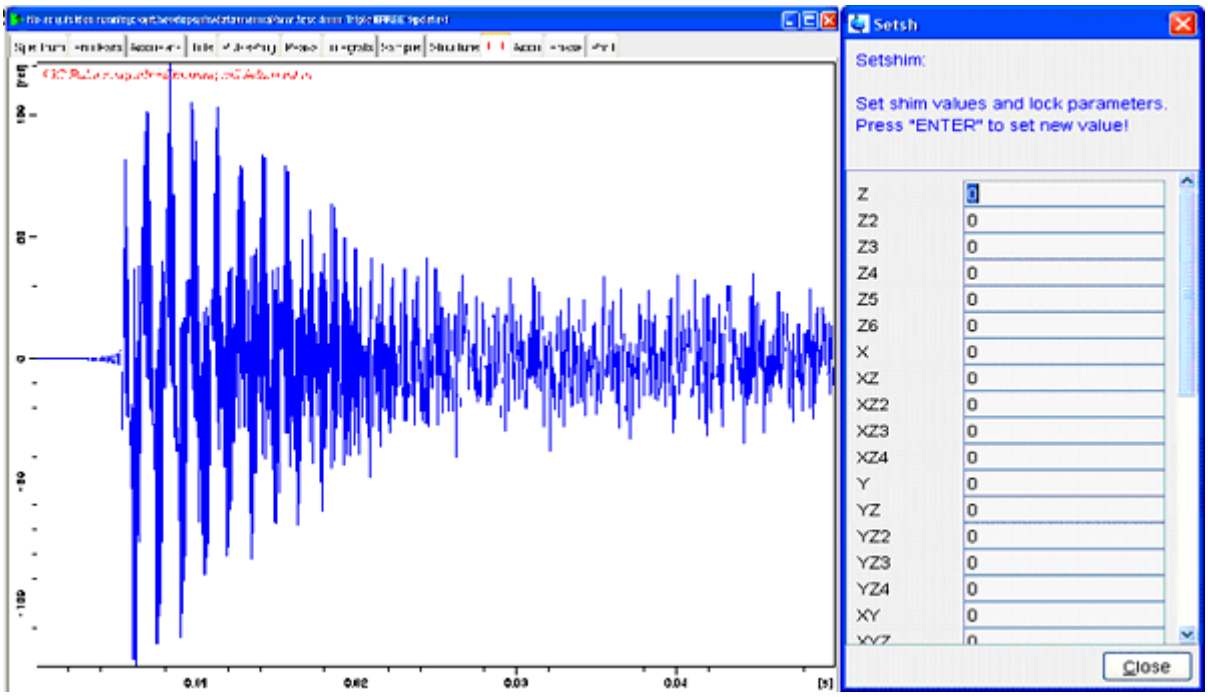

*Figure 4.18. Adamantane ^{13}C FID with 50 msec **aq**. **setsh** Display*

The figure above is an Adamantane ^{13}C FID with 50 msec ***aq***, with ***setsh*** display showing no shim values. N.b.: spinning removes part of the B_0 in homogeneities. Probes which do not use susceptibility compensated coil wire can show much shorter T_2* and require much more shimming effort (only with older probes up to 400 MHz proton frequency).

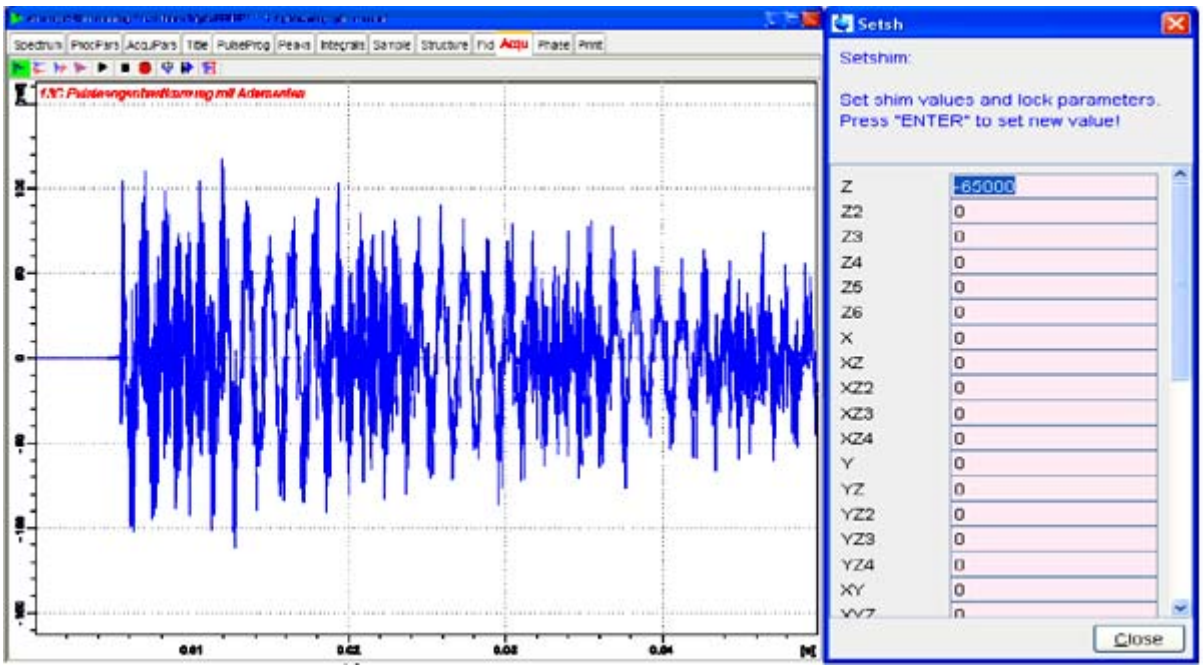

*Figure 4.19. Adamantane ^{13}C FID with 50 msec **aq**. **setsh** with Optimized Z-Shim Value*

For optimum shims (rarely required) set the shims x, y, z^2, xy and x^2-y^2, as well as xz and yz. You may need to increase the acquisition time ***aq*** to see the effect of increasing resolution. Save the shims using the command ***wsh*** followed by a suitable name.

Before the shims are saved, it is recommended to reset the field value in the ***bsmsdisp*** menu to be exactly on resonance with your shift reference sample of choice (protons of adamantane or water in D_2O or silicon rubber).

This allows the command ***probefield*** (TopSpin version 3 and up) to set the field according to probe shims and magnet drift (see below, and ***"Field Setting and Shift Calibration" on page 87***).

Note: For long acquisition times (***aq*** > 0.05 s) the decoupling power level ***pl12*** must be set to +3 dB and d1 must be increased to 6s. To allow longer acquisition times than 50 msec, the ***ZGoption –Dlacq*** must be set in ***ased***, if the pulse program contains the include file aq_prot.incl. Make sure the ***–Dlacq*** option is not left set for the following steps.

Calibrating Chemical Shifts on Adamantane 4.5

In TOPSPIN (as well as in the XWIN-NMR 3.5 release) the frequency list for NMR nuclei follows the IUPAC recommendations (see: R.K. Harris, E.D. Becker, S.M. Cabral de Menezes, R. Goodfellow and P. Granger, *NMR Nomenclature. Nuclear Spin Properties and conventions for Chemical Shifts*, Pure Appl. Chem. Vol. 73, 1795-1818 (2001) for reference).

Set the ^{13}C low field signal of adamantane to 38.48 ppm. This will set the parameter ***SR*** which is used to calculate the chemical shift axis and the peak positions in the spectrum.

Note: All data sets generated from this data set will have the peak positions correctly calibrated, if the magnetic field B_0 is not changed. However, you must make sure that the magnetic field is always the same. It may change, if the magnet has a slight drift, or if different shim settings are loaded. Therefore the same shim file should be loaded and the field be set to the same value using the *BSMSDISP* command. If the magnet drift is noticeable, the calibration should be redone in suitable intervals and the *field* value recorded in the lab notebook.

One can also use a spinner filled with H_2O to set the field position more precisely. Do not spin the sample and make sure the cap is well fitted. Set ***o1p*** to 4.85 ppm, set for proton observe (as described above for adamantane), and use ***gs*** for continuous pulsing and FID display. Change the field value in ***bsmsdisp*** until the FID is exactly on resonance. Then all spectra taken should be correctly referenced with ***sr*** = 0. For more information on correct field setting and shift calibration, see ***"Field Setting and Shift Calibration" on page 87***.

For all these experiments the field sweep must be off! When the BSMS unit is turned off and on again, the sweep will always be on. Running spectra with the sweep on will superimpose spectra at different fields! One can set the sweep amplitude to 0 in order to avoid such an accidental error condition.

Setting Up for Cross Polarization on Adamantane 4.6

Cross polarization is used to enhance the signals of X-nuclei like ^{13}C. The strong proton polarization is transferred (cross polarized) to the X-nuclei coupled to the protons via strong dipolar couplings. To achieve this, the protons and the X-nuclei must nutate at the same frequency. This frequency is the RF field applied to both nuclei at the same time (contact time). If this condition (Hartmann-Hahn-condition) is met, the transfer of proton magnetization to carbon is optimum. Since the proton signal of adamantane is resolved into spinning sidebands even at slow spin rates, this Hartmann-Hahn condition can be set to match for every proton spinning sideband. Using a ramp for the proton contact pulse, the Hartmann-Hahn match is swept over these possible match conditions and becomes insensitive to miss-sets and different spin rates.

Start from the data set used for observing ^{13}C under proton decoupling (**1.4**). Load the pulse program cp (in ***eda*** or typing ***pulprog*** cp). The pulse sequence is depicted in the following figure:

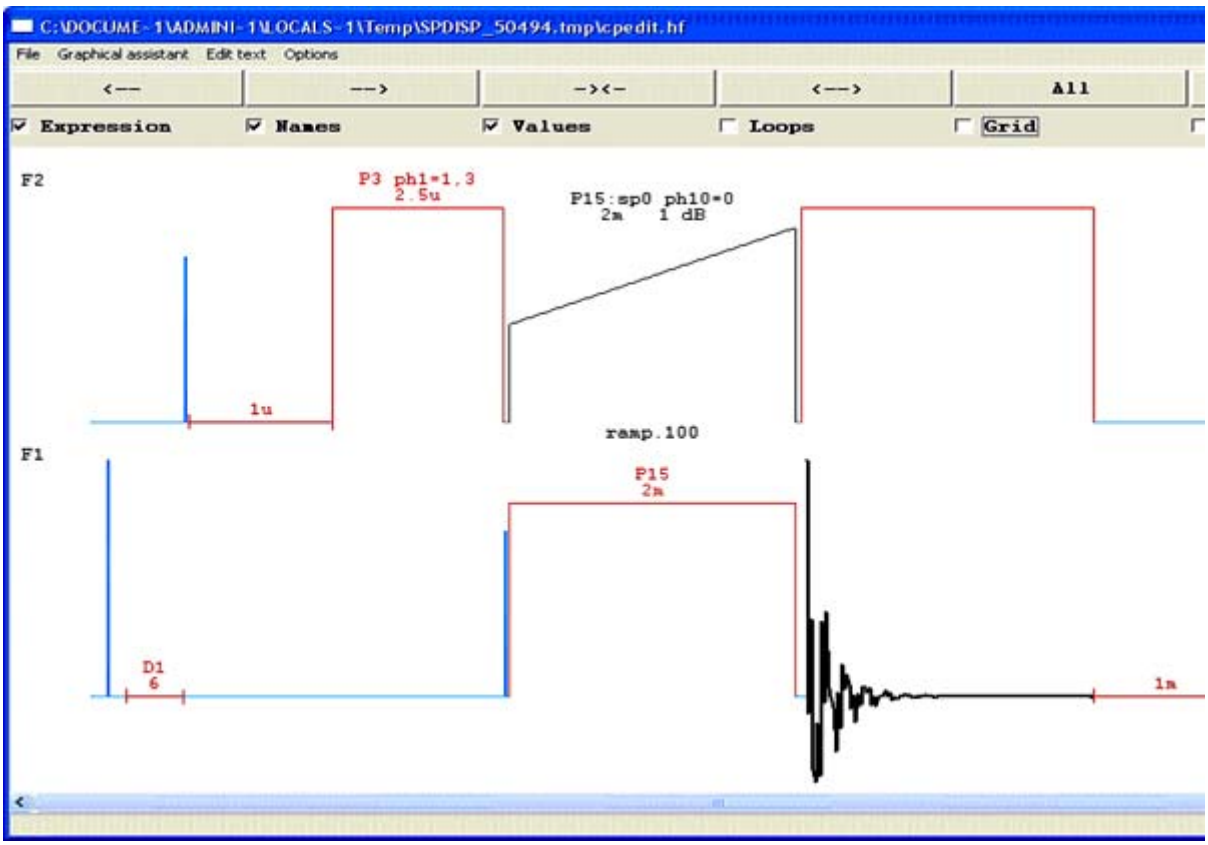

Figure 4.20. A cp Pulse Sequence

The following parameters are set:

- ***pl12***, for the initial 90 degree pulse and the decoupling during acquisition: set for a 4.5 µsec proton 90 degree pulse (as previously determined)
- ***pl1***, for the carbon contact pulse, set for a 4.5 µsec carbon pulse (as previously determined)
- ***p3***, 4.5 µsec
- ***spnam0***, set to ramp.100 to sweep the proton contact RF field from 50 to 100%
- ***sp0***, set to ***pl12*** -3 dB, to account for the lower average RF over the ramp.
- ***p15***, 2-5 msec (after the value, specify m to make it milliseconds, else it is taken as microseconds)
- ***cpdprg2***, select cw
- ***o1***, set between both adamantane peaks
- ***o2***, set to be on resonance on adamantane protons

Acquire 2 or 4 scans, then set plot limits for both peaks, and optimise p3 (+/- 2 µsec) and pl1 (+/- 2 dB) for best signal. **Fig. 21** shows a Hartmann-Hahn match optimization over 4 dB using a ramp contact pulse going from 50 to 100% amplitude.

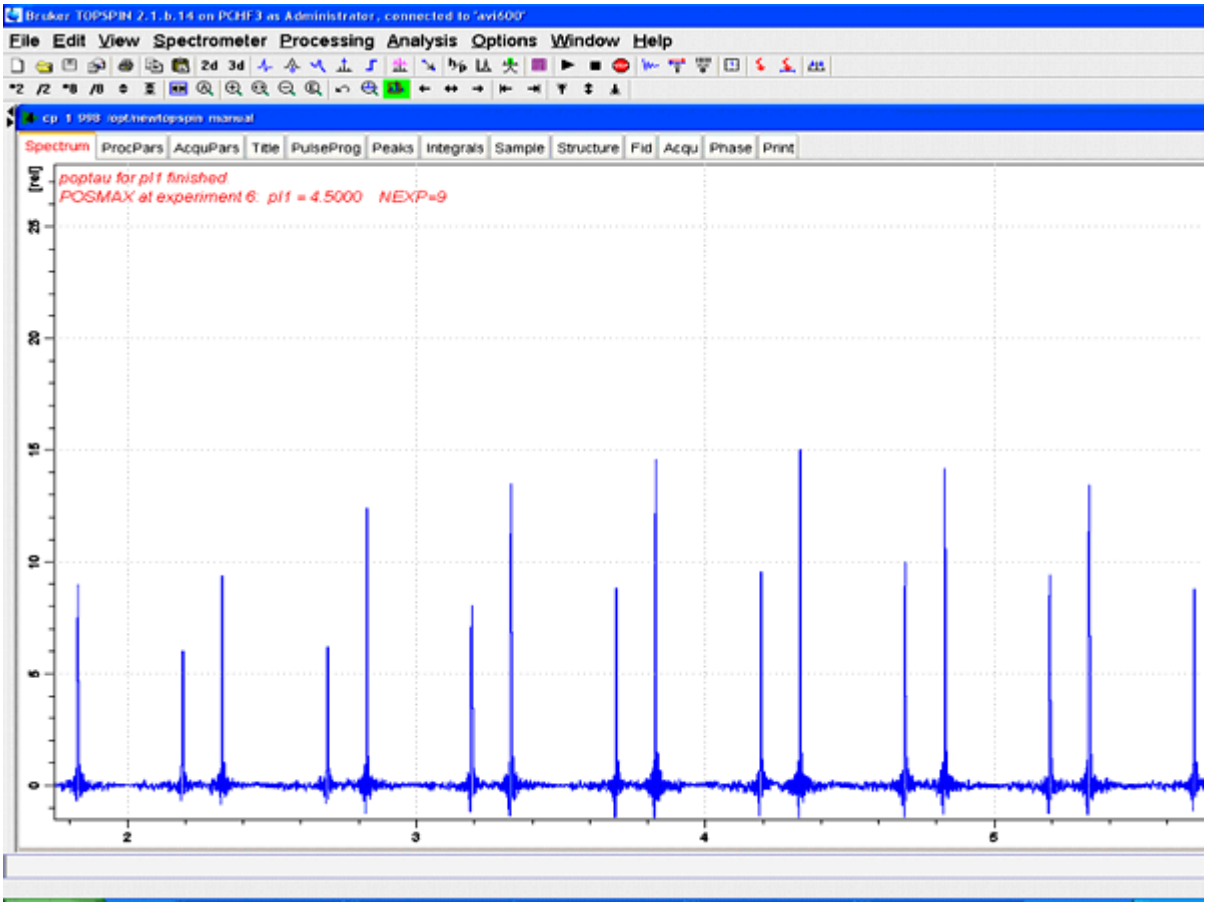

Figure 4.21. Hartmann-Hahn Optimization Profile

The wiggles besides the signals stem from truncation of the FID after 50 msec acquisition time.

To exemplify the existence of several HH-conditions on a spinning adamantane samples, another HH profile (***Figure 4.22.***) is shown where a square proton contact pulse is used. There are several maxima corresponding to matches on the sideband orders n+2, n+2, n+1, n+0, and n-1. The largest intensity is seen for n+/-1, the intensities are very sensitive to the RF-level which is varied in 0.2 dB steps. Using a ramp makes the experiment much more stable and more quantitative. Problems may arise if the proton $T_{1\rho}$ is short, since usually longer contact times must be employed. It makes therefore sense to use a flatter ramp (70-100%) and optimize for the spin rate which is used.

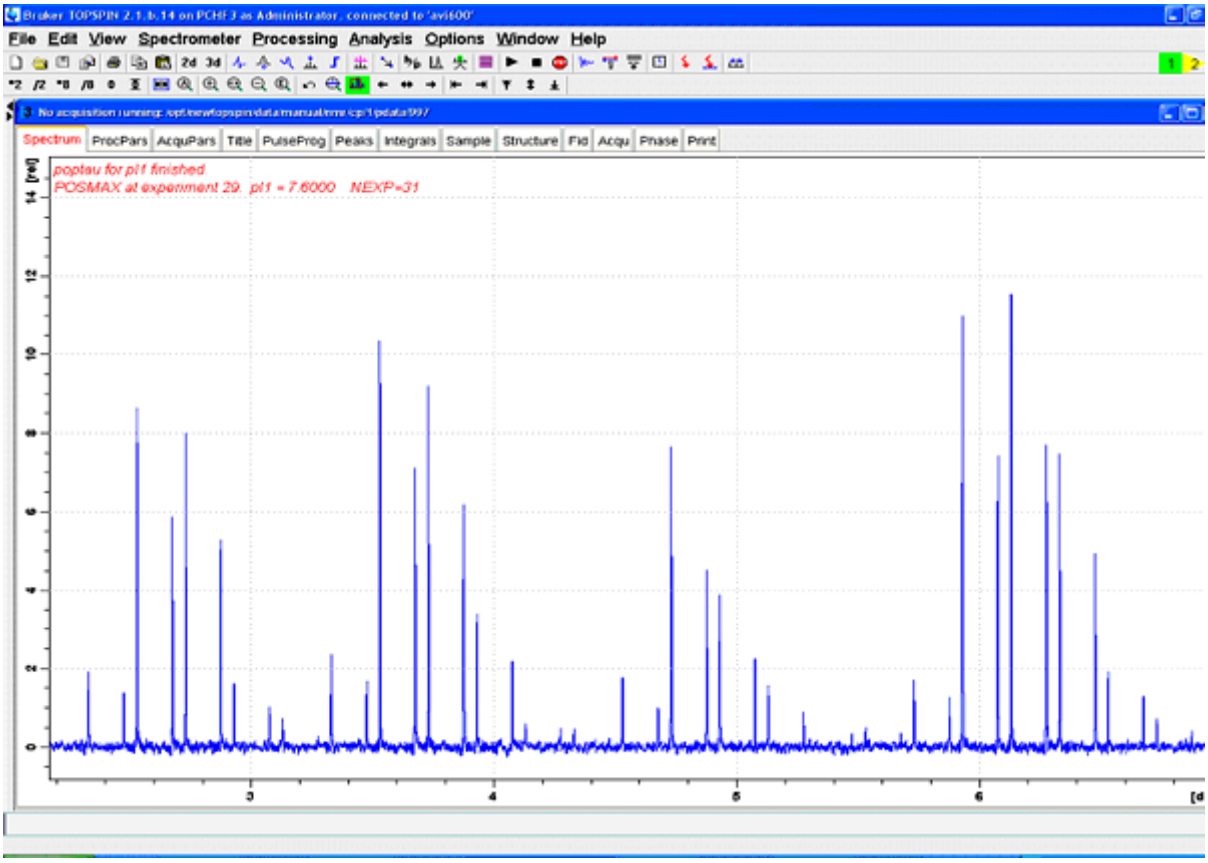

Figure 4.22. Hartmann-Hahn Optimization Profile Using a Square Proton Contact Pulse

The sideband order 0 at 4.8 dB gives a rather small intensity. A ramp sweeping over 3.5-6.5 dB would cover both most efficient HH conditions. Note that increasing the spin rate would shift all maxima except the one at 4.8 dB further out.

Cross Polarization Setup and Optimization for a Real Solid: Glycine 4.7

Adamantane is highly mobile even in the solid state. Therefore it behaves differently from a “hard” solid like glycine. For instance, it is not sensitive to decoupling mis-adjustments, and also not sensitive to miss-sets of the magic angle. It is however extremely sensitive to HH misadjustment. Glycine is therefore used for fine tuning of the decoupling parameters and signal-to-noise assessment. Start with the parameters found for adamantane, using a 50-100% ramp (ramp.100) and ***p15***=2 msec for contact, ***aq*** = 20 msec. Change the sample from adamantane to glycine.

Since glycine may exist in two different crystal modifications with very different CP-parameters, and since packing of the spinner determines crucially the achievable S/N value, it is useful to prepare a reference spinner with pure α-glycine, finely powdered and densely packed. α-glycine is prepared by dissolution of glycine in distilled water and precipitation with acetone, quick filtering and careful drying in a desiccator. Drying is important because wet glycine may readily transform, especially when kept warm, into γ-glycine. α-glycine has two carbons with shifts of 176.03 and 43.5 ppm. γ-glycine shows resonances somewhat shifted to higher field, sharper lines, longer proton T_1 and shorter proton $T_{1\rho}$ which results in longer experiment time and less signal to noise.

Spin the glycine sample at 5 kHz (7mm spinner), or 10 kHz (smaller spinners 4, 3.2 or 2.5), tune and match the probe.

The glycine cp/mas 13C-spectrum taken under the same conditions as adamantane previously will look like in ***Figure 4.23.***, far from optimum:

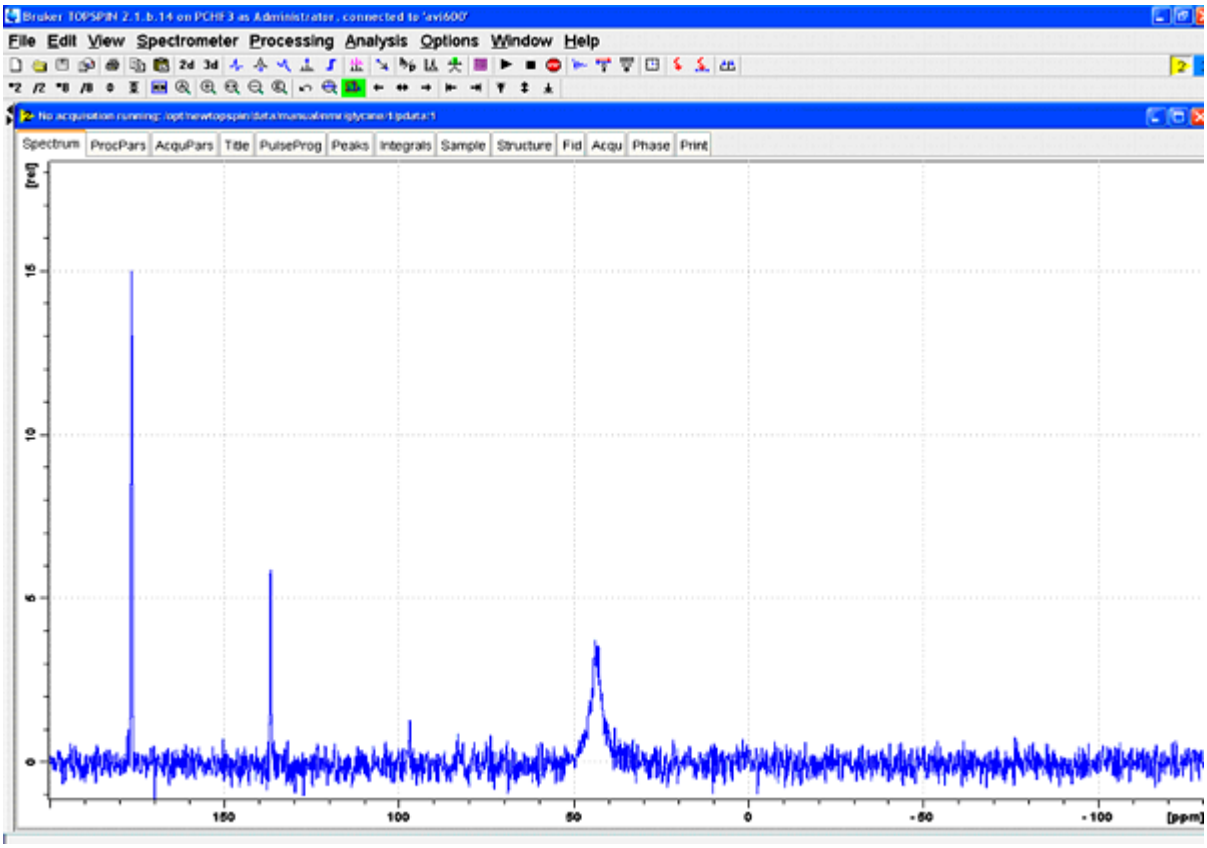

Figure 4.23. Display Showing α-Glycine Taken Under Adamantane Conditions, 4 scans

The figure above shows α-glycine taken under adamantane conditions, 4 scans: Incorrect carrier setting, α-carbon at 43 ppm insufficiently decoupled. Angle is set correctly, because carboxyl peak at 176.03 ppm shows a narrow lorentzian line shape. HH condition looks okay.

Now reset the carrier as shown in ***Figure 4.13.***. ***o1p*** should be around 100 ppm, in the middle of most carbon spectra. Acquire a spectrum, set the plot limits (***Figure 4.14.***, ***Figure 4.15.***) for the peak at 43 ppm, and start ***popt***, optimizing ***o2*** for maximum signal (+/- 2000 Hz around the current position) in steps of 500 Hz. The following result will be obtained:

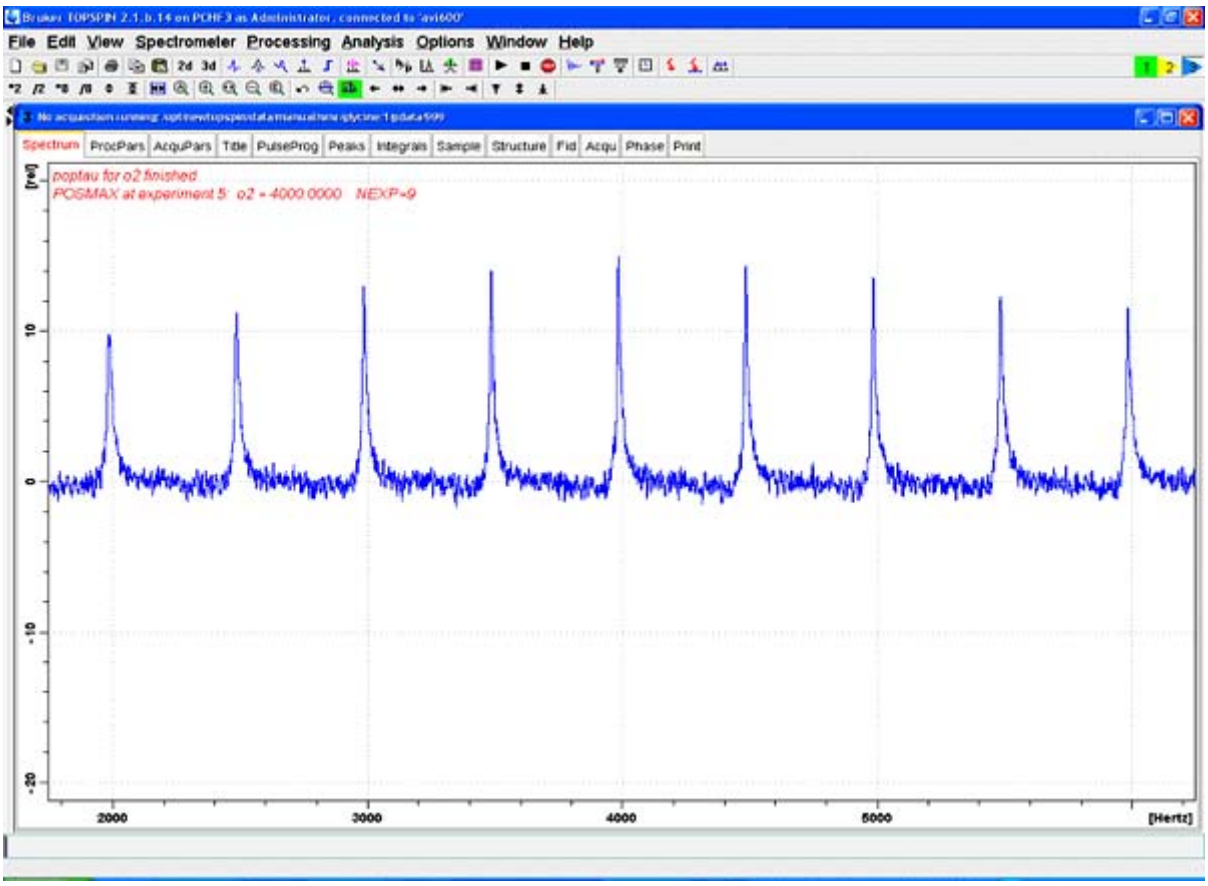

*Figure 4.24. Optimization of the Decoupler Offset **o2** at Moderate Power, Using cw Decoupling*

Since the proton spectrum of glycine extends around 5 ppm, the optimum decoupler offset will be obtained at higher frequency than the adamantane proton peak (around 1.2 ppm). Decoupling is still inefficient, since cw decoupling is used which does not cover the whole proton shift range. Also decoupling power is too low with a proton pulse of 4.5 µsec. Glycine requires about 90 kHz of decoupling RF, corresponding to a 2.7 µsec proton 90 degree pulse. This can be obtained with probes of 4mm spinner diameter and smaller (2.5, 3.2 mm). For a 7 mm probe, 3.5 (4µsec) can be expected at proton frequencies below 500 (at 500) MHz. Use ***calcpowlev*** to calculate the required power level ***pl12*** and set ***p3*** to twice the expected proton pulse width. Check with 4 scans whether a close to zero signal is obtained. Compared to 4.5 µsec, a 2.7 µsec pulse requires about 4.5 dB more power (corresponding to almost 4 times more power!!!).

With ***p3*** properly set, a spectrum like in ***Figure 4.25.*** should be obtained, with about 93 kHz decoupling RF field.

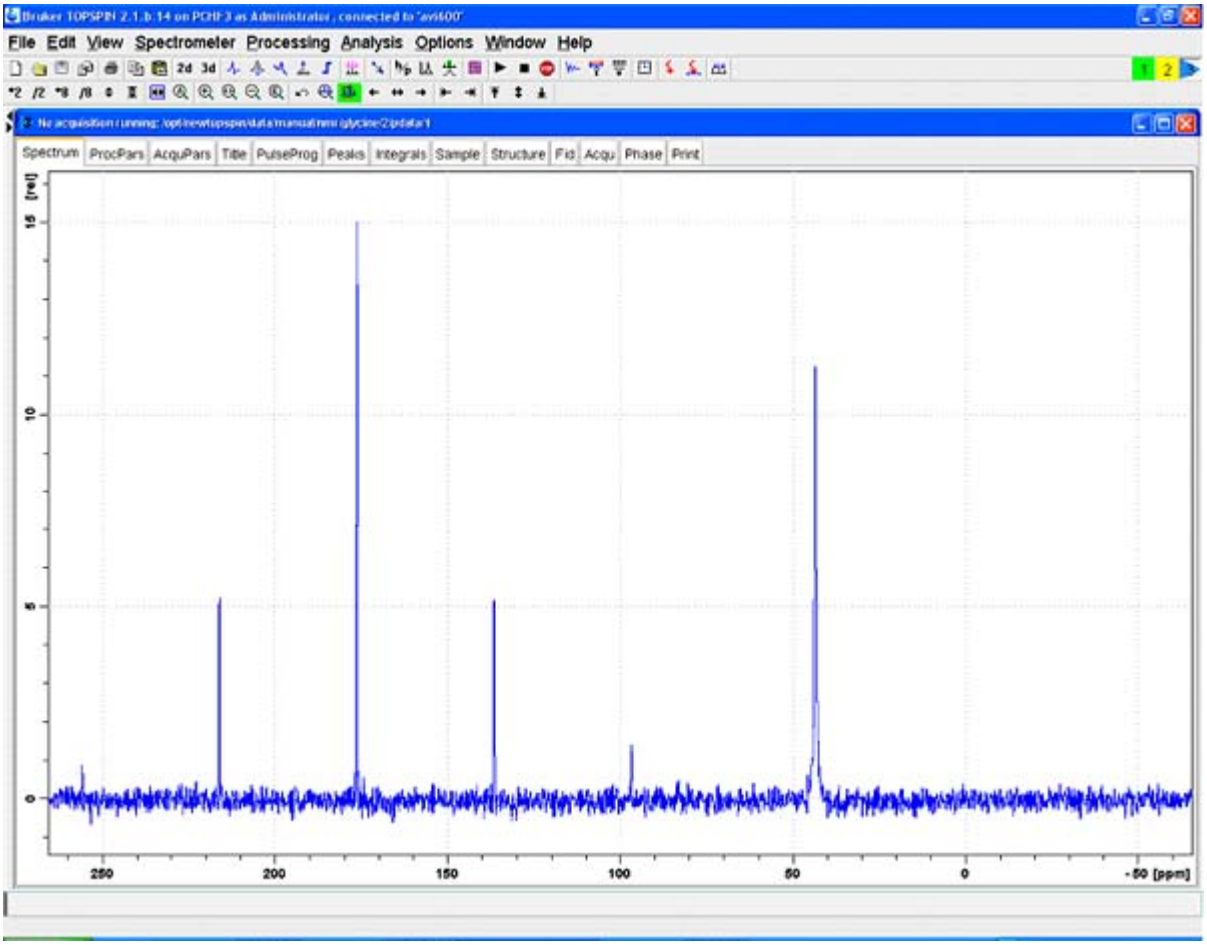

Figure 4.25. Glycine with cw Decoupling at 90 kHz RF Field

In the spectrum above, a lorentzian deconvolution (**Analysis** menu) shows a line width of 71 Hz for the peak at 43 ppm. The line width achievable under optimum decoupling conditions varies with the magnetic field. At fields below 9.4 Tesla (400 MHz) this line is substantially broadened by second order quadrupolar interaction to ^{14}N. At fields above 9.4 Tesla (500 MHz and higher), the residual line width is mostly determined by chemical shift dispersion and insufficient decoupling. Here less than 60 Hz (at 600 MHz) are expected. More efficient decoupling schemes must be applied especially at higher magnetic fields. A more efficient decoupling scheme is spinal64. Select ***cpdprg2*** = spinal64, set ***pcpd2*** to proton 180 degree pulse – 0.2 µsec for a start. A glycine spectrum as shown in ***Figure 4.26.*** is obtained.

Table 4.1. Summary of Acquisition Parameters for Glycine S/N Test

Parameter	Value	Comments
PULPROG	cp	cp.av for AV1 and 2
NUC1	13C	Nucleus on f1 channel
O1P	100 ppm	^{13}C offset
NUC2	1H	Nucleus on f2 channel.
D1	4 s	Recycle delay.
NS	4	Number of scans.
SWP	300 ppm	Spectral width for Glycine.
TD	2048	Number of acquired complex points.
CPDPRG2	SPINAL64	Decoupling scheme f2 channel (^{1}H).
SPNAM0	ramp.100 or ramp 70100.100	For ramped CP.
P15	2 ms	Contact pulse (f1 and f2 channel).
PL1		Set for 4-4.5 µsec P90.
SP0 (or pl2 AV1+2)		Set for 4-4.5 µsec P90 – 2 dB (optimize).
PL12		High power level f2 channel (^{1}H) excitation and decoupling.
P3		90^{o} ^{1}H pulse at PL12 (f2 channel).
PCPD2 or P31 (AV1+2)		SPINAL64 decoupling pulse.
O2P	2.5 - 3 ppm	^{1}H offset - optimize in 400 - 500 Hz steps for maximum signal of aliphatic peak.

Note that the spectral window (***swp***) is set in ppm which makes the acquisition time dependant on the B_0-field at a given ***td*** of 2k. This is intended and accounts for the linewidths dependence on the B_0-field. The glycine lines show a broadening proportional to B_0 due to chemical shift dispersion. To make S/N values more comparable, this accounts for shorter T_2 at higher field.

Table 4.2. Processing Parameters for the Glycine S/N-Test

Parameter	Value	Comment
SI	2-4 k	Twofold or fourfold zero filling.
WDW	No	No apodization used for S/N measurement In this case.
PH_mod	Pk	Phase correction if needed.
BC_mod	Quad	DC offset correction on FID.
FT_mod	Fqc	

Note: No line broadening is applied since the acquisition time is set appropriately.

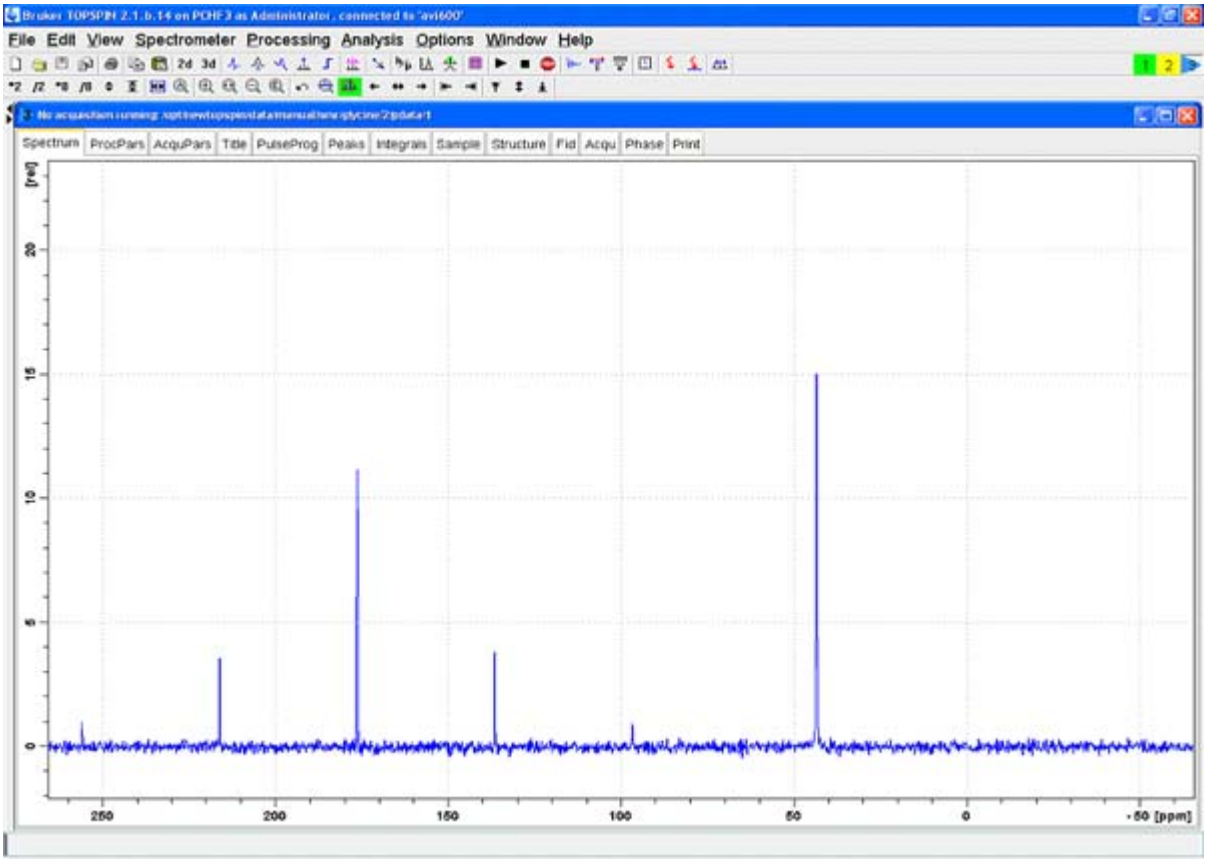

Figure 4.26. Glycine Spectrum with Spinal64 Decoupling at 93 kHz RF field

Here, the line width of the line at 43 ppm is fitted to be about 50 Hz: Correspondingly, the intensity is much higher. The ***sinocal*** routine calculates 80:1 S/N, using 250 to -50 ppm spectrum range, 50 to 40 signal range and 10 ppm noise range. On this triple probe, more than 100:1 is expected. What else needs to be optimized? Two more parameters are essential:

1. The power level at HH contact
2. The decoupling pulse ***pcpd2***.

The spectrum of ***Figure 4.26.*** was taken at contact power levels as set for adamantane. Furthermore, a 50% ramp was used, which has a rather low average RF level corresponding to about 5.7µsec in this case (25% less than 4.5 µsec). This does not spin lock the protons well enough. So the power level of the contact needs to be increased. Set ***spnam0*** = ramp70100.100. Set ***sp0*** and ***pl1*** to about 2 dB less attenuation and check S/N again. Re-optimize the HH condition observing the peak at 176 ppm (which is less strongly coupled to protons and therefore exhibits a sharper HH matching condition) in steps of 0.3 dB. In this case, S/N improves to 100:1. Then optimize the decoupling pulse pcpd2 in steps of 0.2 µsec, observing the peak at 43 ppm (which is more sensitive to decoupling mis-sets). Here, this led to another 10% improvement in S/N.

Good Laboratory Practice requires that evaluation measurements be taken in suitable periods. Store the optimized glycine spectrum together with the following important information:

1. Value of field setting.
2. Name of the shim file.
3. Name of the operator.
4. Probe setup (triple mode or double mode, high range or low range setting, WB probes only, name or part number of the probe).
5. Description of the sample (which reference rotor, weight of glycine and spinner).
6. Any additional comments, for instance the reading of the micrometer setting for the X tuning adjustment (not available on all probes).

Write this information into the title file so it is stored with the data set as well as all other acquisition and processing parameters. Recalling this data set and acquiring a new data set should give the same spectrum within +/- 10% of S/N.

Some Practical Hints for CPMAS Spectroscopy *4.8*

Some general recommendations for reasonable RF-fields used in WB probes:

Table 4.3. Reasonable RF-fields for Max. 2% Duty Cycle

Probe	Nucleus	Decoupling power over 50 ms, 200ms, 500ms. Contact pulse up to 10 ms
2.5mm CPMAS double resonance 35 kHz max sample rotation	^{1}H	115 kHz (2.2µs 90º pulse), 75 kHz, 40 kHz 71 kHz (3.5 µs) contact
2.5mm CPMAS double resonance 35 kHz max sample rotation	^{13}C	83 kHz (3 µs 90º pulse) 71 kHz (3.5 µs)
3.2mm CPMAS double resonance 24 kHz max sample rotation	^{1}H	110 kHz (2.3 µs), 60 kHz, 35 kHz 68 kHz (3.7 µs)
3.2mm CPMAS double resonance 24 kHz max sample rotation	^{13}C	78 kHz (3.2 µs) 68 kHz (3.7 µs)
4 mm CPMAS double resonance probe (15 kHz max. sample rotation)	^{1}H	92.5 kHz (2.7us 90º), 50 kHz, 30 kHz 62 kHz (4 µs)
4 mm CPMAS double resonance probe (15 kHz max. sample rotation)	^{13}C	71 kHz (3.5 µs) 62 kHz (4 µs)
4 mm CPMAS triple resonance probe (15 kHz max. sample rotation)	^{13}C	66 kHz (3.8 µs) 50 kHz (5 µs)
7mm CPMAS double resonance probe (7 kHz sample rotation)	^{1}H	70 kHz (3.6 µs 90º pulse), 35 kHz, 20 kHz 50 kHz (5 µs)
7mm CPMAS double resonance probe (7 kHz sample rotation)	^{13}C	55 kHz (4.5 µs) 50 kHz (5 µs)

Note: Higher RF power levels should only be applied if necessary and within specifications. For special probes, max. allowed RF fields may be lower. Check with your Bruker BioSpin applications support if in doubt.

In order to have quantitative information about the precision of your magic angle, one may measure the line width of the KBr central peak and compare it with the line width of the 5th spinning sideband. If the linewidths compare within ± 8% then the MA-setting is acceptable. The line-width comparison is conveniently achieved with the command ***peakw***, expanding the display first around the center line, typing ***peakw*** and then repeating this with the 5th sideband to either side.

Most cp/mas probes are tunable over a large range of X-frequencies. It can sometimes be fairly difficult to retune a probe to an arbitrary frequency within the tuning range. NEVER just load a nucleus and blindly tune and match the probe, using a small wobble width (***wbsw***) of 10 MHz or less. Instead, either note the current tuning position of the probe into the lab notebook and start retuning to the new nucleus frequency from this frequency on, following the probe response over the whole frequency range using a large ***wbsw*** of 50 MHz. Alternately, check the micrometer setting of the X-tuning adjustment and conclude from that to which nucleus the probe is tuned. Make a list of micrometer settings for the most frequently measured nuclei.

Remember which way to turn the tuning knob to tune to higher and lower frequencies. On most probes, turning the adjustment counter clockwise tunes to higher frequency. Do not change the matching adjustment until you have found the current tuning position of the probe, else you may loose the probe response totally. Do not tune without having the appropriate matching box fitted to the preamp. Fake resonances may appear due to filters between probe and preamp, because filters are also tuned circuits. Remove all filters before tuning over a wide range, and fine tune again (***wbsw*** ≤ 10 MHz) when the probe is tuned close to the desired frequency.

Changing the proton tuning will affect the X-tuning, so always tune the proton channel first, then the X-channel.

Setting a probe from high range to low range mode (lambda/4 switch) will shift the X-tuning to lower frequency by many MHz, the proton frequency will only change by a few MHz.

An empty probe may tune as much as 10 MHz higher on the proton channel compared to a probe with a spinner in.

When a probe has not been used over an extended period, humidity may collect inside the turbine, causing a few harmless arcs (RF-breakthrough) on the proton channel. If the arcing does persist and/or gets worse, have the probe checked. Usually this means that dirt has accumulated inside the turbine or on the RF-coil. Cleaning should be done by a trained person only.

Regular probe performance checks comprise:

- Checking the magic angle setting (KBr)
- Checking the shims (Adamantane)
- Checking S/N performance on glycine

These checks must also be performed after a probe repair. Since a repair may result in a more efficient power conversion, start with slightly reduced power settings.

SB probes flip the stator vertical for sample eject. These probes require some more effort to assure a correct angle setting.

Remember to always approach the magic angle setting from the same side!

To check the reproducibility of the magic angle setting, take a KBr spectrum, stop spinning, eject and reinsert the sample, take another spectrum into a new data set, compare in dual display mode.

If the second spectrum is worse, dial less than 1/8th of a turn **counterclockwise**.

Take another spectrum, compare again.

A laboratory notebook should be kept with the following entries (a suitable form for printout is supplied in the ***"Appendix"***):

- Name of the shim file and field value for every probe.
- Value of power level in dB and power in watt (if available) for proton decoupling (***pl12, pl12W***) and associated pulse lengths ***p3***, **pcpd2**.
- Value of proton contact power level in dB and watt (***sp0, sp0W***).
- Value of carbon contact power level (***pl1, pl1W***) and associated pulse length ***p1***.
- S/N value obtained on glycine, ***SR*** value for shift calibration, line width on α-carbon in Hz.

Note: It is essential that, if spectra taken at different times and/or taken with different probes need to be compared, the shift calibration is executed correctly. If the magnetic field was not the same, the spectra will have different values of Spectrum Reference (*sr*).

To reduce the requirement of readjustment and to make referencing more reliable, the field should be set to be the same for all spectra.

To keep the field the same, 2 parameters must be taken into account:

1. The drift of the magnetic field

2. The difference in shims and field between different probes.

The drift of the magnet should be measured in the following way:

Insert a sample of D_2O and run a proton spectrum just like it was done on adamantane in ***"Calibrating 1H Pulses on Adamantane" on page 65***.

Without changing any parameter, rerun the spectrum every 10 minutes for a full day. This can be done with *popt,* storing the data as a 2D experiment, or use the pulse program zg in a 2D data set, with appropriate settings for *d1* and *td1* so that the drift of the magnet can be followed by the changes in peak positions of the D_2O protons. The pattern of changes in the peak position will reveal whether the changes are solely due to magnet drift, or whether there are additional disturbances to the magnet field. A magnet drift will always be constant towards lower frequency (note.: A freshly charged magnet may also drift to higher frequency, but this will change, so it makes no sense to account for this initial drift). A nonlinear drift pattern indicates temperature changes, abrupt changes reveal magnetic disturbances (elevator, cars or trucks trains, or the keys in your pocket- only if your magnet is not shielded).

From these data, filter out the linear magnet drift. Determine the number of digits the field value in the *bsmsdisp* menu must be changed to set the field back to the exact same value as in the first spectrum. Recalculate this number to a drift time of exactly 1h/24h. Note these values as your magnet drift rate.

This drift rate will only reach a stable and constant value some time after charging, so the drift rate measurement should be repeated until the drift value is constant. This may take some weeks to months (for high field magnets).

The magnet drift value will allow to calculate the time dependant component of the field. The probe dependant component can be established by shimming every probe and setting the field on the same sample, following the same procedure for every probe after shimming. When then the shim file is written, the current (calibrated) field position is written to disk with the shim file.

Executing the AU program (or command, TopSpin version 3.0 and later) *probe field* will now set the field to the appropriate value according to drift and time (taken from the date of the shim file, so the computer clock should be correct) and probe shims (from the current probe setting, so the appropriate probe must be selected in *edhead*). However: this will only work if all shim files contain the precisely determined field value for the same reference compound.

Literature *4.10*

Shift referencing:

1. R.K Harris, E.D. Becker, S.M. Cabral de Menezes, R. Goodfellow, and P. Granger, *NMR Nomenclature. Nuclear Spin Properties and conventions for Chemical shifts*, Pure Appl. Chem. Vol. 73, 1795-1818 (2001)).
2. W.L. Earl, and D.L. VanderHart, *Measurement of ^{13}C Chemical Shifts in Solids,* J. Magn. Res. 48, 35-54 (1982).
3. C.R. Morcombe, and K.W. Zilm, J. Magn. Reson. 162 p479-486 (2003)
4. IUPAC recommendation (Harris et al.):
5. http://sunsite.informatik.rwth-aachen.de/iupac/reports/provisional/abstract01/harris_310801.html

Cross polarization:

1. D. Michel, and F. Engelke, *Cross-Polarization, Relaxation Times and Spin-Diffusion in Rotating Solids,* NMR Basic Principles and Progress 32, 71-125 (1994).
2. G. Metz, X. Wu, and S.O. Smith, *Ramped amplitude Cross Polarization in Magic-Angle-Spinning NMR*, J. Magn. Reson. A 110, 219-227 (1994).
3. B.H. Meier, *Cross Polarization under fast magic angle spinning: thermodynamical considerations*, Chem. Phys. Lett. 188, 201-207 (1992).
4. K. Schmidt-Rohr, and H.W. Spiess, Multidimensional Solid-State NMR and Polymers, Academic Press (1994).
5. S.Hediger, B.H. Meier, R.R. Ernst, *Adiabatic passage Hartmann-Hahn cross polarization in NMR under magic angle sample spinning*, Chem. Phys.Lett 240, 449-456 (1995).

Decoupling Techniques

5

Line shapes in solids are often broadened by dipolar couplings between the spins. If the coupled spins are of the same kind, it is called homonuclear dipolar coupling. heteronuclear dipolar couplings exist between nuclei of different kind. While most dipolar couplings between X-range nuclei can be removed by magic angle spinning, couplings between ^{1}H, ^{19}F and X nuclei cannot easily and efficiently be removed by spinning. Decoupling of homonuclear and heteronuclear interactions can be obtained by different forms of rf-irradiation with or without sample spinning. It is possible to suppress homonuclear couplings without suppressing heteronuclear couplings. Most frequently, the nucleus ^{1}H must be decoupled when X-nuclei like ^{13}C or ^{15}N are observed, since it is abundant and broadens the line shapes of coupled X-nuclei strongly.

Heteronuclear Decoupling 5.1

CW Decoupling 5.1.1

CW decoupling simply means irradiating the decoupled spins (usually protons) with RF of constant amplitude and phase. The decoupling program is called cw or cw13 and it uses ***pl12*** or ***pl13***, respectively. The decoupling programs select the power level and ***pl12*** does not need to be specified in the pulse program, if it is not used elsewhere. In the decoupling program there is also a statement setting the RF carrier frequency, according to the parameter ***cnst21***, which is zero (on resonance) by default. In order to optimize decoupling, one uses the highest permitted rf-field (e.g. 100 kHz for 4mm probes) and optimizes the carrier frequency ***o2*** or ***o2p*** using ***popt***.

The cw –decoupling program is written as follows:

```
0.5µ pl=pl12 ; reset power level to default decoupling power level
1 100up:0 fq=cnst21; reset decoupling carrier frequency to o2+cnst21
jump to 1  ; repeat until decoupler is switched off by do in the
           ; main ppg
```

CW decoupling suffers from the fact that protons have different chemical shifts, so irradiating at a single frequency does not decouple all protons evenly. At higher magnetic fields this becomes more evident, since the separation due to the magnetic field increases. CW decoupling requires fairly high decoupling power to be efficient.

TPPM Decoupling *5.1.2*

TPPM decoupling surpasses the traditional cw decoupling. The decoupling programs tppm15 and tppm20 use a 15 and 20 degree phase shift between the two pulses, respectively. Both operate at power level ***pl12***. The cpd program tppm13 uses 15 degree phase shift, as tppm15, but operates at power level ***pl13***.

In order to optimize the decoupling one optimizes ***pcpd2*** (AV3, or p31, AV1+2) with ***popt*** and the carrier frequency, by varying ***o2*** or ***o2p***. Strongly proton coupled ^{13}C-resonances narrow substantially, especially at high magnetic fields (>300 MHz).

The figure below shows an arrayed optimization using ***popt*** for the TPPM phase tilt and ***pcpd2*** (available in TS2.0 and higher).

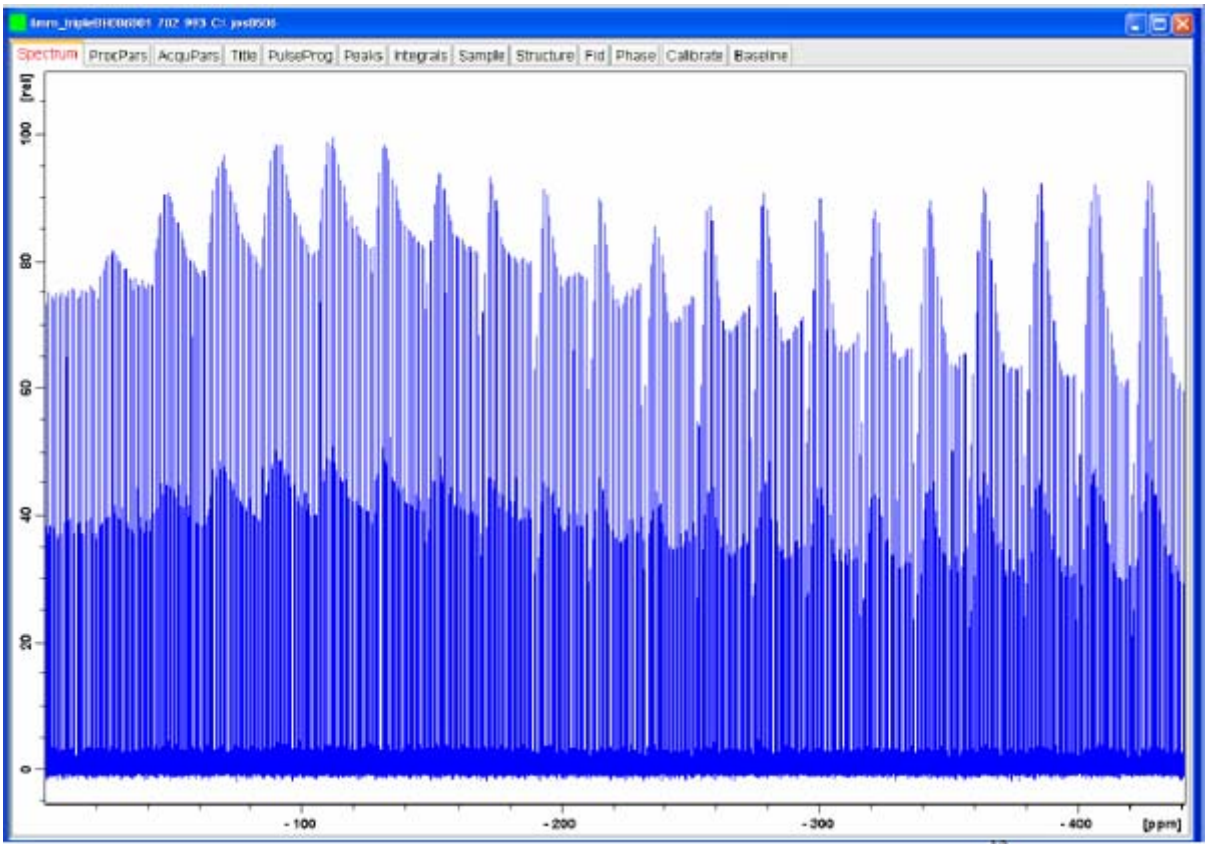

Figure 5.1. Optimization of TPPM Decoupling, on Glycine at Natural Abundance

The figure above shows optimization of TPPM decoupling, on glycine at natural abundance, ^{13}C CPMAS at 5 kHz spin rate. Each block represents a 2° degree increment of the phase toggle and the variation in each block stems from incrementation of the pulse width in 0.2 µs increments. Optimum decoupling was found with a 4.5 µs pulse at a 16° phase toggle. It is obvious that more than one near optimum combinations of phase toggle and pulse length exist.

Reference:

1. A.E. Bennett, C.M. Rienstra, M. Auger, K.V. Lakshmi, and R.G. Griffin; *Heteronuclear decoupling in rotating solids*, J. Chem. Phys. 103 (16); 6951 – 6958 (1995).

SPINAL Decoupling 5.1.3

SPINAL provides adequate decoupling bandwidth even for high field (>400 MHz) instruments at an RF-level of 80 kHz or higher. SPINAL-64 (64 phase permutations) outperforms TPPM and may be used as standard decoupling sequence. SPINAL-64 can be optimized in the same way as TPPM, by incrementing pcpd2 (p31) (the phase shifts are fixed). The decoupling pulse is an approximate 180° pulse.

Reference:

1. B.M. Fung, A.K. Khitrin, K. Ermolaev, J. Magn. Reson. 142, 97-101 (2000).

Swept-Frequency-TPPM 5.1.4

This decoupling method combines TPPM and a frequency variation via. pulse length variation to achieve a wider decoupling bandwidth. The decoupling efficiency is better than TPPM (especially at high fields), and comparable to if not better than SPINAL-64. The corresponding cpd-program is called ***swftppm***.

Reference:

1. R.S. Thakur, N. D. Kurur, and P. K. Madhu, J. Magn. Res. 193, 77 (2008).

XiX Decoupling 5.1.5

XiX decoupling requires high spinning speeds, but decouples at a moderate RF level. 180° proton pulses are used, synchronized to the rotor speed such that recoupling does not occur (***pcpd2***≠n/4*rotor periods). Usually, ***pcpd2*** is selected to be about 1/3 rotor period. The decoupler power level must be adjusted to produce a 180° pulse of (rotor period)/3.

Reference:

1. A. Detken, E. H. Hardy, M. Ernst, and B. H. Meier, Chem. Phys. Lett. 356, 298-304 (2002).

Pi-Pulse Decoupling 5.1.6

Pi–pulse decoupling is a decoupling program, for weaker nuclear interactions like J couplings or weak dipolar interactions, using rotor synchronized 180° pulses. π-pulse decoupling uses the xy-16 phase cycle for large bandwidth. Abundant protons cannot be sufficiently decoupled with this method, but it is very suitable to remove couplings to ^{31}P, which is hard to do by cw or tppm, since the chemical shift range is wide. Likewise, it can be used to decouple dilute spins or spins which are homonuclear decoupled by spinning (^{19}F).

Reference:

1. S.-F. Liu and K. Schmidt-Rohr, Macromolecules 34, 8416-8418 (2001).

Homonuclear Decoupling 5.2

Homonuclear decoupling refers to methods which decouple dipolar interactions between like spins. Those are only prominent between abundant spins like ^{1}H, ^{19}F and ^{31}P (and potentially some others). This interaction cannot easily be spun out in most cases and renders NMR-parameters like chemical shifts of the homonuclear coupled spins or heteronuclear couplings and J-couplings to other (X-)nuclei unobservable.

Multiple Pulse NMR: Observing Chemical Shifts of Homonuclear Coupled Nuclei 5.2.1

Multiple pulse NMR methods are covered in the chapters about CRAMPS of this manual collection. The principle of those methods (CRAMPS, if MAS is used to average CSA interactions simultaneously), is to set the magnetization of the spins into the magic angle, using a suitable pulse sequence. In this case, the dipolar couplings between those spins are suppressed. Short observation windows between pulses allow observation of the signal from the decoupled nuclei.

Reference:

1. S. Hafner and H.W. Spiess, *Multiple-Pulse Line Narrowing under Fast Magic-Angle Spinning,* J. Magn. Reson. A 121, 160-166 (1996) and references therein.

Multiple Pulse Decoupling 5.2.2

Multiple Pulse Decoupling: Observing dipolar couplings and j-couplings to homonuclear coupled nuclei.

Homonuclear couplings between abundant spins (usually protons) superimpose their heteronuclear dipolar couplings to X-spins and J-couplings to X-spins so these (distinct) couplings are not observable. homonuclear decoupling protons while observing X-spins makes these couplings observable. Any method used in multiple pulse NMR (section ***5.2.1***) may be used to achieve this.

BR-24, MREV-8, BLEW-12

Used as heteronuclear decoupling methods, the window between pulses may be shortened or omitted (semi-windowless or windowless sequences). These sequences work well, but have rather long cycle times and are therefore not suitable for fast spinning samples. Else they work in a similar fashion as the sequences covered in the following. BLEW-12 decoupling is supplied as a standard cpd-program. It consists of a windowless sequence of 90° pulses with suitable phases. High RF levels for decoupling provide better resolution.

FSLG Decoupling

The Frequency Switched Lee Goldburg (FSLG) sequence may be used at spin rates up to 15 kHz. It is a homonuclear decoupling sequence which rotates the interaction Hamiltonian around an effective field, aligned at the magic angle (arctan $\sqrt{2}$) with respect to the Zeeman field in the rotating frame. The tilt is achieved by off resonance irradiation at the Lee Goldburg frequency f_{LG} according to the Lee Goldburg condition.

The off-resonance condition depends on the RF-field of irradiation, not very sensitively however. The irradiation frequency jumps between +/- (RF-field)/sqrt(2) for the duration of two 360°pulses on resonance (=293° pulses at the LG-frequency) with a 0/180° phase alternation. The include file <lgcalc.incl> calculates all values according to the RF-field (set in Hz as cnst20) within the pulse program.

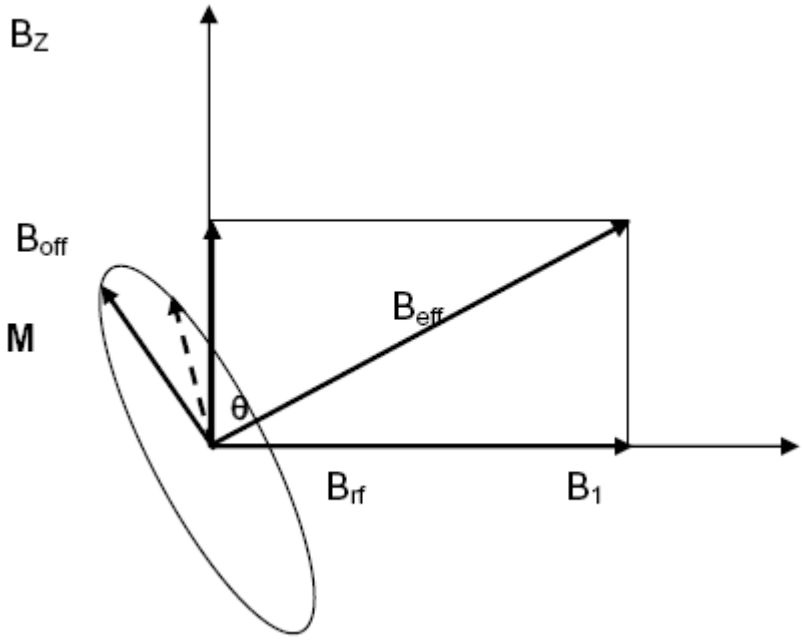

Figure 5.2. Geometry for the FSLG Condition

Note that B_{eff} points along the 1 1 1 direction in the 3 dimensional space (see Reference 2). Note the sign of B_{off} when calculating the actual direction of the effective field. A positive B_{off} and a B_1 with phase 0 results in the effective field being in the positive quadrant along the magic angle in the X-Z plane of the rotating frame.

Two methods are available to achieve such a frequency switch experimentally. One method is simultaneous switching of frequencies and phases. The other method uses phase-modulation. Frequency, time and phase relate to each other as derivative of phase and time as to get 2π = .../. The relationship describes the rate at which a phase of the rf-pulse must be changed in order to achieve a certain frequency offset. Vinogradov et al. describe this approach under the acronym PMLG (Phase Modulated Lee Goldburg).

Used in combination with cp signal generation, both methods allow observing proton-J-couplings to the observed X-nucleus. However, only samples with very narrow lines will produce well resolved J-couplings as shown below on adamantane. Harder solids require careful adjustment and fairly high power levels to show barely resolved couplings, since the linewidths achieved are broader than what can be achieved with standard decoupling sequences like tppm. Since the heteronuclear X-H-coupling remains, there may be spinning sidebands from this coupling, in addition to CSA sidebands.

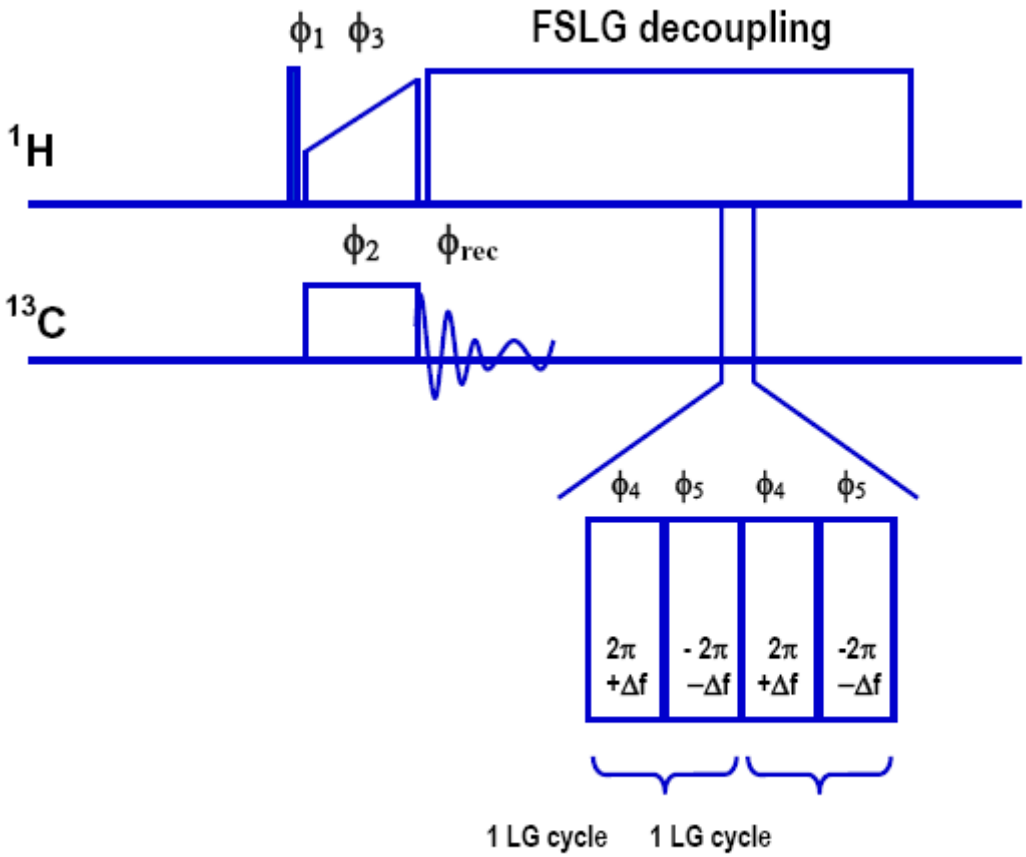

ϕ1=1 3	ϕ2 = 0 0 2 2 1 1 3 3
ϕ3=0	ϕrec= 0 2 2 0 1 3 3 1
ϕ4= 0	ϕ5= 2

Figure 5.3. FSLG Decoupling Pulse Sequence Diagram

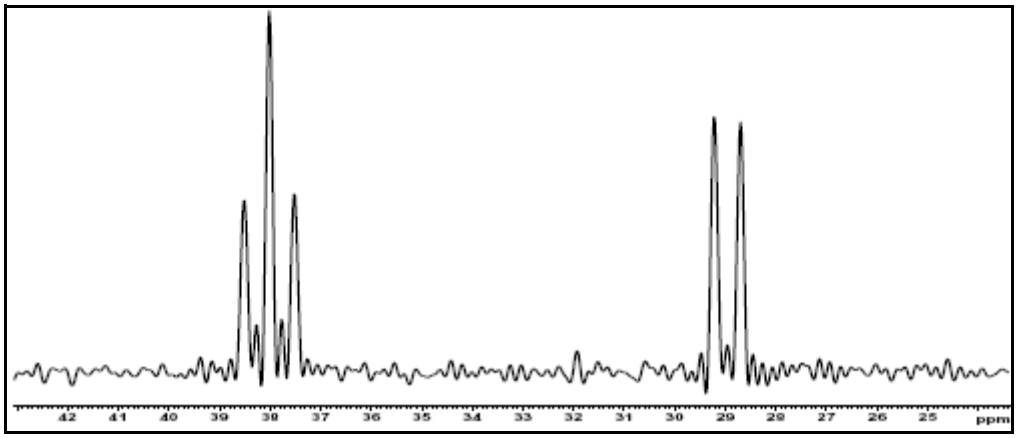

Figure 5.4. Adamantane, FSLG-decoupled, showing the (downscaled) C-H J-couplings.

The figure above shows homonuclear proton decoupling on center packed adamantane sample rotating at 7 kHz, 100 kHz ^{1}H decoupling field. Note that good B_1-homogeneity is required. Use a CRAMPS spinner (12 µl sample volume in a 4mm spinner).

Setting up the experiment:

1. Use center packed adamantane in a CRAMPS rotor, unlabeled and a spinning rate of 10 kHz for adamantane.
2. Start from a data set with well adjusted HH condition on adamantane.
3. Generate a new data set with ***edc***.
4. Readjust decoupling power ***pl12*** and ***p3***, ***pcpd2*** for 70-100 kHz RF field, determine the precise RF field (preferably via a 360° proton pulse ***p3***).
5. Load the pulse program ***fqlg***. This uses frequency shifts with simultaneous phase shifts for FSLG-decoupling at ***pl13***.
6. Set ***pl13*** to achieve the same RF-field as measured in step 4, set ***cnst20*** to the value of RF field in Hz. The pulse program contains the include file <lgcalc.incl> which calculates the required frequency shifts to either side (shown in ***ased*** as ***cnst22*** and ***cnst23***). ***Cnst24*** provides an additional overall offset to compensate for phase glitch. With proper probe tuning and 50Ω match, ***cnst24*** should be close to zero.
7. Set acquisition and processing parameters according to ***Table 5.1.*** and ***Table 5.2.***.

A spectrum like in **fig. 4** should be obtained. If the splitting is worse, optimize with ***pl13*** and ***cnst24***. Usually, somewhat less power than calculated is required.

The FSLG decoupling scheme is also implemented as cpd-program cwlgs. The include file lgcalc.incl is also required. With ***cpdprg2*** = cwlgs, the standard cp pulse program can be used. The **ZGOPTN –Dlacq** (***ased***) should be set in order to allow decoupling times >50 ms.

Table 5.1. Acquisition Parameters

Parameter	Value	Comments
pulprog	fqlg	AV3, use fqlg.av for AV1+2.
d1	4 s	Recycle delay.
ns	4-16	Number of scans.
aq	80 ms	Acquisition time.
spnam0	ramp.100 or, ramp70100.100	For ramped CP.
pl12, p3	set for p3=90°	
sp0, pl1	set for cp	
p15	5-10m	
pl13	set for 70-100 kHz	Optimize for best resolution.
cnst20	70000-100000	Equals the applied RF-field.

Table 5.1. Acquisition Parameters

cnst24	0	To be optimized.
cnst21	0	Reset proton frequency to SFO2.

Table 5.2. Processing Parameters

Parameter	Value	Comment
SI	2*td	Adequate 4fold zero filling.
WDW	no	No apodization.
PH_mod	pk	Phase correction if needed.
BC_mod	quad	DC offset correction.

As mentioned above, frequency shifts can also be generated by a phase gradient shape. A phase change of 360° per second corresponds to a frequency of 1 Hz, as can easily be visualized. The frequency shift which needs to be achieved is ±RF-field/$\sqrt{2}$. Since the pulse duration must achieve a 2π rotation off resonance, corresponding to a 293° flip angle on resonance, it can easily be calculated that a phase change over 209° during a 293° flip angle pulse is required to achieve this.

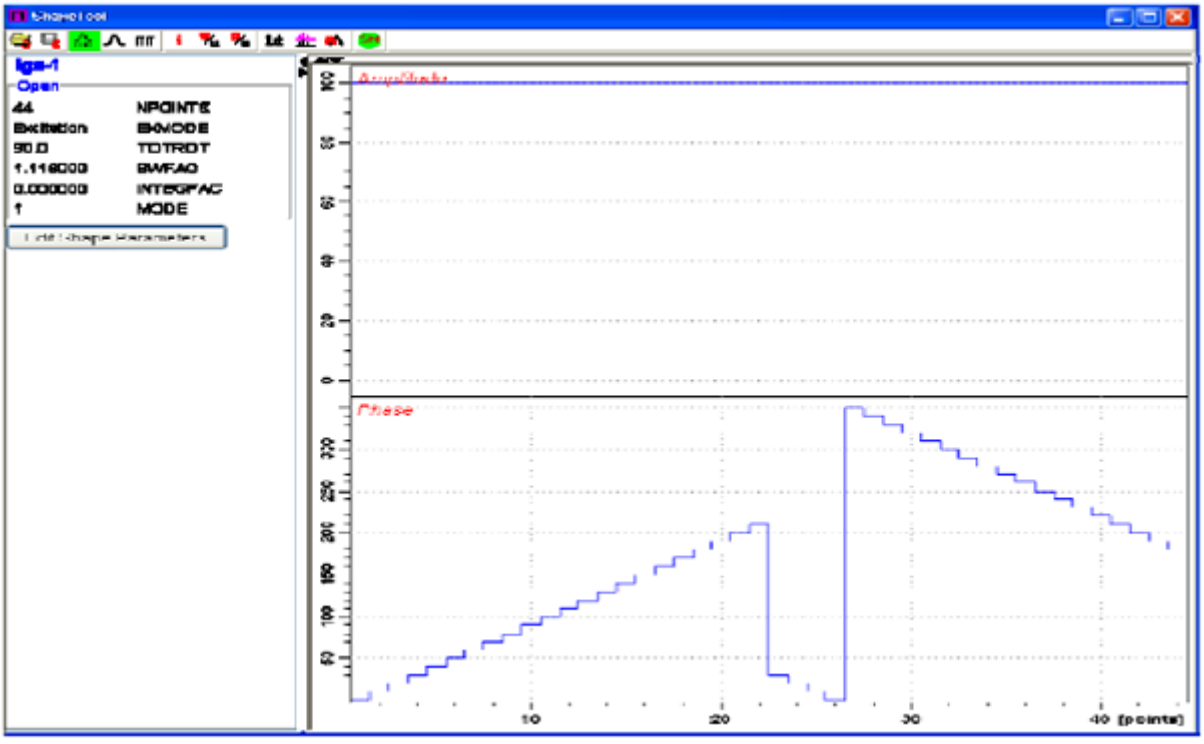

Figure 5.5. Shape with Phase Gradients

In the figure above: Shape with phase gradients for positive and negative offsets and corresponding phase change, ***stdisp*** –display of lgs-1 shape. Amplitude is 100% throughout.

Vinogradov et. al. have published shapes with much fewer steps and different phases. The pulse length for the shape does not depend on the number of steps, but only on the applied RF-field. Using the include file lgcalc.incl, a pulse *p5* is calculated from *cnst20*=RF-field in Hz. The total shape pulse length must be 2**p5*.

To use pmlg decoupling, save the pulse program fqlg under a different filename and change calculations and loop as follows:

define loop counter count; calculate number of LG periods according to aq

"count=aq/(2*p5)"

define pulse pmlg

"pmlg=2*p5"

"sp1=pl13" set shape power to pl13 for LG (TS2.1 only)

.

3 (pmlg:sp1 ph3): f2 for one full PMLG unit, as for lgs-1 shape

lo to 3 times count

References:

1. A. Bielecki, A.C. Kolbert, and M.H. Levitt, *Frequency-Switched Pulse Sequences: Homonuclear Decoupling and Dilute Spin NMR in Solids*, Chem. Phys. Lett. 155, 341-346 (1989).
2. A. Bielecki, A.C. Kolbert, H.J.M. deGroot, R.G. Griffin, and M.H. Levitt, *Frequency-Switched Lee-Goldburg Sequences in Solids*, Advances in Magnetic Resonance 14, 111-124 (1990).
3. E. Vinogradov, P.K. Madhu, and S. Vega, High-resolution proton solid-state NMR spectroscopy by phase modulated Lee-Goldburg experiments, Chem. Phys. Lett. 314, 443-450 (1999) and references cited therein.

DUMBO

DUMBO (Decoupling Uses Mind Boggling Optimization) is a phase modulation scheme where the phase modulation is described in terms of a Fourier series

$$\phi(t) = \sum_{n=0}^{+\infty} a_n \cos(n\omega_c t) + b_n \sin(n\omega_c t)$$

The shape can be created using the AU-program ***DUMBO***. The DUMBO shape file in the release version of TOPSPIN is calculated for 32 µs pulses. To create your own DUMBO shape you can also use the au-program ***dumbo.*** See instructions in the header of the au-program for proper use.

The above pulse program to observe J-couplings with DUMBO decoupling would be written as follows:

define loop counter count ;calculate number of LG periods according to aq

"count=aq/(p10)"

.

3 (p10:sp1 ph3):f2 ;p10 set by AU-program DUMBO (n*32 µsec)

lo to 3 times count

References:

1. D. Sakellariou, A. Lesage, P. Hodgkinson, and L. Emsley, *Homonuclear dipolar decoupling in solid-state NMR using continuous phase modulation, Chem. Phys. Lett. 319, 253-260 (2000).*
2. Lyndon Emsley's home page: http://www.ens-lyon.fr/STIM/NMR/NMR.html

Transverse Dephasing Optimized Spectroscopy 5.3

Decoupling optimized under refocused conditions:

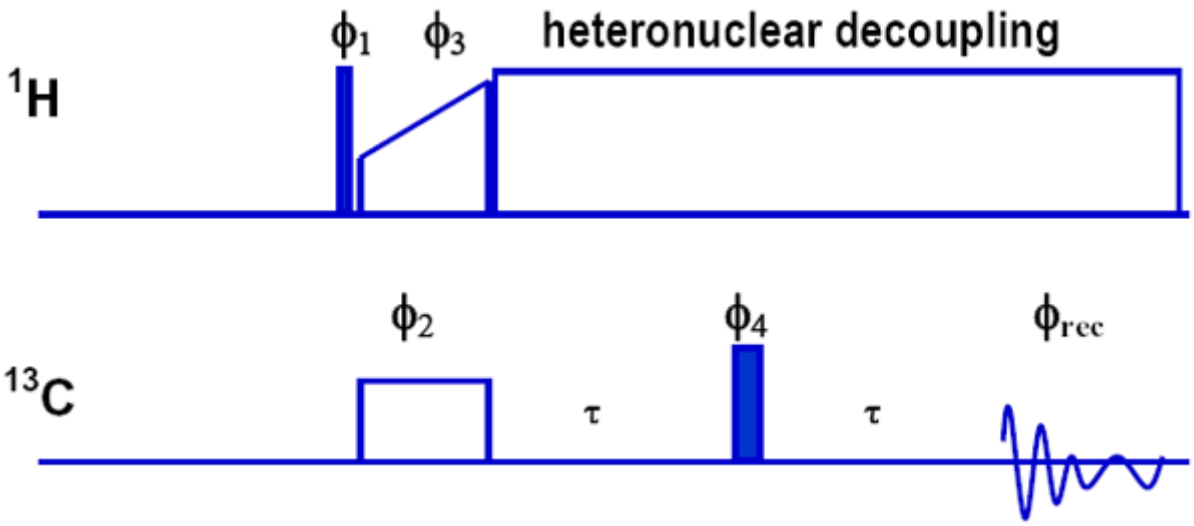

Figure 5.6. Pulse Program for Hahn Echo Sequence

Transverse Dephasing Optimized spectroscopy (G. De Paepe et al. 2003) uses a spin echo sequence for optimizing heteronuclear decoupling. The idea behind it is simply the removal of the normally dominant J_0 term (describing coherent residual line broadening effects) in the transverse relaxation rate R_2 (A. Abragam chapter 8). With the normal CP experiment the observed line broadening (coherence decay time T^*_2) might be caused by other heterogeneous effects, such as distribution of chemical shifts or susceptibility effects and not reflect the true T'_2 (coherence lifetime). The true T'_2 achieved through good heteronuclear decoupling can then be observed with a hahn-echo experiment. Optimization is done by looking for the maximum signal amplitude of the decoupled resonances of interest. Be careful not to exceed the maximum decoupling time with high power decoupling.

Reference:

1. G. De Paepe, N. Giraud, A. Lesage, P. Hodgkinson, A. Böckmann, and L. Emsley, *Transverse Dephasing Optimized Solid-State NMR Spectroscopy,* JACS 125, 13938 – 13939 (2003).

Practical CP/MAS Spectroscopy on Spin 1/2 Nuclei

6

Once good setup parameters have been obtained to observe ^{13}C and get good S/N on glycine, it should be easy to also observe ^{13}C-CP/MAS spectra on other samples and on nuclei different from ^{13}C. Nevertheless, sometimes one comes across samples where it is difficult to observe ^{13}C. This chapter deals with strategies to optimize acquisition parameters for ^{13}C and other spin ½ nuclei.

Possible Difficulties 6.1

Usually, ^{13}C spectra are easily acquired. Several sample properties may however make observation difficult:

1. Low concentration of ^{13}C in the sample.
2. No or too few protons in the sample.
3. Long proton T_1.
4. Long T_{I-S}.
5. Short proton $T_{1\rho}$.

If a nucleus different from ^{13}C should be observed, there are additional potential difficulties:

6. Unknown chemical shift.
7. Unknown Hartmann-Hahn-condition.
8. Unknown relaxation properties (proton T_1, $T_{1\rho}$, T_{I-S}).

Possible Approaches for 13C Samples 6.2

1.Collect as much information about the sample as possible. Do not accept samples for measurement with unknown composition. Request information about:

- possible hazards (upon a rotor explosion)
- concentration of the nucleus to be measured
- structural information about the molecular environment of the nucleus of interest:

- mobility (rigid environment: expect long T_1 and repetition delay),
- proximity to protons (can one use cross polarization)

- conductivity, dielectric loss (expect tuning and RF-heating problems if sample is dielectrically lossy or even conductive)

2. Collect information about the sample first by running an “easy” nucleus:

   Feasibility of cross polarization parameters is the required key information, because it decides the steps to follow.

   If the sample information which you have collected shows that a ^{13}C CP/MAS experiment should be feasible (sample contains more than 20% protonated carbons), load a reference cross polarization data set (S/N test spectrum of glycine), spin the sample at the same spin rate, set contact time (***p15***) to 1ms, wait 1 min., do one scan. There should be a visible signal.

   From there on, optimize the required repetition rate (***d1***), contact time (***p15***), number of scans (***ns***), spin rate (***masr***) and Hartmann-Hahn adjustment until the signal is optimum. In very few cases, the decoupler offset (***o2***) may require readjustment.

   If no ^{13}C-signal is found, the reasons may be:

   - incorrect setup (recheck reference sample)
   - concentration lower than expected
   - unusual relaxation properties (long $T_{I-S,}$ long proton T_1, short proton $T_{1\rho}$).

3. Then the most important information about the sample (proton T_1, proton $T_{1\rho}$) can be obtained by looking at the protons in the sample. Set up for proton observation, set ***swh*** to 100000-500000, ***rg*** to 4 and ***pulprog*** *cpopt* (if not found in the library, copy the pulse program in the appendix), ***p3*** and ***pl12*** for ***p3***=p90. Set ***spnam0*** = ramp.100, ***sp0*** = power level for HH, ***p15*** =100 us. Do 1 scan and fourier transform/phase correct. Using popt, optimize ***d1*** for maximum signal.

   Note: CP/MAS probes usually have a substantial proton background signal. Do not be misled by this, it will not behave like a regular signal:

   - it will grow steadily with longer pulses

   - it will not show spinning sidebands

   - it will cancel when a background suppression pulse program like ***aring*** is used with a full phase cycle.

4. Knowing the required relaxation delay, the following step is to determine the cross polarization (contact time). On protons, we measure the time constant $T_{1\rho}$. Using popt in the previous setup, vary ***p15*** between 100 µsec and 10 ms (even 20 ms at reduced power, if a long T_{I-S} is expected, as the distance between nucleus of interest is long or the mobility is high, leading to a small heteronuclear dipolar coupling between nucleus of interest and protons). This measurement will tell you how long the contact time ***p15*** may be. A value of p15 giving 50% of the initial proton signal amplitude will still give a 2-fold enhancement on ^{13}C. If the proton signal is below 50% at 1ms spin lock time or even less, a full cp-enhancement cannot be expected.

5. Now we know the minimum relaxation delay and the maximum contact time. With these parameters used as d1 and p15, the measurement is just a matter of patience.

Possible Approaches for Non-13C Samples *6.3*

If an arbitrary X-nucleus of spin ½ is under investigation (quadrupolar spins must be treated separately), the strategy follows the one described above, if the sample contains the protons bound to ^{13}C. In this case, running a ^{13}C cp/mas spectrum allows setting and determining all proton parameters (recycle time, contact time) from the ^{13}C setup. To run the X-nucleus, cross polarized from protons, one just needs to set the HH-condition from the known proton RF-field, the spin rate, and the transmitter power at the NMR-Frequency of the X-nucleus such that the effective field at the X-frequency equals the effective field at proton frequency ±spin rate.

Example: setting the HH-condition for ^{15}N from known parameters for ^{13}C-CP/MAS. The gyro-magnetic ration of ^{15}N is lower by a factor of 2.5 compared to carbon (proton frequency: 400 MHz, ^{13}C-frequency: 100 MHz, ^{15}N frequency: 40 MHz). The probe efficiency is about the same for ^{13}C and ^{15}N (but not ^{1}H!), so one needs about 2.5 times higher RF-voltage for the 15N-contact pulse than for the ^{13}C-contact pulse, if the spin rate and the proton RF-field are the same. This is equivalent to 2.5^2=6.25 times the power in watts! So if ased shows ***pl1W*** =150W for a well optimized 13C-CP setup, ^{15}N will require 6.25*150 W= 938 W! This is far above specs, so the same proton contact power level cannot be used, it needs to be lowered. The maximum allowed power for a contact pulse on ^{15}N is 500W. This means that the proton contact power should be lowered by approximately a factor of sqrt (938/500) ≈1.37. Precalculating power levels like this will get the parameters close enough to see a cp-signal on a good test sample, so further optimization is possible. See ***"Test Samples"*** for suitable test samples.

The most efficient way of precalculating power levels for multi-nuclear spectroscopy is the following:

1. Determine the power conversion factor for some nuclei of interest on a suitable test sample, from the low end to the high end of the probe tuning range. This means measuring a precise 360° pulse (make sure it is 360°, not 180° or 540°!) and the associated power level. Make a table in your lab notebook as follows (see ***"Appendix"***):

Table 6.1. Power Conversion Table

Probe: 4mm Triple				
Nucleus Frequency	**P90 (µs)**	**Rf-field (Khz)**	**Power (W or dB)**	**Remarks**
^{1}H/400.13	2.5	100	100	Low range
^{19}F/376.3				Not available
^{15}N/40.5	6.5	38.6	300	Probe in double mode
^{15}N/40.5	6.5	38.6	500	Probe in triple mode C/N
^{29}Si/79.5	6	41.7	300	Double mode low range
^{13}C/100.5	4	62.5	150	Double mode low range
^{13}C/100.5	5	50	200	Triple mode C/N
^{119}Sn/149.1	4	62.5	100	Double mode high range
^{31}P/161.9	3.5	71.4	150	Range switch up, double mode

2. Once these values are measured, any HH condition can be calculated. Assumed you want to cross polarize ^{119}Sn, the sample spins at 12 kHz. The contact time is anticipated to be rather long, because ^{119}Sn atoms are large and far away from protons. So the power level for the contact should not be too high. Let us set the RF-field to 50 kHz for the contact. We decide to apply a ramp shape on the proton contact pulse, covering the ±1 spinning sidebands. This means that we need to apply a ramp from 38 to 62 kHz RF field, plus some safety margin, about 35 to 65 kHz RF field on the proton ramp. For ^{119}Sn we need to apply 50 kHz RF field. Since the RF field is proportional to the amplitude in a shape (RF-voltage output is proportional to shape amplitude value), the shape power must range from 65 kHz to 35 kHz, from 100 to about 50% amplitude. Use ***calcpowlev*** to calculate the changes in dB to achieve the calculated RF fields (enter reference RF-field to calculate required RF field instead of pulse lengths). In our case, the proton contact pulse power sp0 is calculated at + 3.74 dB (65 kHz compared to 100 kHz), the power level for ^{119}Sn is calculated at +1.94 dB (50 kHz compared to 62.5 kHz). Be sure to add the calculated number for a desired RF-field lower than the reference field, subtract the number if the desired RF-field is higher.
3. If such a table is not available, but an oscilloscope is, one can measure the RF- voltage for the X contact pulse of the known (^{13}C) HH condition, calculate the pp-voltage for the unknown HH condition from the NMR-frequencies of the two nuclei, and set this voltage for the unknown HH condition.

Hints, Tricks, Caveats for Multi-nuclear (CP-)MAS Spectroscopy 6.4

1. Since T_1 relaxation tends to be slow in solids, direct observation of hetero-nuclei is usually time consuming, so CP is widely used because the proton T_1 is usually bearable. However, CP can only be used if the hetero-nucleus is coupled to protons (or whatever nucleus the magnetization is drained from). Whereas ^{13}C and ^{15}N usually bear directly bonded protons, this is not the case for many other spin ½ hetero-nuclei. So the magnetization must come from more remote substituents. More remote they may also be because atomic radii increase as one goes to nuclei with higher atomic mass. In short: HH conditions may be very sharp, T_{I-S} may be long, but proton $T_{1\rho}$ may still be short.
2. Chemical shift ranges and chemical shift anisotropies increase with nuclei of higher order number and number of electrons in the outer shell. Therefore one may be confronted with two problems:

   - to find the signal somewhere within the possible chemical shift range
   - to find the signal within a “forest” of spinning sidebands
3. Ease of setup therefore depends largely on the availability of a setup sample with decent T_1, efficient CP, and known chemical shift for referencing. Chapter 2 lists some useful setup samples together with known parameters.

Setup for Standard Heteronuclear Samples 15N, 29SI, 31P 6.5

1. ^{15}N on α-glycine: calculate HH condition as described above. Else:

   Load α-glycine ^{13}C reference spectrum, set observe nucleus N15 in ***edasp***

   - add 2 dB to ***sp0*** (***spnam0=ramp.100***)

- subtract 2 dB from ***pl1*** (more is not required since the transmitter will usually put out 50% more power at ^{15}N frequency)
- set ***p15*** = 3 ms
- acquire 4-8 scans
- optimize HH condition, acquire reference spectrum with ***aq***=25-35 ms

2. ^{29}Si on DSS

   - load α-glycine ^{13}C reference spectrum
   - set observe nucleus to ^{29}Si in ***edasp***
   - add 2 dB to ***sp0***
   - acquire 4 scans with ***aq*** = 35 ms
   - optimize HH condition, acquire reference spectrum

3. ^{31}P on ADP (ammonium dihydrogen phosphate $NH_4\ H_2\ PO_4$)

   - load α-glycine ^{13}C reference spectrum
   - set observe nucleus to ^{31}P in ***edasp***
   - add 6 dB to ***pl1***
   - optimize HH condition, acquire 2 scans, reduce ***rg*** appropriately.

Basic CP-MAS Experiments

7

The following experiments can be run by calling a ^{13}C CPMAS standard parameter, data set, or data, loading the appropriate pulse program and loading the pulse parameters obtained previously during the setup (see ***"Basic Setup Procedures"***). Some attention needs to be paid to special experimental parameters. Most of those parameters are explained in the header section of the pulse programs.

The CPPI experiment series in section ***7.5*** requires measuring the HH match using a constant amplitude contact pulse. This can be accomplished using a rectangular shape ***square.100,*** or using the pulse program ***cplg***.

Pulse Calibration with CP *7.1*

Pulse calibration for ^{13}C pulses after cross polarization using a flip back pulse.

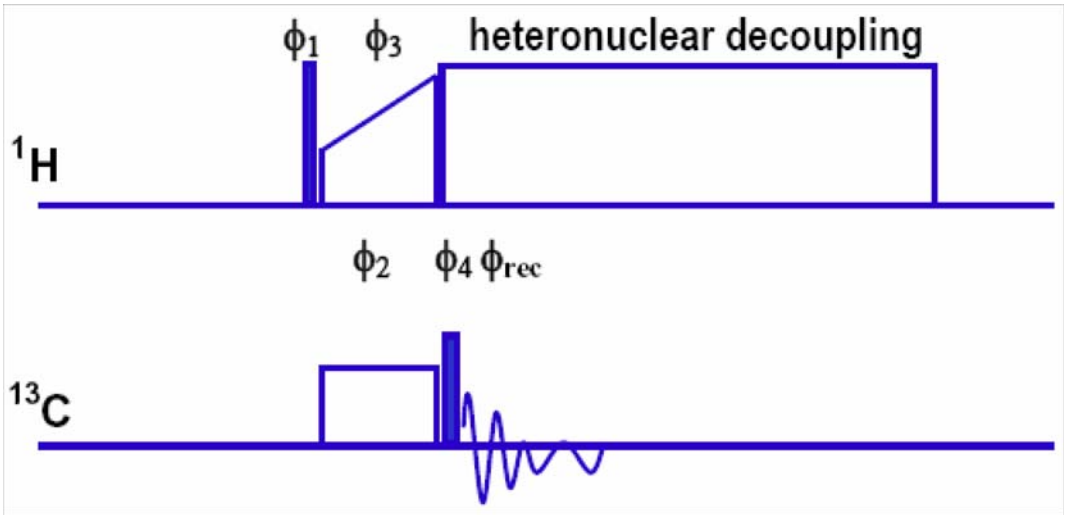

Figure 7.1. Pulse Program for CP with Flip-back Pulse

The experiment can be done directly after the CPMAS setup procedure. Loading the pulse program ***cp90*** and setting ***pl1=pl11*** allows one to measure the X nucleus spin nutation frequency at the HH contact power. Of course, the experiment allows nutation frequencies to be measured at other power levels as well. The typical nutation pattern has a cosine form, so a 90 degree pulse gives null signal. Use glycine spinning at N kHz as before. When using POPT for such measurements the optimization type is “ZERO” so that the program looks for a zero crossing at the automatic data evaluation. To get nutation patterns without phase

distortions, 90° pulses should always be executed close to the observed resonance. Larger offsets give different (shorter) p90 values and phase distortions for pulse lengths close to 180° and multiples thereof.

Table 7.1. Acquisition Parameters

Parameter	Value	Comments
pulprog	cp90	AVIII, cp90.av for older instruments
nuc1	13C	Nucleus on f1 channel
nuc2	1H	Nucleus on f2 channel
sw	300 ppm	Spectral width for Glycine
o1p	45	Close to C-α
td	2048	Number of points sampled

Fine adjustment of the π pulse on ^{13}C can also be done using the TOSS experiment, see next chapter.

Total Sideband Suppression TOSS *7.2*

The TOSS sequences permit complete suppression of spinning sidebands (SSB) in CPMAS experiments. The TOSS sequence consists of the basic CP sequence plus a 2 rotor period sequence with four specially spaced 180º pulses. As is the case for all extra pulses on the X channel in CPMAS experiments (with the exception of symmetry based sequences, see further below), these 180º pulses are set with ***pl11***.

This experiment can be optimized for minimum spinning sideband intensity either by variation of the 180° pulse width or the associated power level ***pl11***.

Two variations of the TOSS sequence exists, the default is TOSS A, which is appropriate for lower spinning speeds. TOSS B, for higher spinning speeds, is selected by setting ***ZGOPTNS*** to ***–Dtossb***. The maximum spinning speed is either determined by common sense – if all sidebands are spun out, TOSS is not needed (low field instruments) – or by the shortest delay, which is ***d26*** in both cases. For TOSS B, ***d26 = 0.0773s/cnst31-p2***, with ***cnst31*** the rotation rate in Hz and ***p2*** the 180º pulse width in µs. For TOSS A, ***d26 = 0.0412s/cnst31-p2***, so the maximum spinning rate is lower.

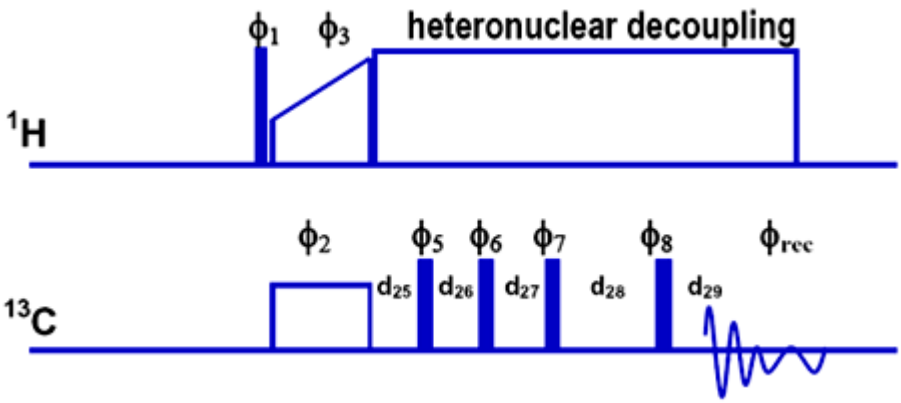

Figure 7.2. Pulse Program for CPTOSS.

If the timing becomes a problem, alternative TOSS schemes need to be found (see e.g. O.N. Antzutkin, *Sideband manipulation in magic-angle-spinning nuclear magnetic resonance*; Progress in Nuclear Magnetic Resonance Spectroscopy 35 (1999) 203-266.). The SELTICS sequence is an alternative.

Set up the experiment using glycine or tyrosine-HCl at a moderate spinning speed. Get a good CPMAS spectrum first then run a TOSS spectrum.

Table 7.2. Acquisition Parameters

Parameter	Value	Comments
pulprog	cptoss ***cptoss243***	
p2		180° pulse on X nucleus
pl11		Power level driving P2 on X-channel
cnst31		Spinning speed in Hz e.g. 5 kHz the entry would be 5000
zgoptns	-Dtossb	Tossb if needed because of high spinning speed or long p2

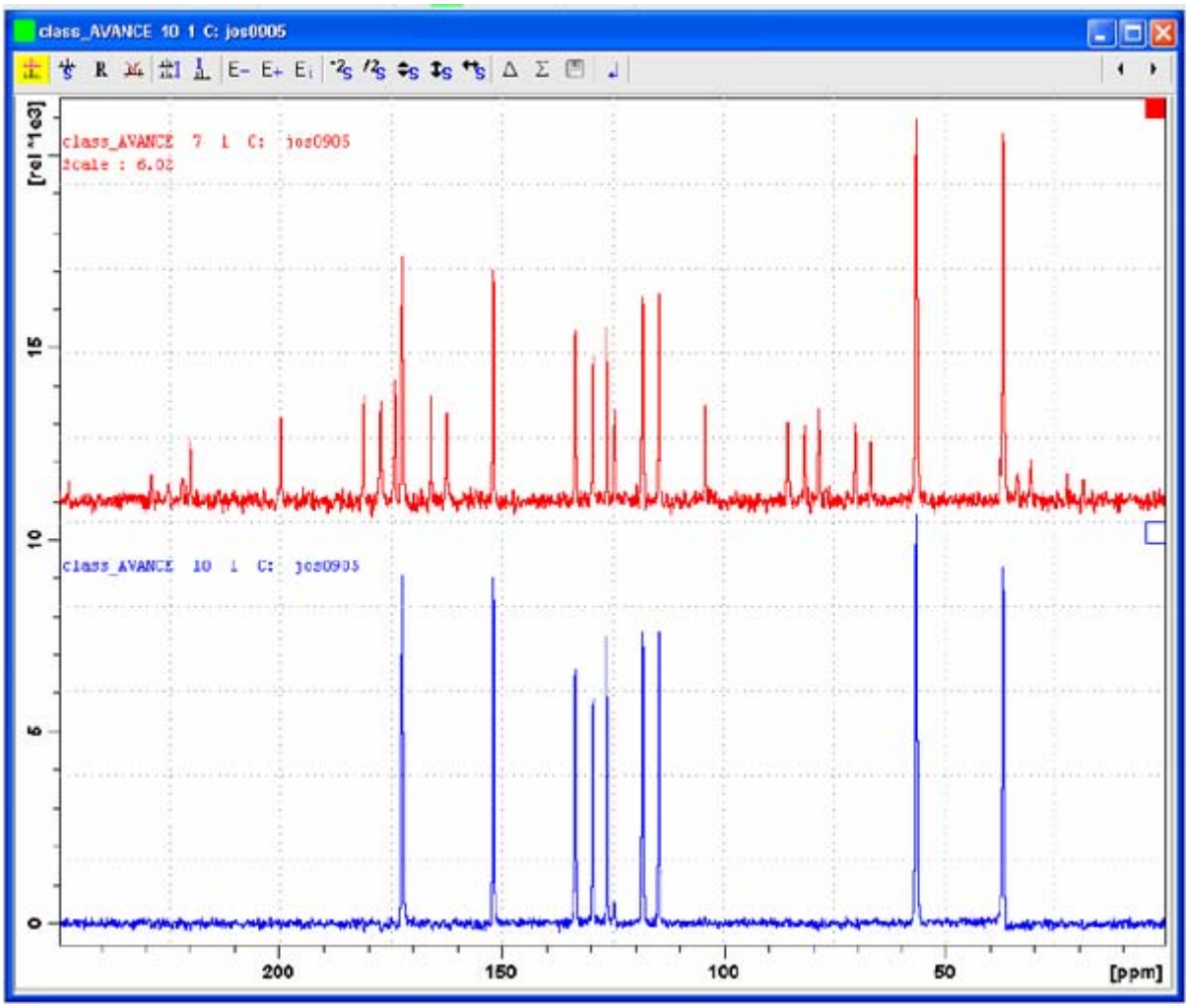

Figure 7.3. Comparison of a CPTOSS and CPMAS Experiment

Figure 7.3. *compares a CPTOSS experiment (lower spectrum) to a CPMAS experiment (upper spectrum) on tyrosine HCl at 6 kHz sample rotation using a 4 mm CPMAS double resonance probe at 500 MHz with 16 accumulated transients.*

The sequence is not perfectly compensated for experimental artifacts and if perfect suppression of SSB is required, one can use a 5 pulse sequence with a long phase cycle, requiring a minimum of 243 transients for complete artifact suppression using the pulse program ***cptoss243***, where the extension.*av* is added in case of the AV2 console. ***Figure 7.4.*** shows the advantage of the well compensated TOSS sequence with its 243 phase cycle steps over the above 4 pulse sequence. Besides the better compensation, the *cptoss243* pulse sequence is also shorter and uses only 1 instead of 2 rotor cycles. This pulse program can be used with fairly high spinning speeds, up to about 12.5 kHz sample rotation, depending, of course, on the width of the employed π – pulses. ***Figure 7.5.*** shows for a comparison the results obtained with the 4 pulse sequence with 256 scans.

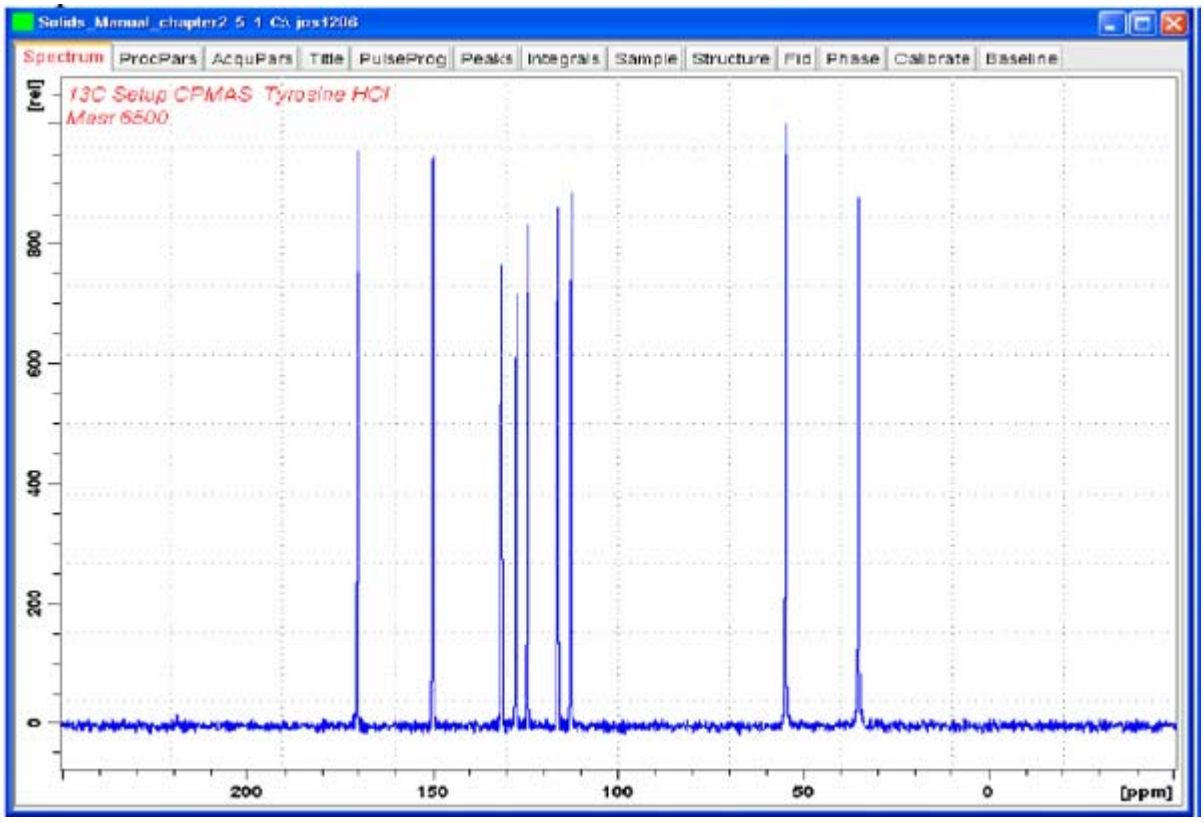

Figure 7.4. CPTOSS243 Experiment on Tyrosine HCl at 6.5 kHz

Figure 7.4. *is a CPTOSS243 experiment on tyrosine HCl at 6.5 kHz sample rotation using a 4 mm CPMAS triple resonance probe at 500 MHz with 243 accumulated transients. No spinning sideband residuals can be observed, with a noise level below 2% peak to peak compared to the highest peak intensity.*

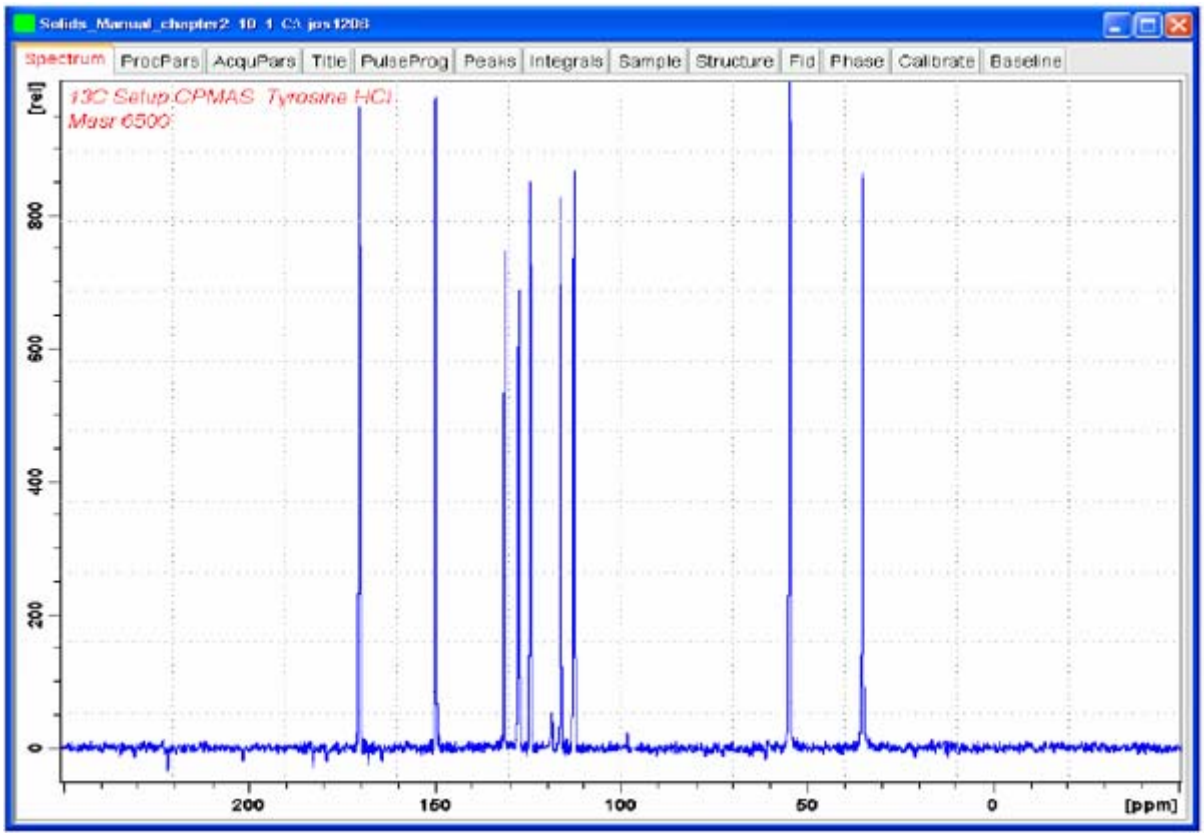

Figure 7.5. CPTOSS Experiment on Tyrosine HCl at 6.5 kHz

Figure 7.5. *is a CPTOSS experiment on tyrosine HCl at 6.5 kHz sample rotation using a 4 mm CPMAS triple resonance probe at 500 MHz with 256 accumulated transients. Spinning sideband residuals can be observed outside a noise level of approximately 2% peak to peak compared to the highest intensity. The residual sidebands have up to 5% intensity compared to the highest resonance.*

SELTICS *7.3*

Like the TOSS experiment, SELTICS (**S**ideband **EL**imination by **T**emporary **I**nterruption of the **C**hemical **S**hift) is an experiment for spinning sideband suppression. Pulses on the ^{13}C channel are driven with ***pl11*** and pulse times are rotor synchronized. For optimum suppression, the shortest pulse ($\tau/24$) of the sequences, where τ_r is the rotor period, should be a $\pi/2$ pulse or stronger. Choose ***pl11*** accordingly. Unlike TOSS, SELTICS is only 0.5 rotor periods long.

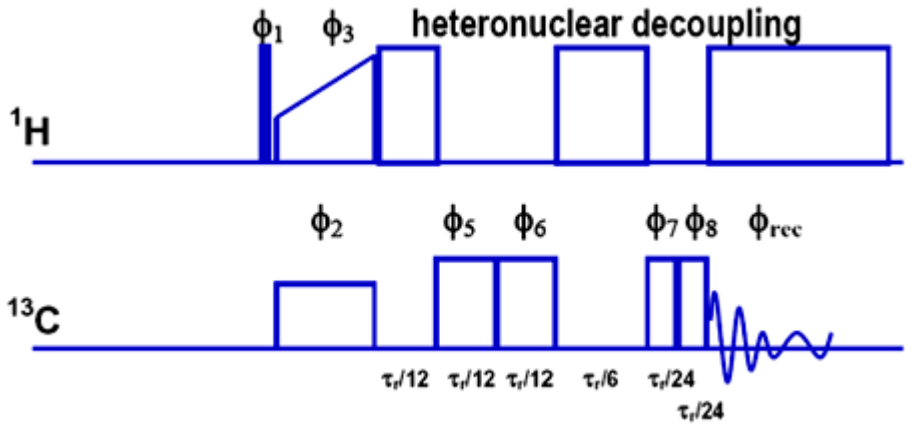

Figure 7.6. Pulse Program for SELTICS.

*In **Figure 7.6.** one can see that the SELTICS experiment takes only ½ rotor period compared to the 2 rotor periods required in the TOSS experiment.*

Use glycine or tyrosine.HCl at reasonable spinning speed.

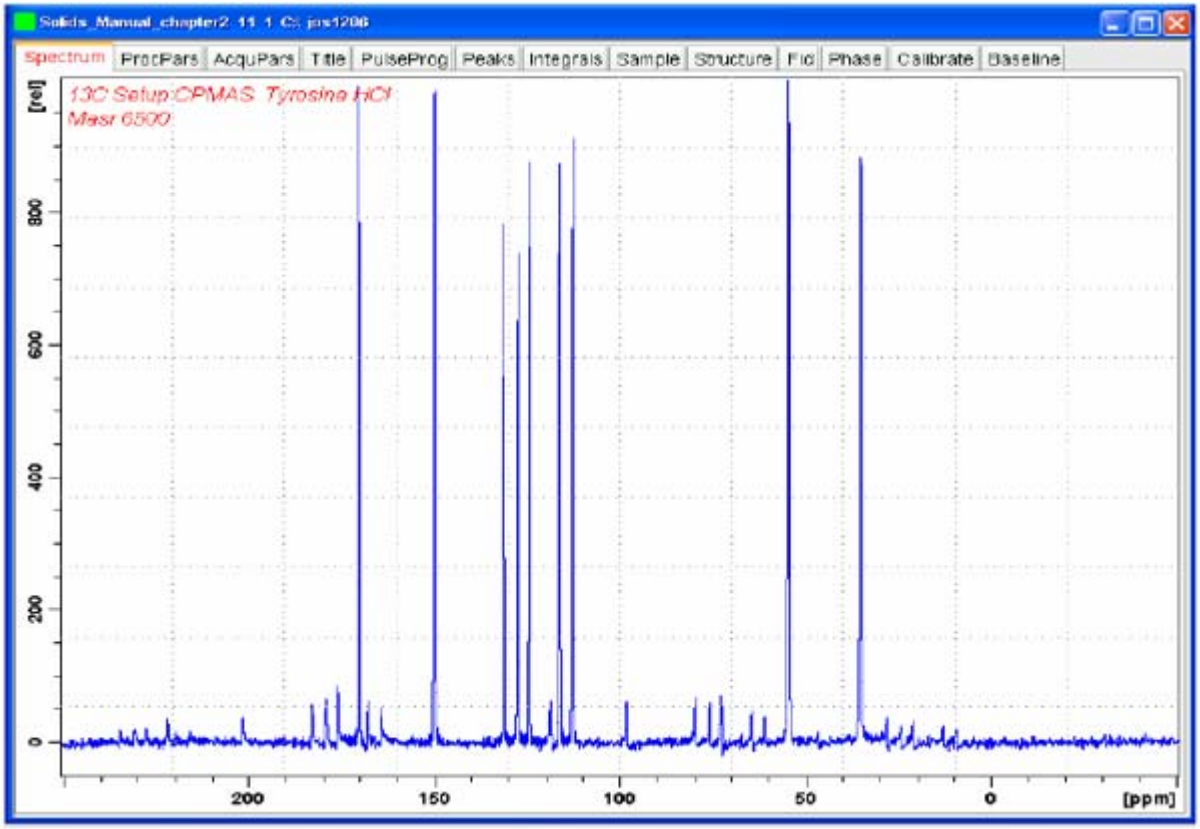

Figure 7.7. SELTICS at 6.5 kHz Sample Rotation on Tyrosine HCl.

*In **Figure 7.7.** the amplitude of the spinning sidebands are reduced to more than 10% compared to the original spectrum without sideband suppression. 256 transients were recorded.*

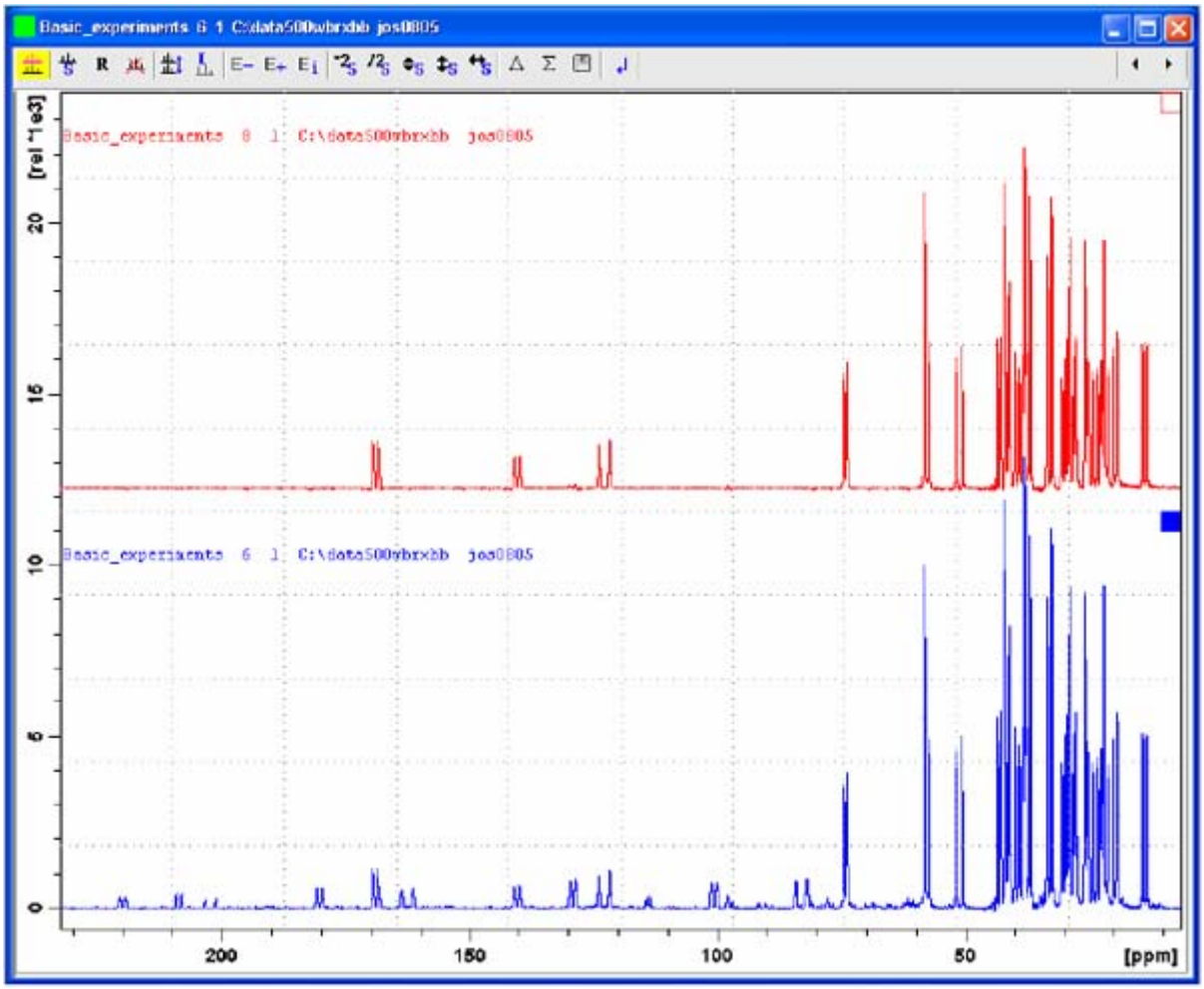

Figure 7.8. Cholesterylacetate Spectrum Using Sideband Suppression

***Figure 7.8.** is a cholesterylacetate spectrum using sideband suppression with the SELTICS sequence at 5 Hz sample rotation (upper spectrum). The lower spectrum is the CPMAS spectrum at 5 kHz sample rotation.*

Non-Quaternary Suppression (NQS) 7.4

The NQS experiment is a simple spectral editing experiment. It relies on the fast dephasing of rare spins coupled to ^{1}H spins through the heteronuclear dipolar interaction. For the dephasing delay ***d3*** one uses between 30 and 80 µs.

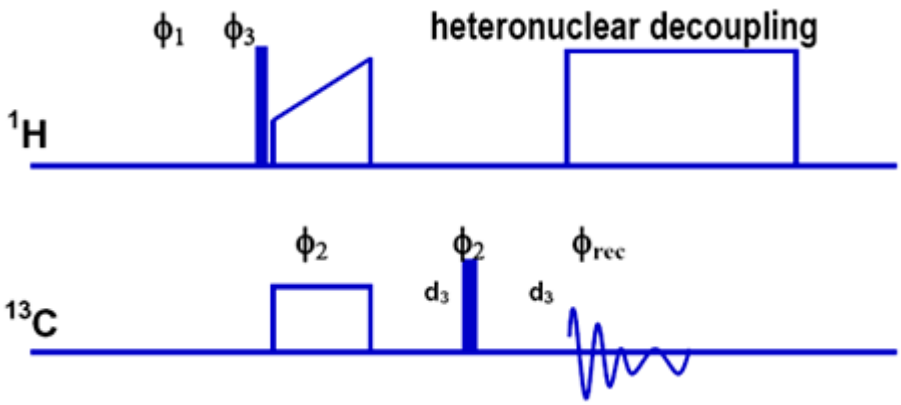

Figure 7.9. Block Diagram of the Non-quaternary Suppression Experiment

The **non-quatemary suppression** experiment is also called the **dipolar dephasing** experiment.

Use glycine or tyrosine spinning at 11 kHz as before.

Table 7.3. Acquisition Parameters

Parameter	Value	Comments
pulprog	cpnqs, cptoss_nqs	
p2		180° pulse on X nucleus.
pl11		Power level driving P2 on X-channel.
d3	30 – 80 µs	Dephasing delay.

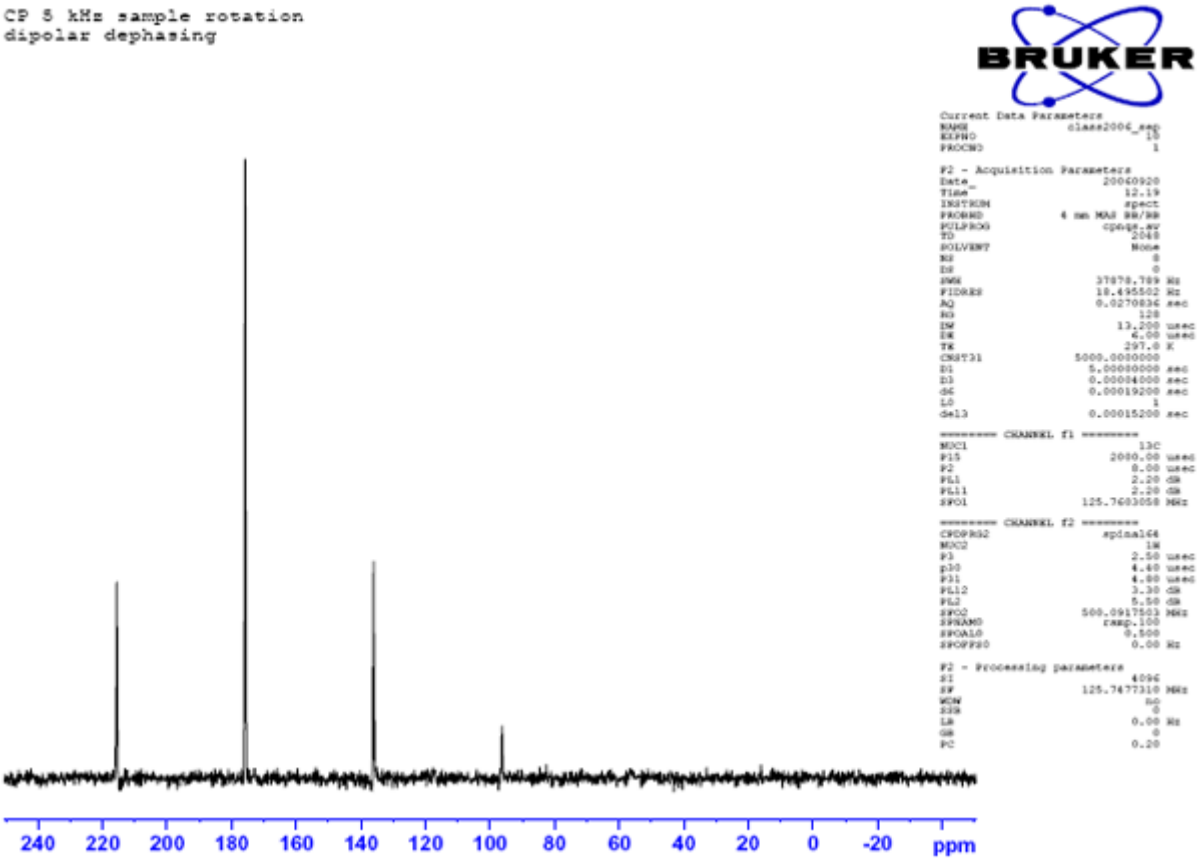

Figure 7.10. Glycine ^{13}C CPMAS NQS Experiment with a Dephasing Delay

Figure 7.10. *is a glycine ^{13}C CPMAS NQS experiment with a dephasing delayd3 = 40 µs so that the total dephasing time is 80 µs. Spinning sidebands are still visible.*

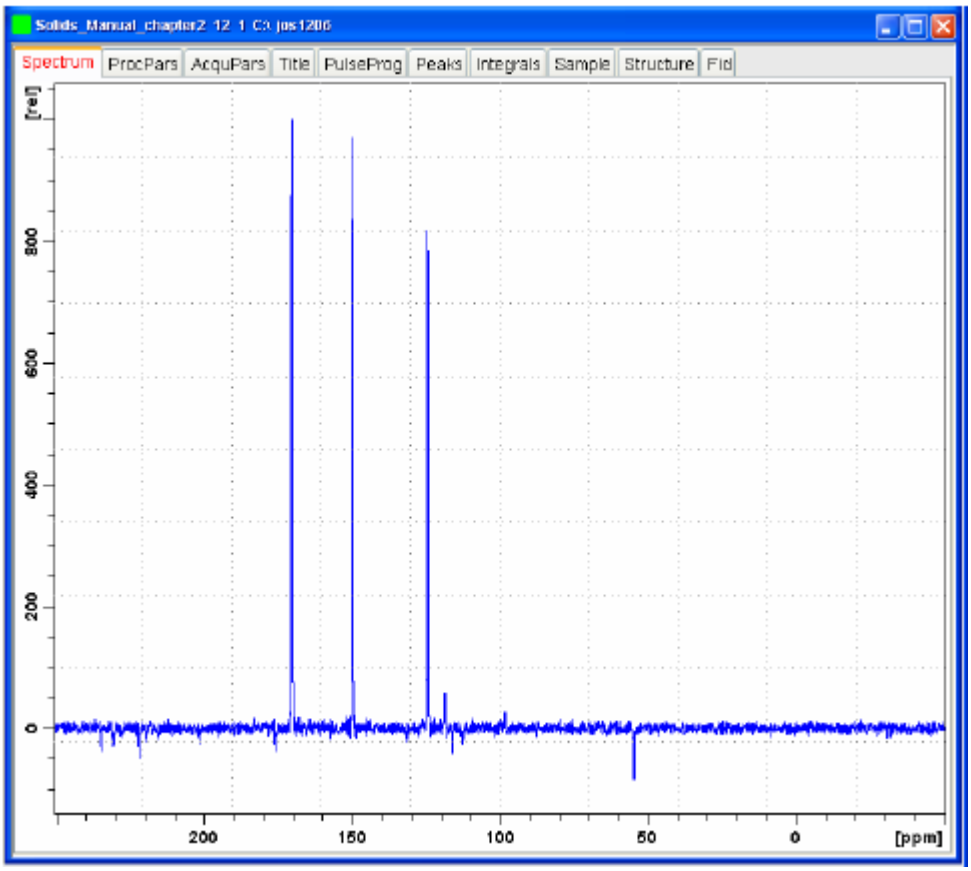

Figure 7.11. Tyrosine ^{13}C CPMAS NQS Experiment with TOSS

Figure 7.11. *is a tyrosine ^{13}C CPMAS NQS experiment with TOSS using a dephasing delay* ***d3*** *= 60 µs. Spinning sidebands are suppressed for a clean spectrum. In this experiment the total dephasing time is 20 µs shorter than that used for the CPNQS experiment on glycine in* ***Figure 7.10.****.*

Spectral Editing Sequences: CPPI, CPPISPI and CPPIRCP 7.5

These spectral editing sequences help to distinguish CH, CH_2, CH_3 and quaternary carbons in ^{13}C spectra. Common to all are various polarization and depolarization times, which properly mixed and combined give a series of spectra, which can be added and subtracted in order to obtain the various sub-spectra. All these sequences use constant-amplitude CP, which should be adjusted for maximum signal intensity. For the *CPPI* and *CPPISPI* sequences, the only parameter needed in addition to the CP parameters is ***p16, for which a good starting value*** is 40 µs to give null signal for CH, negative signal for CH_2, and positive signal for C and CH_3. If necessary, this value can be optimized on a sample similar to the sample of interest for better editing. ***p17,*** for the repolarization step in the *CPPIRCP* experiment, is about 10 – 20 µs.

For this experiment to succeed reliably, one should use moderate spinning speeds around (up to) 10 kHz. At slow rotation rates, no advantage was found in measuring the exact HH match. Running the experiment at constant amplitude CP, optimized for maximum signal, proved to be sufficient.

References for these experiments:

1. X. Wu, K. Zilm, *Complete Spectral Editing in CPMAS NMR*, J. Magn. Reson. A 102, 205-213 (1993);
2. X. Wu, K. Zilm, *Methylene-Only Subspectrum in CPMAS NMR*, J. Magn. Reson. A 104, 119-122 (1993);
3. X. Wu, S.T. Burns, K. Zilm, *Spectral Editing in CPMAS NMR. Generating Subspectra Based on Proton Multiplicities*, J. Magn. Reson. A 111, 29-36 (1994);
4. R. Sangill, N. Rastrup-Andersen, H. Bildsoe, H.J. Jakobsen, and N.C. Nielsen, *Optimized Spectral Editing of 13C MAS NMR Spectra of Rigid Solids Using Cross-Polarization Methods*, J. Magn. Reson. A 107, 67-78 (1994).

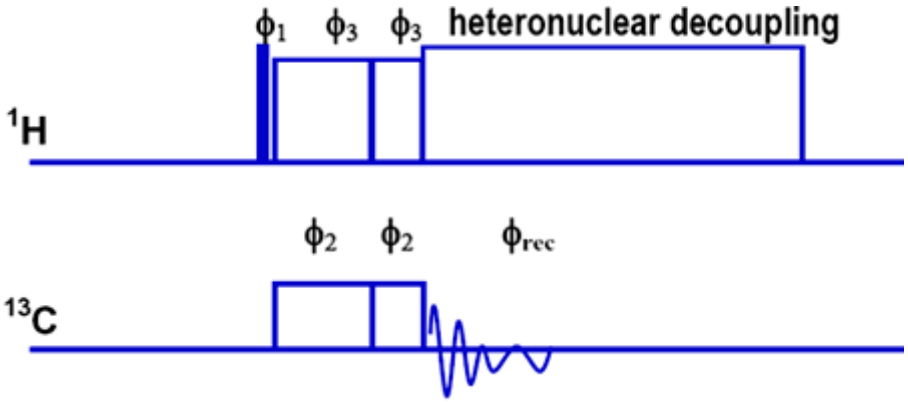

Figure 7.12. Block Diagram of the CPPI Experiment.

Typical pulse widths for the second part of the CP pulse with the phase inversion are 40 µs.

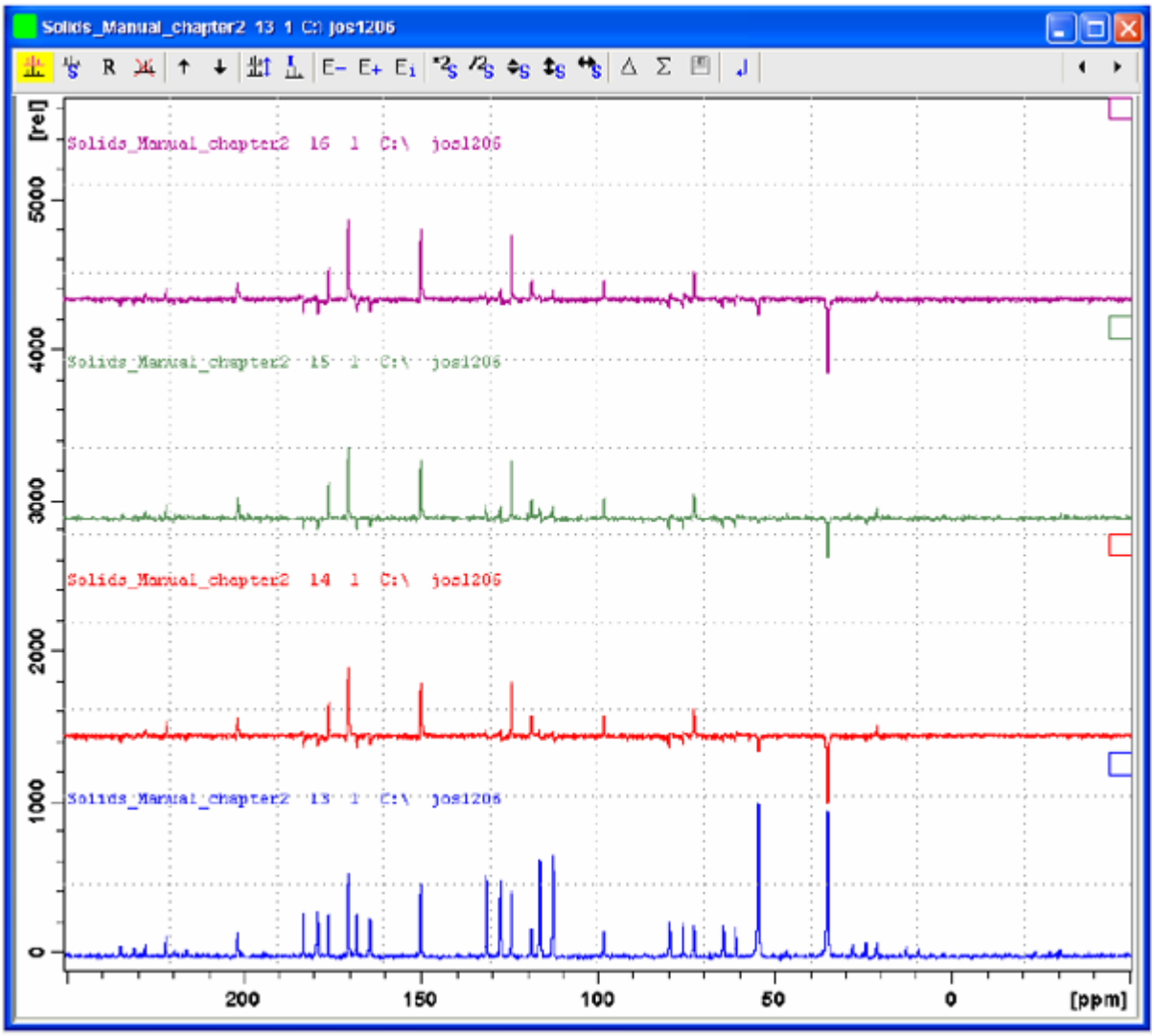

Figure 7.13. CPMAS Spectrum of Tyrosine.HCl at 6.5 kHz

CPMAS spectrum of tyrosine.HCl at 6.5 kHz sample rotation obtained on a 500 WB spectrometer using a 4 mm CPMAS double resonance probe. The red (third) spectrum is a CPPI spectrum where we see the CH_2 resonance at 35 ppm with a negative intensity. The aromatic CH resonances are clearly suppressed, where the C_a shows a slightly negative intensity. The polarization inversion pulse p16 was 40 µs long. The green (second) spectrum is a CPPIRCP experiment with p16=40 µs and p17=10 µs for better nulling of CH resonances, but in this case the aromatic CH resonances gained some intensity back. The purple (first) spectrum is a CPPISPI experiment with a similar performance as for the CPPI spectrum. Our experience is that one can adjust p15 (= 1 ms in this spectrum), p16 (= 30 µs in the purple spectrum) and so edit for pure CH resonances for example. Such tuning needs to be done of course on a known sample, which behaves similarly to the one under investigation, for the editing to be conclusive and correct.

Note: For more editing experiments consider the ***Solid State Attached Proton Test*** experiment, using the *sostapt* pulse program name, or look at 2D editing sequences, based on the FSLG HETCOR experiment.

FSLG-HETCOR 8

This chapter discusses setup and use of the ***F***requency ***S***witched ***L***ee ***G***oldburg ***Het****eronuclear* ***Cor***relation (FSLG HETCOR) experiment.

The FSLG Hetcor experiment correlates ^{1}H chemical shifts with X-nuclei (e.g. ^{13}C, ^{15}N) chemical shifts. The experiment provides excellent ^{1}H resolution in the indirect dimension. Homonuclear decoupling in the ^{1}H evolution period is achieved with an FSLG pulse train. FSLG permits relatively high spinning speeds and makes this experiment available for high field systems, requiring high spinning speeds in order to move spinning sidebands out of the spectral region. Decoupling the protons from the coupled X-nucleus during evolution is not essential, since the high spinning speed already achieves that. One can however improve the heteronuclear decoupling by a π-pulse in the middle of the evolution period (see A. Lesage et. al.).

Mixing is achieved during the cross polarization contact time. Since magnetization transfer from protons to X (e.g. ^{13}C) occurs rapidly, contact times should be kept short in order to avoid long range transfer, leading to unspecific cross peak patterns since the magnetization then has time to flow from any proton to any X-nucleus. A modification of the basic sequence uses cross polarization under a LG frequency offset for the protons. In this case, the proton magnetization detected by the X-nucleus comes from close protons only, since the proton spin lock at an LG offset interrupts the “communication” between the proton spins. A third modification of the basic sequence uses phase modulated pulses instead of frequency shifts. These three modifications to the basic sequence are described in ***"Modifications of FSLG HETCOR"***.

References:

1. H.J.M. deGroot, H. Förster, and B.-J. van Rossum, *Method of Improving the Resolution in Two-Dimensional Heteronuclear Correlation Spectra of Solid State NMR*, United States Patent No 5,926.023, Jul. 20, 1999.
2. B.-J. van Rossum, H. Förster, and H.J.M. deGroot, *High-field and high-speed CP-MAS ^{13}C NMR Heteronuclear dipolar-correlation spectroscopy of solids with frequency-switched Lee-Goldburg homonuclear decoupling,* J. Magn. Reson. A 120, 516-519 (1997).
3. B.–J. van Rossum, *Structure refinement of photosynthetic components with multidimensional MAS NMR dipolar correlation spectroscopy,* Thesis, University of Leiden, Holland; (2000).
4. B.–J. van Rossum, C.P. deGroot, V. Ladizhansky, S. Vega, and H.J.M. deGroot, *A Method for Measuring Heteronuclear (^{1}H-^{13}C) Distances in High Speed MAS NMR*, J. Am. Chem. Soc. 122, 3465-3472 (2000).
5. D.P. Burum and A. Bielecki, *An Improved Experiment for Heteronuclear-Correlation 2D NMR in Solids*, J. Magn. Res. 94, 645-652 (1991).
6. A. Lesage and L. Emsley, *Through-Bond Heteronuclear Single-Quantum Correlation Spectroscopy in Solid-State NMR, and Comparison to Other Through-Bond and Through-Space Experiments,* J. Magn. Res. 148, 449-454 (2001).

Pulse Sequence Diagram for FSLG HETCOR *8.1*

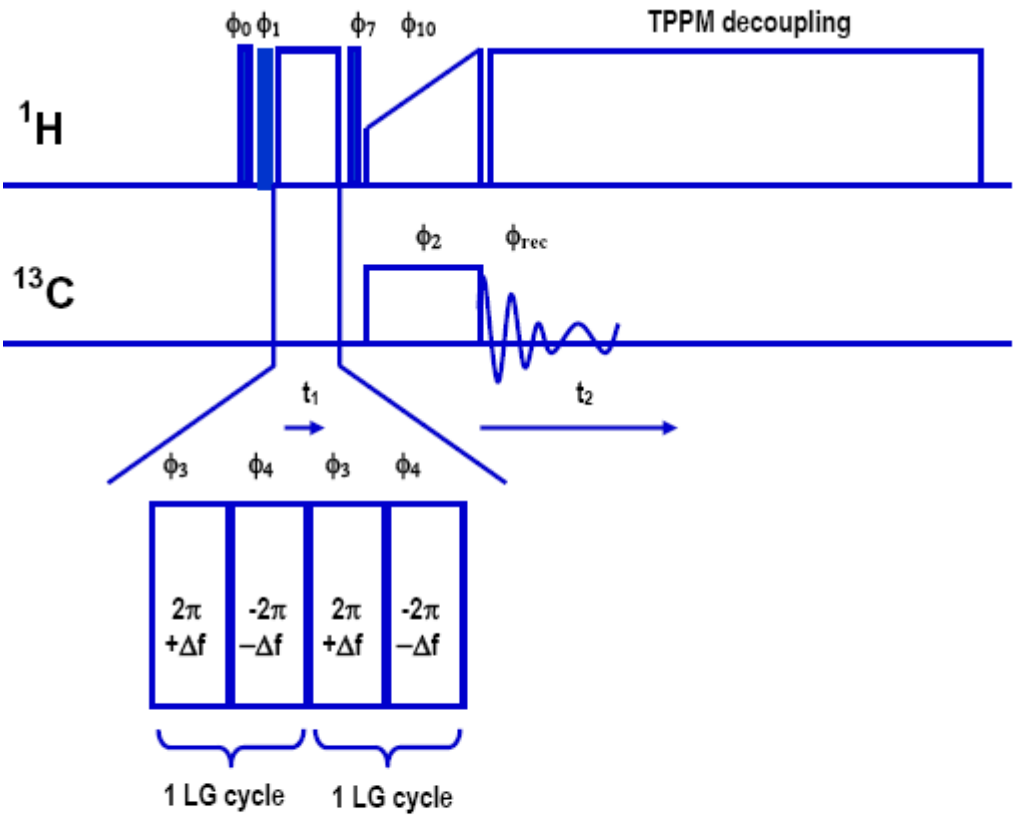

ϕ_0= 1 3 + STATES-TPPI (t_1)	ϕ_1= 1	ϕ_{10}= 0
ϕ_2 = 0 0 2 2 1 1 3 3	ϕ_4 = 2 (-LG)	ϕ_3 = 0 (+LG)
ϕ_7= 3	ϕ_{rec}= 0 2 2 0 1 3 3 1	

Figure 8.1. The FSLG Hetcor Experiment

The FSLG Hetcor experiment consists of 3 basic elements, the homonuclear decoupling sequence during which the ^{1}H chemical shifts evolve, the cross polarization sequence, during which the information of the ^{1}H spin magnetization is transferred to the X-spins, followed by observation of the X-spins under proton decoupling.

Setting up FSLG HETCOR *8.2*

1. This experiment requires a probe of 4 mm spinner size or smaller. One can run it on a 7 mm probe, but the results will not be very convincing.
2. Start from a data set with well adjusted cross polarization and proton decoupling at fairly high RF-fields. Unlike standard multiple pulse decoupling, which only works well at very high RF-fields, FSLG requires only moderately high RF fields. Decent performance is achieved at 80-100 kHz proton field. At lower magnetic fields (200-300 MHz proton frequency) lower RF-fields are adequate, RF fields of 100 kHz and higher perform better at higher magnetic fields (500 MHz and up).
3. Insert a suitable test sample, spin at a suitable speed. We recommend ^{13}C labeled tyrosine hydrochloride, since it has a wide spread (2.5-12ppm) of proton shifts, a short proton T_1, a well resolved ^{13}C-spectrum with quite many lines, and it is readily available. The unlabeled sample can also be used, but requires a few more scans (8-32).
4. Optimize the spin rate such that no overlap occurs between center- and sidebands (especially with the labeled sample, in order to avoid rotational resonance broadening). Re-optimize decoupling and HH-condition. Check the proton RF-field via the proton 90° pulse ***p3***. Set ***pl13*** = ***pl12***, set ***cnst20*** to RF-field in Hz as calculated from ***p3***.
5. Generate a new data set with ***edc***, ***new***. Set pulprog ***lghetfq*** and change to a 2D parameter set using the “123” button in ***eda***. Set ***FnMode*** to STATES-TPPI. Type ***ased*** or click the pulse symbol in ***eda***.

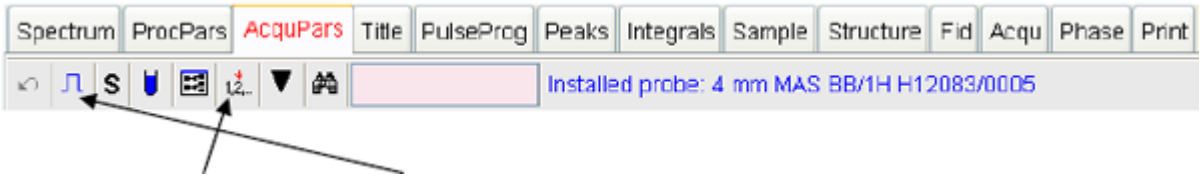

Figure 8.2. The “12...” icon, and the ased icon in eda.

6. Performing ***ased*** will show all parameters which are essential for the acquisition, not all available parameters. In addition, it performs calculations which are specified in the pulse program. Note that all parameters which are calculated are not editable, and will show only, if explicitly used during the main pulse program between ze and exit. In this sequence, the proton chemical shift evolution is influenced by the RF field (***cnst20***) under which the shifts evolve and the type of homonuclear decoupling sequence (FSLG in this case) which scales chemical shifts (by about 0.578 in this case). In order to obtain proton chemical shifts at the standard scale, both parameters are taken into account and an increment along F1 is calculated which yields correct chemical shifts for protons. Transfer this increment to ***IN_F1*** in ***eda*** (***A*** button in ***ased***). This will set the sweep width along F1. Note that the time increment here is generated by a loop counter, counting the periods of FSLG. The loop counter ***l3*** is used to multiply this increment. Usually, l3 is set to 2-4 in order to reduce the F1 sampling width to a reasonable value. ***Cnst24*** is usually set to -1000 - -2000 in order to move the spectrum away from the center ridge in F1.

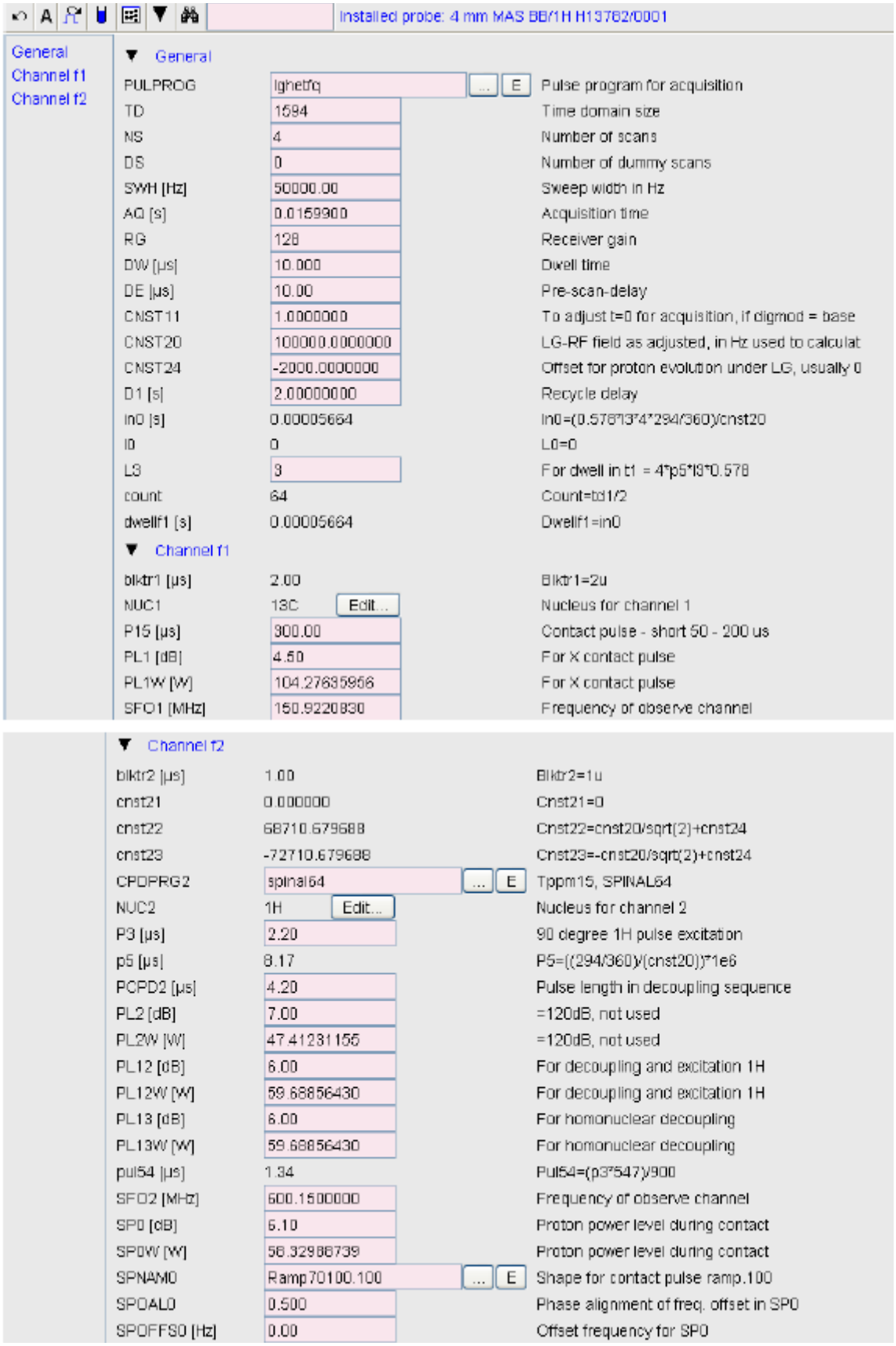

Figure 8.3. The ased Display

In the figure above the frequency offsets for the FSLG part are shown as ***cnst22***, ***cnst23***. They are different because ***cnst24*** shifts the center frequency by 2000 Hz.

Table 8.1. Acquisition Parameters for FSLG-HETCOR (on tyrosine-HCl)

Parameter	Value	Comments
pulprog	lghetfq	FSLG program.
nuc1	13C	
o1p	100 ppm	
nuc2	1H	
cnst20	70-100000	Proton spin nutation frequency with PL13.
cnst24	0 - -2000	Place carrier off during evolution.
pl1		Power level channel 1 for contact pulse.
pl12		Power level channel 2 TPPM/SPINAL decoupling.
pl13		Power level channel 2 FSLG decoupling.
sp0		Power level channel 2 for contact pulse.
spnam0	ramp.100 or simil.	Shape for contact pulse channel f2.
p3	2.5 – 3 µsec	90º pulse channel 2 at pl12.
p15	50 -500 µsec	Contact pulse width.
pcpd2	≈ 2*p3-0.2	SPINAL64 /TPPM decoupling pulse.
cpdprg2	SPINAL64/TPPM15	Decoupling sequence.
F1 1H indirect		
l0	0	Start value 0, incremented during expt.
l3	2- 4	Multiples of FSLG-periods, increment per row.
in_f1	=in0 as calculated	Set according to value calculated by ased.
F2 13C acquisition		
d1	2s	Recycle delay.
sw	310ppm	Sweep width direct dimension.
aq	16-20 msec	
masr	10000-15000 Hz	At 100 kHz RF, 15 kHz is ok.

Table 8.2. Processing Parameters for FSLG-HETCOR (on tyrosine-HCl)

Parameter	Value	Comment
F2 direct dim 13C ***si***	 2-4 k	
wdw	QSINE	SSB 2, 3 or 5
ph_mod	pk	
F1 indirect 1H		
si	256-1048	
mc2	STATES-TPPI	
wdw	QSINE	
ssb	3, 5	
ph_mod	pk	

Results 8.3

A full plot of a FSLG-HETCOR on labeled tyrosine-HCl is shown in the next figure.

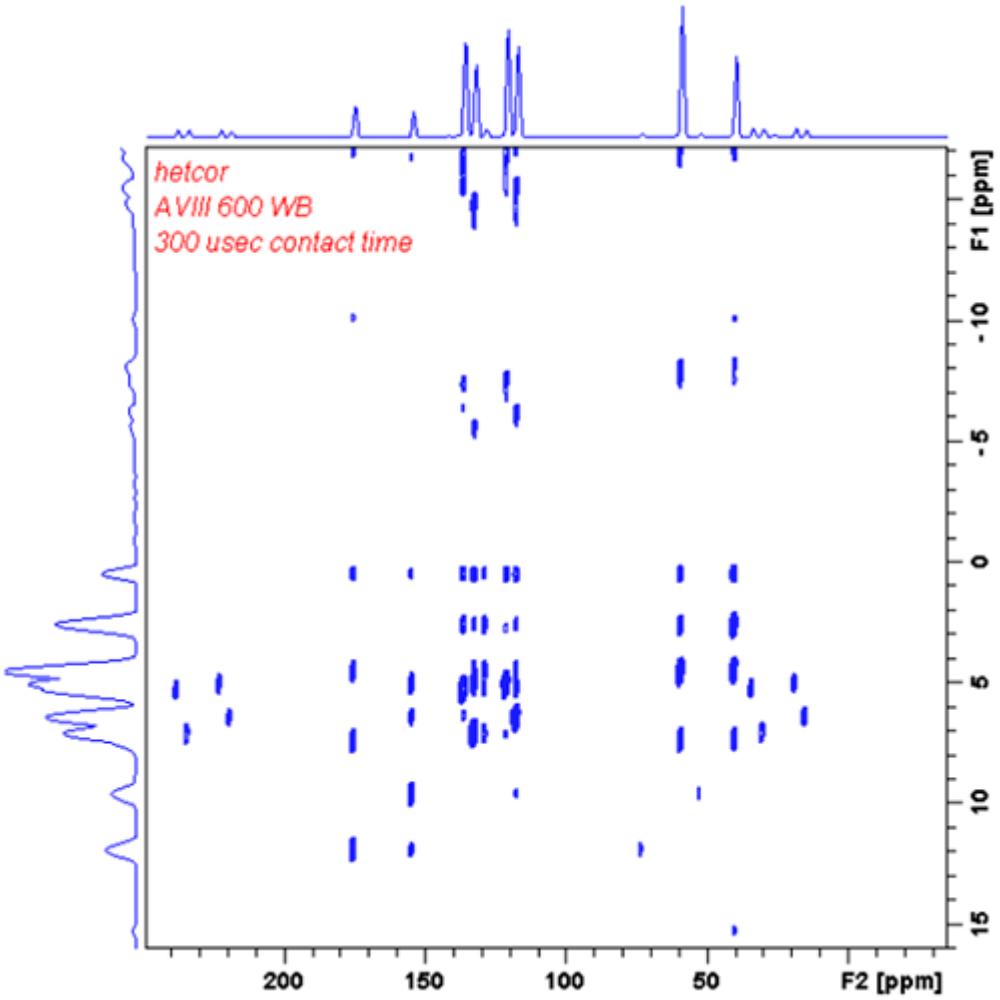

Figure 8.4. FSLG Hetcor Spectrum Tyrosine HCl

The figure above shows a FSLG Hetcor Spectrum Tyrosine HCl with parameters as shown in ***Table 8.1.***/***Table 8.2.***. Full transform with slight resolution enhancement, ***qsine/SSB***=3. Proton shifts calibrated as 2.5 and 12 (most high field/low field peak). Center ridge at 0 ppm along F1 is spin locked signal which does not follow the FSLG-evolution. ***Cnst24*** is used to separate the proton spectrum from this ridge. The contact time of 300 µsec shows many long range couplings. The next figure shows the region of interest excluding the center ridge and the spinning sidebands.

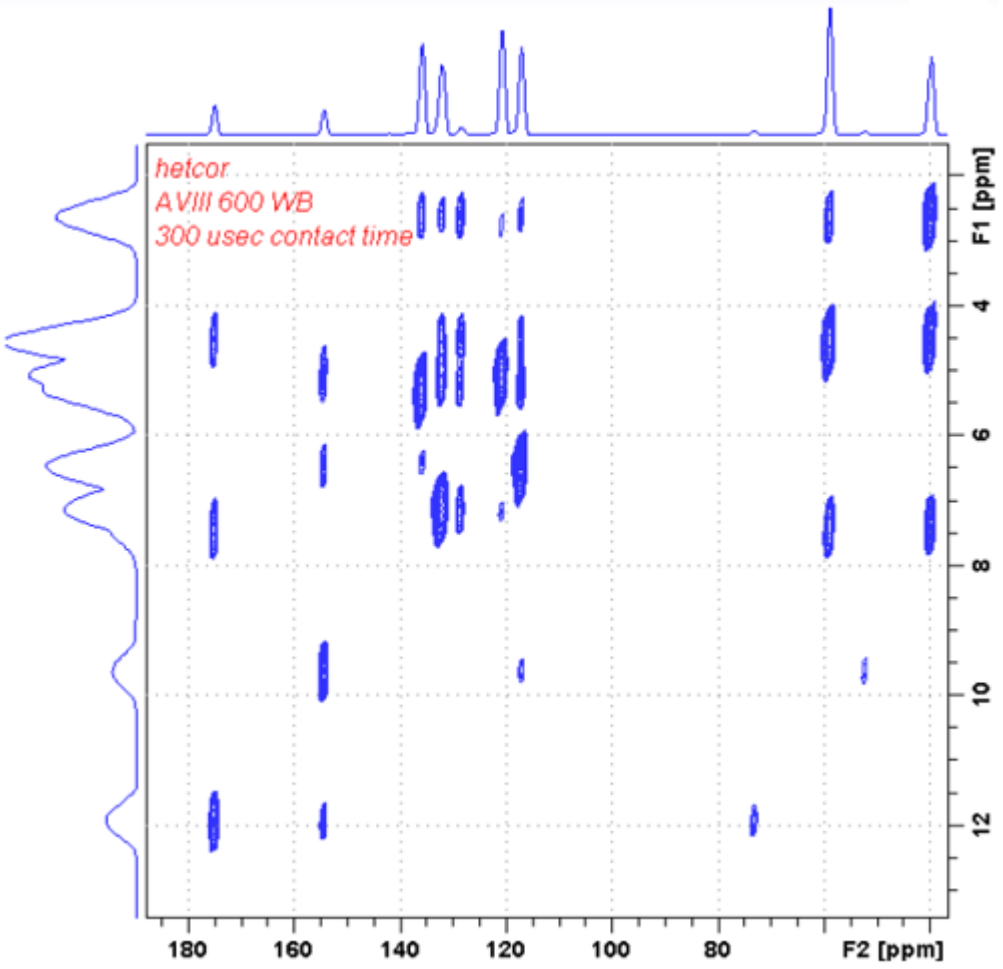

Figure 8.5. FSLG Hetcor Spectrum Tyrosine HCl

The figure above shows a FSLG Hetcor Spectrum Tyrosine HCl with parameters as shown in ***Table 8.1.***/***Table 8.2.***. Full transform with slight resolution enhancement, qsine/SSB=3. Proton shifts calibrated as 2.5 and 12 (most high field/low field peak). Expansion plot.

Modifications of FSLG HETCOR

9

The basic HETCOR sequence can be improved in several respects. The protons which are observed are all coupled to ^{13}C carbons (since we observe these). So the proton shifts evolve also under the residual dipolar coupling and the J-coupling to ^{13}C. This can be refocused by a ^{13}C π-pulse in the middle of the proton evolution. The pulse program ***lghetfqpi*** will serve this purpose.

Furthermore, it may be desirable to compare the proton shift spectrum obtained with X-observation (HETCOR) with the proton spectrum obtained by CRAMPS techniques (see chapters 22, 23, and 24), observing the protons directly. Usually, these experiments use phase modulated shapes (PMLG or DUMBO). In order to make both experiments comparable, it is favored to use the same type of proton shift evolution in both sequences. The pulse programs which use phase gradient shapes to achieve homonuclear proton dipolar decoupling are ***pmlghet*** and ***wpmlghet***. If DUMBO decoupling is desired, the pulse programs are dumbohet or edumbohet. These pulse programs use either windowless pulse trains, or windowed pulse trains which can be timed in exact analogy to the CRAMPS-type sequences wpmlg*2 and dumbo*2. These sequences also suppress the center ridge efficiently so that the carrier frequency need not be shifted out of the proton range during evolution (cnst24=0). In contrary, it is possible to shift the carrier to the proton shift range center.

A third modification addresses the problem of poor discrimination between sites which are strongly and weakly coupled to protons. In the standard sequence this is solely achieved setting contact times short. Of course, this reduces cross peaks from remote couplings more than it reduces cross peaks from directly bonded protons. However, the remote couplings are always present through the homonuclear coupling between all protons. These couplings can however be suppressed by executing the contact with a Lee-Goldburg proton offset. Then the protons are homonuclear decoupled, and the transfer from protons to X only follows the heteronuclear dipolar coupling between those. The pulse program ***lghetfqlgcp*** works completely in analogy to ***lghetfq***, but executes the contact at a proton offset calculated from the proton RF field during the spin lock contact pulse. This modifies the HH condition, which must be reestablished using the pulse program lgcp.

In the following sections, the specifics of these modified sequences are discussed.

Carbon Decoupling During Evolution 9.1

The only difference between ***lghetfq*** and ***lghetfqpi*** is the decoupling π-pulse at the center of the evolution period. All what needs to be set in addition is the X- π-pulse ***p2*** at power level ***pl1***. At fast spin rates and in fully labeled samples, the narrowing effect on the proton spectrum may be small or not noticeable, but on samples with natural abundance it may be noticeable. At long contact times and transfer from many different protons, the line width in the proton spectrum may also be insensitive. In fig. 1, two columns through the most up field aliphatic peak in tyrosine-HCl are shown. The π-decoupled trace (red) is clearly narrower.

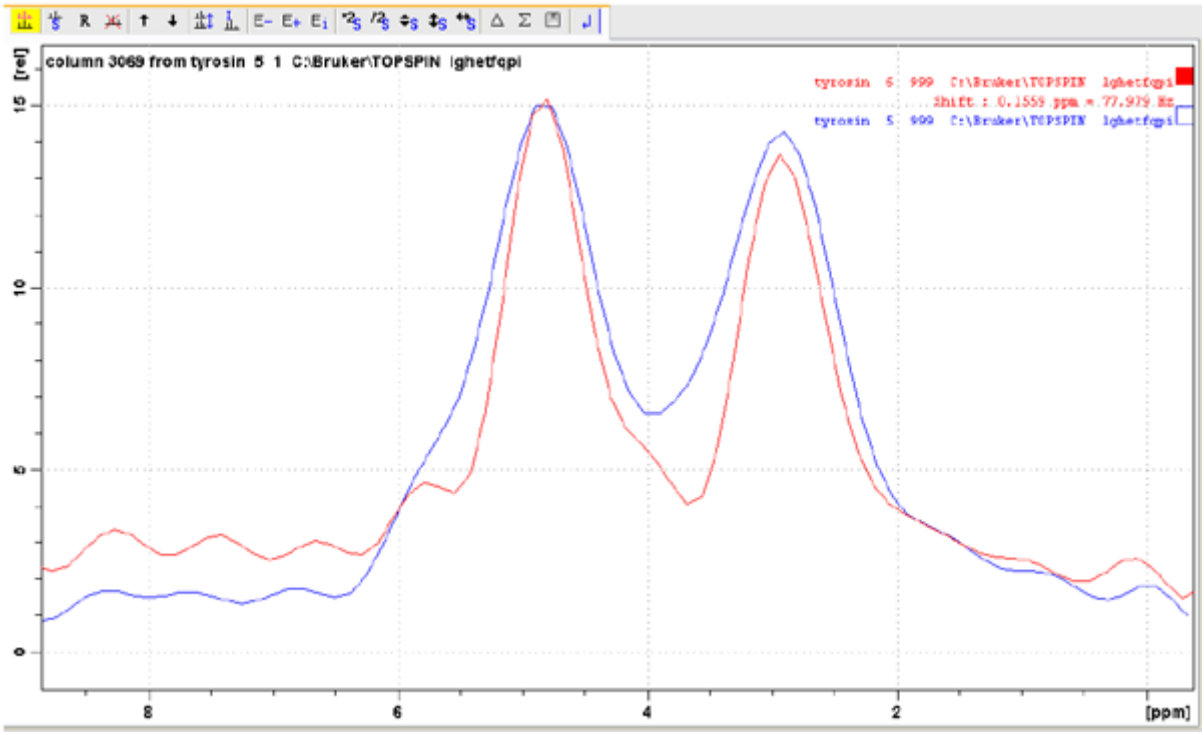

Figure 9.1. Comparison of HETCOR with and without ^{13}C-decoupling

The figure above shows a comparison of HETCOR with and without ^{13}C-decoupling. Natural abundance tyrosine-HCl was run with 50 µsec contact time.

Reference:

1. A. Lesage and L. Emsley, *Through-Bond Heteronuclear Single-Quantum Correlation Spectroscopy in Solid-State NMR, and Comparison to Other Through-Bond and Through-Space Experiments,* J. Magn. Res. 148, 449-454 (2001).

HETCOR with DUMBO, PMLG or w-PMLG, Using Shapes 9.2

These sequences use phase modulated shapes for homonuclear proton decoupling. Apart from some smaller differences, the sequences are in complete analogy to the HETCOR sequence using frequency shifts.

The only differences between these sequences lie in the length and type of shape used for homonuclear decoupling. DUMBO and e-DUMBO (Emsley et al.) use principles known from multiple pulse NMR operating on resonance, whereas pmlg and w-pmlg (Vega et al.) use phase ramps which act like frequency offsets and are therefore derivatives of FSLG.

References:

1. D. Sakellariou, A. Lesage, P. Hodgkinson and L. Emsley, *Homonuclear dipolar decoupling in solid-state NMR using continuous phase modulation,* Chem. Phys. Lett. 319, 253 (2000).
2. Vinogradov, E.; Madhu, P. K.; Vega, S., *High-resolution proton solid-state NMR spectroscopy by phase modulated Lee-Goldburg experiment*, Chem. Phys. Lett. (1999), 314(5,6), 443-450.
3. E. Vinogradov, P.K. Madhu and S. Vega, *Proton spectroscopy in solid state NMR with windowed phase modulated Lee-Goldburg decoupling sequences,* Chem. Phys. Lett. (2002), 354, 193.
4. Leskes, Michal; Madhu, P. K.; Vega, Shimon, *A broad banded z-rotation windowed phase modulated Lee-Goldburg pulse sequence for 1H spectroscopy in solid state NMR,* Chem. Phys. Lett. (2007), 447, 370-374.
5. Leskes, Michal; Madhu, P. K.; Vega, Shimon, *Supercycled homonuclear decoupling in solid state NMR: towards cleaner 1H spectrum and higher spinning rates,* J. Chem. Phys. (2007) in press.

The Sequence pmlghet 9.2.1

This sequence uses windowless phase ramped shapes. One can write these shapes as multiples of FSLG cycles to manipulate the length of the T_1-increment. Usually, 2 FSLG cycles make sense. The pulse program calculates the required shape pulse length from the RF-field during the FSLG-evolution. In pmlghet, a shape with 2 cycles is assumed in the calculation. The sequence is optimized for a simple twofold linear phase ramp (supplied as ***lgs-2***). The carrier may be placed in the middle of the proton spectrum during evolution which may allow using fewer increments and therefore saving time. However, one should be aware of the presence of proton spinning sidebands along F1 which may inappropriately fold in if the spectrum window along F1 is chosen too small.

Processing is done in complete analogy to the FSLG-experiment, as for all following sequences.

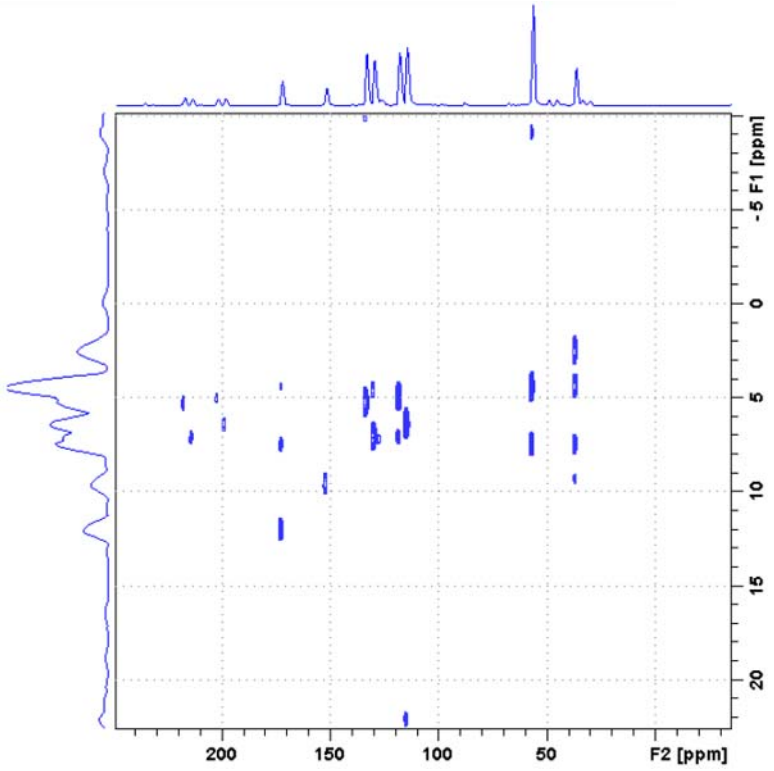

Figure 9.2. HETCOR Using Windowless Phase Ramps

The figure above shows the HETCOR using windowless phase ramped shapes for proton homonuclear decoupling during evolution. The carrier was placed in the middle of the proton spectrum and the usual carrier ridge was suppressed by phase cycling (Leskes et al., Chem. Phys. Lett.). This allows reduced measurement times. Pmlghet, wpmlghet, dumbohet and edumbohet should give rather similar spectra.

Table 9.1. Acquisition Parameters for pmlg-HETCOR (on tyrosine-HCl)

Parameter	Value	Comments
pulprog	pmlghet	Using phase ramps.
nuc1	13C	
o1p	100 ppm	
nuc2	1H	
cnst20	80-100000	Proton spin nutation frequency with PL13.
cnst24	1000-3000	Place carrier within proton spectrum for evolution.
pl1		Power level channel 1 for contact pulse.
pl12		Power level channel 2 TPPM/SPINAL decoupling.
pl13		Power level channel 2 PMLG decoupling.

Table 9.1. Acquisition Parameters for pmlg-HETCOR (on tyrosine-HCl)

sp0		Power level channel 2 for contact pulse.
spnam0	ramp.100 or similar	Shape for contact pulse channel f2.
sp1	set to pl13	To match cnst20.
spnam1	lgs-2	To match ppg calculation of in0, in_f1.
p3	2.5 – 3 µsec	90º pulse channel 2 at pl12.
p15	50 -500µs	Contact pulse width.
pcpd2	≈ 2*p3	SPINAL64 /TPPM decoupling pulse.
cpdprg2	SPINAL64/TPPM15	Decoupling sequence.
F1 ^{1}H indirect		
l0	0	Start value 0, incremented during expt.
l3	2- 4	Multiples of FSLG-periods, increment per row.
in_f1	=in0 as calculated	Set according to value calculated by ***ased***.
F2 ^{13}C acquisition		
d1	2s	Recycle delay.
sw	310ppm	Sweep width direct dimension.
aq	16-20 msec	
masr	10-15 kHz	15 kHz ok at 100 kHz RF-field.

Table 9.2. Processing Parameters for pmlg-HETCOR (as for FSLG on tyrosine-HCl)

Parameter	Value	Comment
F2 direct dim ^{13}C		
si	2-4 k	
wdw	QSINE	SSB 2, 3 or 5.
ph_mod	pk	
F1 indirect ^{1}H		
si	256-1048	
mc2	STATES-TPPI	
wdw	QSINE	
ssb	3, 5	
ph_mod	pk	

w-pmlghet ***9.2.2***

If one wants to compare a solids proton spectrum, acquired via ^{13}C detection (using HETCOR) and a direct detect proton spectrum (using w-pmlg), it is useful to do this using exactly the same parameters (power levels and timings) in both experiments. If w-pmlg is used and optimized for the direct detect experiment, the same parameters will work with w-pmlghet, provided that both experiments are done with the same probe.

Table 9.3. Acquisition Parameters for wpmlg-HETCOR (on tyrosine-HCl)

Parameter	Value	Comments
pulprog	wpmlghet	Phase ramp allows detection window.
nuc1	13C	
o1p	100 ppm	
nuc2	1H	
cnst20	usually >=100 kHz	As prepared with wpmlgd proton detect exp.
cnst24	1000-3000	Place carrier within proton spectrum for evolution.
pl1		Power level channel 1 for contact pulse.
pl12		Power level channel 2 TPPM/SPINAL decoupling.
pl13		Power level channel 2 w-PMLG decoupling.
sp0		Power level channel 2 for contact pulse.
spnam0	ramp.100 or similar	Shape for contact pulse channel f2.
sp1	set to pl13	To match cnst20.
spnam1	m5m or m5p	Both include one FSLG cycle.
p3	2.5 – 3 µsec	90º pulse channel 2 at pl12.
p15	50 -500 µsec	Contact pulse width.
pcpd2	≈ 2*p3	SPINAL64 /TPPM decoupling pulse.
cpdprg2	SPINAL64/TPPM15	Decoupling sequence.
F1 ^{1}H indirect		
l0	0	Start value 0, incremented during expt.
l3	2- 4	Multiples of FSLG-periods, increment per row.
in_f1	=in0 as calculated	Set according to value calculated by ***ased***.
F2 ^{13}C acquisition		
d1	2s	Recycle delay.
sw	310ppm	sweep width direct dimension.
aq	16-20 msec	

edumbohet ***9.2.3***

DUMBO decoupling is as efficient as PMLG decoupling. As discussed in chapters 22 and 23, it requires to spin a bit slower (up to 12-13 kHz) and to place the carrier closer to resonance. Faster spinning is possible with higher power pulses and shorter pulse widths (24 usec or 16 usec). The library of AU-programs in TopSpin includes ***dumbo***, which calculates the desired shapes for windowed and windowless DUMBO shapes. If the windowless version is desired, the e-dumbo shape is preferred. Typing xau dumbo starts a dialog, in which e (for e-dumbo 22), 1 for the number of cycles, 64 for the number of steps, and 0 for an added angle (this value would be added to all phases in the shape). The program sets ***p20*** to 32 µsec as default. This is appropriate for an RF field of 100 kHz. ***Spnam2*** is set to edumbo22_1+0.

Table 9.4. Acquisition Parameters for e-DUMBO-HETCOR (on tyrosine-HCl)

Parameter	Value	Comments
pulprog	edumbohet	windowless dumbo shape.
nuc1	13C	
o1p	100 ppm	
nuc2	1H	
cnst24	1000-3000	Place carrier within proton spectrum for evolution.
pl1		Power level channel 1 for contact pulse.
pl12		Power level channel 2 TPPM/SPINAL decoupling.
pl13	for 100 kHz	Power level channel 2 DUMBO decoupling.
sp0		Power level channel 2 for contact pulse.
spnam0	ramp.100 or similar	Shape for contact pulse channel f2.
sp2	set to pl13	100 kHz for default duration 32 µs.
spnam2	edumbo22_1+0	Both include one e-DUMBO cycle.
p3	2.5 – 3 µsec	90º pulse channel 2 at pl12.
p15	50 -500µs	Contact pulse width.
p20	32 µs	32 µs for 100 kHz field, set by xau dumbo.
pcpd2	≈ 2*p3	SPINAL64 /TPPM decoupling pulse.
CPDPRG2	SPINAL64/TPPM15	Decoupling sequence.
F1 ^{1}H indirect		
l0	0	Start value 0, incremented during expt.
l3	2- 4	Multiples of e-DUMBO period, increment per row.
in_f1	=in0 as calculated	Set according to value calculated by ***ased***.

Table 9.4. Acquisition Parameters for e-DUMBO-HETCOR (on tyrosine-HCl)

F2 ^{13}C acquisition		
d1	2s	Recycle delay.
sw	310 ppm	Sweep width direct dimension.
aq	16-20 msec	
masr	12000-13000	

dumbohet *9.2.4*

This is the windowed version of the previous experiment, analogous to wpmlghet. Run ***xau dumbo***, select d (for dumbo), 1 (for 1 cycle), 0 (for added angle). The calculated shape, dumbo_1+0 will be entered as spnam1, p10 will be set to 32 µsec. The projection of this experiment can be compared to the result of a direct proton detected CRAMPS experiment, using dumbod2. At higher fields, p10 may have to be set to 24 rather than 32 µsec for better resolution. The same pulse length p10, the same shape, the same window (p9) and the same power level should be used in both experiments.

The resolution along the proton dimension is comparable for all these experiments. The FSLG experiment is the most forgiving, requiring just the knowledge of the RF power level for decoupling at a certain RF field. Setting cnst20 to this RF-field (+ 5 or 10%) is all that needs to be set, if the ^{13}C observe parameters are well adjusted.

Table 9.5. Acquisition Parameters for DUMBO-HETCOR (on tyrosine-HCl)

Parameter	Value	Comments
pulprog	dumbohet	Windowed dumbo shape.
nuc1	13C	
o1p	100 ppm	
nuc2	1H	
cnst24	1000-3000	Place carrier within proton spectrum for evolution.
pl1		Power level channel 1 for contact pulse.
pl12		Power level channel 2 TPPM/SPINAL decoupling.
pl13		Power level channel 2 DUMBO decoupling.
sp0		Power level channel 2 for contact pulse.
spnam0	ramp.100 or similar	Shape for contact pulse channel f2.
sp1	set to pl13	100 kHz for default duration 32 µs.
spnam1	dumbo_1+0	Both include one DUMBO cycle.
p3	2.5 – 3 µsec	90º pulse channel 2 at pl12.

Table 9.5. Acquisition Parameters for DUMBO-HETCOR (on tyrosine-HCl)

p15	50 -500μs	Contact pulse width.
p10	32 or 24μs	32 μs for 100 kHz field, 24 μs for better resolution at high magnetic fields (>500 MHz).
pcpd2	≈ 2*p3	SPINAL64 /TPPM decoupling pulse.
cpdprg2	SPINAL64/TPPM15	Decoupling sequence.
F1 ^{1}H indirect		
l0	0	Start value 0, incremented during expt.
l3	2- 4	Multiples of DUMBO-periods, increment per row.
in_f1	=in0 as calculated	Set according to value calculated by ***ased***.
F2 ^{13}C acquisition		
d1	2s	Recycle delay.
sw	310ppm	Sweep width direct dimension.
aq	16-20 msec	
masr	12000-13000	

HETCOR with Cross Polarization under LG Offset *9.3*

Usually, the cross polarization step is executed at less power than what is used for the initial excitation pulse and decoupling during observe. Therefore, a second LG condition must be set for the power level during contact. Furthermore, the HH condition must be re-established, since the proton spin lock pulse now must be a square pulse, not a ramp. The ramp can be transferred to the carbon (F1) side.

The following steps are involved:

1. The RF field for protons during contact must be measured and adjusted. With linearized transmitters, the required power level can be calculated from a known reference pulse width.
2. The LG frequency offset must be calculated from the RF field (RF/sqrt(2)).
3. The HH condition must be reestablished, varying the F1 (^{13}C)-RF field.

As the effective field, required to match for both nuclei at the HH condition, is the vector sum of RF-field and frequency offset, a higher power pulse is required on F1 with increasing offset. So it is recommended not to set the proton power higher than to 50 kHz RF field. For the setup, the pulse program lgcp is used. It contains an include file lgcalc2.incl which will calculate the LG offset from a given RF field specified as ***cnst17***. It will set the calculated offset as ***cnst19*** during contact. In ***ased***, it will calculate also ***cnst16***, which shows the effective field under ***cnst17*** RF field and ***cnst18***, ***cnst19*** offset. The X contact pulse is executed as (ramp)-shape. Any standard ramp is possible, but a flat ramp (70-100% or 90-100%) is preferred. Usually, calculating the required RF field for the HH match can be done in the following way:

1. Load the pulse program lgcp into a standard CP/MAS data set with all parameters set and optimized. Set p14 to about 54° flip angle. Use tyrosine *HCl or the sample of interest.
2. From p3, calculate the power level ***pl2*** for 50 kHz RF field, using calcpowlev.
3. Enter ***cnst17***= 50000, type ***ased***. Read the value of ***cnst16*** (=effective field under ***cnst18***, ***cnst19*** offset (about 61000 Hz). Add or subtract the spin rate used, for instance spinning at 13 yields 74000 or 48000 Hz. If a 30% ramp is used, and ***sp0*** is set to 74000 (with a safety margin of 1000), the HH condition will cover 75000 down to 45000 Hz RF field. This includes both HH sidebands n=±1.
4. Optimize the HH-condition varying ***sp0***, and ***p14***, ***phcor1*** for maximum signal.
5. Run a variation of ***p15*** between 20 and 5000 ms on your sample (or tyrosine *HCl). One should see intensity variations (“dipolar oscillations”) which are normally smeared out by extensive homonuclear dipolar couplings between protons.
6. Set up a 2D data set with the pulse program lgcphetfq. The figures below compare spectra taken with and without LG-offset during cp.

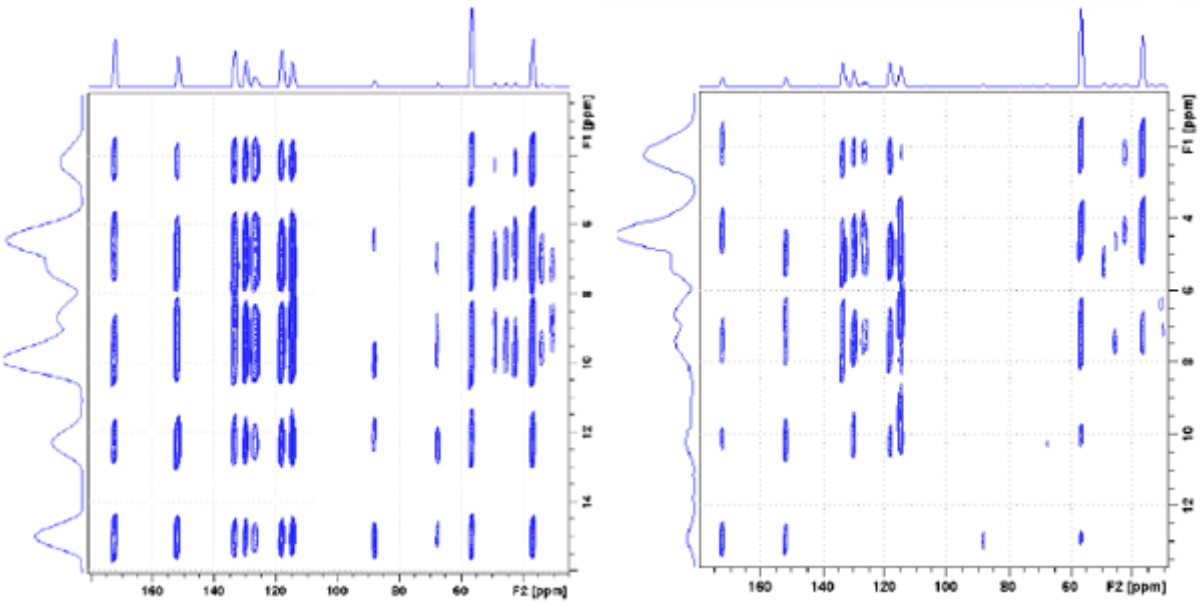

*Figure 9.3. HETCOR on tyrosine *HCl without (left) and with LG contact (1msec contact)*

RFDR 10

Radio Frequency-Driven Recoupling (RFDR) with longitudinal magnetization exchange is a homonuclear dipolar recoupling experiment. This easy setup technique is a zero-quantum recoupling sequence that achieves chemical shift correlation under MAS conditions. The time-dependence of the cross peak amplitudes can be employed to determine inter-nuclear distances. With short dipolar recoupling times, only spins in close spatial proximity lead to cross peak facilitating assignment of ^{13}C resonances in uniformly labelled peptides for instance. RFDR may also be used in order to correlate chemical shifts and crystallographic sites on materials samples.

The homonuclear dipolar recoupling is implemented via the application of rotor-synchronised 180-degree pulses (one inversion pulse per rotor period). The phases of the 180-degree pulses are cycled with Gullion's compensated XY-8 echo sequence in order to achieve efficient recovery of single spin magnetization and to generate an effective dipolar recoupling Hamiltonian during the mixing period. The critical experimental point is to avoid ^{1}H-X recoupling induced by interference between the ^{1}H decoupling rf field and ^{13}C rf recoupling field. This effect can be removed using a ^{1}H decoupling rf field 3 times as strong as the ^{13}C rf field used for recoupling or by using Lee-Goldburg ^{1}H decoupling during the mixing period.

References:

1. T. Gullion, D. B. Baker and M. S. Conradi, *New, compensated Carr-Purcell sequences*, J. Magn. Reson. 89, 479-484 (1990).
2. A. E. Bennett, J. H. Ok, R. G. Griffin and S. Vega, *Chemical shift correlation spectroscopy in rotating solids: Radio frequency-driven dipolar recoupling and longitudinal exchange*, J. Chem. Phys. 96, 8624-8627 (1992).
3. A. E. Bennett, C. M. Rienstra, J. M. Griffith's, W. Zhen, P. T. Lansbury and R. G. Griffin, *Homonuclear radio frequency-driven recoupling in rotating solids*, J. Chem. Phys. 108, 9463-9479 (1998).
4. B. Heise, J. Leppert, O. Ohlenschläger, M. Görlach and R. Ramachandran, *Chemical shift correlation via RFDR: elimination of resonance offset effects*, J. Biomol. NMR 24, 237-243 (2002).

Experiment 10.1

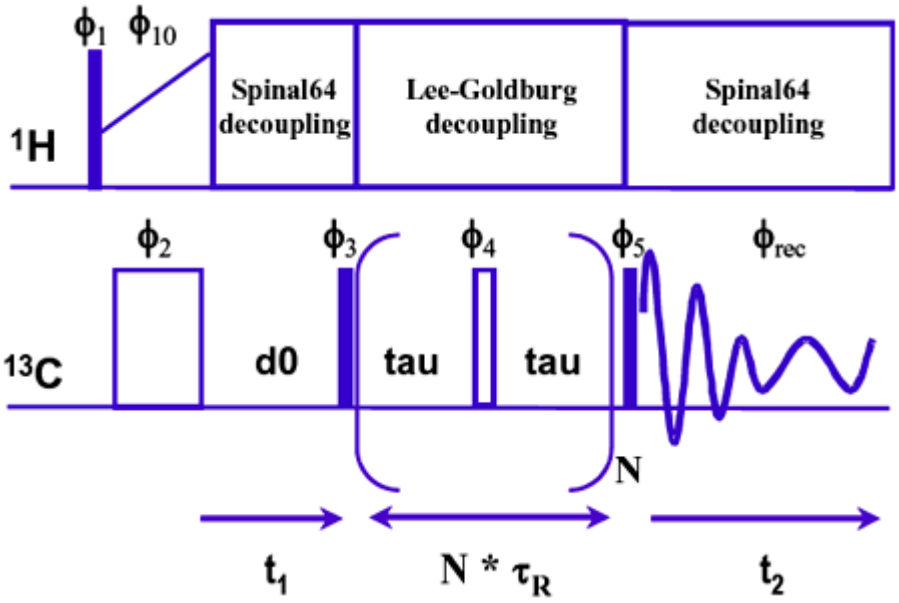

ϕ_1 = 1	ϕ_4 = 0101 1010	
ϕ_2 = 1	ϕ_5 = 0303 0303, 1010 1010	
ϕ_3 = 0123 0321	ϕ_{10} = 0	ϕ_{rec} = 0220 0220, 1331 1331

Figure 10.1. RFDR Pulse Sequence for 2D CPMAS Exchange Experiment

Set-up 10.2

Sample: ^{13}C fully labelled histidine.

Experiment time: Less than 1 hour.

Experiment Setup

First setup the ^{1}H-^{13}C cross polarization and the Hartmann-Hahn match according to the procedures described in ***"Basic Setup Procedures" on page 55***.

An important experimental consideration of the RFDR experiment is that the r.f. field strengths used in the recoupling channel (***pl11***) and the r.f. field on the ^{1}H decoupling channel must be sufficiently different, *ca.* a factor of 3, to avoid rapid de polarization of the carbon signal during the mixing time. This is usually not achievable, so it should be set as high as possible, using a LG-offset.

During the mixing period (***cpds3=cwlg***), as shown in ***Figure 10.1.***, the Gullion compensated echo sequence used for the mixing period is a XY-8 phase cycling (f_4=XYXY YXYX). Consequently, the number of rotor periods for the mixing time (***L1***) must be a multiple of 8.

Data Acquisition 10.3

Sample: ^{13}C fully labelled histidine.

Experiment time: Several hours.

Set-up 2D Experiment 10.3.1

After 1D parameter optimization as previously described, type ***iexpno*** to create a new data file and switch to the 2D mode using the “123” button. Set the appropriate ***FnMode*** parameter in ***eda***. Pulse program parameters are indicated below (***Figure 10.1.*** shows the pulse sequence).

Figure 10.2. The “123” Icon in the Menu Bar of the Data Windows Acquisition Parameter Page

*The “123” icon in the menu bar of the data windows acquisition parameter page (see **Figure 10.2.**)is used to toggle to the different data acquisition modes, 1D, 2D and 3D if so desired.*

Table 10.1. Acquisition Parameters

Parameter	Value	Comments
pulse program	cprfdr.av	Pulse program.
nuc1	^{13}C	Nucleus on f1 channel.
o1p	100 ppm	^{13}C offset, to be optimized.
nuc2	^{1}H	Nucleus on f2 channel.
o2p	2-3 ppm	^{1}H offset, to be optimized.
pl1		Power level for contact time on f1 channel.
pl11		Power level for f1 recoupling and excitation.
pl2		Power level for contact time on f2 channel.
pl12		Power level decoupling f2 channel and excitation.
pl13		Power level LG decoupling f2 channel.
p1		90° excitation pulse on f1 channel.
p2		180° excitation pulse on f1 channel.
p3		90° excitation pulse on f2 channel.
p15		Contact pulse on f1 and f2 channel.
d0	3µ	t1 evolution period.
d1		Recycle delay.
cpdprg2	Spinal64	Spinal64 decoupling on f2 channel.
cpdprg3	***cwlg***	cwlg decoupling on f2 channel.
ns	16	Number of scans.
cnst20	≈100000	Proton rf field in Hz to calculate LG parameters.
cnst21	0	f2 channel offset.
cnst24		Additional Lee-Goldburg offset.
cnst31		Spinning speed in Hz.
l1	for 2-40 msec	Number of rotor cycles for mixing time.
F2 direct ^{13}C		Left column.
td	4k	Number of complex points.
sw	200 ppm	Sweep width direct dimension.
F1 indirect ^{13}C		Right column.
td	256	Number of real points.
sw		Rotor synchronized sweep width, or = 2 sw.

Table 10.1. Acquisition Parameters

in_f1	= dw or rotor period	Synchronised sampling avoids sidebands.
FnMode		STATES or STATES TPPI.

Spectral Processing *10.4*

Table 10.2. Processing Parameters

Parameter	Value	Comment
F1 acquisition ^{13}C		Left column.
si	4k	Number of points and zero fill.
ph_mod	pk	Phase correction if needed.
bc_mod	quad	DC offset correction.
F2 indirect ^{13}C		Right column.
si	256	Zero fill.
mc2		STATES or STATES TPPI.
ph_mod	pk	Phase correction if needed.
bc_mod	no	Automatic baseline correction.

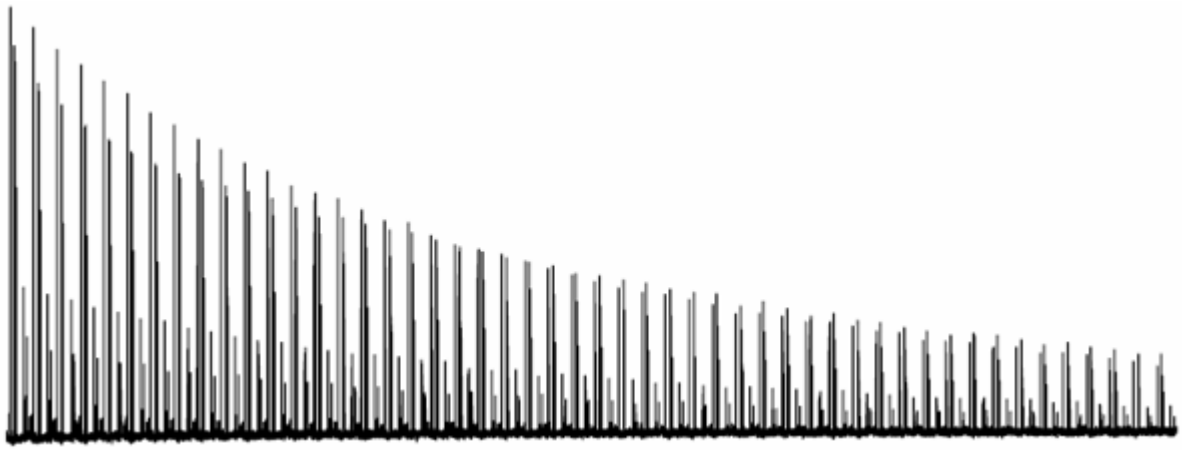

Figure 10.3. ^{13}C Histidine Signal Decay as a Function of the RFDR Mixing Time

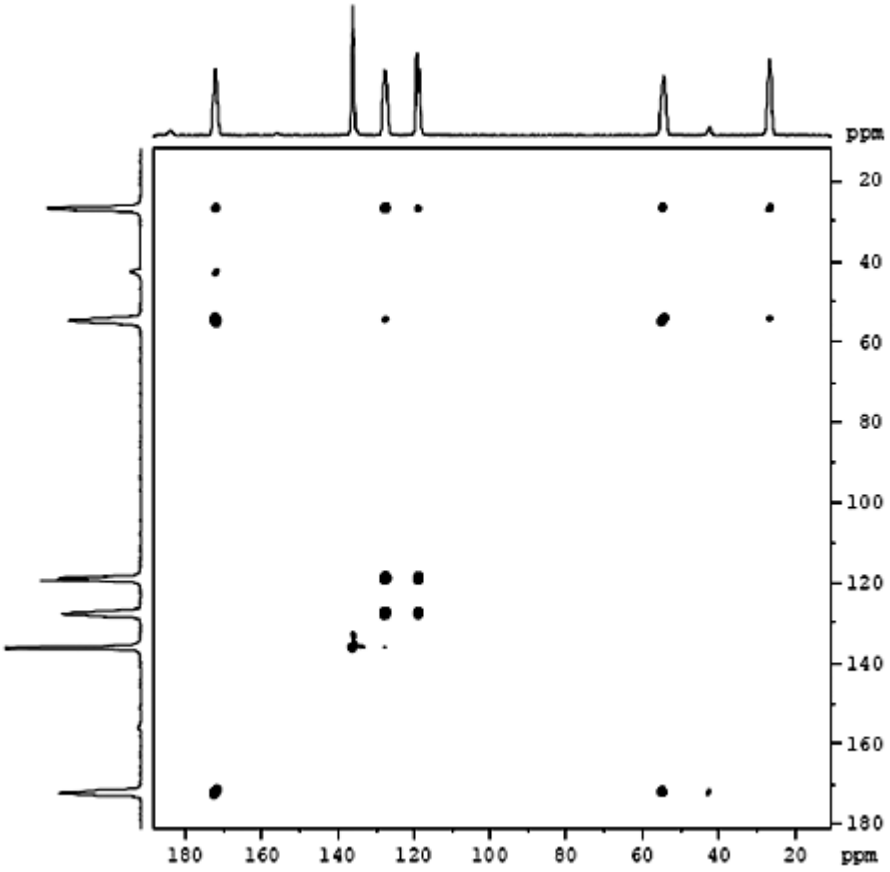

Figure 10.4. 2D RFDR Spectrum of ^{13}C fully Labelled Histidine (RFDR mixing time 1.85 ms).

Proton Driven Spin Diffusion (PDSD) 11

PDSD is a 2D experiment that correlates a spin 1/2 nucleus to another spin of the same species via homonuclear dipolar coupling or chemical exchange. The experiment resembles the NOESY (Nuclear Overhauser Effect SpectroscopY) pulse sequence in the liquid state by replacing the initial 90° pulse with a cross polarization scheme. Since spin diffusion between X-nuclei is measured, cross peak intensities depend on the probability of interaction between different sites, which is low with low natural abundance of NMR-active nuclei. Therefore, these experiments usually require enrichment for nuclei like ^{13}C or ^{15}N in order to allow sensible measurement times.

The pulse program ***cpspindiff*** allows to run several types of PDSD experiments. The CP *preparation* period excites the X nuclei. During the *evolution* time the X magnetization evolves under the effect of the chemical shift interaction. The *evolution* time ends with an X 90° pulse that stores the chemical shift information along the z axis and marks the beginning of the *mixing* time. The X spins communicate through chemical exchange or spin diffusion, depending on the properties of the material and the duration of the *mixing* time. At the end of the *mixing* period, another X 90° (read) pulse and the data *acquisition* follow. The usually strong ^{1}H-X dipolar interaction is removed by high power ^{1}H decoupling during the *preparation* and the *acquisition* time. The ^{1}H decoupling is switched off during the *mixing* to dephase the residual X transverse magnetization. Spin diffusion between X-nuclei is usually very slow and requires very long mixing times since the dipolar coupling between all X-nuclei is small. However, turning the proton decoupling field off during the mix period allows another process to take place: spin diffusion via the proton spin system. Since the rare nuclei are strongly coupled to protons and all protons are strongly coupled to each other, the flip flop transition rate is high along the X_1-H_1-H_2-X_2-pathway. In fact, the spin exchange is almost solely due to proton mediated mechanisms except when chemical exchange is present. At high spin rates, spin diffusion may however still be slow since the X-H spins are decoupled. A simple procedure to recouple the X-H interaction is to irradiate the protons at an RF field of n times the spin rate. These modified sequences are DARR (Dipolar Assisted Rotational Resonance, T. Terao et al.) or RAD (Rf Assisted Diffusion, see C.R. Morcombe et al).

The setup for all these sequences is rather robust, requiring only the ^{1}H to X Hartmann-Hahn condition and the X 90° hard pulse to be set. For RAD and DARR, it is usually sufficient to calculate an RF power level corresponding to n times the spin rate, which is then applied during the mixing period. Rotor synchronization of the *mixing* period is recommended in some cases, where cross peaks due to sidebands need to be suppressed (de Jong et al.) or where spin diffusion is enhanced by matching the spin rate with the chemical shift difference between the sites to be correlated (M. Ernst et al.). PDSD is typically applied to high abundance nuclei or labeled materials to detect through space proximity between spins. This experiment has been often used on proteins as an alternative to Radio Frequency DRiven spin diffusion (see ***"RFDR" on page 137***). RFDR provides similar information to PDSD but with a different *mixing* period. Here the term “frequency driv-

en" relates to recoupling pulses on the X channel, whereas in DARR or RAD the radio frequency that drives the recoupling is the proton RF.

An important aspect of this experiment is that the *mixing* time is a simple delay and no pulse, or only weak rf irradiation (DARR, RAD) is required. Therefore it can be made very long because no technical or experimental problems can arise. So the effects even of small dipolar couplings (requiring long spin diffusion times) can be observed. However the information from this experiment may be ambiguous, because a rather non-selective transfer (within the proton spin system) is utilized.

Nevertheless, even complex molecules like proteins can be surprisingly well characterized by PDSD experiments with different *mixing* times. The buildup of cross peak intensities can be studied and correlated, for instance, to the structure of a macromolecule in the solid state. The same approach has been used to compare different states of a protein, i.e. bound to a membrane or free, as can be found in the recent literature on solid state NMR applied to protein studies.

More elaborate derivatives of PDSD are also known in bio-molecular NMR, where the unspecific spin diffusion within the proton spin system is filtered through a double quantum selection (Lange et al.).

References:

1. N.M. Szeverenyi, M.J. Sullivan, and G.E. Maciel, Observation of Spin Exchange by Two-Dimensional Fourier Transform ^{13}C Cross Polarization Magic Angle Spinning, J. Magn. Reson. 47, 462-475 (1982).
2. A.F. de Jong, A. P. M. Kentgens, and W. S. Veeman, Two-Dimensional Exchange NMR in Rotating Solids: a technique to study very slow molecular motions, Chem. Phys. Lett. 109, 4, 337 (1984).
3. Matthias Ernst and Beat H. Meier, *„Spin Diffusion*" in Isao Ando and Tetsuo Asakura, Eds., „Solid-State NMR of Polymers", pp. 83-122, Elsevier Science Publisher (1998).
4. Matthias Ernst, Arno P.M. Kentgens, and Beat H. Meier, Pure-Phase 2D-Exchange NMR Spectra under MAS, Journal of Magnetic Resonance **138**, 66-73 (1999), and references cited therein.
5. K. Takegoshi, Shinji Nakamura and TakehikoTerao, ^{13}C-^{1}H dipolar-assisted rotational resonance in magic-angle spinning NMR, Chem. Phys. Lett. 2001, 344, 631.
6. F. Castellani, B. van Rossum, A. Diehl, M. Schubert, K. Rehbein and H. Oschkinat, Structure of a protein determined by solid-state magic-angle-spinning NMR spectroscopy, Nature 420, 98-102 (2002).
7. C.R. Morcombe, V. Gapenenko, R.A. Byrd, and K. W. Zilm, Diluting Abundant Spins by Isotope Edited Radio Frequency Field Assisted Diffusion, J. Am. Chem. Soc. 126, 7196-7197 (2004).
8. S.G. Zech, A.G. Wand and A.E. McDermott Protein Structure Determination by High-Resolution Solid-State NMR Spectroscopy: Application to Microcrystalline Ubiquitin, J. Am. Chem. Soc. 127, 8618-8626 (2005).
9. W. Luo, X. Yao and M. Hong Large Structure Rearrangement of Colicin Ia channel Domain after Membrane Binding from 2D ^{13}C Spin Diffusion NMR), J. Am. Chem. Soc. 127, 6402-6408 (2005).
10. A.Lange, S. Luca, and M. Baldus, Structural constraints from proton-mediated rare spin correlation spectroscopy, J. Amer. Chem. Soc.**, 124**, 9704-9705 (2002).

Pulse Sequence Diagram 11.1

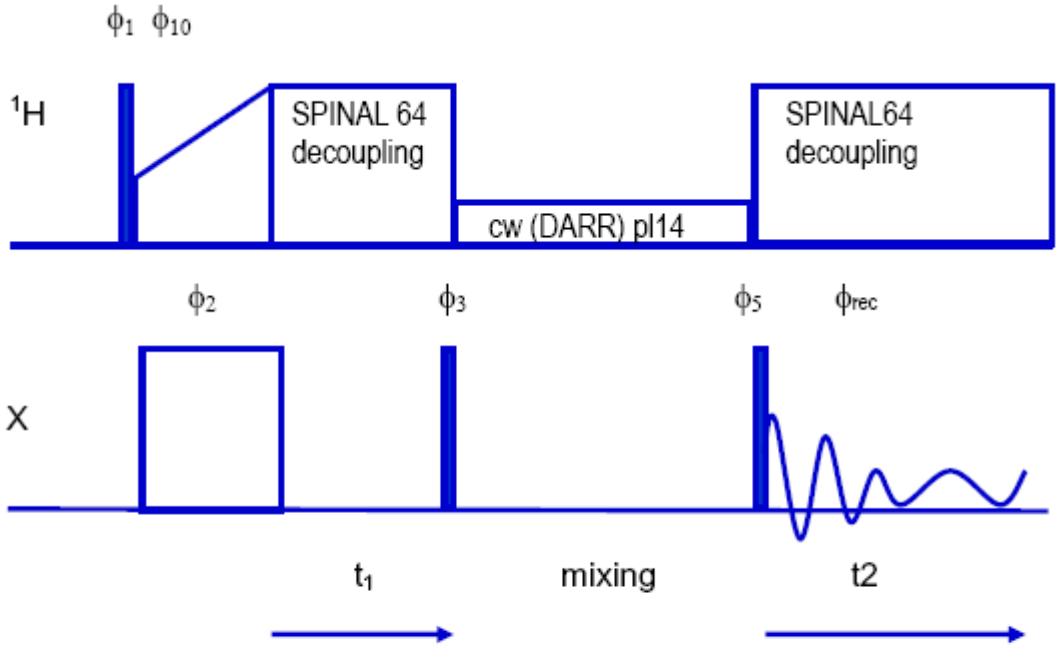

$\phi_1 = 1, 3$	$\phi_2 = 1$	$\phi_3 = 0\,0\,0\,0\,0\,0\,0\,0$ $2\,2\,2\,2\,2\,2\,2\,2$
$\phi_5 = 0\,0\,2\,2\,1\,1\,3\,3$	$\phi_{10} = 0$	$\phi_{rec} = 0\,2\,2\,0\,1\,3\,3\,1$ $2\,0\,0\,2\,3\,1\,1\,3$

Figure 11.1. CPSPINDIFF Pulse Sequence

Basic Setup 11.2

1. On a standard sample (i.e. glycine) determine HH match and decoupling parameters.
2. Check the X 90° hard pulse with *cp90* on the standard sample.
3. If the real sample does tune and match very differently than the setup sample, verify the HH conditions briefly and eventually the X 90° hard pulse.
4. Set the spin rate as high as possible, make sure to avoid rotational resonance conditions (overlap between center bands and sidebands), recheck the HH condition. Set *cnst31*=spin rate.
5. Optimize contact time, o1 and o2 on a ^{13}C 1D CP experiment if necessary.
6. Create a new experiment with either *iexpno* or *edc*.
7. Change to a 2D data set.

8. Type *iexpno* to create a new data file and switch to the 2D mode using the “123” button. Load the pulse program *cpspindiff.*
9. Recheck pulse widths and power levels, using *ased*.
10. Go into *eda* and set parameters for sampling in the indirect dimension, the spectral width *1 swh*. Note, that in TopSpin 2.1 or later the parameter *IN_F1* replaces the parameters *in0* and *nd0*. Usually, *1 swh* equals *swh*. Choose a suitable spin rate such that no RR condition occurs and sidebands do not overlap with peaks, if possible set the sweep width in F1 *1 swh* equal to the spin rate or such that sidebands folding in along F1 do not interfere.
11. Make sure the correct nucleus is selected in the F1 dimension; make sure to choose an appropriate quadrature detection mode in *FnMode* (usually STATES-TPPI).
12. Choose the appropriate sampling time (*td1*) so that the required resolution (*FIDRES*) in the indirect dimension is achieved.
13. Set the desired mixing time as ***d8***. The required multiple of spin periods (from ***cnst31***) is calculated as ***l1***, the real mixing time may deviate by fractions of a rotor period. The required mixing time may vary widely depending on the sample properties, from a few milliseconds to hundreds of milliseconds, if long distance correlations in a mobile sample need to be observed. Note that longer mixing times will result in S/N deterioration, as the mixing time approaches the T_1 of the observed nuclei.

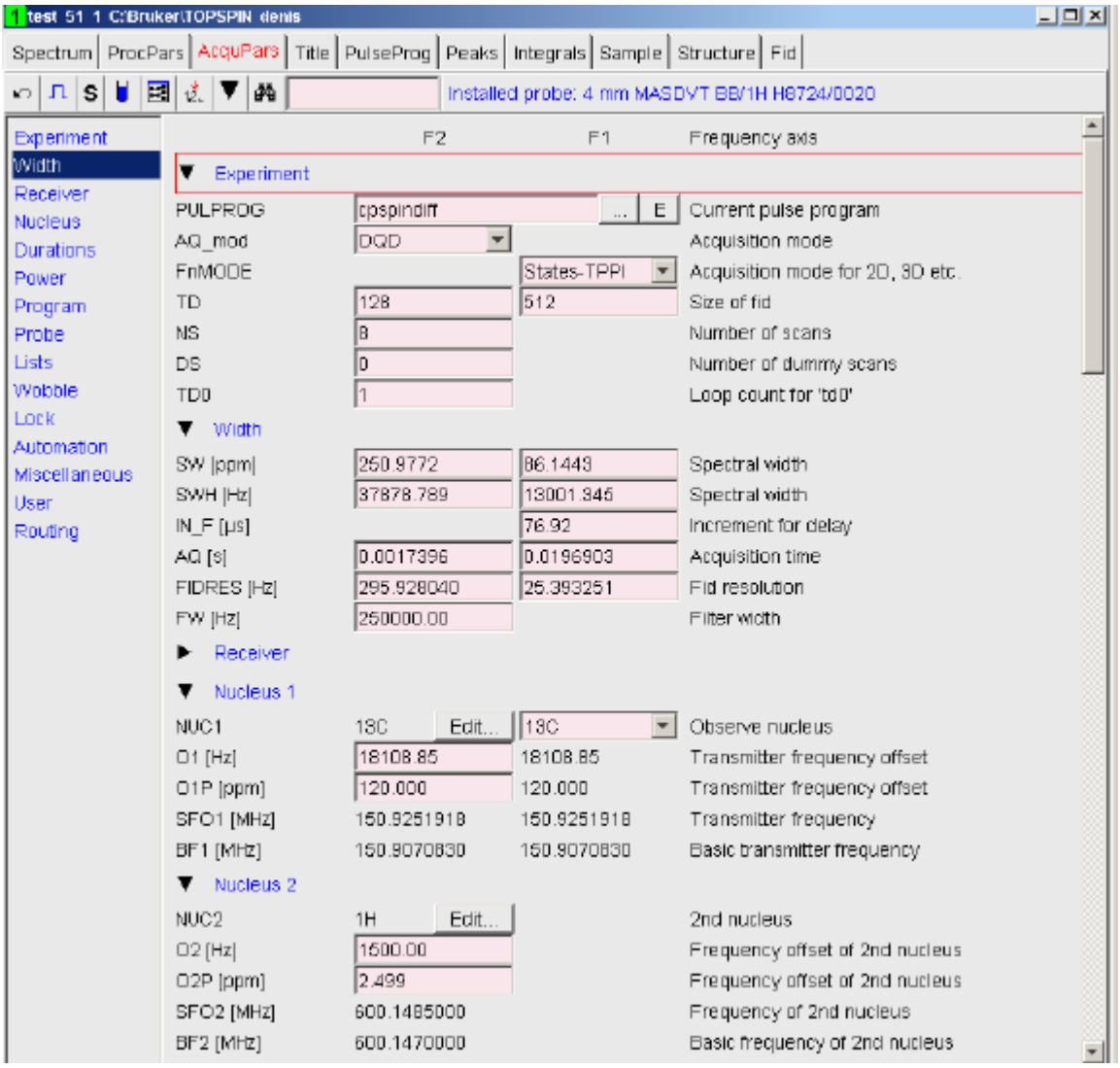

Figure 11.2. The Acquisition Parameter Window (eda)

14. Set *pl14*, if DARR/RAD is desired, else make sure *pl14 = 120 dB*. For DARR/RAD calculate the required power level using calcpowlev, or use the setup procedure shown in 11.7.
15. Start the experiment.

Acquisition Parameters *11.3*

Sample: ^{13}C labelled histidine (labelled tyrosine-HCl).

Experiment time: 90 min. (20 min.).

Table 11.1. Acquisition Parameters

Parameter	Value	Comments
PULPROG	cpspindiff (old: cpnoesy)	Pulse program.
NUC1	^{13}C	Set ^{13}C in both F2 and F1 column.
SW	250 ppm	To be optimized.
O1P	120 ppm	To be optimized.
NUC2	^{1}H	For CP/decoupling only.
O2P	3 ppm	To be optimized for dec.
PL1		For ^{13}C contact.
PL11		For ^{13}C flip pulses.
PL12		For ^{1}H excitation and decoupling.
PL14	for n*spin rate (DARR) or 120	Recoupling.
SP0		For ^{1}H contact using shape.
SPNAM0	ramp.100 or ramp70100.100	For ^{1}H-^{13}C contact.
CPDPRG2	SPINAL64	At PL12.
P1		^{13}C excitation (flip) pulse.
P3		^{1}H excitation pulse.
P15		^{13}C-^{1}H Contact pulse.
PCPD2		Decoupling pulse for spinal64.
D1		Relaxation delay.
D8	5-500 msec	Depending on sample.
CNST31	MAS speed	Used to calculate d31 (rotation period).
L1	calculated from cnst31 and d8	Number of rotor cycles for mixing time.
AQ_MOD	DQD	
TD {F1}	512	Number of points.
SW{F1}	usually = SW	=MASR if possible.
NUC1{F1}	=NUC1	
TD {F2}	128	Number of points.
ND0	1	Not required in TopSpin 2.1.
NS	4*n	
FnMode	TPPI/States/States-TPPI	

Processing Parameters *11.3.1*

Process with *xfb.*

Table 11.2. Processing Parameters

Parameter	Value	Comment
F2 acquisition ^{13}C	**********	Left column.
SI	1k	Number of complex points in direct dimension.
WDW	QSINE	Apodization in t2.
SSB	2-3	
PH_mod	pk	
F1 indirect ^{13}C	**********	Right column.
SI	512	Number of complex points in indirect dimension.
WDW	QSINE	Apodization in t1.
SSB	2-3	
PH_mod	pk	

Adjust the Rotational Resonance Condition for DARR/RAD *11.4*

1. Load the Adamantane sample, spin at the same speed as desired for your sample, match and tune, use a suitable cp setup (same as in section ***11.3***).
2. Set ***CPDPRG2*** to ***cw.***
3. Use the au program calcpowlev to calculate the power level required for a proton decoupling RF field of n × ***masr***, using p3 and pl12 as reference values. Refer to chapter ***"Basic Setup Procedures" on page 55*** for more information).

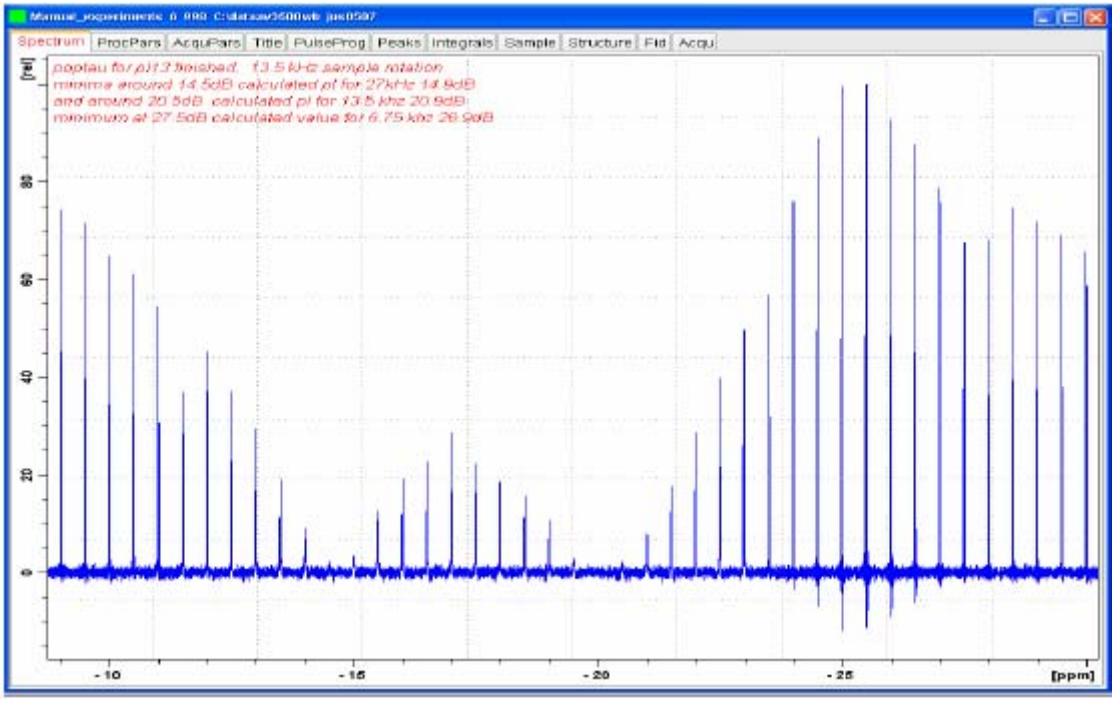

Figure 11.3. POPT Result for the cw Decoupling Power Variation

The figure above shows the POPT result for the cw decoupling power variation from about 50 kHz RF field to about 5 kHz RF field, spinning the adamantane sample at 13 kHz. The minima at 14.5 and 20.5 dB indicate the n = 2 and n = 1 RR conditions (26 and 13 kHz RF field).

4. Vary the decoupler power level ***pl12*** used with cw decoupling as indicated in ***Figure 11.3.*** from a power level value ***pl12*** 1 dB below the calculated n = 1 condition to 1 dB above the calculated n = 2 condition. Bandwidth considerations favor the n = 2 condition, sample heating considerations favor the n = 1 condition. An RF field of 2 × proton chemical shift range is on the safe side.
5. Enter the power level determined above as ***pl14*** recoupling power for DARR or RAD.
6. Using DARR or RAD shorter mixing times are possible.

Example Spectra 11.5

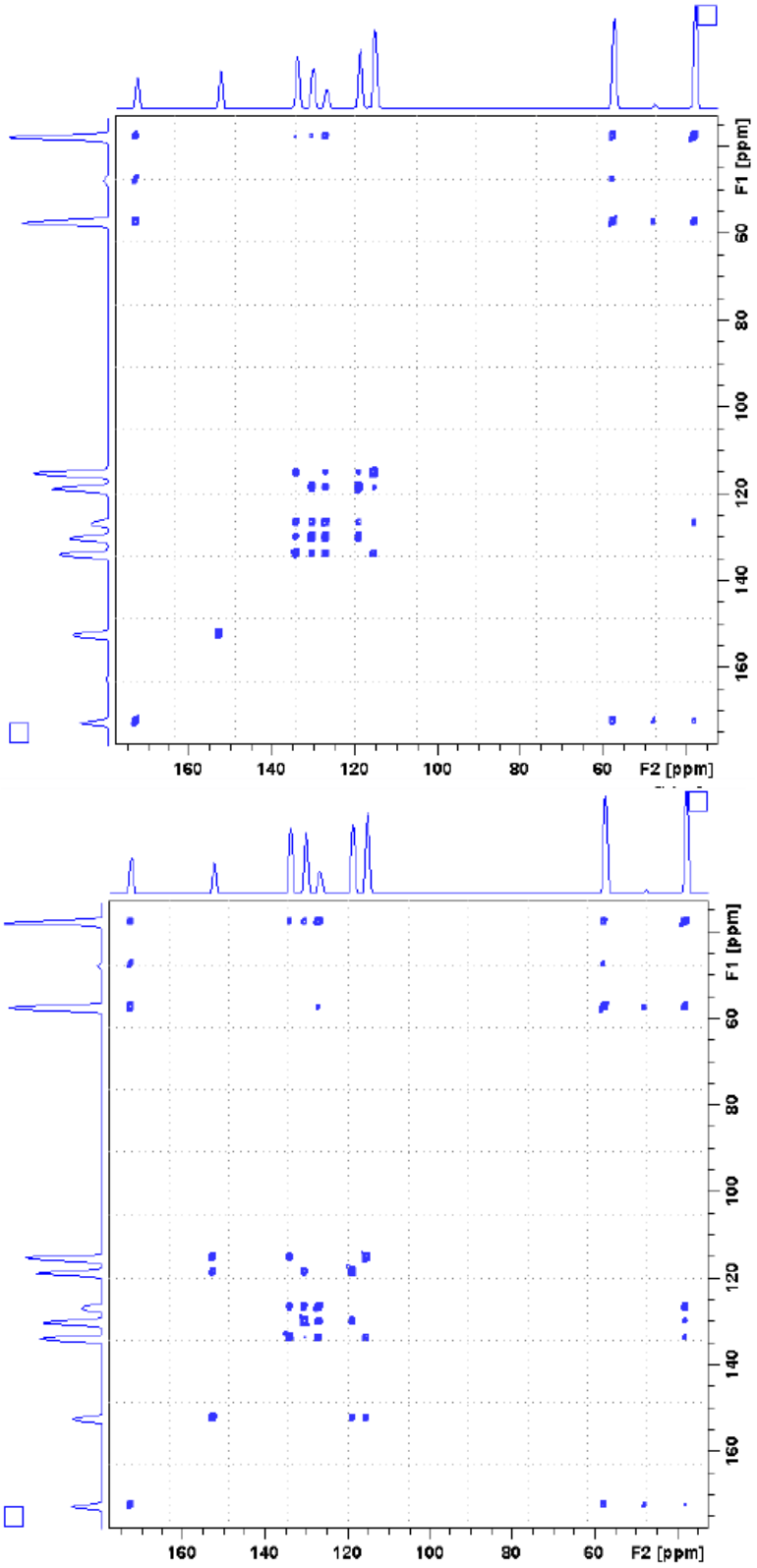

*Figure 11.4. ^{13}C CPSPINDIFF of fully labeled tyrosine*HCl, spinning at 22 kHz, 4.6 msec mix. Upper: PDSD, lower: DARR*

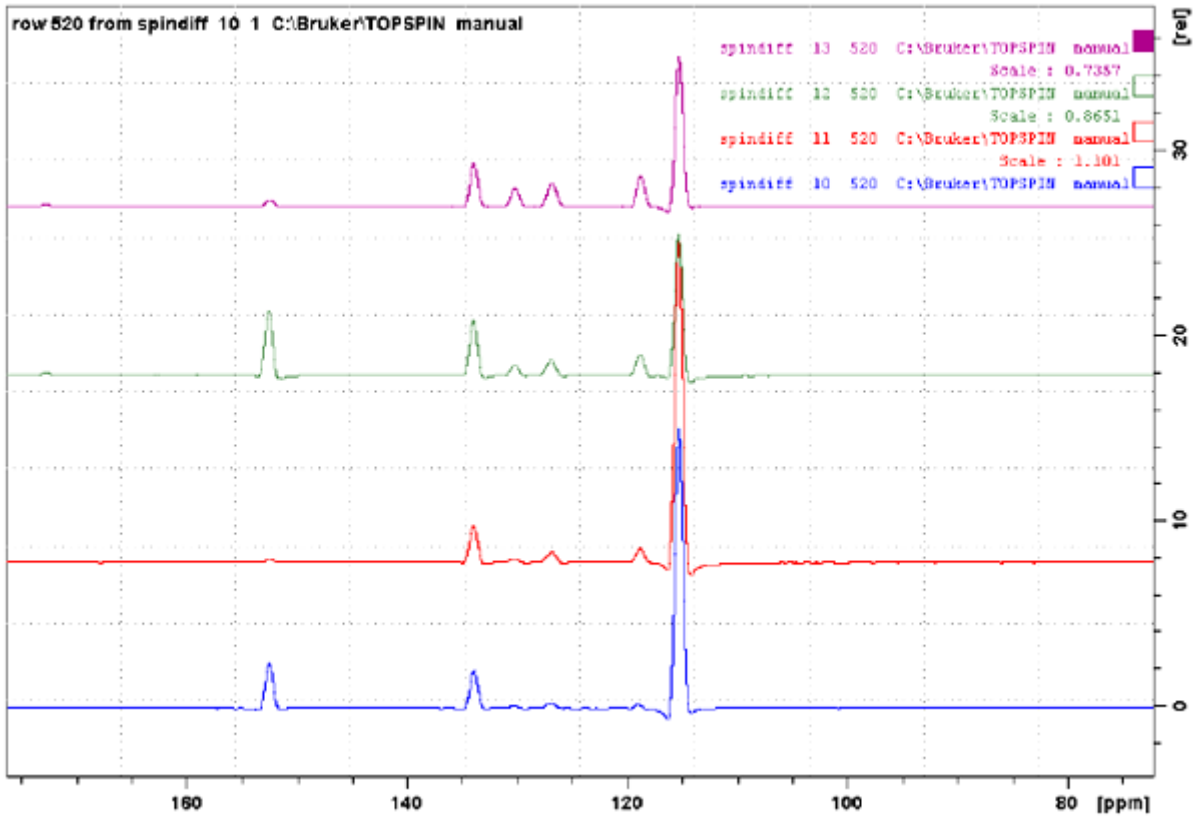

Figure 11.5. Comparison of DARR/PDSD

The figure above is a comparison of DARR/PDSD, with 4.6 and 20 msec mixing time, sample tyrosine-HCl spinning at 22 kHz. Traces through peak at 115 ppm, most high field aromatic carbon. Traces from below: DARR at 4.6 msec mix, PDSD at 4.6 msec mix, DARR at 20 msec mix, and PDSD at 20 msec mix. Note that some cross peak intensities differ substantially!

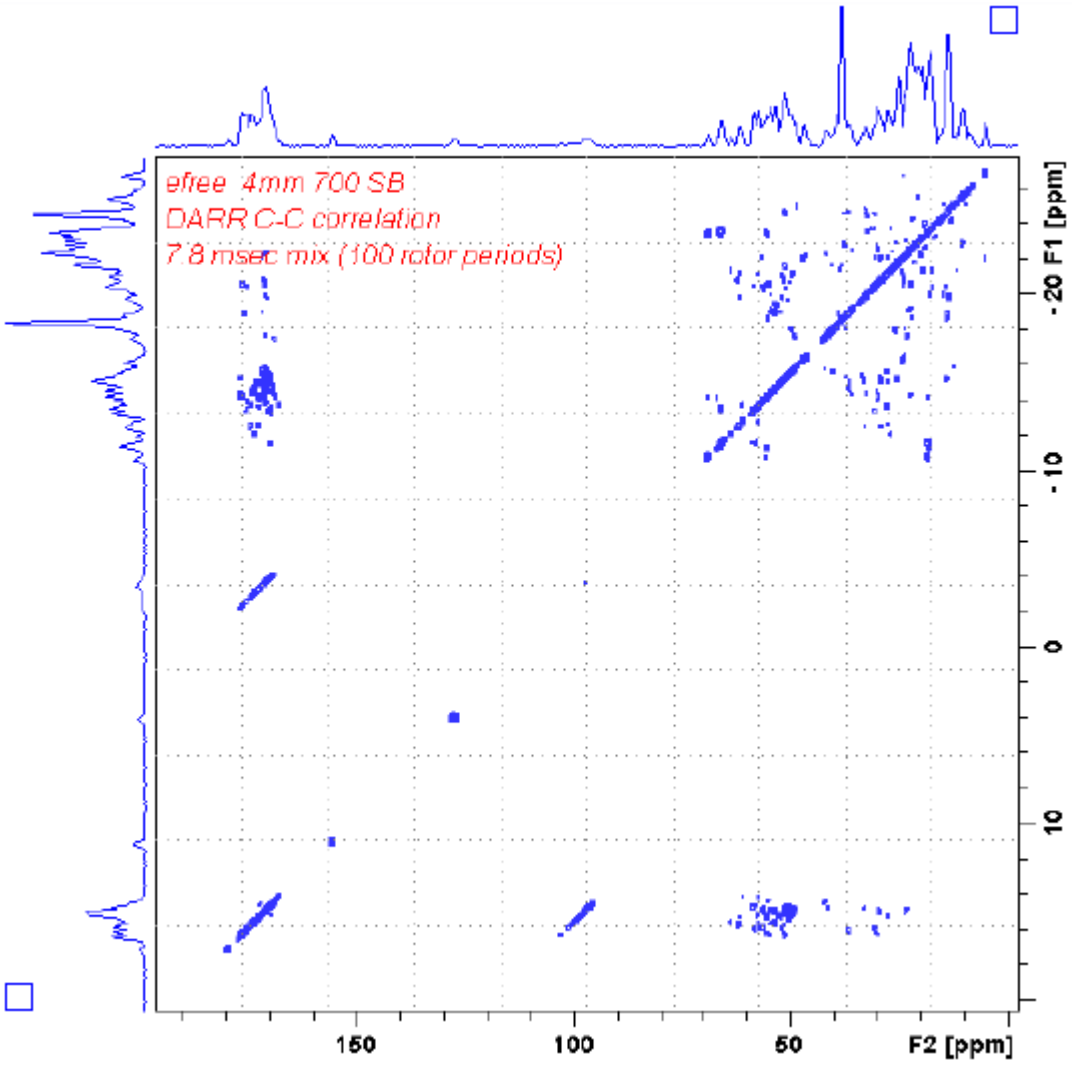

Figure 11.6. ^{13}C DARR of Fully Labelled Ubiquitine Spinning at 13 kHz

Proton Driven Spin Diffusion (PDSD)

REDOR 12

Rotational ***E***cho ***DO***uble ***R***esonance is an experiment based on the heteronuclear dipolar coupling between the observed nuclei. The REDOR sequence investigates this coupling under high resolution MAS conditions.

Dipolar couplings between I (decoupled spin) and S (observed) spins are spun out under MAS if there are no strong homonuclear interactions and if the heteronuclear coupling is not too big. In the case of couplings between most hetero-nuclei (like ^{13}C, ^{15}N and ^{29}Si) this is usually the case (small couplings of a few kHz and dilute spins), if the coupled nucleus is ^{31}P, ^{19}F or even ^{1}H, the coupling may not easily be spun out and the standard REDOR sequence may not be applicable in these cases.

The REDOR sequence reintroduces the heteronuclear dipolar coupling between the spin S and I by applying p pulses every half of a rotor period on the second channel (I), while the S channel is observed. A p pulse at half a rotor period will refocus the dipolar interaction averaged by spinning and dephase the magnetization, leading to an attenuation of the observed signal. Evaluation requires the acquisition of 2 data sets, one with refocusing pulse, the other one without, so that the natural dephasing can be subtracted out from the dipolar dephasing due to the refocusing pulse. Reference experiment (without I refocusing pulse) and dephased experiment (with I refocusing pulse) are subtracted and evaluated. Reference experiment and dephased experiment can be acquired consecutively or in an interleaved mode so that experimental drifts will not cause large errors. Usually, the experiment is set up as a pseudo-2D experiment where the number of rotor periods with p pulses is increased before detection.

The experiment can either be used to investigate isolated spin systems or multi speed systems. In both cases the time dependent difference of the echo S_0 (without the reintroduction of the heteronuclear dipolar coupling) and the second echo experiment S' (with the reintroducing p pulses applied on the I channel) can be used for calculating the distance information for the two involved spins or the second moment of the spin system respectively.

In isolated two spin systems the measured REDOR (dephasing)-curve can be used to determine distance information between the two involved spins. In case of investigating multispin systems the experimental REDOR dephasing curves can only be used to determine the second moment (M_2).

$$\propto \sum 1/r^6 \qquad \text{(Eq. 12.1)}$$

By the relation of the second moment to the distance by, this information in combination with theoretical simulations can be used to determine a mean distance between the involved spins as well.

In the case of very strong dipolar couplings the normal REDOR approach for multispin systems can not be used without introducing severe errors into the calculated second moment. With very strong dipolar couplings, the signal intensity may be lost after very few or only one refocusing pulse, so the decay curve cannot be

measured, and the reference experiment does not show a decay independent of the heteronuclear dipolar coupling. Faster spinning may solve the problem. Alternatively, the constant time (CT-)REDOR sequence may be used, which can help to enhance the performance in these cases and to reduce the experimental time needed dramatically.

Here the refocusing pulse is stepped in small time increments from the beginning of the rotor period, where it has a small effect on the signal intensity, to the middle of the rotor period, where it has the maximum effect.

Finally if one or both of the involved nuclei do have a quadrupolar moment, the here used REDOR sequence should not be used, but there are several different REDOR like experiments in literature which have an enhanced performance on observing quadrupolar nuclei. These are for example the ***R***otational ***E***cho ***A***diabatic ***P***assage ***DO***uble ***R***esonance (REAPDOR) or ***TRA***nsfer of ***P***opulation in ***DO***uble ***R***esonance (TRAPDOR) sequences.

Usually, the setup is chosen such that the more sensitive nucleus is observed. The measured coupling is of course independent from the choice of the nucleus, but there may be reasons to consider carefully, which nucleus is observed. Of course it is tempting to observe the nucleus with higher isotopic concentration, but this is usually not recommended, since it is more difficult to observe a small intensity change on a strong signal (which might be caused by fluctuations) than a bigger difference on the low abundance nucleus caused by the high abundance of the coupling partner. An example: The measurement will be more precise observing ^{13}C and defocus with ^{31}P pulses than vice versa, because the effect on ^{31}P, caused by 1.1% of ^{13}C would be max. 1.1%, a very small change which would require extremely high S/N and extremely high stability in signal generation and spin rate.

Pulse Sequence 12.1

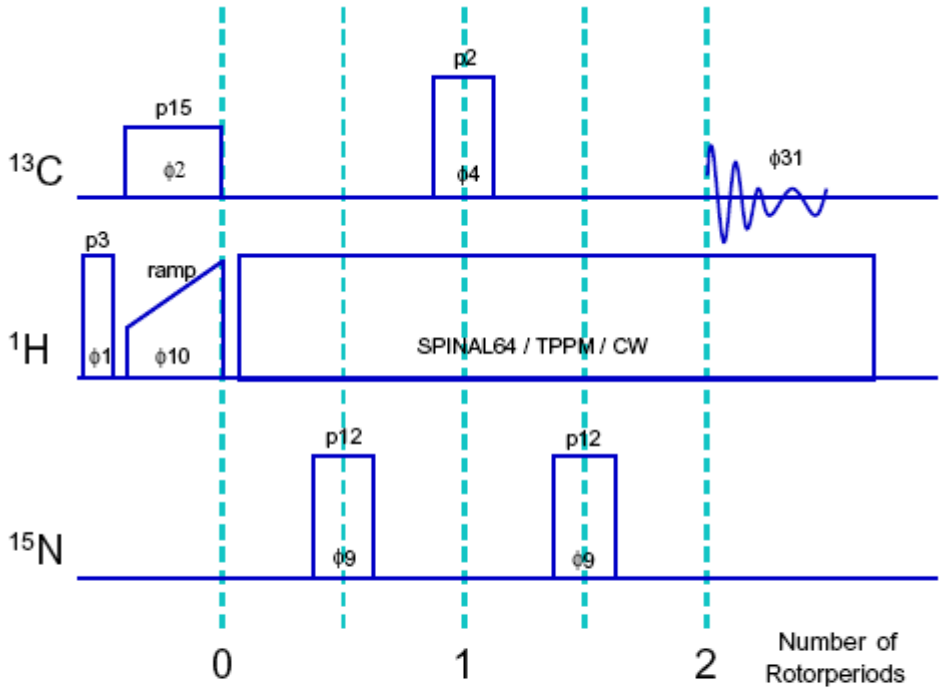

ϕ_1=1 3	ϕ_9=0 1 0 1 1 0 1 0
ϕ_2=0 0 1 1 2 2 3 3	ϕ_{10}= 0
ϕ_4=0 0 1 1 0 0 1 1	ϕ_{31}=0 2 1 3 2 0 3 1

Figure 12.1. REDOR Pulse Sequence

Setup 12.2

The example of setup given here is based on a biological sample, but of course the procedure will not change if you are going to analyze different samples with different combinations of coupled spins.

Sample: fully labelled $^{15}N/^{13}C_a$ Glycine (diluted in natural abundance glycine to 10%). Dilution will reduce long range dipolar interactions strongly and lead to a well defined direct interaction between ^{15}N and $^{13}C_a$, so that a single frequency dipolar modulation is obtained. A triple resonance probe with the X channel tuned to ^{13}C and the Y channel tuned to ^{15}N is required. Set ^{13}C observe with cross polarization from protons. It is recommended that separate preamps are used for C and N so observation can be changed between C and N without rewiring. There should be an X-low pass filter or ^{13}C bandpass filter on ^{13}C, a^{15}N low pass or bandpass on ^{15}N.

MAS rate: 5-10 kHz. The MAS spinning speed should be stable within 1 to 2 Hz in order to get a well refocused echo.

Overall Experimental time, including setup procedure: 3-5 hours.

Packing the sample is critical for the success of the experiment, check your sample is within the central region of the spinner or use a 12ml spinner. The quality of the refocusing p pulses is essential, this can only be achieved with a center packed sample. The coil of a 4mm MAS probe has a length of 10 mm, the sample should be no longer than 5mm, preferably 3mm (CRAMPS spinner or 12 ml HR-MAS spinner).

Setup the CP conditions for the ^{1}H magnetization transfer on both coupled nuclei (X and Y). Use cp90 to determine precise p pulses on both the X and Y channel of your probe.

Accurately setup the p/2 and p pulses for both ^{13}C and ^{15}N according to the standard setup procedures with an accuracy of at least 0.1ms.

After the setup, the pulse lengths for the different channels should be within the same duration and short enough to not exceed an overall duty cycle of about 5%.

One can reoptimise the refocusing pulse on the coupled nucleus using a 1D version of redor, setting the number of experiments (1 td) to 1. Here, the number of refocusing pulses ***l0*** is chosen to a value in a way that there is a noticeable decrease in dephasing experiment (normally this is between ***l0***=1-15), and then the refocusing p pulse is optimized for minimum signal intensity in the dephasing experiment.

Table 12.1. Acquisition Parameters for a ^{13}C observed C/N REDOR

Parameter	Value	Comments
pulse program	cpredori	pulse program
nuc1	^{13}C	nucleus for f1 channel
nuc2	^{1}H	nucleus for f2 channel
nuc3	^{15}N	Nucleus for f3 channel
p3	according to specs	$\pi/2$ pulse on f2 channel
p15	2000	Contact time between f1 and f2
pcpd2	about 2*p3	pulse length for decoupling sequence
p2	according to specs, 6-10 µsec	π pulse on f1
p12	about 10 µsec	π pulse on f3
cnst31	=masr	MAS spinning rate
l0	1	starting value for the desired evolution time, value must be odd
d1	4s	recycle delay
pl1	for HH condition	f1 power level for contact pulse
pl11	according to specs	f1 power level for π pulse
sp0	for HH condition	power level for ^{1}H ramp
pl2	-	not used

Table 12.1. Acquisition Parameters for a ^{13}C observed C/N REDOR

pl12	adequate	power level ^{1}H decoupling
pl3	adequate	power level for f3 π pulse
pl22	120	power level in S_0 experiment for the recoupling pulses
spnam0	ramp	ramp file name for CP
td(f1)	32-256	depending on coupling
aq	20-40 msec	acquisition time in f2
ns	8	number of scans per experiment
fnmode	QF	phase correction mode in the f1 dimension
rg	16-64	receiver gain level
digmod	baseopt or digital	digitizing mode

Data Acquisition *12.2.1*

Setup of the 2D data set:

After the optimization as described above type **iexpno** to create a new data set, afterwards switch to 2D data mode by using the “123” button. Set the time domain for the F1-Dimension according to the maximum desired evolution time of the final REDOR curve. To calculate the value for td1 you have to keep in mind that the REDOR–Program is organized in multiples of two rotation periods (compare with the pulse program scheme).E.g. for a given MAS rate of 10 kHz and a desired overall evolution time of 10 ms you have to set td1 to a value of 200. This will record 100 sets of S_0 and S’ experiments with an maximum evolution time in the last two data rows of the desired 10 ms. The pulse program library supplies the following REDOR sequences:

cpredor: standard REDOR for dipolar couplings > 500 Hz, incrementing in 2 rotor period intervals. Two data sets are required with pl3 set for pulsing (REDOR experiment) or no pulse (=120 dB, reference experiment).

cpredori: stores these data sets in the 2D data frame by interleaving scans of the S_0 and S’ experiments for the same evolution period (see ***Figure 12.2.***).

cpredorxy8: increments in units of 16 rotor periods, for small couplings. Here the XY-8 scheme is used for recoupling pulses which is insensitive to offsets. While in cpredor and cpredori the p pulses should be executed close to resonance, this is not required nor desired in the XY-8 version because the offset dependence is well compensated.

Additionally to the cross-polarization pulse programs all REDOR sequences also exist as a direct excitation version without a cp-Step. These are the programs ***redor, redori*** and ***redorxy8***. The setup procedure of these sequences is identical to the ones explained earlier, but you can skip the CP optimization procedure, which is replaced by a p/2 pulse on the observe channel.

Data Processing 12.2.2

The following refers to the sequence **cpredori**, where the REDOR-experiment and the reference experiment are executed in an interlaced mode (which is less likely to be subject to systematic errors).

The acquired NMR data are arranged in a 2D like structure, every odd row (1, 3, 5,…) contains the REDOR data set with additional p pulses on channel I (S' experiment), every even row (2, 4, 6,…) contains the corresponding echo experiment (S_0 experiment) with the same evolution period t, after the RAW-Data is processed with the "XF2" command (see ***Figure 12.2.***). For further processing you can then either use the function "T1/T2 Relaxation" in the analysis part of Topspin in order to do the integration and/or find the peak maxima of the S_0 and S' intensities automatically or use your favorite deconvolution program for data analysis.

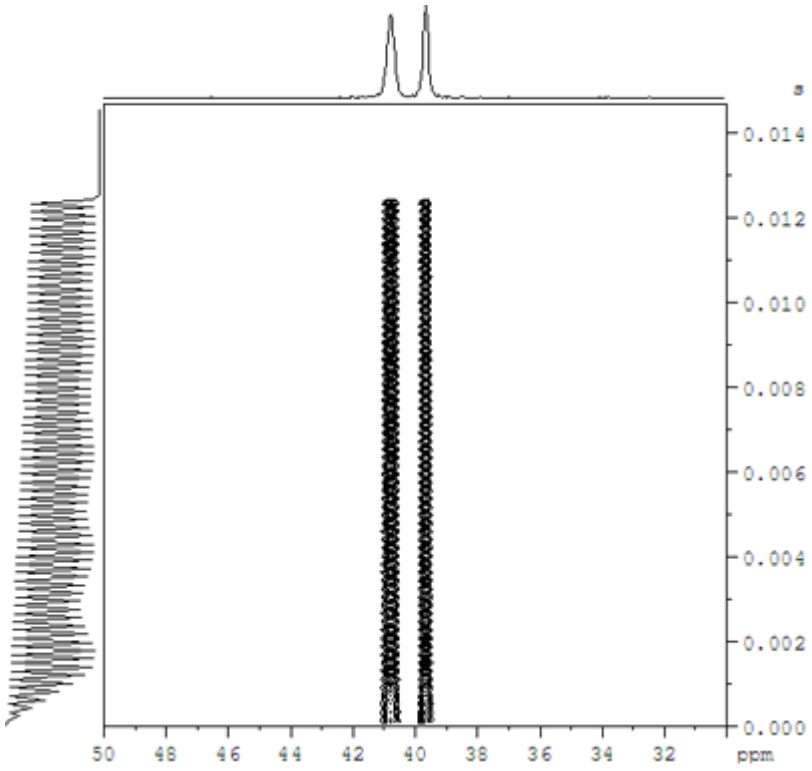

Figure 12.2. 2D data set after "xf2" processing.

In the figure above the data set contains the alternating S' and S_0 experiments

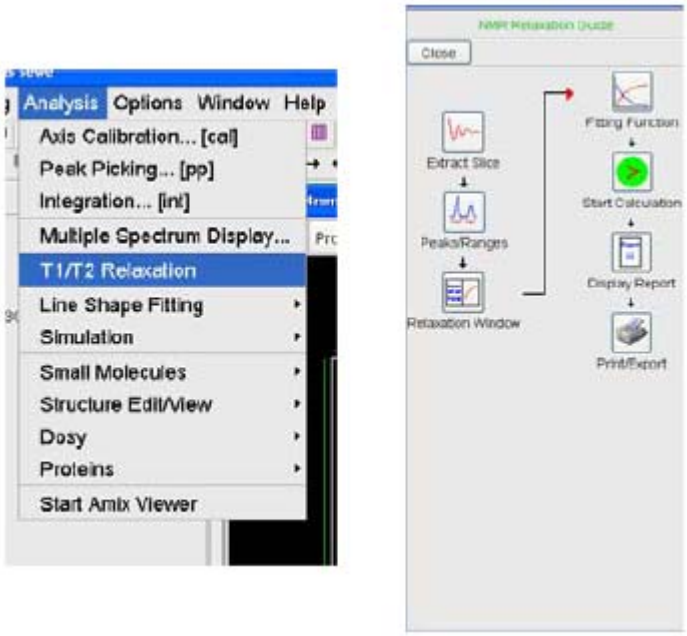

Figure 12.3. T1/T2 Relaxation for further Analysis of the Data Figure and the Analysis Interface

If you are going to use topspin you have to choose T1/T2-Relaxation in the Analysis Menu (see ***Figure 12.3.***) to open the graphical interface for the data analysis (***Figure 12.3.***).

To begin extract the first spectrum by using the extract slice button and select the desired peak by manual peak picking. To save the data use the button shown in ***Figure 12.4.***.

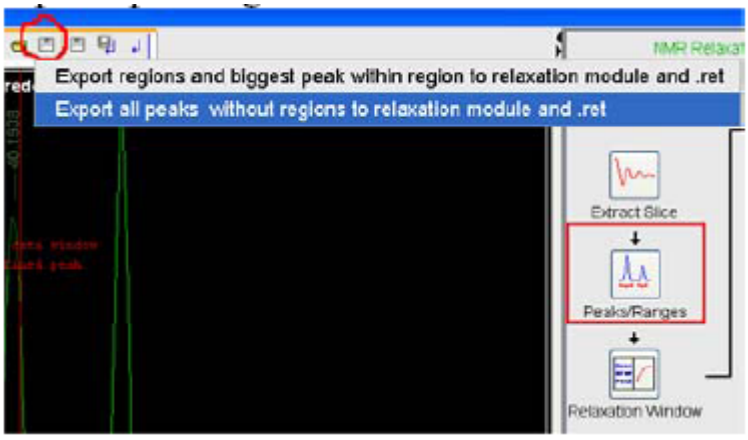

Figure 12.4. Saving Data to Continue to the Relaxation Window

Now after switching to the relaxation window, topspin will show the parameter window which can also be accessed later by clicking the marked button in the upper icon bar (***Figure 12.5.***). Here the value for number of points has to be set to the td2 value and the list file name has to be switched to auto, otherwise the data

preparation will fail (compare ***Figure 12.5.***). By clicking OK, topspin will automatically pick all the intensities for your measured REDOR experiments. These values are then saved in the processed data directory (**\data\user\nmr\experiment\exp#\pdata\1**) in the file "**t1t2.dx**". The intensities are saved in two columns for each peak, while the first column represents a arbitrary x-scale, the measured intensities are within the second column. Remember, because of the used pulse program "cpredori" every odd line contains an intensity value for an REDOR spectrum (S') and every even line the corresponding intensity of the ECHO experiment (S_0).

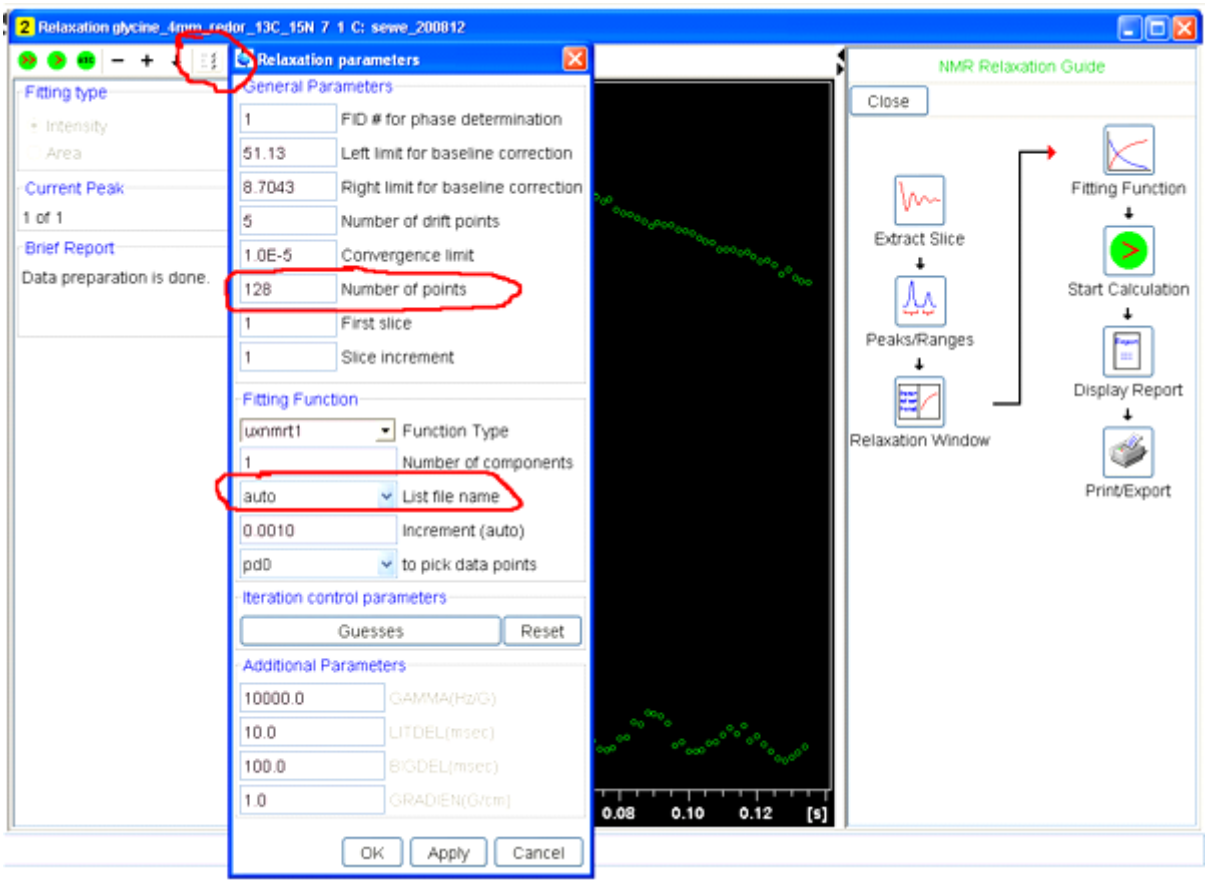

Figure 12.5. Setting the Correct Analysis Parameter

After importing this file into Excel or any other program (using either "Origin" or "Igor" is recommended) for calculating the values for $(S_0\text{-}S')/S_0$, these normalized intensities are plotted versus the evolution time of each spectrum (which is a multiple of "T_R*2") as it is shown in ***Figure 12.6.***. The x-axis is therefore calculated by

$$(1/\mathrm{MASrate}) \cdot (2i - 2) \qquad \text{(Eq. 12.2)}$$

where i is the number of the corresponding data point $(S_0\text{-}S')/S_0$ (the number of the S_0/S' set within the 2D data set). In this experiment MAS spinning speed was 10 kHz resulting in data points every 200ms. Note, only the analysis of the low field shifted peak is shown here, corresponding to the alpha-glycine modification of the measured sample.

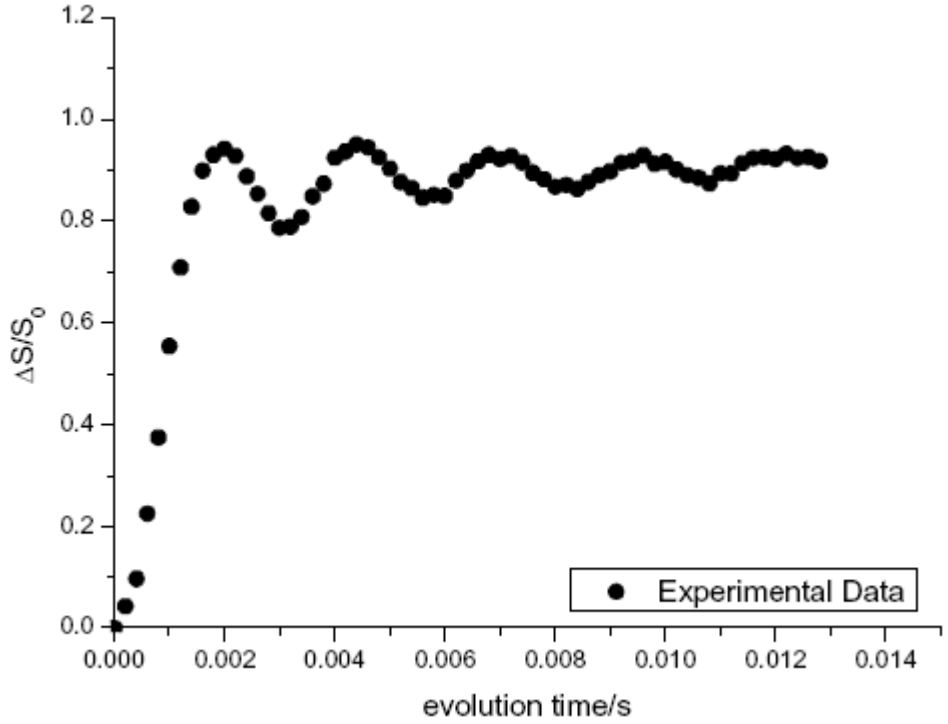

Figure 12.6. Plot of the Normalized Signal Intensity Versus the Evolution Time

There are different methods for the interpretation of the experimentally measured REDOR curves. In the case of isolated two spin systems, like in this case of ^{15}N-$^{13}C_a$-glycine, it is generally possible to fit the experimental dephasing curve by using a combination of bessel functions. This is called the “REDOR transformation” and gives you direct access to the dipolar coupling information for the measured spin system (for details check ***reference 6.***).

The more common way for the interpretation of the experiment is the second moment approach, which is also suitable for multiple spin systems. Here the beginning of the REDOR curve can be fitted by a parabolic approximation up to normalized signal intensities of about 0.2-0.3 (for details see e.g. ***reference 10.***). In the case of very strong dipolar couplings this approach may be restricted to very high MAS spinning speeds, because otherwise it will not be possible to get enough data points within the 0.3 area of the curve (it here may be useful to use a more efficient REDOR technique for strong dipolar coupled systems, like CT-REDOR, see e.g. ***reference 7.***).

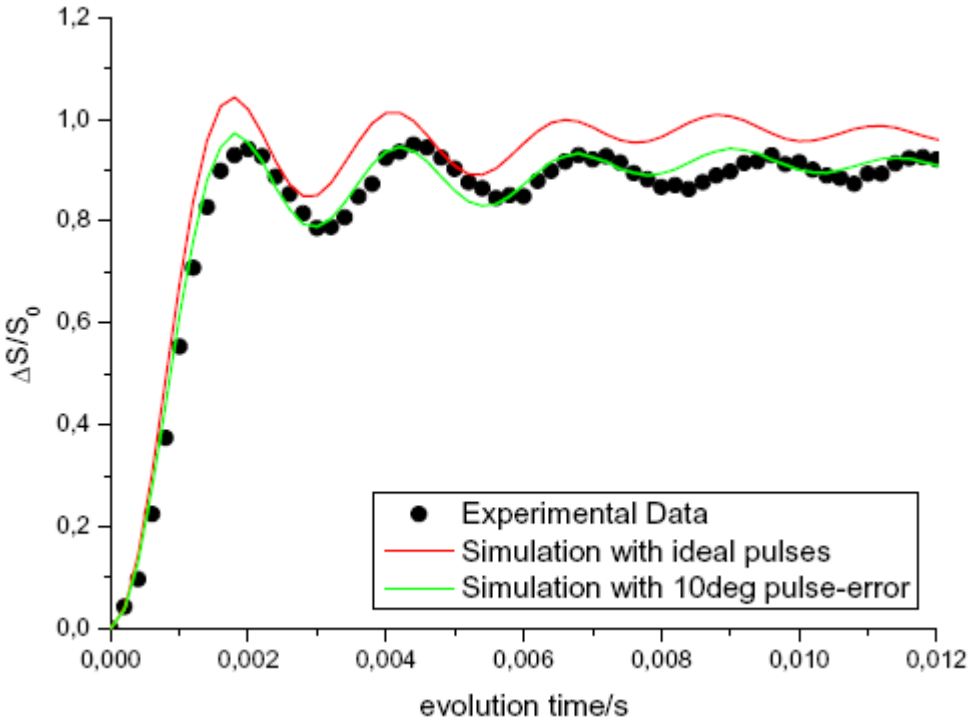

Figure 12.7. Experimental data for the glycine $^{13}C\{^{15}N\}$-REDOR

Red and green curves are the results of different Simpson simulations.

Finally, the complete REDOR curve can be simulated using the SIMPSON (***reference 8.***) NMR simulation package. The following pages will explain the M_2 approach as well as the SIMPSON interpretation of the glycine REDOR data. ***Figure 12.7.*** shows the experimental data points together with two different SIMPSON simulations (for details of the geometry and distance information of the labelled ^{15}N-$^{13}C_a$ spin pair of glycine see ***reference 9.***). The red simulation shows the time dependent evolution assuming ideal p pulse lengths on both the S and I channel (corresponding to an experiment without any errors on both frequency channels for ^{15}N and ^{13}C), leading to a slightly too high theoretical REDOR curve compared to the actual experiment. The green curve shows the same simulation assuming pulse errors of 10% on both channels, corresponding very well with the experimental data.

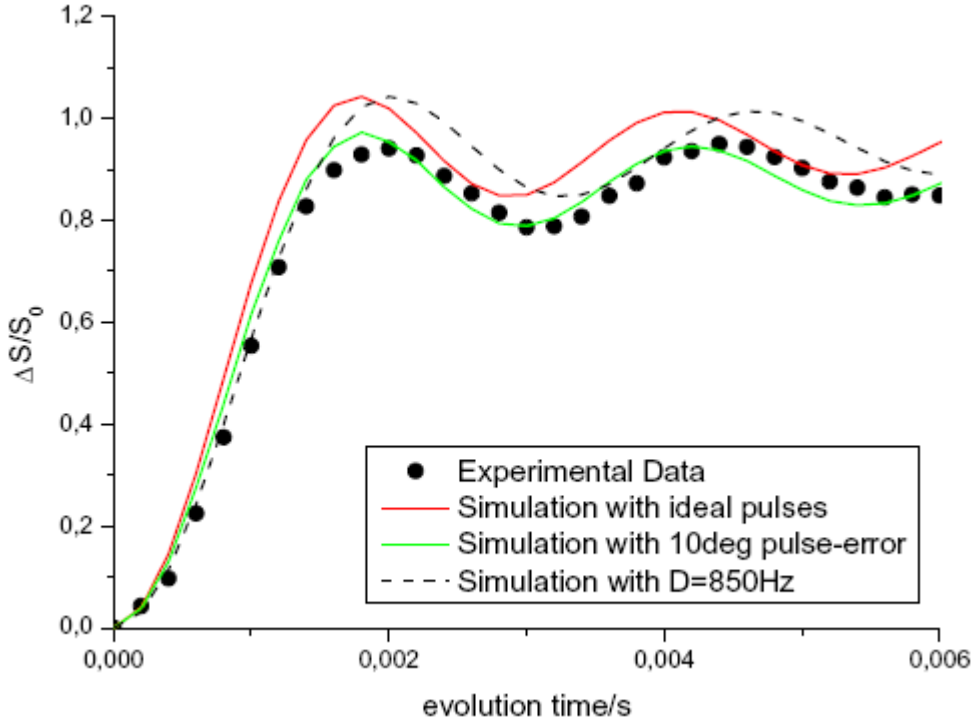

Figure 12.8. Comparison of Experimental Data to a Simulation with Reduced Dipolar Coupling

Figure 12.8. shows a zoomed view of the beginning REDOR curve for the glycine sample. The third, simulated line (broken black line) shows a SIMPSON simulation with ideal pulses on both channels, but varying the dipolar coupling between I and S in order to fit to the experiment. The simulation using a dipolar coupling constant of 850 Hz fits the experimental data points very well. This coupling can be transformed into a distance between ^{15}N and ^{13}C of about 1.53 Å, which is compared to the theoretical value of 1.47 Å (964 Hz) an error within 10%. As you can see, in an unknown spin system, the interpretation by using SIMPSON will always suffer from the fact that a non optimal setup of the experiment will introduce the same error like a reduced dipolar coupling between the analyzed spins; these two effects can not be easily separated from each other during the interpretation process. Therefore it is useful to perform a calibration run like the glycine measurement before analyzing an unknown sample and to set up the complete experiment very carefully in order to calibrate the experiments.

The above shown simulated REDOR curves can now be used to demonstrate the second moment approach in analyzing REDOR experiments. Here a parabolic fit is used to describe the first few points of each curve. In the case of the isolated two spin system of the glycine this parabola is defined by:

$$\Delta S / S_0 = 4 / 3\pi^2 (NT_r)^2 M_2 \qquad \text{(Eq. 12.3)}$$

Using this equation you end up with the values given in ***Table 12.2.*** for the distances and the second moments. The M_2 values given in brackets for the simulat-

ed curves are calculated using the second moment approach, in order to demonstrate the error margins you have to expect by the M_2 approach.

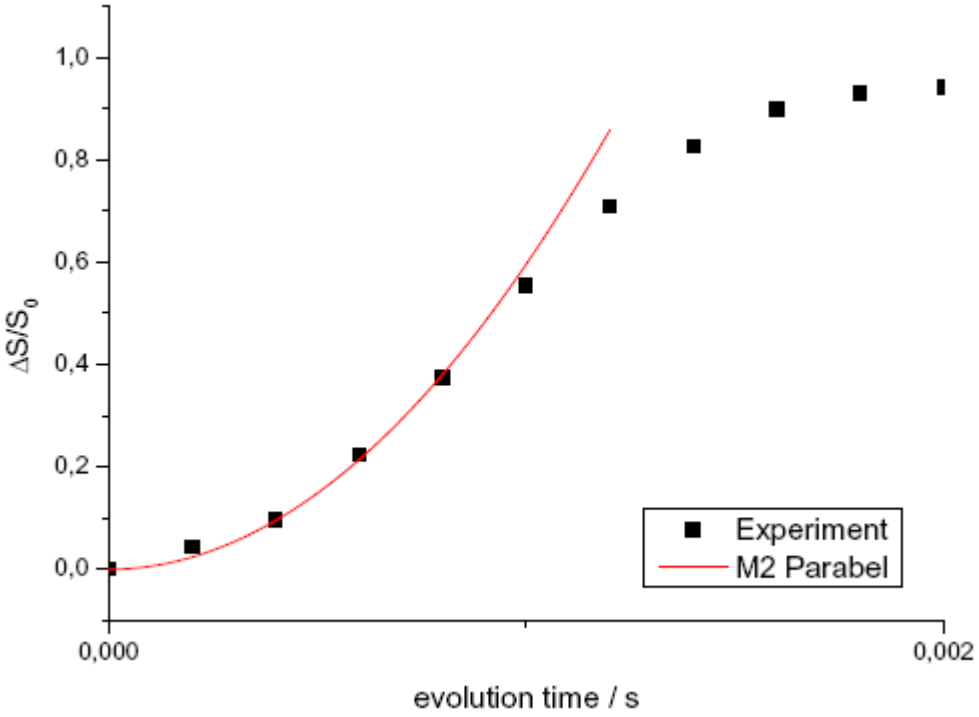

Figure 12.9. Experimental data with the corresponding M_2 parabolic analysis.

Figure 12.9. shows the calculated parabola for the experimental data set. As you can see in the corresponding table the experimental setup reflects the theoretical M_2 within an error margin of 40% while this transforms to an overall distance error of about 10%.

Afterwards the calculated M_2 can be transformed into the dipolar coupling constant by using:

$$\sqrt{15/(16\cdot\pi)^2/0.5/(0.5+1)\cdot M_2} \qquad \text{(Eq. 12.4)}$$

The comparison of the second moment directly calculated from the experimental data with the second moment extracted from the best fitting SIMPSON simulation, gives you in this example 747 Hz compared to 850 Hz. Of course this result can be improved by introducing more data points within the interpretation region of the parabolic fit, which can easily be done by running the experiment again with higher spinning speeds. Afterwards the data sets can be combined before running the interpretation process.

Table 12.2. Results for the M_2 Calculation and the Simulations

Measurement	M_2 [s^{-2}]	Dipolar coupling [Hz]	Distance [Å]
experiment	4.4E6	747	1.6
ideal pulses	7.3 / (6.3)E6	964 / (896)	1.47 / (1.5)
10% pulse error	7.3 / (5.7)E6	964 / (850)	1.47 / (1.53)
850 Hz dipolar coupling	5.7 / (5.0) E6	850 / (800)	1.53 / (1.56)
theoretical (***reference 9.***)	7.3E6	964	1.47

Final Remarks *12.3*

The REDOR sequence is a powerful tool to measure distances in different spin systems. But, as seen above, already a small error during the setup procedure will finally lead to severely stretched distances calculated in the interpretation process of the measured data. Although the results using SIMPSON simulations are in a much better agreement with the expected values, the simulations cannot compensate for the errors introduced by a faulty setup. Additionally it is not always possible to use the simulations for the interpretation of experimental data, e.g. in the case of multispin systems or amorphous systems it may not possible to get reliable input data for the simulations setup.

In any case, in order to be sure of the correct setup of the experiment it is absolutely necessary to proof the experimental setup on a known spin system like the glycine in order to check the robustness of the overall sequence setup. After this validation and calibration process the sequence can then be used to determine distances or M_2 values for unknown samples by using the calibrated experimental setup. Experiments on unknown samples should be measured as close to the calibration run as possible to minimize the influence of experimental fluctuations (pressure changes and consecutive spin rate changes, temperature changes and consecutive pulse power changes and the like).

Of course a qualitative comparison within a set of samples is always possible with the same set of experimental parameters without doing a full calibration run.

References

1. T. Gullion, J. Schaefer, Rotational-echo double-resonance NMR, J. Magn. Reson. 81, 196–200 (1989).
2. T. Gullion, J. Schaefer, Measurement of Heteronuclear Dipolar Couplings by MAS NMR, Adv. Magn. Reson. 13, 58–83 (1989).
3. T. Gullion, Introduction to Rotational-Echo, Double-Resonance NMR, Conc. Magn. Reson. 10, 277–289 (1998).
4. T. Gullion, Measurement of dipolar interactions between spin-1/2 and quadrupolar nuclei by rotational-echo, adiabatic-passage, double-resonance NMR, Chem. Phys. Lett. 246, 325–330 (1995).
5. E. R. H. van Eck, R. Janssen, W. E. J. R. Maas, and W. Veeman, A novel application of nuclear spin-echo double-resonance to alumino phosphates and alumino silicates, Chem. Phys. Lett. 174, 428-432 (1990).
6. K. T. Mueller, Analytic solutions for the Time Evolution of Dipolar-Dephasing NMR Signals, Journal of magnetic resonance A 113, 81-93 (1995).
7. T. Echelmeyer, L. van Wüllen and S. Wegner, A new application for an old concept: Constant time (CT)-REDOR for an accurate determination of second moments in multiple spin systems with strong heteronuclear dipolar couplings, Solid state nuclear magnetic resonance 34, 14-19 (2008).
8. M. Bak, J. T. Rasmussen, N. C. Nielsen, Journal of magnetic resonance 147, 296-330 (2000).
9. G. L. Perlovich, I. K. Hansen and A. Bauer-Brandl, The polymorphism of glycine, Journal of Thermal Analysis and Calorimetry 66, 699-715 (2001).
10. M. Bertmer, H. Eckert, Dephasing of spin echoes by multiple heteronuclear dipolar interactions in rotational echo double resonance NMR experiments, Solid State Nuclear Magnetic Resonance 15,139-152 (1999).

SUPER 13

Overview 13.1

*S*eparation of *U*ndistorted Chemical-Shift Anisotropy *P*owder patterns by *E*ffortless *R*ecoupling (SUPER) correlates CSA powder patterns in the F1 dimension with the isotropic chemical shift in the F2 dimension. The SUPER experiment is based on Tycko's CS – CSA correlation experiment, but provides better compensation for experimental imperfections such as B_1 in-homogeneities and pulse imperfections. Also, both experiments produce scaled powder patterns in F1, and the scaling factor is more favorable in SUPER than the factor 0.39 in Tycko's version. As a consequence, the SUPER experiment does not require high spinning speeds (to fit the F1 lineshape into the rotor-synchronized spectral window) or very strong ^{13}C pulses.

SUPER has several advantages. First of all, it covers a large bandwidth for the isotropic chemical shift. Secondly, no requirements exist for ^{1}H decoupling during the recoupling pulses, because it uses 360º pulses instead of the 180× pulses in Tycko's experiment. Exact 360º pulses automatically decouple the heteronuclear dipolar interaction so that no or only weak ^{1}H decoupling is required during the recoupling pulses. The scaling factor is normally 0.155 so that a spectral width over 40 kHz can be achieved in the indirect dimension. As a consequence, moderate spinning speeds of up to 6.5 kHz can be chosen so that experiments can be performed without serious problems on high field instruments. The limiting factor in the choice of the spinning speed is the rotor synchronization requirement of the recoupling 360º pulses:

$$\nu_{RF} = 12.12\nu_{rot}$$

References:

1. S-F. Liu, J-D Mao, and K. Schmidt-Rohr, *A Robust Technique for Two-Dimensional Separation of Undistorted Chemical-Shift Anisotropy Powder Patterns in Magic-Angle-Spinning NMR*, J. Magn. Reson. 155, 15-28 (2002).
2. R. Tycko, G. Dabbagh, and P.A. Mirau, *Determination of Chemical-Shift-Anisotropy Lineshapes in a Two-Dimensional Magic-Angle-Spinning NMR Experiment*, J. Magn. Reson. 85, 265-274 (1989).

Pulse Program 13.2

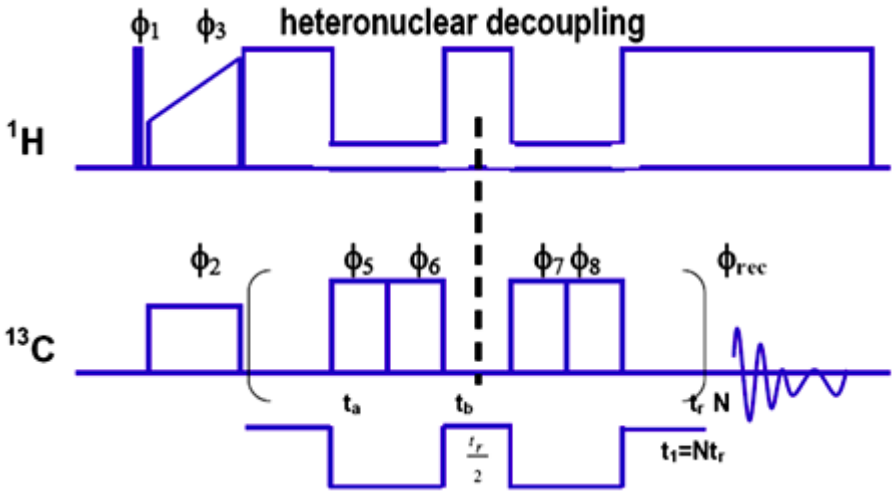

Figure 13.1. Pulse Sequence for 2D CPMAS exchange experiment

2D Experiment Setup 13.3

Sample: Tyrosine HCl natural abundance.

Setup time: Less than 1 hour.

Experiment setup 13.3.1

1. In order to setup the experiment, determine ^{1}H-^{13}C and parameters with variable amplitude on ^{1}H according to ***"Basic Setup Procedures" on page 55***.
2. Verify the pulse parameters on the ^{13}C channel (see ***"Pulse Calibration with CP" on page 105***) and calculate the power level required for the recoupling pulses, i.e. $f_{rf} = 12.2 \times f_{rot}$.
3. Verify pulse width.
4. Calculate power level required for heteronuclear decoupling during the recoupling pulses, ***pl23***, i.e. 20 – 30 kHz or > 25 x f_{rot}. Low power decoupling during the recoupling pulses is permitted because the 360 degree pulses act like heteronuclear decoupling pulses. ***pl22*** during delays should be high.
5. The experiment requires a minimum of 64 transients to complete the phase cycle. Between 32 and 64 experiments are needed for a 2D data set. Depending on the choice for the gamma integral, more transients per slice may be required. The recommended value is 4, which increases the number of required transients per experiment to 256.
6. Run 1D experiment and make sure everything is set properly.
7. Create a new experiment with either ***iexpno*** or ***edc***.
8. Change to 2D data set:

After 1D parameter optimization as previously described, type ***iexpno*** to create a new data file and switch to the 2D mode using the “123” button. Set the appropriate ***FnMode*** parameter in ***eda***. Pulse program parameters are detailed as follows (***Figure 13.1.*** shows the pulse sequence).

Figure 13.2. The “123” Icon in the Menu Bar of the Data Windows Acquisition Parameter Page.

The “123” icon in the menu bar of the data windows acquisition parameter page is used to toggle to the different data acquisition modes, 1D, 2D, and 3D if so desired.

9. Make sure the correct nucleus is selected in F1 dimension, make sure an appropriate quadrature detection mode is selected in ***FnMode*** (TPPI, STATES-TPPI or STATES).
10. Choose the appropriate sampling time **(*td1*)** so that the required resolution **(*FIDRES*)** in the indirect dimension is achieved.
11. Set ***pl11*** to give a pulse nutation frequency of12.12* rotation rate (see chapter 1).
12. Set ***d4,*** the z-filter delay**,** to about 1 ms (integer number of rotor periods if possible).
13. Set ***p2*** to be a 180× pulse at ***pl1*** for the TOSS sequence.
14. Set ***l5*** for the gamma integral, typically = number of spinning sidebands normally 4.
15. Start the experiment.

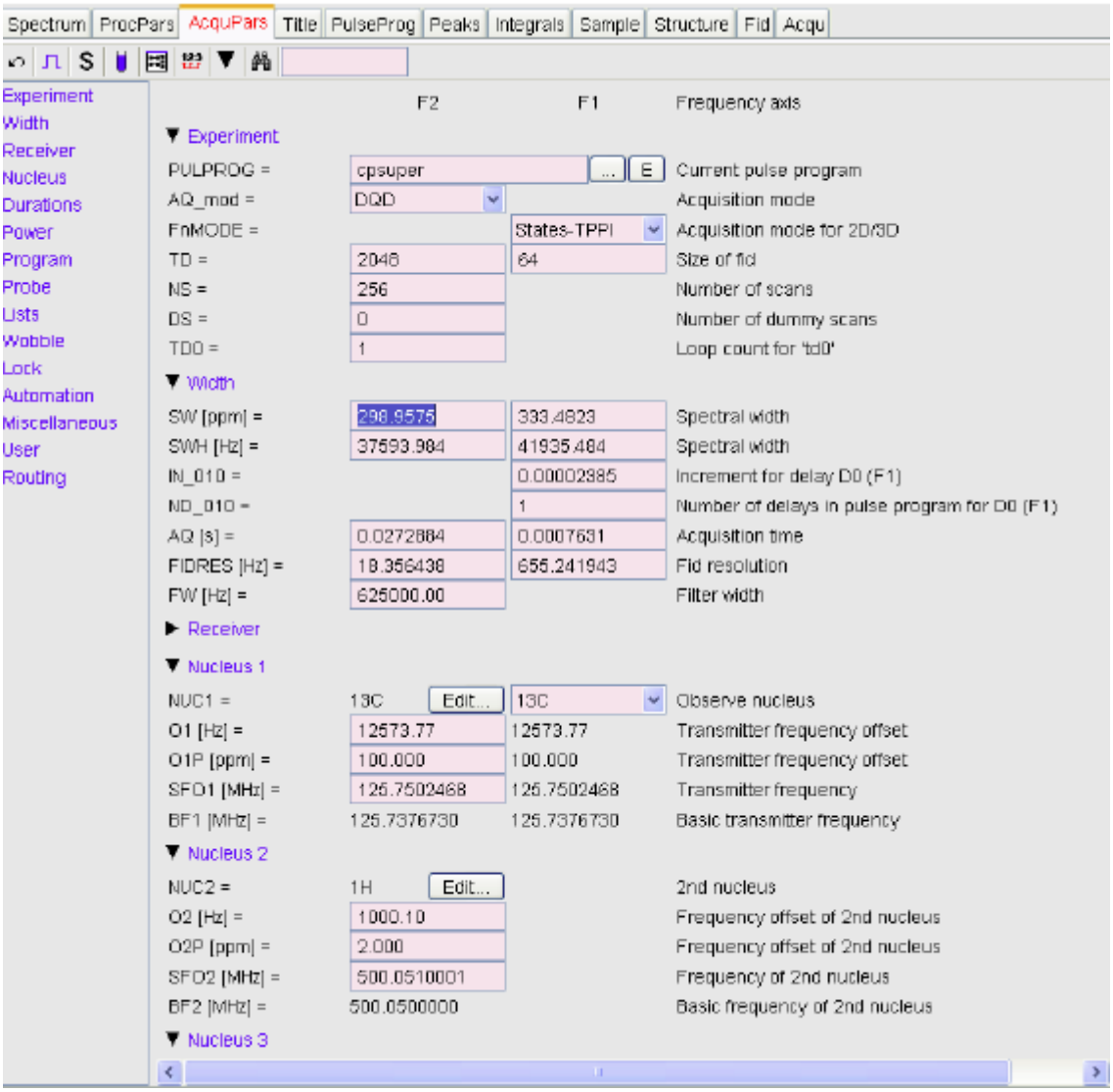

Figure 13.3. The Acquisition Parameter Window (eda)

Data Acquisition *13.4*

Sample: Tyrosine HCl

Experiment time: several hours

Table 13.1. Acquisition Parameters

Parameter	Value	Comments
Pulse program	cpsuper	Pulse program.
NUC1	^{13}C	Nucleus on f1 channel.
O1P	100 ppm	^{13}C offset.
NUC2	^{1}H	Nucleus on f2 channel.
O2P	0 ppm	^{1}H offset (can be optimized for best decoupling).
PL1		Power level for f1 channel.
PL11		Power level for f1 recoupling.
P2		180° pulse on F1 during TOSS with PL1.
PL2		Power level for f2 channel.
PL12		Power level decoupling f2 channel and excitation.
P3		Excitation pulse f2 channel.
P15		Contact pulse – first contact.
CPDPRG2		TPPM or SPINAL64.
NS	64*n*l5	Number of scans.
CNST31		Spinning speed in Hz.
L5		L5/cnst31 counter for increment in t1 and number of gamma integral – typically number of SSB's.
F2 direct ^{13}C		(left column).
TD	2048	Number of complex points.
SW	300 ppm	Sweep width direct dimension.
F1 indirect ^{13}C		Right column.
TD	32 - 64	Number of real points.
FnMode		TPPI, STATES or STATES-TPPI.

Table 13.2. Processing Parameters

Parameter	Value	Comment
F1 acquisition ^{13}C		Left column.
SI	4096	Number of points and zero fill.
WDW	QSINE	Squared sine bell.
SSB	2	90º shifted sine bell.
PH_mod	pk	Phase correction if needed.
BC_mod	quad	DC offset correction.
Alpha	-1	For shearing the spectrum.
F2 indirect ^{13}C		Right column.
SI	128	Zero fill.
MC2	STATES-TPPI	
WDW	QSINE	Squared sine bell.
SSB	2	90º shifted sine bell.
PH_mod	pk	Phase correction if needed.
BC_mod	no	Automatic baseline correction.

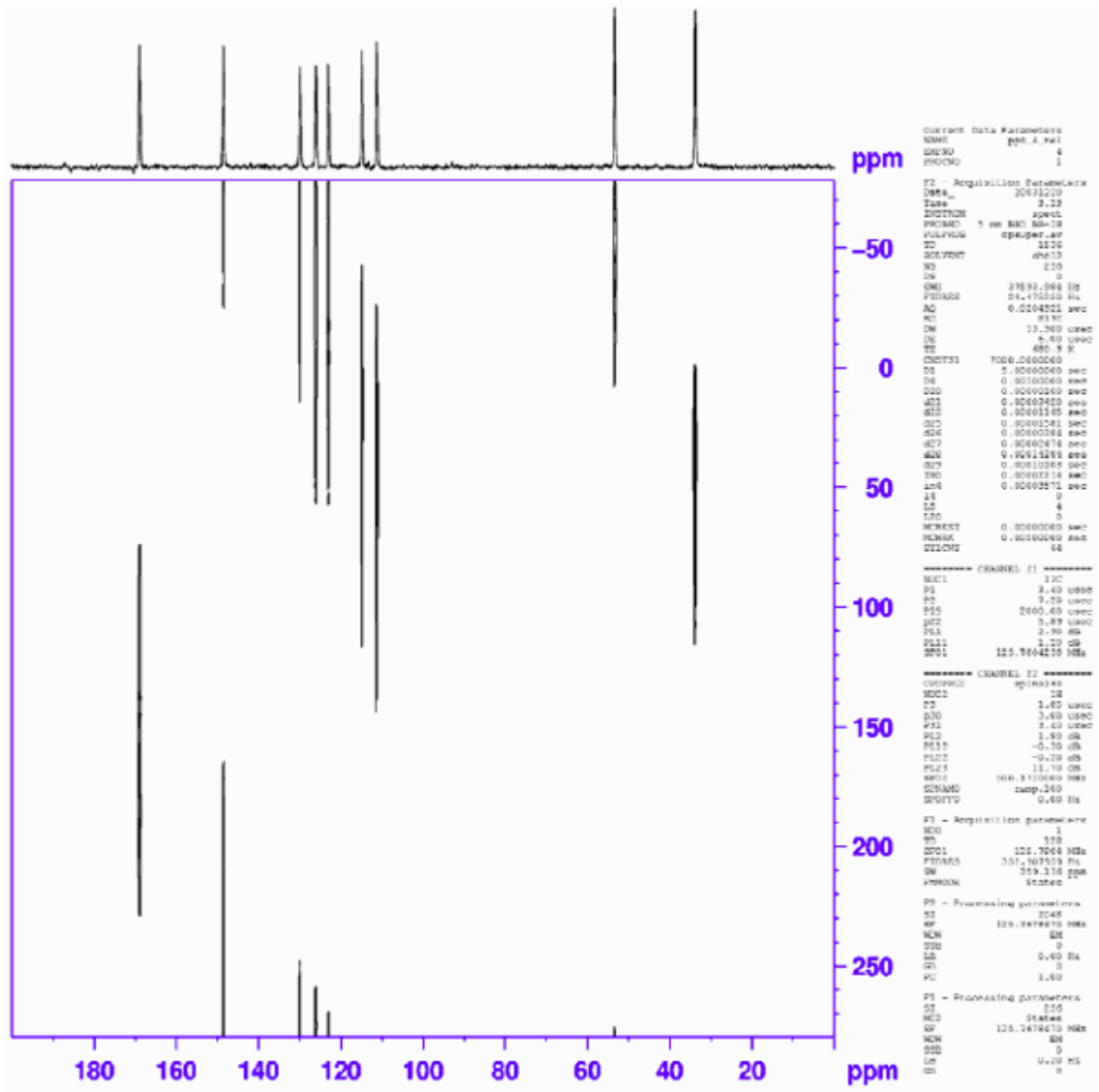

Figure 13.4. The SUPER Spectrum of Tyrosine HCl After Processing Using "xfb"

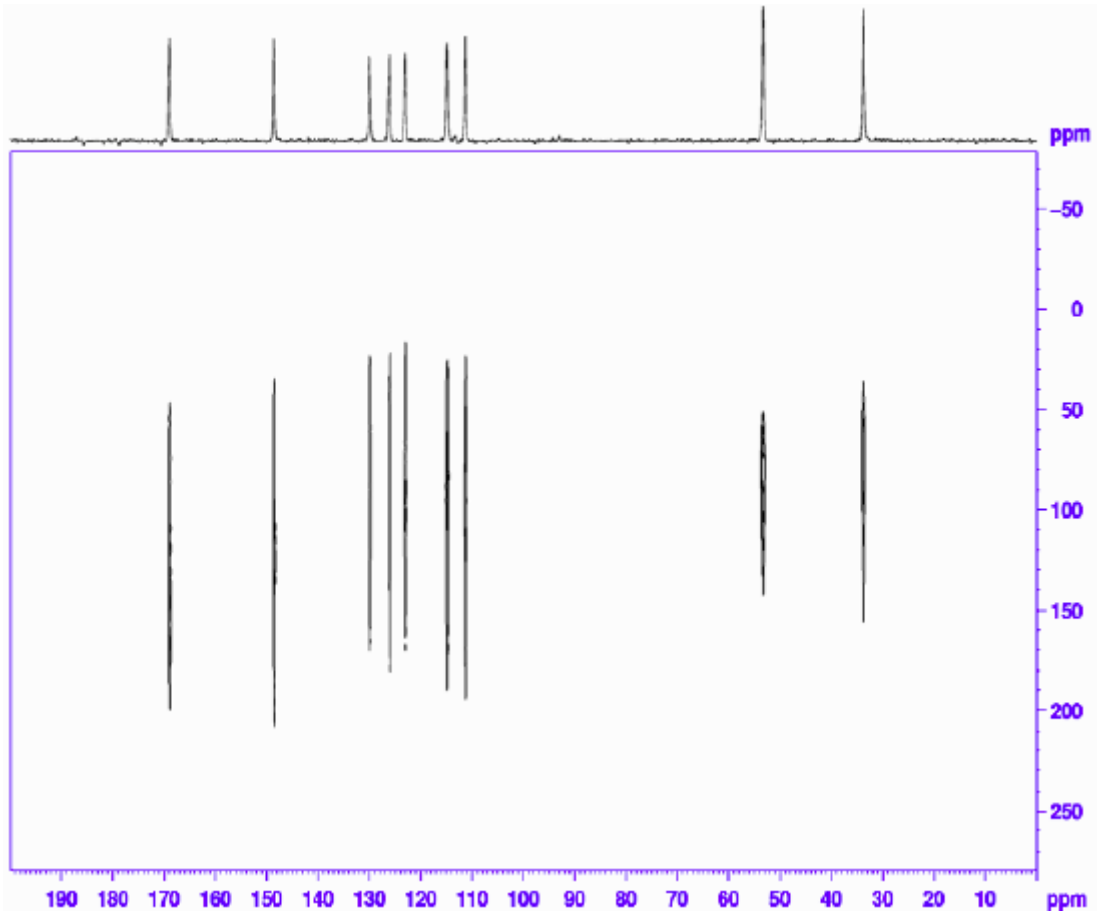

Figure 13.5. SUPER spectrum after tilting the spectrum setting "1 alpha" = -1

The figure above is a SUPER spectrum after tilting the spectrum setting "1 alpha" = -1 and using the command "ptilt1" repeatedly until the CSA lines are within the spectral range.

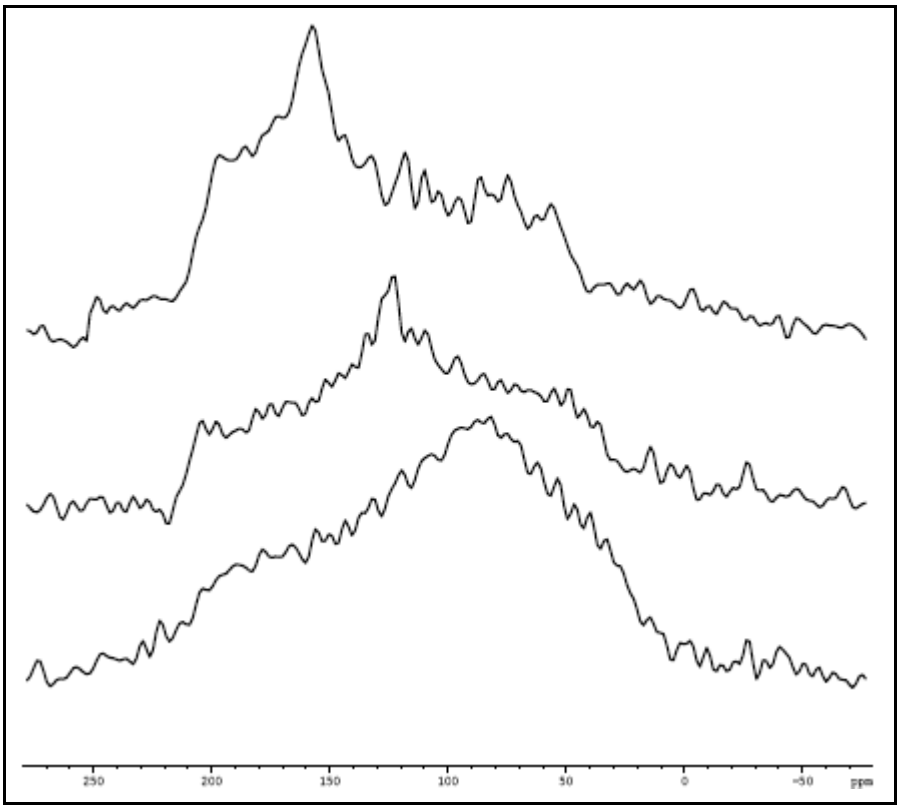

Figure 13.6. Various Cross Sections from the Upper 2D Experiment

The figure above illustrates various cross sections from the upper 2D experiment, from which CSA parameters can be determined.

Symmetry Based Recoupling

14

Sample rotation averages most anisotropic interactions, and therefore removes the information available from them. Therefore, selective recoupling of anisotropic interactions is desired for structural analysis (re-coupling, *re*introduction of anisotropic interactions, like e.g. dipolar *coupling*), in order to regain specific information. The topic has been thoroughly reviewed, by E.A. Bennett et al, and by S. Dusold et al. One strategy is the use of symmetry based recoupling sequences; see M. Hohwy et al (1998) et al. and A. Brinkmann et al. (2000). In these sequences, double quantum coherence are excited via the dipolar homonuclear dipolar coupling. Single quantum coherence are suppressed by phase cycling. The size of the dipolar coupling can be determined from the build-up rate of DQ signal intensity, measured after reconversion into SQ coherence. It should also be mentioned that there are recoupling sequences that do not generate double quantum coherences (DRAWS, DRAMA, and MELODRAMA).

Symmetry-based recoupling sequences recouple specific spin interactions, using cyclic sequences composed of N phase-shifted repetitions of either 2π (C sequences) or π (R sequences) rotation elements. Which interaction(s) are recoupled by a given sequence is determined by the relationship between the sample rotation rate, the spin rotation rate, and the rate of phase shift between the elements. The sequences are denoted as e.g. $CN\frac{\nu}{n}$, where N is the number of elements in the cycle, n is the number of rotor periods spanned by the N elements, and the total phase rotation between the elements is $2\pi/\nu$. In the simplest implementation of a C sequence, the 2π rotation element is simply a 2π pulse, but other elements are possible. Thus the sequence $C7^1_2$ consists of 7 consecutive 2π pulses, with the phase of each pulse shifted by $2\pi/7$ from the previous one. The whole sequence takes two rotor periods, each 2π pulse thus takes $2/7^{th}$ rotor period. The spin nutation frequency and sample rotation frequency are thus related by $\nu_{RF} = (7/2)*\nu_{rotor}$. In practice, the original C7 sequence uses an additional π-phase alternation for every second pulse, so that 14 pulses are executed during 2 rotor periods, requiring $\nu_{RF} = 7*\nu_{rotor}$.

For all C and R sequences, the spin nutation frequency must be accurately matched to the sample rotation rate. Since X-X dipolar couplings are usually small, long mixing times are required to reintroduce the dipolar coupling. When ^1H decoupling is required, it is important to avoid any transfer of magnetization to or from the proton spin system (HH condition), which would destroy the desired information. This means that the effective fields on X and H must be very different. However, proton decoupling must still be efficient as well. It has been shown that the two RF fields should differ by a factor of 3, which in practice is extremely difficult to meet. It has also been shown that at very high spin rates (>16 kHz) decoupling is not necessary at all. A possible trick is also to use off-resonant LG decoupling during the recoupling sequence. This enhances the effective proton field (vector sum of RF field and offset), and sharpens the HH condition since the homonuclear couplings are suppressed.

Another important parameter to observe is the required excitation bandwidth of these sequences. Naturally, going to higher magnetic fields, the higher chemical shift spread requires higher RF fields for the recoupled X-nuclei, requiring even higher RF fields for protons. So the tendency is going to high spin rates (also desired to get rid of spinning sidebands) and turning the decoupling off during recoupling, which represents a much lower RF load to the probes and increases experimental stability substantially.

Table 1 shows the sample rotation rate and the required spin nutation frequencies for the X-nucleus. The spin nutation frequency must be 7 times the sample rotation rate for C7, 5 times the sample rotation rate for SPC5 and 3.5 times the sample rotation rate for SC14. Be careful to obey the maximum allowed spin nutation frequencies for the hardware in use.

It is essential that all these parameters are considered carefully in context with the properties of your sample before the experiment is started, so that the appropriate hardware is used. Especially the choice of the MAS-probe is essential to achieve a sensible setup. ***Table 14.1.*** shows the selection parameters for three standard recoupling sequences.

References:

1. E.A. Bennett, R.G. Griffin, and S. Vega, *Recoupling of homo- and heteronuclear dipolar interaction in rotating solids*, NMR Basic Principles and Progress **33**, 3-77 (1994).
2. S Dusold and A. Sebald, *Dipolar Recoupling under Magic-Angle Spinning Conditions,* Annual Reports on NMR Spectroscopy **41**, 185-264 (2000).
3. M. Hohwy, H.J. Jakobsen, M. Eden, M.H. Levitt, and N.C. Nielsen, *Broadband dipolar recoupling in the nuclear magnetic resonance of rotating solids: A compensated C7 pulse sequence*, J. Chem. Phys. **108**, 2686 (1998).
4. M. Hohwy, C.M. Rienstra, C.P. Jaroniec, and R.G. Griffin, *Fivefold symmetric homonuclear recoupling in rotating solids: Application to double quantum spectroscopy*, J. Chem. Phys. **110**, 7983 (1999).
5. M. Hong, *"Solid-State Dipolar INADEQUATE NMR Spectroscopy with a Large Double-Quantum Spectral Width"*, J. Magn. Reson. **136**, 86-91 (1999).
6. A. Brinkmann, M. Edén, and M.H. Levitt, *Synchronous helical pulse sequences in magic-angle spinning nuclear magnetic resonance: Double quantum recoupling of multiple-spin systems*, J. Chem. Phys. **112**, 8539 (2000).
7. M. Hohwy, C.M. Rienstra, and R.G. Griffin, *Band-selective homonuclear dipolar recoupling in rotating solids*, J. Chem. Phys. **117**, 4974 (2002)
8. C. E. Hughes, S. Luca, and M. Baldus, RF driven polarization transfer without heteronuclear decoupling in rotating solids, Chem. Phys. Letters, **385**, 435-440 (2004).

Pulse Sequence Diagram, Example C7 14.1

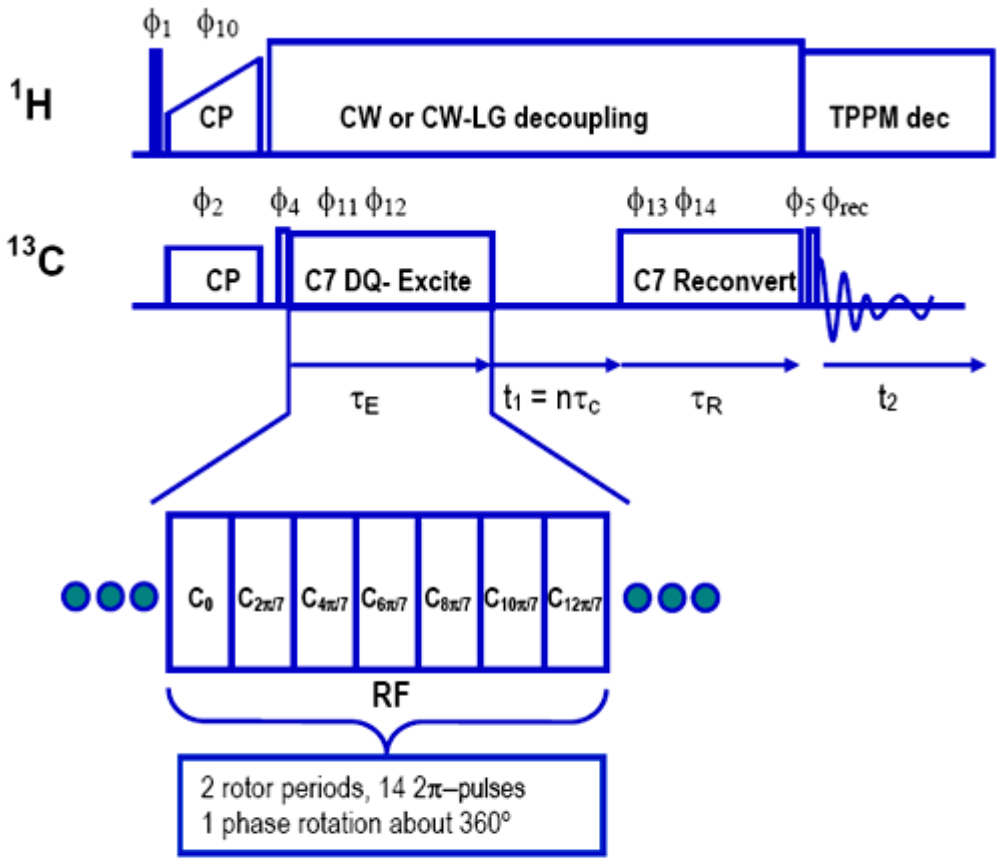

ϕ_1= 0	ϕ_2 = 0	ϕ_4= 3
ϕ_5 = 1 2 3 0	$\phi_{11, 12}$ = φ,φ+180° +QD-phase	$\phi_{13, 14}$ = 90° + (φ,φ+180°) +θ_{DQ}
ϕ_{DQ}= 0 1 2 3	ϕ_{rec}= 0 3 2 1	

Figure 14.1. C7 SQ-DQ Correlation Experiment

Setup 14.2

As mentioned before, it is essential that the parameters of your sample of interest are considered before the experiment is started. ***Table 14.1.*** illustrates the proper choice of hardware for the observe nucleus ^{13}C. Obviously, observation of DQ coherence requires samples with reasonable dipolar couplings and reasonable probability of coupled species. So, running this experiment on ^{13}C samples requires reasonable enrichment. Usually, fully enriched samples are used, sometimes diluted in natural abundance samples to reduce nonspecific long range interactions. As always, rotary resonance conditions (overlap of side- and center bands) should be avoided unless specifically desired.

Running the experiment on enriched ^{15}N samples is of course possible, but one should consider that most samples will not have nitrogen atoms directly attached to each other, so small couplings will prevail, requiring long DQ-excitation and -re-conversion times, with a nucleus that requires high RF power levels to achieve a certain RF-field. On the other side, the shift range is not large, allowing relatively slow spinning. Considering a nucleus like ^{31}P, there is no need for enrichment, but cases with directly bonded ^{31}P-atoms are rare. Phosphates are usually easy, since the shift range is small (couplings are also rather small). If however a large shift range (possible with ^{31}P) needs to be covered, there may be a substantial problem.

Table 14.1. Recommended Probe/Spin Rates for Different Experiments and Magnetic Field Strengths

Sequence	n= (ν_{RF}/ *masr)*	rotor diameter/ *masr* max.	*masr* max. rec. [4] (Hz)	$\nu_{RF}(^{13}C)$ max. (kHz/µs) [5]	$\nu_{RF}(H)$ max. (kHz/µs) [6]	B_o max. (MHz) [8]
POST-C7 [1]	7	7/6000	5000	35 / 7.15	70 / 3.5 +LG	300
		4/15000	9000	63 / 4	100 / 2.5 +LG [7]	500
		3.2/24000	12000	84 / 3	110 / 2.27 +LG [7]	600
		2.5/35000	14000	100 / 2.5	130 / 1.95 +LG [7]	800
SPC5 [2]	5	7/6000	5000	25 / 10	70 / 3.5	300
		4/15000	13000	65 / 3.85	100 / 2.5 +LG [7]	500
		3.2/24000	17000	85 / 3	none	700
		2.5/35000	20000	100 / 2.5	none	900
SC14 [3]	3.5	7/6000	6000	21 / 12	70 / 3.5	200
		4/15000	15000	52.5 / 4.75	100 / 2.5 +LG [7]	500
		3.2/24000	22000	77 / 3.25	none	700
		2.5/35000	28000	100 / 2.5	none	950

1. C7 is not recommended due to restricted excitation bandwidth.
2. SPC5 can be recommended as a standard sequence for 4mm probes and not too high fields.
3. SC14 or sequences with similar RF-field requirements are recommended for small spinners/high fields
4. Maximum speed results from max. possible RF-field
5. Maximum ^{13}C RF fields taken from ^{13}C RF field specification, or ^{1}H RF field specification, considering the requirement of an off HH condition.
6. Maximum RF field for decoupling
7. +LG means cw decoupling with optimized LG-offset frequency at the given RF field in order to avoid HH contact.

8. Maximum magnetic field as proton resonance frequency in MHz. This results from spin rate requirements for 13C observation (to avoid rotary resonance conditions) as well as excitation bandwidth considerations.

Spectrometer Setup for 13C *14.2.1*

1. Load a CPMAS parameter set for ^{13}C.
2. Load a uniformly labeled glycine sample and rotate at the desired rotation rate (see table 1), depending on the recoupling experiment planned and the sample under investigation. Consider possible rotational resonance conditions in the sample of interest!
3. Tune and match the probe, optimize the ^{13}C and ^{1}H pulse parameters for excitation and decoupling.
4. Use the *cp90* pulse program with ***pl11= pl1*** to measure the nutation frequency for ^{13}C, in order to calculate the recoupling conditions (see chapter …. Basic Setup Procedures). Calculate the power levels required by the spin speed (see table 1) using ***calcpowlev***.
5. Set ***pl11*** back to 120 dB (***p1*** to zero) and run 1 experiment with 16 (4) scans as a reference.

Setup for the Recoupling Experiment *14.2.2*

1. Create a new experiment and load the appropriate pulse program (***spc5cp1d***), use the same routing. Set the appropriate sample rotation rate, as required for step 14, set ***cnst31*** equal to the rotation rate.
2. Load the power level calculated for the necessary ^{13}C recoupling B_1-field into ***pl11***, set ***p1*** as determined in step 4.
3. Set ***l0=15*** (should be, but need not be, a multiple of 5 for SPC5 or of 7 for PC7, SC14). This determines the DQ-build-up time (DQ generation). The reconversion time is usually also controlled by ***l0***, it may however be written such as to be independently controlled by a different loop counter. For glycine, about 5msec will be the optimum.
4. Set the decoupling program ***cpdprg1*** to ***cwlg***. Set ***pl13*** such as to yield the desired decoupler RF field during the DQ generation/ reconversion, or set it to 120 if the spin rate suffices to omit decoupling. Set ***cnst20*** = corresponding decoupling RF field.
5. Optimize ***pl11*** for maximum signal intensity.
6. Optimize ***l0*** for optimum signal intensity. In a multi-site spectrum the optima may differ for different spin pairs.

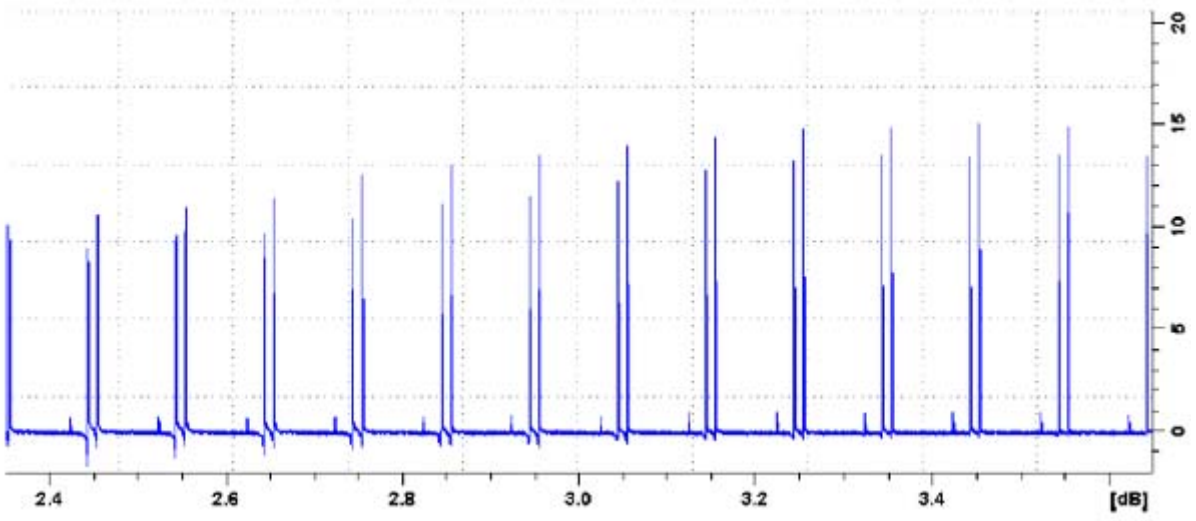

Figure 14.2. Optimization of the RF power level for DQ generation/reconversion on glycine.

*In principle, both peaks must grow together as one approaches the RF=7*MASR condition, but the resonances are differently influenced by non-ideal off-HH conditions. The glycine α-peak is usually hard to get off HH, so it is frequently too small. Optimise the LG-decoupling condition on the glycine α-peak (step 12).*

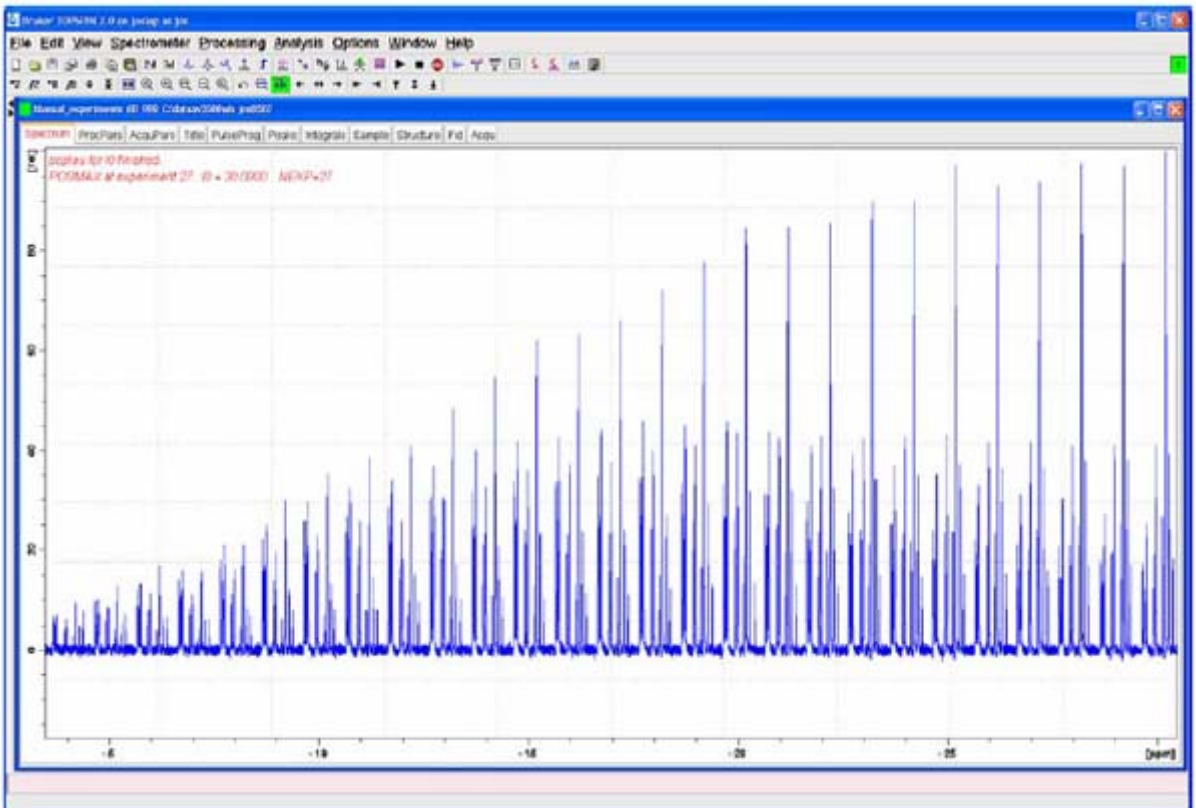

Figure 14.3. Variation of DQ-generation/reconversion time on a uniformly ^{13}C labeled peptide (fMLF).

Both times were incremented in units of 2 rotation periods. One can clearly see the different maxima for the C_a, the alphatic carbons and the mobile CH_3-groups. Spinning speed was 13 kHz.

7. Optimize the ***cwlg*** decoupling if needed by variation of ***cnst20*** in increments of 5000 and check whether a different offset condition helps improving the signal intensity.
8. Run one experiment and compare with the direct CP experiment to measure the DQ recoupling yield.

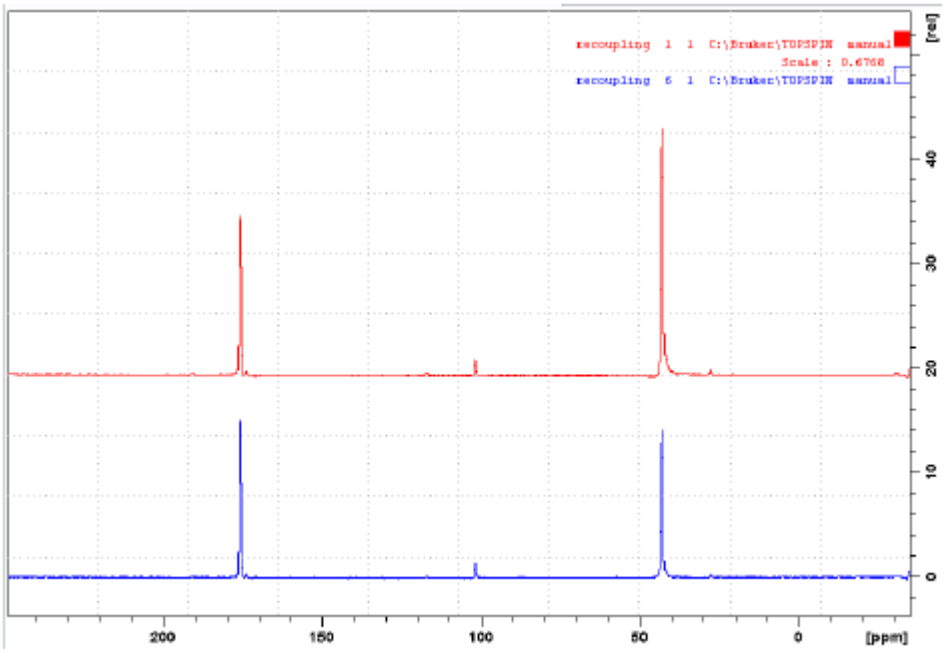

Figure 14.4. PC7 Recoupling Efficiency at a Spinning Speed of 13 kHz

Figure 14.4. *illustrates PC7 recoupling efficiency at a spinning speed of 13 kHz (about 100 kHz RF field), using a 2.5 mm probe. LG decoupling at 125 kHz was used during DQ generation/reconversion. Quite a noticeable loss on the glycine α-peak due to insufficient HH suppression is visible. Efficiency is 67% on the carboxyl peak (AVIII 700 SB).*

Setup of the 2D SQ-DQ Correlation Experiment *14.2.3*

9. Running such a correlation experiment on glycine makes little sense, so insert a sample with more 13C sites (fully labelled tyrosine-HCl, or histidine or any other suitable labelled sample). Optimize ***l0*** for the best compromise in signal intensities.
10. Generate a new data set, set the mode to 2D using the 123 button in ***eda***. Load the pulse program ***spc5cp2d***.
11. Make sure ^{13}C is selected as ***nuc1*** in the F1 dimension, set ***FnMode*** =STATES-TPPI.

12. Set the spectral window along F1. It is desirable to synchronize sampling along F1 with the rotor spin rate in order to eliminate spinning sidebands (fold back onto center band). This may however lead to peak fold over, since achievable spin rates are usually smaller than the spread of DQ-frequencies along F1. This does however not necessarily mean that the spectra are crowded and uninterpretable, because frequently the folding does not lead to cross peak overlap. Of course, the synchronisation to the spin rate need not be used, ***cnst31*** can be set equal to the sweep width along F2 which will normally produce spectra free of folding, but of course, spinning sidebands along F1 will occur and signal intensity will be spread over a larger number of cross peaks. An intermediate sampling rate along F1 can be achieved by incrementing the evolution period synchronised to the phase shifted blocks of the sequence (one PC7-block being 2τ/7, τ=rotor period). This will also not generate sidebands along F1, but provide a larger sweep width and less fold over (M. Hong 1999). Fold over can often be tolerated, ***xfshear rotate*** may be used to shift the spectrum suitably along F1.
13. Set the acquisition time along F1 to about 10 msec for a start. Lines along the double quantum dimension may be narrower than along the single quantum dimension, so a compromise between experiment time and digital resolution along F1 must be found.
14. Start the experiment.

Data Acquisition *14.3*

Sample: Fully 13C labelled tyrosine-HCl, or a suitable fully labelled small peptide

Spinning speed: 5 – 20 kHz, depends on experimental requirements, see ***Table 14.1.***.

Experiment time: 1-4 hours.

Table 14.2. Acquisition parameters for DQ-SQ correlation experiments using symmetry based recoupling sequences

Parameter	Value	Comments
Pulse program	spc5cp2d spc5cp2dlsw sc14cp2d r14cp2d pc7cp2d ……	See ***Table 14.1.*** for hints which sequence to prefer. Rule of thumb: high field: fast spinning, sc14 low field, slow spinning, pc7. Intermediate: spc5. N.b.: sc14 usually has low DQ yield (35%), but that may not matter
NUC1	^{13}C	Nucleus on f1 channel
O1P	100 ppm	^{13}C offset
NUC2	^{1}H	Nucleus on f2 channel
O2P	2-3 ppm	^{1}H offset
PL1	for > 50 kHz ν_{RF}	Power level for f1 channel CP and p1
PL11	dep. on ***masr***	Power level for f1 channel recoupling power

Table 14.2. Acquisition parameters for DQ-SQ correlation experiments using symmetry based recoupling sequences

PL12	as specified	Power level decoupling f2 channel and excitation
PL13	≈pl12, optimize, or 120, fast spinning	Power level decoupling f2 channel during cw or cwlg decoupling
P3		Excitation pulse f2 channel
PCPD2		Decoupler pulse length f2 channel (^{1}H) TPPM
P15		Contact pulse – first contact
D1		Recycle delay
CNST20		Spin nutation frequency at PL13 for cwlg decoupling
L0	for 0.5-10 msec („mix“ in ***ased***)	Use multiples of 5, 7, or 16 (spc5, pc7, sc14) for full phase cycle.
SPNAM0		Ramp for 1st CP step; e.g. ramp: 80 – 100%
SP0		Power level for proton contact pulse
CPDPRG2	SPINAL64	SPINAL64 decoupling
CPDPRG1	cwlg	To avoid HH contacts during DQ-generation, reconversion
NS	4-32	Number of scans (see pulse program phase cycle)
F2 direct ^{13}C		(left column)
TD	1024 or 2048	Number of complex points
SW		Sweep width direct dimension, adjust to experimental requirements
F1 indirect ^{13}C		(right column)
TD	128 - 512	Number of experiments in indirect dimension
SW	see para. 17 above	Sweep width indirect dimension
ND0	1	STATES-TPPI, not required. In TS 2.1

Spectral Processing *14.4*

Processing Parameters

Table 14.3. Processing parameters for DQ-SQ correlation experiments using symmetry based recoupling sequences

Parameter	Value	Comment
F1 acquisition ^{13}C		(left column)
SI	2-4 k	Number of points and zero fill
WDW	QSINE	Sine bell squared
SSB	2-5	Shifted sine bell
PH_mod	pk	Phase correction if needed
F2 indirect ^{13}C		(right column)
SI	256-1024	Zero fill
MC2	STATES-TPPI	
WDW	QSINE	Sine bell squared
SSB	2	90º shifted sine bell

*Processing parameters for DQ-SQ correlation experiments using symmetry based recoupling sequences. The AU program **xfshear** may be used with option **rotate** and argument(+/- δ ppm) to shift the spectrum suitably along F1. Setting 1 **sr** = 2***sr**+**o1** will set the referencing along F1 correctly (just type **sr**, and in f1 enter the value of **sr** for F2 and add *2+o1).*

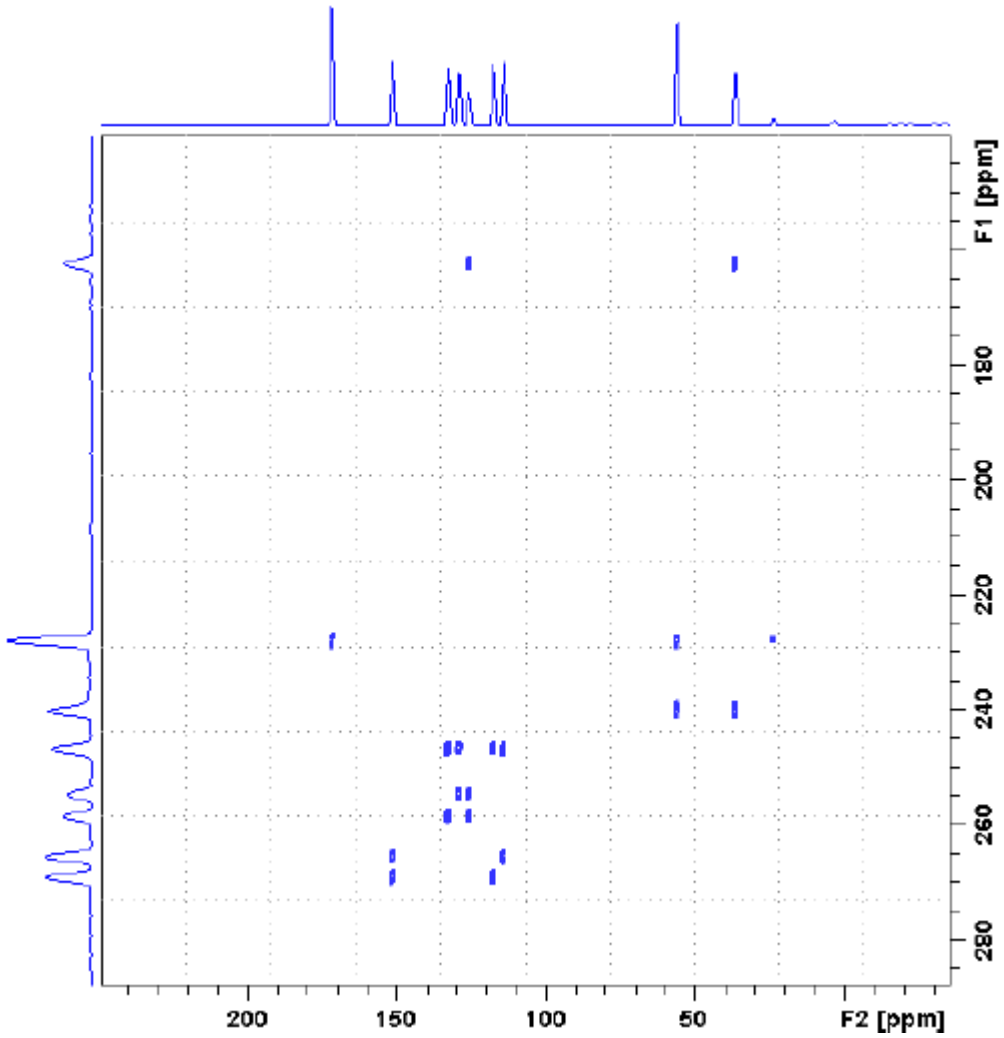

Figure 14.5. SC14 2d SQ-DQ correlation on tyrosine-HCl

SC14 2d SQ-DQ correlation on tyrosine-HCl, 56 rotor periods mixing at 26 kHz, 2.5 mm probe, AV III 700 SB. With the sampling window along F1= spin rate, only the α-β-correlation is folded.

13C-13C Single Quantum Correlation with DQ Mixing *14.5*

Symmetry based DQ recoupling sequences may also be used as mixing periods in SQ-SQ correlation experiments. The experiment resembles the PDSD or RFDR experiments (see ***"Proton Driven Spin Diffusion (PDSD)"*** and ***"RFDR"***) as a NOESY-type correlation will be generated. Similarly, the MELODRAMA (see Bennett et al., Dusold et al.) sequence with $\nu_{RF} = 5*\nu_{rotor}$ may be used here.

Data Acquisition *14.6*

Parameter	Value	Comments
Pulse program	pc7cp2dnoe	Any sequence may be used, make sure to use the correct timing.
NUC1	^{13}C	Nucleus on f1 channel.
O1P	100 ppm	^{13}C offset.
NUC2	^{1}H	Nucleus on f2 channel.
O2P	2-3 ppm	^{1}H offset.
PL1	for > 50 kHz ν_{RF}	Power level for f1 channel CP and p1.
PL11	dep. on ***masr***	Power level for f1 channel recoupling power.
PL12	as specified	Power level decoupling f2 channel and excitation.
PL13	≈pl12, optimize, or 120, fast spinning	Power level decoupling f2 channel during cw or cwlg decoupling.
P3		Excitation pulse f2 channel.
PCPD2		Decoupler pulse length f2 channel (^{1}H) TPPM.
P15		Contact pulse.
D1		Recycle delay.
CNST20		Spin nutation frequency at PL13 for cwlg decoupling.
L0	for 0.5-10msec („mix“ in ***ased***)	Use multiples of 5,7, or 16 (spc5,pc7,sc14)for full phase cycle.
SPNAM0		Ramp for 1st CP step; e.g. ramp: 80 – 100%.
SP0		Power level for proton contact pulse.
CPDPRG2	SPINAL64	SPINAL64 decoupling.
CPDPRG1	cwlg	To avoid HH contacts during DQ-generation, reconversion.
NS	4-32	Number of scans (see pulse program phase cycle).
F2 direct ^{13}C		(left column)
TD	1024 or 2048	Number of complex points.
SW		Sweep width direct dimension, adjust to experimental requirements.
F1 indirect ^{13}C		(right column)
TD	128 - 512	Number of experiments in indirect dimension.
SW	usually = sw (F2)	Sweep width indirect dimension.
ND0	1	STATES-TPPI, not required in TS 2.1.

Spectral Processing *14.7*

Processing parameters: as above

Parameter	Value	Comment
F1 acquisition ^{13}C		(left column)
SI	2-4 k	Number of points and zero fill.
WDW	QSINE	Sine bell squared.
SSB	2-5	Shifted sine bell.
PH_mod	pk	Phase correction if needed.
F2 indirect ^{13}C		(right column)
SI	256-1024	Zero fill.
MC2	STATES-TPPI	
WDW	QSINE	Sine bell squared.
SSB	2-5	90° shifted sine bell.

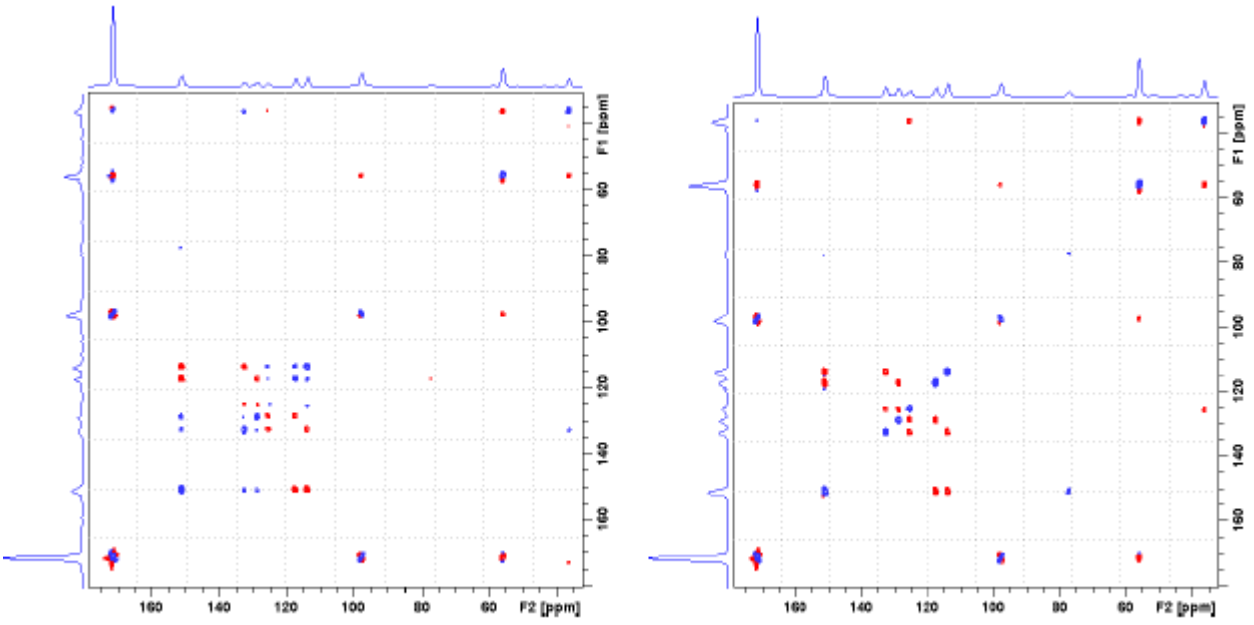

Figure 14.6. PC7 2d SQ-SQ correlation on tyrosine-HCl

PC7 2d SQ-SQ correlation on tyrosine-HCl, 56 rotor periods mixing at 13 kHz, 2.5 mm probe, AV III 700 SB. Left: 84 rotor periods DQ mixing, right:56 rotor periods mixing. The 84 periods mixing time show relayed correlations (positive, blue) which are absent at 56 periods mixing (except for the SSB cross peaks). Direct correlations are negative (red).

PISEMA 15

Polarization Inversion Spin Exchange at the Magic Angle is an experiment that correlates the chemical shift of a spin 1/2 X nucleus with the heteronuclear dipolar coupling to another spin 1/2 nucleus. Most of the applications so far reported have been in the field of structural biology, therefore, the X nucleus is normally ^{13}C or ^{15}N and the other hetero-nucleus ^{1}H. The experiment provides orientation information on the vector connecting the ^{13}C or ^{15}N and the ^{1}H nucleus. The achievable high resolution of the CS as well as the dipole coupling makes the experiment well suited for 3D NMR experiments on aligned systems or single crystals.

Unlike normal FSLG experiments, where the dipolar and CS interactions are scaled by,

$$\cos(\theta_m) = 0.577$$

the scaling factor for the heteronuclear dipolar interaction is

$$\sin(\theta_m) = 0.816$$

because the coupling takes place in the transverse plane of the rotating frame, the spin locked state. (The projection is from the tilted frame (locked ^{1}H spin system) to the transverse plane of the rotating frame system (spin locked ^{15}N spin system), i.e.,

$$\sin(\theta_m) = 0.816$$

the scaling of the heteronuclear dipolar coupling strength.

Through the combination of spin exchange (dipolar flip flop term) and the homonuclear decoupling using FSLG, PISEMA achieves a line width that is an order of magnitude better than its predecessor, the separated local field experiment.

The central line in the dipolar dimension can be caused among other things by a proton frequency offset introducing a constant term in the time domain signal. That offset frequency makes also the splitting larger. See additional test procedures in the paper about „experimental *aspects of multidimensional solid state correlation spectroscopy“*.

PISEMA is not very sensitive to the exact Hartmann-Hahn condition. A mismatch has only little effect on the dipolar coupling. The scaling factor in the indirect dimension depends of the ^{1}H resonance offset and a wrong ^{1}H carrier frequency can cause besides a wrong scaling factor some intensity loss and, as mentioned above, a zero frequency contribution. Diligent adjustment of the LG condition and the rf-carrier is critical for accurate measurement of the dipolar coupling as the splitting increases quadratic with increasing (proton) frequency offset.

Simulations of the spin dynamics show that the heteronuclear term in the Hamiltonian leads to a complicated spectrum for small heteronuclear dipolar couplings (usually introduced by remote protons), see Z. Gan's paper for more information.

References:

1. C.H. Wu, A. Ramamoorthy, and S.J. Opella, *High-Resolution Heteronuclear Dipolar Solid State NMR Spectroscopy*, J. Magn. Reson. A 109, 270-272 (1994).
2. A. Ramamoorthy, C.H. Wu, and S.J. Opella, *Experimental Aspects of Multidimensional Solid State NMR Correlation Spectroscopy*, J. Magn. Reson. 140, 131-140 (1999)
3. A. Ramamoorthy, and S.J. Opella, *Two-dimensional chemical shift / heteronuclear dipolar coupling spectra obtained with polarization inversion spin exchange at the magic-angle sample spinning (PISE-MAMAS),* Solid State NMR 4, 387-392 (1995).
4. Zhehong Gan, *Spin Dynamics of Polarization Inversion Spin Exchange at the Magic Angle in Multiple Spin Systems,* J. Magn. Reson. 143, 136-143 (2000).

Pulse Sequence Diagram *15.1*

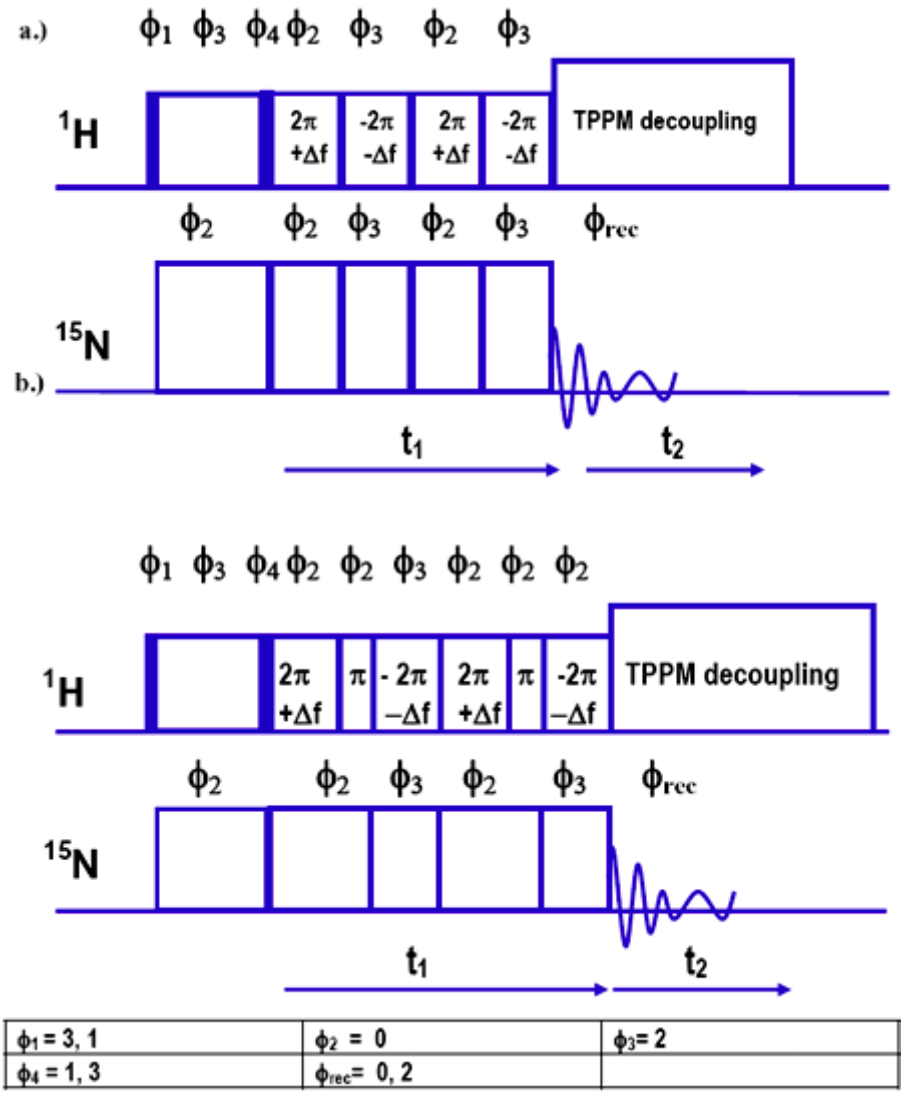

Figure 15.1. Pisema Pulse Sequence

***Figure 15.1.**: Pisema pulse sequence a.) straight PISEMA, b.) "clean PISEMA" variation for further suppression of phase glitches (Ramamoorthy et al. Solid State NMR 4).*

Setup *15.2*

Sample: 15N labelled α-glycine powder for power level determination, 15N labelled acetylated glycine or acetylated valine or leucine for running the PISEMA experiment, preferably as single crystal.

Setup time: 0.5 h on labelled glycine.

Experiment time: 15h on a labelled powder sample, 1-2 h on a good size single crystal.

1. Set up for static 15N CP observation on the α-glycine powder sample, pulse program ***cp***. Use a ramp pulse if the HH condition is unknown, with power level settings for an approximate 5 µsec pulse on both channels.
2. Determine the proton 90 degree pulse ***p3*** at the respective power level, reset the conditions for a square shape and about 50 kHz on both channels for contact. Load the pulse program ***cplg***. With ***cnst17***=0, ***pl2=pl13*** and ***pl1*** all set for 50 kHz, reestablish the HH condition.
3. To adjust the CP condition under a LG-offset, load the pulse program ***cplg***. Cnst 17 sets the LG-offset during the contact, the offset frequencies are calculated as cnst 18 and cnst19. Start with cnst17=0.
4. Two possibilities exist to set the FSLG power levels and offset frequencies.

a. Either, use the appropriate offset frequency for the chosen contact power level of ^{1}H and set ***cnst20*** accordingly to e.g. 50 kHz, i.e ***cnst17 = 50000.0***. This would give an offset frequency of approximately 35 kHz (***cnst19*** should show this number in the ***ased*** display) Then adjust the **^{15}N** power level during the FSLG period to best HH match - which is at a power level of appropriately 20*log(sin(54.7))=**1.8 dB higher** than for the on resonance contact.

If that option is not adequate because of power limitations on ^{15}N, one can also leave the on resonance contact levels of ^{15}N and calculate the offset frequency and power level for ^{1}H. That reduces the required proton RF power by about 70% as compared to the power level for a resonant HH match. For the new nutation frequency (B1 field for LG condition):

$$B_{1LG}(^{1}H) = \sin(\theta_m) * B_{1on\_res}(^{1}H) = 0.82 * B_{1on\_res}(^{1}H)$$

the offset frequency for the Lee-Goldburg condition is:

$$f_{LG} = \cos(\theta_m) * B_{1on\_res}(^{1}H) = 0.578 * B_{1on\_res}(^{1}H)$$

with the inverse of a 360º pulse.

$$B_{1on\_res} = 1/(\tau_{2\pi})$$

Instead of raising the power level for ^{15}N, the power level for **^{1}H is reduced by about 1.7 dB**. Then the new 2π pulse in the tilted frame is:

$$\tau_{2\pi_{LG}} = B_{1on\_res}^{-1} \sin^2(\theta_m) = 0.67 B_{1on\_res}^{-1}$$

In our example of a contact power level of 50 kHz on ^{15}N one would then calculate for ***cnst17 = 40 807.0***, giving an offset frequency of 28855 Hz for the LG frequency, which is calculated automatically.

5. In order to verify all calculated power levels and offset frequencies, optimize for the appropriate power level using the pulse program ***cplg***.
6. Change to the desired PISEMA sample. Since a powder contains all possible spin pair orientations, the measurement of an oriented sample is much recommended, because it is not only much faster, but also allows to judge the performance much better. N-acetly valine can be rather easily grown to sizeable single crystals and has all properties for a good setup sample: decent proton T1, well defined sites and therefore narrow resonances. For a good crystal, the residual proton line width will reflect the quality of the setup. Beware of crystal twinning. The orientation of the sample should be selected carefully.
7. If the sample does tune and match very differently than the setup sample, check the HH conditions briefly and verify that the found parameters are valid. Correct power levels or pulse parameters if needed. This is especially important for saline lipid water mixtures.
8. Depending on the decision taken in (4), set

a. either PL13 = PL2 (case 4a) and set PL11 to the optimized value, higher power, i.e. a value of about 1.8 dB below pl1;

b. or set PL11 = PL1 (case 4b) and PL13 to the obtained value in the cplg experiment, i.e. about 1.8 dB higher than PL2, which is less RF power.

9. Depending on the orientation of the single crystal, O1 and O2 need to be reoptimized since the peak positions will change. Select an orientation that shows the most low-field ^{15}N peak positions, because that will usually correspond to the biggest ^{1}H-^{15}N dipolar couplings.
10. Reoptimise power levels for the HH-contact.
11. Create a new experiment and setup a 2D data set, using the 1,2,3-icon. Load the ***pisema*** pulse program. Go into the ***eda*** window.
12. Make sure the correct nucleus is selected in the F1 dimension.
13. In order to set the t_1 increment, go into the ***ased*** window clicking the pulse symbol, and choose ***I3*** to be 1, 2 or 3. This sets the t_1 increment and the parameter ***in0*** is updated. Use the calculated value and set ***inf1*** in the ***eda*** window correspondingly. Since dipolar couplings between ^{1}H and ^{15}N can be up to 15 kHz, the spectral width (including the experiment scaling factor) should be min. around 20 kHz.

Table 15.1. Acquisition Parameters

Parameter	Value	Comments
PULPROG	Pisema, pisema-clean	Pulse programs.
NUC1	15N	
SW		Reasonable SW in F2.
O1P	90 – 160 ppm	For 15N labeled acetylated glycine.
NUC2	1H	
O2P	to be optimized	For 15N labeled acetylated glycine.
PL1		For 15N contact.
PL11		Or 15N evolution.
PL2		For 1H contact and excitation.
PL12		For 1H heteronuclear decoupling during t2.
PL13		For 1H Evolution under FLSG condition.
P3		1H excitation pulse.
P15		15N-1H Contact pulse.
P6		1H LG 294 degree pulse.
D3	1.4 µs	For frequency & phase setting D*X only.
cnst20		1H spin nutation frequency achieved with PL13.
cnst21	0	Offset from o2 in Hz.
cnst22		+ LG frequency in Hz calculated.
cnst23		- LG frequency in Hz calculated.
L3	1 – 3	Loop counter for appropriate t1 increment.
F2 acquisition 15N	**********	(left column).
AQ_MOD	qsim	
TD	512	No of points.
DW		Dwell time in t2.
F1 indirect 1H	**********	(right column).
TD	64	Number of points.
IN_F1	L3*2*p5*SF or L3*2.5*p5*SF	Scaling factor for PISEMA 0.82 = sin(54.7 deg.) calculated by pulse program.

1. Process the direct dimension with ***xf2***.
2. Accommodate for the *cos* modulated signal by setting thh imaginary part to zero using the au program *zeroim* by typing into the command line *zeroim*.
3. Process the indirect dimension with the command ***xf1***.
4. For more automated processing one can write a short macro using the command *edmac* and the filename ***pisemaft*** for examples: write the following commands using the text editor:

   xf2

   zeroim

   xf1
5. Save and close the ***edmac*** editor.
6. In the future you can do then the processing by simply typing *pisemaft* into the command line or even creating your own icon in TOPSPIN for this purpose.

Table 15.2. Processing Parameters for the Pisema Experiment

Parameter	Value	Comment
F2 acquisition ^{1}H	**********	Left column.
SI	1k	Number of complex points in direct dimension.
WDW	no	Apodization in t2.
F1 indirect ^{15}N	**********	Right column.
SI	128	Number of complex points in indirect dimension.
MC2	QF	

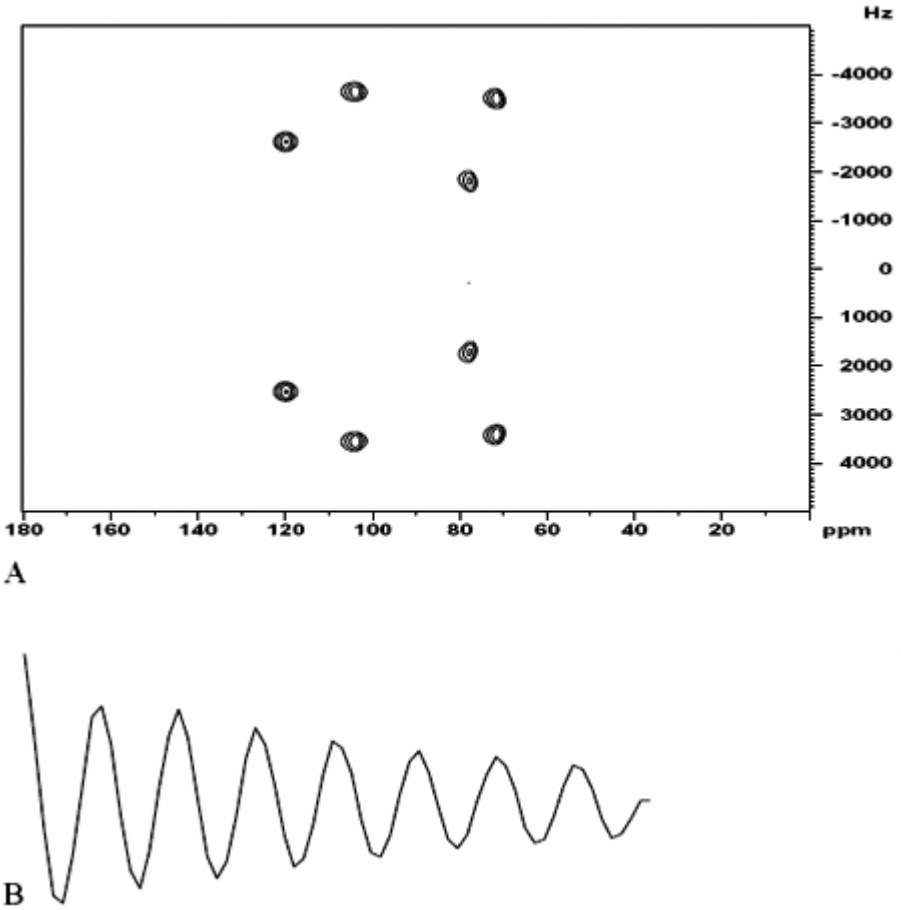

A) PISEMA Spectrum of ^{15}N Labeled Acetylated Valine,
B) FID in t1 over 3.008 ms 64 Data Points

Figure 15.2. PISEMA Spectrum of ^{15}N Labeled Acetylated Valine and FID in t1 over 3.008 ms 64 Data Points

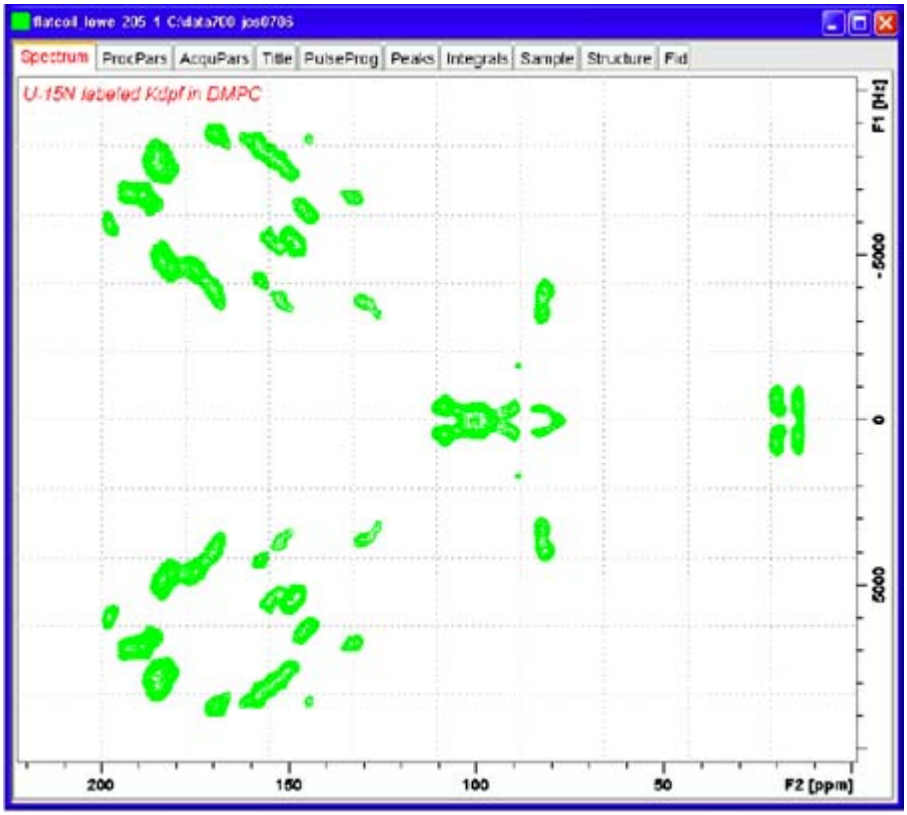

Figure 15.3. PISEMA Spectrum of ^{15}N Labeled Kdpf Transmembrane Protein.

PISEMA spectrum of ^{15}N labeled Kdpf transmembrane protein aligned in DMPC (courtesy of NHMFL, Dr. T. Cross) membrane between glass plates using an E^{FREE} 700 MHz probe.

Relaxation Measurements 16

In NMR experiments, one is generally concerned with measuring resonance frequencies, and relating these to the local molecular environment. To do this the state of the system of spins in the sample must be changed from equilibrium. At equilibrium, the net magnetization due to the spins is aligned along the magnetic field axis. By applying a radio frequency pulse the net magnetization is tilted away from the field axis, and the resulting precessing magnetization generates the observed signal. The pulse has disturbed the system from equilibrium, and over time the system will return to its equilibrium state. This process is called relaxation.

This chapter describes experiments used for measuring relaxation rates in solid-state NMR. A basic description of relaxation is provided in order to define terms and introduce the techniques involved, but discussion of the significance and use of relaxation data is outside the scope of this manual. Many textbooks provide more detail on the theory of relaxation: the classic is Abragam:

> A. Abragam, *Principles of nuclear magnetism*, Oxford: Clarendon Press, (1961)

but simpler descriptions can be found in the books of Slichter and Levitt:

> C.P. Slichter, Principles of magnetic resonance, *Springer* (1996, 3rd ed.)
>
> M.H. Levitt, Spin dynamics: Basics of nuclear magnetic resonance, *Wiley* (2001)

Some discussion of T_{1r} relaxation, including effects of dipolar coupling to proton spins, can be found in:

> D.L. VanderHart and A.N. Garroway, ^{13}C NMR rotating frame relaxation in a solid with strongly coupled protons: polyethylene, *J. Chem. Phys.*, **71**:2773-2787, 1979

Details of the X T_1 experiment with CP are in:

> D.A. Torchia, The measurement of proton-enhanced ^{13}C T_1 values by a method which suppresses artifacts, *J. Magn. Reson.*, **30**:613-616, 1978

The TOPSPIN software includes a tool for processing the data obtained in relaxation measurements, and this will be demonstrated for the different types of relaxation experiment.

Describing Relaxation 16.1

Relaxation of the net magnetization can be described in terms of two processes. After a pulse, the state of the system differs from the equilibrium in two ways: the z-magnetization is not equal to the equilibrium value, and the net magnetization in the transverse plane is non-zero. The return of the z-magnetization to equilibrium is termed longitudinal relaxation, or spin-lattice relaxation, and the return of trans-

verse magnetization to zero is termed transverse or spin-spin relaxation. Both the transverse magnetization and the difference between the current and equilibrium z-magnetization decay exponentially, with time constants denoted T_1 for longitudinal relaxation and T_2 for transverse relaxation. Relaxation also occurs while radio frequency pulses are being applied to the system. Normally this is ignored, but in the case of spin-locking pulses it is important. During cross-polarization, the magnetization on the dilute spins is increased by transfer from another nucleus, but it will also decay, since the radio frequency field (weak compared to the static field B_0) is insufficient to maintain the resulting transverse magnetization. If the pulse on the excitation nucleus is stopped, and only that on the detection nucleus continued, the transverse magnetization will decay exponentially, with a time constant denoted $T_{1\rho}$. This rate of decay will be strongly affected by the amplitude of the spin-locking pulse.

Both of these processes occur via spin energy level transitions. It turns out that the spontaneous transition rate is very low, and thus relaxation is dominated by stimulated transitions. Such transitions are stimulated by local magnetic fields, which fluctuate due to local molecular motion, and the transition rates depend on the strength, and details of the fluctuations, of these local fields. Since the fluctuations are random, the rate of fluctuation is defined by the correlation time of the motion. For efficient relaxation via a particular energy level transition, fields fluctuating with an inverse correlation time close to the frequency of the transition are required. Longitudinal relaxation occurs via transitions on a single spin, and thus requires fields fluctuating with inverse correlation times near to the Larmor frequency. Transverse relaxation occurs also via flip-flop transitions of pairs of spins, which have energies close to zero, and so local fields fluctuating very slowly will cause transverse relaxation. $T_{1\rho}$ relaxation involves transitions at the nutation frequency of the spin-locking pulse, which can be chosen by the experimenter. Measurement of these relaxation rates can therefore provide information about local motions on a range of time scales.

T1 Relaxation Measurements *16.2*

Longitudinal relaxation can be measured using a number of methods – which method is appropriate depends on the sample involved. Here the experiments are demonstrated on glycine, which has a very simple spectrum and will give results using all the methods discussed. In general the only setup required is to calibrate pulses for the nucleus under observation, and to have some idea of the relaxation time constants involved.

Experimental Methods *16.2.1*

The inversion-recovery method is the originally proposed method for measuring T_1 values. The experiment proceeds as follows: firstly, the magnetization is inverted by a 180° pulse. Then, there is a delay during which the magnetization relaxes, and a 90° pulse converts the remaining longitudinal magnetization to transverse magnetization, and an FID is recorded. The intensity of a particular signal in the resulting spectrum depends on the initial intensity, the relaxation delay, and the relaxation time constant T_1 as follows:

$$S(t) = S_E + (S(0) - S_E)\exp(-t/T_1) \qquad \text{(Eq. 16.1)}$$

where *t* is the relaxation delay, S_E is the maximum signal seen when *t* is infinite, *S(0)* is the signal measure with no relaxation delay, and T_1 is the relaxation time constant for the spins giving rise to that signal. Measurement of *S(t)* for a number of relaxation delays allows determination of T_1.

The disadvantage of the inversion recovery experiment is that the delay between scans needs to be somewhat longer than the longest T_1 of the slowest relaxing spins in the sample. If cross-polarization from protons is possible, the initial inversion pulse can be replaced by a cross-polarization step followed by a 90° pulse on the nucleus to be observed. Then, the required delay between scans ***d1*** becomes that for relaxation of the protons. *In most cases, the proton T1 is moderate so inversion recovery (Torchia method) is the method of choice.*

If the T1 relaxation time is extremely long, the saturation-recovery experiment is preferred. Here, the transitions are saturated by a rapid sequence of hard pulses, such that no signal remains. There is then a variable delay, during which relaxation occurs, and then a 90° read-out pulse. If the relaxation delay is very short, no signal is seen, and at long relaxation times the maximum signal is seen. The advantage is that the saturation time required does not need to be many times the longest T_1 value. The state of the system at the start of the experiment is forced by the saturation pulses, so a long recycle delay is not required.

The CP Inversion Recovery Experiment *16.2.2*

Sample: Glycine

Spinning speed: 10 kHz

Experiment time: 20 minutes

Before starting the experiment, the spectrometer should be set up as described in the basic setup procedures chapter, including measurement of the carbon pulse lengths, and the CP spectrum of glycine should be acquired for reference. Since relaxation times are necessarily temperature dependent, control of the sample temperature is desirable. The data shown here were all acquired at an approximate temperature of 20° C. The form of the pulse program is shown in the following figure.

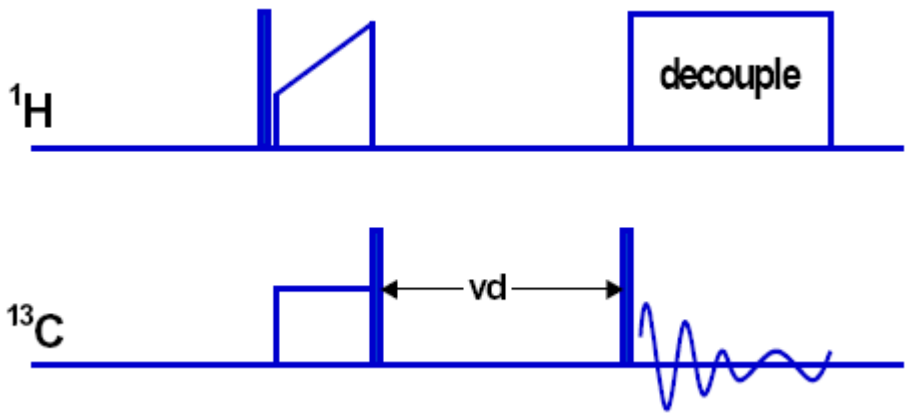

Figure 16.1. The CPX T1 Pulse Sequence

Starting from the glycine spectrum, create a new data set, set parameters according to ***Table 16.1.***, and acquire a 1D spectrum. The relaxation delay after inversion is controlled by a variable delay list – this can be created using ***edlist***, and the name of the list set as the parameter ***vdlist.***

Table 16.1. Parameters for the 1D CP Inversion Recovery Experiment

Parameter	Value	Comments
Pulprog	cpxt1	
Vdlist	See text	Relaxation delays after inversion pulse. Short value – to set spectrum phase correctly.
d1	3s	Needs only to be 3x proton T1
pl1	X HH contact power	standard cp setting
pl11	power for 90 degree pulses	usually pl11<pl1 for short pulses
p1	Measured 90° X pulse length at pl11	adequate for required excitation bandwidth
Ns	2	Should be enough to see a reasonable spectrum.

This pulse program uses the method of Torchia, in which the phase of the contact pulse, and the receiver, is inverted in alternate scans. In the first scan, the first 90° pulse creates –z magnetization, and in the second scan it creates +z. The phase cycling of the receiver means that the difference between the two scans is recorded. For short relaxation delays, neither relaxes significantly, and so the maximum signal is recorded. At longer relaxation delays, both the +z magnetization (which is larger than the equilibrium value as it is created by CP), and the –z magnetization relax, and the recorded signal decays exponentially as a function of the relaxation delay. At long times both have relaxed back to equilibrium, and the two scans yield a zero signal.

The resulting spectrum should be phased to give positive peaks – given the very short recovery delay, no appreciable relaxation will have occurred. Now we can set parameters for the 2D acquisition, as in ***Figure 16.1.***. Since this is a pseudo-2D experiment, the only relevant parameter in F1 is the number of points, which should be the number of entries in the vd list. The most important setting is the range of relaxation delays set in the vd list. Ideally, the list should run from times short enough for no appreciable relaxation to occur, up to a few times the longest T_1 value. Of course, the accurate relaxation time constants are not known in advance, but order of magnitude estimates can be obtained by running the 2D experiment with a small number of relaxation delays, and a small number of scans per slice. The relaxation delays should be approximately equally spaced in log(delay), in order that decays with all time constants in the range are equally well characterized. Data can always be improved either by increasing the number of relaxation delays sampled, or by averaging more FIDs at each relaxation delay. For the glycine sample, a suitable list of times would be:

100ms, 220ms, 450ms, 1s, 2.2s, 4.5s, 10s, 22s, 45s.

Table 16.2. Parameters for 2D Inversion Recovery Experiment

Parameter	Value	Comments
Parmode	2D	
Vdlist	See text	
td(f1)	Number of entries in vd list	
FnMODE	QF	This is not a real 2D experiment.
NS	4, for the glycine sample	Sample dependent – need to see a reasonable spectrum, but must be an even number.

Data Processing *16.2.3*

Once the pseudo-2D data has been recorded, the processing parameters must be set and checked before it can be evaluated using the T_1/T_2 relaxation tool. ***Table 16.3.*** lists the relevant parameters. No processing is done in the indirect dimension (the relaxation dimension), but the size must still be set to a power of two for TOPSPIN to create a processed data file. The size should be next power of two larger than the number of relaxation delays used. The zero points appended are ignored by the relaxation analysis. In principle the line shape in the frequency dimension does not affect the analysis, so exponential multiplication with ***lb*** of the order of the observed line width can be applied to improve the signal-to-noise ratio.

Table 16.3. Processing Parameters for CP T1 Relaxation Experiment

Parameter	Value	Comment
F2 – acquisition dimension		
SI	=TD	Zero fill.
LB		Matched to line width.
WDW	EM	
Ft_mod	FQC	
ABSF1	1000	Limits for baseline correction.
ABSF2	-1000	Should cover entire F2 width.
F1 – relaxation dimension		
SI	Smallest power of 2 greater than TD(F1)	Must be 2n, but any zeros will be ignored.

Once the parameters are set, process the data with ***xf2***, to execute a Fourier transform in the f2 dimension only. The phase can be adjusted from within the relaxation analysis tool, but baseline correction should be carried out with ***abs2.*** Start the relaxation analysis guide with the command ***t1guide***. The sequence of icons guides you through the analysis as follows:

Extract slice: The first spectrum row should be selected for phase correction, as this contains maximum signal. The spectrum should then be phased to give positive peaks.

Define ranges: Here you must define integral regions containing the peaks of interest. The fitting routine can either use the integral of the signal, or the intensity, in which case the maximum signal in each integral region is used. Regions can be defined via the cursor, or between specified limits via a dialogue box. The integral regions need to be saved to a special file, by clicking the disk icon towards the left of the integral window (not the standard save integrals button on the right), and selecting ‘export regions to relaxation module and.ret’.

Relaxation window: Here the intensity or area values from the first integral region are displayed. The icons at the top of this window allow you to move between the integral regions, exclude points from the calculation, display the data on a variety of axes, and start the fit for the displayed region or all regions. ***Figure 16.1.*** shows the decay of the a-carbon signal of glycine as a function of relaxation delay, along with the fit and calculated relaxation parameters. Note that any peaks with integrals or intensities too close to zero will be omitted from the analysis by the software – if you see less points in the relaxation window than were actually recorded, this may be because they have insufficient intensity.

Fitting function: Here the parameters of the fitting calculation are set. The general parameters should be determined automatically, but ensure that the limits for baseline correction are set to cover the whole spectrum. The fitting function depends on the experiment, but in this case the signals decay exponentially, so the function ‘expdec’ should be chosen. The list filename should be ‘vd’ – this will take the specified ***vdlist*** from the data set. Note that when the experiment is run, the selected ***vdlist*** is written into the acquisition data directory as the file “vdlist”, so it is always available, even if the source list is edited. The fitting program can calculate multi exponential fits, but data with very good signal-to-noise is required for this to be accurate. Unless there is obvious overlap of peaks, the assumption is usually that each peak corresponds to a single nuclear site, and thus a single T_1 value.

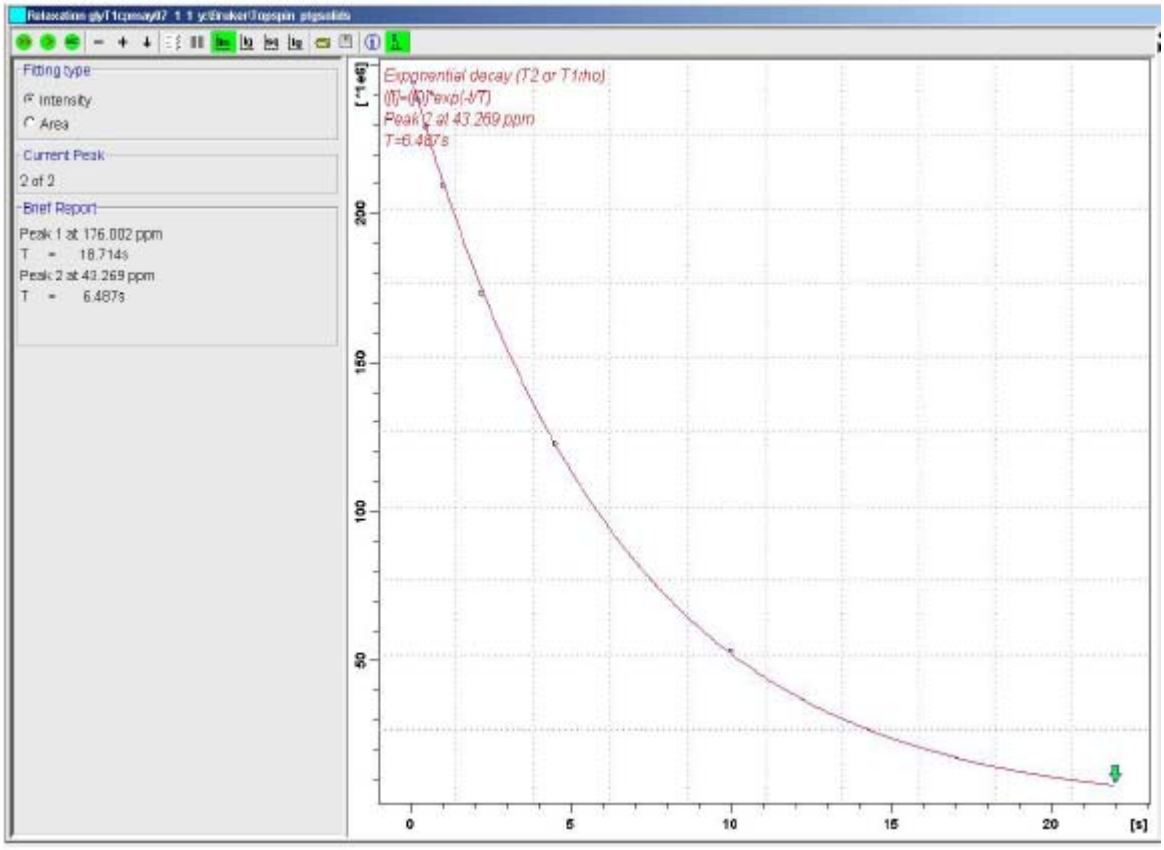

Figure 16.2. Relaxation of Alpha-carbon Signal in Glycine

Start calculation: This will perform the fitting procedure for all regions. The calculated function is displayed as a red line on the same axes as the data points. The plus and minus icons can be used to move through the different regions. If you wish to change whether the fit is based on the integral or the intensity, select the appropriate radio button, and repeat the fit using the icons immediately above. The >> icon will fit all the peaks, the > icon will fit just the current one.

Display report: This displays a text report of the results of the fit, including the details of the fit function, and the calculated values of the parameters in the function. The experimental and calculated data points are also displayed. Note that the experimental data is normalized such that the most intense point has a value of 1. This report file is also saved in the processed data directory when the fit is calculated. If fitting of a single peak is performed, only this result is written to the report. If the 'fit all peaks' option is used, all results will be stored.

The results for glycine at 500 MHz and room temperature should be approximately 18.5s and 6.4s for the carbonyl and alpha-carbon signals respectively - at other field strengths the numbers will be somewhat different. If the signals are really undergoing mono exponential relaxation, the curve should be a good fit to the measured data.

For samples where cross-polarization is not possible, the inversion recovery experiment would be very time consuming, as the recycle delay ***d1*** would need to be approximately 3x the longest T_1 value. For glycine at room temperature, this would mean a delay of about 60s per scan, in addition to the variable relaxation delay. The saturation-recovery experiment removes the need for long ***d1*** by forcing the system into saturation at the beginning of each scan.

Sample: Glycine

Spinning speed: 10 kHz

Time: 20 minutes

Experiment setup

Start from standard carbon CP parameters, and set pulprog to *satrect1*.

Set ***zgoptns*** to –Ddec to turn on proton decoupling. If decoupling is not required on a real sample, this can be left blank to turn off the decoupling.

Set ***p1*** and ***pl1*** to the measured carbon 90-degree pulse parameters (as used in the CP T1 experiment, or see chapter Basic Setup Procedures). Set ***d1*** to a relatively long value for the preparation experiments.

Set the number of pulses in the saturation train, ***l20,*** to zero, and acquire a spectrum. This will give an idea of the amount of signal, and thus how many scans need to be acquired for each relaxation delay.

Create a new data set with ***iexpno***, and set the saturation parameters, ***l20*** = 5-100 and ***d20*** = 1-50 ms respectively.

Acquire a spectrum, and verify that saturation is complete – there should be no signal at all.

Setting up the 2D experiment

Set the parameters for the 2D acquisition as detailed in ***Table 16.4.***.

For the variable recovery delay, the same values can be used as for the inversion recovery experiment.

The recycle delay ***d1*** can be very short, but take care not to exceed the duty cycle limits: high-power pulsing should not exceed 5% of the total scan time. In the case of decoupling, the acquisition time comprises most of the pulsing, so ***d1*** should be >20x ***aq*** – 1 second is reasonable in this case. If the experiment is run without decoupling, then the saturation period is the only significant period of high-power pulsing, and ***d1*** can be shorter.

Acquire the 2D spectrum with ***zg***.

Table 16.4. Parameters for the Saturation Recovery Experiment

Parameter	Value	Comments
Parmode	2D	
Vdlist	See text	
td(f1)	Number of entries in vd list	
FnMODE	QF	This is not a real 2D experiment.
NS	16, for the glycine sample	More scans needed than for the CP experiment, due to reduced signal.

Data Processing

The saturation-recovery data should be processed in the same way as the inversion-recovery data above (see ***Table 16.3.*** for parameters). The only differences are that the fitting function should be satrec rather than expdec, and the slice selected for processing should be the last one (signal is maximum at long recovery times). The calculated relaxation time constants should be the same as those obtained by inversion-recovery.

T1p Relaxation Measurements *16.2.5*

Rotating-frame relaxation measurements, under a spin-locking rf field, can be used to probe motions on shorter domestically than T_1 measurements, with inverse correlation times of the order of the spin-locking rf field strength.

To measure T_{1r} relaxation, after CP a variable length spin-locking pulse is applied to the X nucleus. The remaining X magnetization decays exponentially to zero, as a function of spin-lock time. The parameters of cross-polarization can also be determined from variable-contact-time CP experiments (the function cpt1rho is provided in the relaxation analysis tool for this purpose), but here only simple T_{1r} measurements will be discussed.

It should be noted that the relaxation in a T_{1r} experiment might result from processes other than true T_{1r} relaxation. For example, in glycine, the carbon spins are dipolar coupled to protons, and there is a possible fast relaxation pathway via the protons, which is not T_{1r} relaxation. This is inhibited by having a high spin-lock field strength, but at large field strengths care must be taken over the length of the spin-lock pulse. If apparently non exponential decay is observed, this may result from such alternative relaxation processes.

Experiment setup

Sample: Glycine

Spinning speed: 10 kHz

Time: 20 minutes

1. Start from standard CP parameters. The only additional calibration required is the carbon RF field strength of the spin-lock pulse. This can be set independently of the field strength for the cross-polarization. In principle, the strength of this field can be set to any value (within probe limits) to probe motions on a range of time scales. However, only at relatively large field strengths is true T_{1r} relaxation the only significant relaxation pathway.
2. Set ***pulprog*** to *cp90* and measure the required power level for a 70 kHz RF field (3.57 µs 90 degree pulse).
3. Make a new data set with ***iexpno***, change ***pulprog*** to cpxt1rho and set this measured power as ***pl11***.
4. Set up a variable pulse list for the incrementation of the spin-lock, with the command ***edlist vp***. Check that this list is set as the parameter ***vplist***. Remember that this is a high-power pulse, so the duration should not be too long. For the glycine sample, a possible set of times would be: 1ms, 2ms, 5ms, 10ms, 15ms, 20ms, 25ms, 30ms, 40ms, 50ms. This will not allow the signals to decay completely, so is not ideal, but should not place undue stress on the probe. Often a compromise must be reached between recording an ideal decay curve and avoiding the risk of probe damage.
5. Change ***parmode*** to 2D and set other 2D parameters as for the other relaxation experiments.
6. Acquire spectrum with ***zg***.

Data Processing

The data can be processed in the same way as the other relaxation experiments. The slice with shortest spin-lock time contains most signal, so this slice should be used for processing. The fitting function should be set to expdec, and ***vplist*** should be selected as the list file name, in the fitting function dialogue.

At 500 MHz, with a 60 kHz spin-lock field, the $T_{1\rho}$ values should be approximately 400 ms and 48 ms for the carbonyl and alpha carbons respectively. The data for the alpha carbon does not give a perfect fit to a single exponential, but this may result from the relatively low spin-lock field allowing non-$T_{1\rho}$ relaxation.

Indirect Relaxation Measurements *16.3*

If proton relaxation measurements are desired, the considerable broadening of the proton resonances seen at even high spinning speeds can make resolution of individual components impossible. In such cases, indirect observation of proton relaxation by X-nucleus observation can be used. A typical example would be attempting to observe the proton relaxation of two components of a mixture or multi phase material. In general, the proton spins within a single molecule are sufficiently strongly coupled by the homonuclear dipolar coupling that different relaxation is not seen for the different sites. If the experiments are set up with short contact times, the individual carbon signals will be derived only from directly bonded protons, and thus any differences in proton relaxation within a molecule could be isolated.

Such indirect observation can be implemented conveniently for both T_1 and $T_{1\rho}$ relaxation. For T_1, a proton saturation-recovery step is inserted prior to the cross-polarization step in a standard CP sequence. The proton magnetization immediately prior to CP, and thus the observed carbon signal, depends on the extent of

recovery after the saturation, so the carbon signal as a function of recovery delay gives the proton T_1 value. For $T_{1\rho}$ a variable length proton only spin-lock pulse is applied after the 90-degree pulse in the CP experiment. The proton magnetization after this pulse, and thus the carbon signal after CP, depends on the proton $T_{1\rho}$ relaxation.

Indirect Proton T1 Measurements *16.3.1*

Sample: Glycine

Spinning speed: 10 kHz

Time: 20 minutes

Start from standard CP parameters, as for the X T_1 measurement with CP, and set ***pulprog*** to *cph+1*. Set the saturation loop ***l20*** to zero, and acquire a spectrum, to check signal intensity. Signal to noise should be comparable with the standard CP experiment, so a similar number of scans to that used for the carbon T_1 experiment should suffice.

Saturation parameters can be set as for carbon saturation previously: ***l20*** = 5-100 and ***d20*** =
1-50 ms. Acquire a spectrum with these parameters and verify that there is again no signal.

Make a new data set with ***iexpno*** and set parameters for 2D acquisition, as for the previous experiments. D1 can be short, with the same proviso about duty cycle as the X saturation-recovery experiment. A reasonable set of delays for the vdlist would be: 10 ms, 22 ms, 45 ms, 100 ms, 220 ms, 450 ms, 1 s, 2.2 s, 4.5 s, 10 s.

Data processing

The data should be processed in the same way as for the X saturation recovery experiment. Both the carbonyl and alpha-carbon peaks derive their carbon polarization from the same proton spins, and so analysis of the two peaks should give the same result. If you have a sample containing some gamma-glycine (gives peaks at slightly lower shifts than the more common alpha-glycine form), this should show different T1 values for the two sets of peaks.

At 500 MHz, the proton relaxation time should be approximately 520 ms at room temperature.

Basic MQ-MAS 17

Introduction 17.1

The MQMAS experiment for half integer quadrupole nuclei is a 2D experiment to separate anisotropic interactions from isotropic interactions. In the NMR of half integer quadrupole nuclei the dominant anisotropic broadening of the central +1/2 <-> –1/2 transition (CT), and symmetric multiple-quantum (MQ) transitions, is the 2^{nd} order quadrupole interaction which can only partially be averaged by MAS. The satellite transitions (ST, e.g. the ±3/2 <-> ±1/2 transitions) however, are broadened by a 1^{st} order interaction, which is several orders of magnitude larger than the 2^{nd} order broadening. Under MAS the 1^{st} order interaction of the ST can be averaged but since the spinning cannot be fast compared to the first order broadening (of the order of MHz), a large manifold of spinning side bands remains. The 2^{nd} order broadening of the CT can only be narrowed by a factor of 3 to 4 by MAS so a signal is observed that still reflects this 2^{nd} order broadening, which may be of the order of kHz. Lineshapes resulting from nuclei in different environments are thus likely to be unresolved in a simple 1D spectrum.

The 2D MQMAS experiment exploits the fact that the 2nd order broadening of the symmetric MQ transitions (e.g. +3/2 «-3/2 in a spin 3/2), is related to the 2nd order broadening of the CT by a simple ratio. A 2D spectrum is recorded which correlates e.g. a +3/2 «–3/2 3Q coherence involving the satellite transitions and the +1/2 «–1/2 single quantum coherence of the central transition. This spectrum shows a ridge line shape for each site, with slope given by the ratio of the second order broadening of the two transitions (-7/9 in the case of the 3Q transition). A projection of the 2D spectrum perpendicular to this slope yields an isotropic spectrum free from quadrupolar broadening.

Pulse sequences 17.2

Figure 17.1. and ***Figure 17.2.*** show two of the basic sequences, a 3-pulse and a 4-pulse sequence with z-filter. Both sequences start with an excitation pulse ***p1*** that creates 3Q coherence which is allowed to evolve during the evolution period ***d0***. In the 3-pulse sequence the subsequent conversion pulse ***p2*** flips magnetization back along the z-axis, which after a short delay ***d4*** (to allow dephasing of undesired coherency) is read out with a weak CT selective 90° pulse ***p3***. In the 4-pulse sequence, however, the conversion pulse ***p2*** changes 3Q coherency to 1Q coherency which then passes through a Z-filter of two CT selective 90° pulses in a ***p3-d4-p3*** sequence.

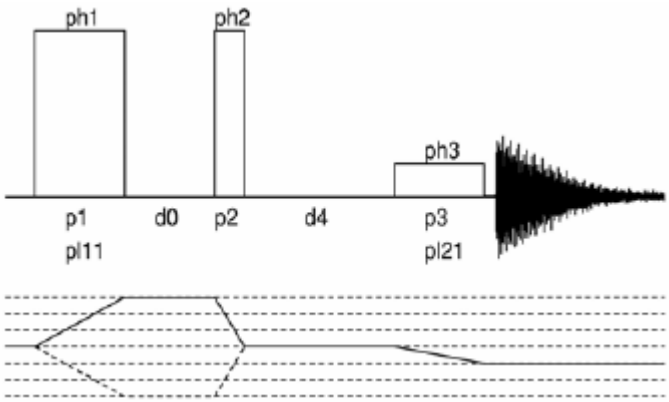

Figure 17.1. A 3-Pulse Basic Sequence with Z-Filter.

Three pulse sequence and coherence transfer pathway for the 3Q MAS experiment with z-filter (mp3qzqf.av). The ratio for pulses p1 and p2 is approximately 3. The corresponding power level pl11 should be set to achieve at least 150 kHz RF field amplitude. p3 should be some tens of µs, corresponding to an RF field amplitude of a few kHz. Delays d0 and d4 are the incremented delay for t1 evolution and 20 µs for z-filter, respectively. Phase lists are as follows, for phase sensitive detection in F1 the phase of the first pulse must be incremented by 30° in States or States-TPPI mode:

ph1 = 0

ph2 = 0 0 60 60 120 120 180 180 240 240 300 300

ph3 = 0 180

receiver = + – – +.

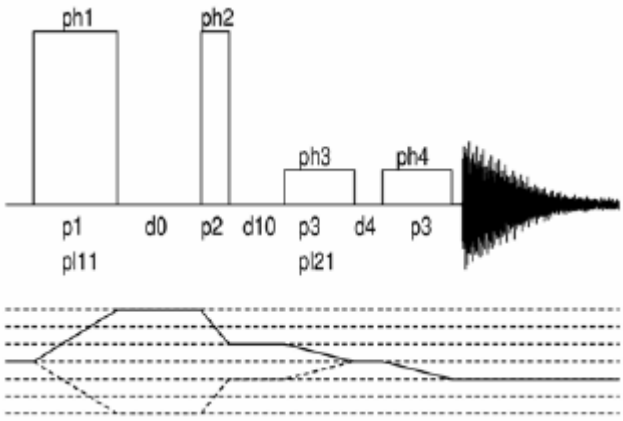

Figure 17.2. A 4-Pulse Basic Sequence with Z-Filter.

Four pulse sequence and coherence transfer pathway for the 3Q MAS experiment with z-filter (mp3qzfil.av). p1 is the same, p2 is usually somewhat shorter than in the three pulse sequence. Corresponding power level pl11 should be set to achieve at least 150 kHz RF field amplitude. p3 should be some tens of µs, corre-

*sponding to an RF field amplitude of a few kHz. Delays d0 and d4 are the incremented delay for t1 evolution and 20 µs for z-filter, respectively. Delay d10 initially is 0 and can be incremented proportional to d0 (in10=in0*7/9), if the observe nucleus has spin I=3/2. Phase lists are as follows, for phase sensitive detection in F1 the phase of the first pulse must be incremented by 30° in States or States-TPPI mode:*

ph1 = 0 60 120 180 240 300

ph2 = 0*24 90*24 180*24 270*24

ph3 = 0

ph4 = 0*6 90*6 180*6 270*6

receiver = {0 180}*3 {90 270}*3 {180 0}*3 {270 90}*3 {180 0}*3 {270 90}*3{0 180}*3 {90 270}*3.

Of course, the sequence with more pulses has slightly inferior sensitivity; however, it is the basic sequence to improve sensitivity by FAM or DFS. The 3-pulse sequence itself can be used directly to enhance sensitivity by soft-pulse added mixing (pulse program *mp3qspam.av*). In ***"MQ-MAS: Sensitivity Enhancement" on page 231*** some of the sensitivity enhancement techniques will be described.

Note that pulse programs suitable for AV and AVII spectrometers have the extension.av, pulse programs for the AVIII have no extension.

Data Acquisition 17.3

Before the 2D experiment on your sample of interest can be started, two set-up steps must be done as described in detail below. All set-up steps should be done on a sample with a) a known MAS spectrum, b) with sufficiently good sensitivity to facilitate the set-up and c) a 2nd order quadrupole interaction in the order of the one expected for your sample of interest. In the first step a low power selective pulse must be calibrated in a single pulse experiment. With this the MQMAS experiment can be optimized using the 2D pulse sequence for t_1=0.

Setting Up the Experiment 17.3.1

Sample: There are a large number of crystalline compounds which can be used to set up the experiment. Please refer to table 1 to select a suitable sample. For the general procedure described here the spin I of the nucleus is not important, of course obtained pulse widths will depend on the spin I, and the Larmor frequency. You can use any arbitrary sample showing a considerable broadening by the 2nd order quadrupole interaction to adjust the experiment, however, reasonable 1D MAS spectra should be obtained quickly for sensitivity reasons.

The set-up must be done in two steps; in the first step a central transition selective pulse that merely excites the central transition must be calibrated. This pulse must be weak enough so that only this transition is affected and it must be short enough so that the central transitions of all sites in the spectral range are excited. As an example, the sinc shape excitation profile of a 20 µs pulse has its zero-crossings at 1/20 µs = ± 25 kHz which means that the central transition signals must not extend beyond this range, otherwise severe line shape distortions will be observed. On the other hand the corresponding RF field amplitude of a 20 µs 90° pulse will be 1/(80 µs*(I+1/2))=12.5 kHz/(I+1/2). This means that $w_{RF} << w_Q$ as a prerequi-

site for a CT selective pulse is most likely to be fulfilled. For the calibration of this pulse a power level around 30 dB with 500 W and 1 kW amplifiers and around 20 dB with 300 W amplifiers should be expected. The pulse program *zg* (which uses ***p1*** and ***pl1***) or *zgsel.av* (which uses ***P3*** and ***PL21***) can be used.

Table 17.1. Some Useful Samples for Half-integer Spin Nuclei

Nucleus	Spin	Spectrometer Frequency[*1)]	d1 [s][*3)]	Sample	Comments
^{17}O	5/2	67.78	2	$NaPO_3$	> 10% enriched
^{11}B	3/2	160.42	>5	H_3BO_3	
^{23}Na	3/2	132.29	10	Na_2HPO_4[*2)]	
^{27}Al	5/2	130.32	5	YAG	
^{27}Al	5/2	130.32	0.5	Al_2O_3	
^{27}Al	5/2	130.32	0.5	VPI-5	
^{27}Al	5/2	130.32	0.5	$AlPO_4$-14	
^{11}B	3/2	160.46	5	H_3BO_3	
^{87}Rb	3/2	163.61	0.5	$RbNO_3$	
^{93}Nb	9/2	122.25	1	$LiNbO_3$	

[*1)] In MHz at 11.7 T (i.e. 500.13 MHz proton frequency)

[*2)] Alternatively $Na_2HPO_4 * 2H_2O$ can be used. For anhydrous Na_2HPO_4 the sample should be dried at 70° C for a couple of hours before packing the rotor in order to eliminate crystal water completely

[*3)] Recycle delays at 11.7 T, longer delays may be required at higher fields

Figure 17.3. shows a comparison of a spectrum excited by a short non-selective pulse with a spectrum that has been obtained by a weak selective pulse. Note that in the latter the spinning sidebands from the satellite transition are no longer visible which is used as an indication that it is not excited.

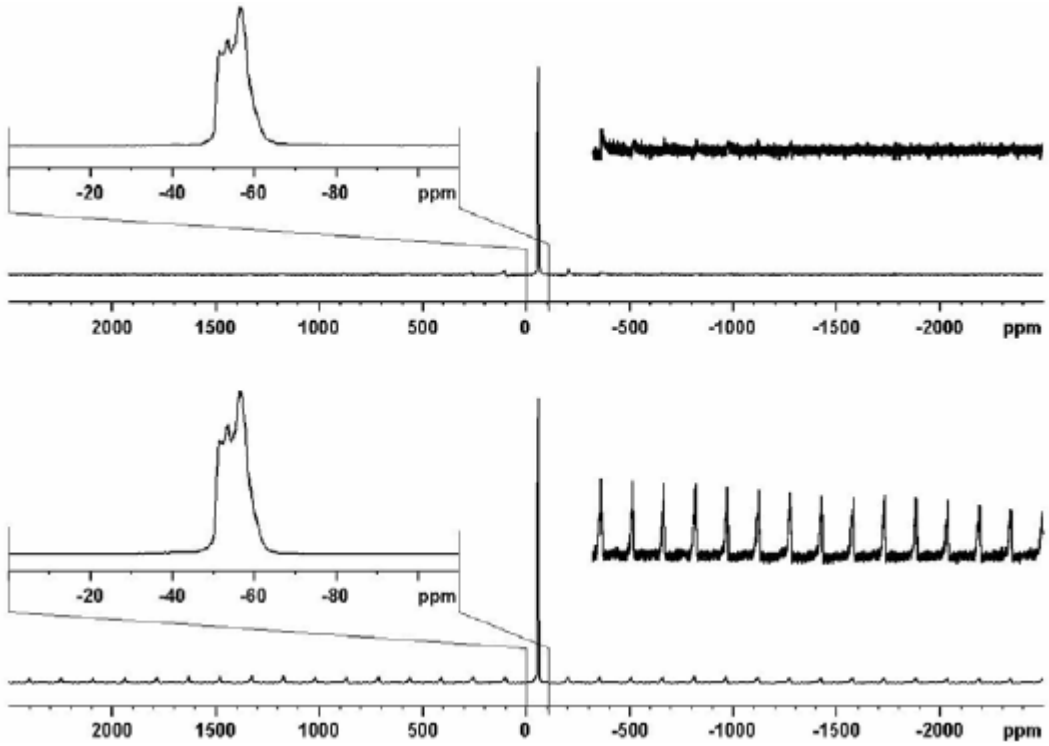

Figure 17.3. Comparison of 87Rb MAS spectra of RbNO3 excited with selective and non-selective pulses.

The lower trace is a spectrum excited with a 1 µs non-selective pulse corresponding to a small flip angle. Above is a spectrum excited with a 20 µs selective 90° pulse. Note that in the latter no spinning side bands from the satellite transition are observed. Spectra are taken on AV500WB at a Larmor frequency of 163.6 MHz with a 2.5 mm CP/MAS probe spinning at 25 kHz.

Figure 17.4. shows the nutation profiles of a non-selective and a selective pulse, respectively. Note that for the selective pulse a fairly precise 180° pulse of a length of $2*\tau_{90°}$ can be determined whereas for a non-selective pulse this is not the case.

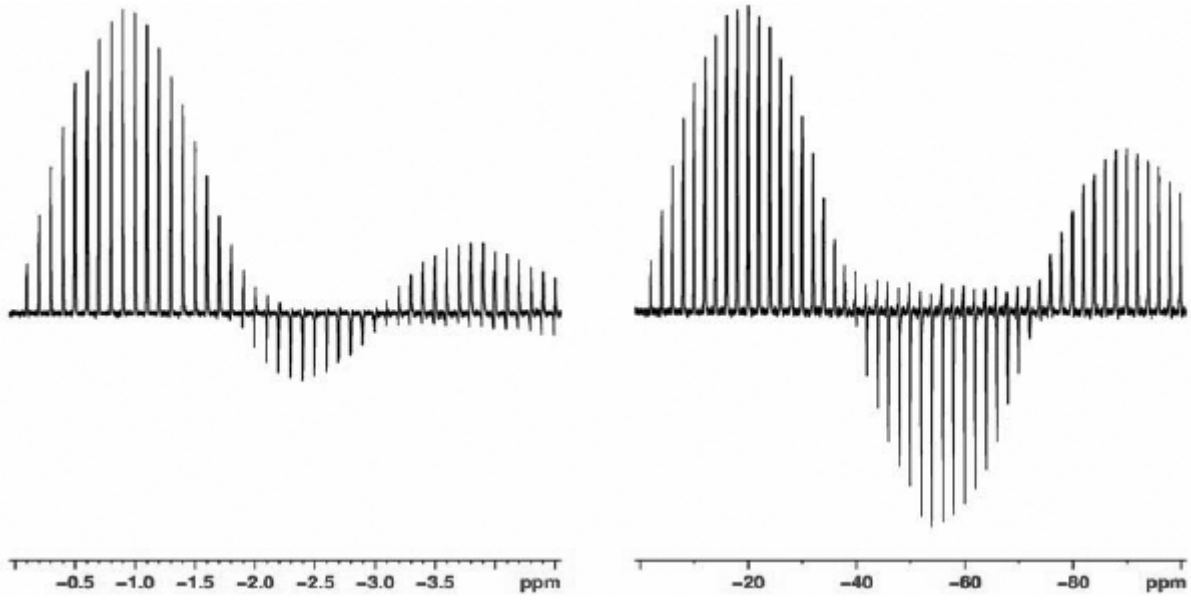

Figure 17.4. Nutation profiles of selective and non-selective pulses.

Left diagram shows signal intensity of ^{87}Rb resonances in RbNO3 as a function of a non-selective pulse at approx. 150 W RF power, the right diagram shows the signal intensity as function of a selective pulse at less than approx. 0.5 W. Spectra are taken on AV500WB at a Larmor frequency of 163.6 MHz with 2.5 mm CP/MAS probe spinning at 25 kHz. Note the different scaling of x-axis, which is displayed as "ppm" but corresponds to the used pulse lengths in µs (apart from the sign).

Once the central transition selective 90° pulse is calibrated the parameters can be copied to a new data set with ***iexpno***, and the MQMAS pulse program can be loaded. Available pulse programs are *mp3qzqf* and *mp3qzfil*. The first is a 3-pulse sequence, the second a 4-pulse sequence. The sequence with fewer pulses will be slightly more sensitive, whilst the 4-pulse sequence can be used as an initial set-up for experiments with sensitivity enhancement methods like DFS or FAM (see ***"MQ-MAS: Sensitivity Enhancement" on page 231*** describing sensitivity enhancement methods).

In ***Table 17.2.*** the starting parameters for the set-up are displayed. This table gives typical values for the pulses and powers that should be close to the final values confirmed by the optimization procedure. Parameters like ***O1***, ***TD***, ***SWH***, ***RG***, should already be set in the standard 1D spectrum. For 4 mm probes these pulse lengths are about the limit of what can be achieved, for 2.5 mm probes somewhat shorter pulses can be obtained. For I = 3/2 and I = 5/2 nuclei the ratio of p1/p2 ≈ 3.

For ***pl11*** an initial value that corresponds roughly to 300 W can be used. Optimization will be done on the first increment of the 2D sequence, i.e. ***d0*** = 1 µs. Two strategies for the optimization procedure can be followed; either the pulse lengths ***p1*** and ***p2*** or the power level ***pl11*** can be optimized for maximum signal amplitude. However, the latter can be disadvantageous because a power level above the probe limit might be applied, in order to clearly determine the optimum power. In the case of 300 W amplifiers the maximum signal amplitude may not be obtained even at full power, with the chosen pulse lengths.

Table 17.2. Initial Parameters for Setup

Parameter	Value	Comments
Pulprog	mp3qzqf.av or mp3qzfil.av	Pulse program.
NS	12*n (zqf) 96*n (zfil)	Full phase cycle is important.
D0	1u	Or longer, t_1-period.
D1	5 * T_1	Recycle delay, use dummy scans if shorter.
D4	20 µs	Z-filter delay.
P1	3.6 µs	Excitation pulse at pl11.
P2	1.2 µs	Conversion pulse at pl11.
P3	20 µs	90° selective pulse at pl21 taken from previous pulse calibration.
PL1	=120 dB	Not used.
PL11	start with ≈ 300 W	Power level for excitation and conversion pulses.
PL21		Power level for selective pulse, approx. pl11+30 dB taken from previous pulse calibration.

Hence, it is always better to optimize the pulse lengths ***p1*** and ***p2***. In this case ***p2*** should be optimized before ***p1*** because the signal intensity is much more sensitive to this pulse length. A suitable set-up for the parameter optimization procedure ***popt*** is shown in following figure.

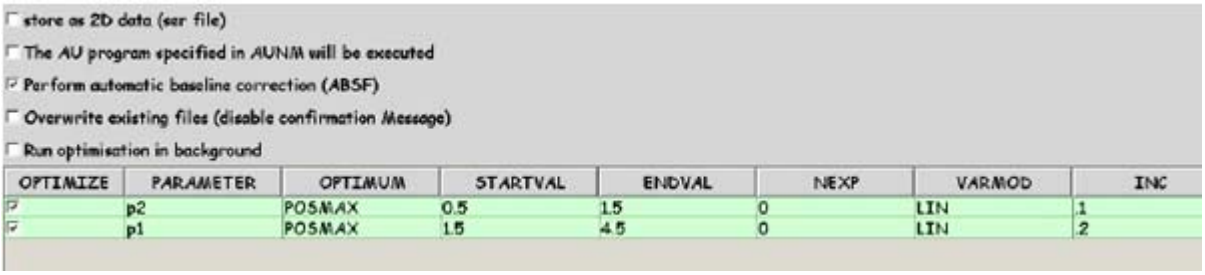

Figure 17.5. Example for popt Set-up for Optimization of p1 and p2.

*In the first step **p2** is optimized to which the experiment is the more sensitive. In the second step **p1** is optimized using the optimum value found for **p2** in the first step.*

For more details about using the ***popt*** procedure to optimize a series of parameters please refer to the manual. ***Figure 17.6.*** shows the signal amplitudes as functions of pulse lengths ***p2*** and ***p1***.

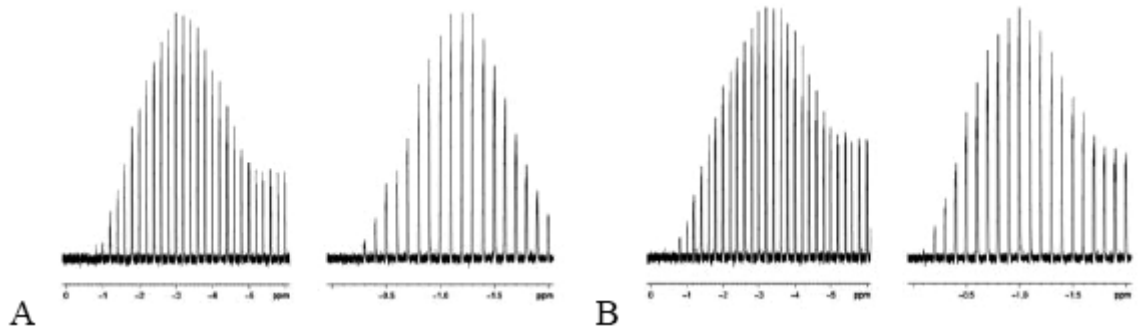

*Figure 17.6. Signal Intensities of 87Rb Resonances in RbNO3 as Function of **p1** and **p2**.*

*Each pair of diagrams in A and B shows the signal intensities as function of the excitation pulse p1 and the conversion pulse **p2**. In A the 3-pulse sequence and in B the 4-pulse sequence was used. Note that the signal intensity is much more sensitive to the proper length of the conversion pulse. Maximum intensities were 3.0 µs and 1.2 µs in A and 3.2 µs and 1.0 µs in B, respectively. This corresponds to approximate RF field amplitudes of 160 kHz. Spectra are taken on an AV500WB at a Larmor frequency of 163.6 MHz with a 2.5 mm CP/MAS probe spinning at 25 kHz. Note the different scaling of the x-axes, for **p1** they range from 0 to 6 µs, for **p2** from 0 to 2 µs.*

Two Dimensional Data Acquisition *17.3.2*

Once the pulses are calibrated everything is ready for the 2D data acquisition. Create a new data set and change *parmode* to 2D. In the acquisition parameters for the (new) indirect F1 dimension the following parameters must be set according to the following table.

Table 17.3. F1 Parameters for 2D Acquisition

Parameter	Value	Comments
FnMode	States or States-TPPI	Acquisition mode for 2D.
TD	see text	Number of FID's to be acquired.
SWH	"masr"	Equals spinning frequency for rotor synchronization, from this IN_010 is calculated correctly, if ND_010 is already set.
NUC1		Select the same nucleus as for F2 so that transmitter frequency offset is correctly set (important for referencing).[1]
D10	0	Used in mp3qzfil.av only.
IN10	=in0*7/9	Used in mp3qzfil.av for nuclei with spin I=3/2 only, so that no shearing FT is required.

[1] Note the difference in increment handling in Topspin 2.1 and higher.

Some further comments and explanations on the parameters listed above:

FnMode must be States or States-TPPI so that the shearing FT can be performed for processing. If the pulse program *mp3qzfil.av* is used, no shearing is required in case of nuclei with spin I=3/2 if ***in10*** is set correctly in which case a split-t_1 experiment is performed. **td** determines the number of FID's to be accumulated in the indirect dimension. This value is determined by the line width and resolution that can be expected in the indirect MQ dimension (F1) and which depend on the properties of the sample. In crystalline material fairly narrow peaks can be expected so a maximum acquisition time in F1 of 2 to 5 ms is expected. In disordered materials where the line width is broader and determined by chemical shift distribution a total acquisition time in F1 of 1 ms may be sufficient. The total acquisition time **aq** in F1 equals (***td***/2)****in_010***.

For rotor synchronized experiments ***in_010*** = 1/spinning frequency so will typically be between 100 µs (10 kHz spinning) and 28.5 µs (35 kHz spinning), so only 10 to 40 experiments in amorphous samples but 50 to 200 experiments in crystalline samples might be required. The rotor synchronization means that the spectral range in F1 is limited. Depending on the chemical shift range, spinning frequency, and quadrupole interactions the positions of the peaks may fall outside this range. In such a case care must be taken when interpreting the spectrum. Acquisition with half-rotor synchronization to double the spectral window in F1 may help. However, in this situation one set of spinning sidebands appears and it must be avoided that the spinning side bands of one peak fall on top of other peaks. Some sort of rotor synchronization is always recommended because spinning side bands in the indirect dimension extend over a very wide range, which cannot be truncated by e.g. filtering. Therefore, rotor synchronization together with States or States-TPPI phase sensitive acquisition helps to fold spinning sidebands from outside back onto centre bands or other side bands.

Data processing *17.4*

Processing parameters should be set according to the following table:

Table 17.4. Processing Parameters for 2D FT

Parameter	Value	Comments
F2 (acquisition dimension)		
SI		Usually set to one times zero filling.
WDW	no	Don’t use window function.
PH_mod	pk	Apply phase correction.
BC_mod	no	No DC correction is required after full phase cycle.
ABSF1	1000 ppm	Should be outside the observed spectral width.
ABSF2	-1000 ppm	Should be outside the observed spectral width.
STSR	0	Avoid strip FT.
STSI	0	Avoid strip FT.
TDoff	0	Avoid left shifts or right shifts before FT.
F1 (indirect dimension)		
SI	256	Sufficient in most cases.
WDW	no	Don’t use window function, unless F1 FID is truncated.
PH_mod	pk	Apply phase correction.
BC_mod	no	No DC correction is required after full phase cycle.
ABSF1	1000	Should be outside the observed spectral width.
ABSF2	-1000	Should be outside the observed spectral width.
STSR	0	Avoid strip FT.
STSI	0	Avoid strip FT.
TDoff	0	Avoid left shifts or right shifts before FT.

Data obtained with *mp3qzfil.av* from nuclei with spin I = 3/2 can be processed with ***xfb***, if ***IN10*** has been set appropriately to run a split-t_1 experiment. If this is not the case data can be sheared in order to align the anisotropic axis along the F2 axis. This is done with the AU program ***xfshear***. The AU program checks the nucleus to determine the spin quantum number, checks the name of the pulse program and decides what type of experiment has been performed. In case the nucleus is unknown to the program, or the pulse program has a name that does not contain a string “nq” nor “nQ” (with n=3, 5, 7, 9), the required information is asked for by the program, in order to calculate the shearing correctly.

Note that using a user designed pulse program that contains e.g. a string “5q” but performs a 3Q experiment (and vice versa) will yield erroneous shearing. When started the AU program prompts for “Apply ABS2?” and “F1 shift in ppm:”. It is advisable to calculate a baseline correction after F2 Fourier transform. Note that the range defined by ABSF1 and ABSF2 is used for this. You should make sure that

the limits are at least as large as the spectral width to allow baseline correction of the whole spectrum. The “F1 shift in ppm” allows shifting the spectrum (including its axis) in the vertical direction for cases where peaks are folded due to a limited spectral window in a rotor synchronized experiment. For the first processing both prompts are typically returned. At the end of the processing the AU program corrects the apparent spectrometer frequency of the indirect dimension by a factor $|R\text{-}p|$, where *R* is defined in equation [1] and *p* is the order of the experiment (e.g. 3 for 3QMAS):

(Eq. 17.1)

$$R = \frac{m(18I(I+1) - 8.5m^2 - 5)}{18I(I+1) - 3.5}$$

This ratio is calculated from the spin quantum number *I* of the nucleus and the magnetic spin quantum number *m,* which is determined by the experiment, e.g. 3/2 in case of a 3Q experiment of an order *p*=3. The program stores the “F1 shift” that was calculated and will prompt for it when data are processed next time. If the same F1 shift should be applied as before the AU program can be called with the option “lastf1”. Before giving some further explanations about the experiment, ***Figure 17.7.*** shows the 2D ^{87}Rb 3QMAS spectrum of $RbNO_3$.

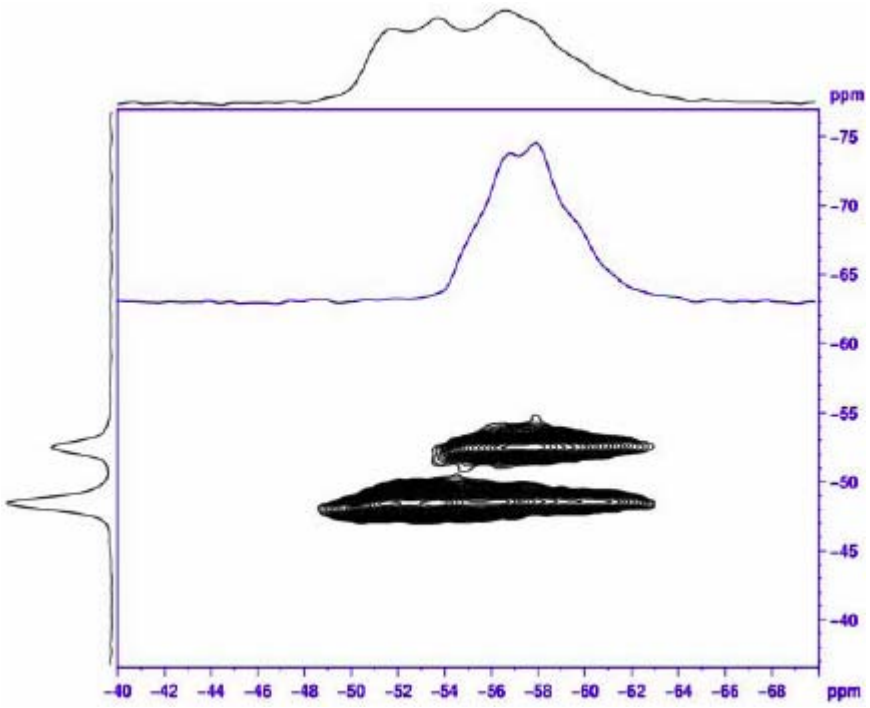

Figure 17.7. 2D ^{87}Rb 3QMAS Spectrum of RbNO3.

Top and left projections are the summations over the signal ranges. The spectrum included in the 2D map is a cross section through the resolved peak resonating at approximately 53 ppm. Note that at 11.7 T two of the three sites cannot be resolved in the 2D spectrum. The spectral range shown in F1 corresponds to the spinning frequency. Spectra are taken on AV500WB at a Larmor frequency of 163.6 MHz with a 2.5 mm CP/MAS probe, spinning at 25 kHz.

Since the quadrupole parameters are usually unknown before performing the experiment the positions of the peaks in the indirect dimension cannot be predicted. Therefore, it may happen that a peak is positioned at the border of the spectral range in the F1 dimension or even folded. When using ***xfshear*** the prompt “F1 shift in ppm:” can be used to shift the spectrum including its axis upfield (negative value) or low field (positive value) accordingly. For data which don’t need a shearing transformation, the ppm axis in F1 can be correctly calibrated by running the AU program xfshear with the option „rotate”. It will calibrate the F1 axis and perform the 2D FT. ***Figure 17.8.*** compares the same 2D 3Q MAS spectrum processed with no shift and an additional shift of 5 ppm, respectively. We see that without the additional shift, the uppermost peak is at the border of the spectral range and the projection shows that the edge of this peak reenters into the spectral range from the opposite side. In summary the AU program ***xfshear*** can be called with the following options:

lastf1: Use the F1 shift value from last processing
abs: Do abs2 after F2 Fourier transform of data
noabs: Don’t do abs2 after F2 Fourier transform of data
rotate: don’t calculate shearing, only use F1 shift to rotate spectrum along F1 axis
ratio: Use different value for ratio R, value can either be entered or passed.

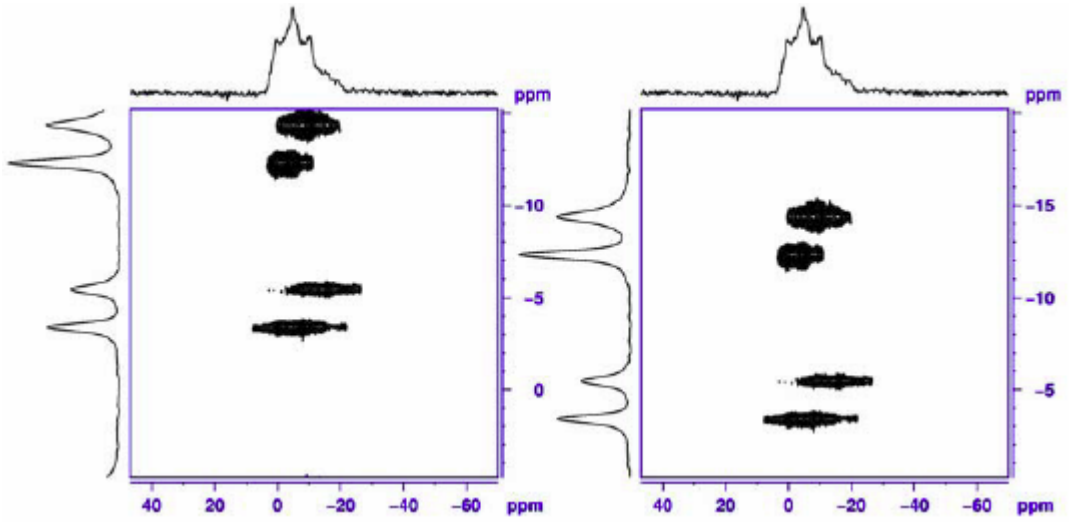

Figure 17.8. Comparison of Differently Processed 2D ^{23}Na 3Q MAS Spectra of Na4P2O7.

The left spectrum was processed with an additional F1 shift of 0 ppm, the right spectrum with +5 ppm. Spectra are taken on an AV500WB at a Larmor frequency of 132.3 MHz with a 4 mm CP/MAS probe spinning at 10 kHz. Note that the F1 range equals the spinning frequency of 10 kHz in both cases.

Obtaining Information from Spectra 17.5

The referencing procedure in ***xfshear*** defines the axis in the MQ dimension such that:

(Eq. 17.2)

$$\delta_{MQ} = \delta_{iso} - \frac{10}{17}\delta_{qis}$$

The value of δ_{qis} is given by:

(Eq. 17.3)

$$\delta_{qis} = -\frac{3\left(4I\left(I+1\right)-3\right)}{\left(4I\left(2I-1\right)\right)^2} * \frac{Q_{cc}^2}{\omega_0^2}\left(1+\frac{\eta^2}{3}\right) * 10^5$$

In ***(Eq. 17.3)*** *I* is the spin quantum number, Q_{cc} the quadrupolar coupling constant, ω_0 the Larmor frequency, and *h* the asymmetry parameter. This makes δ_{MQ} µ ω_0^{-2}, which causes the MQ positions to be field dependent. An interesting behavior results as one compares spectra at different fields. Plots of the function δ_{MQ} over ω_0^{-2} are shown in ***Figure 17.9.*** for an arbitrary sample with two sites. If the isotropic chemical shifts of the two sites are identical, then it is obvious that the separation of the two lines increases as the field decreases (plot A). In the opposite case of identical quadrupole couplings separation increases as the field is increased (plot B). In cases where a difference in isotropic chemical shift δ_{iso} exists and the sites have different quadrupole couplings the relative positions depend on which site has the larger quadrupole coupling. The separation of the lines will always increase as the field decreases (plots C and D), but in some cases a crossover of the shift positions may be observed as the field B_0 is altered (plot C).

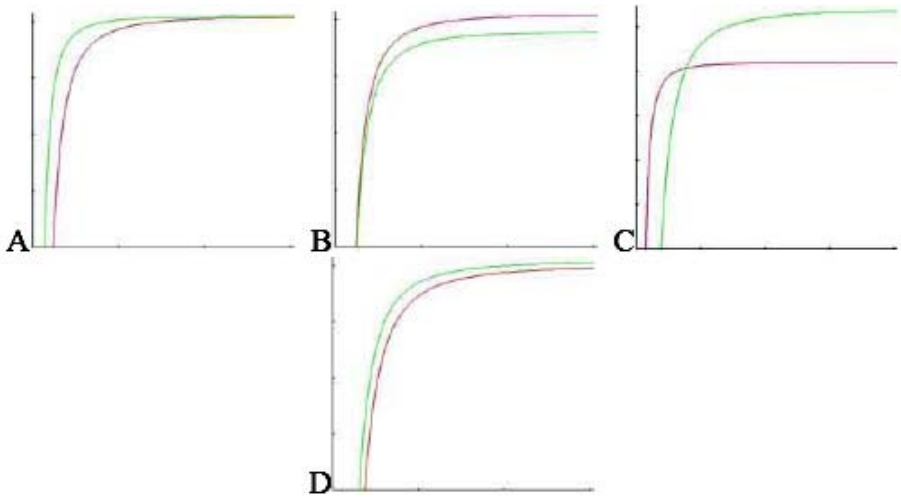

Figure 17.9. Calculated Shift Positions δ_{MQ}

Calculated shift positions δ_{MQ} as function of the static magnetic field B_0 for two different sites with arbitrary δ_{iso} and δ_{qis}. The x axis in each plot is the static magnetic field B_0 increasing from left to right; the y axis δ_{MQ} increases from bottom to top. Plot A is for identical δ_{iso}, plot B for identical quadrupole coupling and. In plots C

and D shift positions for two sites with large and small d_{iso} and large and small δ_{qis} and with large and small δ_{iso} and small and large δ_{qis} are plotted, respectively.

This behavior is independent of the spin quantum number and of the order *p* of the experiment. Higher quantum order experiments are possible for half integer spin quantum numbers >3/2, however, corresponding pulse programs are not provided in the pulse program library. They can easily be derived from the 3Q pulse program by changing the phase cycle. In the 3-pulse sequence (*mp3qzqf*) e.g. ph2 should be changed for the 5Q experiment to:

ph2 = 0 0 36 36 72 72 108 108 144 144 180 180 216 216 252 252 288 288 324 324

An 18° phase increment of the phase ph1 of the first pulse is required for States or States-TPPI phase sensitive acquisition. For a full phase cycle a multiple of 20 scans must be used.

For the 4-pulse sequence (*mp3qzfil*) the phases should be changed to:

ph1 = 0 36 72 108 144 180 216 252 288 324

ph2 = 0*40 90*40 180*40 270*40

ph3 = 0

ph4 = 0*10 90*10 180*10 270*10

receiver = {0 180}*5 {90 270}*5 {180 0}*5 {270 90}*5 {180 0}*5 {270 90}*5{0 180}*5 {90 270}*5.

Again an 18° phase increment of the first pulse for States or States-TPPI phase sensitive detection in F1 is needed. Thus a full phase cycle can be performed with a multiple of 160 scans.

The usefulness of such a 5Q experiment is limited, and there are several drawbacks: Firstly, the sensitivity is much inferior to the 3Q experiment because of the lower transition probability and a less efficient excitation. Secondly, the shift range (in ppm) in the indirect dimension is much smaller when a rotor synchronized experiment is performed. The factors $|R\text{-}p|$ are listed in ***Table 17.5.***. The shift positions in the MQ dimension in a sheared spectrum are the same for all orders p and therefore, no additional information can be expected. However, the observed line widths are slightly reduced in the higher order experiments so in special cases some enhancement of resolution can provide additional information.

Table 17.5. Values of |R-p| for Various Spins I and Orders p

Spin I	R(p=3)	|R-p| (p=±3)	|R-p| (p=±5)	|R-p| (p=±7)	|R-p| (p=±9)
3/2	-7/9	3.78	-	-	-
5/2	19/12	1.42	7.08	-	-
7/2	101/45	0.76	3.78	10.58	-
9/2	91/36	0.47	2.36	6.61	14.17

The spectral width in the MQ dimension of the sheared spectrum is given by spinning speed / $|R\text{-}p|$ in a rotor synchronized experiment. A 5Q experiment e.g. gives a 7.08/1.42 = 5 times smaller spectral range in the indirect dimension than a 3Q experiment.

We see that a 5Q experiment has a 5 times smaller range than the 3Q experiment and therefore, folding of peaks will always occur even at fast spinning. For even higher quantum orders the shift ranges are 7 and 30 times smaller for 7Q and 9Q than for the 3Q experiment, respectively. ***Table 17.6.*** summarizes ppm ranges for the maximum spinning frequencies of 2.5, 3.2, and 4 mm probes, respectively. A Larmor frequency of 100 MHz is assumed. One can see that the ranges become less than the typical chemical shift range for many nuclei. The expression $|R\text{-}p|$ acts like a scaling factor that scales the frequency scale directly. Mathematically this is solved in the AU program ***xfshear*** in such a way that the observe Larmor frequency is multiplied by the factor Á*R-p* Á to redefine an apparent Larmor frequency in the MQ dimension.

Table 17.6. Chemical Shift Ranges for all MQ Experiments for All Spins I

Spin *I* and MQ Experiment	15 kHz [4 mm probe]	25 kHz [3.2 mm probe]	35 kHz [2.5 mm probe]
3/2	39.6 ppm	66.0 ppm	92.4 ppm
5/2 3Q 5/2 5Q	105.6 ppm 26.1 ppm	176.0 ppm 35.2 ppm	246.4 ppm 49.3 ppm
7/2 3Q 7/2 5Q 7/2 7Q	197.4 ppm 39.5 ppm 14.1 ppm	329.0 ppm 65.8 ppm 23.5 ppm	460.6 ppm 92.1 ppm 32.9 ppm
9/2 3Q 9/2 5Q 9/2 7Q 9/2 9Q	319.2 ppm 63.2 ppm 45.6 ppm 10.6 ppm	532.0 ppm 160.4 ppm 76.0 ppm 17.7 ppm	744.8 ppm 144.9 ppm 106.4 ppm 24.8 ppm

Figures are calculated for a Larmor frequency of 100 MHz.

From the isotropic shift and the shift position in the MQ dimension the so-called *SOQE* parameter can be calculated, d_{qis} being given by equation 2:

(Eq. 17.4)

$$SOQE = Q_{cc}^2\left(1+\frac{\eta^2}{3}\right) = \delta_{qis} f(I)\frac{\omega_0^2}{10^5}$$

with

(Eq. 17.5)

$$f(I) = -\frac{(4I(2I-1))^2}{3(4I(I+1)-3)}$$

f(I) equals 4, 16.67, 39.2, and 72 for I=3/2, 5/2, 7/2, and 9/2, respectively. So one can see that for a given value of Q_{cc} the second order quadrupole induced upfield shift d_{qis} decreases as the spin *I* increases. With d_{qis} always being negative this has a direct influence on the appearance of the sheared 2D spectra.

Figure 17.10. shows 2D ^{17}O 3QMAS spectra at 11.7 T and 18.8 T where the Larmor frequency of this nucleus is 67.8 and 108.4 MHz, respectively. The sample is

sodium metaphosphate $NaPO_3$ in the glassy state. The enrichment of ^{17}O is approx. 30 to 33%. It contains 2 oxygen positions: there are bridging oxygen (P-O-P) and non-bridging oxygen (P-O-Na).

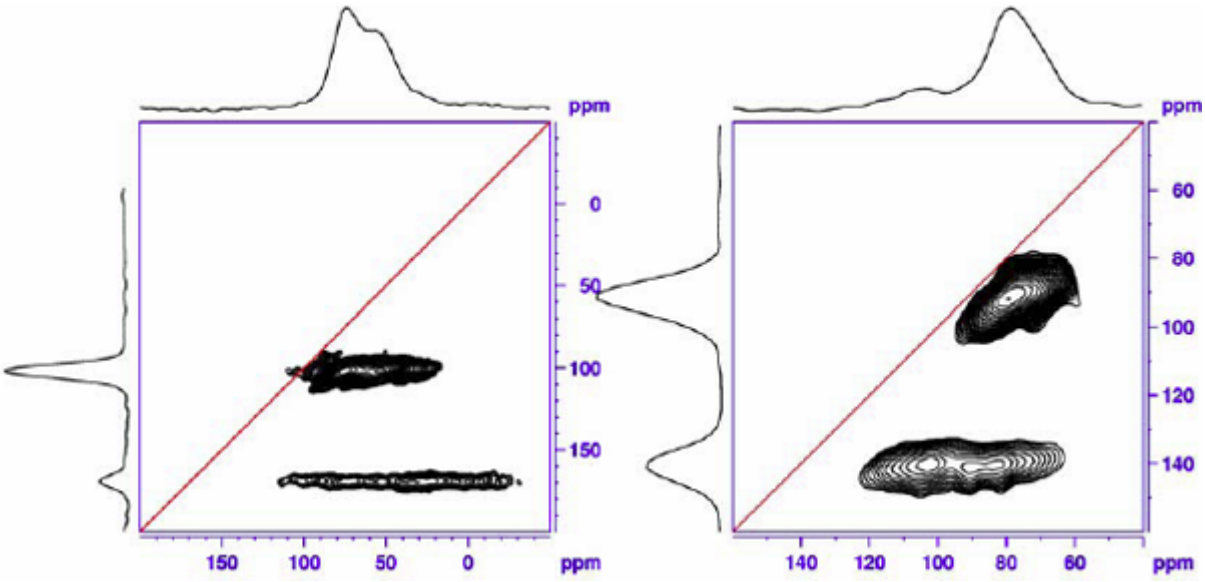

Figure 17.10.^{17}O MQMAS of NaPO3 at 11.7 T (67.8 MHz) on the left and 18.8 T (108.4 MHz) on the right.

The red lines in the spectra indicate the isotropic chemical shift axis. Approximate quadrupole parameters of the two sites are Qcc ≈ 7.7 MHz, h ≈ 0.36, diso ≈ 125 ppm for the lower peak and Qcc ≈ 4.5 MHz, h ≈ 0.16, diso ≈ 85 ppm for the upper peak (sample courtesy of Alexandrine Flambard, LCPS, Univ. de Lille).

The bridging oxygen give rise to the lower peaks in the 2D spectra of ***Figure 17.10.***, the non-bridging ones give rise to the upper peak. An additional red line is drawn into the spectrum which represents the diagonal, meaning *d(F2) = d(F1)*. One can see that all line positions must be below this diagonal because the negative quadrupole induced shift is scaled down and subtracted from the isotropic shift to give the MQ shift. In the example shown in ***Figure 17.10.*** two sites are visible with distinct differences in their spectroscopic parameters. In the sheared spectra we find the lower peak at 170 ppm (11.7 T) and 140 ppm (18.8 T), respectively, in the 3Q dimension. This peak is dispersed parallel to the F2 axis which means that its line width is mainly due to second order quadrupole broadening. The upper peak at 100 ppm (11.7 T) and approx. 90 ppm (18.8 T) in the 3Q dimension has a much smaller quadrupole coupling which can immediately be recognized from the fact that the peak is much closer to the diagonal. It is very nice example where the second order broadening which is still the dominant interaction at 11.7 T is so much reduced at 18.8 T that the width of the peak is now determined by the distribution of chemical shift. This is expressed in the fact that the peak is dispersed along the diagonal.

Figure 17.11. shows the results of the fitting with the solids line shape analysis package included in TopSpin. The spectra used for that have been extracted from rows of the 2D spectrum shown in ***Figure 17.10.***.

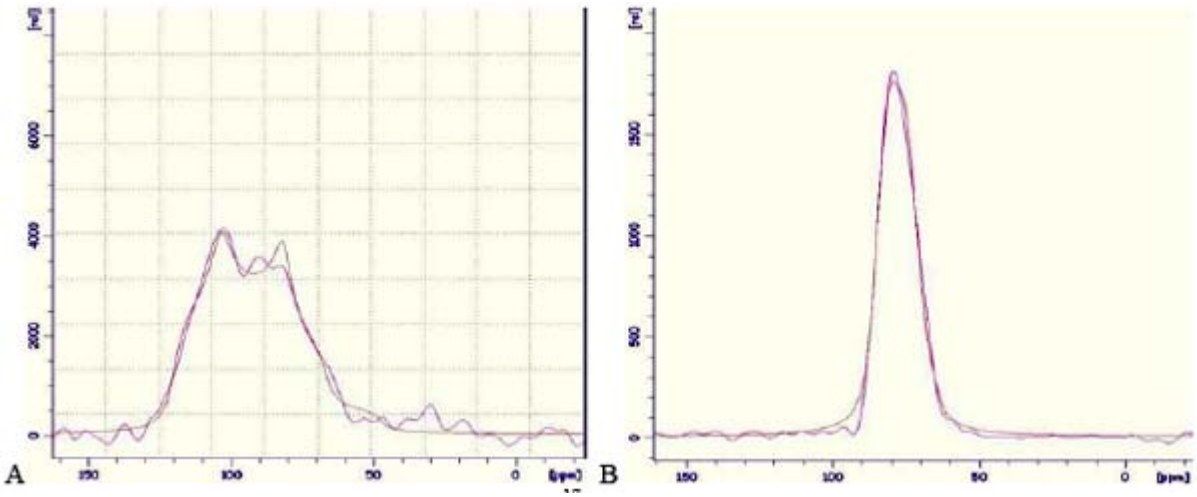

Figure 17.11.Slices and Simulations of the 18.8 T ^{17}O MQMAS of NaPO3.

Fitted parameters are A) Qcc ≈ 7.7 MHz, h ≈ 0.36, diso ≈ 125 ppm and B) Qcc ≈ 4.5 MHz, h ≈ 0.16, diso ≈ 87 ppm for the upper peak (sample courtesy of Alexandrine Flambard, LCPS, Univ. de Lille).

Spectra that are sheared can be evaluated graphically as follows, as shown in ***Figure 17.12.***. In addition to the (red) isotropic chemical shift axis indicated as "axis CS" with the slope $\Delta\delta$ (F2)/$\Delta\delta$ (F1) = 1 there are two more lines drawn. The (blue) axis indicated as "axis Qis" is the quadrupole induced shift axis with the slope $\Delta\delta$ (F2)/$\Delta\delta$ (F1) = -17/10. This axis is identical for all different spins *I* and all orders p of the MQMAS experiments. This axis can be shifted, retaining the same slope, so that it intersects a spectral line in its centre of gravity. Through the intersection point of the Qis axis with the CS axis a third line can be drawn parallel to the F2 axis. This is the dotted black line in ***Figure 17.12.***. The shift value that is read from the F1 axis at this position is the isotropic chemical shift of that particular site, and the Qis is then given by ***(Eq. 17.2)***.

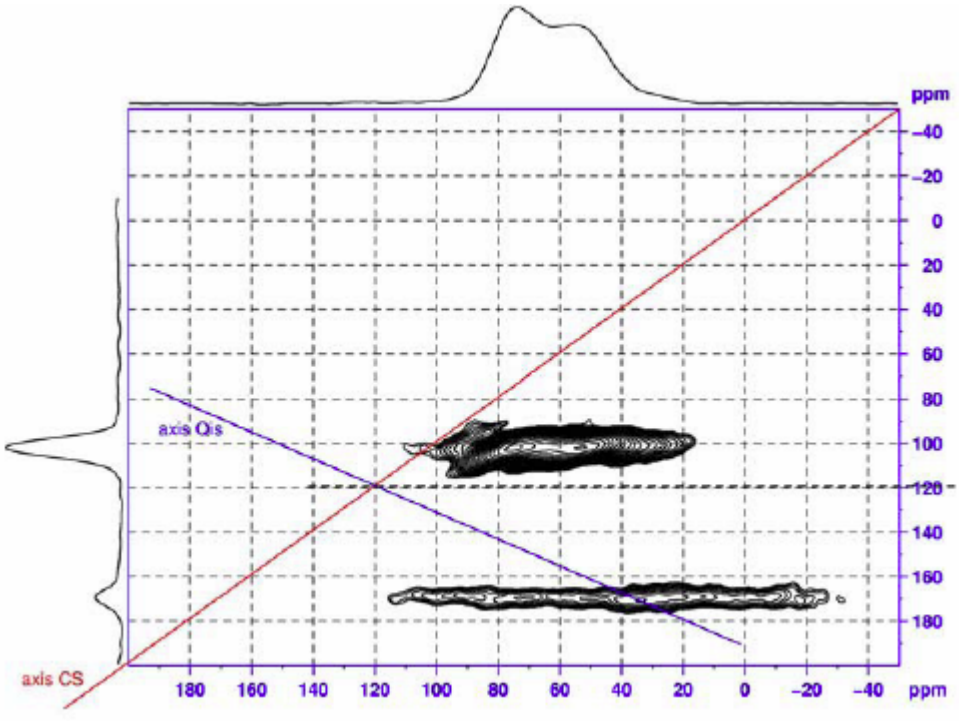

Figure 17.12.Graphical Interpretation of the Spectrum from ***Figure 17.10.****.*

In the 11.7 T spectrum this gives quadrupole induced shifts δ_{qis} of ≈ -75 ppm and ≈ -20 ppm for the two sites, respectively. At 18.8 T the δ_{qis} of the lower peak in the 2D spectrum decreases to ≈ -30 ppm, whereas it cannot be determined graphically anymore for the upper peak since the chemical distribution broadens the peak in the F1 dimension more than the theoretical δ_{qis} of ≈ -5 ppm.

MQ-MAS: Sensitivity Enhancement 18

The MQMAS experiment on half integer quadrupole nuclei is an extremely insensitive experiment. This is due to the low efficiencies of both the excitation of 3Q coherence and their conversion to observable magnetization. Several approaches have been taken to enhance the efficiency of the excitation and conversion, mainly focusing on the conversion, as this is the least efficient step. Adiabatic pulses can be used for the conversion instead of a single high power CW pulse, and alternative phase cycling schemes have also yielded improvements. Improving the efficiency of the MQ excitation pulse has been tried but no generally applicable scheme exists so far. Before describing the optimization procedures, some experimental approaches used in combination with these enhancement techniques are introduced.

Split-t_1 Experiments and Shifted Echo Acquisition *18.1*

The excitation pulse in the MQMAS experiment creates 3Q coherence that can be refocused into an observable SQ echo by the conversion pulse. As the t_1 period is incremented in successive slices of the 2D experiment this echo position relative to the conversion pulse changes as a function of the duration of the actual t_1 delay. If this observable (SQ) magnetization can be refocused again, by a central transition selective 180° pulse, a shifted echo acquisition can be implemented. The delay between the conversion pulse and the 180° pulse or the delay prior to the start of the acquisition must be incremented proportional to t_1. This results in a split-t_1 experiment where the top of the shifted echo appears at a constant position after the final pulse throughout the entire 2D experiment. The position of the echo top depends on the spin *I* of the observed nucleus. If the delay before the selective 180° pulse is long enough, the signal will have decayed and the full build up and decay of the echo can be recorded. By this method a phase modulated data set is acquired with a full echo that contains twice the intensity of the simple MQMAS experiment (if transverse relaxation can be neglected). At the end of the t_1 period of the split-t_1 experiment, there is no net evolution under the second order quadrupole broadening. This is the case because the evolution of the MQ coherence in the first part of t_1 is cancelled out by the evolution of the SQ coherence in the part of t_1 after the conversion pulse (the lengths of the two periods are related by the ratio of the second order broadening of the MQ and SQ coherence). The resulting 2D spectrum thus requires no shearing transformation to make f2 the isotropic dimension.

Whether this experimental trick is useful for your sample of interest can easily be determined by running a simple Hahn-echo experiment, where the delay τ in the 90°-τ-180° sequence is adjusted so that the FID of the signal is decayed before the 180° pulse is applied. This is shown in ***Figure 18.1.***. The FID generated by the initial 90° pulse is not sampled, but after it is decayed it is refocused with a 180°

pulse into a so-called shifted echo, meaning that the position of the echo can be shifted by adjusting the delay ***d6***.

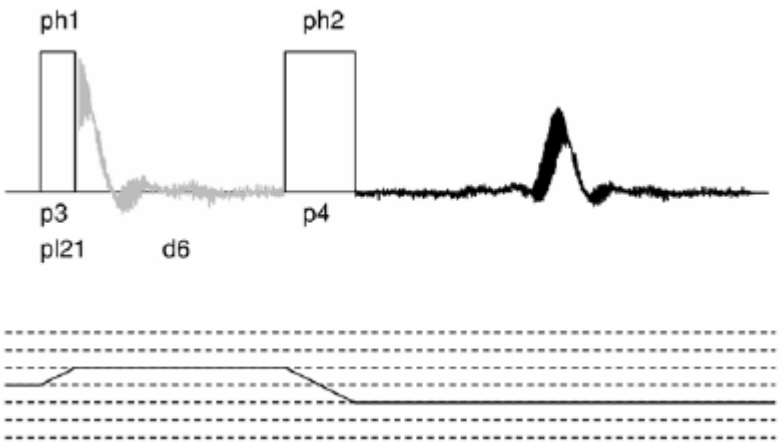

Figure 18.1. Hahn Echo Pulse Sequence and Coherence Transfer Pathway.

*After the initial 90° pulse **p3** the magnetization dephases and is refocused by the 180° pulse **p4**. If the τ delay **d6** is long enough a full echo can be acquired.*

If data acquisition starts immediately after the second pulse the whole echo will be acquired. The integrated intensity of the echo will be almost twice the intensity of the single FID; it is just T_2 relaxation during τ that leads to attenuation. In MAS experiments it is advisable to synchronize the echo with the sample rotation i.e. make τ an integer multiple of rotor periods. For FT of the shifted echo FID there is a slight “inconvenience” as shown in ***Figure 18.2.*** because after a normal FT the signal looks quite unconventional. To obtain the usual spectrum a magnitude calculation can be done on 1D spectra, with the loss of phase information. Alternatively, and in particular in 2D spectra it is possible to apply a large 1st order phase correction ***phc1*** to compensate for the time delay before the echo top. The value of this is:

$$phc1 = -\frac{d6}{dw} \cdot 180° \qquad \text{(Eq. 18.1)}$$

This value can be entered into the processing parameters and a phase correction *pk* can be performed. After this the 0th order phase correction still needs to be adjusted interactively. The best method is to phase the spectrum to give minimum signal intensity and add or subtract 90° to the obtained value (click 90 or -90 in the TopSpin phasing interface).

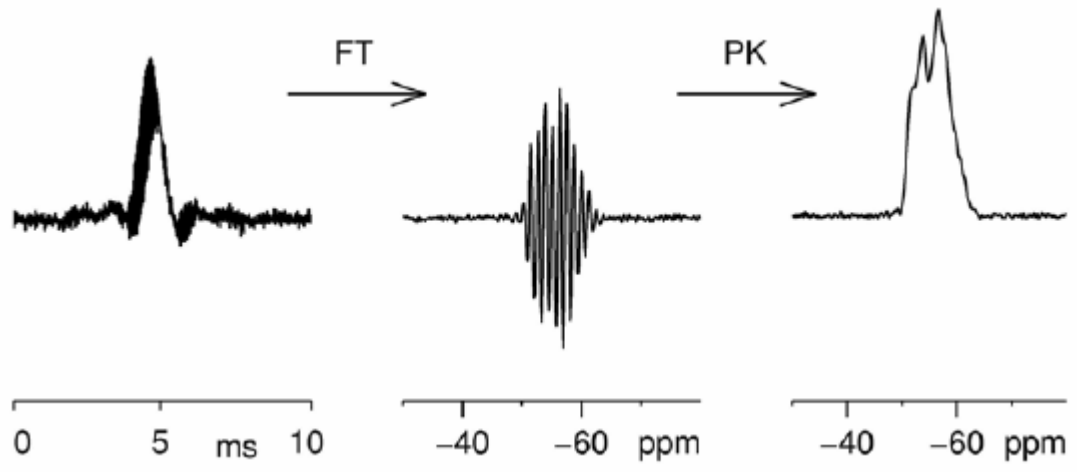

Figure 18.2. Processing of Hahn Echo. Left is the Shifted Echo.

The middle shows the spectrum after FT. On the right is the spectrum with the correct first order phase correction.

Implementation of DFS into MQMAS Experiments 18.2

Two pulse sequences are available to implement a double frequency sweep (DFS). ***Figure 18.3.*** shows the 4-pulse sequence with z-filter, *mp3qdfsz.av*. The principle of this sequence is already described in the chapter ***"Basic MQ-MAS" on page 213***, with a CW pulse instead of a DFS for conversion. ***Figure 18.4.*** shows a 3-pulse sequence with a shifted echo acquisition in a split-t_1 experiment, *mp3qdfs.av*. In both sequences the same sweep is used. Both sequences start with an excitation pulse ***p1*** that creates 3Q coherence which is allowed to evolve during the evolution period ***D0***. The sweep during ***P2*** is used to change (non-observable) 3Q coherency to observable SQ coherency. In the 4-pulse sequence they pass through a z-filter by a sequence of CT selective 90°-90° pulses ***P3-D4-P3***. In the 3-pulse sequence a delay ***D6*** is introduced so that the obtained signal can first dephase and then be refocused with a 180° CT selective pulse.

Optimization of the Double Frequency Sweep (DFS) 18.2.1

At this point it is assumed that the pulses ***p1***, ***P3***, and ***P4*** together with their corresponding power levels ***PL11*** and ***PL21*** are already calibrated as described in the chapter ***"Basic MQ-MAS" on page 213***. Starting from this set-up a data set should be created into which either of the two DFS pulse programs is loaded.

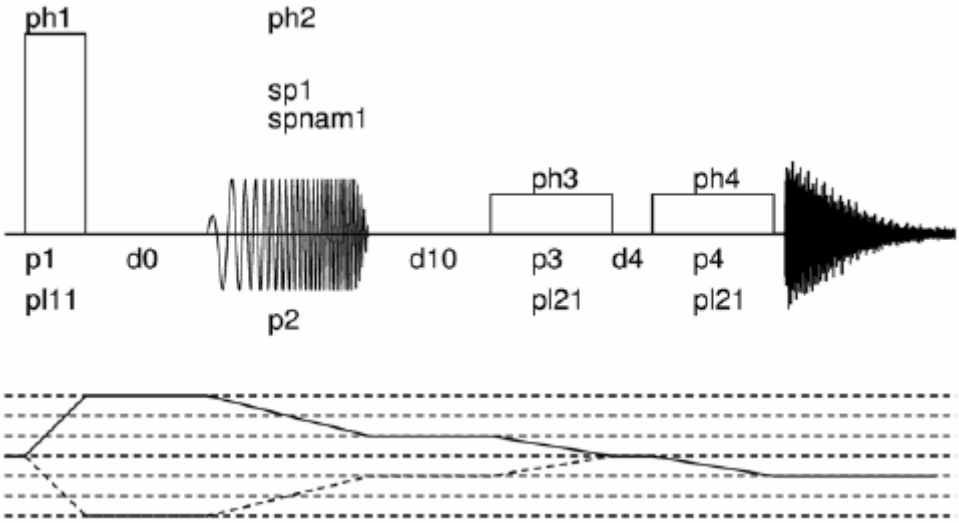

Figure 18.3. Four Pulse Sequence and Coherence Transfer Pathway for the 3Q MAS Experiment

Four pulse sequence and coherence transfer pathway for the 3Q MAS experiment with z-filter (mp3dfsz.av) and double frequency sweep (DFS). Excitation pulse p1 and selective pulses P3 are the same as for mp3qzfil.av. Delays ***D0*** *and* ***D4*** *are the incremented delay for t_1 evolution and 20 µs for z-filter, respectively. Delay* ***D10*** *can be incremented for spin I = 3/2 nuclei proportional to* ***D0****. Power level and duration of the sweep P2 must be optimized. Phase lists are as follows, for phase sensitive detection in F1 the phase of the first pulse must be incremented by 30° in States or States-TPPI mode:*

ph1 = 0 60 120 180 240 300

ph2 = 0*24 90*24 180*24 270*24

ph3 = 0

ph4 = 0*6 90*6 180*6 270*6

receiver = {0 180}*3 {90 270}*3 {180 0}*3 {270 90}*3

{180 0}*3 {270 90}*3 {0 180}*3 {90 270}*3.

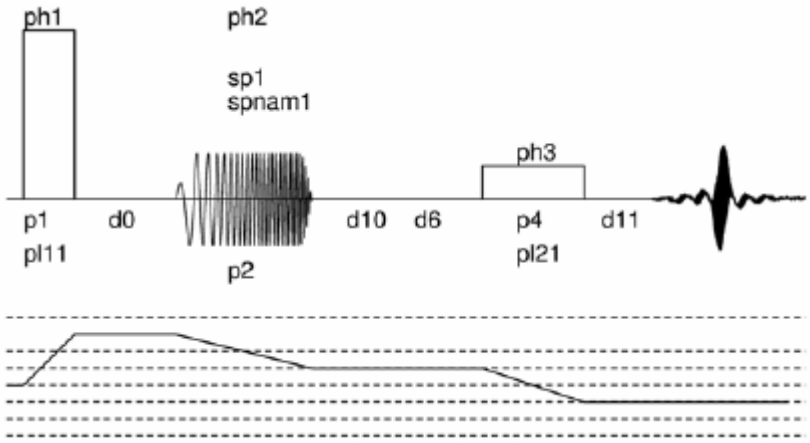

Figure 18.4. Three Pulse Sequence and Coherence Transfer Pathway

*Three pulse sequence and coherence transfer pathway for the 3Q MAS experiment with z-filter (mp3qdfs.av). Excitation pulse **p1** is the same as for mp3qzfil.av, **P4** is a central transition selective 180° pulse (usually 2*p3). Delays **D0** is the incremented delay for t_1 evolution. Delays **D10** or **D11** must be incremented proportional to **D0**. Power level and duration of the sweep **P2** must be optimized. Phase lists are as follows, 2D data are acquired in QF mode, which means that no phase incrementation is required:*

ph1 = 0 30 60 90 120 150 180 210 240 270 300 330

ph2 = 0

ph3 = 0*12 90*12 180*12 270*12

receiver = {0 270 180 90}*3 {180 90 0 270}*3

Initial parameter values are listed in ***Figure 18.1.***. A few of these parameters need further explanation:

D6**:* Is calculated as (1s**L1*/*CNST31*)-(*P4*/2)-(*P2*/2). This ensures that the delay from the centre of the sweep to the middle of the 180° pulse is an integer multiple of the rotor period. ***L1 must be set so that ***D6*** becomes long enough for a full echo to build up. If we assume the FID has decayed after 3 ms, spinning frequency is 25 kHz, and the 90° pulse is 20 µs, then ***L1*** should be between 70 and 80 so that ***D6*** is between 2.77 and 3.17 ms.

P2**:* Is calculated as 1s/(CNST31*******L0***). The duration of the sweep can be adjusted depending on T_2 of the sample. The sweep should not be longer than one rotor period, for many samples you may find that a quarter of a rotor period or even less is sufficient.

In ***ased*** the values of the two parameters ***D6*** and ***P2*** are greyed, because they cannot be set anymore. They are calculated in the pulse program from the parameters explained below, which must be set accordingly:

L0**:* Defines the fraction of a rotor period for the duration of the sweep ***P2, usually between 1 and 8.

L1**:* Defines ***D6 to be an integer number of rotor periods.

The sweep will be defined by further parameters:

***CNST1**:* Start frequency (in kHz) of the sweep; the sweep should start slightly off resonance, usually 30 to 50 kHz from the resonance of the central transition.

***CNST2**:* End frequency (in kHz) of the sweep; the sweep should cover the satellite transition, but this is often broader than the band width of the probe of approximately 1 MHz. Therefore, it does not make sense to have this value bigger than 1000.

Table 18.1. Initial Parameters for the DFS Experiment

Parameter	Value	Comments
pulprog	mp3qdfs.av, or mp3qdfsz.av	Pulse program.
NS	48*n (dfs) 96*n (dfsz)	Full phase cycle is important.
D0	3 µs	Or longer, t_1-period.
D1	5 * T_1	Recycle delay, use dummy scans if shorter. If d1 is too short artefacts in the 2D spectrum may show up.
D4	20 µs	Z-filter delay, mp3qdfsz.av only.
D6	see text	Calculated in pulse program mp3qdfs.av only.
D10	= 4µs	
D11	= 0	Used in mp3qdfs.av only.
P1	≤ 3.6 µs	Excitation pulse at pl11.
P2	see text	Calculated in pulse program.
P3	20 µs	90° selective pulse at pl21 used in mp3qdfsz.av only.
P4	40 µs	180° selective pulse at pl21 used in mp3qdfs.av only.
PL1	=120 dB	Not used.
PL11		Power level for excitation pulse, use value from standard MQMAS optimization.
PL21		Power level for selective pulse, approx. pl11+30 dB taken from previous pulse calibration.
spnam1	dfs	Set by AU program zg_dfs.
sp1	to be optimized	Power level for dfs.
aunm	zg_dfs	AU program to calculate sweep.
L0	see text	Fraction of rotor period for sweep.
L1	see text	Number of rotor cycles for synchronization used in mp3qdfs.av only.
cnst1	see text	Start frequency of sweep (in kHz).
cnst2	see text	End frequency of sweep (in kHz).
cnst3	50	(in ns) timing resolution for sweep.
cnst31	“masr”	Spinning frequency.

CNST3**:* (in ns) = 50. This is the maximum timing resolution that can be obtained on a shaped pulse, with AV or AVII hardware. However, if ***cortab is defined for that nucleus, 100 ns is the maximum timing resolution possible in a shaped pulse.

***CNST31**:* Magic angle spinning frequency, used for the calculation of the duration of the sweep and the echo delay.

The calculation of the sweep is done via an AU program called ***zg_dfs***. It calculates the sweep according to the parameters given above and stores it as a shape file, which is called dfs. After the calculation the AU program starts the acquisition. In order to ensure that the correct sweep is always used, it is advisable to enter the name of this AU program into the parameter ***aunm***, and start all acquisitions using the command ***xaua***. All that needs to be optimized now is the appropriate RF power level for the sweep, defined as parameter ***sp1***. As a first guess a value of 3 dB less RF power than for the excitation pulse should be used (i.e. ***SP1*** = ***PL11*** + 3 dB). You may use ***popt*** for the optimization, where ***SP1*** is decremented by 1 dB up to the same power level used for the excitation pulse (e.g. from 20 dB to 0 dB). Initially a sweep of one whole rotor period (i.e. ***L0*** = 1) can be used. The optimization of ***SP1*** can be repeated e.g. for half a rotor period, a quarter of a rotor period and so on. With a shorter sweep you will find that higher RF power will be needed.

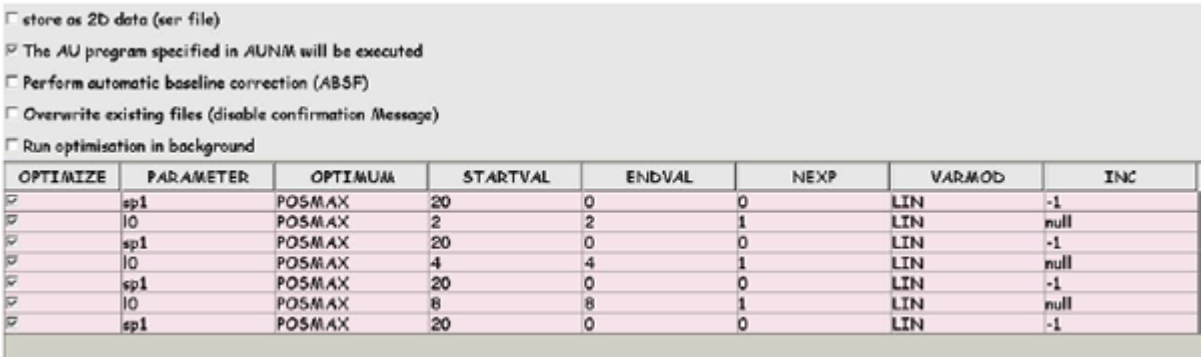

☐ store as 2D data (ser file)
☑ The AU program specified in AUNM will be executed
☐ Perform automatic baseline correction (ABSF)
☐ Overwrite existing files (disable confirmation Message)
☐ Run optimisation in background

OPTIMIZE	PARAMETER	OPTIMUM	STARTVAL	ENDVAL	NEXP	VARMOD	INC
☑	sp1	POSMAX	20	0	0	LIN	-1
☑	l0	POSMAX	2	2	1	LIN	null
☑	sp1	POSMAX	20	0	0	LIN	-1
☑	l0	POSMAX	4	4	1	LIN	null
☑	sp1	POSMAX	20	0	0	LIN	-1
☑	l0	POSMAX	8	8	1	LIN	null
☑	sp1	POSMAX	20	0	0	LIN	-1

Figure 18.5. Example for popt to Set-up for Optimization of DFS.

*Note that the option "The AU program specified in AUNM will be executed" is checked. This ensures that the sweep is recalculated for the variation of **I0** and stored in the shape file dfs. The initial value of **I0** is 1.*

Figure 18.5. shows a ***popt*** window with successive optimization of ***SP1*** for several fractions of rotor periods ***I0***. Note that the check mark for "The AU program specified in AUNM will be executed" MUST be set, in order to force recalculation of the shape for each step of the optimization. In this case acquisition is run with the command ***xaua***, which ensures that the correct sweep is stored in the shape file dfs. In the above example optimization proceeds such that in the first run ***SP1*** is varied from 20 to 0 in 21 steps. Then ***L0*** is set to 2 and ***SP1*** is again varied from 20 to 0. Then ***I0*** is set to 4 and so on. ***Figure 18.6.*** shows results of the variation of the RF power level of sweeps with different durations. Experiments have been run at 20 kHz and optimization procedures for 1, 0.5, 0.25, and 0.125 rotor periods corresponding to 50, 25, 12.5, and 6.25 µs respectively have been run. One can see that as the duration of the sweep is reduced the required RF field amplitude is higher. This is true when the spinning frequency is kept constant and the sweep is a smaller fraction of a rotor period and when the sweep is kept at e.g.

one rotor period and the spinning frequency is increased (and hence the rotor period decreased). On “real life” samples the differences between signal intensities at one rotor period compared to e.g. ¼ rotor periods will be more pronounced than on a crystalline model compound. Since the spinning frequency is usually determined by the spectrum itself, the only degree of freedom is the amplitude of the sweep. In the example chosen here any of the conditions will provide a good quality spectrum, and the condition with the biggest enhancement at the least power is to be preferred.

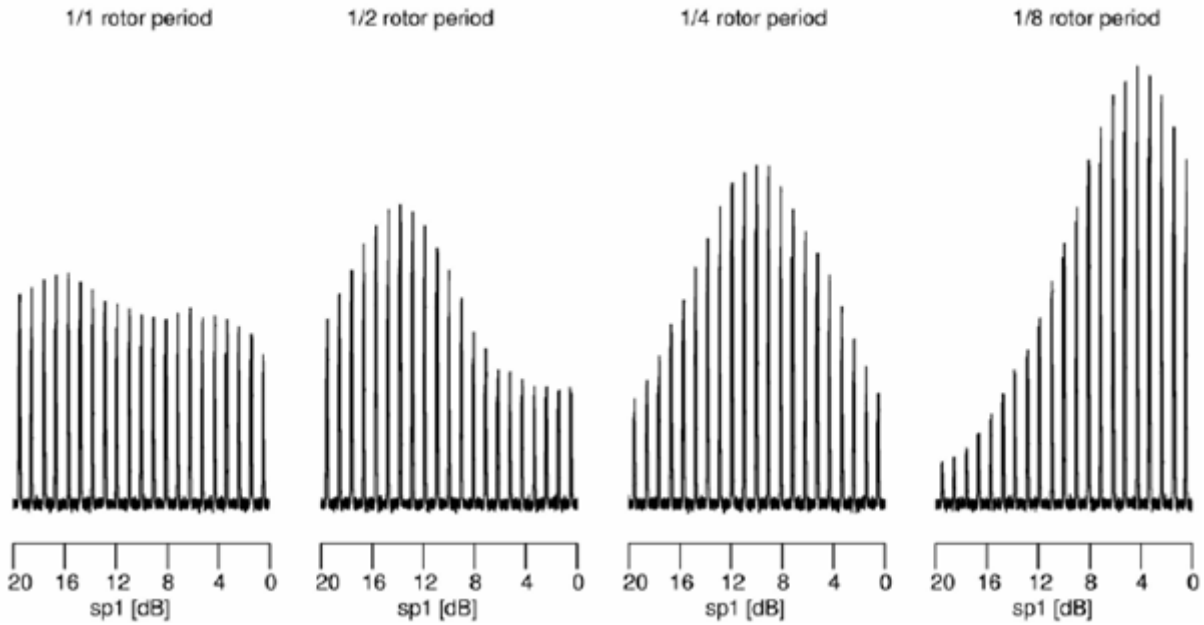

Figure 18.6. Signal Intensities of ^{87}Rb in $RbNO_3$

Signal intensities of ^{87}Rb in $RbNO_3$ as function of duration and RF field amplitude for double frequency sweeps.

2D Data Acquisition *18.2.2*

After the parameters for the DFS are adjusted the 2D data acquisition can be prepared. In tables 2 and 3 the important parameters are listed for the two pulse sequences. Parameters are listed separately for F1 and for the pulse program relevant parameters which should be set in ***eda*** and ***ased***, respectively.

The 3-pulse sequence used in *mp3qdfs.av* creates a phase modulated data set and therefore, FnMODE must be QF. However, since a whole echo acquisition is performed a pure absorption mode spectrum can be obtained. Increments for ***D10*** and ***D11*** must be set correctly so that a standard two-dimensional FT can be applied.

Using the 4-pulse sequence *mp3qdfsz.av* FnMode must be States or States-TPPI, so that the shearing FT can be performed for processing. However, no shearing is required in case of nuclei with spin I=3/2 where a split-t_1 experiment can be performed, in which case ***IN10*** must be set correctly.

For both sequences, TD in F1 determines the number of FID's to be accumulated in the indirect dimension. This value is determined by the line width and resolution that can be expected and which depend on the properties of the sample. In crystalline material fairly narrow peaks can be expected so that a maximum acquisition time in F1 of 2 to 5 ms is expected. In disordered material where the line width is broader and determined by distribution a total acquisition time in F1 up to may be 1 ms may be sufficient. The total acquisition time aq in F1 equals (***TD***/ 2)****IN_010***. For rotor synchronized experiments ***IN_010*** = 1/spinning frequency so will typically be between 100 µs (10 kHz spinning) and 28.5 µs (35 kHz spinning), so only 100 to 250 experiments might be required. The rotor synchronization immediately means that the spectral range in F1 is limited. Dependent on chemical shift range, spinning frequency, and quadrupole interactions the positions of the peaks may fall outside this range. In such a case care must be taken when interpreting the spectrum. Acquisition with half-rotor synchronization to double the spectral window in F1 may help. However, in this situation one set of spinning sidebands appears and it must be avoided that the spinning side bands of one peak fall on top of other peaks. Some sort of rotor synchronization is always recommended because spinning side bands in the indirect dimension extend over a very wide range, which cannot be truncated by e.g. filtering. Therefore, rotor synchronization together with States or States-TPPI phase sensitive acquisition helps to fold spinning sidebands from outside back onto centre bands or other side bands.

Table 18.2. Parameters for 2D Data Acquisition of 3-pulse Shifted Echo Experiment mp3qdfs.av.

Parameter	Value	Comments
pulprog	mp3qdfs.av	
F1 parameters:		In *eda.*
FnMode	QF	Acquisition mode for 2D.
TD	see text	Number of FID's to be acquired.
ND_010	1	There is only one d0 delay in the sequence.
SWH	"masr"	Equals spinning frequency for rotor synchronization, from this in0 is calculated correctly, if ND_010 must be set first.
NUC1		Select the same nucleus as for F2 so that transmitter frequency offset is set the same in both dimensions (essential for referencing).
pulse program parameters:		In *ased.*
D10	0	
IN10	=IN0*7/9 0	For spin *I* = 3/2, for all other spin I.
D11	0	
IN11	0 =IN0*19/12 =IN0*101/45 =IN0*91/36	For spin *I* = 3/2, For spin *I* = 5/2, For spin *I* = 7/2, For spin *I* = 9/2.

Table 18.3. Parameters for 2D Data Acquisition of 4-pulse Z-filtered Experiment mp3qdfsz.av.

Parameter	Value	Comments
pulprog	mp3qdfsz.av	
F1 parameters:		In *eda.*
FnMode	States or States-TPPI	Acquisition mode for 2D.
TD	see text	Number of FID's to be acquired.
SWH	"masr"	Equals spinning frequency for rotor synchronization, from this in0 is calculated correctly, ND_010 must be set first.
NUC1		Select the same nucleus as for F2 so that transmitter frequency offset is set the same in both dimensions (essential for referencing).
Pulse program parameters:		In *ased.*
D10	0	
IN10	=IN0*7/9 0	For spin I=3/2, so that no shearing FT is required. For all other spin I.

Data Processing *18.2.3*

Processing parameters should be set according to ***Table 18.4.***. Data obtained with mp3qdfs.av can be processed with ***xfb*** alone, if ***IN10*** or ***IN11*** have been set appropriately to run a split-t_1 experiment. Since a whole echo is accumulated FT along F2 from $-\Delta > t > +\Delta$ is done which necessitates a large 1st order phase correction to compensate for the start of the acquisition before the echo top. This correction can easily be calculated as given in ***(Eq. 18.1)***and should be stored into the parameter ***PHC1***. This gives an approximate value, which can be precisely adjusted in the interactive phase correction routine. The phase of the spectrum must be corrected such that there is no signal in the imaginary part, as described above.

Table 18.4. Processing Parameters

Parameter	Value	Comments
F2 (acquisition dimension)		
SI		Usually set to one times zero filling.
WDW	no	Don't use window function.
PH_mod	pk	Apply phase correction.
BC_mod	no	No DC correction is required after full phase cycle.
ABSF1	1000 ppm	Should be outside the observed spectral width.
ABSF2	-1000 ppm	Should be outside the observed spectral width.
STSR	0	Avoid strip FT.
STSI	0	Avoid strip FT.
TDoff	0	Avoid left shifts or right shifts before FT.
F1 (indirect dimension)		
SI	256	Sufficient in most cases.
WDW	no QSINE	Don't use window function. Only use if FID in F1 is truncated.
SSB	2	$\pi/2$ shifted squared sine bell.
PH_mod	pk	Apply phase correction.
PHC1		$-$(d6/dw)*180.
BC_mod	no	No dc correction is required after full phase cycle.
ABSF1	1000	Should be outside the observed spectral width.
ABSF2	-1000	Should be outside the observed spectral width.
STSR	0	Avoid strip FT.
STSI	0	Avoid strip FT.
TDoff	0	Avoid left shifts or right shifts before FT.

Data obtained with *mp3qdfsz.av* can be processed with the AU program ***xfshear***, unless in case of nuclei with spin I = 3/2 where a straight 2D FT can be used if a split-t_1 experiment has been recorded by setting ***IN10*** appropriately. The information obtained from the DFS enhanced spectra is the same as from the standard MQMAS experiments. Please refer to the chapter ***"Basic MQ-MAS" on page 213*** for further details regarding the shearing transformation and the information obtained from MQMAS spectra.

Fast Amplitude Modulation - FAM 18.3

It must be mentioned at this point that similar approaches have been made where the frequency of irradiation is established by a fast modulation of the amplitude of the pulses. This is realized by a repetitive train of either $[\text{pulse-delay-pulse-delay}]_n$ or $[\text{delay-pulse-pulse-delay}]_n$. Pulses and delays in these trains are of the same length. The phases of the pulses are alternating +x and –x which creates a fast cosine type amplitude modulation. The frequency of this amplitude modulation appears to the spin system as an irradiated frequency.

Two pulse programs are available, *mp3qfamz.av* and *mp3qfam.av*. They correspond to the pulse sequences depicted in ***Figure 18.3.*** and ***Figure 18.4.***, but the shaped pulse realizing the DFS is replaced with a sequence ***D2-P2-P2-D2*** embedded in a loop repeated by loop counter ***L2*** and with power level ***PL14*** for the pulses. These sequences are only useful for spin *I* = 3/2 nuclei. There are also sequences for higher spins, which are not included in the pulse program library. In those cases it is recommended to use DFS. The difference between FAM and DFS can be understood in such a way that FAM establishes the irradiation of a single distinct frequency whereas DFS continuously irradiates (sweeps) over a range of frequencies. These frequencies must lie in the range of the satellite transitions, therefore a single frequency irradiation is sufficient for spin *I* = 3/2. Higher spins have more satellite transitions and therefore, a correspondingly larger number of irradiation frequencies are required. DFS is here the most convenient solution.

Start values for the parameters determining FAM are listed in ***Table 18.5.***.

Table 18.5. Parameters for FAM

Parameter	Value	Comments
PL14	PL11 + 3 dB	Less RF power than for a CW pulse is sufficient.
P2	0.8 µs	
D2	= P2	Calculated in the pulse program.
L2	2	

All other parameters are in full analogy to the other MQMAS pulse programs, in particular for z-filtering and creating the shifted echo. What is left is to find the best conditions for FAM optimizing ***PL14***, ***P2***, and ***L2*** consecutively. This can conveniently be performed with the parameter optimization procedure ***popt***, where two or three iterations can automatically be performed.

Soft Pulse Added Mixing - SPAM 18.4

A simple and ingenious experimental trick can immediately give a signal enhancement. Starting from the standard 3-pulse sequence the phase cycling of reconversion pulse ***P2*** and the CT selective 90° pulse ***P3*** is eliminated. This changes the coherence transfer pathway from $0 \rightarrow \pm 3 \rightarrow 0 \rightarrow -1$ to $0 \rightarrow +3 \rightarrow -1, 0, +1 \rightarrow -1$ and $0 \rightarrow -3 \rightarrow -1, 0, +1 \rightarrow -1$. It has been shown that this leads to a substantial gain in sensitivity. However, it requires that data are acquired in echo/anti-echo mode in order to store the two different coherence transfer pathways in consecutive FID's in the serial file.

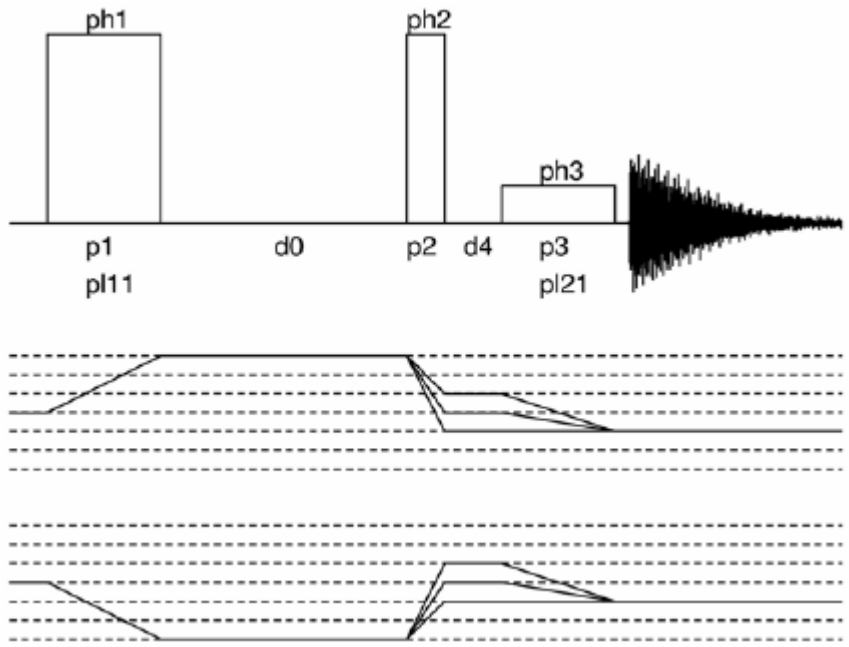

Figure 18.7. Pulse Sequence and Coherence Transfer Pathways for SPAM 3QMAS.

It is extremely convenient that the setup of the pulse lengths and power levels can be done with the pulse program *mp3qzqf.av*. The setup procedure is exactly the same as described for this experiment in the chapter ***"Basic MQ-MAS" on page 213***. Before the start of the 2D data acquisition all that needs to be set is the pulse program, *mp3qspam.av*, and a small number of other parameters. These are listed in ***Table 18.6.***:

Table 18.6. Further Parameters for 2D Data Acquisition of SPAM MQMAS Experiment mp3qspam.av

Parameter	Value	Comments
pulprog	mp3qspam.av	
Further F1 parameters:		In *eda.*
FnMode	Echo/Anti-echo	Acquisition mode for 2D.
Further pulse program parameters:		In *ased.*
D4	0.5 µs	Not 20 µs like in mp3qzqf.av.
l4	1	Set by the pulse program, internally used counter.
l5	see text	Number of anti-echos to be acquired 0 > L5 > td{F1}/2.
l6	3 1	For spin *I* = 3/2. For all other spins.

FNMODE: Even though this parameter is not evaluated by the pulse program it will be used by the processing AU program ***xfshear***.

D4: A very short delay is used here, just to allow for amplitude and phase switching.

I4: This loop counter is internally used for checking if the echo or anti-echo is currently being acquired.

I5: In the acquisition of echo-anti-echo 2D spectra signals from the echo and anti-echo pathways are stored into consecutive FID's in the serial file. In MQMAS experiments these echos and anti-echos behave differently. For t_1 = 0 both signals have their echo top immediately after the selective 90° pulse. As t_1 is incremented the top of the echo appears at later point in time whereas the top of the anti-echo appears at an earlier point in time. It means that the contribution of the anti-echo becomes less and less until finally the signal fades out completely and only noise is sampled. It can be advantageous to terminate the acquisition of this noise in order to increase the overall S/N and save spectrometer time. However, in the processing of echo-anti-echo data two consecutive FID's are linearly combined in the following way:

$$re1 = -im2 - im1 \quad re2 = re2 - re1$$
$$im1 = re2 + re1 \quad im2 = im2 - im1 \qquad \text{(Eq. 18.2)}$$

Where *re* and *im* refer to the real and imaginary points of FID's 1 and 2. Hence, acquiring a smaller number of anti-echos than echos leads to the usual truncation effects (wiggles in the spectrum). Furthermore, since both signals contribute to the phase information care must be taken that the pure absorption line shape of the 2D peaks is not obscured. Therefore, in case of doubt it is probably the best idea to set ***L5*** = ***TD***{F1}/2. If less anti-echos are to be accumulated the question is how many anti-echos to acquire - this depends on the sample. In amorphous or disordered materials the FID decays rapidly and so does the anti-echo. In such a case 4 to 8 anti-echos may be sufficient. In the case of crystalline materials it takes many more t_1 increments before the anti-echos decay. Hence, the number of anti-echos should be of the order of half the number of echos. It is always better to acquire more anti-echos than are really needed, because then you can be sure that you acquire a 2D spectrum with a reliable 2D absorption line shape. Never risk gaining sensitivity or saving experimental time at the expense of quality of lineshapes.

II6: the value of this loop counter is needed to set the phases of the soft pulses correctly and define what is an echo and what is an anti-echo (which are different for spin *I* = 3/2 and all the other spin quantum numbers).

Processing of these spectra is done in analogy to spectra obtained with *mp3qzqf.av*. However, phase correction in the acquisition dimension F2 cannot be determined on the first FID. Therefore, ***xf2*** must be applied first and then F2 phase correction can be determined on either the first slice, in case of nuclei with spin *I* = 3/2, or the second slice for all other nuclei. 2D processing is then done with the AU program ***xfshear***. Alternatively ***xfshear*** can be used first, with a subsequent 2D interactive phase correction.

STMAS 19

The STMAS experiment for half integer quadrupole nuclei is a 2D experiment to separate anisotropic interactions from isotropic interactions. In the NMR of half integer quadrupole nuclei the dominant anisotropic broadening of the central +1/2 ↔ –1/2 transition (CT), and symmetric multiple-quantum (MQ) transitions, is the 2nd order quadrupole interaction which can only partially be averaged by MAS. The satellite transitions (ST, e.g. the ±3/2 ↔ ±1/2 transitions) however, are broadened by a 1st order interaction, which is several orders of magnitude larger than the 2nd order broadening. Under MAS the 1st order interaction of the ST can be averaged but spinning cannot be fast compared to the first order broadening (of the order of MHz), a large manifold of spinning side bands remains. The 2nd order broadening of the CT can only be narrowed by a factor of 3 to 4 so a signal is observed that still reflects this 2nd order broadening.

The 2D STMAS experiment exploits the fact that the 2nd order broadening of the ST transitions (e.g. + 3/2 ↔ +1/2 in a spin 3/2), is related to the 2nd order broadening of the CT by a simple ratio. A 2D spectrum is recorded which correlates a single quantum coherence of the satellite transitions (usually one of the inner transitions, ± 3/2 ↔ ± 1/2), and the + 1/2 ↔ –1/2 single quantum coherence of the central transition. The resulting 2D spectrum yields an isotropic projection where the 2nd order broadening has disappeared. The information content is in full analogy to the MQMAS experiment.

Experimental Particularities and Prerequisites 19.1

In contrast to the MQMAS experiment the first pulse in the STMAS experiment excites single quantum (SQ) coherency. The signal which is thus generated consists of contributions from both the CT and the ST. In ***Figure 19.1.*** the contribution of the CT shows up in the cosine curve starting at the (blue) filled rectangle resembling the initial pulse.

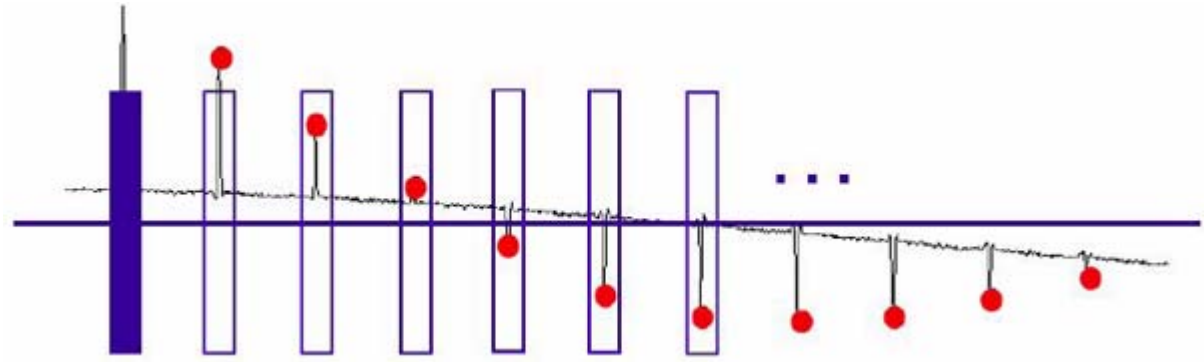

Figure 19.1. Principle of 2D Data Sampling in STMAS Experiments.

The (blue) filled rectangle on the left symbolizes the first pulse, which starts the evolution period t_1. After each revolution of the rotor, rotational echo's show up

which are indicated by the (red) filled circles. The open rectangles symbolize the second pulse (one pulse at the end of each individual t_1 increment). They must always occur precisely on top of the rotational echo. For each increment the t_2 data acquisition, which is not shown here, starts after the second pulse.

In the following discussion we will ignore this part completely. It showed up in the original experiments but can be completely suppressed by a double quantum filter. The contribution of the ST “rides” on top of the CT signal like spikelets. Since MAS efficiently averages the 1st order quadrupole interaction of the ST, the corresponding MHz broad signal is now narrowed into a huge number of spinning side bands. These coherency originating from the ST dephase rapidly and refocus into rotational echoes with each rotor cycle. A pulse precisely on top of such a rotational echo can transfer the SQ coherency from the ST to SQ coherency of the CT, the signal from which can then be acquired under standard MAS conditions. The evolution in the indirect dimension is achieved in such a way that the delay between the two pulses, which is the evolution period t_1, is incremented by integer multiples of the rotor period.

Two extremely important points must be considered for the experimental realization of the STMAS experiment. Firstly, the spinning frequency must be kept absolutely constant. The duration of the rotational echoes in the STMAS experiment is determined by the width of the satellite transition, giving a length of e.g. 1 µs for a satellite transition of 1 MHz width. If the rotor period varies from that specified in the parameters, the calculated delay in the pulse program is incorrect and the pulse misses the echo top, so less or no signal intensity is obtained. ***Table 19.1.*** summarizes the time deviation that occurs when the spinning frequency fluctuates by ± 1 Hz and ± 10 Hz at various desired spinning frequencies. One can see that when the t_1 increment accumulates to as much as 100 rotor periods it is possible to miss an echo completely. For example, if the duration of the rotational echo is 1 µs it will be missed when the deviation is larger, which is the case for a 1 Hz deviation at 10 kHz, but requires a fluctuation of 10 Hz at 30 kHz spinning.

Table 19.1. Time deviation of the rotor period for spinning frequency variations of ± 1 and ± 10 Hz for various spinning frequencies.

Fluctuation of … Hz @ desired spinning frequency	Deviation from precise rotor period after 1 rotor period	Deviation from precise rotor period after 100 rotor periods
10 Hz @ 30 kHz	11 ns	1.1 µs
1 Hz @ 30 kHz	1.1 ns	110 ns
10 Hz @ 20 kHz	25 ns	2.5 µs
1 Hz @ 20 kHz	2.5 ns	250 ns
10 Hz @ 10 kHz	100 ns	10 µs
1 Hz @ 10 kHz	10 ns	1 µs

Typically the spinning frequency must be stable within ≤1 Hz throughout the entire 2D data acquisition. Secondly, the accuracy of the magic angle setting is extremely important. The sidebands resulting from the first order broadening are narrowed from the full first order line width by a factor of $(3\cos^2\theta-1)$, hence for a deviation of $d\theta$ from the magic angle the broadening is $3\cos\theta\sin\theta d\theta$, which close to the magic angle is $\sqrt{2}d\theta$. The magnitude of the interaction that must be narrowed in the pres-

ent case is in the order of MHz so even a small deviation causes a severe broadening in the STMAS spectrum. This can easily be understood as the rotational echoes decay much more rapidly when the magic angle is off. Experimentally it has been found that the precision for setting the angle must be ≤ 0.002°. The dependence on the accuracy is so important that the experiment itself must be used to find the most precise magic angle setting. It is obvious that this can only be done on a well-known sample, as we will see later in the chapter. In order to achieve the necessary precision for the adjustability of the angle a special goniometer screw with an adapted gear transmission ratio is provided for the magic angle setting knob as an upgrade for Bruker WB MAS probes. Once the best angle setting is found it is advisable to leave the probe in the magnet. Sample changes, however, on the WB probes doesn't change the setting noticeably.

Pulse Sequences *19.2*

Figure 19.2. and ***Figure 19.3.*** show two of the basic sequences, which are 4-pulse sequences with z-filter (*stmasdqfz.av* and *stmasdqfe.av*). Both sequences start with a non-selective excitation pulse *p1* that creates SQ coherency on the innermost ST which is allowed to evolve during the evolution period ***D0***. Shortly before the end of the t_1 period there is a selective 180° pulse ***P4***. This provides a double quantum filter by which magnetization of the CT transition is eliminated which will otherwise give a strong diagonal signal from a CT –> CT coherence transfer pathway. The t_1 period is terminated with the second non-selective pulse ***P2***.

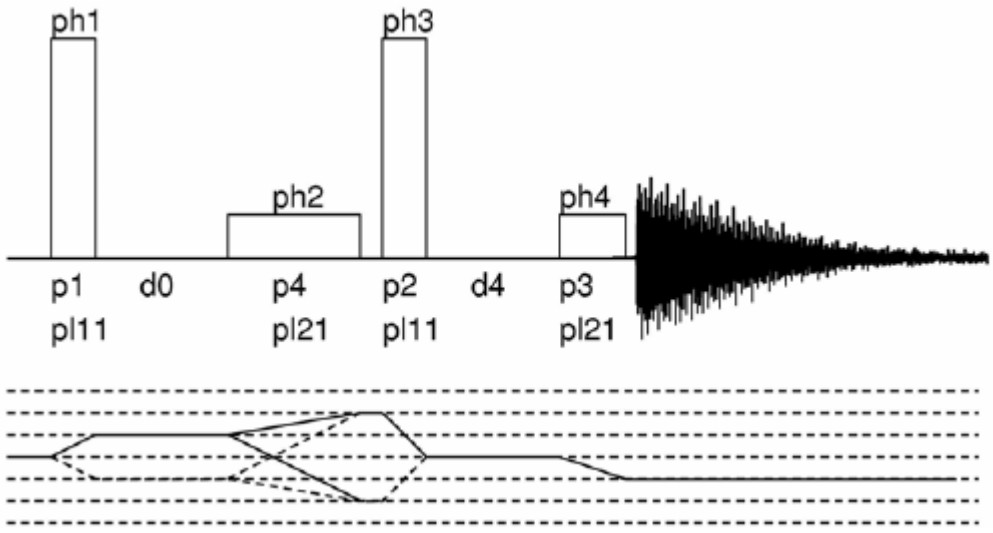

Figure 19.2. Four-pulse sequence and coherence transfer pathway for the double quantum filtered STMAS experiment with z-filter (stmasdqfz.av)

*Pulses **p1** and **P2** are non-selective pulses. The corresponding power level **PL11** should be set to achieve around 100 kHz RF field amplitude. **P3** and **P4** are CT selective pulse 90° and 180° pulses of about 20 and 40 µs, respectively, corresponding to an RF field amplitude of a few kHz. Delays **D0** and **D4** are the incremented delay for t_1 evolution and 20 µs for z-filter, respectively. Phase lists are as follows, for phase sensitive detection in F1 the phase of the first pulse must be incremented by 90° in States or States-TPPI mode:*

ph1 = 0 2

ph2 = 0 0 2 2

ph3 = 0 0 0 0 1 1 1 1 2 2 2 2 3 3 3 3

ph4 = 0*8 1*8 2*8 3*8 4*8

receiver = 0 2 2 0 2 0 0 2 0 2 2 0 2 0 0 2 1 3 3 1 3 1 1 3 1 3 3 1 3 1 1 3
2 0 0 2 0 2 2 0 2 0 0 2 0 2 2 0 3 1 1 3 1 3 3 1 3 1 1 3 1 3 3 1.

In the *stmasdqfz.av* pulse sequence this pulse flips the magnetization back along the z-axis. After a short z-filter delay ***D4*** a CT selective 90° pulse ***P3*** creates transverse magnetization. In the *stmasdqfe.av* pulse sequence the non-selective pulse ***P2*** converts the ST SQ coherence into CT SQ coherence. This is allowed to evolve for another delay ***D6*** after which it refocuses into an echo by a CT selective 180° pulse. When either the ***D6*** before the 180° pulse or ***D7*** after the 180° pulse is incremented proportionally to the t_1 period a split-t_1 experiment as described in chapters 16 and 17 for some MQMAS experiments will be performed.

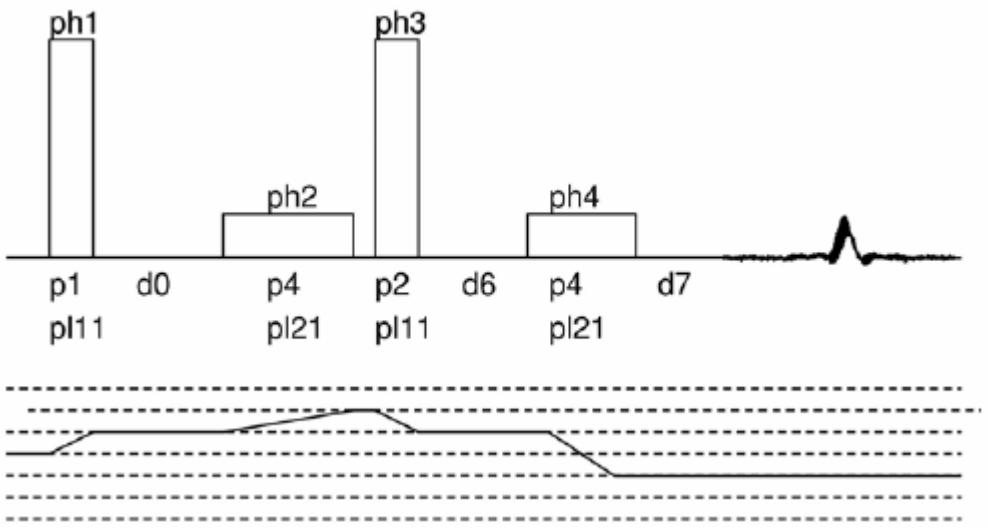

Figure 19.3. Four pulse sequence and coherence transfer pathway

*Four pulse sequence and coherence transfer pathway for the double quantum filtered STMAS experiment with shifted echo acquisition (stmasdqfe.av). Pulses **p1** and **P2** are non-selective pulses. Corresponding power level **PL11** should be set to achieve around 100 kHz RF field amplitude. **P3** and **P4** are CT selective pulse 90° and 180° pulses of about 20 and 40 µs, respectively, corresponding to an RF field amplitude of a few kHz. Delay **D0** is the incremented delay for t_1 evolution, **D6** and **D7** can be incremented proportional to **D0** depending on the spin of the observed nucleus. Phase lists are as follows, incrementation of the phase of the first pulse is not required because a phase modulated data set is acquired with FnMODE being QF:*

ph1 = 0 180 90 270

ph2 = 0*4 90*4 180*4 270*4

ph3 = 0*16 90*16 180*16 270*16

ph4 = 0

receiver = ph3-ph1-ph2

Experiment Setup 19.3

Before the 2D experiment on your sample of interest can be started some setup steps must be done as described in detail below. All setup steps should be done on a sample with:

- A known MAS spectrum,
- With sufficiently good sensitivity to facilitate the set-up, and,
- A 2nd order quadrupole interaction of the order of the one expected for your sample of interest.

In a first step, a low power selective pulse must be calibrated in a single pulse experiment. After this the STMAS experiment can be optimized using the 2D pulse sequence for the first t_1 increment.

Setting Up the Experiment 19.3.1

Sample: There are a large number of crystalline compounds that can be used to set-up the experiment. Please refer to ***Table 19.2.*** to select a suitable sample. For the general procedure described here the spin I of the nucleus is not important, of course the obtained pulse widths will depend on the spin I, and the Larmor frequency. For the STMAS experiment, in contrast to MQMAS, it is advisable to use a well-known sample for the setup because the accuracy of the magic angle setting is extremely critical.

Table 19.2. Some Useful Samples for Some Nuclei with Half Integer Spin

Nucleus	Spin	Spectrometer frequency*1)	d1 [s]*3)	Sample	Comments
^{17}O	5/2	67.78	2	$NaPO_3$	> 10% enriched
^{11}B	3/2	160.42	>5	H_3BO_3	
^{23}Na	3/2	132.29	10	Na_2HPO_4 *2)	
^{27}Al	5/2	130.32	5	YAG	
^{87}Rb	3/2	163.61	0.5	$RbNO_3$	
^{93}Nb	9/2	122.25	1	$LiNbO_3$	

*1) In MHz at 11.7 T (i.e. 500.13 MHz proton frequency).

*2) Alternatively $Na_2HPO_4 * 2H_2O$ can be used. For anhydrous Na_2HPO_4 the sample should be dried at 70° C for a couple of hours before packing the rotor in order to eliminate crystal water completely.

*3) Recycle delays at 11.7 T, longer delays may be required at higher fields.

As for MQMAS the setup must be done in two steps; in the first step a central transition selective pulse that merely excites the central transition must be calibrated. This pulse must be weak enough so that only the central transition is affected and it must be short enough so that the central transitions of all sites in the spectral range are excited. These conditions are typically fulfilled by a 20 µs pulse. For the calibration of this pulse a power level around 30 dB with 500 W and 1 kW amplifiers and around 20 dB with 300 W amplifiers should be expected. The pulse program *zg* (which uses ***p1*** and ***pl1***) or *zgsel.av* (which uses ***P3*** and ***PL21***) can be used. For more details please refer to chapter 16.

Once the central transition selective 90° pulse is calibrated the STMAS pulse program can be loaded. Available pulse programs are *stmasdqfz.av* and *stmasdqfe.av*. Both are double quantum filtered 4-pulse sequences, the first with a z-filter, the second with a shifted echo. If this second sequence is to be used a proper setting of the timing for the shifted echo is required, to allow collection of the full echo signal. This is explained in chapter 17, where a shifted echo can be used in DFS enhanced MQMAS experiments.

In ***Table 19.3.*** and ***Table 19.4.*** the starting parameters for the setup of the two sequences are given. Typical values for the pulses are entered so one should see some signal for further optimization. Parameters like ***O1***, ***TD***, ***SWH***, ***RG***, should already be set in the standard 1D spectrum. Since the experiment is not as dependent on the pulse lengths or the applied RF field amplitude as MQMAS, pulse lengths between 1 and 2 µs, which can be achieved with every probe with 4mm or smaller rotor diameter, are sufficient.

Table 19.3. Initial Parameters for the Set-up of stmasdfqz.av.

Parameter	Value	Comments
pulprog	stmasdqfz.av	Pulse program.
NS	16*n	For set-up the full phase cycle is not so critical.
D0	see text	Calculated in pulse program.
D1	5 * T_1	Recycle delay, use dummy scans if shorter.
D4	20 µs	Z-filter delay.
P1	1.5 µs	Excitation pulse at pl11.
P2	1.5 µs	Conversion pulse at pl11.
P3	20 µs	90° selective pulse at pl21 taken from previous pulse calibration.
PL1	=120 dB	Not used
PL11	start with ≈ 150 to 300 W	Power level for excitation and conversion pulses.
PL21		Power level for selective pulse, approx. pl11+30 dB taken from previous pulse calibration.

For ***PL11*** an initial value that corresponds to 150 to 300 W can be used. Optimization will be done on the first increment of the 2D sequence, which is calculated within the pulse program according to „D0=(1s***L0***/***CNST31***)-***P1***/2-***P4***-0.3µ-***P2***/2“,

because it is essential that the centres of the pulses ***P1*** and ***P2*** are exactly an integer number of rotor periods apart. In this formula ***P1***, ***P2***, and ***P4*** are the RF pulses as listed in table 2, ***CNST31*** must be set equal to the spinning frequency. This means that the first increment can last between 100 µs (10 kHz spinning) and 28.5 µs (35 kHz spinning). Since ***P4*** is the 180° selective pulse, which can be as long as 40 µs, ***L0*** must be set large enough to avoid the situation where the calculated *d0* is negative. Optimization of the pulses ***P1*** and ***P2*** can be done using ***popt*** in full analogy to the optimization of the pulses in MQMAS.

Table 19.4. Initial Parameters for the Set-up of stmasdfqe.av.

Parameter	Value	Comments
pulprog	stmasdqfe.av	Pulse program.
NS	16*n	For set-up the full phase cycle is not so critical.
D0	See text	Calculated in pulse program.
D1	5 * T_1	Recycle delay, use dummy scans if shorter.
D6	See text	
D7	See text	
P1	1.5 µs	Excitation pulse at pl11.
P2	1.5 µs	Conversion pulse at pl11.
P3	20 µs	90° selective pulse at pl21 taken from previous pulse calibration.
PL1	=120 dB	Not used.
PL11	Start with ≈ 150 to 300 W	Power level for excitation and conversion pulses.
PL21		Power level for selective pulse, approx. pl11+30 dB taken from previous pulse calibration.

Two Dimensional Data Acquisition *19.3.2*

Once the pulses are calibrated the 2D data acquisition can be used to find the correct and precise magic angle setting. Create a new data set and change *parmode* to 2D. The acquisition parameters for the (new) indirect F1 dimension must be set according to ***Table 19.5.***.

Similar considerations for the maximum t_1 period, determined by the number of FID's to be acquired and the t_1 increment, can be made as for MQMAS. Because the shift range in ppm is twice a big as in 3QMAS a larger increment can be used to give an equivalent shift range, the increment being calculated from the spinning speed. Since the magic angle is probably not yet perfect 32 to 64 FID's will be sufficient initially. Processing parameters are described in the next section.

Table 19.5. F1 Parameters for the 2D Data Acquisition.

Parameter	Value	Comments
F1 parameters:		In *eda.*
FnMode	States TPPI, or States QF	2D acquisition mode for stmasdqfz.av. 2D acquisition mode for stmasdqfe.av.
TD	see text	Number of FID's to be acquired.
SWH	"masr"	Equals spinning frequency for rotor synchronization, from this IN0 is calculated correctly, if ND_010 is already set.
NUC1		Select the same nucleus as for F2 so that transmitter frequency offset is correctly set (important for referencing).
Pulse program parameters:		In *ased.*
D6	0	Used in stmasdqfe.av only.
IN6	=IN0*8/9	Used in stmasdqfe.av for I = 3/2.
D7	0	Used in stmasdqfe.av only.
IN7	=IN0*7/24 =IN0*28/45 =IN0*72/55	Used in *stmasdqfe.av* for I = 5/2. Used for I = 7/2. Used for I = 9/2.

In ***Figure 19.4.*** two 2D plots of the ^{87}Rb STMAS experiment on $RbNO_3$ are compared. The spectrum on the left was obtained after the first execution of the experiment. The spectrum on the right was obtained after several iterations of resetting the angle and rerunning the spectrum. From this it is obvious that the spectrum of the sample for the setup must be known because otherwise it is impossible to judge whether a shoulder or a splitting is due to an incorrectly set angle or another signal from another site in the sample.

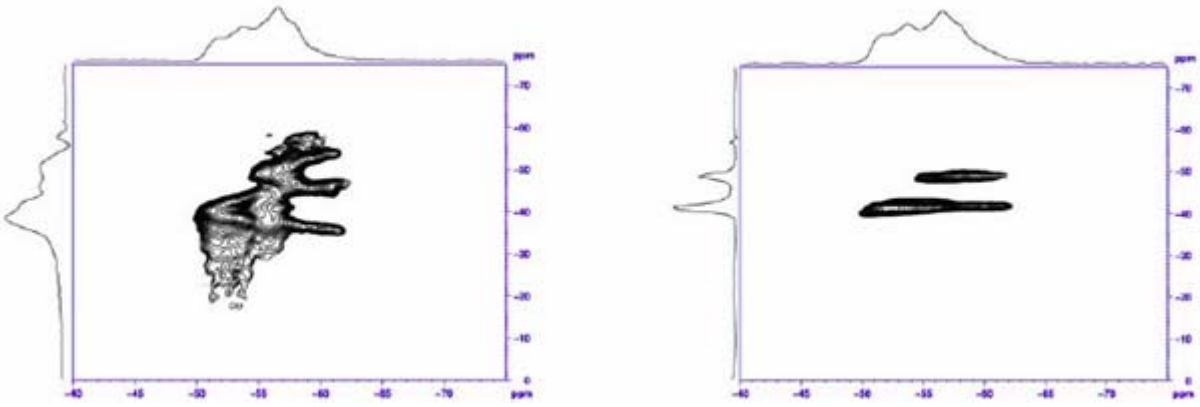

Figure 19.4. 87Rb STMAS Spectra of RbNO3

While the left spectrum has been obtained after adjusting the magic angle with KBr, the right spectrum can be obtained after several iterations of readjusting the angle and rerunning the 2Dspectrum.

Data Processing 19.4

Processing parameters should be set according to the table below:

Table 19.6. Processing Parameters for the 2DFT

Parameter	Value	Comments
F2 (acquisition dimension)		
SI		Usually set to one times zero filling.
WDW	No	Don't use window function.
PH_mod	Pk	Apply phase correction.
BC_mod	No	No DC correction is required after full phase cycle.
ABSF1	1000 ppm	Should be outside the observed spectral width.
ABSF2	-1000 ppm	Should be outside the observed spectral width.
STSR	0	Avoid strip FT.
STSI	0	Avoid strip FT.
TDoff	0	Avoid left shifts or right shifts before FT.
F1 (indirect dimension)		
SI	256	Sufficient in most cases.
WDW	no	Don't use window function, unless F1 FID is truncated.
PH_mod	pk	Apply phase correction.
BC_mod	no	No DC correction is required after full phase cycle.
ABSF1	1000	Should be outside the observed spectral width.
ABSF2	-1000	Should be outside the observed spectral width.
STSR	0	Avoid strip FT.
STSI	0	Avoid strip FT.
TDoff	0	Avoid left shifts or right shifts before FT.

Data obtained with *stmasdqfe.av* can be processed with ***xfb*** only, if ***IN6*** or ***IN7*** have been set appropriately to run a split-t_1 experiment. Data acquired with the pulse program *stmasdqfz.av* should be processed with the AU program ***xfshear***. For information about this program please refer to chapter 16. In an analogous way to MQMAS spectra the apparent Larmor frequency in the indirect dimension is recalculated by multiplying the real Larmor frequency with the corresponding value of $|R\text{-}p|$. The values for the different spin quantum numbers are summarized in ***Table 19.7.***, for experiments using the inner ST (± 3/2 ↔ ± 1/2). R determines the shearing ratio, i.e. the slope in a non-sheared spectrum, $|R\text{-}p|$ is the scaling factor for referencing in the indirect dimension. Using this procedure the shift positions in the indirect dimension are identical (in ppm) to all MQMAS experiments, and the information obtained is the same.

Refer to the chapter ***"Basic MQ-MAS" on page 213*** for details about the information obtained from such spectra.

Table 19.7. Values of R and |R-p| for the Various Spin Quantum Numbers Obtained in the STMAS Experiment

Spin I	R	|R-p| (p = ± 1)
3/2	-8/9	1.889
5/2	7/24	0.70833
7/2	28/45	0.3777
9/2	55/72	0.263111

Double-CP 20

Double Cross Polarization (DCP) experiments use two consecutive cross polarization steps. Usually, the first step transfers from protons to one type of X-nucleus (to achieve high sensitivity), the second step transfers to a different (Y) nucleus in order to probe the dipolar coupling between X and Y. The sequence of transfers is in principle arbitrary, but usually sensitivity is an issue, so transfer from protons (to generate a large magnetization) and detection on the nucleus of higher sensitivity (to gain signal intensity) is the standard procedure. Detection of the most sensitive nucleus, protons, is also possible, but is difficult if the homonuclear proton-proton dipolar coupling is strong (see ***"CRAMPS: General" on page 271***).

In this chapter, the most popular double CP experiment is described. Here, the first CP step transfers magnetization from protons to ^{15}N. Then, in a second cross polarization step, magnetization is transferred from ^{15}N to ^{13}C; the signal is finally detected on ^{13}C under suitable proton decoupling. The purpose of this experiment is to gain information about the C-N dipolar coupling which in turn provides special information.

Naturally, the C-N-, or in general, the X-Y dipolar coupling is much smaller than any dipolar coupling involving protons. For C-N, it is <2.5 kHz. This has some experimental consequences:

1. There is no need to decouple ^{15}N while observing ^{13}C, since the coupling is spun out already at moderate spin rates.
2. The Hartmann-Hahn condition for this cross polarization is extremely sharp and must be adjusted very carefully for every spin rate.
3. The magnetization transfer is substantially slower than from protons, meaning that contact times are usually longer.
4. The transfer occurs (unlike CP from protons) not out of a bath of abundant spins, but behaves (especially at high spin rates) more like a transfer between spin pairs.
5. Labeled samples must be used so that an observable number of coupled spins is present.

Advanced experimental schemes use tangential pulses to provide adiabatic conditions during the cross polarization (S. Hediger et al.) or provide only selective polarization transfer, Specific CP (Baldus et al.).

References:

1. J. Schaefer, T.A. Skokut, E.O. Stejskal R.A. McKay, and J.E. Varner, Proc. Nat. Acad. Sci. USA **78**, 5978 (1981).
2. J. Schaefer, E.O. Stejskal, J.R. Garbow, and R.A. McKay, Quantitative Determination of the Concentrations of ^{13}C-^{15}N Chemical Bonds by Double Cross-Polarization NMR, J. Magn. Reson.59,150-156 (1984).
3. M. Baldus, A.T. Petkova, J. Herzfeld, and R.G. Griffin, Cross Polarization in the tilted frame: assignment and spectral simplification in heteronuclear spin systems. Mol. Physics 5, 1197-1207 (1998).

Pulse Sequence Diagram, Double CP (DCP) 20.1

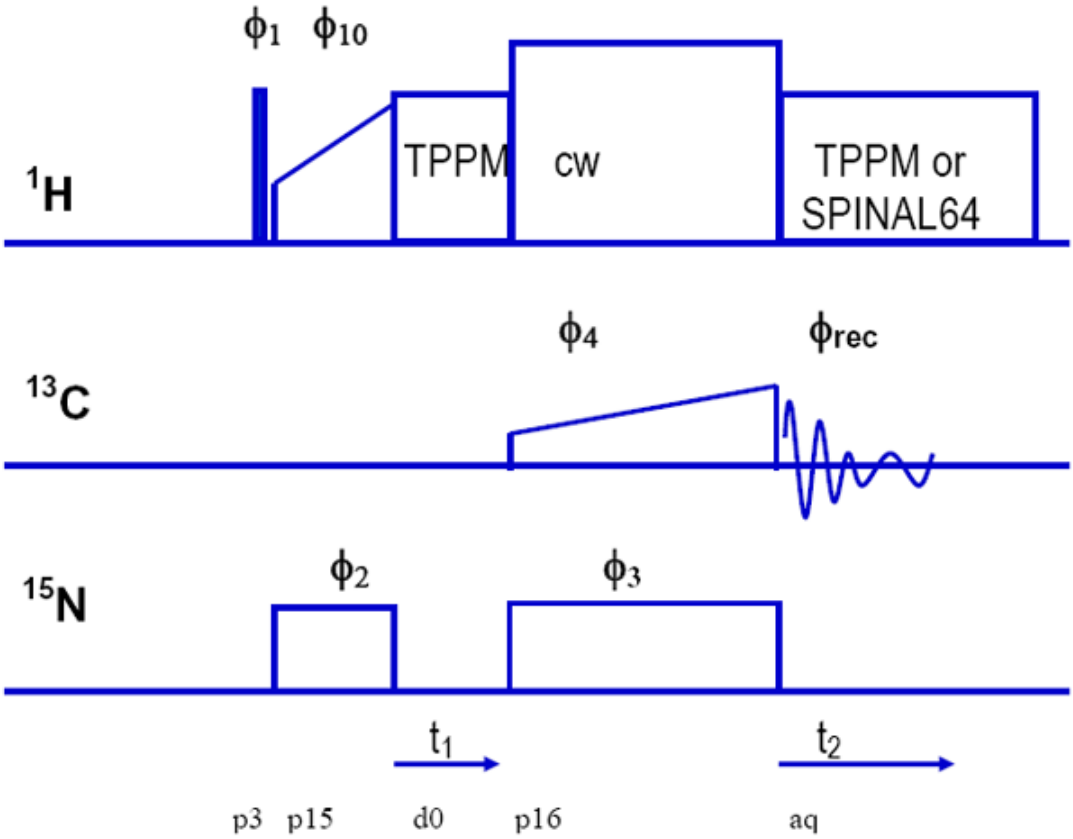

ϕ_1= 1, 3	ϕ_2= 0 + States-TPPI (t_1)	ϕ_4= 0 0 0 0 1 1 1 1 2 2 2 2 3 3 3 3	ϕ_{rec}=0 2 2 0 3 1 1 3 2 0 0 2 1 3 3 1
	ϕ_3= 0 0 0 0 2 2 2 2		

Figure 20.1. Pulse sequence diagram for 1D (t_1=0) and 2D double CP experiments.

Double CP Experiment Setup 20.2

Double CP 2D Experiment Setup 20.2.1

1. Prepare your probe for triple resonance applications H/C/N
2. Load a sample of glycine, ^{15}N and C_1,-C_2 (or only C_2-) ^{13}C labelled. Make sure the sample is α-glycine, you will get nowhere with γ-glycine, since the proton $T_{1\rho}$ is very short and CP just does not work with high efficiency. Rotate at 11 kHz. The sample may be fully labelled or diluted with natural abundance glycine. A restricted volume rotor is preferred. If a different spin rate is used, a different shape must be generated for the second CP step.

3. Check the ***edasp*** routing and set up 3 RF channels for C, H and N, such that the lower power amplifier (500W or less) is used for ^{13}C. (^{15}N may require more than 500W). Set for ^{13}C observation.

4. Make sure the preamplifiers in use are set up for the appropriate frequencies. The following external RF filters are required: proton bandpass, ^{13}C bandpass, and ^{15}N low pass. The channel isolation required between X and Y (here ^{13}C and ^{15}N) is usually sufficient with a bandpass on one of the channels, but a filter to remove the proton decoupling RF interference is required for X and Y. This means that one of the band pass filters on X or Y may be replaced by a proton reject, X low pass filter. If the channel isolation between X and Y is not adequate, the probe cannot be tuned.

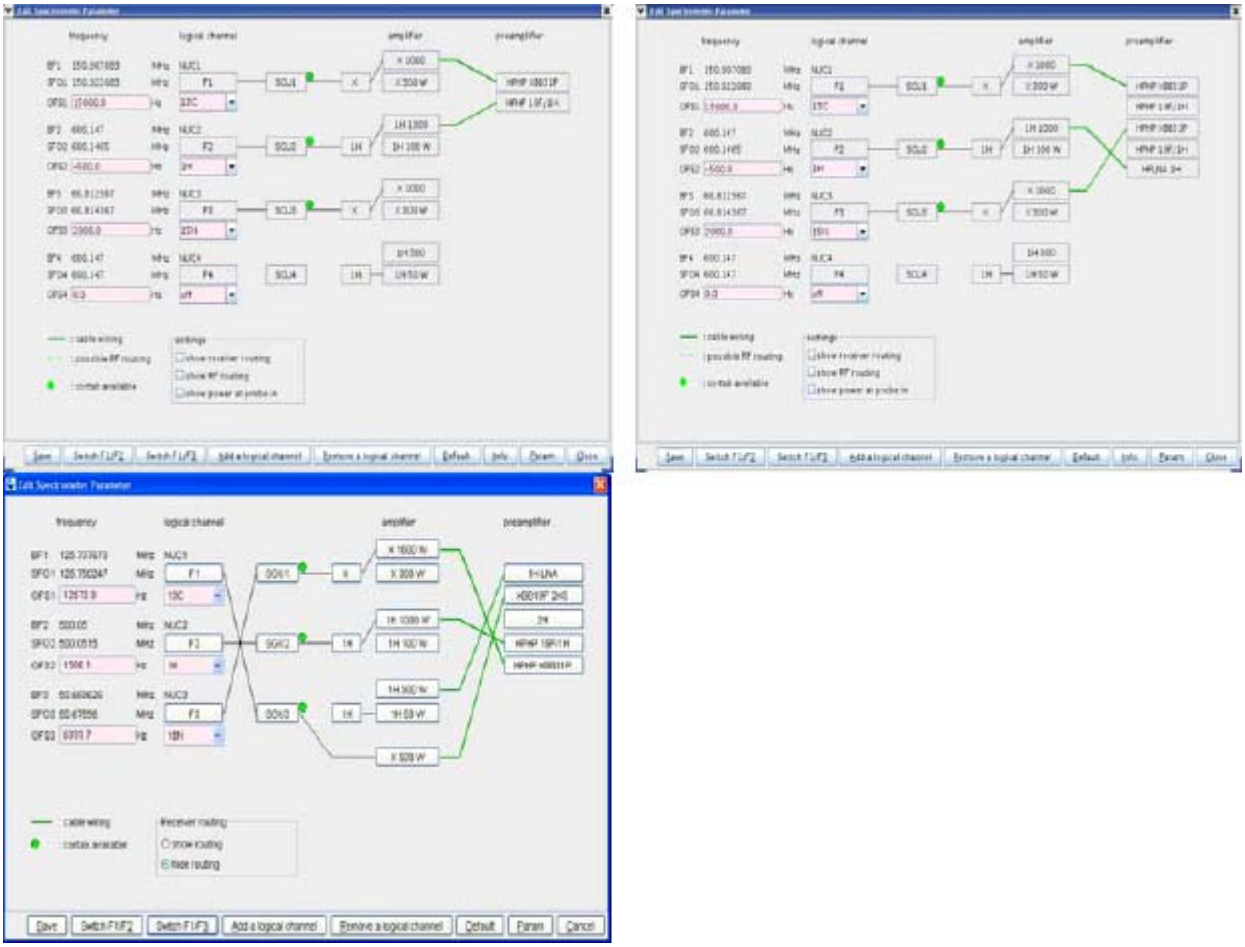

Figure 20.2. The edasp routing tables for H-C-N double CP.

Three examples are shown: Setup with only one X-HP-preamplifier (must be recabled for ^{13}C and ^{15}N setup), setup with 2 X-BB HP-preamplifiers and 2 HP transmitter, and setup with one HP transmitter and one 500W transmitter. The higher frequency nucleus is set for the lower power amplifier.

5. Set up for standard ^{13}C CP operation in triple mode. Remember that a double tuned probe has better signal to noise and requires less power on X than a triple probe.

6. Optimize decoupling and CP condition, run a reference ^{13}C CP/MAS spectrum of the labelled glycine sample, using 16 scans. This reference spectrum will serve to measure the efficiency of the DCP magnetization transfer.
7. To set up the conditions for the N to C transfer, one must define the RF field at which the transfer is to take place, and find the appropriate power levels to achieve these RF fields. In order to minimize losses due to insufficient excitation bandwidths and $T_{1\rho}$ relaxation, the contact should be executed at high power. However, there are limitations in terms of what the probe can take, and there are losses due to unwanted HH contact to the proton spin system. On the other hand, in many samples (bio-samples) the spread of chemical shifts that one wants to cover is not extremely wide or one even wants to execute the transfer selectively ("Specific-CP"). An RF field of 35 kHz is a decent compromise. So, using the ***cp90*** pulse program, and moving the carrier close to the C_α-peak, determine a power level ***pl11*** which corresponds to 35 kHz RF (7.14 µsec 90 ° pulse). However, since the sample spins at 11 kHz, the HH condition will require 46 or 24 kHz on one nucleus and 35 kHz on the other nucleus. If you decide to account for the spin rate on the ^{13}C side, calculate the required power levels for 24 and 46 kHz (= 35 kHz RF field +/- 11 kHz spin rate) RF field using ***xau calcpowlev***. Now the ^{13}C channel is set.

^{15}N Channel Setup *20.2.2*

8. Create a new experiment using edc.
9. Setup the proper routing by going into ***edasp***. Click the switch F1/F3 button to get ^{15}N on channel 1.

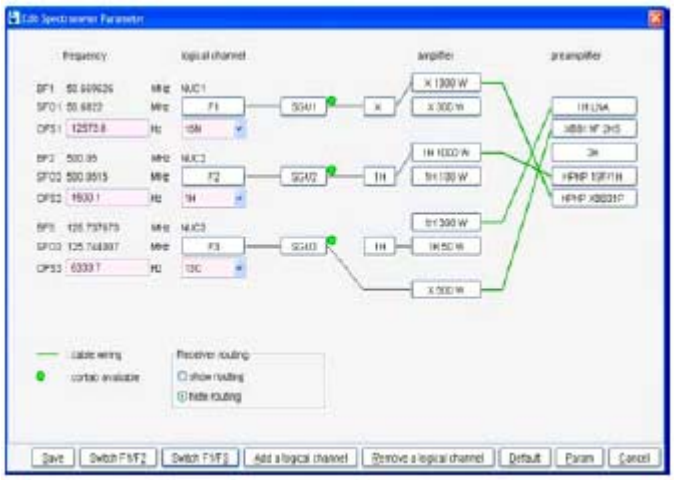

Figure 20.3. Routing table for triple resonance setup change for ^{15}N pulse parameter measurement and CPMAS optimization.

10. If available, set ***pl1*** and ***sp0*** for a proton/^{15}N HH condition in triple mode. On a labelled sample, even the previous settings for ^{13}C should give a signal which allows optimizing the HH condition.
11. When the HH condition is optimized, find the power level to achieve a 35 kHz RF field (7.14 µsec 90 ° pulse, carrier close to the ^{15}N-resonance). It is essential to optimize the first proton to nitrogen HH contact. This is not as trivial as

one might think, since the transfer efficiency depends strongly on the timing and RF fields of the HH match. The proton $T_{1\rho}$ of the glycine NH_2 protons (from which the nitrogen is polarized) is fairly short, so the polarization transfer is not efficient. On a fully labelled sample, a maximum enhancement factor of 8.3 is possible (5 protons transfer to one nitrogen). Comparing the cross polarized ^{15}N spectrum to the directly observed spectrum (using ***hpdec*** and 90 degree pulses at 4 sec repetition) one can measure the enhancement factor rather easily. Without optimization, the enhancement factor may be as low a 5fold. It should be at least 6.5fold, more than 7.5fold is hard to achieve. To achieve a good result, the HH RF-fields should be set as high as possible with a contact time of 4 msec (higher proton RF fields yield a longer proton T1ρ and allow longer contact times). Of course, the RF field is limited by transmitter power and probe breakthrough limits. Note the optimum power levels (***sp0*** and ***pl1***) and contact time (***p15***).

Setup of the Double CP Experiment *20.2.3*

1. Read the reference carbon data set and generate a new data set using ***edc*** or ***iexpno***.
2. Select the pulse program doubcp. Set the optimum ^{15}N cp parameters as found in the previous step (set ***sp0***, ***p15*** and ***pl3*** for proton to ^{15}N cp). Set ***o3*** close to the ^{15}N peak position.
3. Now we have to select the appropriate parameters for the nitrogen to carbon magnetization transfer. In the standard ***doubcp*** pulse program, ***p16*** is used as the second contact time, and the shapes ***sp1*** and a square pulse at ***pl5*** are specified for the ^{13}C and ^{15}N contact, so ***p16***, ***sp1*** (^{13}C power level) and ***pl5*** (^{15}N power level) are the relevant parameters. The C-N contact consists of a square pulse on one channel and a ramp or adiabatic shape on the other channel. Using a square pulse on the ^{15}N channel is preferred, but the sequence can be rewritten to use a ^{13}C square pulse and have the shape on the ^{15}N channel.

Table 20.1. Recommended Parameters for the DCP Setup

Parameter	Value	Comments
Pulse program	doubcp	AVIII, Topspin 2.1 only, else use doubcp, doubcp.av
nuc1	^{13}C	Nucleus on f1 channel
o1p	100 ppm	^{13}C offset
nuc2	^{1}H	Nucleus on f2 channel
o2p	2-4 ppm	^{1}H offset, optimize
nuc3	^{15}N	Nucleus on f3 channel
o3p	≈35 glycine ≈120 histidine ≈65 -130 protein	^{15}N offset depending on sample
sp1		Power level for f1 channel, NC contact pulse
pl3		Power level for ^{15}N channel HN contact
pl5		Power level for ^{15}N channel, NC contact pulse
pl12		Power level decoupling f2 channel and excitation
pl13		power level during second contact, cw dec.
cnst24		offset for cw decoupling during p16
p3		Excitation pulse f2 channel
pcpd2		Decoupler pulse length f2 channel (^{1}H) TPPM
p15	3-5 msec	Contact pulse – first contact
p16	5-12 msec	Contact pulse – second contact f1 – f3 channel
d1	5-10s histidine 4s α-glycine	Recycle delay
spnam0		Ramp for 1st CP step; e.g. ramp: 80 – 100%
sp0		Power level for Ramp HN contact pulse 1H
spnam1	ramp45-55, tcn5500, or square.100	ramp, tangential contact pulse ***tcn5500*** on C, or square
spnam2	square.100 or ramp45-55, tcn5500	square on N, or ramp/tangential pulse
cpdprg2	SPINAL64	SPINAL64 decoupling
ns	2, 4, or 16	Number of scans

4. Now we select the shape to use for the C-N contact. To find the HH contact more rapidly (it is a very narrow condition) it is recommended to start with a ramp shape. In order to find a HH condition independent of the type of shape, it is recommended to select shapes which are all centred around 50% amplitude, which allows arbitrary amplitude modulation without changing the HH condition. For a start, generate a ramp shape from 45 to 55% with 100 slices, using shape tool (***stdisp***). Store the ramp as ramp4555.100. Select this ramp as ***spnam1***.

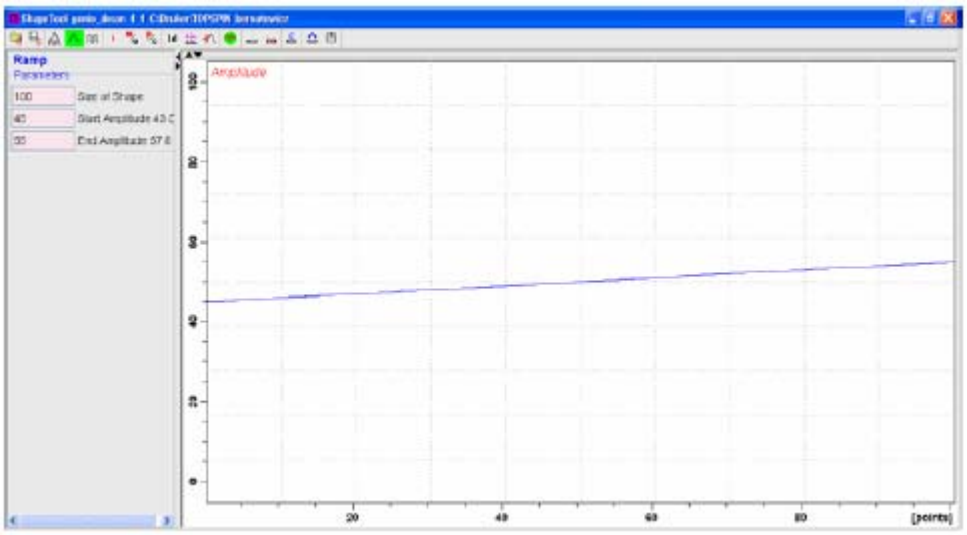

Figure 20.4. Shape Tool display with ramp shape from 45 to 55%.

The amplitude factor is 50%, corresponding to 50% RF field or a power level change of 6 dB, since the amplitude corresponds directly to the pulse voltage.

5. Since the shape is centred around 50%, the RF voltage here is down by a factor of 2 (= 6 dB in voltage), the power must be increased by 6 dB to get the same RF field as with a 100% square pulse.
6. Usually, the ramp shape is set on ^{13}C (but it can also be used on ^{15}N). Set ***pl5*** to 46 or 24 kHz RF field on ^{15}N. Set ***spnam1*** to ***ramp4555.100,sp1*** to 35 kHz RF field on ^{13}C - 6 dB. Set ***pl13=pl12*** for a start, set ***p16*** to 5 msec. Optimise the power level ***pl5***. A variation over -1 to +1 dB in steps of 0.2 dB should be ample. In order to be sure, one can optimise ***sp1*** and ***pl5*** as an array, ***sp1*** in steps of 0.5 dB, ***pl5*** in steps of 0.2 dB. Use a full phase cycle to avoid signal from a direct proton to carbon transfer (which is cancelled by the phase cycle). Optimise ***p16*** between 5 and 15 msec. See **fig. 6** for an optimization of ***pl5*** (^{15}N square pulse power).
7. With a ramp shape for the N-C transfer, one should get 40-50% DCP efficiency (***Figure 20.7.***), compared to the reference direct ^{13}C CP spectrum. If this cannot be achieved, even with careful HH matching, the following parameters should be checked:
8. Re-optimize ***p16,*** the optimum should be > 10 msec. If the signal gets worse with longer contact time, there is a loss due to direct ^{13}C-^{1}H contact. Minimise this loss in the following way:

9. Never use a pulsed proton decoupling schemes during ***p16***. Frequency shifted Lee-Goldburg decoupling is no alternative, since the signal will broaden and decay with shorter T_2. Use cw decoupling during ***p16***, and carefully optimize the decoupling power (***pl13***) for maximum signal. A slight offset may be set using ***cnst24***.

10. Instead of a 45-55% ramp, a tangential amplitude modulation shape can be used. Since this shape provides 100% transfer efficiency on a spin pair system (compared to 50% of a standard rectangle or ramp shape), the DCP efficiency can be increased. With such a shape, one can get 50-70% DCP efficiency. To generate such a shape in ***stdisp***, select TanAmpMod as a shape model, select solids notation, select 1000 points, set the spin rate to half the actual spin rate (5500), set the RF field to the actual RF field used on this channel, select 400 for the dipolar coupling, and 50% for the scaling factor. Save the shape as tcn5500 (if not already available), and select this name for ***spnam1***. The efficiency should be noticeably better. Reoptimise the first HH contact, decoupling and ***p16***. More than 50% should definitely be obtained.

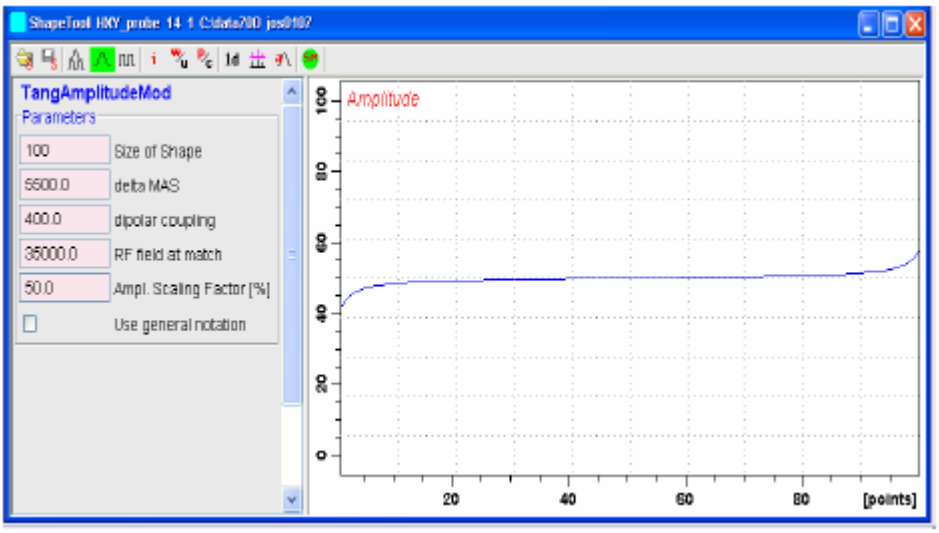

Figure 20.5. Shape Tool display with a tangential shape for adiabatic cross polarization.

The amplitude factor is 50%, corresponding to 50% RF field or a power level change of +6 dB (4 fold power in TopSpin 3.0 and later), since the amplitude corresponds directly to pulse voltage.

11. Optimize the DCP condition on the rectangular pulse, using 0.1 dB steps over a range of +/-1 dB around the optimum found with the ramp.

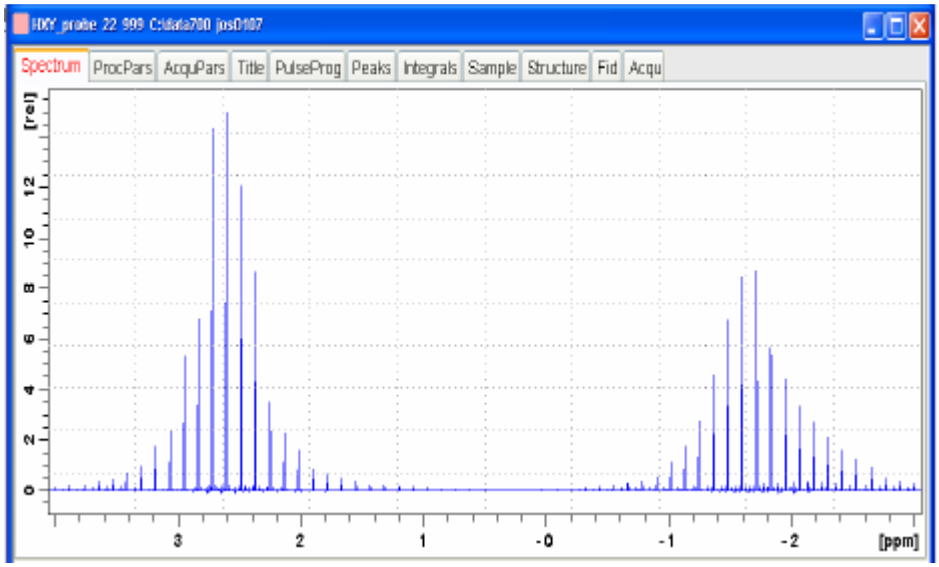

Figure 20.6. Double CP optimization of PL5 in increments of 0.1 dB.

Note how narrow the optimum DCP conditions are. However, with diligent preparation, one should be very close to the optimum with the first try.

12. Run an experiment with 16 scans and compare the signal amplitude with the signal intensity of the ^{13}C CPMAS experiment with the same number of scans, using dual display. The intensity ratio of the aliphatic resonance of the CPMAS compared to the one obtained with the DCP experiment gives the DCP yield, see ***Figure 20.7.***.

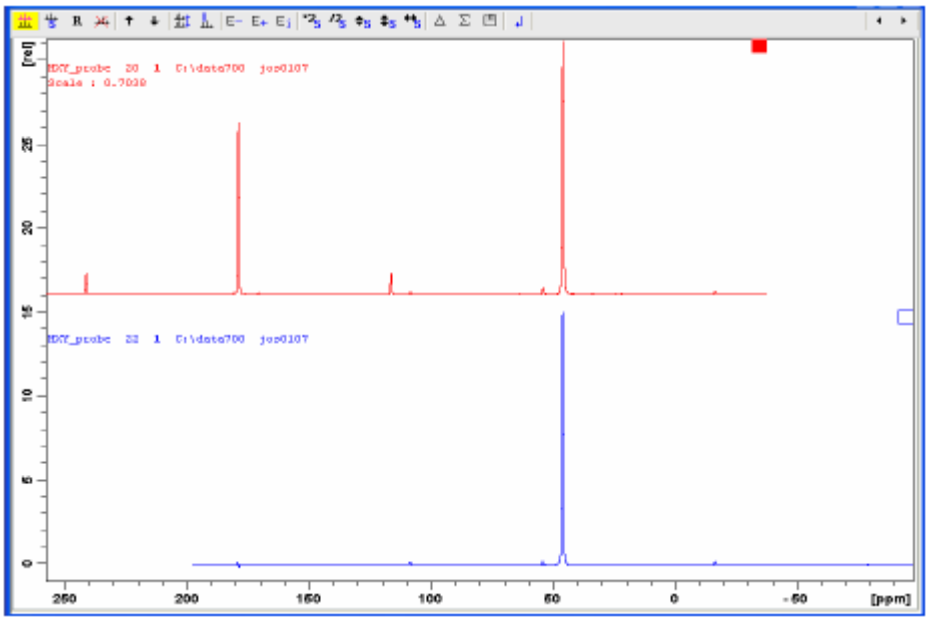

Figure 20.7. Double CP yield, measured by comparing CPMAS and DCP amplitudes of the high field resonance.

Note that the C_1 carbon receives very little magnetization under these conditions, the transfer is rather selective.

The setup for DCP can be rather much sped up and simplified by a python program named dcpset.py. This program will ask for the 90° pulse widths and associated power levels and for the spin rate and calculate the appropriate power levels for the HH condition for all pulses except for the proton channel.

Contact solids@bruker.de to receive this python program and some instructions for use. This program serves as an example on how the experiment setup can be controlled by the high level script language.

Setup of the 2D Double CP Experiment *20.2.4*

1. Load a suitable sample, spin it up, set the desired temperature and match and tune the probe. As a simple setup sample, full ^{13}C, ^{15}N-histidine may be used (***d1***=10s, 2-4 scans, ***p15***=1msec, ***p16***=3msec).A labeled oligopeptide or small protein will of course provide a more interesting spectrum. With proteins, good results should only be expected if the preparation is micro-crystalline. In such a case, water, salt and cryo-protectant (glycol, glycerol) will very likely be present. This means that the probe proton channel will be detuned to lower frequency, and tuning may be difficult, if not impossible at high proton frequencies and salt contents. In such cases, E^{free} probes are recommended.
2. Run standard 1D cp ^{13}C and ^{15}N experiments; determine the required offsets for all frequencies and the required sampling windows.
3. Re-optimize the H-N and N-C HH conditions.
4. Generate a new data set and switch to 2D data mode, using the “123”-icon in ***eda***.
5. In ***eda***, set the pulse program to ***doubcp***. Set FnMode as desired, usually STATES-TPPI.
6. Make sure the correct nucleus (^{15}N) is selected in the F1 dimension.
7. Set the sampling windows for both dimensions from the previously acquired 1D spectra.
8. Both acquisition times in F2 and F1 should be considered with care, since the decoupler is on at high power during both periods. Especially for biological samples, where the RF heating may be high and the samples are temperature sensitive, it is essential not to use overly long acquisition times and high duty cycles. Remember that the heating effect is generated inside the sample where the temperature increases within milliseconds, whereas cooling requires transfer of the energy to the outside of the spinner, which takes seconds! E^{free} probes eliminate these problems to a large extent.
9. The basic double-CP experiment can be extended into many different variations. One example is the double transfer N-C_α-C_β, where the second transfer step is made selective so only α-carbons are polarized from the nitrogen, then magnetization is transferred from the α-carbons to the adjacent β-carbons. This can be done by a simple PDSD or DARR proton spin diffusion step, or by a ^{13}C-^{13}C homonuclear recoupling step (HORROR, DREAM, or other). Likewise, the N-C_α-C_x experiment transfers from the α-carbons to all (X) carbons which are in close enough proximity to the α-carbons. Check with your applications support for appropriate pulse programs.

Sample: ^{15}N, ^{13C}-labeled histidine, peptide or protein.

Spinning speed: 10 – 15 kHz, depending on ^{13}C spectral parameters (rotational resonance must be avoided)

Experiment time: 30 min. – several hours

Acquisition Parameters:

Table 20.2. Recommended Parameters for the DCP 2D Setup

Parameter	Value	Comments
Pulse program	doubcp	Pulse program
nuc1	^{13}C	Nucleus on f1 channel
o1p	100 ppm	^{13}C offset
nuc2	^{1}H	Nucleus on f2 channel
o2p	2-4 ppm	^{1}H offset, optimize
nuc3	^{15}N	Nucleus on f3 channel
o3p	65 – 150 ppm	^{15}N offset depending on sample
pl1		Power level for f1 channel, NC contact pulse
pl3		Power level for ^{15}N channel HN contact
pl5		Power level for ^{15}N channel, NC contact pulse
pl12		Power level decoupling f2 channel and excitation
p3		Excitation pulse f2 channel
pcpd2		Decoupler pulse length f2 channel (^{1}H) TPPM
p15	1-5 msec	First contact, optimize on ^{15}N cp spectrum
p16	3-10 msec	Second contact f1 – f3 channel, optimize on 1D dcp spectrum
d1	5-10 s for histidine	Recycle delay, optimize on 1d
spnam0		Ramp for 1st CP step; e.g. ramp: 80 – 100%
sp0		Power level for Ramp HN contact pulse 1H
spnam1	tcn5500	Tangential or ramp contact pulse
spnam2	square.100	Shape on ^{15}N channel
cpdprg2	SPINAL64	SPINAL64 decoupling
ns	2 or 16	Number of scans
F2 direct ^{13}C		(left column)
td	2k	Number of complex points

Table 20.2. Recommended Parameters for the DCP 2D Setup

sw	≈200 ppm	Sweep width direct dimension, adjust to experimental requirements
F1 indirect ^{15}N		(right column)
td	128-.512	Number of real points
sw	≈100-150 ppm	Sweep width indirect dimension

Spectral Processing *20.4*

Processing parameters

Table 20.3. Recommended Processing Parameters for the DCP 2D

Parameter	Value	Comment
F1 acquisition ^{13}C		(left column)
si	2-4k	FT-size
wdw	QSINE	Squared sine bell
ssb	2-5	Shifted square sine bell, >2: res. enhancement
ph_mod	pk	Phase correction if needed
F2 indirect ^{15}N		(right column)
si	512-1024	Zero fill
mc2	STATES-TPPI	
wdw	QSINE	Squared sine bell
ssb	2-5	

Example Spectra 20.5

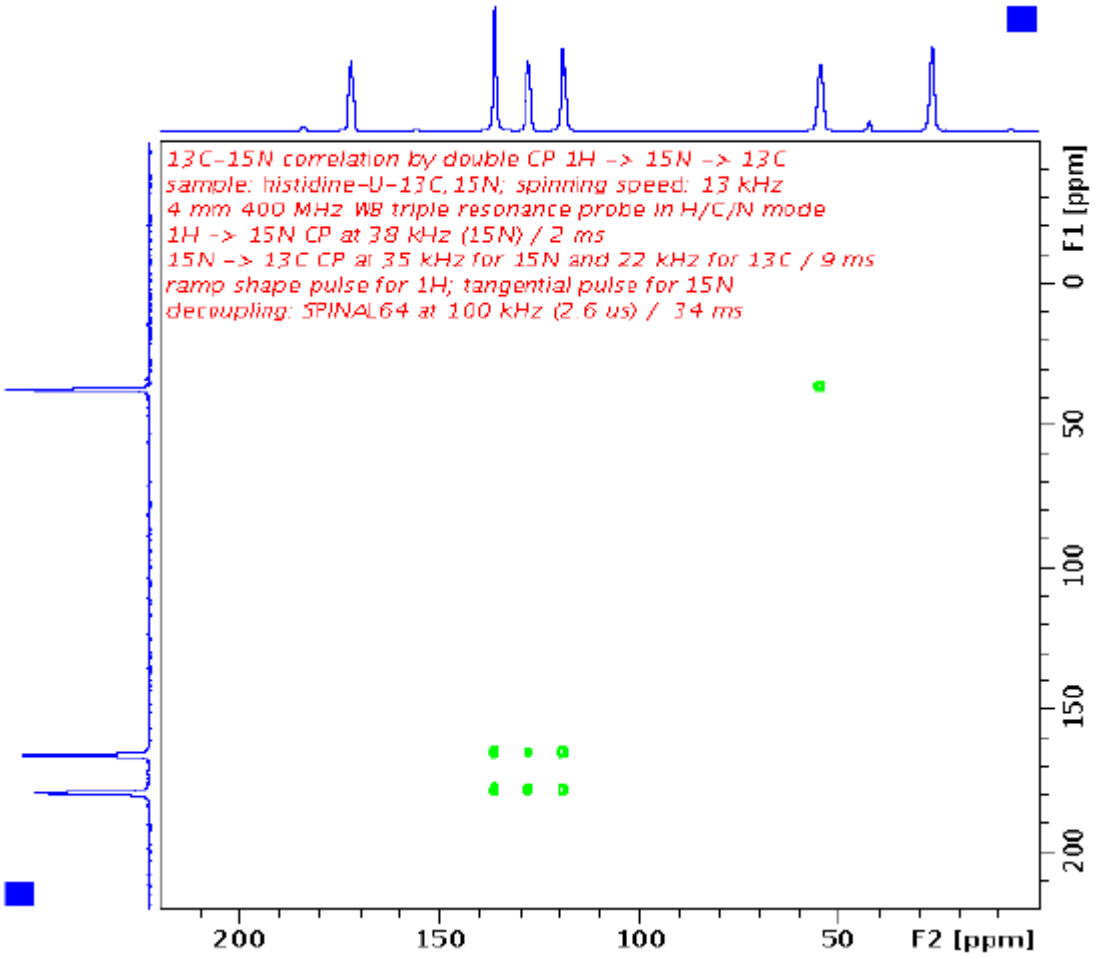

Figure 20.8. C-N correlation via Double CP in histidine (simple setup sample). 4mm Triple H/C/N Probe.

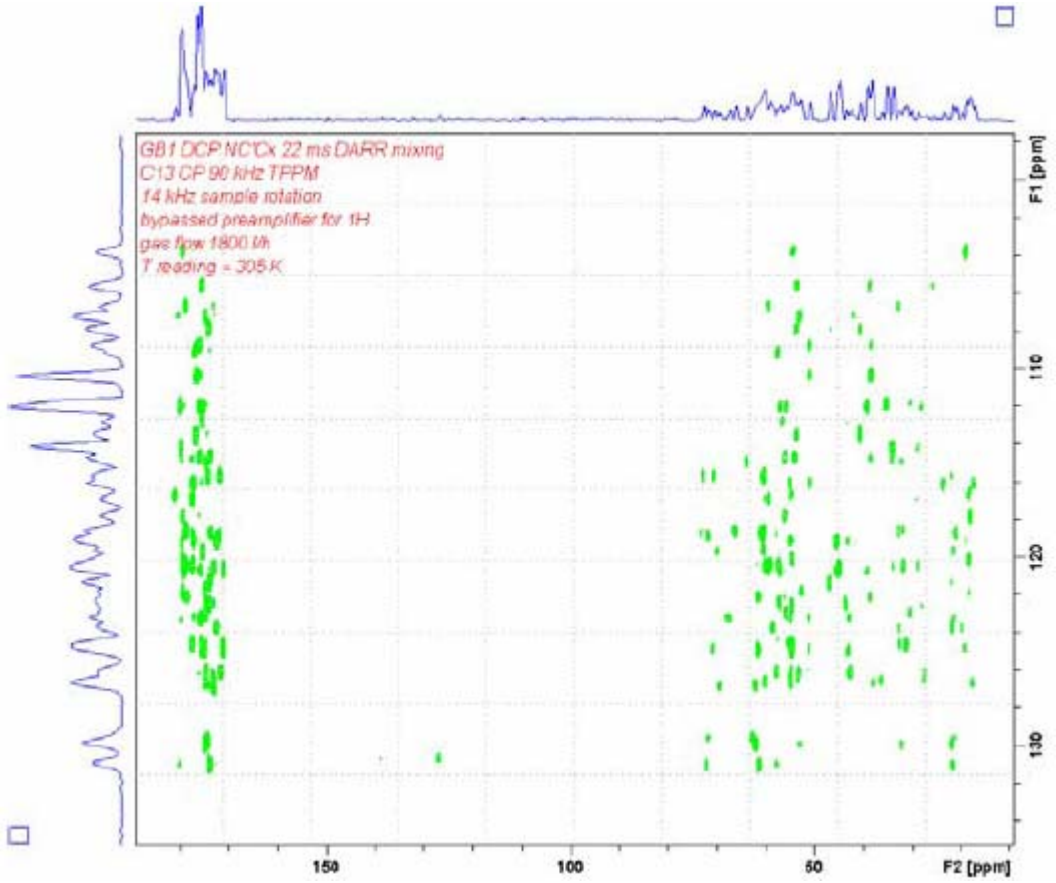

Figure 20.9. $NC_\alpha C_x$ correlation experiment with 22 ms DARR mixing period for Cα-Cx spin diffusion on GB1 protein run using an E^{FREE}-Probe.

DARR transfer from C_α to C_β or C_x generates positive cross peaks, HORROR or DREAM transfer generates negative cross peaks. See the chapter on spin diffusion experiments for more information about DARR or PDSD.

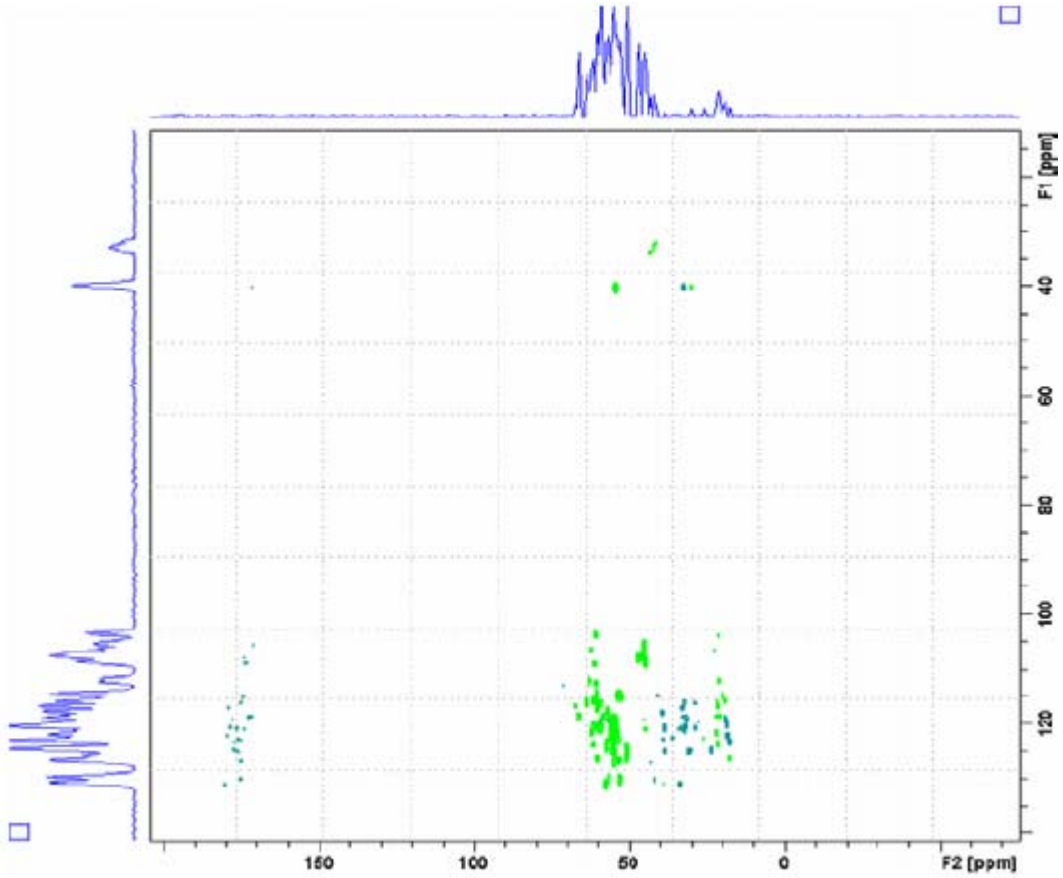

Figure 20.10.NC$_a$C$_x$ correlation experiment with 4.2 ms SPC5-DQ mixing period for C$_a$C$_x$ spin diffusion on GB1 protein run using an E^{FREE}-Probe at 14 kHz sample rotation and 100 kHz decoupling.

See the chapter on recoupling experiments for the SPC5 setup and for more information about DQ recoupling sequences. Note the inverse phase of the cross peaks generated by the DQ-mixing step.

Double-CP

CRAMPS: General 21

CRAMPS is an acronym standing for “Combined Rotation And Multiple Pulse NMR Spectroscopy”. Multiple Pulse Spectroscopy had long been thought not to work under spinning around the magic angle, but in fact it does work, as long as the pulse cycle times are substantially shorter than the rotation period.

CRAMPS suppresses homonuclear dipolar interactions between the abundant spins (mostly protons) and chemical shift anisotropy simultaneously through the combination of multiple pulse techniques and magic angle spinning. J-couplings and large heteronuclear dipolar couplings are not suppressed.

Reference:

1. L.M. Ryan, R.E.Taylor, A. J. Patt, and B. C. Gerstein, *An experimental study of resolution of proton chemical shifts in solids: Combined multiple pulse NMR and magic-angle spinning*, J. Chem. Phys. 72 vol.1, (1980).

Homonuclear Dipolar Interactions 21.1

Homonuclear dipolar interactions among spins with a strong magnetic moment and high natural abundance - mainly ^{1}H or ^{19}F, and to a much smaller extent ^{31}P - are usually very large unless averaged by high mobility. Especially in the case of protons, spin exchange is usually rapid compared to routinely achievable rotation periods, meaning that MAS alone cannot suppress the homonuclear dipolar broadening. Even spin rates in the order of 70 kHz, which is no longer a mechanical problem, cannot fully average this interaction in rigid solids. As chemical shift differences among the coupled nuclei become larger, the interaction becomes more heterogeneous and MAS can suppress it more efficiently. This is the reason why fast spinning alone works much better on ^{19}F or ^{31}P than on protons. heteronuclear dipolar coupling, such as between ^{13}C and ^{1}H, can in principle be spun out, but only if the homonuclear coupling between protons is small, or averaged by motion or a suitable pulse sequence. CRAMPS sequences therefore play an important role also in experiments where X-nuclei are observed.

Multiple Pulse Sequences 21.2

Dealing with a heteronuclear dipolar coupling is easy: continuous high power irradiation of one coupling partner will decouple it from the other nucleus, as in the case of ^{13}C observation while decoupling protons. However observing a nucleus while decoupling it from like spins at the same time is obviously not trivial, since the signal cannot be observed under the much higher decoupling RF. Observation of the signal and decoupling pulses must therefore be alternately applied. Suppression of a homonuclear dipolar interaction occurs when the magnetization vector of the coupled spins is tilted into the magic angle. This condition can be achieved either by 4 л/2 pulses of suitable phase and spacing (multiple-pulse methods), or by off-resonance irradiation of suitable offset and RF-field (Lee-

Goldburg). To observe the signal, a gap within the pulse sequence must be supplied, which is long enough to observe one or several data points while the magnetization vector points along the magic angle. This condition obviously persists only for a time period short compared to the transverse relaxation of the signal. To observe the time dependence of the signal, the sequence must be repeated and more data points accumulated until the signal has decayed under the influence of residual broadening. Obvious problems of this experiment are the requirement to observe a relatively weak signal shortly after a strong pulse (dead time problem) and the requirement to time the sequence in such a way that the magnetization vector is accurately aligned with the magic angle (requires precise pulse lengths and phases, and it requires RF fields strong compared to the interaction and shift distribution). Many sequences have been devised after the original WHH-4 (or WaHuHa) sequence which yield better results due to better error compensation (MREV-8, BR-24, C-24, TREV-8, MSHOT). Modern hardware has made the setup and application of these sequences a lot easier since pulse phase and amplitude errors are negligible, higher magnetic fields have led to better chemical shift dispersion and also to shorter dead times. The resolution achieved with long, highly compensated sequences like BR-24 is very good, but their applicability at limited spin rates (because of the need for the cycle time to be short with respect to the rotor period) often presents a problem.

References:

1. S. Hafner and H.W. Spiess, *Multiple-Pulse Line Narrowing under Fast Magic-Angle Spinning,* J. Magn. Reson. A 121, 160-166 (1996) and references therein.
2. M. Hohwy, J. T. Rasmussen, P. V. Bower, H. J. Jakobsen, and N. C. Nielsen. *^{1}H Chemical Shielding Anisotropies from Polycrystalline Powders Using MSHOT-3 Based CRAMPS*, J. Magn. Res.133 (2), 374 (1998), and references cited therein.

W-PMLG and DUMBO *21.3*

W-PMLG and DUMBO are shorter sequences which avoid turning high power pulses rapidly on and off, which is what most multiple pulse sequences do. This avoids undesired phase glitches. Also, they use higher duty cycles during the decoupling period. As a result, the sequences are simpler and shorter, requiring fewer adjustments and allowing higher spin rates.

Both sequences use repetitive shaped pulses with detection in between. PMLG uses the principle of a ***F***requency ***S***witched ***L***ee ***G***oldburg (FSLG) sequence (continuous irradiation with a net RF field along the magic angle), where the frequency shifts are replaced by a phase modulation. DUMBO basically works like a windowless MREV-type pulse sequence where the individual pulses are replaced by a single pulse with phase modulation.

References:

1. E. Vinogradow, P.K. Madhu, and S. Vega, High-resolution proton solid-state NMR spectroscopy by phase modulated Lee-Goldburg experiment, Chem. Phys. Lett. 314, 443-450 (1999).
2. D. Sakellariou, A. Lesage, P. Hodgkinson and L. Emsley, *Homonuclear dipolar decoupling in solid-state NMR using continuous phase modulation,* Chem. Phys. Lett. **319**, 253 (2000).

Quadrature Detection and Chemical Shift Scaling *21.4*

Under homonuclear decoupling, the magnetization precesses in the transverse plane of a tilted rotating frame whose new z-axis is along the direction of the effective field. The projection of this plane into the X-Y plane is therefore an ellipse, and the signal intensities sampled in the two quadrature channels along the x and y direction are different, since these are the major and the minor axes of the projected ellipse. As can be seen from fig. 1, the X and Y observe direction will see a signal of different amplitude. This means that quadrature images will always be present, if quad detection is used. In the case of single detection, the signal may be smaller or larger depending on the receiver phase. The standard procedure is to use quad detection and suppress the quad images by a suitable phase cycling scheme. This is however not as straightforward as it is with standard excitation/ observation. The quad phase cycling must occur in the precession plane, so a prepulse is required to tilt the initial magnetization into the direction of the precession axis. Usually, a combination of 2 pulses is used for initial excitation ($90^{o}_{x,y,-x,-y}$ + (90^{o} -55^{o})$_{adjust}$).

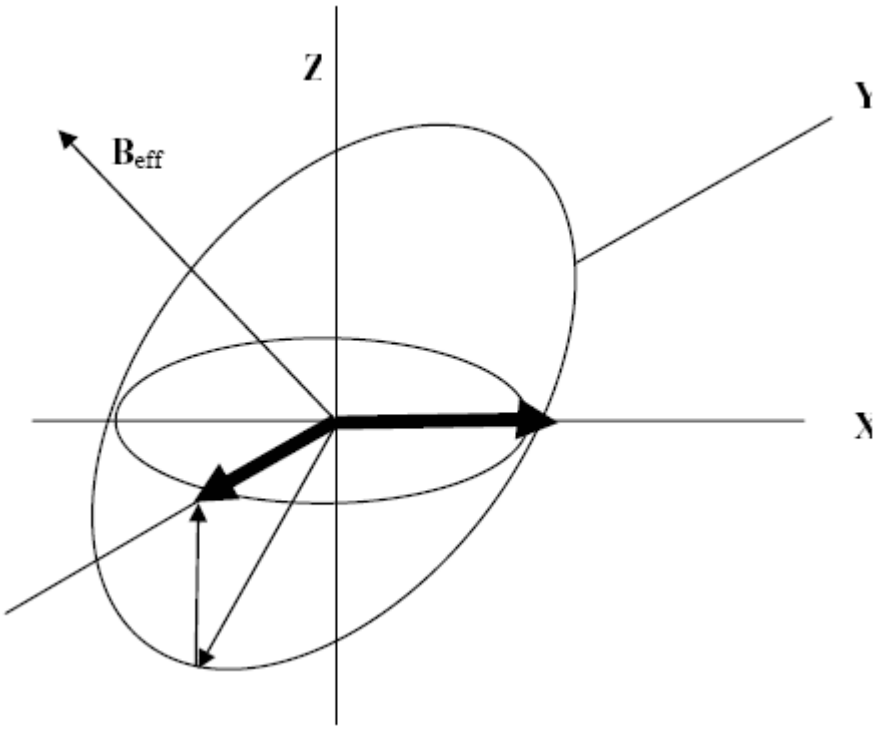

Figure 21.1. Difference in Amplitude of the Quadrature Channels X and Y

The difference in amplitude of the quadrature channels X and Y, caused by the tilted precession plane. Along X, the full amplitude is observed, along Y only the component in the XY-plane is detected.

As the spins precess around a tilted effective field and not only around the direction of the external field, the precession frequencies are changed, which means that the observed chemical shifts are changed. As the frequencies are always smaller than in the standard excitation/observation scheme, the chemical shift

range appears scaled down. The scaling factor depends on the pulse sequence used. To achieve a spectrum comparable to spectra acquired conventionally, the shift range must be scaled up again by this scaling factor, i.e. the spectral window given by the repetition rate of the pulse sequence must be multiplied by this scaling factor in order to place the resonances correctly. This scaling factor can be calculated from the tilt angle, but is also slightly dependant on the offset and RF-field. Since the correct chemical shifts are usually unknown, one must be aware of the fact that the shifts may not be as precise as they are in high resolution liquids experiments. An example of shift calibration, taking the scaling factor into account, will be given in the practical chapter.

CRAMPS 1D

22

As outlined above, many sequences are available to achieve homonuclear dipolar decoupling. We want to concentrate on those that allow fast spin rates and are easy to set up. The performance of DUMBO and W-PMLG is very similar. The pulse sequence is also very similar on AV3 instruments, just different shapes and different timings are loaded.

Pulse Sequence Diagram of W-PMLG or DUMBO 22.1

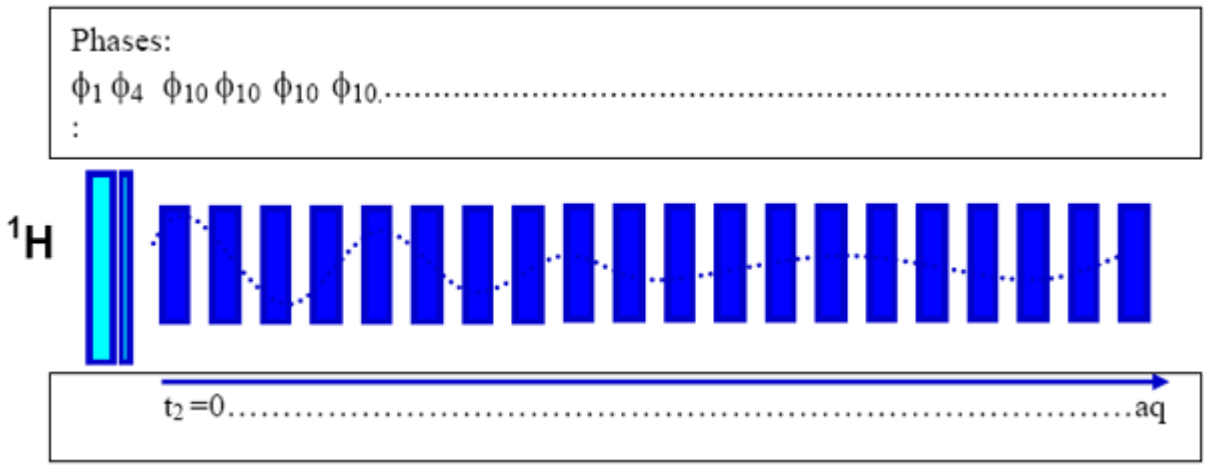

Figure 22.1. Pulse Sequence Diagram

Table 22.1. Phases, RF-Levels, Timings

Phases	RF Power Levels	Timing
ϕ_1 = CYCLOPS, 1 2 3 0	pl12=set for around 100 kHz	p1 around 2.5 µsec.
ϕ_4 = 0 +cnst25, adjust	ditto.	p4 about 45 degrees, adjust.
ϕ_{10} = 0	sp1: set for 100-130 kHz	WPMLG: p5, 1.2-1.5 µsec or calculated from cnst20=RF field DUMBO: p10 set by xau dumbo.
ϕ_{31} = CYCLOPS, 0 1 2 3		

Pulse Shapes for W-PMLG and DUMBO *22.2*

Both shapes are purely phase modulated pulses, their amplitudes are constant throughout. The PMLG shape is a standard shape delivered with the software (***wpmlg1***, ***m5m***, ***m5p***). DUMBO shapes are generated using the standard AU-program dumbo. Calling dumbo with ***xau dumbo*** will ask for the slice length of the shape (usually 1 µsec), the number of slices (usually 32), generate the shape and load the name of this shape into the current parameter set, it will also set the length of the shaped pulse, ***p10***, to 32 µsec. N.B.: at magnetic fields higher than 500 MHz, it is recommended to replace the standard 32 µsec timing by 24 µsec timing and increasing the power level accordingly, since this has been found to give better results.

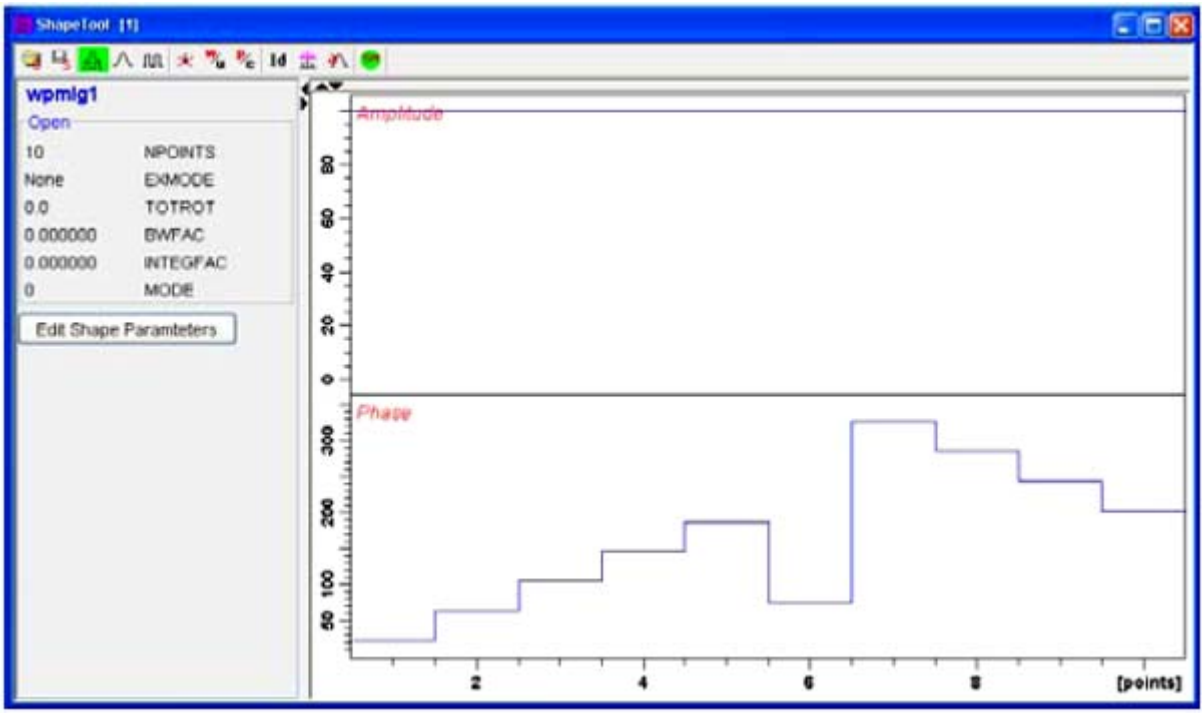

Figure 22.2. PMLG Shape for wpmlg, sp1

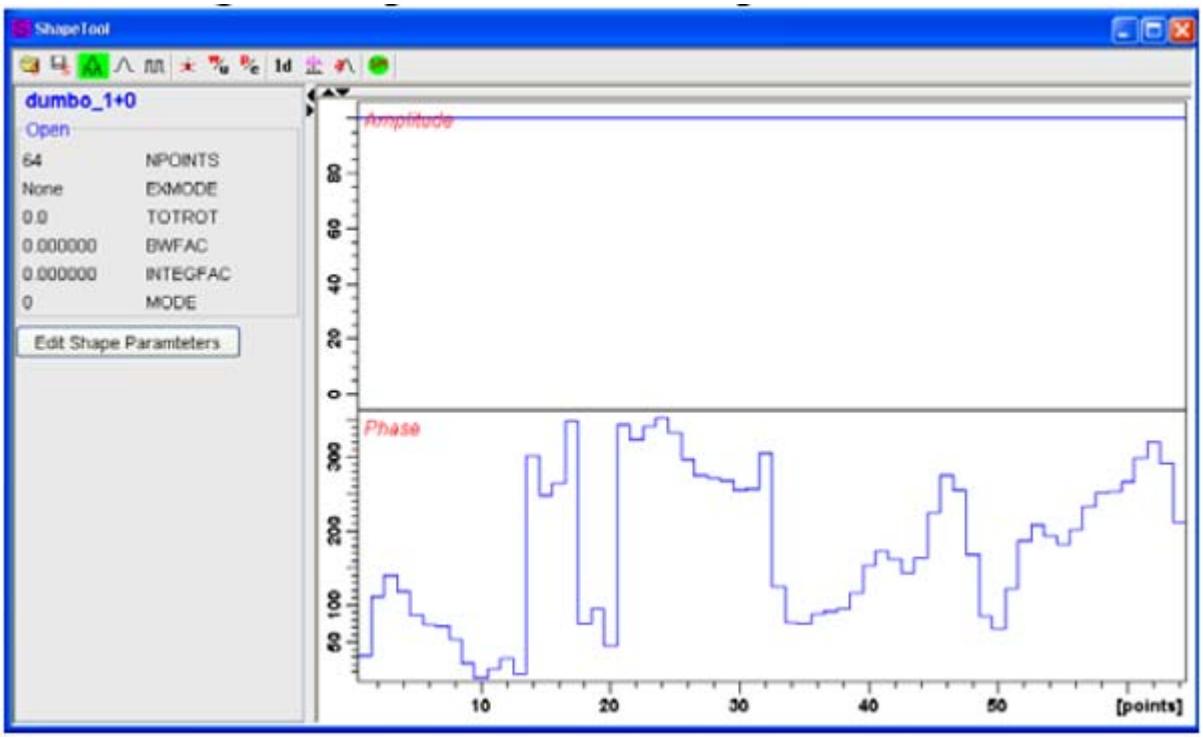

Figure 22.3. Shape for DUMBO, sp1

Analog and Digital Sampling Modi *22.3*

AV3 instruments allow different acquisition modi, one which resembles the previous mode of analogue filtering in so far as the down-conversion is done without simultaneous digital filtering, whereas the digital mode always down converts and filters simultaneously. Remember that at a standard sampling rate of 20 MHz (the fixed sampling rate of the DRU) down-conversion must be done to obtain data sets of reasonable sizes. The pulse programs dumboa and wpmlga are written for the pseudo analog mode without digital filtering, ***dumbod*** and ***wpmlgd*** are written for the digitally filtered mode.

Analog Mode Sampling 22.3.1

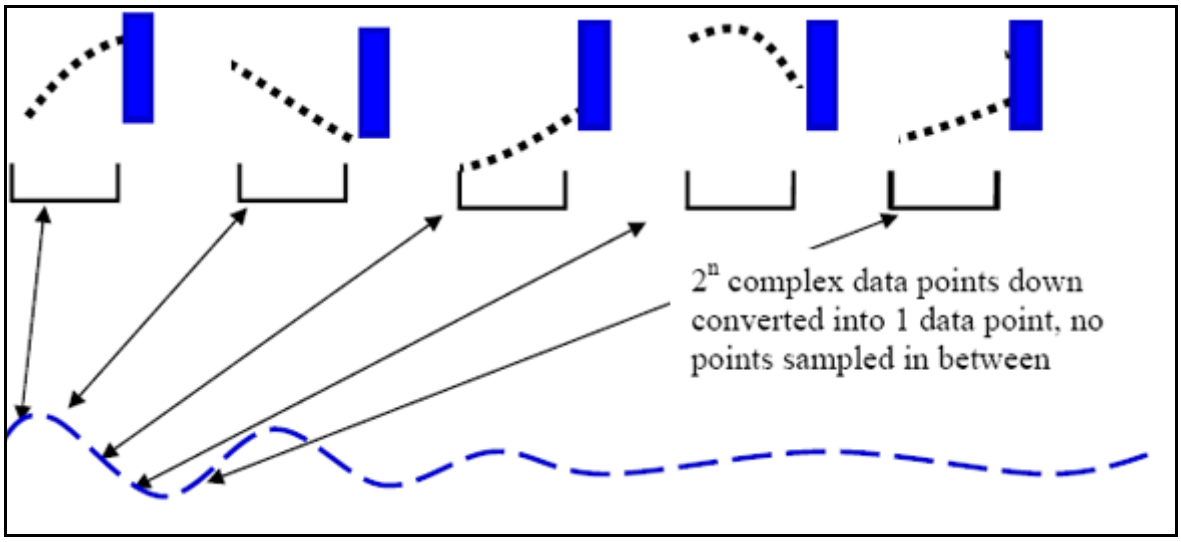

Figure 22.4. Analog Sampling Scheme

Digital Mode Sampling 22.3.2

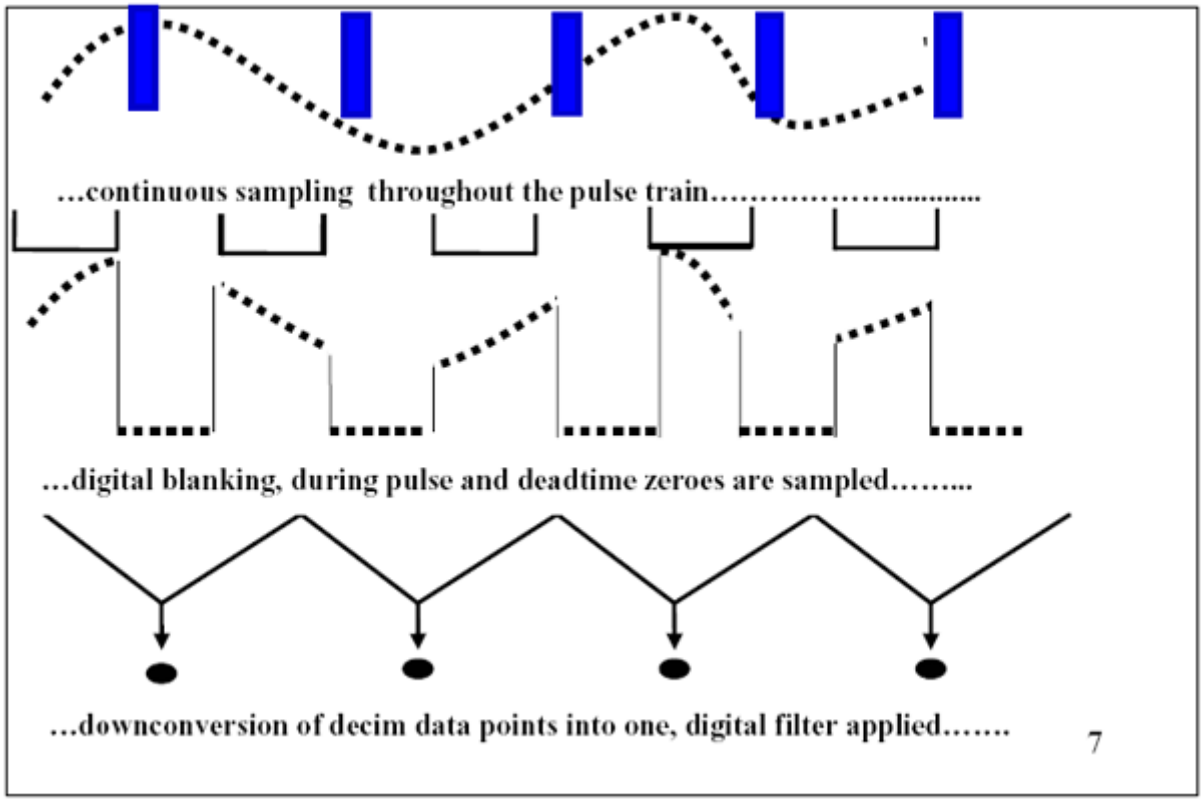

Figure 22.5. Digital Sampling Scheme

Setup 22.4

At frequencies of 400 MHz and higher, double or triple resonance CP-MAS probes may be used on the proton channel, at lower fields a CRAMPS probe is required due to the increased ring down time at lower field. Spinner diameters of 4mm or smaller are preferred, since we want to spin over 10 kHz. Since only one nucleus is observed, no filters are required and should be avoided. Good impedance matching between probe and transmitter is important in order to optimise the effect of the pulses on the spins. If the RF cable has been too strongly bent or the connectors been twisted, the cable may not have 50 Ohms and the result will always be bad. Likewise, if the preamp is burnt, it is not possible to get good results.

The fewer connectors are between probe and preamp, the better you can expect the 50 Ohm match to be. In ***edasp***, set F1 for ^{1}H-observation, select the high power proton amplifier and high power preamplifier. Tune and match as usual. It is assumed that the magic angle is precisely set, which can easily be achieved with KBr on a double resonance probe, or on $BaClO_3{*}H_2O$, looking at the proton signal, much like one does on the Br^{79} resonance.

Shimming will also be important, since protons are observed, and on some samples, good resolution is expected. Looking at the protons in adamantane, find the power level for a 2.5 µsec 90^{o} pulse. Set the B_0-field or ***o1*** to be close to resonance (see chapter Basic Setup Procedures for more details). Calibrate the adamantane proton shift to 1.2 ppm. Then load a spinner with α-glycine (precipitate from cold water with acetone and dry, if you are not sure about the composition of your sample). A spinner with 50 µl or less sample volume is preferred since high H_1-homogeneity is desired, although it is by far less important than is commonly stated in the literature.

Parameter Settings for PMLG and DUMBO 22.5

Table 22.2. PMLG Analog Mode

Parameter	Value	Comment
pulprog	wpmlga	Runs on AV 3 instruments only.
pl12 sp1	for 100 kHz RF field dto, set cnst20=100 000	To be optimized during setup.
spnam1	wpmlg1, m5m or m5p	
p1	2.5 µsec	As for 100 kHz RF field.
p8	1.2µsec	
p14	0.7 µsec	To be optimized.
cnst25	140	To be optimized.
p9	4 – 2.6 µsec	To be optimized.
p5	1.5 µsec or calculated from cnst20	To be optimized.
d1	4s	For α-glycine.

Table 22.2. PMLG Analog Mode

l11=anavpt	4	2, 4, 8, 16 or 32.
o1p	10 or -1	To be optimized.
swh	$1e^6/2*(2*p9+10*p5)*0.6$	To be corrected for proper scaling.
rg	16-64	
td	512	Up to 1024.
si	4k	
digmod	analog	
MASR	12-15 kHz	Depending on cycle time.

Table 22.3. DUMBO, Analog Mode

Parameter	Value	Comment
pulprog	dumboa	Runs on AV 3 instruments only.
pl12 sp1	for 100 kHz RF field up to 130 kHz	To be optimized during setup.
spnam1	dumbo1_64	Set by xau dumbo.
p1	2.5 µsec	For 100 kHz RF field.
p8	1.2µsec	
p14	0.7 µsec	To be optimized.
cnst25	140	To be optimized.
p9	4 – 2.6 µsec	To be optimized.
p10	32 µsec or 24 µsec	Set by xau dumbo.
d1	4s	For α-glycine.
l11=anavpt	4	2, 4, 8, 16 or 32.
o1p	5	To be optimized.
swh	$1e^6/2*(2*p9+p10)*0.5$	To be corrected for proper scaling.
rg	16-64	
td	512	Up to 1024.
si	4k	
digmod	analog	
MASR	10-12 kHz	Depending on cycle time.

Fine Tuning for Best Resolution 22.6

For fine tuning, the following parameters are important:

P9 sets the width of the observe window. The shorter it is, the better the resolution. However, the natural limit is the size of the sampling period and the dead time of the probe. Preamp and receiver play no significant role in the total dead time. A CP/MAS probe usually has a fairly narrow bandwidth (long dead time), so ***p9*** <3µsec is only possible at frequencies 400 and higher. With ***l11*** 4-8, ***p9*** can be chosen shorter for better resolution, but at the cost of S/N. Sampling more data points during d9=***l11****0.1 µsec with larger values of ***l11***, will increase S/N slightly but requires more time within the window, may require a longer p9 and therefore degrade resolution.

Since the decoupling bandwidths are not very large, ***o1*** should be close to resonance, especially for DUMBO. For PMLG, this is less critical. The power level for the shapes should be adjusted in steps of 0.2 dB. The splitting of the two high field lines (the protons in the $–CH_2-$ are in-equivalent in the solid state) should be below the 50% level.

Fine Tuning for Minimum Carrier Spike 22.7

The tilt pulse ***p14*** and its phase (***cnst25***) determine the size of the carrier spike. Optimise both parameters alternately for minimum spike, and make sure the spike does not overlap with a resonance by choosing ***o1*** appropriately. N.B: changing ***o1*** will lead to different values for ***cnst25***.

Correcting for Actual Spectral Width 22.8

Since the sampling rate is governed by the multi-pulse sequence repetition rate, the foreground parameter ***swh*** has no real meaning. Once all tuning procedures are done, calculate the real spectral width ***swh*** according to the formula given in the parameter tables and run a new experiment. After FT, the spectrum should have an approximately correct spectral width. Calibrate the middle position between the two $–CH_2-$ peaks to 3.5 ppm, the NH_3-peak should then be at about 7.5 ppm. Since the actual peak positions depend on the probe tuning, you will have to recalibrate for your sample using one or more known chemical shifts. If the peak separation is incorrect, change the status parameter ***swh*** by typing ***s swh*** and scaling it appropriately. Some pulse programs are written such that upon ***ased***, the (approximately) correct sweep width is shown and can be set as an acquisition parameter.

Digital Mode Acquisition 22.9

Most parameters stay the same as adjusted in analog mode.

Table 22.4. Parameters for Digital Mode

Parameter	Value	Comment
pulprog	dumbod or wpmlgd	AV 3 instruments only.
digmod dspfirm	digital sharp or medium	
aqmod	qsim or dqd	
swh	50000-10000	Depending on spectral range and o1.

The correction for the scaling factor must be done after acquisition, changing the status parameter ***swh*** by typing ***s swh*** and dividing the value by the scaling factor (about 0.578 for WPMLG, 0.47 for wpmlgd2 and 0.5 for DUMBO). Some pulse programs are written such as to show the correct sweep width in ***ased***, which can then be set appropriately as ***s swh*** before transform.

Examples 22.10

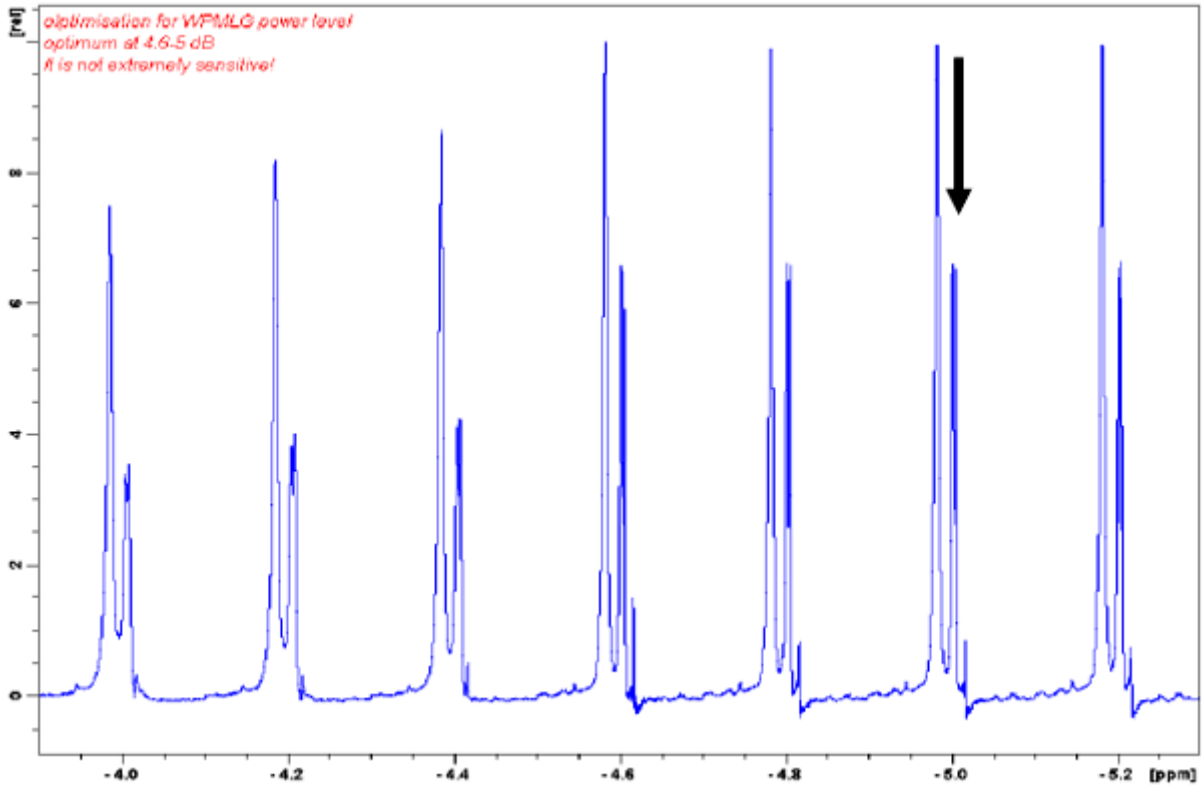

Figure 22.6. Optimizing sp1 for Best Resolution

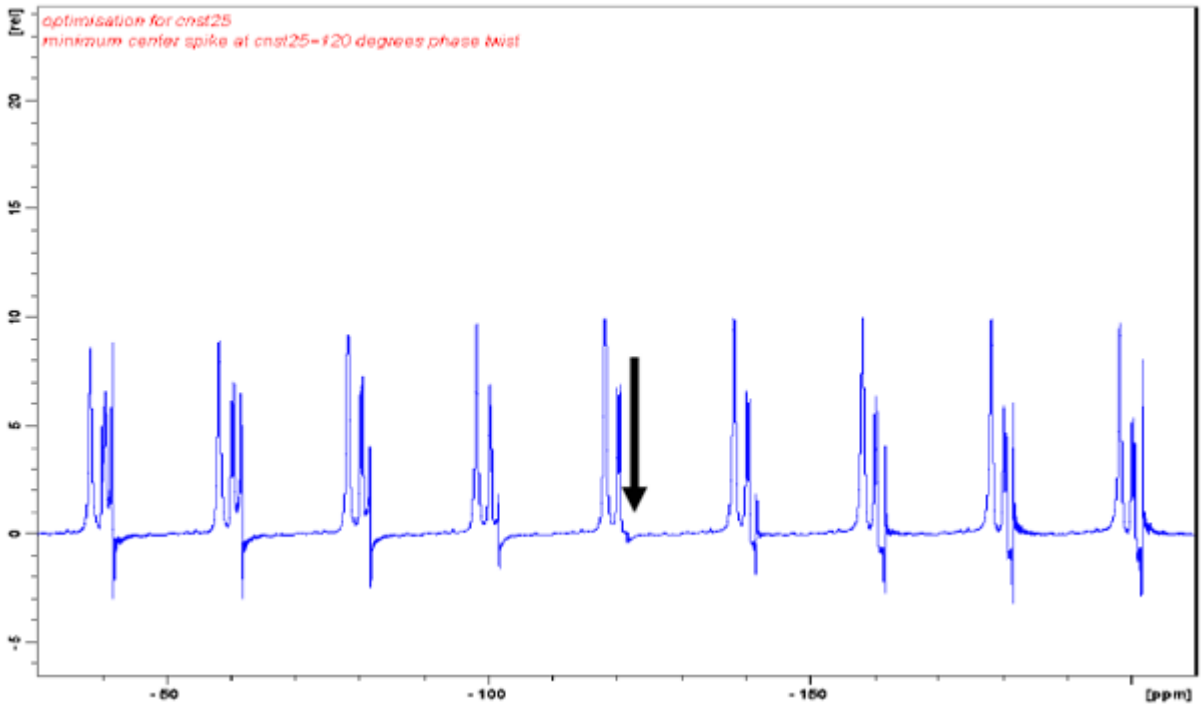

Figure 22.7. Optimizing cnst25 for Minimum Carrier Spike, Optimized at 120°C

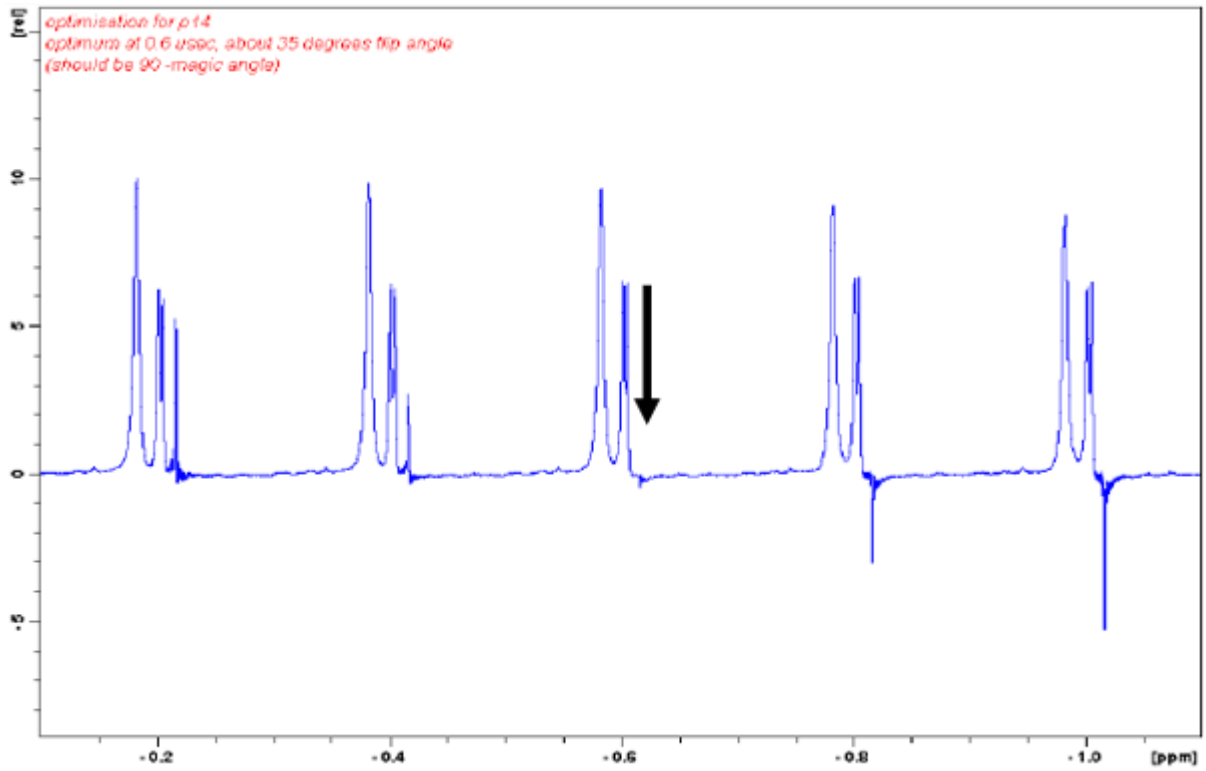

Figure 22.8. Optimizing p14 for Minimum Carrier Spike, Optimized at 0.6 µsec

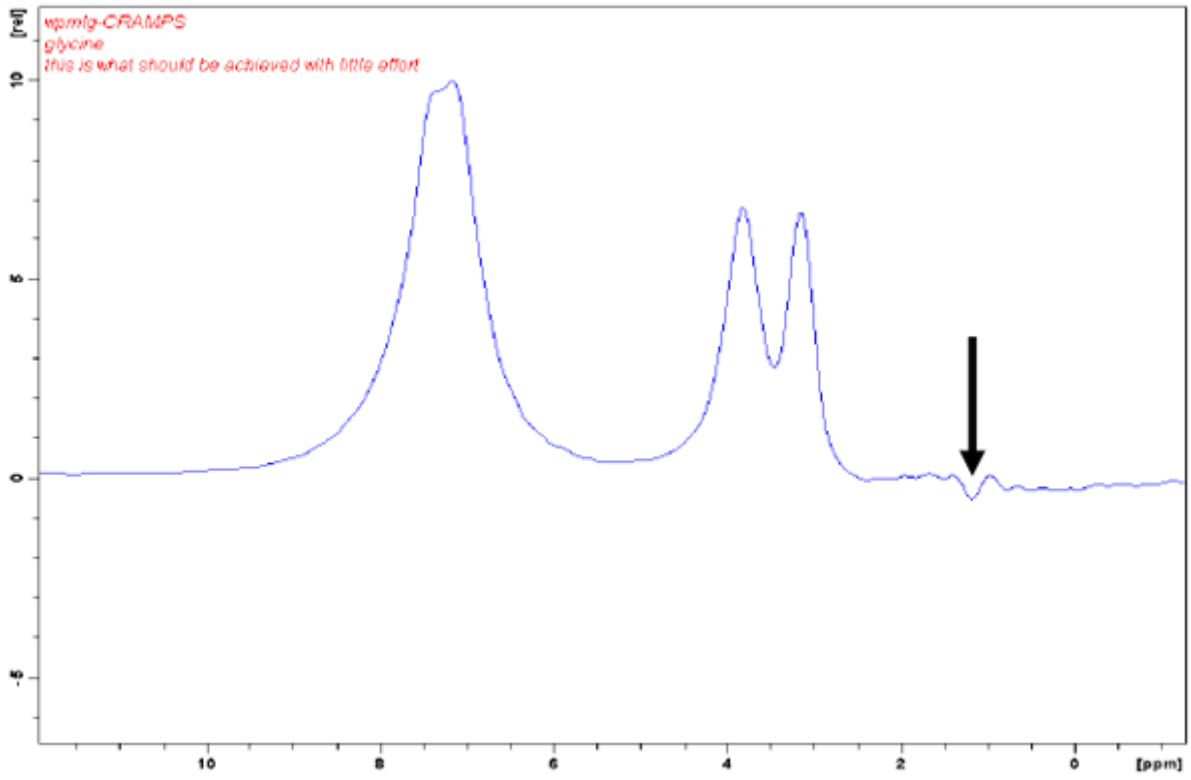

Figure 22.9. WPMLG-CRAMPS After Optimization, Digital Acquisition

Modified W-PMLG 23

Recently, a modified version of WPMLG was published by Leskes et al., which suppresses the carrier spike completely and therefore allows placing the carrier frequency ***o1***, ***o1p*** arbitrarily. This is achieved by a 180 degree phase alternation between consecutive WPMLG-pulses. The magic angle tilt pulse is then not required anymore. This reduces setup time and enhances experimental possibilities significantly.

Reference:

1. M. Leskes, P.K. Madhu and S. Vega, *A broad-banded z-rotation windowed phase modulated Lee–Goldburg pulse sequence for ^1H spectroscopy in solid-state NMR,* Chem. Phys. Lett. 447, 370 (2007).

Pulse Sequence Diagram for Modified W-PMLG 23.1

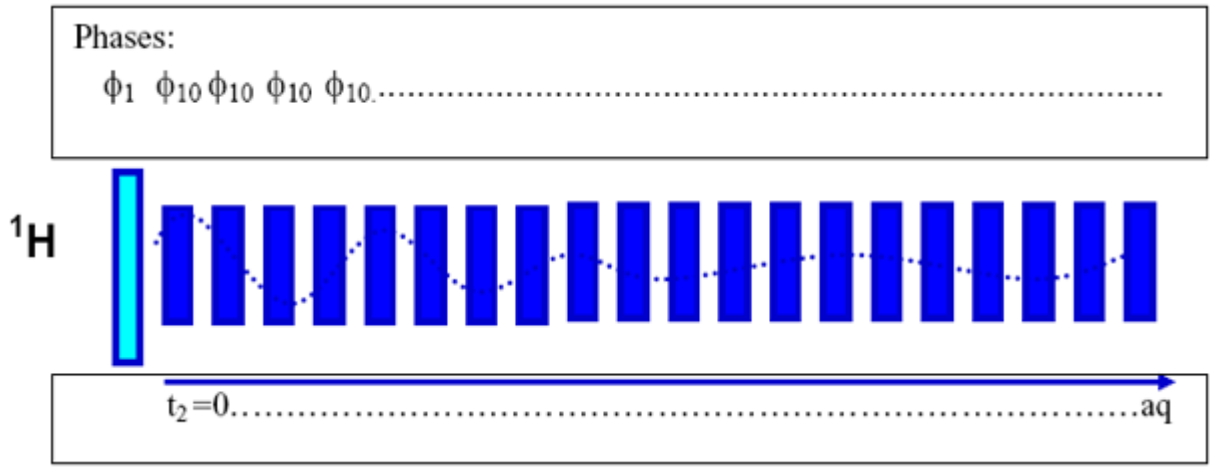

Figure 23.1. Pulse Sequence Diagram

Table 23.1. Phrases, RF-Levels, Timings

Phases	RF Power Levels	Timing
ϕ_1 = CYCLOPS, 1 2 3 0	pl12=set for around 100 kHz	p1 around 2.5 µsec
ϕ_{10} = **0 2**	sp1: set for 100-130 kHz=cnst20	WPMLG: calculated from cnst20=RF field
ϕ_{31} = CYCLOPS, 0 1 2 3		

Pulse Shapes for W-PMLG *23.2*

PMLG-shapes: m3p, m3m, m5m, m5p

All these shapes perform similarly. M3p and m3m use 6 phases, m5p and m5m use 10 phases to generate the phase ramp. Obviously, 6 phases generate a phase ramp with less resolution, but shorter possible duration. With the timing resolution available on AV instruments, there is no need to prefer the coarse phase ramp. The letters m and p refer to the sense of phase rotation which is opposite between m and p. If probe tuning is not perfect, m or p may give different results depending on the carrier position. The overall added phases of 0 and 180 degrees on consecutive shape pulses are set by the phase program (phase list ph10).

```
##TITLE= m5p
##JCAMP-DX= 5.00 Bruker JCAMP library
##DATA TYPE= Shape Data
##ORIGIN= Bruker BioSpin GmbH
##OWNER= <hf>
##DATE= 2005/11/29
##TIME= 14:47:39
##$SHAPE_PARAMETERS=
##MINX= 1.000000E02
##MAXX= 1.000000E02
##MINY= 1.125000E01
##MAXY= 3.487500E02
##$SHAPE_EXMODE= None
##$SHAPE_TOTROT= 0.000000E00
##$SHAPE_TYPE= Excitation
##$SHAPE_USER_DEF=
##$SHAPE_REPHFAC=
##$SHAPE_BWFAC= 0.000000E00
##$SHAPE_BWFAC50=
##$SHAPE_INTEGFAC= 6.534954E-17
##$SHAPE_MODE= 0
##NPOINTS= 10
##XYPOINTS= (XY...XY)
1.000000E02, 20.78
1.000000E02, 62.35
1.000000E02, 103.92
1.000000E02, 145.49
1.000000E02, 187.06
1.000000E02, 7.06
1.000000E02, 325.49
1.000000E02, 283.92
1.000000E02, 242.35
1.000000E02, 200.78
##END
```

```
##TITLE= m3p
##JCAMP-DX= 5.00 Bruker JCAMP library
##DATA TYPE= Shape Data
##ORIGIN= Bruker BioSpin GmbH
##OWNER= <hf>
##DATE= 2005/11/29
##TIME= 14:47:39
##$SHAPE_PARAMETERS=
##MINX= 1.000000E02
##MAXX= 1.000000E02
##MINY= 1.125000E01
##MAXY= 3.487500E02
##$SHAPE_EXMODE= None
##$SHAPE_TOTROT= 0.000000E00
##$SHAPE_TYPE= Excitation
##$SHAPE_USER_DEF=
##$SHAPE_REPHFAC=
##$SHAPE_BWFAC= 0.000000E00
##$SHAPE_BWFAC50=
##$SHAPE_INTEGFAC= 6.534954E-17
##$SHAPE_MODE= 0
##NPOINTS= 6
##XYPOINTS= (XY...XY)
1.000000E02, 214.64
1.000000E02, 283.92
1.000000E02, 353.21
1.000000E02, 173.2
1.000000E02, 103.92
1.000000E02, 34.64
##END
```

Setup 23.3

Fine tuning is done in the same way as with the original sequence, except that the carrier is placed on a convenient position within the spectrum. There is no need to minimise the carrier spike, it should be all gone. Somewhat higher power is required for the wpmlg-shapes.

Parameter Settings for PMLG and DUMBO 23.4

Table 23.2. PMLG, Analog Mode

Parameter	Value	Comment
pulprog	wpmlga2	Runs on AV 3 instruments only.
pl12 sp1	for 100 kHz RF field dto, set cnst20=100 000	To be optimized during setup.
spnam1	m5m or m5p	
p1	2.5 µsec	As for 100 kHz RF field.
p8	1.2 µsec	
p9	4 – 2.6 µsec	To be optimized.
p5 not used	calculated from cnst20	To be optimized.
d1	4s	For α-glycine.
l11=anavpt	4	2, 4, 8, 16 or 32.
o1p	3 - 8	To be optimized.
swh	$1e^6/2*(2*p9+10*p5)*0.47$	To be corrected for proper scaling.
rg	16-64	
td	512	Up to 1024.
si	4k	
digmod	analog	
MASR	12-15 kHz	Depending on cycle time.

Table 23.3. DUMBO, Analog Mode

Parameter	Value	Comment
pulprog	dumboa2	Runs on AV 3 instruments only.
pl12 sp1	For 100 kHz RF field up to 130 kHz	 To be optimized during setup.
spnam1	dumbo1_64	Set by xau dumbo.
p1	2.5 µsec	For 100 kHz RF field.
p8	1.2µsec	
p9	4 – 2.6 µsec	To be optimized.
p10	32 µsec or 24 µsec	Set by xau dumbo.
d1	4s	For α-glycine.
l11=anavpt	4	2, 4, 8, 16 or 32.
o1p	5	To be optimized.
swh	$1e^6/2*(2*p9+p10)*0.5$	To be corrected for proper scaling.
rg	16-64	
td	512	Up to 1024.
si	4k	
digmod	analog	
MASR	10-12 kHz	Depending on cycle time.

Fine Tuning for Best Resolution *23.5*

Fine tuning is done by optimizing power levels, pulse widths and carrier offset as before, the carrier spike is gone, spikes at both sides may appear.

Correcting for Actual Spectral Width *23.6*

The modified sequence has a slightly different scaling factor of 0.47.

Digital Mode Acquisition *23.7*

Most parameters stay the same as adjusted in analogue mode.

Table 23.4. Parameters for Digital Mode

Parameter	Value	Comment
pulprog	dumbod2 or wpmlgd2	AV 3 instruments only.
digmod dspfirm	digital sharp or medium	
aqmod	qsim or dqd	
swh	50000-10000	Depending on spectral range and o1.

The correction for the scaling factor must be done after acquisition, changing the status parameter ***swh*** by typing ***s swh*** and dividing the value by the scaling factor (about 0.47 for WPMLG and 0.5 for DUMBO).

Modified W-PMLG

CRAMPS 2D 24

CRAMPS methods allow measurement of chemical shifts in the presence of strong homonuclear dipolar interactions. Therefore, CRAMPS-type sequences can be applied to measure chemical shifts of protons (where these sequences work most efficiently, and where fast spinning cannot easily be used). As an example, the proton-X heteronuclear chemical shift correlation experiment (see chapter 5) uses FSLG to suppress homonuclear dipolar couplings between protons to resolve the proton chemical shifts. CRAMPS-type pulse sequences must be used in both dimensions if proton chemical shifts are to be correlated.

Two types of proton-proton correlation experiment will be described here:

1. Proton-proton shift correlation via spin diffusion (similar to the high resolution NOESY-experiment). In this case, the dipolar coupling between protons acts during the mixing period. The size of the off-diagonal cross peaks indicates the size of the dipolar coupling between the correlated sites.
2. Proton-proton DQ-SQ correlation (similar to the high resolution INADEQUATE) correlates proton chemical shifts with DQ-frequencies of dipolar coupled sites.

The modifications according to the chapter ***"Modified W-PMLG"*** are implemented in order to remove the carrier spike. Without a carrier spike, 2D experiments are much easier and faster to set up. Being able to set the carrier close to the desired spectral range, one can make the total acquired window smaller as well along F2 (using digital mode) as along F1.

References:

1. P. Caravetti, P. Neuenschwander, R.R. Ernst, Macromolecules, **18**, 119 (1985).
2. S.P. Brown, A. Lesage, B. Elena and L. Emsley*, Probing Proton-Proton Proximities in the Solid State: High-Resolution Two-Dimensional ^{1}H-^{1}H Double-Quantum CRAMPS NMR Spectroscopy,* J. Am. Chem. Soc. **126**, 13230 (2004).

Proton-Proton Shift Correlation (spin diffusion) *24.1*

The standard CRAMPS setup must be executed first (see chapter ***22***, ***23***). Any homonuclear dipolar decoupling scheme may be used, but in the following the experiment is described using windowed pmlg (w-PMLG). The reasons are the following:

1. At fast spin rates over 10 kHz, only w-PMLG and DUMBO work well. The sequence can easily be modified to use DUMBO, replacing the w-PMLG shapes by DUMBO-shapes and modifying the shape timing accordingly.
2. W-PMLG is easy to set up, since it is rather insensitive to power level missets and frequency offsets. When the experiment setup for the 1D experiment has been executed, no further setup is required for the 2D experiment. Start from the 1D experiment on your sample (the recommended setup sample is glycine) and generate a 2D data set by clicking on the symbol 1, 2 in the headline of the acquisition parameters.

Pulse Sequence Diagram 24.2

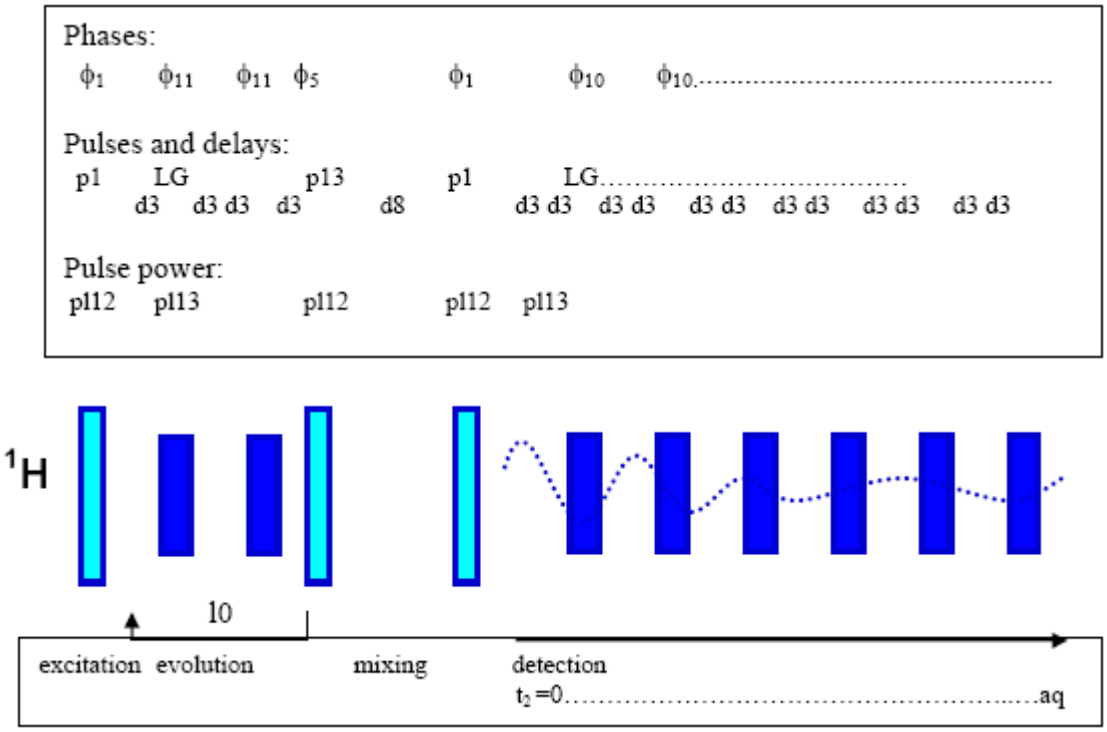

Figure 24.1. Pulse Sequence Diagram

This sequence is written in such a way that the windowed PMLG-unit is used both for detection and for the shift evolution along F1. This was done to minimize the setup requirements. In principle, a windowless sequence can be used as well and should give better resolution along F1. The power level for a windowless sequence is however usually slightly different from the windowed sequence, so this needs to be adjusted separately. Likewise, decoupling during t1 could be implemented using real frequency shifts as in the HETCOR sequence (see ***"Decoupling Techniques" on page 89***). If a windowless sequence is incorporated, the windows d3 must of course be removed. A simple windowless FSLG-unit can be used, with a shape like lgs-2 or lgs-4 having duration of twice or 4 times the length of the w-pmlg pulse.

Table 24.1. Acquisition Parameters

Parameter	Value	Comment
pulprog	wpmlg2d.	AV 3 instruments only, topspin 2.1 or later.
FnMODE	STATES-TPPI.	Any other method may be used with appropriate changes in ppg.
NUC1, NUC2	1H.	

Table 24.1. Acquisition Parameters

sw, swh along F1	Same as for F2.	Needs to be corrected before transform pulse program calculates approximate values to be set before transform (***ased***).
td	512-1k.	Depending on resolution.
1 td	128-256.	Depending on resolution.
spnam1	wpmlg1, m5m or m5p as in 1d.	DUMBO may be used with modified timing.
spnam2	lgs-2 or lgs-4 if used.	Set l3=2 or 4, depending on desired sw1 DUMBER-22 with modified timing.

Table 24.2. Phases, RF-levels, and Timings

Phases	RF Power Levels	Timing
$\phi_0 =$ 0, STATES-TPPI	pl12 = set for around 100 kHz	p1 around 2.5 µsec.
$\phi_1 =$ CYCLOPS, 1 2 3 0	pl12	p1
$\phi_5 = 2$		
ϕ_{10} = 0 2	sp1,sp2: set for 100-130 kHz RF-field or pl13 for both set in ppg	WPMLG: calculated via cnst20. DUMBO: p10 set by xau dumbo.
ϕ_{11} = 0 2	dto.	dto.
$\phi_{31} =$ CYCLOPS, 0 1 2 3		d8 = desired mixing time, 50-1000 µs.

Data Processing *24.3*

The spectral width in both dimensions assumes the absence of shift scaling. In order to account for the shift scaling effect of the sequence, one has to increase the spectral width by the scaling factor. Before doing the 2D-fourier transformation, type ***s sw*** to call the status parameters for both F2 and F1 and replace both values by <current value>/0.6. After ***xfb***, the relative peak positions will be (approximately) correct, but the absolute peak positions must be corrected by calibrating a known peak position to the correct value. The pulse program is written such that the correctly scaled sweep widths are calculated and indicated upon ***ased***. These values are set as status parameters before transform as indicated above.

Table 24.3. Processing Parameters

Parameter	Value	Comment
mc2	STATES-TPPI	
wdw	QSINE	Slight-moderate resolution enhancement is usually required.

Table 24.3. Processing Parameters

ssb	3 or 5	
si	2k -4k	
1 si	512 – 1k	

Examples *24.4*

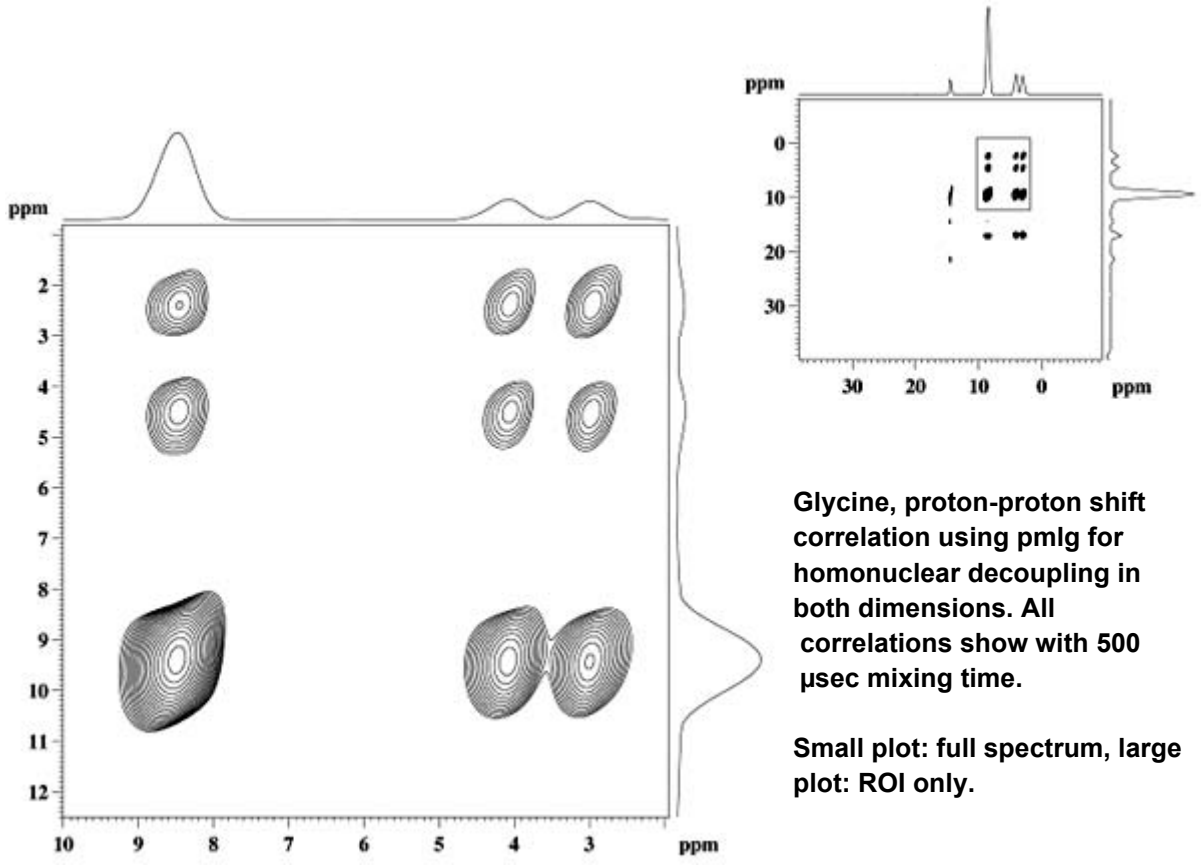

Glycine, proton-proton shift correlation using pmlg for homonuclear decoupling in both dimensions. All correlations show with 500 µsec mixing time.

Small plot: full spectrum, large plot: ROI only.

Figure 24.2. Setup and Test Spectrum of Alpha-glycine

The figure above shoes the setup and test spectrum of alpha-glycine (N.B. glycine samples containing gamma glycine will show additional peaks!). The protons attached to the alpha-carbon are in-equivalent and strongly coupled. The cross peaks at 3 and 4 ppm will show at a mixing time as short as 50 µsec, the cross peaks to the NH_3-protons at 9 ppm require 200 -300 µsec to show. The mixing time here was 500 µsec. A sequence without carrier spike suppression was used here.

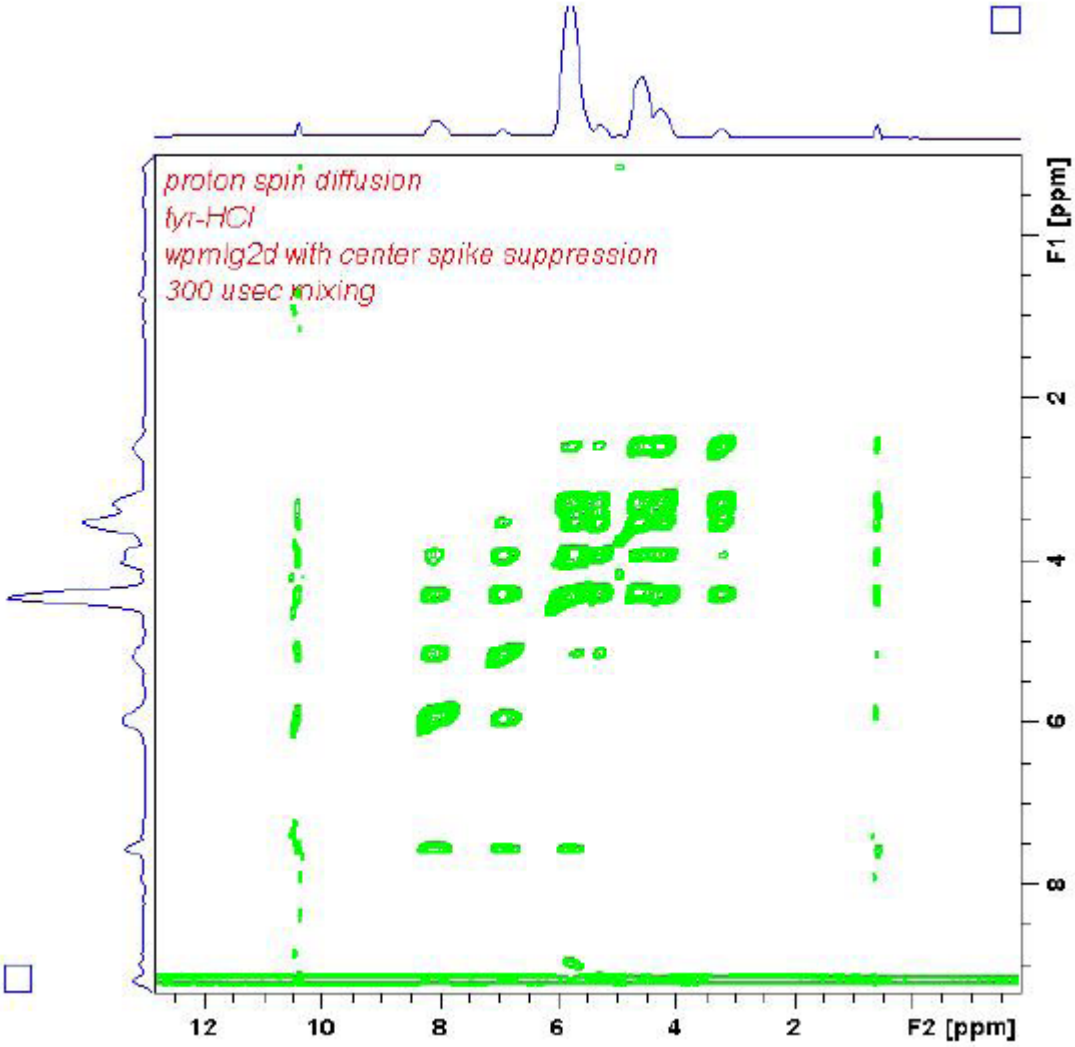

Figure 24.3. Spectrum of Tyrosine-hydrochloride

The mixing time was 300 µsec to show all connectivities. Full plot to show that smaller sweep widths can be chosen when the carrier can be conveniently placed within the spectrum.

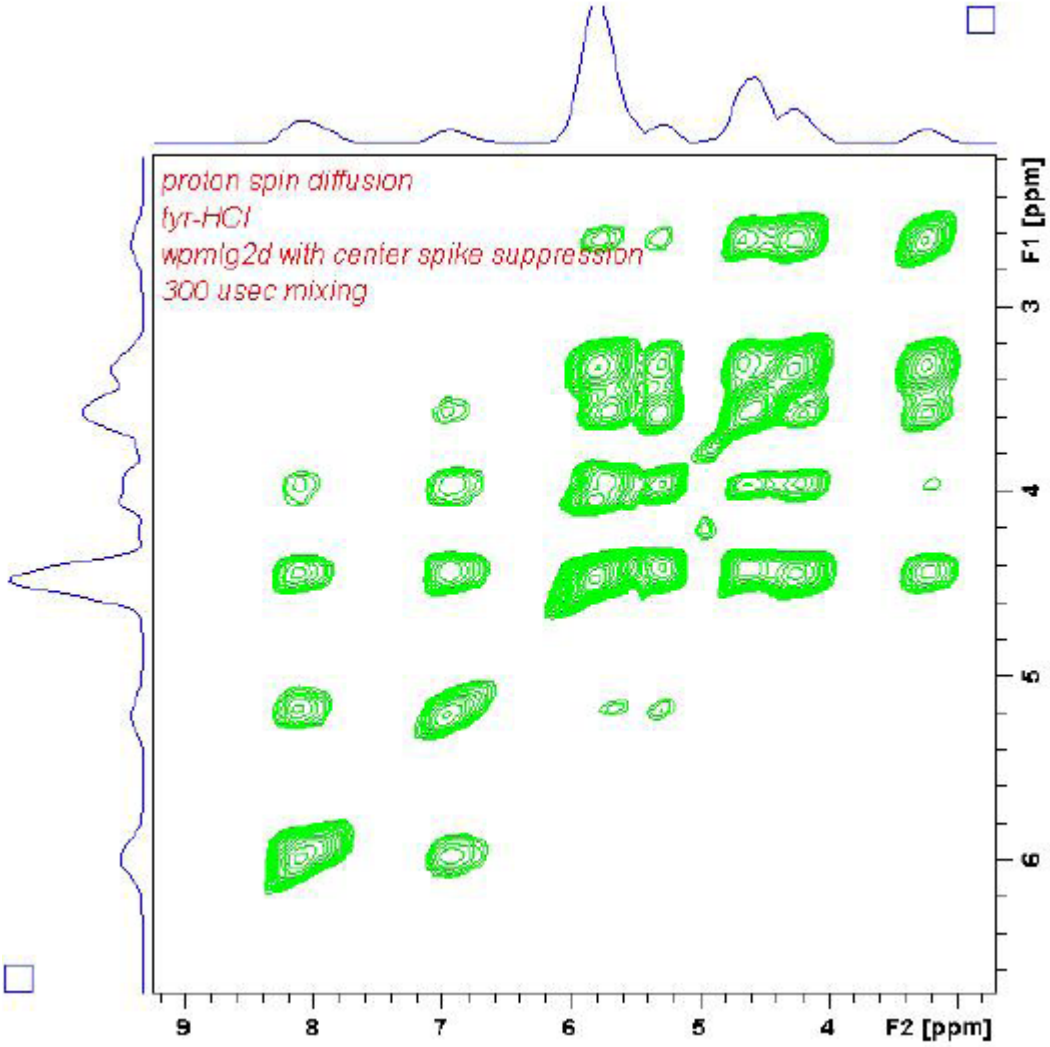

Figure 24.4. Expansion of the Essential Part of the Spectrum

Proton-Proton DQ-SQ Correlation *24.5*

This experiment correlates proton shifts (F2) with double quantum frequencies (sum of shifts of the correlated sites). Double quantum transitions are excited and reconverted by a post-C7 or similar sequence.

Pulse Sequence Diagram 24.6

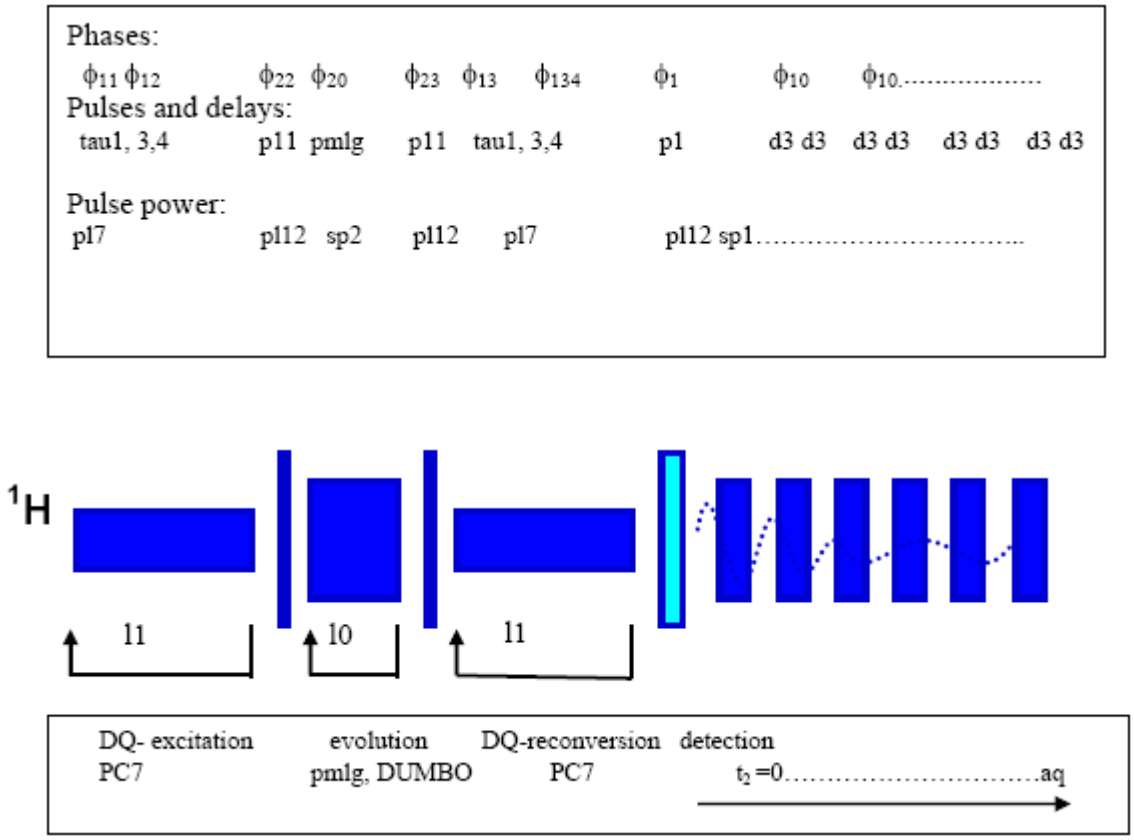

Figure 24.5. Pulse Sequence Diagram

When applied to X-nuclei like ^{13}C, the RF field during this sequence must be carefully matched to the 7-fold spin rate, since the dipolar couplings are small, and care must be taken that the excitation bandwidth of the sequence chosen covers the whole shift range of the X-nucleus. In the case of protons, this is rather forgiving, since the shift range to be covered is small, and the required power levels are easily achieved for protons. Usually it is enough to calculate the required power level from the spin rate and the known proton 90 degree pulse using the au program ***calcpowlev.*** Assume the spin rate is 14000 Hz and post-C7 is used. The required RF field is then 7*14000=98000 Hz. The known proton 90 degree pulse is 2.5 µsec=1/4*2.5e-6 =100000 Hz. Type ***calcpowlev*** and enter 100000, return, then enter 98000, return. The output will be “change power level by 0.18 dB”. The power level for the p-C7 sequence is therefore 0.18 dB to higher attenuation than what is required for a 2.5 µsec pulse.

Table 24.4. Acquisition Parameters

Parameter	Value	Comment
pulprog	wpmlgdqsq	AV 3 instruments only, topspin 2.1 or later.
FnMODE	STATES-TPPI	Any other method may be used with appropriate changes in ppg.
NUC1, NUC2	1H	
sw, swh along F1	same as for F2	Needs to be corrected before transform pulse program calculates approximate values upon ***ased***.
td	512-1k	Depending on resolution.
1 td	128-256	Depending on resolution.
cnst31	spin rate, 10-15 000	Depending on available RF field.
l1	number of pc7-cycles	2-7 depending on dipolar coupling.
spnam1	m5m or m5p as in 1d setup	DUMBO may be used with modified timing.
spnam2	lgs-2 or lgs-4 if used.	Set l3=2 or 4, depending on desired sw1 DUMBER-22 with modified timing.

Table 24.5. Phases, RF-Levels and Timing

Phases	Rf Power Levels	Timing
$\phi_{11,12}$ = POST-C7=$\phi_{13,14}$ $\phi_{11,12}$ incremented for DQ-evol. $\phi_{11,12}$ incremented for DQ-select	pl7 set for RF=7*spin rate	tau1,3,4 calculated from cnst31.
ϕ_1 = CYCLOPS	pl12	p1
$\phi_{22} = 3$	pl12	p11, ~45°
$\phi_{23} = 1$	pl12	p11
$\phi_{10} = 0$	sp1: set for 100-130 kHz RF-field	WPMLG: calculated via cnst20 DUMBO: p10 set by xau dumbo.
ϕ_{31} = DQ selection		

Data Processing 24.7

The spectral width in both dimensions assumes the absence of shift scaling. In order to account for the shift scaling effect of the sequence, one has to increase the spectral width by the scaling factor. Before doing the 2D-fourier transformation, type ***s sw*** to call the status parameters for both F2 and F1 and replace both values by <current value>/0.6. After ***xfb***, the relative peak positions will be (approximately) correct, but the absolute peak positions must be corrected by calibrating a known peak position to the correct value.

Table 24.6. Processing Parameters

Parameter	Value	Comment
mc2	STATES-TPPI	Or whatever used.
wdw	QSINE	Slight-moderate resolution enhancement is usually required.
ssb	3 or 5	
si	2k -4k	
1 si	512 – 1k	

Examples 24.8

These spectra were both taken without the modification according to ***"CRAMPS 2D" on page 291***, so the offset is placed to the down field side and the spectrum width was chosen larger than necessary. The small plots show the full spectrum.

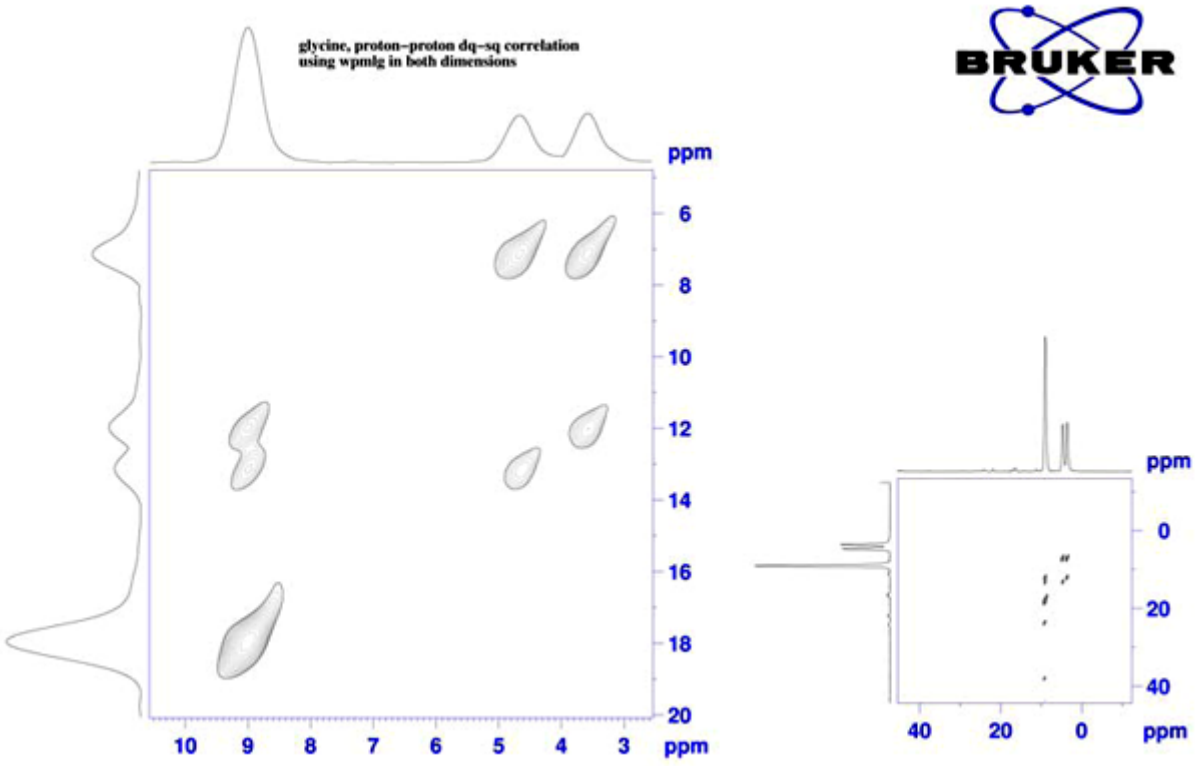

Figure 24.6. Glycine, Proton-Proton DQ-SQ Correlation Using WPMLG in Both Directions

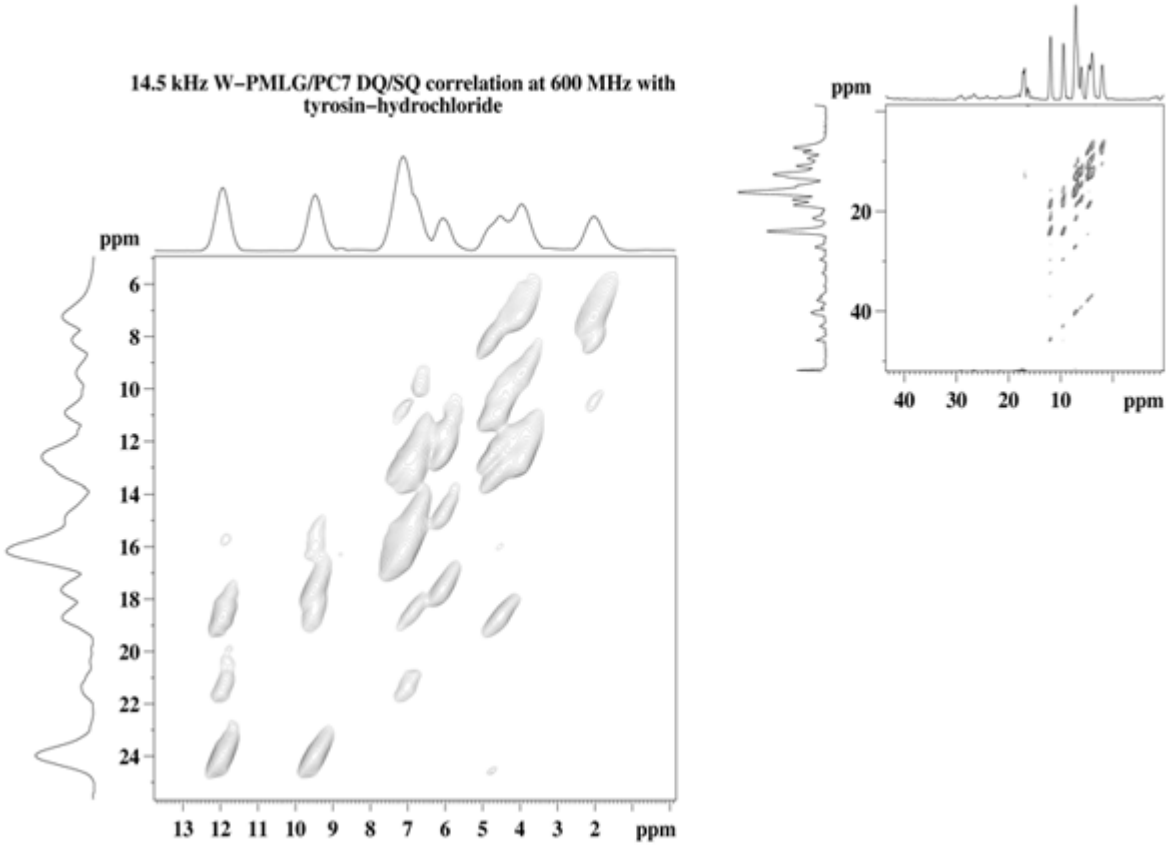

Figure 24.7. 14.5 kHz W-PMLG/PC7 DQ/SQ Correlation at 600 MHz with Tyrosine-Hydrochloride

Appendix A

Form for Laboratory Logbooks A.1

The form on the following page may be printed and filled out by every user using the instrument to trace eventual problems and provide information for the next user.

Another copy may be printed for every user's own laboratory notebook. One form per probe used should be filled out. The following form serves as an example:

Operator	**used from:**		**to:**						
HF	10.12.07 10.00h		13.12.07 18.00h						
Probe:	**shim file:**		**B_0-field:**						
4mm triple C/N/H	triple4.hf		390 SR -360.14						
Sample:	**Experiment:**		**pulses**	**(us)**	**pl(n)**	**(dB/watt)**		**ok?**	**S/N:**
Glycine	CP S/N test	F1 ^{13}C	p90: contact: mix: else:	3.5 2m - -	pl11 pl1	3 3.5	150 120	y	100
		F2 ^{1}H	p90: contact: decouple: mix: else:	2.5 2m 4.6 - -	pl12 sp0 pl12	4 5	120 100		
		F3	p90: contact: decouple: mix: else	- - - 					

stored under filename: glycine-4 /opt/topspin/reference 1 1

comments: spinning at 10 kHz ok, mains pressure at 6 bars, linewidth α-C 50 Hz, O2= 1500,spinal decoupling

Operator	used from:	to:						
Probe:	shim file:	B_0-field:						
		SR:						
Sample:	**Experiment:**	**pulses**	**us**	**pl(n)**	**dB**	**watt**	**ok?**	**S/N:**
	F1	p90: contact: mix: else:						
	F2	p90: contact: decouple: mix: else:						
	F3	p90: contact: decouple: mix: else						
Sample:	**Experiment:**							
stored under filename:								
comments:								

2. Pulse program cpopt:

```
;cpopt (TopSpin 2.1)

;single pulse excitation, acquisition without decoupling

;Avance III version
;parameters:
;d1 : recycle delay
;p3 : proton excitation pulse length as in cp
;pl12 : decoupling/excitation power level for cp
;spnam0 : usual shape for cp
;sp0 : usual shape power for cp contact

;$COMMENT=single pulse excitation, acquisition without decoupling
;$CLASS=Solids
;$DIM=pseudo-2D
;$TYPE=direct excitation
;$SUBTYPE=relaxation measurement
;$OWNER=Bruker
;cnst11 : to adjust t=0 for acquisition, if digmod = baseopt
"acqt0=1u*cnst11"

1 ze
2 d1
  (p3 pl12 ph1):f1
  (p15:sp0 ph10):f1
  go=2 ph31
  wr #0
exit

ph1= 0 2
ph10= 1
ph31= 0 2
```

3. Power conversion table:

power conversion table				
probe: 4mm triple				
nucleus/frequency	p90 (us)	RF-field (kHz)	power (W)	remarks
^{1}H/				
^{19}F/				
^{15}N/				
^{15}N/				
^{29}Si/				
^{13}C/				
^{13}C/				
^{119}Sn/				
^{31}P/				

Figures

1 Introduction 9

2 Test Samples 11

3 General Hardware Setup 15

Figure 3.1. All Connections to the Back of the Preamplifier 16
Figure 3.2. Transmitter Cables (only) Wired to Back of the Preamplifier 17
Figure 3.3. The edasp setpreamp Display 18
Figure 3.4. Additional Connections to the Preamplifier Stack. 19
Figure 3.5. Matching Box Setup for High Power X-BB Preamplifiers 20
Figure 3.6. Standard Double Resonance CP Experiment, Bypassing the Proton Preamp 22
Figure 3.7. Standard CP Experiment, Proton Preamp in Line 22
Figure 3.8. Triple Resonance Experiment, without X-Y Decoupling 23
Figure 3.9. Triple Resonance Experiment, with X-Y Decoupling 23
Figure 3.10. Triple Resonance 1H/19F-Experiment 24
Figure 3.11. 19F/1H Combiner/Filter Set 24
Figure 3.12. Quadruple Resonance HFXY Experiment (WB probes ≥ 400 MHz only!) 25
Figure 3.13. PICS Probe Connector and Spin Rate Monitor Cable on a WB Probe 25
Figure 3.14. Spin Rate Monitor Cable Connector for 2 Different Types of SB Probes 26
Figure 3.15. WB DVT Probe MAS Tubing Connections 28
Figure 3.16. VTN Probe MAS Tubing Connections Note: WVT Probes are VTN-Type Probes 28
Figure 3.17. WB Probes: Eject/Insert Connections 29
Figure 3.18. WB Probes: DVT, Probe Connections for RT and HT Measurements 29
Figure 3.19. SB VTN Probe MAS Connections 30
Figure 3.20. SB DVT probe MAS connections. 31
Figure 3.21. WB Probe MAS VTN and WVT, and DVT Probe Connections 32
Figure 3.22. WB Probe MAS DVT Connections 33
Figure 3.23. SB Probe MAS VTN 34
Figure 3.24. SB Probe MAS DVT Connections 34
Figure 3.25. WB Wideline or PE Probes 35
Figure 3.26. WB Wideline or PE Probe Connections 35
Figure 3.27. Low Temperature Heat Exchanger for VTN Probes (old style) 36
Figure 3.28. Low Temperature Heat Exchanger for DVT Probes 37
Figure 3.29. Low Temperature Liquid N2 Dewar with DVT Probe/Heat Exchanger 38
Figure 3.30. Bottom view of Low Temperature DVT Probe/Heat Exchanger 39
Figure 3.31. Low Temperature Setup with B-CU X (or B-CU 05) 40
Figure 3.32. Low temperature setup with B-CU X 41
Figure 3.33. RF Setup of a Wideline Single Frequency Probe 42
Figure 3.34. Possible Modifiers for Probe Tuning Ranges (400 MHz and up only) 44
Figure 3.35. λ/4 (low range) and λ/2 Mode (high range), 400 MHz Probe 45
Figure 3.36. A λ/4 only probe (left) and a λ/4 - λ/2 probe (right) 46
Figure 3.37. Without/with Parallel Capacitance to Shift the Tuning Range to Lower Frequency 47
Figure 3.38. Parallel Coil to Shift the Tuning Range to Higher Frequency 48

Figure 3.39. Mounting a Triple Insert Into a Triple Probe 49
Figure 3.40. Example of a 600 WB NMR Instrument Site 51
Figure 3.41. Short Display, Pulse Routing Only for C/N/H DCP or REDOR Experiment, observing 13C (above) and 15N (below) 52
Figure 3.42. Long Display, Pulse and Receiver Routing 53
Figure 3.43. Pulse on F2, Observe on F1 - Routing 54
Figure 3.44. The edasp Display for a System with two Receiver Channels 54

4 Basic Setup Procedures 55

Figure 4.1. Routing for a Simple One Channel Experiment 57
Figure 4.2. Probe Connections to the Preamplifier 59
Figure 4.3. Pop-up Window for a New Experiment 60
Figure 4.4. ased Table with Acquisition Parameters for the KBr Experiment 61
Figure 4.5. Graphical Pulse Program Display 62
Figure 4.6. Display Example of a Well-tuned Probe 63
Figure 4.7. Display Example of an Off-Matched and Off-Tuned Probe 64
Figure 4.8. Display Example Where Probe is Tuned to a Different Frequency 64
Figure 4.9. FID and Spectrum of the 79Br Signal of KBr used to Adjust the Magic Angle 65
Figure 4.10. Routing for a Double Resonance Experiment using High Power Stage for H and X-nucleus 66
Figure 4.11. Routing for a Double Resonance Experiment, Changed for Proton Observation 67
Figure 4.12. Proton Spectrum of Adamantane at Moderate Spin Speed 68
Figure 4.13. Setting the Carrier on Resonance 69
Figure 4.14. Expanding the Region of Interest 70
Figure 4.15. Save Display Region to Menu 70
Figure 4.16. The popt Window 71
Figure 4.17. The popt Display after Proton p1 Optimization 72
Figure 4.18. Adamantane 13C FID with 50 msec aq. setsh Display 74
Figure 4.19. Adamantane 13C FID with 50 msec aq. setsh with Optimized Z-Shim Value 74
Figure 4.20. A cp Pulse Sequence 76
Figure 4.21. Hartmann-Hahn Optimization Profile 77
Figure 4.22. Hartmann-Hahn Optimization Profile Using a Square Proton Contact Pulse 78
Figure 4.23. Display Showing α-Glycine Taken Under Adamantane Conditions, 4 scans 79
Figure 4.24. Optimization of the Decoupler Offset o2 at Moderate Power, Using cw Decoupling 80
Figure 4.25. Glycine with cw Decoupling at 90 kHz RF Field 81
Figure 4.26. Glycine Spectrum with Spinal64 Decoupling at 93 kHz RF field 83

5 Decoupling Techniques 89

Figure 5.1. Optimization of TPPM Decoupling, on Glycine at Natural Abundance 90
Figure 5.2. Geometry for the FSLG Condition 93
Figure 5.3. FSLG Decoupling Pulse Sequence Diagram 94
Figure 5.4. Adamantane, FSLG-decoupled, showing the (downscaled) C-H J-couplings. 94
Figure 5.5. Shape with Phase Gradients 96
Figure 5.6. Pulse Program for Hahn Echo Sequence 98

6 Practical CP/MAS Spectroscopy on Spin 1/2 Nuclei 99

7 Basic CP-MAS Experiments 105

Figure 7.1. Pulse Program for CP with Flip-back Pulse 105
Figure 7.2. Pulse Program for CPTOSS. 107

Figure 7.3. Comparison of a CPTOSS and CPMAS Experiment 108
Figure 7.4. CPTOSS243 Experiment on Tyrosine HCl at 6.5 kHz 109
Figure 7.5. CPTOSS Experiment on Tyrosine HCl at 6.5 kHz 110
Figure 7.6. Pulse Program for SELTICS. 111
Figure 7.7. SELTICS at 6.5 kHz Sample Rotation on Tyrosine HCl. 111
Figure 7.8. Cholesterylacetate Spectrum Using Sideband Suppression 112
Figure 7.9. Block Diagram of the Non-quaternary Suppression Experiment 113
Figure 7.10. Glycine 13C CPMAS NQS Experiment with a Dephasing Delay 114
Figure 7.11. Tyrosine 13C CPMAS NQS Experiment with TOSS 115
Figure 7.12. Block Diagram of the CPPI Experiment. 116
Figure 7.13. CPMAS Spectrum of Tyrosine.HCl at 6.5 kHz 117

8 FSLG-HETCOR 119

Figure 8.1. The FSLG Hetcor Experiment 120
Figure 8.2. The “12...” icon, and the ased icon in eda. 121
Figure 8.3. The ased Display 122
Figure 8.4. FSLG Hetcor Spectrum Tyrosine HCl 125
Figure 8.5. FSLG Hetcor Spectrum Tyrosine HCl 126

9 Modifications of FSLG HETCOR 127

Figure 9.1. Comparison of HETCOR with and without 13C-decoupling 128
Figure 9.2. HETCOR Using Windowless Phase Ramps 130
Figure 9.3. HETCOR on tyrosine *HCl without (left) and with LG contact (1msec contact) 136

10 RFDR 137

Figure 10.1. RFDR Pulse Sequence for 2D CPMAS Exchange Experiment 138
Figure 10.2. The “123” Icon in the Menu Bar of the Data Windows Acquisition Parameter Page . 139
Figure 10.3. 13C Histidine Signal Decay as a Function of the RFDR Mixing Time 141
Figure 10.4. 2D RFDR Spectrum of 13C fully Labelled Histidine (RFDR mixing time 1.85 ms). ... 142

11 Proton Driven Spin Diffusion (PDSD) 143

Figure 11.1. CPSPINDIFF Pulse Sequence 145
Figure 11.2. The Acquisition Parameter Window (eda) 147
Figure 11.3. POPT Result for the cw Decoupling Power Variation 150
Figure 11.4. 13C CPSPINDIFF of fully labeled tyrosine*HCl, spinning at 22 kHz, 4.6 msec mix. Upper: PDSD, lower: DARR 151
Figure 11.5. Comparison of DARR/PDSD 152
Figure 11.6. 13C DARR of Fully Labelled Ubiquitine Spinning at 13 kHz 153

12 REDOR 155

Figure 12.1. REDOR Pulse Sequence 157
Figure 12.2. 2D data set after “xf2” processing. 160
Figure 12.3. T1/T2 Relaxation for further Analysis of the Data Figure and the Analysis Interface 161
Figure 12.4. Saving Data to Continue to the Relaxation Window 161
Figure 12.5. Setting the Correct Analysis Parameter 162
Figure 12.6. Plot of the Normalized Signal Intensity Versus the Evolution Time 163
Figure 12.7. Experimental data for the glycine 13C{15N}-REDOR 164
Figure 12.8. Comparison of Experimental Data to a Simulation with Reduced Dipolar Coupling . 165
Figure 12.9. Experimental data with the corresponding M2 parabolic analysis. 166

13 SUPER 169

Figure 13.1. Pulse Sequence for 2D CPMAS exchange experiment 170
Figure 13.2. The “123” Icon in the Menu Bar of the Data Windows Acquisition Parameter Page. 171
Figure 13.3. The Acquisition Parameter Window (eda) 172
Figure 13.4. The SUPER Spectrum of Tyrosine HCl After Processing Using “xfb” 175
Figure 13.5. SUPER spectrum after tilting the spectrum setting “1 alpha” = -1 176
Figure 13.6. Various Cross Sections from the Upper 2D Experiment 177

14 Symmetry Based Recoupling 179

Figure 14.1. C7 SQ-DQ Correlation Experiment 181
Figure 14.2. Optimization of the RF power level for DQ generation/reconversion on glycine. 184
Figure 14.3. Variation of DQ-generation/reconversion time on a uniformly 13C labeled peptide (fM-LF). 184
Figure 14.4. PC7 Recoupling Efficiency at a Spinning Speed of 13 kHz 185
Figure 14.5. SC14 2d SQ-DQ correlation on tyrosine-HCl 189
Figure 14.6. PC7 2d SQ-SQ correlation on tyrosine-HCl 191

15 PISEMA 193

Figure 15.1. Pisema Pulse Sequence 194
Figure 15.2. PISEMA Spectrum of 15N Labeled Acetylated Valine and FID in t1 over 3.008 ms 64 Data Points 199
Figure 15.3. PISEMA Spectrum of 15N Labeled Kdpf Transmembrane Protein. 200

16 Relaxation Measurements 201

Figure 16.1. The CPX T1 Pulse Sequence 203
Figure 16.2. Relaxation of Alpha-carbon Signal in Glycine 207

17 Basic MQ-MAS 213

Figure 17.1. A 3-Pulse Basic Sequence with Z-Filter. 214
Figure 17.2. A 4-Pulse Basic Sequence with Z-Filter. 214
Figure 17.3. Comparison of 87Rb MAS spectra of RbNO3 excited with selective and non-selective pulses. 217
Figure 17.4. Nutation profiles of selective and non-selective pulses. 218
Figure 17.5. Example for popt Set-up for Optimization of p1 and p2. 219
Figure 17.6. Signal Intensities of 87Rb Resonances in RbNO3 as Function of p1 and p2. 220
Figure 17.7. 2D 87Rb 3QMAS Spectrum of RbNO3. 223
Figure 17.8. Comparison of Differently Processed 2D 23Na 3Q MAS Spectra of Na4P2O7. 224
Figure 17.9. Calculated Shift Positions dMQ 225
Figure 17.10. 17O MQMAS of NaPO3 at 11.7 T (67.8 MHz) on the left and 18.8 T (108.4 MHz) on the right. 228
Figure 17.11. Slices and Simulations of the 18.8 T 17O MQMAS of NaPO3. 229
Figure 17.12. Graphical Interpretation of the Spectrum from ***Figure 17.10.***. 230

18 MQ-MAS: Sensitivity Enhancement 231

Figure 18.1. Hahn Echo Pulse Sequence and Coherence Transfer Pathway. 232
Figure 18.2. Processing of Hahn Echo. Left is the Shifted Echo. 233
Figure 18.3. Four Pulse Sequence and Coherence Transfer Pathway for the 3Q MAS Experiment .. 234
Figure 18.4. Three Pulse Sequence and Coherence Transfer Pathway 234

Figure 18.5. Example for popt to Set-up for Optimization of DFS. 237
Figure 18.6. Signal Intensities of 87Rb in RbNO3 238
Figure 18.7. Pulse Sequence and Coherence Transfer Pathways for SPAM 3QMAS. 243

19 STMAS 245

Figure 19.1. Principle of 2D Data Sampling in STMAS Experiments. 245
Figure 19.2. Four-pulse sequence and coherence transfer pathway for the double quantum filtered STMAS experiment with z-filter (stmasdqfz.av) 247
Figure 19.3. Four pulse sequence and coherence transfer pathway 248
Figure 19.4. 87Rb STMAS Spectra of RbNO3 252

20 Double-CP 255

Figure 20.1. Pulse sequence diagram for 1D (t1=0) and 2D double CP experiments. 256
Figure 20.2. The edasp routing tables for H-C-N double CP. 257
Figure 20.3. Routing table for triple resonance setup change for 15N pulse parameter measurement and CPMAS optimization. 258
Figure 20.4. Shape Tool display with ramp shape from 45 to 55%. 261
Figure 20.5. Shape Tool display with a tangential shape for adiabatic cross polarization. 262
Figure 20.6. Double CP optimization of PL5 in increments of 0.1 dB. 263
Figure 20.7. Double CP yield, measured by comparing CPMAS and DCP amplitudes of the high field resonance. 263
Figure 20.8. C-N correlation via Double CP in histidine (simple setup sample). 4mm Triple H/C/N Probe. 267
Figure 20.9. NCαCx correlation experiment with 22 ms DARR mixing period for Cα-Cx spin diffusion on GB1 protein run using an EFREE-Probe. 268
Figure 20.10. NCaCx correlation experiment with 4.2 ms SPC5-DQ mixing period for CaCx spin diffusion on GB1 protein run using an EFREE-Probe at 14 kHz sample rotation and 100 kHz decoupling. 269

21 CRAMPS: General 271

Figure 21.1. Difference in Amplitude of the Quadrature Channels X and Y 273

22 CRAMPS 1D 275

Figure 22.1. Pulse Sequence Diagram 275
Figure 22.2. PMLG Shape for wpmlg, sp1 276
Figure 22.3. Shape for DUMBO, sp1 277
Figure 22.4. Analog Sampling Scheme 278
Figure 22.5. Digital Sampling Scheme 278
Figure 22.6. Optimizing sp1 for Best Resolution 282
Figure 22.7. Optimizing cnst25 for Minimum Carrier Spike, Optimized at 120°C 283
Figure 22.8. Optimizing p14 for Minimum Carrier Spike, Optimized at 0.6 µsec 283
Figure 22.9. WPMLG-CRAMPS After Optimization, Digital Acquisition 284

23 Modified W-PMLG 285

Figure 23.1. Pulse Sequence Diagram 285

24 CRAMPS 2D 291

Figure 24.1. Pulse Sequence Diagram 292
Figure 24.2. Setup and Test Spectrum of Alpha-glycine 294

Figure 24.3. Spectrum of Tyrosine-hydrochloride 295
Figure 24.4. Expansion of the Essential Part of the Spectrum 296
Figure 24.5. Pulse Sequence Diagram 297
Figure 24.6. Glycine, Proton-Proton DQ-SQ Correlation Using WPMLG in Both Directions 300
Figure 24.7. 14.5 kHz W-PMLG/PC7 DQ/SQ Correlation at 600 MHz with Tyrosine-Hydrochloride ... 301

A Appendix ***303***

Tables

1 Introduction 9

2 Test Samples 11

Table 2.1. Setup Samples for Different NMR Sensitive Nuclei 11

3 General Hardware Setup 15

4 Basic Setup Procedures 55

Table 4.1. Summary of Acquisition Parameters for Glycine S/N Test 82
Table 4.2. Processing Parameters for the Glycine S/N-Test 83
Table 4.3. Reasonable RF-fields for Max. 2% Duty Cycle 85

5 Decoupling Techniques 89

Table 5.1. Acquisition Parameters 95
Table 5.2. Processing Parameters 96

6 Practical CP/MAS Spectroscopy on Spin 1/2 Nuclei 99

Table 6.1. Power Conversion Table 101

7 Basic CP-MAS Experiments 105

Table 7.1. Acquisition Parameters 106
Table 7.2. Acquisition Parameters 107
Table 7.3. Acquisition Parameters 113

8 FSLG-HETCOR 119

Table 8.1. Acquisition Parameters for FSLG-HETCOR (on tyrosine-HCl) 123
Table 8.2. Processing Parameters for FSLG-HETCOR (on tyrosine-HCl) 124

9 Modifications of FSLG HETCOR 127

Table 9.1. Acquisition Parameters for pmlg-HETCOR (on tyrosine-HCl) 130
Table 9.2. Processing Parameters for pmlg-HETCOR (as for FSLG on tyrosine-HCl) 131
Table 9.3. Acquisition Parameters for wpmlg-HETCOR (on tyrosine-HCl) 132
Table 9.4. Acquisition Parameters for e-DUMBO-HETCOR (on tyrosine-HCl) 133
Table 9.5. Acquisition Parameters for DUMBO-HETCOR (on tyrosine-HCl) 134

10 RFDR 137

Table 10.1. Acquisition Parameters 140
Table 10.2. Processing Parameters 141

11 Proton Driven Spin Diffusion (PDSD) 143

Table 11.1. Acquisition Parameters 148
Table 11.2. Processing Parameters 149

12 REDOR *155*

Table 12.1. Acquisition Parameters for a 13C observed C/N REDOR 158
Table 12.2. Results for the M2 Calculation and the Simulations 167

13 SUPER *169*

Table 13.1. Acquisition Parameters 173
Table 13.2. Processing Parameters 174

14 Symmetry Based Recoupling *179*

Table 14.1. Recommended Probe/Spin Rates for Different Experiments and Magnetic Field Strengths 182
Table 14.2. Acquisition parameters for DQ-SQ correlation experiments using symmetry based recoupling sequences 186
Table 14.3. Processing parameters for DQ-SQ correlation experiments using symmetry based recoupling sequences 188

15 PISEMA *193*

Table 15.1. Acquisition Parameters 197
Table 15.2. Processing Parameters for the Pisema Experiment 198

16 Relaxation Measurements *201*

Table 16.1. Parameters for the 1D CP Inversion Recovery Experiment 204
Table 16.2. Parameters for 2D Inversion Recovery Experiment 205
Table 16.3. Processing Parameters for CP T1 Relaxation Experiment 205
Table 16.4. Parameters for the Saturation Recovery Experiment 209

17 Basic MQ-MAS *213*

Table 17.1. Some Useful Samples for Half-integer Spin Nuclei 216
Table 17.2. Initial Parameters for Setup 219
Table 17.3. F1 Parameters for 2D Acquisition 220
Table 17.4. Processing Parameters for 2D FT 222
Table 17.5. Values of |R-p| for Various Spins I and Orders p 226
Table 17.6. Chemical Shift Ranges for all MQ Experiments for All Spins I 227

18 MQ-MAS: Sensitivity Enhancement *231*

Table 18.1. Initial Parameters for the DFS Experiment 236
Table 18.2. Parameters for 2D Data Acquisition of 3-pulse Shifted Echo Experiment mp3qdfs.av. .. 239
Table 18.3. Parameters for 2D Data Acquisition of 4-pulse Z-filtered Experiment mp3qdfsz.av. 240
Table 18.4. Processing Parameters 241
Table 18.5. Parameters for FAM 242
Table 18.6. Further Parameters for 2D Data Acquisition of SPAM MQMAS Experiment mp3qspam.av 243

19 STMAS *245*

Table 19.1. Time deviation of the rotor period for spinning frequency variations of ± 1 and ± 10 Hz for various spinning frequencies. 246
Table 19.2. Some Useful Samples for Some Nuclei with Half Integer Spin 249
Table 19.3. Initial Parameters for the Set-up of stmasdfqz.av. 250
Table 19.4. Initial Parameters for the Set-up of stmasdfqe.av. 251
Table 19.5. F1 Parameters for the 2D Data Acquisition. 252
Table 19.6. Processing Parameters for the 2DFT 253
Table 19.7. Values of R and çR-pç for the Various Spin Quantum Numbers Obtained in the STMAS Experiment 254

20 Double-CP *255*

Table 20.1. Recommended Parameters for the DCP Setup....260
Table 20.2. Recommended Parameters for the DCP 2D Setup 265
Table 20.3. Recommended Processing Parameters for the DCP 2D 266

21 CRAMPS: General *271*

22 CRAMPS 1D *275*

Table 22.1. Phases, RF-Levels, Timings 275
Table 22.2. PMLG Analog Mode....279
Table 22.3. DUMBO, Analog Mode....280
Table 22.4. Parameters for Digital Mode 282

23 Modified W-PMLG *285*

Table 23.1. Phrases, RF-Levels, Timings 285
Table 23.2. PMLG, Analog Mode 287
Table 23.3. DUMBO, Analog Mode....288
Table 23.4. Parameters for Digital Mode 289

24 CRAMPS 2D *291*

Table 24.1. Acquisition Parameters....292
Table 24.2. Phases, RF-levels, and Timings....293
Table 24.3. Processing Parameters....293
Table 24.4. Acquisition Parameters....298
Table 24.5. Phases, RF-Levels and Timing 298
Table 24.6. Processing Parameters....299

A Appendix *303*

Tables

Index

Symbols

(NH4)2SeO4 12
(NH4)H2PO4 11

Numerics

13C Matching Box 59
1H HP Preamplifier 59
79Br Signal 65
90° pulse 55

A

Adamantane ..... 11 – 12
ADP 103
AgNO3 13
AlPO-14 11
analog mode 277
Anatas 12
as hydroquinon 11
ased 60
AU-program DUMBO 97

B

B0-field 82
background signal 100
background suppression 100
BaClO3*H2O 279
Basic Setup Procedures 55
Beff 93
BF1 58
BLEW-12 92
BN 11
Boric Acid 11
BR-24 ..... 92, 272
breakthrough 56
bsmsdisp 75
bypassing the preamp 73

C

C-24 272
calcpowlev 72
Calibrating 75

Carrier 69
Cd(NO3)2*4H2O 12
Chemical Shifts 75
Clathrate 11
cnst20 121
Co(CN)6 12
Compressors 56
conductivity 100
contact time 76
CORTAB 58
cpdprg2 81
CPPI ..... 105, 116 – 117
CPPIRCP ..... 116 – 117
CPPISPI ..... 116 – 117
CRAMPS 271
Cross polarisation 76
cross polarisation 55
cross polarization under a LG frequency offset 119
Cu-metal powder 11
CW decoupling 89

D

D2O 12
d-DMSO2 12
Default 58
dielectric loss 100
digital mode 277
d-PE 12
dpl 70
d-PMMA 12
dry gas 56
dryers 56
DSS 12, 103
–Dtossb 106
DUMBO 97, 134, 272

E

eda 57, 121
EDASP 58
edasp 57
edc 59
e-DUMBO 133
experiment button 61

F

frequency 57
Frequency Switched Lee Goldburg 92, 272
Frequency Switched Lee Goldburg Heteronuclear Correlation 119
FSLG 272
FSLG Decoupling 92
FSLG pulse 119

G

Ga2O3 11
gas 56
gas in air 11
Glycine 11
Good Laboratory Practice 84
graphical display 61
group 71

H

H3SeO3 12
Hartmann-Hahn 77
Hartmann-Hahn-condition 76
Heteronuclear Decoupling 89
Hg 12
Hg(acetate)2 12
HH conditions 78
HH profile 78
high 66
High power decoupling 56
Homonuclear decoupling 92
Homonuclear dipolar interactions 271
HP-HPPR modules 73
HPLNA 1H modules 73

I

IN_F1 121
inversion-recovery 202
irradiation frequency 58

K

K2Pt(OH)6 12
K2S 12
KBr 12, 55, 65
KCl 12
KMnO4 12

L

Lee Goldburg condition 92
LG Offset 135
Li (org.) 12
LiCl ..... 11 – 12
local motions 202
logical channel 57
longitudinal relaxation 201

M

magic angle 55, 92
Malonic Acid 11
matching box 58
monoexponential 207
MREV-8 ..... 92, 272
MSHOT 272
Multiple Pulse Decoupling 92
Multiple pulse NMR 92

N

Na2HPO4 11
Na3P3O9 11
new 65
nexp 71
NH4Cl 12
NH4VO4 11
nonexponential decay 209
NQS 113
nrf 55

O

observe nucleus 58
offset O1 58
oil-free gas 56
optimize 71
optimum posmax 71

P

Pb(p-tolyl)4 12
PbNO3 12
PCPD2 82
pcpd2 ..... 83, 90
peakw 85
phase modulated pulses 119
phase-modulation 93
Pi-pulse decoupling 91
PMLG 93
pmlg 130
pmlghet 129
popt 71, 90
poptau.exe 71
power conversion factor 101
Power Conversion Table 101
powmod 58, 66
powmod high 66
preamp 58
preamplifier 58
Profile ..... 77 – 78
Proton Bandpass Filter 59

proton T1 99
proton T1ρ 78, 99
Proton-Proton DQ-SQ Correlation 296
pseudo-2D 205
PTFE 11
Pulprog 61
PVDF 11

Q

Q8M8 12

R

RbClO4 11
RbNO3 11
relaxation 201
Resonance 69
RF voltages 56
RFDR 137
RF-efficiency 55
RF-field 55
RF-performance 55
RF-power 55
RF-routing 55

S

Sampling 277
saturation recovery 208
saturation-recovery experiment 203
save button 71
Save Display Region to 70
SB probes 86
scaling factor 274, 282
SELTICS ..... 107, 110 – 111
semi-windowless 92
sensitivity 55
setsh 73
SFO1 58
SGU1 58
shimming 55
Silicone paste 11
Silicone rubber 11
sinocal 83
skip 71
Skip optimization 71
Sm2Sn2O7 11
Sn(cyclohexyl)4 11
SnO2 11
spin nutation frequencies 55
spin rate monitor 55
SPINAL 91
SPINAL decoupling 91

spin-lattice relaxation 201
spin-locking pulse 202
spinning gas 55
spin-spin relaxation 202
spnam0 84
sr 75
SSNMR 55
start optimize 71
stop optimization 71
susceptibility compensated 74
SwitchF1/F2 66

T

T1 ..... 99, 202
T1/T2 relaxation 205
T1r 202
T1ρ 99
T2 202
TI-S 99
TMSS 12
Torchia method 203
TOSS 107
tp90 55
TPPM decoupling 90
transmitter 58
transverse magnetization 201
TREV-8 272

V

variable delay 203
variable pulse list 210
varmod 71

W

WaHuHa 272
WHH-4 272
windowless sequences 92
wobb 62
wobb high 67
W-PMLG 272

X

X Low Pass Filter 59
xau angle 65
X-BB Preamplifier 59
XiX decoupling 91

Y

Y(NO3)3*6H2O 13

Z

ZGoption –Dlacq 75
ZGOPTNS 106
α-carbon at 43 ppm 80
α-glycine 12, 79
γ-glycine 79

Index

End of Document

Bruker BioSpin, your solution partner

Bruker BioSpin provides a world class, market-leading range of analysis solutions for your life and materials science needs.

Our solution-oriented approach enables us to work closely with you to further establish your specific needs and determine the relevant solution package fromour comprehensive range, or even collaborate with you on new developments.

Our ongoing efforts and considerable investment in research and development illustrates our long-term commitment to technological innovation on behalf of our customers. With more than 40 years of experience meeting the professional scientific sector's needs across a range of disciplines, Bruker BioSpin has built an enviable rapport with the scientific community and various specialist fields through understanding specific demand, and providing attentive and responsive service.

Bruker BioSpin Group

info@bruker-biospin.com
www.bruker-biospin.com